

V.I. Djunin · A.V. Korzun



# Hydrogeodynamics of Oil and Gas Basins



Springer

# Hydrogeodynamics of Oil and Gas Basins

V.I. Djunin<sup>†</sup> · A.V. Korzun

# Hydrogeodynamics of Oil and Gas Basins

 Springer

V.I. Djunin<sup>†</sup>

Dr. A.V. Korzun  
Lomonosov Moscow State  
University  
Faculty of Geology  
Leninskie Gory  
Moskva  
Russia 119992

Translated by Ivan Basov

The Russian language edition of the book Гидрогеодинамика нефтегазоносных бассейнов was first published by Nauchnyi Mir, Moscow, in 2005.

«Гидрогеодинамика нефтегазоносных бассейнов»

© В.И. Дюнин, А.В. Корзун, 2005

© Научный мир, 2005

“Hydrogeodynamics of Oil and Gas Basins”

Copyright © 2005, by Nauchnyi Mir and Djunin V.I., Korzun A.V.

ISBN 978-90-481-2846-4

e-ISBN 978-90-481-2847-1

DOI 10.1007/978-90-481-2847-1

Springer Dordrecht Heidelberg London New York

Library of Congress Control Number: 2009937414

© Springer Science+Business Media B.V. 2010

No part of this work may be reproduced, stored in a retrieval system, or transmitted in any form or by any means, electronic, mechanical, photocopying, microfilming, recording or otherwise, without written permission from the Publisher, with the exception of any material supplied specifically for the purpose of being entered and executed on a computer system, for exclusive use by the purchaser of the work.

*Cover illustration:* Cover Image(s) © 2009 JupiterImages Corporation

Printed on acid-free paper

Springer is part of Springer Science+Business Media ([www.springer.com](http://www.springer.com))

*Dedicated to late Boris Ivanovich Kudelin, who was a pioneer in the study of deep underground drainage at the Chair of Hydrogeology in the Geological Department of the Moscow State University.*

# Preface

Existing views on geodynamics (recharge, migration, discharge) of fluids at deep layers of petroliferous basins are summarized. The infiltration and elision theories explaining development of fluid pressures in deep formations are called into question based on quantitative estimates available for some artesian (petroliferous) basins. Using the West Siberian, Pechora, Terek-Kuma, Bukhara–Karshi, and other petroliferous basins as examples, the stratum-block structure of deep formations is substantiated for stratified systems of platform in inter- and intramontane depressions. It is shown that petroliferous reservoirs at great depths are characterized, regardless of lithology, by largely fissure-related capacity and permeability (clayey rocks included) changeable in space and through geological time. Much attention is paid to development of abnormally high formation pressures. Peculiarities in heat and mass transfer at deep levels are considered for different regions. The energetic formation model substantiated for deep fluids explains different anomalies (baric, thermal, hydrogeochemical, mineralogical, and others) at deep levels of platforms. Based on hydrogeodynamic considerations, the theory of oil origin and formation of hydrocarbon fields is proposed. The book is of interest for oilmen, hydrogeologists, geologists, and specialists dealing with prospecting of petroliferous deposits as well as industrial, mineral, and thermal waters in deep formations of stratified sedimentary basins.

# Contents

<b>1 Existing Views on Fluidodynamics in Petroliferous Formations . . .</b>	<b>1</b>
References . . . . .	11
<b>2 Investigation Methods of Deep Fluidodynamics . . . . .</b>	<b>15</b>
2.1 Methods of Formation Pressure Reducing . . . . .	16
2.2 Assessment of Directions of Density-Variable Fluid Flows by the “Filtration Force” Method . . . . .	25
2.3 The Direct Method of Assessing Density-Variable Deep Fluid Flow Directions . . . . .	26
2.4 Modeling Methods in the Studies of Deep Fluid Flows . . . . .	27
2.5 Compilation Methods of Regional Potentiometric Maps for Petroliferous Formations . . . . .	30
2.6 Methods of Compiling Hydrogeodynamic Maps . . . . .	33
2.7 Investigation Methods of Temperature and Concentration Fields . . . . .	34
References . . . . .	35
<b>3 Role of Regional Infiltration Recharge Sources in the Formation of Deep Fluids and Petroliferous Basin Hydrodynamic Zoning . . . . .</b>	<b>37</b>
3.1 Role of Petroliferous Basin Periphery in Recharge of Deep Fluids . . . . .	37
3.2 Hydrodynamic Zones in Petroliferous Basins . . . . .	41
References . . . . .	45
<b>4 Elision Recharge and Paleomigration of Deep Fluids . . . . .</b>	<b>47</b>
References . . . . .	56
<b>5 Genesis of Abnormally High Formation Pressures . . . . .</b>	<b>59</b>
5.1 The Relaxation Period of Abnormally High Formation Pressures . . . . .	61
5.2 Possibilities for Development of Fluidodynamic Horizontal Boundaries in Clayey Sequences . . . . .	63
5.2.1 Variant 1 . . . . .	67
5.2.2 Variant 2 . . . . .	67

5.2.3	Variant 3 . . . . .	69
5.2.4	Variant 4 . . . . .	69
5.2.5	Variant 5 . . . . .	69
5.2.6	Variant 6 . . . . .	69
5.2.7	Variant 7 . . . . .	70
5.3	Main Factors and Processes Responsible for Development of Abnormally High Formation Pressures . . . . .	72
5.3.1	Elision Processes . . . . .	72
5.3.2	Dehydration of Clay Minerals . . . . .	73
5.3.3	Tectonic Forces (External Factor) . . . . .	74
5.3.4	Additional Recharge . . . . .	81
5.3.5	Catagenetic Processes . . . . .	83
5.3.6	Chemical Processes . . . . .	84
5.3.7	Temperature Changes . . . . .	84
	References . . . . .	87
<b>6</b>	<b>Development of Filtration Properties in Deep Formations of Petroliferous Basins . . . . .</b>	<b>89</b>
6.1	Development of Reservoir Properties in Terrigenous Formations . . . . .	90
6.1.1	Sedimentation Settings . . . . .	90
6.1.2	Catagenetic Rock Transformations . . . . .	94
6.1.3	Compaction . . . . .	94
6.1.4	Dissolution . . . . .	97
6.1.5	Cementation . . . . .	99
6.1.6	Tectonics . . . . .	105
6.1.7	Hydraulic Fracturing . . . . .	106
6.2	Development of Reservoir Properties in Carbonate Rocks . . . . .	108
6.2.1	Compaction . . . . .	109
6.3	Formation of Clayey Reservoirs . . . . .	112
6.3.1	Geostatic Compaction . . . . .	113
6.3.2	Temperature and Mineralization . . . . .	113
6.3.3	Mineralogical Composition of Clayey Rocks . . . . .	115
6.4	Permeability of Saliferous Rocks . . . . .	126
6.5	Conclusions . . . . .	127
	References . . . . .	128
<b>7</b>	<b>Fluidodynamics in Deep Formations of the West Siberian Petroliferous Basin . . . . .</b>	<b>131</b>
7.1	Geological and Tectonic Structure . . . . .	131
7.1.1	Lower–Middle Jurassic Complex ( $J_{1-2}$ ) . . . . .	131
7.1.2	Upper Jurassic–Lower Valanginian Complex ( $J_3-K_{1v}$ ) . . . . .	133
7.1.3	Lower Cretaceous–Cenomanian Complex ( $K_{1a}-K_{2sm}$ ) . . . . .	133
7.1.4	Upper Cretaceous–Paleogene Complex ( $K_2-P$ ) . . . . .	134



7.1.5	Paleogene–Quaternary Complex (P–Q) . . . . .	134
7.1.6	Tectonics . . . . .	134
7.2	Hydrogeological Conditions of the Basin . . . . .	137
7.2.1	Aptian–Cenomanian Aquifer (K <sub>1</sub> a–K <sub>2</sub> sm) . . . . .	137
7.2.2	Neocomian Petroliferous Complex (K <sub>1</sub> v–b) . . . . .	138
7.2.3	Lower–Middle Jurassic Petroliferous Complex (J <sub>1–2</sub> ) . . . . .	139
7.3	Some Peculiarities in Filtration Properties of Rocks . . . . .	141
7.4	Influence of Peripheral Areas of the Basin on Fluidodynamics in Petroliferous Formations . . . . .	147
7.4.1	Characteristic of Areas Providing Recent Infiltration Recharge of Deep Fluids . . . . .	147
7.4.2	Characteristic of Present-Day Deep Fluid Discharge Areas . . . . .	150
7.4.3	Discharge Stimulated by Recovery of the Lower Hydrogeological Stage Due to Erosion . . . . .	152
7.4.4	Discharge Along Tectonic Fractures and Brecciation Zones . . . . .	154
7.4.5	Discharge in the Form of Ascending Migration of Deep Fluids Through Low-Permeability Rocks . . . . .	154
7.5	Influence of the Elision Recharge on Formation Pressures at Deep Levels . . . . .	160
7.6	Fluidodynamics of Deep Formations in Central Areas of the Basin . . . . .	165
7.6.1	Salym Field . . . . .	166
7.6.2	Western Surgut Field . . . . .	170
7.6.3	Kharasavei Field . . . . .	174
7.6.4	Ust-Balyk Field . . . . .	176
7.7	Vertical Paleomigration of Deep Fluids . . . . .	180
7.8	Main Conclusions . . . . .	183
	References . . . . .	183
<b>8</b>	<b>Fluidodynamics in Hydrocarbon-Bearing Formations of the Northern Pechora Petroliferous Basin . . . . .</b>	<b>187</b>
8.1	Geological Structure . . . . .	187
8.1.1	Paleozoic Group (PZ) . . . . .	187
8.1.2	Cambrian System (C) . . . . .	187
8.1.3	Ordovician System (O) . . . . .	189
8.1.4	Silurian System (S) . . . . .	189
8.1.5	Devonian System (D) . . . . .	189
8.1.6	Carboniferous System (C) . . . . .	191
8.1.7	Permian System (P) . . . . .	191
8.1.8	Mesozoic Group (MZ) . . . . .	192
8.1.9	Triassic System (T) . . . . .	192
8.1.10	Jurassic System (J) . . . . .	193
8.1.11	Cretaceous System (K) . . . . .	193
8.1.12	Cenozoic Group (KZ) . . . . .	193

8.2	Tectonics . . . . .	194
8.3	Hydrogeological Conditions . . . . .	195
8.3.1	Upper Jurassic–Cretaceous Confining Sequence (J <sub>3</sub> -K) . . . . .	196
8.3.2	Jurassic Aquifer (J) . . . . .	196
8.3.3	Upper Permian–Triassic Aquifer (P <sub>2</sub> -T) . . . . .	197
8.3.4	Lower Permian (Kungurian) Confining Sequence (P <sub>2</sub> kg) . . . . .	197
8.3.5	Upper Viséan–Artinskian Aquifer (C <sub>1v3</sub> -P <sub>1ar</sub> ) . . . . .	197
8.3.6	Viséan Confining Sequence (C <sub>1v1</sub> ) . . . . .	198
8.3.7	Upper Frasnian–Tournaisian Complex (D <sub>3f3</sub> -C <sub>1t</sub> ) . . . . .	198
8.3.8	Kynov–Sargaevo (Lower Frasnian) Confining Sequence (D <sub>3kn-sr</sub> ) . . . . .	198
8.3.9	Middle Devonian–Lower Frasnian Aquifer (D <sub>2</sub> -D <sub>3f1</sub> ) . . . . .	199
8.3.10	Ordovician (Silurian)–Lower Devonian Aquifer (O–D <sub>1</sub> ) . . . . .	199
8.3.11	Vendian–Lower Cambrian Aquifer (V–C) . . . . .	200
8.3.12	Riphean Aquifer (R) . . . . .	200
8.4	Methods Used for the Analysis of Fluid Geodynamics in Deep Formations of the Pechora Petroliferous Basin . . . . .	200
8.5	Fluid Dynamics in Deep Formations of Individual Well-Studied Structures . . . . .	208
8.6	Regional Peculiarities of Fluidodynamics in the Pechora Petroliferous Basin . . . . .	210
8.6.1	Silurian–Lower Devonian Petroliferous Complex . . . . .	212
8.6.2	Upper Permian–Triassic Petroliferous Complex . . . . .	214
8.7	Abnormally High Formation Pressures in the Northern Pechora Petroliferous Basin . . . . .	215
8.8	The Temperature Field in Deep Formations . . . . .	218
8.9	Distribution of Deep Fluid Mineralization . . . . .	225
8.10	Typification of Hydrodynamic Blocks . . . . .	232
8.10.1	Blocks of the First Type . . . . .	233
8.10.2	Blocks of the Second Type . . . . .	234
8.10.3	Blocks of the Third Type . . . . .	235
8.10.4	Blocks of the Fourth Type . . . . .	235
8.10.5	Blocks of the Fifth Type . . . . .	236
8.10.6	Blocks of the Sixth Type . . . . .	236
8.11	Conclusions . . . . .	236
	References . . . . .	237
<b>9</b>	<b>Fluidodynamics in Deep Formations of the Eastern Ciscaucasia Petroliferous Basin . . . . .</b>	<b>239</b>
9.1	Geological Structure . . . . .	239
9.1.1	The Jurassic System . . . . .	239
9.1.2	The Cretaceous System . . . . .	241

9.1.3	The Cenozoic Group . . . . .	241
9.1.4	The Quaternary System ( <i>Q</i> ) . . . . .	242
9.2	Tectonics . . . . .	242
9.3	Hydrogeological Conditions . . . . .	244
9.3.1	The Maikop Aquifer . . . . .	245
9.3.2	The Paleocene–Eocene Aquifer . . . . .	245
9.3.3	The Upper Cretaceous Petroliferous Complex . . . . .	246
9.3.4	The Lower Cretaceous Petroliferous Complex . . . . .	247
9.3.5	The Upper Jurassic Petroliferous Complex . . . . .	247
9.3.6	The Lower–Middle Jurassic Petroliferous Complex . . . . .	248
9.3.7	The Permian–Triassic Petroliferous Complex . . . . .	249
9.4	Influence of Peripheral Parts of the Basin on Fluidodynamics in Deep Petroliferous Complexes . . . . .	250
9.5	Influence of Elision Recharge on the Formation of Deep Fluid Pressures . . . . .	261
9.6	Local Fluidodynamics in Individual Structures of the Basin . . . . .	263
9.6.1	The Russkii Khutor Severnyi Settlement . . . . .	267
9.6.2	The Zapadno-Mekteb Field . . . . .	269
9.6.3	The Velichaevsk Area . . . . .	269
9.6.4	The Achikulak Area . . . . .	269
9.6.5	The Ozek-Suat Area . . . . .	272
9.7	Abnormally High Formation Pressures . . . . .	274
9.8	Regional Fluidodynamics in the Eastern Ciscaucasia Petroliferous Basin . . . . .	275
9.9	Conclusions . . . . .	286
	References . . . . .	286
<b>10</b>	<b>Fluidodynamics in Deep Formations of the Bukhara–Karshi Petroliferous Basin . . . . .</b>	<b>287</b>
10.1	Stratigraphy . . . . .	287
10.1.1	Mesozoic Group (MZ) . . . . .	287
10.1.2	Cenozoic Group (KZ) . . . . .	289
10.2	Tectonics . . . . .	290
10.2.1	Bukhara Step . . . . .	290
10.2.2	Chardzhou Step . . . . .	291
10.3	Hydrogeological Conditions . . . . .	292
10.3.1	Turonian–Paleocene Petroliferous Complex . . . . .	292
10.3.2	Albian–Cenomanian Petroliferous Complex . . . . .	292
10.3.3	Jurassic Petroliferous Complex . . . . .	292
10.4	Influence of Peripheral Basin Areas on Fluidodynamics in Petroliferous Complexes . . . . .	293
10.4.1	Turonian–Paleocene Groundwater Complex . . . . .	293
10.4.2	Albian–Cenomanian Petroliferous Complex . . . . .	295
10.4.3	Jurassic Petroliferous Complex . . . . .	296
10.5	Local Fluidodynamics in Particular Basin Structures . . . . .	296

10.6	Abnormally High Formation Pressures . . . . .	298
10.7	Regional Fluidodynamic Features of the Basin . . . . .	303
10.7.1	Jurassic Petroliferous Complex . . . . .	303
10.7.2	Albian–Cenomanian Petroliferous Complex . . . . .	303
10.7.3	Turonian–Paleocene Petroliferous Complex . . . . .	303
10.7.4	Main Inferences . . . . .	304
	References . . . . .	304
<b>11</b>	<b>Heat and Mass Transfer in Deep Formations of Petroliferous Basins . . . . .</b>	<b>305</b>
11.1	Palynological Analysis: Evidence for Vertical Migration of Deep Fluids . . . . .	305
11.2	Anomalies in Deep Formations and Vertical Ascending Migration of Deep Fluids . . . . .	307
11.3	Main Inferences . . . . .	316
	References . . . . .	316
<b>12</b>	<b>Genesis of Boundaries Forming the Stratum-Block Structure of Deep Formations in Petroliferous Basins . . . . .</b>	<b>319</b>
	References . . . . .	325
<b>13</b>	<b>Principal Formation Model of Deep Fluids in Petroliferous Basins . . . . .</b>	<b>327</b>
	References . . . . .	341
<b>14</b>	<b>Oil Origin and Formation of Hydrocarbon Accumulations . . . . .</b>	<b>343</b>
14.1	Hydrogeological Aspects of Oil Origin and Formation of Hydrocarbon Fields . . . . .	344
14.2	Recent Hypotheses (Theories) of Oil Origin . . . . .	347
14.2.1	Sedimentary-Migratory Hypothesis . . . . .	347
14.2.2	Shortcomings of the Sedimentary-Migratory Oil Origin “Theory” . . . . .	351
14.2.3	Isotopic Composition of Gases . . . . .	353
14.2.4	Mineral (Inorganic) Theory . . . . .	357
14.2.5	Artificial Synthesis of Hydrocarbons . . . . .	360
14.2.6	Optical Properties of Oils . . . . .	360
14.2.7	The Mineral–Organic Hypothesis . . . . .	364
14.2.8	Subaqueous Hydrothermal Vents . . . . .	367
14.2.9	Hydrothermal Springs on Continents . . . . .	370
14.2.10	Hydrothermal Hydrocarbon Accumulations . . . . .	374
14.3	Principal Inferences . . . . .	375
	References . . . . .	376
	<b>Conclusion . . . . .</b>	<b>381</b>
	<b>Index . . . . .</b>	<b>387</b>

# Introduction

This book is a substantially revised and added edition of *Deep Hydrogeodynamics of Petroliferous Basins* published in 2000. Despite a relatively short period after its publishing, extensive empirical data on deep levels of petroliferous basins (PB) appeared in the geological literature. Taking into consideration these new materials, we summarized available extensive information that includes theoretical, experimental, and empirical data on petroliferous basins obtained by geochemical, geodynamic, fluidodynamic, and other studies.

Deep formations of petroliferous basins and their basement are least studied. At the same time, precisely they enclose most hydrocarbon (HC) accumulations. Fluids of deep formations play a significant role in the formation, preservation, and destruction of mineral deposits. The solution of the problem related to the formation of deep fluids could shed light on many aspects of practical geology and help in developing complex criteria for exploration of mineral deposits, primarily HC included.

Therefore, this book contains a special chapter dedicated to the problem of oil origin and formation of hydrocarbon fields.

The authors consider the problem of oil origin and formation of hydrocarbon fields from the hydrogeological standpoint analyzing local and regional regularities in the formation of deep fluids in petroliferous basins, primarily spatial position of recharge, discharge, and transit areas.

In this book, we tried to take into account all the facts supporting different “theories” of oil origin: organic (sedimentary-migratory, biogenic, fluidodynamic, and other variants of the organic theory), mineral (inorganic, emanation) based on concepts of wide development of Earth’ degassing processes, and other hypotheses.

The problem of formation of deep fluids is still far from its solution. This is primarily explained by the complex nature of the study object.

1. *The complexity of the study object* consists in the following:

- (a) deep fluids are characterized by spatially variable density, which gives birth to methodical difficulties in estimating directions and velocities of fluid movement. In practice, this results in situation, when using the same factual data different researchers compile potentiometric maps for the same region with differently oriented (frequently, opposite) directions of deep fluid movement. The

- assessment of prospects, for example, of the petroleum reserve potential based on these maps causes serious doubts;
- (b) the formation of deep fluids occurs in medium deformed in the elastic manner. This means that all the hydrogeological interpretations should take into consideration the external influence or impact of natural geodynamic processes as well as anthropogenic load on environments disturbed by the human economic activity (decrease in formation pressures due to exploitation of mineral deposits or their increase due to pumping of liquid industrial wastes). The necessity in consideration of the external influence on the fluid-rock system leads to significant complexation of equations that are used for describing fluid migration in these conditions;
  - (c) the formation of deep fluids is frequently accompanied by phase transitions in the fluid-rock system. Under successively changeable thermodynamic conditions (pressure, temperature), these interrelated processes lead to substantial changes in capacity and filtration properties of fluid-hosting rocks, chemical and gas composition of fluids and their temperature, formation of secondary minerals, i.e., partial or complete transformation of both rocks and fluid. Interrelationships between these processes are reflected, for example, in the following. Due to geodynamic processes, some areas of sedimentary cover in petroliferous basins experience compression, while others are subjected to extension. The increase in the external pressure (which is distributed between solid and liquid phases) results in the enhanced dissolubility of many minerals and rocks, particularly in areas where contacts of the solid phase are minimal (convex fissure walls, contacts between grains of incoherent sediments, and others), while the pressure is maximal all other factors being equal. In such a situation, the solid phase passes partially into solution to increase its concentration and density. In extension areas, the process is reverse: the pressure drop results in the transition of dissolved matter into the solid phase. These processes proceed with consumption or liberation of heat, which results in temperature changes in the fluid-rock system.

Due to diversity of the mineralogical–lithological composition as well as heterogeneity of thermal, hydrogeodynamic, and stress fields, these processes proceed with different intensities and consequences at each point, which form substantial heterogeneity of many geological and physical fields.

Precisely due to these reasons, *the formation of deep fluids is both a hydrogeological and, to a great extent, a geological problem*. Ignoring achievements of allied geological sciences (history of geological development, geodynamics, geochemistry, lithology, mineralogy, ground mechanics, thermodynamics, and others), its solution is practically impossible. Therefore, a complex approach to its solution is required.

2. *The second important cause* is the lack of appropriate methods for the study of hydrogeology of petroliferous formations. Unfortunately, one-sided approach is now dominant: separate aspects of this problem are studied while others are ignored.

For example, all the inferences on hydrogeodynamics are largely based on the analysis of potentiometric surface without considering capacity and filtration properties of host rocks.

When studying the formation of deep fluids, researchers propose frequently a new hypothesis and consider it as being the main one forgetting that many factors are responsible for this process, i.e., the complex approach and comprehensive analysis with the quantitative assessment (at least, its factor-diapason aspect) of all the possible processes that determined together or separately the formation of deep fluids in petroliferous basins are ignored.

In this respect, the illustrative example is an idea of the compressive movement of deep fluids at elision stages of petroliferous basin development, which became popular during the last decades. This idea is based on the real physical process: compaction of rocks, clayey varieties included, during the entire geological history of a petroliferous basin, when all the water types (interstitial, fixed, crystallization) became released to enter subsequently well-permeable rocks and increase the elevated formation pressures in them. Moreover, the formation pressure is higher in areas where clayey rocks are thicker and subsided to deeper levels (maximal volumes of fluids are released precisely from these rocks). Since this process is real, deep fluids should move from most subsided parts of petroliferous basins toward their periphery. Neither rates of the rock load growth and their relationships with velocities of formation pressure relaxation nor relations between filtration resistances of high- and low-permeability rocks, nor relations between infiltration and elision recharge modes relative to time and area units, nor other parameters are taken into consideration. Such a simplified (up to primitivity) approach leads to illusory interpretations of movement directions of deep fluids based, however, on the real physical process. Let us note apparent absurdity of the compression hypothesis of deep fluid movement, which is used by researchers for compiling potentiometric maps based on data on thicknesses of clayey rocks and their occurrence depths. Unfortunately, this hypothesis is also used for prognostic estimates of the petroleum reserve potential of the basin or its separate parts.

The diffusion theory of brine formation at deep levels of stratified platform sections developed by S.I. Smirnov represents another example of the one-sided approach to the hydrogeological study of deep formations in petroliferous basins, when a single physical process participates, together with many others, in the formation of deep subsurface fluids. In this case, salt beds (loads), which are frequently destructed during geological development due to molecular diffusion, are a priori assumed; other geological and physical processes and events are simply ignored. This researcher uses well-developed mathematical apparatus applied for calculations in the thermodynamics, which provides illusion of reliability of his inferences.

Similarly illustrative in the one-sided approach to the solution of the problem of deep fluid formation is the theory of failuation proposed by A.G. Arie. This researcher explains movement of deep fluids at the molecular level in finely dispersed rocks under pressure gradients lower as compared with its initial value.

The thorough studies show, however, that both horizontal and vertical gradients of deep fluids are substantially higher (one to two orders of magnitude or exceeding unity) than that in undersurface aquifers. In addition, the fact that all the rocks at greater depths are largely characterized by fissure-related permeability with clays transformed into rocks with rigid structural–crystalline connections, which are also characterized by fissure capacity and permeability, is ignored.

With respect to the theory of oil origin, which is discussed over a century, the one-sided approach is reflected in the following. For example, adherents of the organic theory of oil origin completely ignore achievements in the laboratory oil synthesis, some geochemical inconsistencies between properties of dispersed organic matter from source rocks and oils, some achievements in deep-sea investigations interpreting them in favor of the organic theory of oil origin, occurrence of large (sometimes, giant) hydrocarbon fields in crystalline rocks, which are inconsistent with real natural conditions, and others.

3. *The third reason* that determines difficulties in solution of the problem connected with the formation of deep fluids is extremely irregular knowledge of deep formations in petroliferous basins with respect to their lateral and vertical distributions. Laterally, sampling sites are located tens to, sometimes, hundreds of kilometers away from each other, while in the section they are separated usually by distances of tens to hundreds of meters. The high cost of drilling and sampling of deep formations in petroliferous basins prevents from the desirable knowledge degree. This should be taken into consideration in solving practical tasks and estimating reliability degree of the results and inferences.

Some of the scientific hydrogeological problems concerning deep formations can be formulated in the following way: (a) forces responsible for migration of deep fluids if they do migrate; (b) spatial position of recharge areas, migration paths, and discharge sites of deep fluids; (c) role of host rocks (clayey formations included) in the formation of deep fluids; (d) paleohydrogeological formation aspects of deep fluids; (e) interaction between the petroliferous basins basement and its sedimentary cover; (f) geodynamics and formation of deep fluids; and others.

Many of the cited problems have no final solution, and results of investigations obtained from different areas are frequently inconsistent with each other.

The purpose of investigations presented in this book was the study of hydrogeodynamics of deep formations constituting the stratified cover of platforms. Particular tasks were as follows: (1) the analysis of available methods for formation pressure reducing and substantiation of the method used in these studies; (2) the study of the formation pressure (hydrodynamic potential) field in natural and, locally, disturbed environments; (3) the assessment of the role of petroliferous basin peripheral parts in the formation of deep fluids; (4) the study of formation conditions of filtration properties peculiar to fluid-hosting rocks at great depths and their spatial and temporal changes; (5) the study of hydrogeochemical and thermal fields; (6) the study of formation and preservation conditions of abnormally high formation pressures; (7) the assessment of the role of elision processes in the formation of deep fluids; (8) the assessment of the role of recent geodynamic processes in the formation of



formation pressure fields; (9) the study of hydrodynamic relations between the basement and the sedimentary cover; (10) development of the principal model of deep subsurface fluid migration; (11) the analysis of arguments and counterarguments of the two main oil origin hypotheses in light of new information on deep formations of sedimentary cover and basement.

These tasks are accomplished with different completeness, which is largely explained by extremely irregular knowledge of petroliferous formations both in the regional and in the stratigraphic aspects.

The work is based on the analysis and generalization of initial (only data on borehole tests were used) and published information on hydrodynamic and hydrogeochemical sampling of deep boreholes, tectonics (geodynamics), palynology, filtration properties of rocks from deep formations, and others.

In the course of investigations, we applied the complex analysis of available material on deep (petroliferous) formations and used modeling of hydrogeodynamic conditions for particular objects at different scales: from large regions (Pechora, West Siberia, and Terek-Kuban petroliferous (artesian) basins) to their particular areas. Modeling was used for solving test tasks in the factor-diapason formulation for assessing influence of different processes on the formation of deep fluids.

Four petroliferous basins were selected to serve main study objects: West Siberian, eastern Ciscaucasia, Pechora, and Bukhara–Karshi. They differ substantially from each other in age, structural–tectonic, geological, and hydrogeological conditions; composition of host rocks; and other features. In addition, fluidodynamic conditions of the Dnieper-Donets and Pripyat depressions as well of three Fergana intermontane depressions were studied. Because of the limited volume of the book, only some of the data on the last structures are presented here.

It should be emphasized that in our understanding fluids are gas, water, oil, and melted rocks that migrate under influence of pressure gradient. Fluidodynamics includes both ascending near-vertical migration of fluids (gas–water mixture of different compositions and temperatures) and movement of infiltration and elision waters and fluids of different geneses along sedimentary strata, i.e., spatial three-dimensional movement.

# Chapter 1

## Existing Views on Fluidodynamics in Petroliferous Formations

The theory of vertical hydrodynamic zoning represents a basis for recent conceptions of regional fluidodynamics in petroliferous basins. V.S. Il'in and V.L. Lichkov were the first to propose in the late 1920s and 1930s a hydrodynamic criterion: a local base level of erosion separating ground and artesian waters, i.e., they defined, in fact, two hydrodynamic zones, which reflected natural vertical zoning determined by different fluidodynamics.

In 1931, P.I. Butov introduced the notions of “active” and “passive” water-exchange zones. F.F. Makarenko and N.K. Ignatovich, who studied formation conditions of groundwaters and their chemical compositions in the Matsesta area (1937–1939) and East European Platform (1939), respectively, arrived at the conclusion that three hydrodynamic zones are distinguishable in the section. The last author developed and published in 1947 a scheme that includes the three following hydrodynamic zones in the section of artesian basins [18].

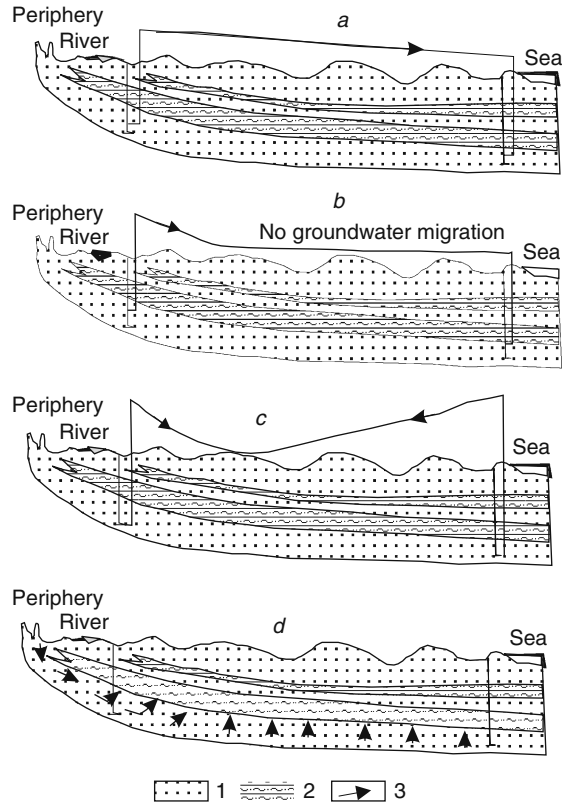
The zone of active water exchange with large “hydrodynamic reserves” of fresh groundwater is influenced by exogenic factors such as the climate, topography, and river network.

The zone of “hampered groundwater circulation” is characterized by reduced filtration velocities and discharges and, correspondingly, by enhanced water-exchange duration.

The zone of stagnant water regime (relative immobility), where the groundwater flow is observable only at the geological time scale (Fig. 1.1b). The zone is marked by development of several physicochemical processes (exchange, diffusion, sorption, osmosis, and others) that produce specific chemical composition of groundwater.

Subsequently, some main aspects of the hydrodynamic zoning scheme by Ignatovich were subjected to modification and additions or even revision in works by other researchers. For example, M.A. Gatal'skii considered it necessary to define the fourth hydrodynamic zone: the zone of “significant water exchange,” which is sandwiched, in his opinion, between the Ignatovich's zones of the active and passive water exchange. Gatal'skii substantiated the fourth zone by distinct brine drainage in coastal areas. According to this author, the zone of significant water exchange is located below the local base level, although being characterized by substantial

**Fig. 1.1** Principal distribution of pressures and directions of groundwater migration within the petroliferous basins. (1) Permeable rocks; (2) low-permeability rocks; (3) direction of groundwater migration. (a-d) different directions of fluid migration.



filtration rates as well as variable chemical composition and mineralization of groundwater, which is determined by their significant exchange with the surface.

I.K. Zaitsev (1967) shares the opinion that the vertical section of the basin usually comprises three hydrodynamic zones with free, hampered, and highly hampered water-exchange modes, which he unites in two hydrodynamic stages based on flow intensity, direction of migration, and formation conditions of groundwater: upper and lower. The first of them comprises the zones with free and hampered water exchange and is characterized by intense water migration, which is largely determined by the hydrostatic pressure. The lower hydrodynamic stage corresponds to the zone of highly hampered water exchange. Within this stage, fluid migrates slowly under the influence of tectonic movements that are responsible for formation pressures exceeding normal hydrostatic values. Based on hydrostatic pressures within the lower hydrodynamic stage, the artesian basins are subdivided into three types [36]:

- (1) Artesian basins where the lower hydrodynamic stage is characterized by the formation pressures exceeding the normal hydrostatic one. Fluids migrate from most subsided parts of the basin toward its periphery (Fig. 1.1c) or upward

- along tectonic fractures (North Caspian, Terek-Caspian, Azov-Kuban, Rioni-Kura, and others located in tectonically active regions).
- (2) Artesian basins with the lower hydrodynamic stage characterized by the normal hydrostatic pressure and stagnant groundwater regime (Fig. 1.1*b*). The discharge is insignificant occurring along tectonically weakened zones (Moscow, Volga-Kama, Severnaya Dvina).
  - (3) Artesian basins where the lower hydrodynamic stage is marked by redistribution of pressures in response to the changed hypsometric position due to recent tectonic movements (West Siberian).

Nevertheless, the quantitative criterion for defining hydrodynamic zones was not formulated at that time. A.N. Kamenskii (1954) proposed an averaged water-exchange coefficient for the entire aquifer, but it was rejected because of scarcity of empirical material for calculations at that time. The researchers determined boundaries of hydrodynamic zones usually based on the geological structure of the region as well as on mineralization and chemical composition of fluids.

In works by V.A. Vsevolozhskii, the hydrogeological stage characterized by “uniform formation conditions of regional dynamics of groundwater flows” represents a largest stratification–hydrodynamic unit [33]. This author considers “character and connection degree of groundwater with the present-day surface” that serves as the upper hydrodynamic boundary of the basin to represent a general parameter that determines formation conditions of the subsurface discharge of the hydrodynamic stage. Hydrodynamic stages are bordered by regional confining beds. Vsevolozhskii divides the sedimentary cover of the artesian basin into four hydrogeological stages.

The first (upper) structural–hydrogeological stage comprises the portion of the platform cover where groundwater is closely connected with the upper hydrodynamic boundary. This stage is marked by the formation of local groundwater flows determined by present-day topography and river network.

The second structural–hydrogeological stage includes aquifers of the section, which outcrop along the periphery of the basin and, consequently, have hydraulic connection with the present-day surface, although being isolated largely from the latter and first structural–hydrogeological stage by the regional confining bed. The stage is characterized by regional dynamics of groundwater flows controlled by positions of main recharge and discharge areas. Local groundwater flows can exist at this stage as well.

The third (lower) structural–hydrogeological stage unites aquifers that have no hydraulic connection with the present-day surface of the basin. Its lack implies that the internal structure of the basin and inner recharge sources are largely responsible for the formation of deep subsurface flows. These factors also form local flows.

The fourth stage is represented by the basin basement, which differs from other stages by its heterogeneous structure and anisotropy of filtration-capacity properties.

Based on different connection degree between groundwater and surface flows and “prevalent influence of exogenic or endogenic” factors, Vsevolozhskii defines three hydrodynamic zones in the artesian basin that correspond, to a variable extent, to structural–hydrogeological stages.

The first hydrogeological stage encloses the boundary between two hydrodynamic zones that corresponds to the roof of the first concealed confining sequence. The upper zone is characterized by free exchange with surface waters and corresponds to the zone of free (intense) water exchange (after Ignatovich). The lower hydrodynamic zone lacks free connection with the surface. The groundwater discharge and recharge occurs largely on account of vertical filtration through low-permeability sequences. In the accepted classification, this zone corresponds to the zone of the hampered water exchange.

The second hydrogeological stage demonstrates deteriorating exchange with surface waters and decreasing rates and filtration discharges down the section and toward central parts of the basin. Based on changes in the groundwater discharge, all three hydrodynamic zones with different water-exchange rates are distinguished within the second stage.

The first zone (“marginal recharge area”) comprises the peripheral part of the basin and represents a zone of intense water exchange in its formation conditions of groundwater dynamics. The second zone is characterized by the sharply decreased discharge of lateral flows and largely hampered vertical groundwater discharge into overlying aquifers, which results in decreased water-exchange rates. This zone may be considered as a zone of relatively hampered water-exchange or “transitional” zone. The third hydrodynamic zone is remarkable for lack of recharge that is forming in peripheral parts of the basin. Groundwater migration occurs only as hampered filtration. The zone includes the deepest portion of the second hydrogeological stage and the entire third stage.

According to the accepted classification, this is the zone of highly hampered water exchange.

Based on changes in proportion of horizontal and vertical filtration resistances, gradients, and discharges along the flow, Djunin [7, 9] defines three hydrodynamic zones.

The first zone (“marginal recharge area”) comprises the peripheral part of the basin and represents a zone of intense water exchange, according to formation dynamics of groundwaters.

The second zone is characterized by very low discharges of lateral flows and prevalence of hampered vertical groundwater discharge into overlying formations, which results in the increased water-exchange period. This is a zone of relatively hampered water-exchange or transitional zone.

The third hydrodynamic zone is remarkable for lack of the recharge in peripheral parts of the basin. Migration occurs only due to hampered ascending filtration of fluids provided by internal recharge sources.

In line with the accepted terminology, this is a zone of highly hampered water exchange (Fig. 1.1d).

Now, nobody has any principal objections against defining three hydrodynamic zones in the section of artesian basins (principles of their defining and names can be different). At the same time, views on hydrogeodynamics of fluid in deep parts of their sections corresponding to the zone of highly hampered water exchange are contradictory. There are two main standpoints.

According to the first of these standpoints, the last zone is characterized by groundwater migration (Fig. 1.1a), while adherents of the second one believe that groundwater in this zone is relatively or completely immobile (Fig. 1.1b).

M.A. Gatal'skii (1956) asserts that brines confined to the zone of stagnant regime migrate slowly (1–5 m/year) and participate in the water exchange. The chemical composition of groundwater, which attracts elevated attention, represents only a “product of transformation by hydrodynamic process.”

With regard to Middle–Upper Devonian complexes of the Volga-Urals petroliferous province, G.P. Yakobson believes that groundwater migration is characteristic of all the zones, deepest parts of the lithosphere included (Fig. 1.1a). He estimated the groundwater flow velocity as being 4–20 cm/year.

A.M. Ovchinnikov supposes that all waters experience the hydrodynamic pressure, which originates in peripheral parts of the basin and spreads then through the entire water-pressure system to provide water movement with different velocities. In this connection, he notes that the zone of highly hampered water exchange is sometimes called incorrectly as a zone of stagnant regime (Fig. 1.1a).

E.V. Pinneker (1977) calculated the duration of water exchange for the entire section of the Angara-Lena artesian basin. For this purpose, he divided the section into hydrodynamic zones based on the position of the drainage base and data on intensity of resource renewal, migration velocity, and age of groundwater and taking into consideration development history and geological structure of the basin. According to his calculations, the period of water exchange for the zone of highly hampered regime lasts from 5 to 50 Myr.

New additional information on the zone of highly hampered water exchange and discovery of abnormally high formation pressures (AHFP) in ancient basins led to principally different concepts of deep hydrogeodynamics. They are based on the hypothesis of compression (elision) groundwater migration [19–22, 24, 31 and others]. Similar to the first standpoint, it implies regional flows. According to this hypothesis, clayey, finely dispersed sediments capture during their deposition large volumes of waters. Under subsequent compacting (catagenesis), clayey rocks release water, which migrates into reservoir sequences. The thicker the clay formations in the section, the larger the volume of water squeezed out. This results in the AHFP formation in deep parts of the section and groundwater migration from most subsided parts (feeding areas) of the artesian basin toward its elevated periphery (discharge areas).

In this case, artesian basins are marked by the surface that separates infiltration and elision flows, i.e., the section is divided in two hydrodynamic isolated stages (A.A. Kartsev, V.V. Kolodii, and many others). The upper stage comprises the zone of intense and hampered water exchange and is characterized by downward migration along bed dips under the influence of the hydrostatic pressure gradient. The lower stage corresponds to the zone of highly hampered water exchange and dominant ascending filtration of fluids under the compression pressure (Fig. 1.1c). Such a subdivision of the section implies no influence of the hydrostatic pressure originated in peripheral parts of the artesian basin on deep groundwater hydrodynamics.

Using the West Turkmen petroliferous province as an example, V.V. Kolodii calculated that the clay sequence 1 km thick with the distribution area of 40,000 km<sup>2</sup> yields water volume of  $5 \cdot 10^{12}$  km<sup>3</sup>.

Kortsenshtein [25] believes that at least 75% of sedimentation waters return to the sedimentation basin due to primary squeezing. Some share of remaining 25% is consumed by high-absorbency diagenesis of clay minerals, while residual waters enter reservoir sequences to become mixed with infiltration groundwater and migrate toward discharge areas. These processes proceed mainly at the initial stage of water-pressure system development. With the integral water-pressure system thickness of 6 km, the thickness of the clayey sequence and aquifer of 3 and 3 km, respectively, the distribution area of 1,000 · 500 km, the filtration velocity of 1 cm/year, the porosity of reservoir sediments 20%, and the decrease in porosity by 25% due to compression, maximal volume of sedimentation waters squeezed from clayey rocks should be as large as 3.75<sup>5</sup> km<sup>3</sup>. In this case, the flow with the annual yield of 0.6 km<sup>3</sup> should exist during approximately 0.6 Myr, which is an insignificant duration in terms of the geological time.

In parallel with studies of recent deep hydrogeodynamic conditions, intense paleohydrologic investigations were also in progress. A.N. Semikhatov was the first to pay attention in 1947 to recurrence of hydrogeological processes in subsurface sequences reflected in the accumulation of seawater in deposited sediments and its subsequent replacement by fresh waters during sea regression. The complete hydrogeological cycle consists of elision (sedimentation), infiltration, and, sometimes, endogenic stages of water exchange.

In other words, it is implied that waters enter deep aquifers from three sources: (1) release from rocks during their catagenetic transformations; (2) infiltration recharge within orogenic structures surrounding the artesian basins; (3) endogenic solutions, which migrate from the basement and, possibly, upper mantle during periods of tectonic activation. Correspondingly, geostatic, hydrostatic, and endogenic (deep type) hydrodynamic regimes are defined (A.A. Kartsev, E.V. Pinneker). Moreover, these regimes function simultaneously, although separately in different intervals of the section and in different periods.

The present-day regime reflects a certain stage of geological history of the artesian basin.

E.V. Pinneker (1977) defined three stages in hydrodynamic development of artesian basin: geostatic, transitional, and hydrostatic.

The geostatic development stage is determined by tectonic stresses, compacting processes, lithogenesis, and ascending migration of fluids from the basement. This stage is characteristic of young artesian basins, which were developing for a long time as marine basins. After basin closing, its entire section was involved into elision fluid migration from central parts of the basin toward the periphery (West Turkmen segment of the South Caspian basin).

The endogenic regime (regime of the deep type) is usually untypical of the entire artesian basin. It functions only in areas of elevated tectonic and volcanic activity where results in the intense ascending groundwater migration. This occurs at any stage of basin development. In such areas, formation pressures exceed usually

hydrostatic values beginning from depths shallower than 1 km. At the transitional stage, infiltration waters penetrate into the upper part of the lithosphere, and the hydrostatic pressure involves the upper stage, while the geostatic pressure continues dominating the lower stage. These stages are hydrodynamically independent of each other (Ciscaucasian Trough, Turan and West Siberian plates, Lena-Vilyui Depression).

The hydrostatic regime becomes dominant when action of the hydrostatic pressure spreads over the entire aquifer system. Such a regime is developed only in old artesian basins. The successive basin development is frequently distorted, with the hydrostatic regime being replaced by the geostatic one and vice versa (eastern Ciscaucasia region).

These different views on groundwater fluidodynamics of the zone of highly hampered water exchange are characterized by a feature in common: all of them are based on the assumption of the hydraulic mechanism responsible for the transfer of formation pressures. This determines the lateral hydrodynamic unity of all the parts of artesian basins and the possibility of formation-pressure transfer over distances of tens, hundreds, and, even, thousands of kilometers.

Under the influence of new information, these classical views have recently been subjected to transformations.

For example, the role of orogenic structures surrounding the basin is now thought to be less significant in the recharge of deep waters. In 1967, G.P. Yakobson noted insignificant influence of the river runoff from the Urals on the hydrodynamic regime in the Middle–Upper Devonian petroliferous complex. This complex outcrops in the Uralian slope and is characterized by maximal values of formation pressures. Similar inferences were obtained for the Cisuralian region (V.F. Krotova, 1962), Kopet Dag (A.V. Kudel'skii, 1964), and Ukrainian Shield [3]. According to Zaidel'son [35], “water exchange in deep formations is realized in form of the selective flow along most permeable zones, not in form of its frontal movement.”

In our opinion [8–12], the groundwater formation of artesian basins is characterized by the following features: (1) independence of water formation in deep zones of highly hampered water exchange from peripheral areas in all the artesian basins, regardless of their ages and geological structures; (2) development of blocks hydrodynamically unrelated or poorly related to each other; (3) dominant role of vertical infiltration, which occurs intermittently and results in the formation of new minerals; (4) variability in the chemical and gas composition of fluids at relatively short distances, which indicates the nonequilibrium state of the hydrodynamic system and is confirmed by the abnormally high formation pressure and contrast lateral and vertical differentiation of the pressure field.

This standpoint is recently accepted by many researchers and confirmed for many regions. For example, the Jurassic aquifers of West Siberia are characterized by “chaotic pressures of formation waters, which indicates hydrodynamic disconnection” [28]. Similar inference on the block structure is obtained for aquifers of the eastern Ciscaucasia region [23], Apsheron Peninsula [1], and Alma-Ata [13] and Pripyat depressions [5, 4]. The stratum-block patterns are expressed in both large



and small local tectonic structures. For example, the Surgut Arch hosts blocks with different hydrodynamic conditions, hydrochemical parameters, and zoning [8, 30]. Rustamov [32] revealed the complicated distribution of pressures for separate fields of the Srednyaya Kura Depression with gradients up to 1,000 m of the water column. Djunin [8, 9] established a system of isolated blocks in the Salym oil field, which restrict lateral migration and stimulate dominant vertical movement of groundwater.

In their recent works on regional hydrogeodynamics of deep formations in the Pechora artesian basin, Fartukov [14] and Korzun [26] arrived at the conclusion on its heterogeneous patterns in deep parts of the section through the entire distribution area of aquifers and on autonomous development of separate areas that are characterized by different intensity and direction of fluid-exchanging processes.

Many foreign researchers share similar views and believe that the sedimentary basin consists of separate areas isolated from each other by hydraulic barriers, which is confirmed by numerous examples for particular regions [6, 17].

The stratum-block structure of deep formations may be determined by the existence of internal recharge sources. In opinion of many researchers, release of interstitial and crystallization water during all the stages of lithogenesis is one of such sources. Nevertheless, this process cannot provide water volumes sufficient for disturbances in the distribution of formation pressures [8, 9]. The quantitative assessment of the process is given below.

Fluids which intrude during periods of tectonic activation from deep levels of the crust to migrate upward and even discharge to the surface under certain conditions are another potential recharge source. These fluids are frequently characterized by different chemical and gaseous compositions as well as thermobaric parameters as compared with solutions enclosed in rocks. This may result in the distortion of the thermodynamic equilibrium in the water–gas system, hydrofracturing, phase transformations, physicochemical reactions, and mineral precipitation.

All these processes change the interstitial (fissure) space in rocks to decrease their porosity up to its complete disappearance, which results in the formation of relatively impermeable barriers and, correspondingly, hydrodynamically isolated blocks [9].

In addition, the value and distribution of formation pressures is influenced by the stress state of enclosing rocks, which represent in fact recharge sources particularly in areas of elevated tectonic activity. Gaev and Khomevski [15] believe that “migration of fluids is explainable only by geodynamics. The mechanism of extensions and isolation of separate crustal blocks that is responsible for the formation, development, and closure of fissures and is of the pulsating oscillation-impact mode serves simultaneously as a powerful hydrodynamic tool.” These authors define three hydrodynamic layers in the hydrosphere: upper, intermediate, and lower. They refer the pulsating mode of the movement to the lower hydrodynamic layer and call it as “hydrodynamic” or “tectono-hydrodynamic.”

Vartanyan with co-authors [34] established empirically the development of the hydrogeodeformation field (HGDF) at deep levels of the lithosphere. It is characterized by globally sustained rapid pulsating changes in the stress state of the lithosphere due to changes in natural (exo- and endogenic, cosmogenic) or technogenic stresses. Such oscillations are manifested in the form of thermobaric and physicochemical anomalies in development areas of deformation processes.

In his numerous works, Arie [2] proves the possibility of fluid migration under low gradients (less than initial) at the molecular level and terms such movement as “filuation.”

Kuvaev [29] believes that density convection plays a significant role in the formation of hydrodynamic peculiarities. In his opinion, available hydrodynamic models ignore the “effect of eddy mixing of the brine at the microlevel.”

Thus, no uniform views exist nowadays on groundwater formation conditions in the zone of hampered water exchange.

E. F. Stankevich (1971) defined several viewpoints on water dynamics in deep formations of artesian basins of the platform type. With our modifications and additions, they are the following.

#### **Based on the principle of groundwater mobility/immobility**

- (1) Beginning from a certain level, groundwaters are stagnant or relatively stagnant (B.L. Lichkov, N.K. Ignatovich, N.I. Tolstikhin, E.V. Posokhov, N.K. Zaitsev, E.F. Stankevich, and others). Most of researchers consider lack of the substantial present-day water exchange with surface waters as indicating the stagnant regime (Fig. 1.1b).
- (2) Groundwater moves through the entire sedimentary cover with variable velocity from recharge areas toward areas of their regional discharge (A.I. Silin-Bekchurin, M.A. Gatal'skii, V.P. Yakutseni, V.A. Krotova, I.K. Zerchaninov, M.I. Zaidel'son, E.V. Pinneker, Yu.V. Mukhin, and others) (Fig. 1.1a).
- (3) Groundwater moves due to the elision recharge from subsided parts of the artesian basin toward its periphery (A.V. Kartsev, Yu.V. Mukhin, I.K. Zaitsev, V.V. Kolodii, A.Ya. Khodzhakuliev, and many others) (Fig. 1.1c).
- (4) Some development stages of artesian basins are characterized by ascending groundwater movement due to the influx of juvenile waters (V.F. Derpgol'ts, E.S. Gavrilenko, L.N. Elyanskii, P.N. Kropotkin, E.V. Pinneker, V.A. Krotova, A.A. Dzyuba, V.I. Djunin, and many others.) (Fig. 1.1d).

#### **Based on driving force**

- (1) Waters move under the influence of the pressure gradient (head) [A.A. Kartsev, Yu.V. Mukhin, I.K. Zaitsev, V.V. Kolodii, A.I. Silin-Bekchurin, M.A. Gatal'skii, V.P. Yakutseni, V.A. Krotova, I.K. Zerchaninov, M.I. Zaidel'son, E.V. Pinneker, and many others (overwhelming majority)].

- (2) Gravity forces stimulate jet flows of waters with different density, owing to which waters with higher density subside, while waters with lower density rise (A.B. Ronov, M.G. Valyashko, A.I. Polivanova, A.A. Kuvaev). In other words, these researchers consider gravity or “density convection” (after, Kuvaev [27]) as a main driving force.
- (3) Waters move under the influence of their subsurface evaporation or any other removal from the formation. They move downward toward areas of maximal subsidence of the formation (V.A. Sulin, M.E. Al'tovskii, N.V. Kulakov, A.A. Brodskii, and others).
- (4) Groundwaters move at the molecular level: diffusion (after S.I. Smirnov; filtration or water migration in fine-grained rocks under the gradient that is lower as compared with the initial one (after A.G. Arie).
- (5) Groundwater movement is substantially influenced by permanent tectonic forces, which change the stress field (G.S. Vartanyan, G.V. Kulikov, V.I. Djunin, and others).

### **Based on spatial position of recharge sources**

- (1) The recharge takes place in peripheral parts of artesian basins in surface discharge areas (infiltration recharge) (B.L. Lichkov, N.K. Ignatovich, N.I. Tolstikhin, A.I. Silin-Bekchurin, M.A. Gatal'skii, V.P. Yakutseni, V.A. Krotova, I.K. Zerchaninov, M.I. Zaidel'son, E.V. Pinneker, Yu.V. Mukhin, and others).
- (2) Recharge sources are located in the innermost subsided areas of aquifers (waters released during catagenesis of sedimentary rocks) (A.V. Kartsev, Yu.V. Mukhin, I.K. Zaitsev, V.V. Kolodii, S.B. Vagin, E.A. Baskov, and many others).
- (3) The intermittent recharge is realized owing to endogenic processes (cryptic hydrothermal activity) (V.F. Derpgol'ts, E.S. Gavrilenko, L.N. Elyanskii, P.N. Kropotkin, E.V. Pinneker, V.A. Krotova, V.I. Djunin, V.N. Florovskaya, G.N. Dolenko, A.A. Dzyuba, and many others).

A very important point unites practically all these standpoints: *all of them imply hydrodynamic interrelationships between all elements of the section through the entire distribution area and potential transfer of formation pressures over large distances (tens, hundreds, and even thousands of kilometers).*

We share the following standpoint, which is substantiated in this work. It implies the following: (1) the restricted role of peripheral parts of the basin in hydrogeodynamics of deep aquifers (petroliferous formations); (2) the block (stratum-block) structure of deep formations in artesian basins; (3) the substantial role of intermittent endogenic factors; and (4) the significant role of tectonic forces in the formation of the present-day formation-pressure field.

Tectonics of lithospheric plates is of great significance for formation conditions and localization of hydrocarbon fields as well as for their prognosis and exploration. One of the recent classifications is given in [16].

According to plate tectonics, sedimentary basins experience stages of their divergent and convergent evolution. The divergent stage includes riftogenic and

spreading phases with formation of genetically different sedimentary basins. Riftogenic sedimentary basins are subdivided into intracontinental (aulacogens), continental-oceanic (Dnieper-Prpyat), and pericontinental (fragments of continental) types. Spreading sedimentary basins are divided into two types: pericontinental with the shelf, continental slope, its foot, and abyssal zone in their structure and intracontinental that are formed in the rear part of pericontinental basins.

The basins are characterized by four main sedimentation types: riftogenic, pericontinental, intercontinental, and pelagic with different structures of sedimentary and volcano-sedimentary rock complexes, lithology and diagenetic transformations, sedimentation and mass accumulation rates. Pericontinental, intercontinental, continental-island arc, and intercontinental-island arc sedimentary basins accumulate up to 95–98% of organic matter. Of total organic matter contained in Holocene sediments of the World Ocean, 97.5% accumulated on the underwater margin (pericontinental sedimentary basins of all types), 10% of which are buried in shelf sediments and 87.5% on the continental slope and at its foot, and only 2.5% in the abyssal zone. Fossilization coefficients in these different zones are 0.4, 0.73, and 0.11%, respectively. According to the oil-generating potential, sedimentary basins form the following succession: pericontinental (passive continental margins), intercontinental–spreading–riftogenic, continental–oceanic–riftogenic, intercontinental-island arc, spreading, and intracontinental. Such a succession “is confirmed by discovery of giant oil and gas fields in the Brazil, Nigerian, Angola, and other passive continental margins at water depths exceeding 1200 m” [16, p. 44]. This model is also tested in the Siberian Platform and, in opinion of the authors, can be used as a scientific basis for prognosis and exploration of hydrocarbon fields.

## References

1. Aliev F Sh, Bairamov T A (1993) On geological structure and hydrogeological conditions of the Apsheron Peninsula. *Otechestvennaya geologiya* 3:73–78
2. Arie A G (1984) Physical basics of groundwater filtration. Nedra, Moscow
3. Babinets A E, Shestopalov V M, Litvak D R (1980) Water exchange in platform-type artesian basins of Ukraine in natural and disturbed environments. In: *Hydrogeology, engineering geology, and construction materials*. Nauka, Moscow
4. Bagdasarova M V (2000) Recent hydrothermal systems and their relation with formation of oil and gas fields. In: *Basics of new technologies in oil and gas industry*. Nauka, Moscow
5. Bagdasarova M V (2001) Fluid systems of oil accumulation zones and geodynamic oil and gas fields. *Geologiya nefi i gaza* 3:50–56
6. Dewers T, Ortoleva P (1994) Nonlinear dynamical aspects of deep basin hydrogeology: fluid compartment and fluid release. *Amer J Sci* 6: 713–755
7. Djunin V I (1981) Investigation methods and principles of deep formation hydrodynamics. VIEMS, Moscow
8. Djunin V I (1985) Investigation methods of the deep subsurface flow. Nedra, Moscow
9. Djunin V I (2000) Hydrodynamics of deep formations in petroliferous basins. *Nauchnyi mir*, Moscow

10. Djunin V I, Korzun A V (2001) Geological formation model of deep groundwaters and origin of hydrocarbon fields. In: Proceedings of the 5th international conference "New ideas in geosciences." Moscow
11. Djunin V I, Korzun A V (2001) Fluidodynamics and formation of hydrocarbon fields. Mineral resource base of Russia in 21st century. In: Materials of the scientific-practical conference. Arkhangel'sk
12. Djunin V I, Korzun A V (2003) Fluid migration: Oil origin and formation of hydrocarbon accumulation. Nauchnyi mir, Moscow
13. Dmitrovskii S V, Kim E K, Malakhov V D, Ostrovskii V N (1993) Influence of the block structure in the Alma-Ata depression on formation of groundwater resources. *Otechestvennaya geologiya* 3:67–73
14. Fartukov A M (1990) Hydrodynamic localization condition of oil accumulations in Carboniferous-Lower Permian sediments of the northern Timan-Pechora petroliferous basin. Candidate dissertation (Geol-Miner)
15. Gaeva A Ya, Khometovskii A S (1982) On deep hydrodynamics (exemplified by the East European Platform). *DAN SSSR* 263:967–970
16. Gorbachev V F, Kovalenko V S (2001) Lithosphere plate tectonics as a source of information on formation conditions, formation, localization, predicting and prospecting of oil and gas fields. In: Abstracts of the International Conference Oil and gas genesis and formation of their accumulations in Ukraine as a scientific basis for predicting and prospecting new fields. Chernigov
17. Hubbert M K, Willis D G (1957) Mechanics of hydraulic fracturing. *J. Petrol. Technol* 9:34–42
18. Isaev V P (2002) Recent sediments degassing in Cenozoic depressions of the Baikal rift zone. *Geologiya nefi i gaza* 4:5–9
19. Kartsev A A (1980) Hydrogeological prerequisites for manifestation of superhydrostatic pressures in petroliferous areas. *Geologiya nefi i gaza* 4:40–43
20. Kartsev A A (1992) Oil and gas hydrogeology. Nedra, Moscow
21. Kartsev A A, Vagin S B, Baskov E A (1969) Paleohydrogeology. Nedra, Moscow
22. Kartsev A A, Vagin S B, Serebryakova L K (1980) Paleohydrogeological reconstructions for revealing oil- and gas-accumulation zones (exemplified by western Ciscaucasia). *Byul. MOIP* 1:132–140
23. Kissin I G (1964) The East Ciscaucasia artesian basin. Nauka, Moscow
24. Kolodii V V (1966) Hydrodynamic and paleohydrodynamic conditions in Pliocene sediments of the West Turkmen depression. *Sov Geol* 12:50–62
25. Kortsenshtein V N (1977) Water-pressure systems of largest gas and gas condensate fields. Nedra, Moscow
26. Korzun A V (1996) Hydrodynamics of deep formations in the northern Pechora artesian basin. Candidate dissertation (Geol-Mineral), MGU, Moscow
27. Krayyushkin V A (2001) Non biotic petroleum resource potential. In: Abstracts of the International Conference Oil and gas genesis and formation of their accumulations in Ukraine as a scientific basis for predicting and prospecting new fields. Chernigov
28. Kruglikov N M, Nelyubin V V, Yakovlev O N (1985) Hydrogeology of the West Siberian petroliferous megabasin and peculiarities in hydrocarbon formation. Nedra, Leningrad
29. Kuvaev A A (1995) Problems of brine migration in groundwater flows. Review information series. Protection of man and environments in gas industry. IRTs Gazprom, Moscow
30. Matusovich V M, Chistyakova N F (1993) Hydrogeochemical and hydrogeodynamic peculiarities of oil fields in the Surgut area. In: Multiobjective hydrogeochemical studies in connection with prospecting mineral resources and groundwater protection. Tomsk
31. Mukhin Yu. V (1965) Compaction of clayey sediments. Nedra, Moscow
32. Rustamov R I (1993) Results of hydrodynamic studies obtained during exploration of oil fields in the Srednyaya Kura depression. Crucial problems of petroleum hydrogeology. Nauka, Moscow
33. Vsevolozhskii V A (1991) Basics of hydrogeology. MGU, Moscow

34. Vvedenskaya A Ya, Bakhtin V V (1977) Influence of thermobaric formation conditions on screening properties of clayey confining beds above accumulations with abnormally high formation pressures. *Trudy VNIGNI* 397:85–91
35. Zaidel'son M I (1972) Dynamics of subsurface brines in the Paleozoic productive complex of the Urals-Volga region. In: *Problems of petroleum hydrogeology*. Kuibyshev
36. Zubkov M. Yu, Sitdikov A Sh (1994) Secondary reservoirs in the pre-Jurassic complex of the Ur'ev field. *Geologiya nefi i gaza* 4:5–9

## Chapter 2

# Investigation Methods of Deep Fluidodynamics

The study of hydrogeodynamic conditions in deep aquifers (petroliferous formations) is now based on compiling different-scale potentiometric maps. The correctly compiled potentiometric maps make it possible to estimate directions of deep fluid flows and hydrodynamic interaction between petroliferous complexes in the vertical section as well as regional and local petroleum reserve potential in addition to other parameters (hydrochemistry, temperature, gas composition of fluids, and others). Without the knowledge of peculiarities in the geological and tectonic structure and reservoir properties of rocks, potentiometric maps allow, however, only possible (potential) flows of deep fluids to be estimated. At the same time, it is impossible to determine direction of their migration without potentiometric maps that reflect the field of formation pressures in particular regions. Therefore, the accuracy of potentiometric maps is of particular importance.

The present-day irregular knowledge degree of the lateral and vertical distribution of deep fluids, completeness, and adequacy of corresponding information allows only directions of possible (potential) flows of deep fluids to be determined. The results are substantially dependent on the methods used for processing information on hydrodynamic characteristics of deep fluids. Moreover, these estimates are frequently ambiguous even in case of application of a single method. For example, application of the method of reduced formation pressures (after A.I. Silin-Bekchurin) with different positions of the comparison plane and substantiation of the empirical curve demonstrating dependence of changes in the fluid density on sampling depth may lead to opposite interpretation of direction for deep fluid flows, which is frequently observed in the practical activity.

When studying regional hydrodynamics of deep fluids, researchers frequently propose some hypothesis (for example, elision movement or deep groundwater movement determined only by position of regional recharge and discharge areas when regional flows are usually outlined), which is thought to be the main one. It is easy to prove the latter finding necessary arguments among extensive factual materials. For example, the elision concept of past- and present-day fluid migration taken as a basis provides regional flows directed from deepest parts of petroliferous basins toward their peripheral areas. To the contrary, if the concept of the dominant role of surrounding folded structures and petroliferous basin marginal parts in the

motion of subsurface fluids (hydraulic principle) is accepted, regional flows should be directed from peripheral areas of the basin toward its most subsided areas (marine and oceanic basins). Thus, both situations are characterized by one-sided approach, which makes impossible the comprehensive analysis (as thorough as possible) and quantitative assessment of all the potential processes that determine (combined or separately) the formation of deep fluids in stratified petroliferous basin systems and, primarily, their flow directions.

The following materials are required when studying the formation of deep fluids, hydrodynamics included: (1) sampling data on deep boreholes contained in test certificates (i.e., initial materials): depths (intervals) of sampling with geological positioning, formation pressures, temperature, chemical and gas composition of fluids; (2) geological materials: structural, tectonic, and lithological-facies maps, geological sections, schematic maps illustrating location boreholes for every structure; and (3) information on reservoir properties of rocks, newly formed minerals, geodynamics, palynological complexes, and others.

The adequacy degree of available primary information is one of the main problems in fluidodynamic interpretations, which requires particular attention. All information should be taken only from borehole test certificates, not from reports, where it is processed to variable extent by the authors of these reports, who use unknown methods. In addition, primary information should be subjected to the preliminary analysis, processing, and selecting. The following data should be rejected or taken with precaution: calculated values of formation pressures obtained from the recovery curve; insufficiently recovered values of formation pressures; minimal pressure values measured at the same depth in the same borehole; pressures measured during borehole testing or its hydrodynamic sampling or during exploitation of different deposits (oil and gas, industrial, mineral, and thermal waters).

## 2.1 Methods of Formation Pressure Reducing

As is known, liquid moves under the influence of three forces: pressure gradient, gravitation, and inertia. Inasmuch as velocity of deep fluid flows is insignificant, the inertia can be neglected.

In hydraulics, there is a notion “hydrostatic pressure,” which is determined as follows:

$$P = P_0 + \rho gz, \quad (2.1)$$

where  $\rho$  is the water density,  $g$  is the gravitational acceleration,  $z$  is the sampling depths, and  $P_0$  is the external pressure.

The hydrostatic pressure value ( $\rho gz$ ) is different in every point of space and, consequently, depends on coordinates. Equation (2.1) is valid under permanent density along  $X$ ,  $Y$ , and  $Z$  axes and gravitational acceleration.



The first of these conditions is sometimes not fulfilled for deep formations of petroliferous basins, since they are characterized by significant variations in density in all directions.

In order to take into account a fluid density variable in the vertical plane ( $\rho(Z)$ ), Silin-Bekchurin [11] suggested to determine the reduced pressure from the equation (it should be emphasized that *density changes only through the vertical section* and remains permanent in the horizontal plane)

$$P = P_0 + g \int_{z_2}^{z_1} \rho(z) dz, \quad (2.2)$$

where  $P$  is the formation pressure reduced to some comparison plane  $Z_1$  and  $P_0$  is the formation pressure measured at depth  $Z_2$ . Other designations are as in equation (2.1). This equation does not take into account lateral changes in fluid density, which is practically unobservable in natural objects.

For the particular situation, when downward density changes can be described by linear function, this author proposed a simplified equation instead of equation (2.2)

$$P = P_0 + (\rho_1 + \rho_2)zg/2, \quad (2.3)$$

where  $\rho_1$  is the water density in the sampling point,  $\rho_2$  is the water density at the comparison plane, and  $z$  is the distance from the sampling point to the comparison plane. This equation was subsequently termed as the Silin-Bekchurin's formula and his method as the method of formation pressure reducing. Precisely, equation (2.3) gained wide recognition due to its simplicity and subsequent criticism in the geological literature [1 and many others], which was explained by ambiguity of its results.

The use of equations (2.2) and (2.3) for calculation of reduced pressures in natural objects by different researchers revealed that (a) absolute values of reduced pressures for the same point are different depending on the selected comparison plane and (b) different researchers obtain different flow directions for the same natural objects. All these called in question possibility of application of the method under consideration in traditional form and resulted in long searches for obviating a difficulty.

Most of investigations were aimed at "specifying" the Silin-Bekchurin's method of formation pressure reducing, which concerned more exact empirical dependence between density changes and depths (exponential, logarithmic, polynome of the  $n$ -degree, and others) or more accurate determination of the water density value with account for formation conditions, i.e., at search of density dependence on fluid gas saturation, pressure, and temperature in formation environments [9 and many others].

Zerchaninov (1962) was the first to pay attention to variations in values of groundwater density in the horizontal plane and impossibility of its account in the Silin-Bekchurin's formula. This researcher notes that "two conditionalities are used in calculations of reduced pressures: (1) arbitrary selection of the comparison plane

and (2) hypothetical assumption of constancy of groundwater density at the same depth through significant areas.” He states that the analysis of different calculation variants shows that “changes in the altitude of the comparison plane result in changes of relative values of reduced heads.” It should be noted that such a relation is natural (equation 2.2), since the formation pressure depends on the height of the liquid column, although in case of constancy of the fluid density in the horizontal plane, the gradient between two points (boreholes) should remain constant despite different absolute values of reduced formation pressures. Precisely this is a purpose of hydrogeodynamic interpretations (fluid flow direction).

The first statement is true. It follows from equations (2.1) and (2.2), which take into account potential energy value, and, consequently, depends on the height or the position of the comparison plane.

As for the second statement, constancy of the density in the horizontal plane was the main condition for the Silin-Bekchurin’s equation (2.2).

Let us dwell only on the method of local gradients considered in one of the recent works dedicated to hydrodynamics of liquid with variable density.

Rejecting the possibility of the application of the formation pressure reducing method, Shestakov and Khodzhakuliev [10] suggested to calculate the “local gradient” of the head between two points of a bed (boreholes) with that of  $P_1$  and  $P_2$ , ordinates  $Z_1$  and  $Z_2$ , water densities  $\rho_1$  and  $\rho_2$ , and located at a distance  $L$  from each other:

$$I = \Delta P / \rho^0 g L + \rho \Delta Z / \rho^0 L,$$

$$\Delta P = P_1 - P_2, \Delta Z = Z_1 - Z_2,$$

where  $\rho$  is the average fluid density between considered points [if data on vertical changes in density are unavailable, density is calculated as an average arithmetic  $\rho = 0.5(\rho_1 + \rho_2)$ ],  $\rho^0$  is a selected density value to which heads in the particular area are reduced (average value or fresh water density).

The thorough analysis of this equation shows that in this case, formation pressures between two pairs of boreholes are reduced with reduction of fluid density to some average value of density of fresh waters. In addition, it is evident that the equation for calculation of local gradients differs from equation (2.3) only by the constant multiplier  $\rho^0 L$ .

Indeed, by multiplying equation  $I = \Delta P / \rho^0 g L + \rho \Delta Z / \rho^0 L$  by  $g \rho^0 L$ , we obtain:  $\Delta P^\# = \Delta P + \rho g \Delta z$ . In this equation,  $\Delta P^\#$  is the difference between reduced pressures between two points or some value of pressure  $P^\#$ ;  $\Delta P$  is the difference between measured formation pressures in two boreholes or some value of  $P$ ;  $\Delta z$  is the difference between sampling intervals and comparison plane or some value of  $z$ ; and  $\rho$  is the average value of fluid density between considered points. If data on vertical changes in density are unavailable, density is calculated as an average arithmetic  $\rho = 0.5(\rho_1 + \rho_2)$ . Thus, we obtain the following equation:  $P^\# = P + g z (\rho_1 + \rho_2)$ . This is nothing else but the simplified Silin-Bekchurin’s equation (equation 2.3); thus, the proposed method of local gradients is just the masked Silin-Bekchurin’s formula.

In addition, contraposition of two figures presented in [10] is also incorrect. The regional flow of deep fluids demonstrated on one of them may also be presented in the form of gradients: to show directions of possible flows between borehole pairs instead of interpolating between points.

The statement that the method of formation pressure reducing cannot be used [10] is incorrect and conflicts with hydraulic laws of physics. The hydrostatic pressure is a measure of potential energy (depends on height or position of the comparison plane). This is readily seen from equation (2.1). It is reasonable to recollect the Bernoulli's equation, which is based on the analysis of kinetic (is not taken into consideration in the movement of deep fluids due to low velocities) and potential energy of inflowing and outflowing liquid and related work.

Potential energies of two bodies (two liquid columns included) are comparable when they (liquid columns) are measured in the same plane. The necessity of reducing heads to a single plane when studying hydrodynamics of fresh groundwaters in the zone of intense water exchange is undoubted. In this case, the sea level is accepted to serve the comparison plane. Flow directions are estimated using heads at certain altitudes (plane of reducing). The change in density is ignored due to its negligible values in the zone of intense water exchange, where it is practically constant, varying around  $1,000 \text{ kg/m}^3$ .

*The only method which is useful for determining of direction of the density-variable fluid flow between two or several points is the method of formation pressure reducing.* There is no other way as it follows from classical laws of physics related to liquid hydraulics.

Reviewing critically available methods, Gurevich [6, 7] notes justly that the Silin-Bekchurin's method is substantiated from both physical and mathematical standpoints (this is undoubted). The method of formation pressure reducing is, however, inapplicable for real natural objects, since it is inconsistent with the important condition in most situations:

$$\partial\rho/\partial x = \partial\rho/\partial y = 0. \quad (2.4)$$

This condition means that the fluid density in the horizontal plane should remain constant. Only in this situation, the integral value in equation (2.2) will be the *only* and the gradient between reduced pressures will remain constant by both value and direction despite their different values, which is connected with the selection of the comparison plane. It should be remembered that this determination of fluid flow direction is a main task in the study of hydrodynamics of deep fluids with permanently variable density.

Gurevich recommends reasonably considering the method of pressure reducing as approximate and as such it can be used when approximation is insignificant. This researcher suggests estimating precisely this approximation (error in formation pressure reducing). He argues that the method of formation pressure reducing can be used only in situations when difference between reduced formation pressures between two points (boreholes) is greater than uncertainty of the integral in equation (2.2), i.e., when

$$\Delta P_{z_1}^{z_2} \text{indef} J_{z_1}^{z_2} + 2\delta P_{z_1}^{z_2}, \quad (2.5)$$

Where  $\Delta P_{z_1}^{z_2}$  is the difference between reduced pressures in two points determined in line with equation (2.2);  $\text{indef} J_{z_1}^{z_2} = \max \int_{z_1}^{z_2} \rho_1(z) dz - \min \int_{z_1}^{z_2} \rho_2(z) dz$  reflects the value of integral uncertainty that depends on the scatter of points in the horizontal plane and is restricted by empirical functions  $\rho_1(z)$  and  $\rho_2(z)$ ; and  $2\delta P$  is an error related to inaccuracy in determining formation pressure in boreholes [6, 7].

This inequality “provides only correct determination of direction of the pressure gradient and (under available permeability) approximate general direction of groundwater flow” [6, 7].

Borevskii (1971) notes that inaccuracy in pressure reducing during regional interpretations should always be significant due to a variety of hydrodynamic settings. At the same time, it is always possible to define the study object, where applicability condition of the formation pressure reducing method is fulfilled [1]. This statement is unproved. For example, for the Pechora petroliferous basin, it is not confirmed. In this region, the difference between reduced formation pressures of two compared points (boreholes) is greater as compared with uncertainty of the integral in equation (2.2), i.e., greater than error in formation pressure reducing through the entire Khoreiver Depression, Sorokin Swell, and Kolva Megaswell.

Let us pay more attention to two important aspects in reducing formation pressures.

(1) Selection of the comparison plane for the assessment of reduced pressures, which provoked criticism of the Silin-Bekchurin’s method from many researchers and which stimulated the search of new ways for determination of directions of fluids flow with variable density.

It should be kept in mind that pressure is a potential energy (which follows from equations (2.1), (2.2), and Bernoulli equations), which means that it depends on the height. Therefore, the value of the reduced fluid pressure is unnecessarily dependent on the selected comparison plane. Under the constant fluid pressure in the horizontal plane, values and directions of gradients between points should always remain constant despite different values of reduced pressures.

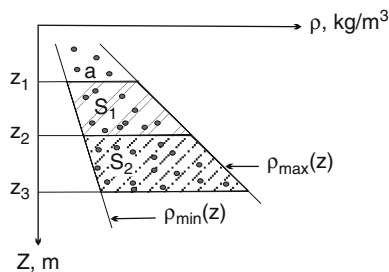
For the assessment of the role of comparison plane selection in case of changeable density at the horizontal plane, let us compile the plot of vertical density changes with account for the scatter of depth changes in the horizontal plane (Fig. 2.1).

If the formation pressure measured in the point “a” (plane  $Z_1$ ) is reduced to the plane  $Z_2$ , the error of reducing should geometrically be equal to the area  $S_1$ . When the pressure is reduced from the plane  $Z_1$  to the plane  $Z_2$ , the reducing error should increase to become geometrically equal to the sum of two areas  $S_1$  and  $S_2$  (area  $S_3$ ).

It follows from the aforesaid that the farther the comparison plane located from the sampling point, the greater the reducing error in changes of the fluid density in the horizontal plane [3, 6, 7].

If all the points of the plot  $\rho(z) + z$  are located along the single straight (curve), absolute values of reduced pressures should change depending on the selected

**Fig. 2.1** The assessment of errors in formation pressure reducing



comparison plane, although gradient of reduced pressures between two (or several) points should remain constant, since areas  $S_1$  and  $S_2$  are equal to zero.

The role of the selected comparison plane in reducing formation pressures can be exemplified by the Sorokin Swell of the Timan-Pechora petroliferous basin with the assessment of an error that depends on the position of the comparison plane in the vertical section.

For this purpose, separate plots of correlation between changes in fluid density and sampling depth were compiled for each structure of the swell. Then, an error of reducing was estimated with account for the selected comparison plane as well as the possibility of the usage of the formation pressure reducing method for each structure in the northern part of the Timan-Pechora petroliferous basin.

The field of points in plots  $\rho(z)$  was bounded by straight lines, which simplified calculations without damage to the trustworthiness of inferences (for example, find of empirical function of fluid density dependence on depths) and increased their "reliability margin." Comparison planes were selected at altitudes of  $-2,400$  (average position between maximal and minimal sampling depths) and  $-4,000$  m (maximal sampling depth of petroliferous formations).

Table 2.1 presents errors of formation pressure reducing for some structures of the Sorokin Swell under different positions of comparison planes. The table clearly shows that the error of reducing to  $-2,400$  m is below  $0.5$  mPa, while that of reducing to  $-4,000$  m increases to range from  $2$  to  $3.9$  mPa. In measuring points that are located close to the comparison plane of  $-4,000$  m and reduced to the latter, the error decreases substantially. For example, in the sampling point located at  $4,068$  m in Borehole Naul'skaya-56, the error of reducing to depths  $2,400$  m is  $1.48$  mPa and decreases practically up to zero ( $0.01$  mPa) at a depth of  $4,000$  m. Similar situation is observed in Borehole Varandeiskaya-7, where errors are  $3.02$  and  $0.1$  mPa. In other cases, the reducing error varies from  $0.002$  to  $0.5$ . Thus, the farther the sampling interval from the comparison (reducing) plane, the greater the error.

It means that in order to decrease the error in formation pressure reducing, it is necessary to minimize the distance between the comparison plane and the sampling point. Therefore, the comparison plane should be selected in the middle between minimal and maximal sampling points in aquifers. When potentiometric maps are compiled for separate petroliferous formations without the necessity

**Table 2.1** Errors of formation pressures reduced to different comparison planes

Borehole	Formation pressure (mPa)	Altitude of measured formation pressure (m)	Reduced pressure (mPa) $K = -2,400$	Reducing error $K = -2,400$	Reduced pressure (mPa) $K = -4,000$	Reducing error $K = -4,000$
<i>Varandei area</i>						
1	17.0	1,699.1	24.68	0.29	42.78	3.76
2	57.9	4,250.9	36.07	1.63	54.41	0.4
3	16.95	1,678.5	24.85	0.3	42.96	3.77
3	17.86	1,643.5	25.93	0.31	44.04	3.79
3	12.7	1,643.0	22.89	0.35	41.01	3.89
4	19.0	1,789.1	25.71	0.27	43.81	3.71
5	12.7	1,448.0	23.05	0.36	41.17	3.9
7	28.44	2,573.8	26.40	0.1	44.6	3.02
8	19.42	1,758.9	26.45	0.28	44.56	3.73
9	17.65	1,640.4	25.95	0.31	44.06	3.8
10	16.59	1,654.3	24.75	0.31	42.86	3.79
10	18.64	1,677.3	26.55	0.33	44.66	3.78
<i>Naul area</i>						
51	18.8	1,607	27.46	0.38	4.5	3.58
52	24.5	2,235	26.34	0.1	43.99	3.29
52	15.14	1,374	26.27	0.45	43.76	3.65
52	23.92	2,244	25.66	0.09	43.31	3.29
52	24.04	2,235	25.88	0.1	43.53	3.29
52	11.14	1,144	24.67	0.51	42.1	3.7
53	25.0	2,281	26.33	0.07	43.99	3.26
53	15.47	1,422	26.09	0.44	43.59	3.63
54	12.6	1,234	25.19	0.49	42.65	3.68
54	25.4	2,337	26.1	0.04	43.77	3.23
55	11.1	1,169.5	24.36	0.5	41.8	3.7
56	46.9	4,068	27.33	1.48	45.17	1.71
56	46.9	4,110	26.81	1.53	44.66	1.66
57	25.5	2,250	27.17	0.09	44.83	3.28
58	15.8	1,464	25.98	0.43	43.49	3.62
59	12.83	1,230	25.46	0.49	42.92	3.68
59	15.1	1,430	25.64	0.44	43.14	3.63
59	23.7	2,345	24.31	0.03	41.99	3.23
59	22.2	2,254	23.83	0.09	41.48	3.28
61	20.6	1,962	25.44	0.24	43.04	3.43
61	12.2	1,192.5	25.22	0.5	42.67	3.69
61	12.0	1,121	25.76	0.51	43.19	3.71

of studying hydrodynamic interaction between them in the vertical section, the comparison plane should be located in the middle of these formations. In modeling multilayer sequences (system of petroliferous and intervenient formations), the comparison plane should be placed in the middle of the examined interval of the section and be common for all the petroliferous formations, which offers opportunity to study hydrodynamic interaction of the stratified system in the vertical section.

Supplementing the Gurevich method, it should be emphasized that the pressure reducing error must be lower as compared with gradients of measured formation pressures at the same or close depths of hydrodynamic sampling. Therefore, in areas where the knowledge is sufficient, it is necessary to compile plots of correlation between changes of formation pressures and sampling depths and determine gradients of formation pressures measured at the same or close depths, which should be compared with error estimated using the method by Gurevich. If the error appears to be lower as compared with measured formation pressures at the same or close comparison planes, the method of reduced pressures may be used for the analysis of hydrogeodynamic situation in particular objects. Otherwise, the reliable analysis of hydrogeodynamic settings is impossible.

(2) Now, let us dwell on specifying dependence  $\rho(z)$  and reducing fluid densities to formation conditions.

Figure 2.2 demonstrates changes in fluid densities for several fields of the Bukhara-Karshi petroliferous basin (for the entire basin). The plots are compiled with account for the influence of different factors on density; for water density determined in standard conditions (laboratory) (Fig. 2.2a); for water density determined in formation conditions with account for temperature and compressibility (Fig. 2.2b); and in formation conditions with account for gas saturation, temperature, and compressibility (Fig. 2.2c). The field of points is bounded by straight lines. They could be limited by any nonlinear empirical curve, but this is unimportant for the problem under consideration. Each of these lines is described by empirical equations of straight lines shown in corresponding figures.

The figures display that regardless of factors that determine fluid density, the latter changes substantially in the horizontal plane particularly at great depths. For example, at a depth of 2,600 m, it changes from 1,000 to 1,100 kg/m<sup>3</sup> (Fig. 2.2c), which means that the method of pressure reducing cannot be applied. Nevertheless, the error in reducing of formation pressures can be estimated.

For standard conditions (variant 1), formation conditions (variant 2), and formation conditions with account for gas saturation (variant 3), errors (meters of water column) are 270, 246, and 220 m, respectively.

These estimates show that, first, there is no need to make laborious investigations and calculations for reducing density to formation conditions. Change in the absolute error, i.e., maximal discrepancy between variants 1 and 3, is 50 m (approximately 0.5 mPa), which is frequently less as compared with the error in measurements of formation pressures at great depths, particularly when they are anomalously high. The maximal relative error between variants 1 and 3 is <19%. Similar results are also obtained for the eastern Ciscaucasia region. Thus, reducing fluid densities to formation conditions provides no desirable effect, resulting only in additional labor and time expenditures.

The estimated error values of reduced pressures (meters of the water column) are obtained during the assessment of possible error (under integration from 3,200 to 400 m) from the maximal sampling depth to the middle altitude. Figure 2.2 shows that this error in reducing is related to the maximal scatter of points in the lower part of the section (with brine occurrences): divergence of straight lines

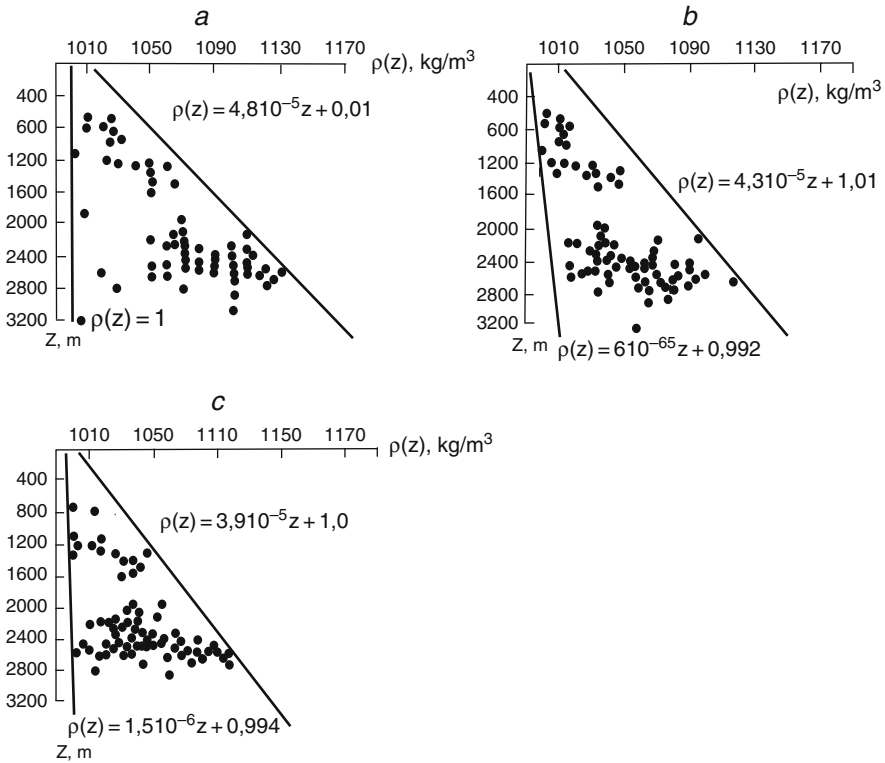


**Fig. 2.2** Correlation between density and depth in some fields of the Bukhara-Karshi petroliferous basin. (a) Density of water in normal conditions; (b) the same in formation conditions with account for temperature and pressure; (c) the same in formation conditions with account for gas saturation, temperature, and pressure

bounding the point field. If the integration way is increased (another comparison plane is selected), the error should increase as well. For example, under integration within the interval of 2,600–400 m for variants 1, 2, and 3, respective errors should be 180, 162, and 164 m; maximal absolute error in this case will decrease up to 27 m (relative error 10%). Integration within the interval 1,000–400 m will result in pressure reducing errors of 2, 26, and 24 m, respectively; maximal absolute error is 2 m (relative error 7.7%).

Thus, calculations demonstrate that the absolute and relative errors decrease with the decrease in scatter of points in the horizontal plane within assigned integration limits. We always changed one of the integration limits in order to pass into the area with the minimal scatter of points, where straight line bounding the point field converge. Thus, the less the distance from the measuring point, the lower the error in formation pressure reducing, all other factors being the same.



## 2.2 Assessment of Directions of Density-Variable Fluid Flows by the “Filtration Force” Method

When the method of reduced pressures is inapplicable [difference between reduced formation pressures between two compared points (boreholes) is greater as compared with uncertainty of the integral in equation (2.2)], Gurevich recommends to immediately assess the value and direction of the filtration force vector following from the equation  $\vec{F} = -\nabla P + \rho \vec{g}$ .

Calculation of filtration force is recommended to determine replacing the differential form of the general filtration law  $\vec{v} = (1/\mu)K(-\nabla P + \rho \vec{g})$  by the finite-difference one. In this case,  $\partial P/\partial l_i \cong (P_0 - P_i)/\Delta l_i$ .

In this equation,  $P_0$  is the pressure in the point (borehole), from which filtration force vectors are determined relative to the closest three points with measured formation pressures  $P_i$  and  $\Delta l_i$  is the distance to these three points.

In this case, projection of filtration force vectors along axes  $x$ ,  $y$ , and  $z$  is recorded in the following way:

$$F_x = -\{(P_0 - P_1)[(y_0 - y_2)(z_0 - z_3) - (y_0 - y_3)(z_0 - z_2)] + (P_0 - P_2)[(y_0 - y_3)(z_0 - z_1) - (y_0 - y_1)(z_0 - z_3)] + (P_0 - P_3)[(y_0 - y_1)(z_0 - z_2) - (y_0 - y_2)(z_0 - z_1)]\}U;$$

$$F_y = -\{(P_0 - P_1)[(x_0 - x_3)(z_0 - z_2) - (x_0 - x_2)(z_0 - z_3)] + (P_0 - P_2)[(x_0 - x_1)(z_0 - z_3) - (x_0 - x_3)(z_0 - z_1)] + (P_0 - P_3)[(x_0 - x_2)(z_0 - z_1) - (x_0 - x_1)(z_0 - z_2)]\}U;$$

$$F_z = -\{(P_0 - P_1)[(x_0 - x_2)(y_0 - y_3) - (x_0 - x_3)(y_0 - y_2)] + (P_0 - P_2)[(x_0 - x_3)(y_0 - y_1) - (x_0 - x_1)(y_0 - y_3)] + (P_0 - P_3)[(x_0 - x_1)(y_0 - y_2) - (x_0 - x_2)(y_0 - y_1)]\}U - \rho^* g;$$

$$U = (z_0 - z_1)[(x_0 - x_2)(y_0 - y_3) - (x_0 - x_3)(y_0 - y_2)] + (z_0 - z_2)[(x_0 - x_3)(y_0 - y_1) - (x_0 - x_1)(y_0 - y_3)] + (z_0 - z_3)[(x_0 - x_1)(y_0 - y_2) - (x_0 - x_2)(y_0 - y_1)],$$

where  $\rho^*$  is  $1/4 \sum_0^3 \rho_i$ ;

$$F_{xy} = (F_x^2 + F_y^2)^{1/2}; \quad F = (F_x^2 + F_y^2 + F_z^2).$$

The following angles are recommended to be taken as determining the vector  $F$ :  $\theta$  between the direction of the vector  $F$  and the horizontal plane considering angles counted upward and downward as positive and negative respectively, and  $\beta$  between the axis  $x$  and the vector  $F_{xy}$  counted clockwise.

$$\begin{aligned}
\theta &= \arcsin(F_z/F); \\
\beta &= \arctg(F_y/F_z) \quad \text{under } F_z \gg 0 \text{ and } F_y \gg 0, \\
\beta &= \arctg(F_x/F_y) + 90^\circ \quad \text{under } F_z \gg 0 \text{ and } F_y \gg 0, \\
\beta &= \arctg(F_y/F_x) + 180^\circ \quad \text{under } F_z \gg 0 \text{ and } F_y \gg 0, \\
\beta &= \arctg(F_x/F_y) + 270^\circ \quad \text{under } F_z \gg 0 \text{ and } F_y \gg 0.
\end{aligned}$$

When axes  $x$  and  $y$  are directed northward and eastward, respectively,  $\beta$  is the azimuth angle indicating the direction of the vector  $F_{xy}$  horizontal component.

Application of this method is constrained by several conditions related to substantiation of selected points, between which calculations are performed. These constraints consist in the following: (1) changes in density values as well as coefficients of permeability and porosity within the calculation area should be insignificant and (2) points should be located far away from boundaries and areas with contrasting changes in the subsurface fluid flows.

The accomplishment of these conditions is possible when areas between points are lacking fractures and contrasting lithological changes and when the scale of filtration heterogeneity is substantially greater as compared with distances between selected points, which should be located within the same structure or its part.

The above-mentioned constraints show that the filtration force method requires detailed and reliable geological substantiation, which is frequently impossible due to the insufficient information. The method may be used for the assessment of the potential flow and its direction only in rare situations because of the stratum-block structure of deep formations in petroliferous basins and the development of impermeable or poorly permeable boundaries between blocks, i.e., due to contrasting heterogeneity in capacity and filtration properties of rocks.

This conclusion is well illustrated by the eastern Ciscaucasia petroliferous basin, where the method of filtration force was applied for determining value and direction of the flow vector (and compared with other methods).

### 2.3 The Direct Method of Assessing Density-Variable Deep Fluid Flow Directions

In connection with continuing disputes on possibility/impossibility of the usage of the formation pressure reducing method, we propose the approach that allows the assessment of gradients without reducing formation pressures based only on factual data with their subsequent comparison with gradient directions obtained by the pressure reducing method [4, 8].

It is evident that when formation pressure values are measured in two different boreholes at the same depth, there is no need in reducing them, i.e., in such a situation, we can confidently solve the dilemma of the presence or the absence of the gradient between these two boreholes (without account for technical errors in measuring formation pressures). Inasmuch as sampling depths are practically always different, it is possible to select the best studied intervals of the section with insignificant differences. For assessing lateral gradients of fluid flow direction in particular

objects, we accepted the thickness of selected sampling intervals in petroliferous formations to be 20–30 m. In this case, neglecting changes in fluid density in such a narrow section interval, we can speak about the presence (absence) of the gradient under the pressure differential over 0.2–0.3 mPa between two or several points (boreholes).

We used largely the method of reduced formation pressures accompanied by the assessment of reducing error in particular natural objects (Chapters 7–10). For the eastern Ciscaucasia region, the Gurevich method [7] was used for the calculation of “filtration force” vector value and its direction, an addition to the reducing method combined with the error assessment. The direct method was applied when the knowledge degree was sufficient.

## 2.4 Modeling Methods in the Studies of Deep Fluid Flows

Modeling methods are usually used for solving many different tasks. We used modeling for solving the following particular tasks:

- (1) estimating the duration of periods with abnormally high formation pressures;
- (2) revealing the distribution of pressures in clayey formations during their compacting (equation of filtration consolidation without account for skeleton creeping) for the area with regularly moving boundary (growth of the geostatic load);
- (3) defining the distribution of pressures under the variable stress (under the influence of external forces such as tectonic stresses). These tasks were solved in the test regime with the factor-diapason assessment.

The methods used for assessing directions and values of vertical and horizontal formation pressure gradients can be used only for some well-studied areas, which are irregularly scattered through regions. In addition, what is most important, the results obtained by these methods prevent from receiving the idea on hydrogeodynamics for the entire region, particularly for poorly studied areas irregularly scattered between well-studied structures, i.e., it is impossible to obtain the spatial picture characterizing the distribution of formation pressures and *regional* hydrogeodynamics of petroliferous formations. The idea on the regional hydrogeodynamics can be obtained only modeling large regions and considering the system of such formations with intervenient poorly permeable sequences (caprocks) successively replacing each other upward the section.

In this connection, we performed modeling for the northern part of the Timan-Pechora petroliferous basin (in the northern part of the Pechora Syncline), which also included the entire section from the Ordovician–Silurian to Permian–Triassic (plane-spatial task) (Chapter 8).

For the West Siberian petroliferous basin, the modeling was aimed at the solution of the plane task: assessment of the redistribution of lateral and vertical fluid

expenditures in the section and role of peripheral parts of the basin as a regional recharge source in dynamics of deep fluids; the Salym oil fields was also modeled.

No quantity estimates (velocities, expenditures, intensity of hydrodynamic connections between separate petroliferous formations) were expected from this modeling since, first, there was no such necessity and second, it was impossible to obtain them because of the following causes: (a) poor and irregular knowledge of both lateral and vertical peculiarities practically for all the regions: (b) low reliability of primary information, which is determined by purposes and conditions of sampling usually conducted in order to sample separate elements of the section for oil, gas, or other hydrocarbons; (c) traditional unavailability of information on filtration parameters or reservoirs and caprocks. The processes responsible for their formation vary both through space and, likely, time and their ambiguous estimate is now impossible.

The main purpose of modeling was obtaining the principally correct solution consistent with available factual material and revealing only general regularities in regional hydrogeodynamics of deep fluids. Regional modeling of geofiltration tasks was performed in the stationary regime for natural (undisturbed by exploitation) conditions.

For the Pechora petroliferous basin (northern part), hydrogeological conditions were schematically presented in the form of a four-member sequence (Silurian–Lower Devonian, upper Frasnian—Tournaisian, upper Visean—Artinskian, and Upper Permian–Triassic complexes) with three low-permeable layers [caprocks: lower Frasnian (Kynov-Sargaev), Visean, and Lower Permian (Kungurian) fluid-confining sequences] overlain by permafrost rocks.

Modeling was conducted using information on all the boreholes and with account for maximal quantity of data on geological structure of the region and its tectonics. Geofiltration modeling included the entire region and the entire examined section. The model represents a four-member system at scale 1:200,000 for the entire territory and separately for the Sorokin Swell at scale 1:50,000.

For each petroliferous formation (reservoir), the filtration equation appears in the following way (in the stationary regime):

$$\begin{aligned} \partial/\partial x(kt\partial P/\partial x) + \partial/\partial y(km\partial P/\partial y) + k_0^u/m_0^u(P_u - P) \\ + k_0^d/m_0^d(P_d - P) + W + \alpha\partial P_0/\partial t = 0, \end{aligned}$$

where  $P$  is the reduced formation pressure (equation 2.2),  $P_u$  is the reduced formation pressure in the underlying reservoir,  $k_0^u/m_0^u$  and  $k_0^d/m_0^d$  are the permeability and the thickness of overlying and underlying caprocks, respectively,  $k$  and  $m$  are the permeability and the thickness of the reservoir,  $P_0$  is the external pressure (for example, tectonic stress),  $\alpha$  is the coefficient that takes into account thickness, porosity, and compressibility of rocks and water,  $t$  is the time, and  $W$  are internal feeding and discharge sources.

It should be noted the external impact (for example, geodynamic processes) imitates additional recharge with the variable sign. For example, under compression the formation pressure in the fluid-rock system increases (positive recharge source), while extension results in the opposite process. During modeling of zones

with abnormally high formation pressures, the recharge was assigned to be constant (although minimal) with permeability of the boundary layer being  $n \cdot 10^{-(10-11)}$  m/day.

The study region was subdivided by the rectangular irregular net into blocks (their linear sizes varied from 1 to 8 km) so that all the available boreholes and geological boundaries (primarily, tectonic fractures) appeared to be located in centers of blocks.

Boundary conditions were substantiated by all the available information:

- of the first type when boundaries were marked by boreholes with measured formation pressures;
- of the second type with the zero expenditure along faults (sometimes, it was obtained in the course of the reversed task solution);
- of the third type at the boundary with the sea or in some blocks of the study region (usually, at boundaries between large structural elements).

The task was solved in the stationary regime since no oil and gas fields or industrial and thermal water deposits were developed in the study area, except for fields in the southern part of the Kolva Megaswell. Thus, the area retained natural hydrogeodynamic conditions and its geological processes that influence the formation of deep fluids are characterized by rates that are substantially lower as compared with the redistribution of pressures within the formation and have no impact on present-day hydrogeodynamic conditions [4]. The exception is seismic processes, but the area is characterized by low seismicity.

The reversed task solution was accompanied by correction of permeability of petroliferous formations and fluid-confining beds. The solution was considered to be accomplished when model values of pressures corresponded to their natural (factual) counterparts, and horizontal and vertical gradients coincided with both value and direction. The solution accuracy was 0.5 mPa (2%), which is equal to the maximal error in pressure reducing. Correction of the model during the task solution should be accompanied by decrease in permeability of petroliferous formations up to  $10^{-(4-5)}$  m/day and interlayer permeability up to  $10^{-(10-11)}$  m/day, i.e., it was necessary to assign impermeable boundaries. Sometimes, boundary conditions of the second type with the zero expenditure should be assigned.

The reversed task solution resulted in obtaining formation pressure values for the entire study region, which was used for compiling hydrogeodynamic schematic map for all the petroliferous formations and hydrogeodynamic profiles. In addition, modeling allowed the value and direction of the vertical gradient (i.e., interstratal interaction) to be estimated (Chapter 8). The analysis of its results revealed peculiarities in regional dynamics of deep subsurface fluids in the northern Timan-Pechora petroliferous basin located in the northern part of the Pechora Syncline (Kolva Megaswell in the west, Sorokin Swell in the east, Chernyshev Ridge in the south, and sea basin in the north).

Comparison of directions of lateral gradients obtained by different methods demonstrates that best correspondence is observed between directions of gradients based on factual measurements of the formation pressure and obtained by the method of formation pressure reducing with the assessment of their reducing errors. The method of local gradients and paired successive reducing of formation pressures provides relatively ambiguous results. This is explained likely by the fact that changes in the water density between points, which were used in calculations, were ignored. This is particularly important when vertical distances between these points are significant and changes in the fluid density in the same direction are also substantial.

The distribution of formation pressures through the study region derived from modeling is consistent with the direction of lateral gradients obtained by the method of formation pressure reducing with the assessment of the reducing error and direct method.

## 2.5 Compilation Methods of Regional Potentiometric Maps for Petroliferous Formations

Regional potentiometric maps of deep fluids in petroliferous formations are compiled for regional prognoses of the petroleum resource potential. Reliability of these prognoses is determined by the trustworthiness of maps that reflect directions of deep fluid flows.

During the study of *regional fluidodynamics* of petroliferous formations, one to two values of formation pressures are selected among their many values in local high-order structures (which represent a single point at the regional scale). These values of reduced formation pressures are either averaged or some value is selected for one of several boreholes. This value is then interpolated along with similar randomly selected points in neighboring structures or even in some remote structures. The selected particular values of reduced formation pressure usually remain unsubstantiated. They are selected randomly or according to the researcher's standpoint on regional character of the fluid flows, which introduces significant subjectivity into regional hydrogeodynamic interpretations. Precisely because of this reason, regional potentiometric maps compiled by different researchers for the same productive formation differ from each other.

Such an approach to compilation of regional potentiometric maps undoubtedly distorts the real fluidodynamic situation. Moreover, if geological structure of the area (boundaries between structures, tectonic fractures, zones of layer pinching out, facies replacements, and others) is ignored, reliability of regional fluid geodynamic maps and estimates of the petroleum resource potential based on such maps cast serious doubts.

Therefore, it is clear that the study of regional fluidogeodynamics is impossible *without investigation of the fluid geodynamic situation in limited well-studied areas*

(structures) with account for information on hydrodynamic and hydrogeochemical sampling, geothermal, and filtration properties of fluid-hosting rocks.

Such an approach (from particular to general or study of situation in local structures with subsequent regional generalization) differs substantially from that used nowadays. It allows the whole drilled and sampled borehole stock to be used with maximal account for the geological structure, tectonic settings, and other features, i.e., the complex analysis of all available information. Such an approach provides the results that reflect most adequately the natural situation [5, 2, 8].

Our studies of fluid geodynamic conditions in particular regions (Chapters 7–10) and separate areas and objects (compilation of potentiometric maps) were carried out at scale 1:10,000–1:50,000. Large-scale schematic maps were subsequently used for compilation of maps of the smaller scale.

Figures 2.3–2.5 illustrate schematic fluid flows in the eastern Ciscaucasia region (Lower Cretaceous aquifer), the upper Frasnian–Tournaisian aquifer of the Pechora Syncline, and the Lower Cretaceous complex of West Siberia, respectively. The maps reflect regional flows. They are based on the classical approach of averaging the formation pressure in separate areas and using the only averaged value for them or data on separate boreholes.

Below, we give insets to these schematic maps compiled with account for all trustworthy information available for all the structures (Chapters 7–9). These insets demonstrate that regional flows of deep fluids cannot exist in principle because of the stratum-block structure of deeply subsided parts of petroliferous basins.

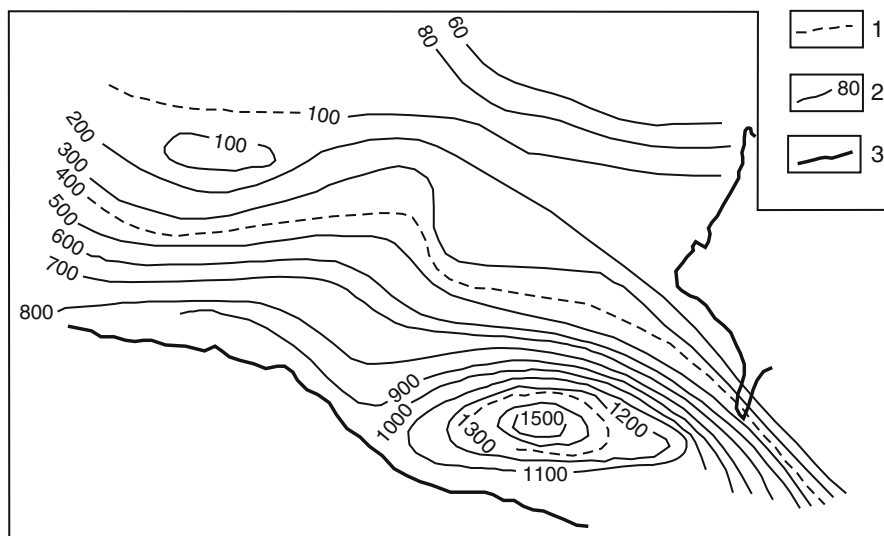


**Fig. 2.3** Schematic potentiometric map of the groundwater surface in Lower Cretaceous sediments of the eastern Ciscaucasia region (after V.A. Krotova). (1) Outcrops of Lower Cretaceous sediments; (2) isolines of reduced levels (m); (3) Caspian Sea shoreline

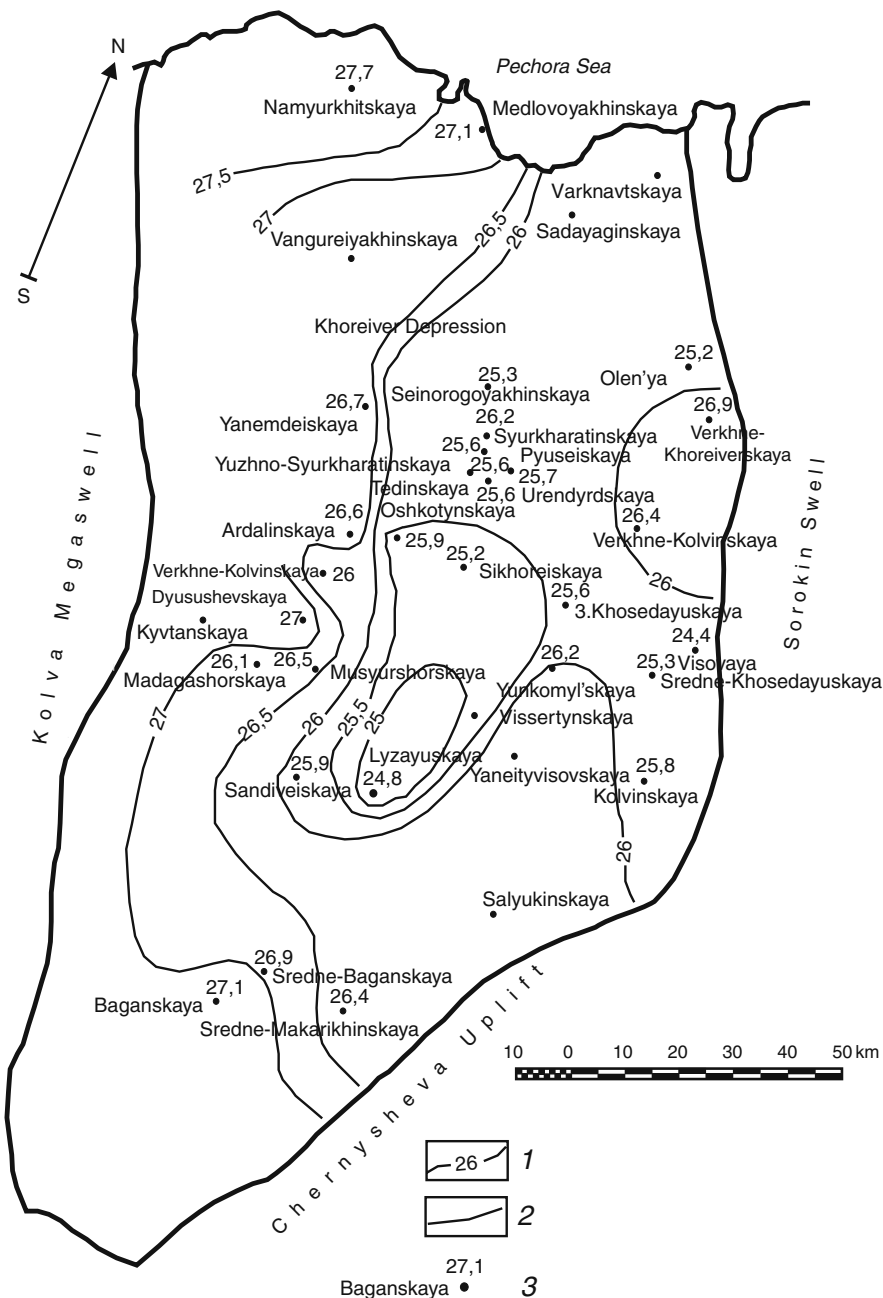
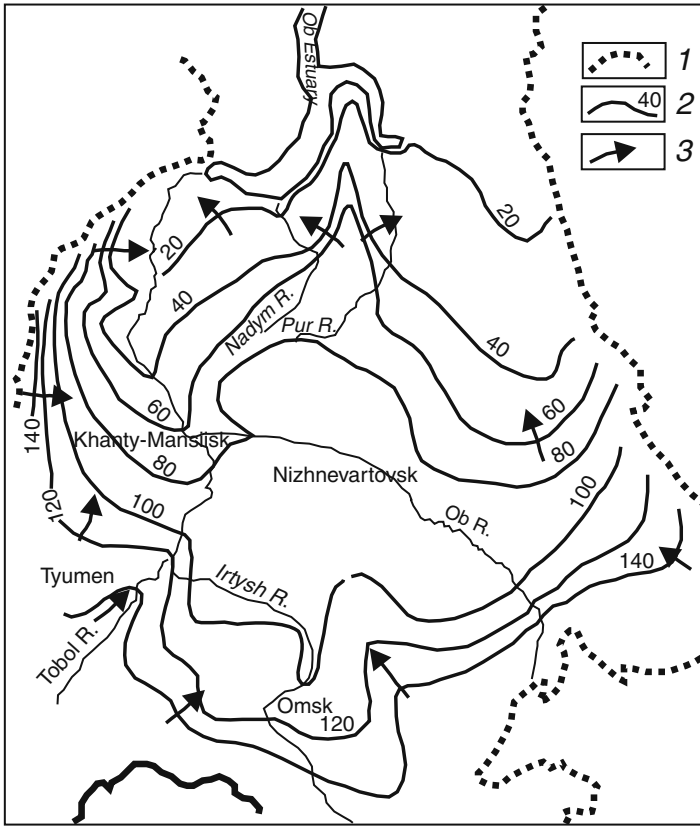


Fig. 2.4 Schematic potentiometric map of the groundwater surface in upper Frasnian–Tournaisian sediments of the Khoreiver Depression (Pechora petroliferous basin) [8]. (1) Isoline of the hydrodynamic potential (mPa); (2) boundaries of the Khoreiver depression; (3) structures and values of the hydrodynamic potential (mPa)





**Fig. 2.5** The map of groundwater dynamics in the Hauterivian–Barremian sequence of the West Siberian petroliferous basin (after V.V. Nelyubin). (1) Boundaries of the aquifer; (2) piezoisolines; (3) directions of groundwater flows

## 2.6 Methods of Compiling Hydrogeodynamic Maps

In order to unambiguously answer the question as to what determines the regional decrease in reduced formation pressures (heads) of fluids from the periphery of the petroliferous basins toward their central most subsided parts, both potentiometric maps and hydrodynamic maps or schemes are needed [orthogonal net of heads (reduced fluid pressures) and flow directions]. In addition, schematic changes in lateral expenditures of fluids along lines (bands) of the flow (in case of availability of information on filtration properties of reservoirs) should be outlined, which allows main fluid geodynamic zones with different intensity of water exchange to be defined [2–4].

Flow lines (bands) in maps of the potentiometric surface and hydrodynamic calculations (lateral expenditures per unit of the flow width) shed light on fluidodynamics in marginal zones of petroliferous basins and reveal peculiarities

in hydrodynamic relationships of deep fluids with its upper hydrogeological stage and surface.

For example, hydrodynamic schematic maps may reflect areas with the closed formation of subsurface drainage, which excludes the influence of marginal zones of artesian basins on the formation of deep groundwaters (Chapters 7, 9, and 10). Such a situation appears in areas with well-developed river network and deep lakes, which play the determining role in draining the basin and groundwater formation (southern West Siberia). In addition, the maps offer opportunity to outline hydrodynamic zones with different intensity of fluid exchange: intense, slow, and very slow.

The schematic maps of changes in lateral expenditures are compiled based on hydrodynamic maps [orthogonal net of isolines of formation pressures (heads) and flow lines]. Calculations are performed in line with the Darcy's law (necessary condition is the availability of the map of hydrogeological parameters) for every nod of the hydrodynamic network along lines or bands of the flow. This procedure results in the map with point values of lateral expenditures. Linear or other interpolations between points provide the map of lateral expenditures per unit of the flow width through the area.

In our opinion, schematic maps of changes in lateral groundwater expenditures are most convenient for presentation of factual material and corresponding calculation results since they characterize with sufficient detail regional regularities in expenditures of subsurface fluids as well as gradients, flow velocities, and total flow values (vertical hydrodynamic interaction between neighboring petroliferous formations or aquifers). In addition, they also make it possible to compare hydrodynamic conditions of separate productive formations, to establish duration of the fluid exchange, and to define hydrodynamic zones in the petroliferous basin (Chapters 7, 9, and 10). The informative value of such maps increases when they are accompanied by plots that reflect regional changes in fluid expenditures along flow lines in different geomorphologic, geological–structural, and hydrogeological settings.

## **2.7 Investigation Methods of Temperature and Concentration Fields**

When studying fluidodynamics of petroliferous formations, the researcher usually encounters difficulties such as shortage or, sometimes, insufficient trustworthiness of initial hydrodynamic information. This determines the necessity in the analysis of hydrogeodynamic and other data, which may indirectly shed light on hydrogeodynamics of separate regions. These are primarily the temperature and mineralization of the fluid. As is known, the spatial distribution and formation pressures are influenced by physicochemical, tectonic, and other processes, in addition to hydrodynamic factors. These processes result in changes in the temperature, mineralization, and chemical and gas composition of the fluid. In this connection,

the analysis of temperature fields and mineralization as well as separate chemical components may help in understanding the hydrogeodynamic situation.

The available viewpoints on the temperature field imply regular temperature increase with depth (geothermal gradient). Compilation of maps and sections is usually based on the averaged vertical temperature gradients for separate areas or boreholes within these areas. Moreover, subsequent interpretations that deal with deep surfaces and petroliferous formations may lead to confusing inferences. For example, the use of the averaged vertical gradient may result in zero or insignificant lateral temperature gradient both in separate areas and between them and, consequently, in simplified conception of the temperature field distribution or its complete distortion.

In order to exclude errors related to temperature recalculation for single temperature surfaces, the temperature field was analyzed in well-studied areas with selection of temperature measurements in the narrow interval of the section (20–30 m). The temperature difference, which exceeded 1°C (normal temperature gradient is 3°C per 100 m), provided grounds for suggesting the *lateral* temperature gradient between two points (boreholes).

Similar approach was also used in studies of hydrogeochemical field. Such studies are usually accompanied by compilation of maps illustrating the distribution of mineralization and different chemical groundwater components. In this case, a single mineralization value is selected to characterize the entire aquifer (petroliferous complex), which is incorrect taking into consideration significant thicknesses of these formations (usually, a few hundreds of meters). To avoid such a situation, the mineralization field was studied in local structures in the central part of the Khoreiver Depression, in several structures of the Surgut Arch (West Siberian petroliferous basin), and in other areas with available sufficient and trustworthy information. For determining existence and direction of mineralization gradient between points (boreholes), mineralization values (or its separate chemical components), which were measured at close depths with the interval not exceeding 50 m, were selected. The compiled schematic maps of lateral mineralization gradients made it possible to study its spatial distribution within well-studied structures [8].

In addition, disembodied (which is explained by extremely irregular knowledge of deep formations in basins) on palynological spectra, tectonics, mineralogy, geochemistry, reservoir properties of formations and caprocks, and others, data published in numerous articles, monographs, and initial reports were used for substantiation of main inferences.

## References

1. Bondarenko S S, Barevskii L V, Dzyuba A A (1983) Migration peculiarities of deep groundwater. In: Basics of hydrogeology. Hydrogeodynamics. Nauka, Moscow
2. Djunin V I (1981) Investigation methods and principles of deep formation hydrodynamics. VIEMS, Moscow
3. Djunin V I (1985) Investigation methods of the deep subsurface flow. Nedra, Moscow

4. Djunin V I (2000) Hydrodynamics of deep formations in petroliferous basins. Nauchnyi mir, Moscow
5. Durmish'yan A G (1977) On the problem of abnormally high formation pressures and its role in oil and gas prospecting. Trudy VNIGRI 397:55–69
6. Gurevich A E (1969) Groundwater, oil, and gas migration. Nedra, Leningrad
7. Gurevich A E (1985) Practical manual for the study of groundwater migration during exploration of mineral resources. Nedra, Leningrad
8. Korzun A V (1996) Hydrodynamics of deep formations in the northern Pechora artesian basin. Candidate dissertation (Geol-Mineral), MGU, Moscow
9. Nelyubin V V, Kamenev A P (1976) Calculation of formation water pressure in boreholes. In: Problems of hydrogeology and engineering geology. Tyumen
10. Shestakov V M, Kodzhakuliev A Ya (1988) Analysis of geohydrodynamic conditions in deep aquifers in connection with the study of their petroleum resource potential. Vestnik MGU Ser Geol 2:56–61
11. Silin-Bekchurin A I (1949) The method of approximate calculation of filtration and subsurface brine flow rates based on piezometers. Trudy laborat hydrogeol problem AN SSSR 2:158–182

# Chapter 3

## Role of Regional Infiltration Recharge Sources in the Formation of Deep Fluids and Petroliferous Basin Hydrodynamic Zoning

### 3.1 Role of Petroliferous Basin Periphery in Recharge of Deep Fluids

At present, solution of most scientific and practical tasks is based on conceptions of regional hydrodynamically integrated flows of deep fluids. In this connection, it seems reasonable to consider the role of peripheral parts of petroliferous basins (regional recharge sources) in hydrodynamics of deep formations.

The following question should primarily be answered: do fluids formed in peripheral parts of petroliferous basins (regional infiltrations recharge sources) possess energy sufficient for overcoming horizontal filtration resistance at distances of hundreds to thousands of kilometers and subsequent overcoming of vertical filtration resistance in marine and oceanic basins, which are thought to represent regional discharge zones?

To answer this question, we should consider proportions of vertical ( $R_z$ ) and horizontal ( $R_{x,y}$ ) filtration resistances to subsurface fluids with account for increment of filtration areas away from marginal petroliferous basin parts and stratified systems of negative structures in general (synclines, inter- and intramontane depressions).

$$R_{x,y} = \Delta x,y/km; R_z = m_0/k_0 \Delta x, \Delta y, \quad (3.1)$$

where  $m$  and  $m_0$  are thicknesses of high- and low-permeable sediments, respectively,  $k$  and  $k_0$  are filtration (permeability) coefficients of high- and low-permeable sediments, respectively, and  $\Delta x, y$  are respective increments of filtration areas along axes  $x$  and  $y$ .

Petroliferous basins are characterized by distinct discrepancy between the distribution area of sediments (hundreds of thousands and millions of square kilometers) and their thicknesses (a few kilometers). Due to such geometrical sizes of basins, the flow of subsurface fluids along bedding of oil- and gas-bearing formations directed toward their peripheries experiences progressively increasing horizontal filtration resistance ( $R_{x,y}$ ) directly proportional to the migration way of fluids, which is readily

seen from equation (3.1). The integral ascending discharge of fluids increases permanently in the same direction on account of increased integral vertical resistance ( $R_z$ ) due to the increased area of ascending filtration ( $\Delta x \cdot \Delta y$ ), i.e.,  $\frac{Q_{x,y}}{\sum Q_z} \rightarrow 0$ .

It follows that owing to the gradual increment of the filtration area along the fluid flow at some distance from boundaries of regional infiltration recharge sources, horizontal filtration resistance appears to be comparable with the integral vertical filtration resistance.

For simplification, let us suggest that thicknesses of the reservoir and intervening low-permeability sediments are equal or increase proportionally away from marginal zones of negative stratified structures (any difference in thicknesses has no principal significance), while permeability of caprocks (largely clayey sediments) was  $10^5$ – $10^6$  times lower as compared with that of reservoirs. Then, the ratio between filtration resistances should be recorded as

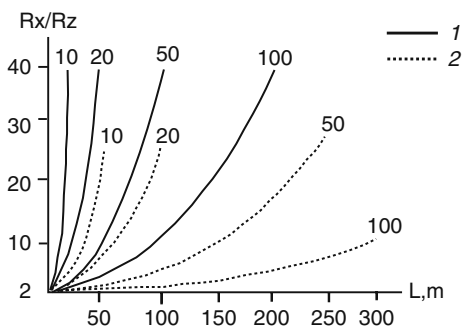
$$R_{x,y}/R_z = (\Delta x/m)^2 \cdot (10^6 - 10^5), \quad (3.2)$$

It follows from equation (3.2) that horizontal filtration resistances increase proportionally to the square of a distance from marginal petroliferous basin zones along bed dipping, while integral vertical resistance decreases with the same velocity (Fig. 3.1). The figure demonstrates that the horizontal filtration resistance becomes higher as compared with its vertical counterpart at a distance from a few to tens of kilometers depending on the rock thickness and ratios between permeability of reservoirs and low-permeability rocks.

Consequently, fluids move in two directions: lateral and vertical within a relatively narrow zone along margins of artesian basins. At large distances (tens of kilometers and more), the integral vertical filtration of fluids becomes prevalent against the background of the reduced lateral filtration (Fig. 3.1).

Thus, in order to accomplish the minimal work, it is more “profitable” for the subsurface fluid flow to overcome resistance of low-permeability rocks than move toward progressively increasing filtration resistance along rock bedding under their dipping toward central parts of petroliferous basins (negative stratified structures).

**Fig. 3.1** Changes in the ratio between vertical and horizontal filtration resistances away from the basin periphery. (1) Under ratios of filtration coefficients  $10^5$  m/day; (2) the same under  $10^6$  m/day. Numerals near curves designate thickness of reservoirs and caprocks, m.



Transition to the area with dominant vertical migration of subsurface fluids is natural and universal and should be considered as reflecting general regularity for negative stratified structures (artesian basins, inter- and intramontane depressions) [3].

As is shown below for particular objects (Chapters 7, 9, and 10), this regularity is manifested regardless of geological and structural–tectonic peculiarities, age, and hydrological conditions of petroliferous basins. Regional and local peculiarities determine only spatial changes in subsurface fluid flows. In any case, the entire fluid flow formed in regional recharge zones enters indirectly through a system of aquifers and low-permeability rocks first the river network and then sea and oceanic basins with the surficial drainage.

When the river network is lacking, for example, in arid and semiarid areas of the Turan Plate, Kalmykia, and other regions, deep fluids enter near-surface formations and discharge through evaporation. Precisely such a process is responsible for the reversed hydrochemical zoning in these areas reflected in high mineralization of groundwater, which decreases downward up to certain depths.

Equation (3.1) ignores changes of filtration properties of reservoirs and low-permeability sequences. As is shown below (Chapter 6), transmissibility (product of the thickness and filtration coefficient) of reservoirs of the petroliferous basin platform cover decreases with subsidence of aquifers (to certain depth). In marginal zones, permeability of clayey sediments is maximal due to their enrichment in sandy material. These lithological regularities result in even greater changes of proportions between horizontal and vertical resistances in favor of the vertical fluid filtration component.

Indeed, in the equation  $R_{x,y} = \Delta x,y / km$ , denominator decreases. It means that away from marginal petroliferous basin zones, filtration resistance along rock bedding increases progressively with their dipping. Consequently, the lateral fluid flow on its way should spend more energy for overcoming resistance. With account for the decreased filtration resistance of reservoirs along rock bedding, the distance, where the vertical infiltration resistance should be lower as compared with the horizontal one, should be reduced much significantly than shown in Fig. 3.1.

Under constant values of transmissibility in rocks, changes in lateral expenditures are described by the exponential function [1–3] with the variable being more complicated, although also decreasing. It is clear that transmissibility decrease along with the subsurface fluid flow should be accompanied by more significant decrease in lateral expenditures. If the change in transmissibility is accepted for the marginal petroliferous basin zone in the form of the exponential function [3], ratio between unit fluid expenditures should be as follows:

$$\frac{Q_1}{Q_2} = \frac{(km)_1 \Delta H_1 / \Delta L}{(km)_2 e^{-\alpha \Delta L} \Delta H_2 / \Delta L} \quad \text{and} \quad \frac{Q_1}{Q_2} = \gamma e^{\alpha \Delta L} \gamma = \text{const.} = \frac{(km)_1 \Delta H_1}{(km)_2 \Delta H_2},$$

It means that in the field of reservoir rock properties with the irregular structure, gradients, velocities, and expenditures of subsurface fluids at the same distance

should decrease (with given regularity in transmissibility changes)  $e^{\alpha\Delta L}$  times faster than that in the uniform medium.

Lateral fluid expenditures are decreasing gradually or with significant variations at relatively short distances. Changes in fluid unit expenditures along flow lines (as well as gradients) are determined by intensity of the hydrogeodynamic interrelationships of stratified elements of the petroliferous formation (aquifer) section between each other and with the surface.

The aforesaid is confirmed by modeling and hydrodynamic calculations (Chapters 7, 9, and 10), which were used for compiling maps and plots illustrating changes in fluid expenditures from the periphery toward the central part of the petroliferous basin. For compiling hydrodynamic maps, schemes, and plots illustrating changes in lateral unit expenditures of fluids in particular objects, the value of the unit expenditure in areas of outcropping rocks was accepted to be 100% along one of the flow lines. The ratio between this value and that of unit expenditures along other flow lines was used for compiling the schematic plane map illustrating changes in lateral unit expenditures of subsurface fluids for Aptian–Cenomanian and Lower–Middle Jurassic aquifers of West Siberia.

Development of tectonic fractures that frequently separate platforms from orogenic structures stimulates undoubtedly reduction of lateral fluid expenditures along the profile from peripheral parts of the basin toward its center. Regardless of their hydrogeological role (permeable or impermeable), these fractures serve always as hydrodynamic boundaries, which hinder lateral migration of subsurface fluids. When they are impermeable, this is quite natural. When faults and fault-line zones are permeable in some areas, they serve as conduits for vertical fluid discharge, which results in partial or complete reduction of the lateral fluid flow.

Thus, changes in proportions of vertical and horizontal filtration resistances and development of faults or large river drains (frequently connected with different-order faults) determine natural reduction of lateral expenditures and deep fluid flow velocities away from marginal zones of stratified negative structures.

The vertical fluid discharge (usually by flowing) distributed through some area occurs via low-permeability, largely clayey, rocks. Development of different-order near-vertical faults or the river network results in the concentrated discharge (frequently reflected in the potentiometric surface of deep fluids) within narrow, sometimes, linear local zones [1, 3].

Thus, there are grounds to state that the significant role of regional fluid recharge sources is manifested only within the relatively narrow band adjacent to regional infiltration recharge sources, *while regional flows of subsurface fluids (hundreds to thousands of kilometers) in stratified systems of negative structures are impossible. This is true of all the regions.*

Unfortunately, when estimating the petroleum resource potential of regions, researchers proceed usually from the concept of regional fluid flows through the entire distribution area of some elements in stratified systems of petroliferous basins. In light of the above-mentioned considerations, such an approach to the assessment of the regional migration of deep fluids is incorrect.



### 3.2 Hydrodynamic Zones in Petroliferous Basins

The concept of hydrodynamic zoning of petroliferous basins is based on different depths of subsurface fluid recharge by surface basins and flows (local and regional) and position of regional confining beds in the section.

These principles, although being correct in essence, introduce significant uncertainty into the spatial position of hydrodynamic zones and can be used, when all other factors are equal, which is a rare situation due to significant changes in natural conditions even within a single petroliferous basin. Boundaries of hydrodynamic zones are determined by both position of local and regional fluid drainage levels and geological structure of particular petroliferous basin areas, development of faults, bedding patterns, lithology, and other factors.

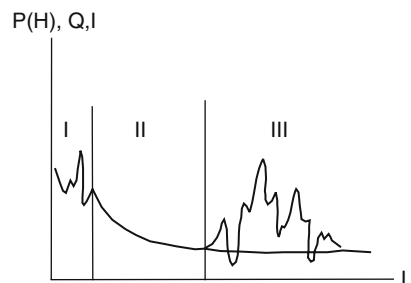
The difficulties related to defining hydrodynamic zones, particularly their plane configuration, stimulate searches for new approaches to the solution of this problem.

Figure 3.2 demonstrates in schematic form the principal model of the subsurface fluid formation along the flow line parallel to subsided aquifers (formations) from marginal parts of petroliferous basins toward their deepest areas [1–3, 5].

In Zone I, subsurface flow is closely connected with surface factors and experiences significant spatial variations due to highly differentiated relief, shallow occurrence of aquifers, development of the river network and different-order recharge zones, small thickness of overlying low-permeability rocks, and high content of sand admixture in them. These areas are characterized by substantial changes in gradients, velocities, and expenditures of subsurface fluids at relatively short distances. By terminology of most researchers (Chapter 1), this area corresponds to the zone of the intense water exchange.

When reservoirs subside or the section includes thick low-permeability formations that immediately contact marginal zones and overlie aquifers, this zone (of intense water exchange) is practically missing or vague. In most cases, position of local recharge and discharge areas in marginal zones determines, however, complicated migration of subsurface fluids (Chapters 7, 9, and 10). This zone is most unstable with respect to gradients, velocities, and expenditures of groundwater. It is influenced only by exogenic factors.

**Fig. 3.2** The principal model of changes in formation pressures ( $P$ ) (heads  $H$ ), lateral expenditures ( $Q$ ), and pressure gradients away from the periphery of the basin. (I, II, III) zones with the intense, low, and very low water exchange, respectively



Zone II of subsided aquifers that is overlain by low-permeability and other petroliferous formations (aquifers) with progressively increasing thickness contacts immediately Zone I.

Zone II is largely characterized by diffused vertical fluid discharge against the background of permanently decreasing lateral flow. This determines reduction of gradients, velocities, and expenditures practically up to zero, which is explained by changes in proportions of vertical and horizontal filtration resistances. This zone is bordered on its outer side (marginal zone of negative stratified structures) by subsurface hydraulic watershed. From the latter, parameters of fluid flow (formation pressures, velocities, expenditures, gradients) change gradually toward internal subsided petroliferous basin areas along a zone of the intense water exchange, if there is any, or along boundaries of petroliferous complexes (aquifers), when the latter is missing.

By its position, this zone can be considered as transitional between zones with intense and slow water exchange. Therefore, both surface and internal factors may influence the formation of subsurface fluids and, primarily, hydrodynamics.

Most subsided parts of stratified negative restructures (Fig. 3.2) host a zone with the very slow (passive) water exchange (Zone III). The subsurface fluid flow is local being determined mainly by the internal structure of the area and its tectonic fractures. The zone is characterized by dominant vertical filtration under the influence of endogenic factors. Its recharge sources are determined by internal processes. Various anomalies mark this zone: hydrodynamic, hydrochemical, thermal, gas, and others. When anomalies are missing, parameters of the fluid flow experience weak gradual changes.

The boundary between zones with intense and slow water exchange is located close to the local recharge area most remote from marginal negative structures (Fig. 3.2). It is incorrect to draw the boundary between these zones based, for example, on the hypsometric position of the drainage base level, since the depth of the draining influence of the river network depends on the combined influence of many factors that determine dynamics of subsurface fluids and interaction between petroliferous formations (aquifers).

For complex negative structures with local and regional relative confining beds, the depth of the complete draining influence under equal influx along bedding and vertical discharge of fluids may be derived from the following equation [4]:

$$m_0 = \Delta H_v k^0 L^2 / \Delta H_l T, \quad (3.3)$$

where  $L$  is the width of the discharge zone derived from the ratio between vertical positions of subsurface fluid levels ( $\Delta H_v$ ),  $\Delta H_l$  is the difference between levels of the lateral flow in the discharge area,  $T$  is the transmissibility of host rocks, and  $k_0$  is the permeability of low-permeability rocks.

Calculations performed in line with equation (3.3) and with real values of parameters show [4] that the complete drainage of aquifers is possible with the integral thickness of low-permeability rocks up to 200 m and that of the zone with intense

water exchange up to 500 m and more. The depth of incomplete drainage may naturally be substantially thicker.

Thus, the position of the zone with intense water exchange in the section can be derived from the above equation. In the plane, the boundary of this zone is determined based on the totality of points calculated for different geological–structural, hydrogeological, and geomorphologic conditions.

The other method used for mapping zones with intense and slow water exchange is based on the analysis and calculation of unit expenditures along the hydrodynamic grid of fluid flows with account for the transmissibility map.

In this case, the boundary between zones with different water exchange is located between zones with strong deformation of the fluid flow and its gradual changes accompanied by increase in flow parameters (formation pressures (heads) gradients, velocities) toward internal subsided parts of negative structures (Fig. 3.2, Chapters 7, 8, and 10).

For substantiating boundaries of hydrodynamic zones, plots of changing flow parameters (primarily, expenditures, gradients, and heads) along the flow lines (flow bands) are needed [3]. The plots compiled in relative coordinates, for example,  $q(x)/q(0)-x/L$  (where  $q(0)$  is the expenditure of subsurface fluids along the boundary of negative structures (beginning of coordinates),  $q(x)$  is the same in every point  $x$  located at the flow line, and  $L$  is the integral flow line) should demonstrate all the regularities in changes of the subsurface fluid flow along bedding surfaces (Chapters 7–10). They may help, for example, in defining internal recharge areas (sources) and discharge areas of subsurface fluids as well as in understanding their role in the formation of the subsurface flow.

When internal recharge and discharge areas are missing, the curve should be smooth and remain in limits of Zone II along the coordinate axis. Otherwise,  $q(x)$ ,  $J(x)$ , and  $P(x)$  or  $H(x)$  should be characterized by extreme values, which can decrease up to zero (complete load) or exceed unity (additional recharge).

Extreme values are also observed under sharp changes in filtration properties of rocks, for example, under development of impermeable boundaries such as healed faults, pinching-out zones, and others. It is clear, however, that in this case extreme values of fluid flow parameters should not exceed unity.

Schematic maps illustrating lateral changes in unit expenditures of subsurface fluids are more informative as compared with potentiometric maps since they characterize, in sufficient detail, regional changes in expenditures of subsurface fluids, their gradients, migration velocities, and flow values. They allow comparison between hydrodynamic conditions in marginal zones of negative stratified structures. The information value of such schematic maps is higher in combination with plots that reflect regional changes in expenditures of subsurface fluids along flow lines in different geomorphological, geological–structural, and hydrogeological environments.

This method proposed for defining boundaries between hydrodynamic zones reveals principal changes in the subsurface flow along the flow line and general spatial (vertical and lateral) regularities of its formation in negative stratified structures.

The boundary between zones with the slow and very slow water exchange may be established proceeding from the following considerations. Inasmuch as filtration resistances (and their ratios) influence substantially the redistribution of the subsurface flow along beddings of aquifers, the decelerating lateral movement along beds is accompanied by the increasing *integral* discharge through the zone of the slow water exchange (Zone II, Fig. 3.2). In this connection, expenditures and migration velocities of subsurface fluids decrease with simultaneous flattening of their potentiometric surface in the horizontal plane toward subsiding areas of petroliferous complexes (aquifers). In a certain point of a bed (along the flow line), these expenditures and velocities may decrease to become comparable with rates of other processes, molecular diffusion included.

The Pecle criterion may be used for assessing the influence of mass transfer, convective, and diffusion components:

$$P_e = xv/d,$$

where  $x$  is a characteristic size of the filtration area (migration),  $v$  is the filtration velocity, and  $d$  is the coefficient of molecular diffusion. According to I.S. Pashkovskii, under  $P_e < 0.1$ , the convective component can be neglected. The mass transfer in such a situation occurs only due to molecular diffusion.

In other words, when the subsurface fluid flow velocity reaches certain values, migration of substances (water included) in the zone with very slow water exchange is determined by other processes. This boundary can be considered as representing the boundary between zones with low and very slow water exchange. Along the flow line, it is located in the area, where over 90% of infiltration recharge is discharged into overlying sediments.

N.A. Ogil'vi and A.N. Klyukvin (1978) noted that downward decrease in filtration velocities and growth of heat flow are accompanied by suppression of filtration processes at some depths and prevalence of substance migration under influence of thermal fields, i.e., migration of subsurface fluids under hydrostatic pressure from external (peripheral) areas of negative stratified structures is restricted at some distances and depths, where other processes (primarily, endogenic) play dominant role.

This criterion applied for defining boundaries between zones of slow and very slow water exchange is difficult for the practical use due to unavailability of required parameters: migration velocities of subsurface fluids, diffusion coefficients, and thermal conductivity.

For practical purposes, the traditional hydrodynamic method can be used. In line with this method, the boundary between zones of the slow and very slow water exchange separates areas with gradual changes in relative unit expenditures and velocities and those with their sharp changes in the zone with the very slow water exchange (Fig. 3.2).

When the zone with the very low water exchange is lacking anomalous areas (very rare situation), the boundary between these zones can probably be placed at the level with  $q(x)/q(0) < 0.1$  (<10%). In our opinion, such a threshold is determined

by the fact that results of hydrodynamic calculations of unit (per unit of the flow width) expenditures are beyond the accuracy of filtration parameters and reduced levels (pressures) and include unavoidable errors related to construction of the hydrodynamic grid for the subsurface fluid flow.

Thus, the 2D hydrodynamic zoning model of negative stratified structures can be represented by two zones with strongly deformed flows of subsurface fluids separated by a zone with gradual changes in expenditures, gradients, and velocities. Deformation of the subsurface fluid flow in the zone of intense water exchange is determined by influence of surface factors such as climate, relief, density and incision depths of the river network, and others, all other things being equal. In the zone with the very slow water exchange, it is determined by internal factors: tectonic fractures, quasi-periodical changes in the stress field, impacts related to recent geodynamic processes, and hydrothermal activity.

The principal model proposed for the formation of fluids in oil- and gas-bearing basins (similar model is applicable for inter- and intramontane basins), which is substantiated by models for natural conditions, displays very limited (or negligible) role of peripheral areas of basins usually represented by orogenic structures in hydrogeodynamics of subsurface fluids within deep petroliferous formations (aquifers) and lack of regional flows of subsurface fluids.

Consequently, classical ideas on the formation of the artesian flow based only on hydraulic principles are inconsistent with observations and should, therefore, be revised. While the situation with marginal zones of negative stratified structures (Fig. 3.2, Zones I and II) is clear, many aspects of hydrodynamics of deep formations remain ambiguous (Fig. 3.2). Regularities in the formation of subsurface fluids in this largest zone of petroliferous basins are considered below.

## References

1. Djunin V I (1981) Investigation methods and principles of deep formation hydrodynamics. VIEMS, Moscow
2. Djunin V I (1985) Investigation methods of the deep subsurface flow. Nedra, Moscow
3. Djunin V I (2000) Hydrodynamics of deep formations in petroliferous basins. Nauchnyi mir, Moscow
4. Vsevolozhskii V A (1991) Basics of hydrogeology. MGU, Moscow
5. Vsevolozhskii V A, Djunin V I (1996) Analysis of regularities in hydrodynamics of deep formation systems. Vestnik MGU. Ser Geol 3:61–72

## Chapter 4

# Elision Recharge and Paleomigration of Deep Fluids

The main task of this chapter is to assess the influence of elision recharge on the formation of formation pressures (heads) of subsurface fluids and vectors of their migration.

Compaction of sediments, clays included, is a real observable process. Numerous experimental works on the study of density and porosity of Cambrian clays sampled in different areas of northwestern European Russia demonstrated that they are compacted in line with the logarithmic law within the pressure range of 2–70 mPa despite diagenetic and catagenetic processes during >500 Ma, repeated stresses, and relaxations (for example, advance and retreat of glaciers). It should be noted that density and porosity of clays change downward precisely in line with this law.

By subsequent studies, this regularity was established also for Jurassic clay of the Moscow Basin, different-age clays of the West Siberian OGB, Fergana Depression, Ciscaucasia, and many other regions, where sedimentary sections include clayey members. Differences consist only in constant coefficients of the empirical curve:

$$\varepsilon = A + B \cdot \lg Z,$$

where  $\varepsilon$  is a porosity coefficient,  $Z$  is the depth, and  $A$  and  $B$  are empirical coefficients for each region.

It is established also that the geological time acts as a compacting agent, i.e., elastic and plastic deformations of clays become irreversible. *It should be emphasized that all geological processes are irreversible.*

The sampling depth ( $H$ ), density ( $\rho$ ), and porosity coefficient ( $\varepsilon$ ) are initial data for plotting curves of natural compaction. It should be remembered that the porosity coefficient reflects ratio between volumes of interstices and sediment.

The plots  $\varepsilon$ – $Z$  or  $\varepsilon$ – $p(z)$  reflect both stages in development of clays: sedimentation and denudations.

Development of basic principles for recent and paleohydrodynamic reconstructions of petroliferous basins (inter- and intramontane depressions) is of scientific and practical significance. Concepts of compression-induced migration of subsurface fluids at different stages of geological history are widely used for solving different problems: formation of subsurface fluid chemistry; migration and hydrocarbon

accumulation conditions and related peculiarities in the formation and destruction of oil and gas fields; prognostic assessment of the petroleum resource potential for separate areas of negative stratified structures. During recent years, these problems are considered in different details in many publications [4, 5, 9, and others].

The characteristic of peculiar features in paleomigration of subsurface fluids (position and role of their main recharge and discharge areas, vectors and velocities of migration, duration of water exchange) at different stages of geological development of structures, the recent one included, represents a main purpose in reconstructing paleohydrogeodynamics of negative stratified structures.

Reconstruction of fluid paleomigration at infiltration development stages of negative stratified structures with continental hiatuses is a very difficult task. For its solution, integral influence of different factors should be taken into consideration: climate, topography in combination with geological–structural conditions, and river network patterns. In addition, main regularities in regional hydrogeodynamics of deep fluids characteristic of infiltration stages in development of negative stratified structures that are relatively well studied for recent sedimentary basins with thick clayey sequences are of importance for this procedure.

Main regularities in migration of deep fluids at sedimentation stages in development of negative stratified structures (marine sedimentation periods) represent a substantially more difficult task for investigation. At the same time, it is thought precisely that these regularities may determine, to significant extent, hydrogeodynamic and hydrochemical zoning patterns in recent negative stratified structures.

In this connection, main approaches to the characteristic of fluid paleomigration concern largely reconstruction of sedimentation stages. Moreover, such reconstructions are based on concepts of relatively simple regularities in fluid paleomigration at these stages in development of negative stratified structures.

The recent concepts of subsurface fluid migration at the sedimentation stage are based on the elision type of water exchange [7, 8, and others]. As is believed, the elision movement of fluids is directed from areas with maximal subsidence, where reservoirs are overlain and underlain by sequences of fine-grained sediments. Due to compaction of clays, they release significant volumes of water, which moves toward areas with shallower subsidence of rocks (Fig. 1.1c). It is assumed that also separate elements of the section (reservoir) are characterized by the hydrodynamic uniformity through the entire distribution area.

Thus, direction of fluid migration in petroliferous formations and complexes (aquifers) is thought to be determined largely by the hypsometric position of their separate parts and thicknesses of underlying and overlying clayey sediments, which are considered as serving a main “supplier” of free water at elision stages in development of negative stratified structures. The maps of paleoisopiezes are compiled based on paleogeographic and paleogeological maps. Reservoir outcrops are usually interpreted as discharge areas for deep fluids, while most subsided zones of the basin are considered as their recharge areas.

The main shortcoming of such constructions consists in the fact that areas with the water exchange of the elision type are considered separately from areas of the same water-pressure system, which retains water exchange of the infiltration type

(eastern and western Ciscaucasia region, West Siberia, Timan-Pechora region, West Turkmen petroliferous basins, and others).

The main task of paleoreconstructions consists in assessing the role of sedimentation waters released from clayey sediments (water from the crystalline lattice of clay minerals included) in producing formation pressures (heads) and determining vectors of migration of deep fluids during the elision stage in development of stratified structures with account for areas of the bedded formation system, which retain conditions of the infiltration water exchange (infiltration recharge). The distribution of heads in the aquifer of the artesian basin during the elision stage may be described by the following equation:

$$\frac{\partial}{\partial x} \left[ T(x,t) \frac{\partial H}{\partial x} \right] + \frac{\partial}{\partial z} \left[ T(z,t) \frac{\partial H}{\partial z} \right] + Q[P(x,z),t] = a \frac{\partial H}{\partial t}, \quad (4.1)$$

where  $H$  is the head in the bed,  $T$  is the transmissibility depending on coordinates and time,  $Q[P(x,z),t]$  is the water volume entering reservoirs from compacting clayey rock under the geostatic load,  $a=m/\mu$  is the piezoconductivity,  $m$  is the reservoir thickness, and  $\mu$  is the water yield.

In order to understand the distribution of heads (pressures) of subsurface fluids and, consequently, assess vectors and velocities of their migration, we should solve equation (4.1) with assigned boundary and initial conditions. Thus, the task comes to correct substantiation of boundary conditions and search for trustworthy values of coefficients. Similar to solutions of other geological problems, the principle of actualism and geological investigation methods, modeling included, may be used.

When developing paleohydrodynamic reconstructions, we should keep in mind that one of the most important purposes consists in determining geometry of aquifers and position of main recharge and discharge areas of subsurface fluids using paleogeological maps, schemes, and sections. The geometry of petroliferous formations (aquifers) is determined using paleogeological maps, schemes, and sections. With account for available data on regional dynamics of deep fluids, outcrops of reservoirs can be considered as potential recharge areas.

Approximate quantitative estimates of potential fluid recharge may be derived from the distribution of subsurface flow values with account for general regularities in changes of permeability, sizes of formation outcrops, and paleoclimatic conditions. Specification of second-class boundary conditions is most correct. This excludes errors, which may appear if conditions of the first type are assigned since the hypsometric position of outcrop areas is subjected to permanent changes due to tectonic movements of different signs.

In all the situations, when the reservoir is overlain by low-permeability formation, hampered vertical filtrations (flow) of fluids serve as their main discharge type. At the same time, possible existence of areas with the intense local load related to erosional incisions, fracture zones, lithological windows, and other factors, which can be taken into account by assigning additional (internal) boundary conditions, cannot be ruled out.



In line with the accepted model, the second-class boundary condition (expenditure as a function of time, which is permanent in the particular case) should be assigned at the elision development stage of negative stratified structures. For the roof of the clayey sequence, second-class boundary conditions can be specified. The expenditure value at this boundary is determined by the volume of interstitial waters released from underlying clayey sediments during their compacting. For the roof of the overlying clayey bed, the boundary with the constant pressure (head) is imposed. If the level in the sedimentation basin is accepted to represent the comparison plane, the pressure (head) at the upper boundary should be equal to zero. At the infiltration development stage of negative stratified structures, boundary conditions remain the same, except for that at the upper boundary, which is uncertain and can be substantiated considering only the development history of the particular areas (Chapters 7 and 9).

The permeability of sedimentary rocks and regularities in its temporal and spatial changes are the most important parameters. Variations in reservoir transmissibility are determined by sedimentation conditions, weathering, leaching, sediment reworking, compacting, and many other processes (Chapter 6). Under the influence of all these processes, reservoir transmissibility decreases usually from the periphery of negative stratified structures (source areas of detrital material, karst development, and others) toward their central subsided parts [1–3, 11].

The growth of the geostatic pressure due to reservoir subsidence results in substantial decrease in its transmissibility with all other things being equal. Thus, reservoir transmissibility at the elision development stage of negative stratified structures represents a function of both time and coordinates, while at the infiltration stage, only that of coordinates. When reconstructing paleoconditions of the aquifer or petroliferous basin as a whole, we should introduce certain corrections for present-day transmissibility values, since the impact of the formation pressure, epigenetic, and other processes is able to change transmissibility by several orders of magnitude particularly in areas with maximal amplitudes of subsidence or uplifting.

The assessment of the influence of elision processes on the formation of heads (formation pressures) of deep fluids was aimed at the solution of the task with the factor-diapason estimate of different parameters that influence development of fields of deep fluid formation pressures.

Integration of equation (4.1) is a test task, which does not take into account members describing changes in the stress state of rocks, since their influence may be significant under very high sedimentation rates ( $>10^{-2}$  m/year) or under intense tectonic movements and earthquakes (Chapter 5). In addition, the main purpose of this chapter is to assess only influence of elision recharge on the formation of heads (formation pressures) of fluids and vectors of their migration.

The boundary conditions were substantiated proceeding from the following considerations. According to [5–8], most subsided parts of negative stratified structures (regions of recent sedimentation such as the Caspian, Kara, Black, and Pechora seas) represent recharge areas. From these areas, subsurface fluids move along bedding surfaces toward outcrops of reservoirs. Consequently, the central part of the

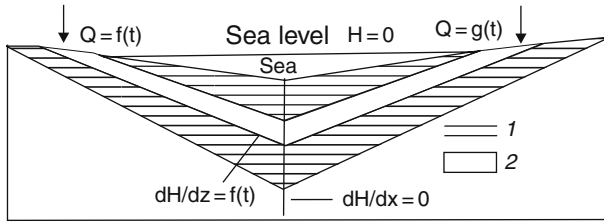


**Fig. 4.1** The principal model of boundary conditions. (1) Clayey sediments; (2) sandy sediments.

basin should host a certain “hydraulic watershed,” which can be considered as an impermeable boundary (Fig. 4.1).

For the area of outcropping sediments, the second-class boundary condition is assigned with the permanent expenditure that is formed on account of infiltration recharge. For the upper boundary of the basin, the imposed head was equal to zero (the sea level was taken for the comparison plane). The base of the reservoir was accepted to be impermeable. The expenditure of interstitial waters squeezed from underlying clays was set immediately into the reservoir.

Thus, half of the model is characterized by the following conditions (Fig. 4.1). The reservoir 1,000 km long resting upon clayey sediments subsides with a certain permanent velocity in every point. The maximal subsidence velocity (sedimentation rate) is characteristic of the point most remote from the infiltration recharge area and decreases up to zero in the area of reservoir outcropping.

With subsidence of the reservoir, the latter becomes overlain by sediments with the maximal thickness of 1,500 m in the most subsided point. The thickness of clays in the outcropping area is equal to zero. The change in the subsidence velocity and thickness of clayey sediments between these two points is governed by the linear law. The permeability of overlying sediments is accepted to be constant and equal to  $10^5-10^6$  m/day. The transmissibility of the reservoir is assigned as a variable, according to equation (4.2):

$$T(x) = T_0 e^{-0.14\beta^*z\alpha}, \tag{4.2}$$

where  $T(x)$  is the transmissibility in any point  $x$ ,  $T_0$  is the transmissibility in the reservoir outcropping area (accepted to be 3,000 m<sup>2</sup>/day),  $\beta^*$  is a coefficient of irreversible rock compacting (accepted to be  $30 \cdot 10^{-4}$  cm<sup>2</sup>/kg),  $z$  is the depth of reservoir subsidence, and  $\alpha$  is the parameter depending on the structure of the interstitial space of rocks.

The transmissibility of the reservoir in any section was accepted constant, although it depends usually on both coordinates.

The expenditure in the recharge area  $Q$  and integral recharge from underlying and overlying clayey sediments  $q$  regardless of the direction of interstitial fluid migration were assigned to the reservoir (which increases trustworthiness of results) and accepted to be voluntary under their different proportions. Moreover, inasmuch as

the subsidence depth of the reservoir changed with time in line with the linear law, additional recharge  $q$  changed, in line with the same law, from maximal values in the area with the deepest subsidence of a bed to zero in its outcropping area.

The solution of this task revealed a very important point: the distribution of heads and migration velocity of subsurface fluids in the system under consideration represents the *substantially stationary* process, where it is characterized at each moment by its own distribution of heads (pressures) of subsurface fluids.

For obtaining the solution close to the true one, it is necessary [10] that the ratio between temporal network resistances ranged from 6 to 10. In our situation,

$$R/R_z = T \cdot 365 \cdot \Delta t / \Delta x^2 \mu = 6 - 10, \quad (4.3)$$

Or

$$\Delta t / \Delta x \leq 10 / 365 \cdot 10^4 = 2.7 \cdot 10^{-6}$$

where  $\alpha = T/\mu$  is a coefficient of piezoconductivity, which is at least  $10^4$  m<sup>2</sup>/day,  $\Delta x$  is the width of a block, and  $\mu$  is the water yield.

Proceeding from this ratio and accepting the block being 10 or 100 km wide,  $\Delta t$  should be equal to 270 or 27,000 years. During such a short period, formation pressure cannot experience any significant increase and, consequently, water quantity released from clays should also be insignificant.

According to radiocarbon analysis of bottom sediments from different water basins, the average sedimentation rate of mud is 16 mm/kyr ( $1.6 \cdot 10^{-4}$  m/year) ranging from maximal 68 mm/kyr ( $6.8 \cdot 10^{-4}$  m/year) to minimal 1 mm/5,000 years ( $2 \cdot 10^{-8}$  m/year).

The maximal sedimentation rate in geosynclinal regions does not exceed usually  $10^{-4}$  m/year; in platform-type basins, it is substantially lower. With such a sedimentation rate and time being 270 and 27,000 years, the thickness of the sediment layer should be 0.027 and 2.7 m, which should result, under average density of 2,300 kg/m<sup>3</sup>, in the formation pressure increase by 0.006 or 0.06 mPa.

Under the assigned transmissibility and water yield coefficient of  $10^{-4}$ , the ratio is feasible under simultaneous increase in both time and block width. In this connection, it is necessary to take the period being comparable with duration of the basin development or even longer, *which leads to inference on stationarity of the process under consideration*.

For example, increase in time by an order of magnitude (with the sedimentation rate of  $10^{-4}$  m/year) results in the growth of the formation pressure by 0.6 mPa, which is evidently insufficient for any significant change in the water influx from clayey sediments. The tenfold growth of the block width results in the necessity to consider the whole layer as a single block (the task becomes senseless). It is easy to see that the ratio  $R_1/R_2$  for the overlying clayey sequence is unfeasible.

Figure 4.2 presents the results obtained by solving the task in question with different parameters (Table 4.1). It illustrates the distribution of fluid heads in the reservoir 1,000 km long with the transmissibility ( $T_0$ ) of 3,000 m<sup>2</sup>/day. The

**Fig. 4.2** The distribution of subsurface fluid heads along the flow from the periphery of the artesian structure toward its center (results of the test task solution)

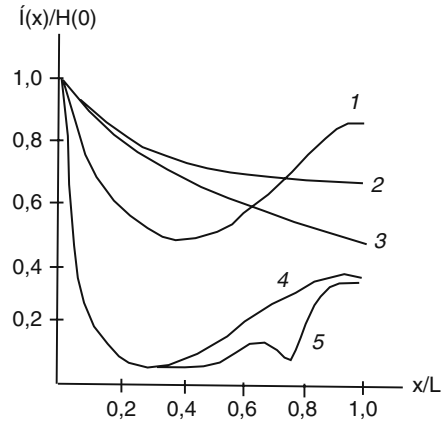


**Table 4.1** Parameters used in the assessment of elision recharge influence on the formation of deep fluid heads (1–5 are numbers of curves in Fig. 4.2.)

Parameters	1	2	3	4	5
Length of the basin (km)	1,000	500	500	1,000	1,000
Initial transmissibility	3,000	300	3,000	300	300
Permeability of clays (m/day)	$10^{-5}$	$10^{-6}$	$10^{-5}$	$10^{-5}$	$10^{-5}$
Integral recharge from clays for the entire section per 1 m of the width ( $m^3/year$ )	$3.2 \cdot 10^3$	$3.2 \cdot 10^3$	$3.2 \cdot 10^3$	$3.2 \cdot 10^3$	$3.2 \cdot 10^3$
Ratio between infiltration recharge value and additional recharge from clays	1.7	10	10	1.7	1.7
Growth rate of positive structures relative to the velocity of general basin bottom subsidence				0.5 at the point 0.45 L and 0.3 at the point 0.75 L	

transmissibility value varies in line with equation (4.2). The reservoir is successively subsided to depths of 300, 600, 1,200, and 1,500 m (maximal subsidence in the area most remote from its outcropping area  $x/L$ ;  $L$  is the length of the reservoir). The reservoir is overlain during its subsidence by substantially clayey sediments with the permeability of  $10^{-5}$  m/day. The expenditure per unit of the width in the point  $x/L = 0$  (area of infiltration recharge) was assigned to be  $15 m^3 \cdot 10^3/year$  ( $5.5 \cdot 10^3 m^3/year$ ).

The integral expenditure of additional recharge from clays with account for the entire length of the flow with the unit width was accepted to be  $3.2 \cdot 10^2 m^3/year$  (linearly changing expenditure from zero in the reservoir outcropping area to  $5.6 m^3/year$  per 1 m of the width at a distance of 1,000 km). These values of elision recharge exceed significantly real volumes (Chapters 7 and 9 and data in [8 and others]). Thus, the ratio between fluid expenditure at the external boundary (infiltration recharge area) and integral expenditure of elision recharge is  $Q/q = 1.7$ .

The modeling results in Fig. 4.2 (Curve 1) show that the area of the outcropping reservoir has nothing to do with the discharge area of elision waters released from clayey sequences. Infiltration waters discharge in form of diffused ascending filtration at a distance of 300–350 km away from the reservoir outcropping area. Released interstitial waters also discharge in form of diffused filtration in the central part of the petroliferous basin (right of the area with the minimal head). The formation of relatively low heads in the right part of the plot (model area with the maximal head value) is explained by the fact that the accepted  $Q/q$  ratio is two to three orders of magnitude lower as compared with real values. In this case, the discharge area of released interstitial waters does not reach reservoir outcrops.

The subsidence and growth of thicknesses of clayey sediments are accompanied by general increase in fluid heads and simultaneous decrease in head gradients so that the point with the minimal value of the relative head moves away from the infiltration recharge area, which results in the increased area of the diffused discharge of infiltration groundwater.

Of interest is the problem of reservoir permeability influence on the distribution of fluid heads under additional recharge from clays. The solution presented in Fig. 4.2 (Curve 1) is obtained under relatively high transmissibility ( $T_0 = 3,000 \text{ m}^2/\text{day}$ ); at deep levels of negative stratified structures, it is substantially lower. Figure 4.2 (Curve 4) demonstrates the distribution of heads under transmissibility  $T_0 = 300 \text{ m}^2/\text{day}$  (periphery of the negative structure) with all other factors being the same. In this situation, maximal head values at the point  $x/L$  decreased more than twice. In addition, the tenfold transmissibility decrease resulted in the shift of the point with the relative piezominimum to the left ( $>100 \text{ km}$  under the thickness of overlying clays of 1,500 m), which resulted in significant reduction of the discharge area of fluids that migrated from land.

The permeability of overlying clayey sediments is one of the main factors responsible for the formation and distribution of heads in the system under consideration. In previous variants, the permeability of clayey sediments was accepted to be  $10^{-5} \text{ m/day}$ . Figure 4.2 (Curve 2) demonstrates the distribution of heads in the reservoir with length  $L = 500 \text{ km}$  and maximal transmissibility value  $T_0 = 300 \text{ m}^2/\text{day}$  (solid lines). For comparison, the figure shows also changes of heads under permeability of clayey sediments of  $10^{-5} \text{ m/day}$  (Fig. 4.2, Curve 4). The ratio between expenditure at the boundary and integral expenditure of interstitial waters released from clayey sediments is  $Q/q = 9$ . This ratio is close to the real value, although it is still relatively low (Chapters 7 and 9). Regularities in transmissibility changes and the distribution of expenditures of waters from clays are similar to these parameters considered above.

The curves show that under the given ratio between expenditure and permeability of the upper clayey sequence of  $10^{-6} \text{ m/day}$ , no areas with elevated head values are formed in the central area of the depression (Fig. 4.2, Curves 2, 3). Interstitial waters released from compacting clayey sequences discharge in this part of the depression in form of hampered vertical filtration through overlying low-permeability sediments. The influx of released interstitial fluids shows no notable influence on the distribution of subsurface fluid heads. Under the permeability of the clayey

overlying sediments being  $10^{-5}$  m/day, the central part of the depression is marked by the limited ( $x/L = 0.7-1.0$ ) area with relatively elevated head values (relative increase in heads  $0.1 H(x)/H(0)$  and less).

In all the previous variants, we considered peculiarities in the distribution of heads in the system under regular subsidence of the reservoir with some constant velocity  $V$ . In real situations, separate parts of stratified systems in negative structures are sometimes characterized by movements with different signs and intensities. In this connection, negative and positive structures of the second and higher orders, position of which should influence the distribution of fluid heads (pressures), may be formed in internal areas of stratified systems.

The formation of the positive structure results in the relative (local relative to the entire system) reduction of reservoir subsidence velocity and depth. This leads, in turn, to a decrease in the thickness of overlying clayey sediments (decreased sedimentation rates or development of local erosion) and, consequently, to less intense growth of the geostatic load and local decrease in expenditures of released interstitial waters that enter the reservoir. In addition, cores of positive structures may be characterized by relatively elevated permeability of clayey sediments (local changes in sedimentation conditions or intense fissuring) and local zones of intense "open" discharge of subsurface fluids (erosion areas, zones of tectonic fractures).

For assessing the role of the tectonic factor, we have studied the distribution of heads in areas with different subsidence velocities (Fig. 4.2, Curve 5). The figures demonstrate the distribution of heads through the section under general regular subsidence (Curve 1) and in situation when positive structures are forming with velocities of  $0.5$  and  $0.3 V$  in respective points  $x/L = 0.45$  and  $0.75$  (Curve 5).

The results derived from modeling allow the following inferences.

When a single water-pressure system hosts two or several areas with different water exchange types, the distribution of heads (pressures) and vectors of subsurface fluid migration in the bed area located in the recent sedimentation domain is determined by interaction between the flow of infiltration waters and interstitial fluids released from clayey sequences during their catagenesis. Under conditions of the regular subsidence, the ratio between expenditures of infiltration and elision waters ( $Q/q$ ) and permeability of overlying sediments are main factors that determine head values and vectors of subsurface fluid migration.

The boundary between areas with different water exchange types is marked by the zone of dynamic equilibrium between the lateral influx (from the infiltration recharge area) and hampered vertical discharge of deep fluids. Inasmuch as in natural conditions, expenditures of lateral flows per time unit are incomparably higher as compared with expenditures of squeezed interstitial waters, the transitional zone extends from the boundary of the recharge area to the shelf area of the sedimentation basin; the transit flow of released interstitial solutions toward areas with outcropping reservoir cannot exist in such a situation.

The width of the transitional zone (in different variants under consideration) varies from 150–200 to 400 km and more being determined mainly by the ratios between expenditures ( $Q/q$ ), on the one hand, and horizontal and vertical filtration

resistances on the other (Chapter 3). Due to regular increase in expenditures of fluids entering through the lower boundary of the reservoir, the width of the transitional zone should become reduced from lower toward upper reservoirs.

The elision water exchange type properly designates the diffused ascending discharge of subsurface fluids (released interstitial solutions), which is observed in the deepest parts of stratified systems in negative structures beyond the transitional zone.

When recent sedimentation basins host areas and zones with different subsidence velocities, the general distribution of heads is complicated due to development of additional centers of the localized discharge. The influence of local areas with the “open” discharge areas related to zones of tectonic dislocations and deep faults influences the distribution of heads even more significantly.

It should be emphasized that the above-mentioned modeling data are based exclusively on classical elision concepts, which imply primarily hydrodynamic unity of separate portions of the section in stratified systems of negative structures. In reality, deep layers of stratified systems in negative structures represent a stratum-block system, as is shown below. Therefore, elision processes may play a certain role in the formation of formation pressures within separate blocks. This is possible, however, only in the situation, when boundaries of blocks were impermeable during the entire period of catagenesis of clayey rocks, i.e., during hundreds of millions of years, which is unlikely; it means that the role of water released from clayey rocks (and from other lithologies as well) in the formation of formation pressures should be quantitatively estimated for each particular region or its segment, when this is necessary for solution of practical tasks.

Thus, compression (elision) transformation of clayey rocks plays insignificant role in the formation of the regional field of formation pressures. Its any notable contribution into this process is possible only in ideal conditions of complete isolation.

The elision processes are substantially stationary in terms of the geological time.

## References

1. Djunin V I (1981) Investigation methods and principles of deep formation hydrodynamics. VIEMS, Moscow
2. Djunin V I (1985) Investigation methods of the deep subsurface flow. Nedra, Moscow
3. Djunin V I (2000) Hydrodynamics of deep formations in petroliferous basins. Nauchnyi mir, Moscow
4. Kartsev A A (1980) Hydrogeological prerequisites for manifestation of superhydrostatic pressures in petroliferous areas. *Geologiya nefti i gaza* 4:40–43
5. Kartsev A A (1992) Oil and gas hydrogeology. Nedra, Moscow
6. Kartsev A A, Vagin S B, Baskov E A (1969) Paleohydrogeology. Nedra, Moscow
7. Kartsev A A, Vagin S B, Serebryakova L K (1980) Paleohydrogeological reconstructions for revealing petroliferous zones (exemplified by western Ciscaucasia). *Byul. MOIP* 1:132–140
8. Kolodii V V (1966) Hydrodynamic and paleohydrodynamic conditions in Pliocene sediments of the West Turkmen Depression. *Sov Geol* 12:50–62

9. Lyubomirov B N (1963) Paleohydrogeological formation conditions of oil and gas accumulations in the Timan-Pechora region. *Sov Geol* 4:27–32
10. Pavlovskaya L N (1967) The study of accuracy in modeling unstable filtration at the grid of ohmic resistances (in line with the Libman's method). In: Proceedings of the coordinative meeting on hydraulic engineering. Energiya, Leningrad
11. Vsevolozhskii V A (1991) Basics of hydrogeology. MGU, Moscow



## Chapter 5

# Genesis of Abnormally High Formation Pressures

Development of abnormally high formation pressures (AHFP) at deep levels of stratified systems in negative structures is one of the remarkable features of their hydrodynamics. By their values, they are frequently comparable with the geostatic pressure or even exceed the latter. The abnormally high formation pressures are observable practically in all the stratified systems of negative structures regardless of their age and geological structure. Their discovery stimulated intense development of elision concepts of the hydrodynamics in negative stratified structures.

The desire to explain the nature of abnormally high formation pressures gave birth to many hypotheses. The origin of such pressures is frequently explained by mutually exclusive factors or some of them appear to be preferable.

This unique geological phenomenon that is characterized by the universal distribution is of both scientific and undoubted practical significance. Recovery of stratified system with abnormally high formation pressures results in substantial complications during drilling operations and corresponding rise in their cost.

Different researchers who study the origination problem of abnormally high formation pressures are anonymous in a single point: *their development and any prolonged existence require the isolated segment of the stratified system, i.e., impermeable or very poorly permeable boundaries of different geneses.*

Due to complexity of the problem, lack of an anonymous standpoint on genesis of abnormally high formation pressures, and its importance for understanding many aspects in the formation of deep fluids, it deserves special consideration.

The term “abnormally high formation pressures” is understood by different specialists in different ways. For example, oilmen consider it as a pressure that exceeds by 10–20% the conditional hydrostatic one, which is equal to the pressure of the column of liquid with density of  $1,000 \text{ kg/m}^3$  and height from the recovery point to the Earth’s surface. Anomalous pressures are thought to be also related to the hypsometric position of the wellhead relative to the bed outcropping area. Such a concept leads frequently to confusing inferences, according to which the normal pressure in the formation is interpreted as an anomalous one.

Figure 3.2 (Area III) demonstrates clearly that the pressure inconsistent in some areas with the regional (normal) distribution of formation fluid pressures (determined by the hypsometric position of regional recharge and discharge zones, structure of the aquifer, and its interaction with neighboring similar formations)

characterized by maximal or minimal values in a certain point of the flow line should be interpreted as the abnormally high formation pressure.

The extremum in the distribution of the formation pressure indicates additional recharge sources with different signs. The source sign determines maximum or minimum (plus corresponds to abnormally high and minus to abnormally low pressures). Intensity of the source determines the absolute extremum value, i.e., indicates how the abnormally high formation pressure differs from the normal one.

For example, low values of subsurface fluid pressures in limited areas beneath river valleys can be considered as anomalously low. In this situation, the discharge of head fluids results in negative anomalies, which are observable against the background of the regional distribution of formation pressures.

When studying causes responsible for the abnormally high formation pressure development, one should establish nature of the additional recharge source with the positive sign. Some researchers introduced the notion of the anomaly coefficient, which corresponds to the ratio between the measured formation pressure and the conditional hydrostatic one. When the anomaly coefficient value exceeds 1.1–1.2, the pressure is considered anomalous. Further, we share such an approach.

The development of abnormally high formation pressures should be considered in temporal dynamics comparing velocities of potentially responsible processes with velocities of their relaxation. These factors should be considered in terms of thermodynamics. According to the latter, in the closed system (necessary condition of the abnormally high formation pressure preservation), its internal energy is determined by three parameters: pressure, volume, and temperature. The change in one or two of these values results in the change of others.

The equation of the closed system state (the first law of thermodynamics) is the following (neglecting insignificant velocity of fluid movement):

$$\begin{aligned} dU &= \delta Q + \delta A \text{ or } dU = \delta Q + P_{ext}dV + \delta A^*, \\ \text{or } dU &= CdT + P_{ext}dV + \delta A^*, \end{aligned} \quad (5.1)$$

where  $dU$  is change in internal energy of the system,  $Q$  is quantity of heat received by the system,  $P_{ext}dV$  is work spent for overcoming the external pressure,  $\delta A^*$  is work spent for overcoming other external forces,  $C$  is thermal capacity, and  $T$  is absolute temperature.

Before going to the role of each of the summands in equation (5.1), it is necessary to find out one of the main points: isolation of some part of the bed. This is a main question because for changes in the internal energy of the system, for example, for any durable existence of the abnormally high formation pressure, the system should be closed. Otherwise, the pressure in the latter should not experience substantial changes under any high temperature or strong compression, since an additional volume of liquid should leave the system in response to such an impact. The answer to the question about the closure of the system (bed segment) and duration of abnormally high formation pressure existence will help in solving the problem of its origin.

By hydrodynamic isolation [1–3, 17, and others] we mean bordering of the reservoir segment by tectonic fractures in plane and clayey sediments and salts with low or zero permeability in the section is meant.

The clayey rocks are permeable to some extent (their permeability may be comparable with that of the reservoir). Moreover, recent studies show that during some periods of geological development of stratified system in negative structures even salts may be permeable (Chapter 6). Due to some permeability of rocks regardless of their lithology (with other factors being the same), abnormally high formation pressures should decrease after sometime up to normal hydrostatic levels. In this connection, the question arises as to how long the abnormally high formation pressure can exist in the relatively isolated segment of the stratified system.

## 5.1 The Relaxation Period of Abnormally High Formation Pressures

According to V.F. Linetskii (1959), the period during which the pressure decreases from its peak to normal hydrostatic values spans several million years. M.K. Kalinko believes that it is two orders of magnitude longer amounting to tens and hundreds of million years. Gurevich [11] argues that the Linetskii's assessment is overestimated approximately 20,000 times (being several hundred years long). In his opinion, Linetskii used for his calculations the formula suitable for formations with the free surface. V.V. Kolodii and Yu.V. Kalyuzhnyi estimate the relaxation period of anomalous pressures as ranging from 50 hundreds to tens of millions of years depending on the bed subsidence depth.

Gurevich [11] cites his calculated data on the abnormally high formation pressure existence period for the following conditions: a sandy lens 50 m thick with the filtration coefficient of 5 m/day is separated by two clayey members each 100 m thick from over- and underlying reservoirs. The formation pressure at the base of the upper reservoir is 10.2 mPa and at the roof of the lower one, 12.75 mPa. Formation pressures of fluids in under- and overlying reservoirs remain constant. The excess pressure in the sandy lens results from the instant pulse to reach 30.6 mPa.

The following assumptions were made: (1) linear filtration in clayey sediments is governed by Darcy's law; (2) clayey sediments are not elastic; (3) formation pressures at the roof and base of the upper and lower clayey members, respectively, remain constant. The last assumption is quite justifiable since the velocity of the redistribution of formation pressures in highly permeable rocks is several orders of magnitude higher as compared with that characteristic of clayey sediments.

Taking into consideration ambiguous estimates of the abnormally high formation pressure relaxation period (differences are four to five orders of magnitude), we integrated at the computer the known filtration equation for multilayer sequences for the same conditions as in [11] and with similar assumptions, but the second one was taken into account (the elasticity coefficient of clayey rocks was accepted to be  $2\text{--}10^{-4}$  mPa).

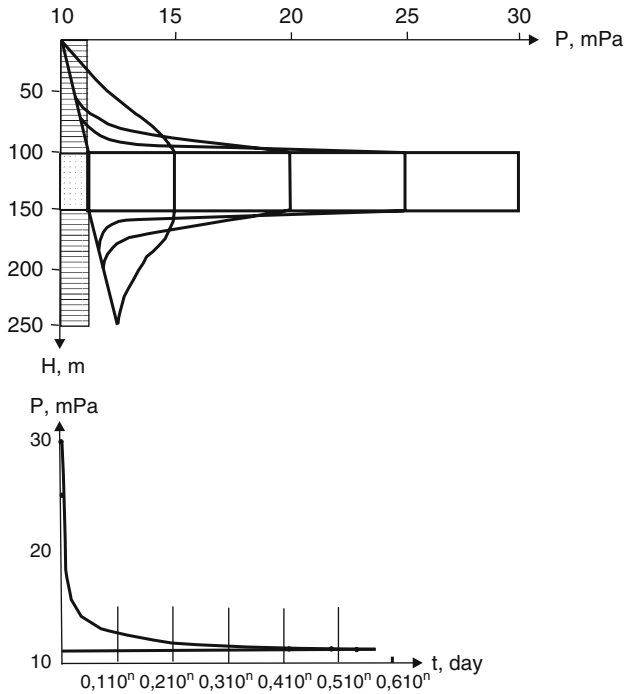


**Fig. 5.1** Relaxation of anomalous pressure in the sandy lens sandwiched between clayey sediments 100 m thick. The parameter  $n$  corresponds to the degree in the permeability coefficient

Figure 5.1, which presents the obtained results, demonstrates dynamics of reduction of the formation pressure in the sandy lens 50 m thick sandwiched between two clayey sequences each 100 m thick. In the figure,  $n$  is a parameter equal to permeability of clayey sediments. For example, with clay permeability of  $10^{-7}$  m/day, the period of complete relaxation of pressures should be  $0.4 \cdot 10^7$  years.

The formation pressure decreases most significantly during first days and years, when it differs notably from anomalous values. With the lowest clay permeability coefficient of  $10^{-9}$ , the formation pressure decreases up to the initial one during  $3.5 \cdot 10^9$  years (Fig. 5.1, Table 5.1).

Such permeability values for clays are obtained, however, only in experimental conditions for special samples, which exclude assessment of fissure permeability. In massive rocks, these values range from  $10^{-3}$  to  $10^{-6}$  m/day (Chapter 6). This means that the maximal period of abnormally high formation pressure existence (period of pressure reduction from maximal to the minimal one) should be  $1.4 (10-10^3)$  years in the absence of completely impermeable boundaries, i.e., period of its existence in geological terms is negligible.

I.G. Kissin received similar values. According to his calculations, the period of abnormally high formation pressure relaxation is 3,000 years [17].

**Table 5.1** Period of pressure reduction from the anomalous to normal values

Curves in	Period of pressure reduction, year			
Fig. 5.1	Permeability of clays, m/day			
	$10^{-2}$	$10^{-4}$	$10^{-6}$	$10^{-9}$
1	Initial distribution of pressures			
2	The same after instant pressure increase			
3	$1.43 \cdot 10^{-4}$	$1.43 \cdot 10^{-2}$	1.43	1,430
4	$6.8 \cdot 10^{-4}$	$6.8 \cdot 10^{-2}$	6.8	6,800
5	$6.1 \cdot 10^{-3}$	$6.1 \cdot 10^{-1}$	61	61,000

If the thickness of the clayey sequence in the model exceeds 100 m, the period of pressure reduction should increase proportionally to the thickness change, since the vertical filtration resistance for the unit area is determined by the ratio  $k_0/m_0$ . With the thickness of clayey sediments being 1,000 m, the relaxation period should increase an order of magnitude to amount to  $1.4 \cdot (10^2-10^4)$ , not  $1.4 \cdot (10-10^3)$ .

When estimating the role of catagenetic transformation of clayey rocks in development of formation pressures by modeling, I.K. Gavich demonstrated, using the Albian–Cenomanian aquifer of the South Mangyshlak basin as an example, that with the permeability and porosity coefficients ranging from  $10^3$  to  $10^{-7}$  m/day and from 1.0 to 0.5, respectively, the compacting and squeezing process takes 100 to  $10^4$  years in the case of clay thickness of 100 m and lower.

The aforesaid allows preliminary conclusion that the observable present-day abnormally high formation pressure formed 20 ka ago; in any event, their origination is limited by the Quaternary Period.

In addition, it is clear that under normal conditions clayey sediments can hardly be considered to represent reliable confining beds (caprocks). Any prolonged existence of anomalous pressures may be provided only by ideal isolating conditions. Possibilities for the formation of absolute confining beds are considered in Chapters 6 and 12. It should be emphasized that under *normal conditions* any hydrodynamic system is partly open and is able, therefore, to transfer pressures in all directions. The problem is only in the openness degree, i.e., what permeability is characteristic of the boundary layer (third-class boundary conditions). For example, according to modeling of the Kolva Megaswell (Pechora petroliferous basin), permeability of the boundary layer for abnormally high formation pressure preserving in the Inzyrei field should be  $10^{-(11-12)}$  m/day.

## 5.2 Possibilities for Development of Fluidodynamic Horizontal Boundaries in Clayey Sequences

It is thought that clayey sediments play an extremely significant role in the formation of deep fluids and abnormally high formation pressures. It is a priori agreed that velocity of the redistribution of formation (interstitial) pressures in clayey

sediments is substantially lower as compared with that characteristic of many geological processes, the confining pressure increment included. In the opinion of A.T. Durmish'yan (1977) and many other researchers, the latter assumption provides the formation of anomalously high interstitial pressures (special abbreviation AHIP was introduced) and hydrodynamic interface (hydraulic watershed that represents an impermeable boundary), from which interstitial waters in compacting sediments migrate toward their roof and base to enter reservoirs and form abnormally high formation pressure in them. In this situation, abnormally high formation pressure under clayey sediments and inside them is preserved until this watershed exists, and, consequently, the period of its relaxation may be substantially longer than it is indicated above.

In this connection, Mukhin [21] assumes that the clayey sequence should enclose a point where the interstitial pressure is higher than that at the roof and base of clayey sequences. The interstitial pressure in this point is accepted to be equal to the geostatic one while in neighboring reservoirs to normal hydrostatic. In such a situation, clays should enclose interfaces and two opposite flows of interstitial solutions and be characterized by lack of interaction between neighboring parts of the section via intervenient clayey sequences. The position of the interface between differently oriented flows of released interstitial waters is determined by this author as (equation is given without inference) follows:

$$h = m \frac{P_\rho - P_\gamma}{2P_\rho - (P_\gamma - P_n)},$$

where  $P_\rho$  is interstitial pressure inside the clayey sequence,  $P_\gamma$  is pressure at the roof of the clayey sequence, and  $P_n$  is pressure at the base of the clayey sequence.

The absurdity of this equation is evident from the following considerations. If pressures at the roof and base of the clayey sequence are equal, the equation should take the following form:

$$h = m/2(1 - P_v/P_\rho).$$

If the interstitial pressure is higher as compared with that at boundaries (in the situation under consideration, at the base of the clayey sequence), as the author affirms, the hydraulic interface falls into the negative area!

Under the correct statement of a question, the possibility of the existence of the interstitial pressure equal to the geostatic one should be proven or the distribution of interstitial pressures in the vertical section be obtained using the known physical and mathematical model with substantiated initial and boundary conditions and filtration parameters of clayey sediments.

Gurevich [11] formulated and solved this task more correctly, although he assigned equal boundary conditions for the roof and base of clayey sequence (equal values of formation pressures). Therefore, he received the expected and same result: existence of the interface and two vectors of fluid migration. The result is expected because no equal values of formation pressures at the roof and base of the clayey

sequence exist in natural conditions, particularly with its great thickness. Formation pressures increase usually downward.

Inasmuch as this problem is of importance, let us solve the task of the distribution of interstitial pressures inside the forming clayey sequence and its subsidence based on the equation of filtration consolidation (without creeping effect) of clayey rocks proposed in [10]

$$\frac{dP}{dt} = \frac{d\sigma^*(q)}{dt} + \frac{dP^0}{dt} + \alpha \frac{d}{dt} \left( k \frac{dP}{dz} \right), \quad (5.2)$$

where  $P$  is interstitial pressure inside the clayey sequence,  $\sigma^*(q)$  is the share of stresses in rock framework determined by the external load and own mass of the rock framework (geostatic pressure),  $P^0$  is the share of stresses of the rock framework determined by boundary values of heads,  $\alpha = (1 + \varepsilon_{av})/\rho a^*$ ,  $\varepsilon_{av}$  is the average value of the porosity coefficient,  $\rho$  is water density,  $a^*$  is the coefficient of rock compacting, and  $k$  is coefficient of permeability of clayey rocks depending in general on the coordinate  $z$  and time.

Values  $\sigma^*(q)$  and  $P^0$  determined from boundary conditions are elements of the equilibrium equation, which is used for deducing equation (5.2). The equilibrium equation is recorded in the following form:

$$\sigma^* + P = q + P^0 + \rho^*(m_0 - z), \quad (5.3)$$

where  $\sigma^*$  is stress of the rock framework at the point  $z$  (origin of coordinates at the clayey sequence base),  $P = P^0 + \rho^*(m_0 - z)$  is interstitial pressure at the same point,  $q$  is external load,  $P^0$  is part of the external load determined by the weight of liquid column,  $\rho^*$  is clay density, and  $m_0$  is the thickness of the clayey member.

Let us use equations (5.2) and (5.3) for solving the next test task proceeding from the fact that the horizontal component of filtration velocity is equal to zero, only vertical filtration exists, and water movement in clays is governed by Darcy's law.

Let us imagine a clayey element of the section and assume that its thickness in the sedimentation basin increases from zero to some value with the constant velocity  $v$ . With the thickness growth, this element of the clayey sequence subsides to the depth equal to the thickness increment. The depth of the sedimentation basin is accepted to be constant in time. The roof and base of the clayey sequence are permeable. The origin of coordinates is located at the base of the forming clayey sequence.

Let us assume also that under the regular subsidence of the element of the clayey sequence, the pressure at its base grows with the same velocity (the normal vertical distribution of the hydrostatic pressure) and is equal to zero at its roof (under permanent depth  $H$  of the sedimentation basin  $dH/dt = 0$ ). After reaching some thickness, clayey element of the section becomes overlain by sediments with different lithology and filtration properties characteristic of reservoirs. Under such a statement of a question, initial and boundary conditions should be recorded in the following form:

$$\begin{aligned}
 t = 0 \quad z = 0 \quad P = 0] \\
 t > 0 \quad z > 0 \quad P = vt\} \\
 t > 0 \quad z = vt \quad P = 0]
 \end{aligned}
 \tag{5.4}$$

Values of  $\sigma^*$  and  $P^0$  will be equal:

$$\sigma^*(q) = \rho[m(t) - z]; P_{z=0}^0 = P(t); P_{z=vt}^0 = \text{const.}, \tag{5.5}$$

With account for (5.5), equation (5.2) will take the following form:

$$dP/dt = (\rho^*/\rho + 1)v + \alpha d/dz(kdp/dz). \tag{5.6}$$

Thus, we are dealing with the usual Furies equation with the internal recharge source of permanent intensity (neglecting changes in rock density and interstitial solutions), regularly moving boundary, and boundary conditions described by (5.4).

Equation (5.6) demonstrates that appearance of function extremum inside the study area is theoretically possible, i.e., maximal value of the interstitial pressure relative to fluid pressure values at the interface between two opposite flows (upward and downward or, in other words, toward the roof and base of the clayey sequence).

The analysis of equation (5.6) shows also that the possibility for appearance of the function (pressure) extremum is determined only by two parameters with all other things being the same: sedimentation rates (velocity of the external load increment at any point) and permeability of the medium, which are highly variable, while porosity and compaction coefficients as well as density of interstitial waters experience insignificant changes.

The analytical solution of equation (5.6) with boundary conditions (5.4) and constant value of the medium permeability coefficient represents a system of the Volterra-type integral equations with the upper limit, which is relatively difficult to be solved.

Therefore, equation (5.6) with boundary conditions (5.4) was integrated at the computer, which made it possible to solve several test tasks with different parameters and account for their spatial and temporal changes. For simplification, a new function was introduced:

$$P = (\rho^*/\rho + 1)v + U$$

After this, equation (5.6) comes to the usual equation of thermoconductivity without external sources, although with time-variable boundary conditions:

$$\begin{aligned}
 z = 0 \quad t > 0 \quad U = vt(\rho^*/\rho - 1) \\
 z = vt \quad t > 0 \quad U = -\rho^*/\rho vt.
 \end{aligned}$$

Initial conditions remain former:  $t = z = 0, U = 0$ .



Values of porosity and compaction coefficients were deleted from the plot (Chapter 6). Initial values of the permeability coefficient were derived from the same plot. Water and clay densities were accepted to be 1,000 and 2,300 kg/m<sup>3</sup>, respectively. The sedimentation rate (increment of the external load) was taken proceeding from the possibility to obtain the extremum of the interstitial pressure under real values of other parameters, i.e., to estimate what extreme conditions are required for the appearance of the interface between opposite (upward–downward) flows of released interstitial solutions.

Integration was performed with different values of indicated parameters (Fig. 5.2). For convenient analysis of different variants, plots were compiled in relative coordinates: value of the interstitial pressure at any point  $P(z)$  of the clayey sequence element is related to the value of the interstitial pressure at its base  $P(0)$  and any point  $z$  is related to the integral thickness of the clayey sequence element that formed by the moment  $t$ .

### 5.2.1 Variant 1

The task is solved under  $K = 10^{-8}$  m/day,  $V = 10^{-3}$  m/year, and  $a^* = 10^{-3}$  cm<sup>2</sup>/kg. Figure 5.2a demonstrates the solution results.

All the parameters were accepted constant prior to subsidence of the base of the clayey sequence element to a depth of 500 m and its thickness of 500 m.

Under the clayey member thickness of 80 m, the interface appears between two flows of released interstitial solutions: upward and downward (area  $P(z)/P(0) > 1$ ). With the thickness growth, the interface moves upward. Extremum values of the interstitial pressure grow continuously relative to the maximal pressure at the member base to reach 1.75 under the thickness of 500 m, i.e., anomalously high interstitial pressures with the anomaly coefficient 1.75 are forming inside the clayey sequence.

### 5.2.2 Variant 2

Conditions are the same with account for changes in the coefficient of permeability. The latter was assigned in line with Curve 1 (Chapter 6) with its initial value  $10^{-8}$  m/day. In addition, when the thickness of the clayey member is 500 m, it is subsided up to depth corresponding to that of the base at 2,500 m. It is assumed that the clayey member 500 m thick becomes overlain by high-permeability sediments with the constant bulk density of 2,300 kg/m<sup>3</sup>. Since the moment when the thickness of the layer reached 500 m, changes were introduced into equilibrium equation (5.3) and boundary conditions (5.4).

The change in the vertical permeability coefficient results in the increase in maximal values of the interstitial pressure with all other factors being the same (thickness of 500 m) from 1.75 to 1.8 (Fig. 5.2b). Under subsequent subsidence (>500 m), the hydrodynamic interface approaches the middle of the clayey

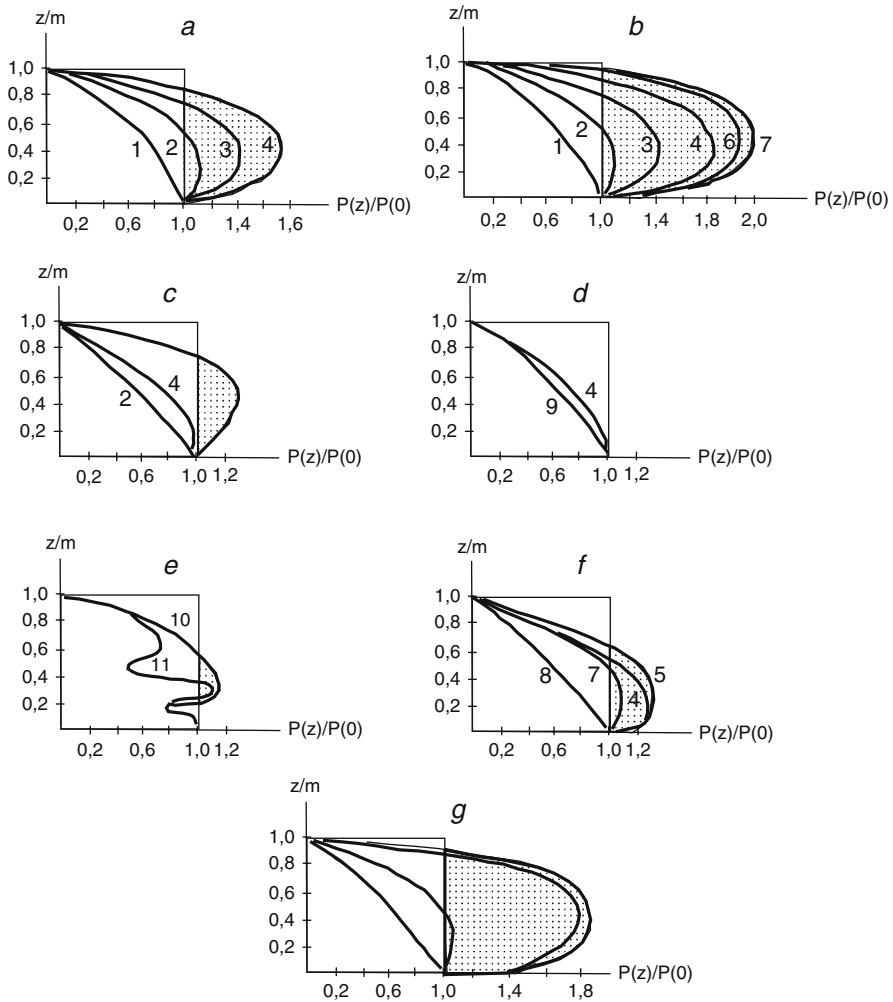


**Fig. 5.2** The distribution of the interstitial pressure in compacting clays. Variants (a–g) with different parameters: (1–4) with clay thickness, m: (1) 30, (2) 100, (3) 250, (4) 500; (5–8) with occurrence depths of the clayey sequence base, m: (5) 1,500, (6) 2,000, (7) 2,500 and sedimentation rates of  $10^{-4}$  m/year or permeability coefficient of  $10^{-4}$  m/day, (8) 2,500; (9–11) with the clay thickness of 130 m: sedimentation rates of  $10^{-5}$  m/year with one (10) or two (11) sandy members; (12) with account for changes of the compacting coefficient; (13) without account for the compacting coefficient; (14) with account for changes in coefficients of porosity, compacting, and filtration; (15) the same with the sedimentation rates of  $10^{-4}$  m/year. The shaded area corresponds to the zone with abnormally high formation pressures

member. The extremum of the interstitial pressure increases to reach the maximal value at depth of 2,500 m, where the anomaly coefficient is 2.1, which is very close to the geostatic pressure. It is conceivable that in the extreme case the anomaly coefficient may reach the value of 2.3 (i.e., average rock density).

### 5.2.3 Variant 3

Conditions are the same, except for the initial value of the coefficient of permeability, which is accepted to be  $10^{-7}$  m/day (Fig. 5.2c). It should be emphasized that while the permeability coefficient value in the layer adjacent to the roof (thickness 25–125 m) is  $10^{-7}$  m/day, in the layer of the same thickness, but adjacent to its base, it is  $10^{-8}$  m/day. The figure shows the substantial influence of the permeability coefficient in the vertical section: the anomaly coefficient decreases from 1.83 to 1.08 (1.7 times) under the thickness of the clayey member of 500 m and from 2.1 to 1.4 (1.5 times) under the subsidence of the clayey member base to a depth of 2,500 m.

### 5.2.4 Variant 4

As compared with Variant 1, the permeability coefficient value is  $10^{-7}$  and sedimentation rate values are reduced to  $10^{-4}$  m/year. With these values accepted for parameters, no maximum of the interstitial pressure appears inside the clayey member (Fig. 5.2d). The distribution of the interstitial pressure is largely determined by head values at boundaries of the clayey sequence.

### 5.2.5 Variant 5

When the thickness of the clayey member reached 130 m, conditions imitating occurrence of one and two sandy interbeds, which could serve as migration paths for released interstitial waters from the study element of the clayey member, were assigned at 22 and 67 m from its base (Fig. 5.2e). The figure demonstrates that normal interstitial pressures are forming in sandy interbeds and adjacent clayey sediments. Inasmuch as no pure clayey sediments exist in natural conditions and they may be dominant in the section composed of alternating clayey and sandy rocks, the possibility for the formation of abnormally high interstitial pressures is excluded. Similar conditions should be characteristic also of areas with tectonic jointing that forms near-vertical weakened zones, via which relaxation of excess interstitial pressures is possible.

### 5.2.6 Variant 6

Dissimilar to Variant 2, it takes into account changes in the permeability coefficient related to both sediment compacting and temperature. In this situation, the change of the permeability coefficient was specified in line with Curve 2 (Chapter 6).

Under subsidence to depth 100 m, the interstitial pressure inside the clayey sequence first grows regularly to reach the maximal value  $P(z)/P(0) = 1.3$  at 75 m

above the base of the clayey member (Fig. 5.2f). Under further subsidence, the temperature growth reduces the interstitial pressure, which amounts only to 1.1 at a depth of 2,500 m (at the member base it is 1.0). It means that the interstitial pressure is substantially lower (1.9 times) as compared with its value in Variant 2 (2.2).

Curve 9 was obtained with the sedimentation rate reduced an order of magnitude (from  $10^{-3}$  to  $10^{-4}$  m/year). The decrease in the increment rate of the geostatic pressure shows unambiguously that the distribution of interstitial pressures inside the clayey member is described in this case practically by the straight line and their values are determined only by hydrostatic pressure values at the roof and base of the clayey member, i.e., velocities of the interstitial pressure redistribution under the permeability coefficient value of  $10^{-7}$  m/day exceed substantially the sedimentation rate.

### 5.2.7 Variant 7

The compaction of clayey sediments is accompanied by changes in their porosity and, correspondingly, porosity and compaction coefficients (Fig. 5.2 g). The last two parameters are elements of the consolidation equation as constant values. It is assumed that their change may be neglected when studying compaction of clayey sediments and migration of interstitial solutions. At the same time, no quantitative estimates are available at present.

Variant 7 takes into account temporal changes of these parameters (under the assigned sedimentation rate). The parameters were considered constant only within limits of each time interval under consideration and changes were taken into account only along the coordinate; corresponding corrections were introduced for subsequent time interval in every block.

Curve 12 (Fig. 5.2 g) illustrates the assessment results for the subsidence depth of 2,500 m: no substantial changes are observed in comparison with Curve 13, which takes into account changes in the permeability coefficient only under compaction. The anomaly coefficient increases from 2.1 (Curve 13) to 2.14 (Curve 12), i.e., only by 0.04. Consequently, changes in coefficients of the permeability and compaction of clayey sediments influence insignificantly the formation of the interstitial pressure in compacted sediments.

For illustrating the role of different factors, the last figure presents also curves that describe the distribution of interstitial pressures with account for all the above-mentioned variants (with the subsidence depth of 2,500 m in all of them). Curve 14 takes into consideration changes in the porosity, compaction, and permeability coefficients with account for compaction and temperature. Curve 15 reflects the same parameters and their changes, but with sedimentation rate of  $10^{-4}$  m/year.

Thus, the analysis of all the results reveals that the hydraulic watershed (impermeable boundary between opposite flows of interstitial solutions) appears only

under values of parameters that differ substantially from their counterparts observed in natural conditions: coefficient of permeability of clayey rocks  $<10^{-7}$  m/day and sedimentation rates  $>10^{-3}$  m/year. Such high sedimentation rates are untypical of both platform and geosynclinal domains. They should be considered as anomalous. All the remaining situations are characterized by the normal distribution of interstitial pressures that depend only on values of the hydrostatic pressure at boundaries of the clayey sequence. In addition, the results indicate the substantially stationary filtration regime, when velocity of the redistribution of interstitial pressures (velocity of outflow) is significantly higher as compared with that characteristic of the formation pressure increment.

In order to solve correctly the differential thermoconductivity equation by the finite-difference method, temporal and network resistances should be of the same order differing from each other only 6–10 times, no more [22].

With regard to the above-mentioned task, the ratio between these resistances may be recorded as

$$R_1/R_z = k \cdot 365 / (v \cdot \mu \cdot \Delta t) = 6 - 10,$$

where  $\mu = (\rho a \cdot m) / (1 + E_{av})$ .

Under  $v = 10^{-5}$  m/year (most characteristic of platform domains), thickness of the clayey member of 100 m, permeability coefficient of  $10^{-7}$  m/day, compaction coefficient of  $10^{-4}$  cm<sup>2</sup>/kg, and porosity coefficient of 0.5,  $\Delta t$  should exceed  $10^7$  years.

This value exceeds more than five times the period required for accumulation of the clayey sequence 100 m thick. This indicates, in turn, that under real natural parameters (the value of the permeability coefficient for clayey sediments is underestimated as compared with observable natural values), the distribution of interstitial pressures at any moment should be determined only by values of the hydrostatic pressure at boundaries of the clayey sequence.

It means that migration of released interstitial solutions is characterized by the substantially stationary filtration regime. Thus, the interface between two opposite fluid flows cannot appear in compacting clayey sediments, particularly taking into consideration that compaction and mineral transformation of clayey sediments occur mostly up to the depths of 1,800–2,500 m (Chapter 6); abnormally high formation pressures develop largely below these depths.

It should be emphasized that (1) all the factors responsible for development of abnormally high formation pressures should be considered only with account for velocities of the redistribution of pressures, i.e., it is necessary to compare velocities of processes that form the abnormally high formation pressure zones with velocities of processes that destroy them; (2) processes resulting in the formation of anomalous pressures should be either constant or intermittent (recurrent), which yields conditions favorable for preservation of anomalous pressures in relatively closed systems during long periods.

### 5.3 Main Factors and Processes Responsible for Development of Abnormally High Formation Pressures

The processes resulting in abnormally high formation pressures are subdivided into two groups: external and internal. In addition, permanent (characterized usually by slow velocities) and one-time (recurrent intense and, frequently, high-velocity) processes are definable.

#### 5.3.1 *Elision Processes*

Most of the researchers share the standpoint on influence of elision process on development of abnormally high formation pressures. According to the latter, the increasing geostatic load results in compaction of rocks, which is evident from their downward reducing porosity [6, 12–16]. Clayey sediments experience the strongest compaction. Their compaction and catagenetic transformation are accompanied by the release of large volumes of water, some of which penetrates into relatively isolated segments of aquifers.

The growth of the geostatic load takes part in the formation of abnormally high pressures in a dual manner: decreasing the volume of the system (when outflow is missing) and by the influx of additional feeding from compacted clays. The additional recharge may also be yielded by dehydration of clay minerals and their secondary crystallization at the catagenetic stage.

These processes exist undoubtedly in natural conditions, which is confirmed by factual data. When estimating their role in the formation of pressures, abnormally high included, the researcher should take into consideration their scale and assess them based on reliable physical and mathematical methods and with account for their evolution.

The adherents of the significant role of elision processes in the formation of pressures in deeper parts of the section of stratified negative structures admit a priori that abnormally high formation pressures appear due to differences in velocities of the geostatic load increment and redistribution of interstitial pressures in clayey sequences. The geostatic load grows faster as compared with its redistribution. As is shown above, this is far from reality.

For approving significant role of elision processes, they use frequently insufficiently substantiated mathematical models or incorrect calculation parameters.

For example, V.V. Kolodii and Yu.V. Kalyuzhnyi introduce the so-called coefficient of outflow difficulty, which is, in their opinion, an inverse value of the infiltration velocity multiplied by the ratio between maximal and factual areas of the “transverse outflow channel.” Using this coefficient, the authors arrive at the conclusion that abnormally high formation pressures may appear and exist during tens of millions of years at a depth of 15 km. Leaving aside the proposed model, we should only note that the authors use in their calculations parameters of maximal and factual areas of transverse outflow channels, while for gradients they accept

values characteristic of the horizontal component of the filtration velocity. If most characteristic  $k_0/m_0$  values are used, the abnormally high formation pressure relaxation period at a depth of 15 km is higher only an order of magnitude as compared with that at a depth of 1.5 km, i.e., it is a few tens of thousands of years.

Anikeev [2] adduced most weighty objections against participation of the geostatic pressure in the abnormally high formation pressure development. Some of them deserve citing: (1) in similarly isolated conditions, abnormally high formation pressures should change gradually, not in the jump manner as it is; (2) the abnormally high formation pressure gradient increase is inconsistent with the growth of the geostatic pressure; (3) the abnormally high formation pressure distribution is discrete in contrast to universal compaction of clayey rocks; (4) the sedimentation process was replaced long ago by denudation, which destroys abnormally high formation pressures.

These objections can hardly be refuted. Unfortunately, they are ignored so far. The objections may be added by inferences that were derived from modeling the equation of filtration consolidation with different parameter values. This is primarily the inference on *stationarity of compaction processes*.

The adherents of the geostatic pressure influence on abnormally high formation pressure development cite very impressive estimates of released interstitial waters (hundreds of cubic kilometers). At the same time, if we recalculate these values for the unit of area and time, we obtain insignificant values. For example, only 330  $\text{m}^3/\text{m}^2$  of interstitial waters was released from the Upper Jurassic–Lower Cretaceous aquifer of West Siberia (Chapter 7) or approximately  $6 \cdot 10^{-9} \text{ m}^3/\text{m}^2/\text{day}$ .

All the aforesaid indicates that elision processes cannot result in development of abnormally high formation pressures.

### 5.3.2 Dehydration of Clay Minerals

Dehydration of clay minerals and release of crystallization water due to epigenetic processes (diagenesis and catagenesis) are discussed in Chapters 6 and 13. Crystallization water is mostly released in the depth interval of 1,800–2,500 m at temperatures of 70–90°C, i.e., at relatively shallow depths.

In addition, epi- and catagenetic transformations of clayey rocks are characterized by the montmorillonite→chlorite→hydromicas trend. The study of clayey rocks [11] indicates that the permeability of hydromica clays is two to three orders of magnitude higher as compared with the montmorillonite phase (Chapter 6). Consequently, catagenetic transformations of clay minerals should be accompanied by increase in their filtration properties and outflow of released crystallization water.

This should be stimulated by the formation of rigid structural-crystalline bonds in the plastic clay–argillite–shale succession, which results in its reduced plasticity, increased tendency for fissuring, and eventual replacement of the interstitial permeability by the fissure-related one. This is confirmed by the discovery of several commercial oil accumulations in argillites (for example, in the Bazhenovka Formation of the Salym field in West Siberia and others).

Thus, the significant role of dehydration of clay minerals in development of abnormally high formation pressures seems unlikely.

### ***5.3.3 Tectonic Forces (External Factor)***

Tectonic forces are another factor, which is able to change the volume of a relatively isolated system and, thus, result in development of abnormally high formation pressures. We exclude from consideration tectonic movements of epeirogenic character since their velocities are substantially lower as compared with rates of the formation pressure redistribution. They are comparable with sedimentation rates and cannot be responsible for the formation of anomalous pressures.

The relation between abnormally high formation pressures and tectonics (or more exactly geodynamics) is evident from the fact that this phenomenon is most frequently observed in areas adjacent to the Alpine fold belt (Caucasus, Central Asia, Carpathians, and others) and in tectonically active regions (Chapters 8 and 10). Zones of tectonic stresses exist also in older stratified negative structures (Kolva Megaswell in the Pechora petroliferous and others) and aulacogens in ancient platforms (Pripyat and Dnieper-Donets depressions).

Similar to geostatic compression, tectonic forces result in reducing the system volume. In addition, these forces stimulate development of fractures, which can serve as conduits for ascending thermal (or cold) solutions from deep formations and their migration into relatively isolated beds. At the same time, dissimilar to geostatic forces, they are, first, differently oriented being able to provide uniform compression and, second, characterized by high velocities (earthquakes, volcano eruptions, and others) to be sometimes instantaneous (seismic waves).

When they increase gradually, their velocities exceed rates of geostatic compacting significantly. For example, "slow" movements are characterized by the following values. The Caucasus experiences differentiated vertical different-sign movements with the velocity of a few to 20 mm/year and higher. In Armenia and the South Urals, the maximal velocity of the horizontal displacement of some blocks is 5.6 cm/year and up to 7 mm/year, respectively. In the Californian coast of the United States, recent movements along the San Andreas Fault are as rapid as 30 mm/year. Respective vertical displacements in Central Kyzylkums and Kamchatka in the Avachinskii Volcano area reach 10 and up to 50 mm/year. The Apsheron Peninsula experiences differently oriented vertical movements: maximal velocity of uplifting is 12 mm/year and subsidence up to 50 mm/year in some blocks. Moreover, velocities increased twice during the last 50 years [7–9, 18].

Comparison between secular movements (sedimentation rates in geosynclinal areas are  $10^{-(1-2)}$  mm/year) and velocities of recent vertical movements shows that the latter are higher at least two to three orders of magnitude.

Accumulating gradually stress in the fluid-rock system, seismic processes are manifested almost instantaneously, i.e., their velocity significantly exceeds that of redistribution of pressures in stratified systems. Of great significance are both the scale of neotectonic processes and their recurrent patterns. Seismically active



areas experience many shocks, which is important for retaining abnormally high formation pressures. For example, the Mongol–Baikal seismic zone experiences up to 1,000 shocks during a year (two to three per day). Up to 1,000–1,500 different-magnitude earthquakes are registered during a year in the eastern Ciscaucasia region (two to three events per day on the average).

Changes in the formation pressure in response to intense tectonic processes are sometimes observable immediately [2, 18]. During the pass of seismic waves through fluid-saturated rocks, formation pressures either increase or decrease simultaneously in all the layers. This results in either well flowing or fall of the water level in all the wells below the initial one. Some springs stop flowing; others start working, while a third increase their yield, which is retained for a long time (weeks, months). For example, after the earthquake in Arvia Tekhachani (United States), the yield of one of the springs increased more than four times. This was followed by the gradual decrease to reach a year later the level exceeding its initial yield three times.

After the Tashkent earthquake (1966), the lowered level in exploitation wells was first compensated and 5 months later, it was 3 m higher as compared with its initial level. After the strong shock, the pressure in one of the wells increased by 0.2 mPa, while in the other well hydrohypes formed a dome, which is possible only under additional recharge, as is justly stated in [18]. The earthquake in Dagestan (1970) was followed by changes in the yield of exploitation wells at a distance of 100–250 km. In one of the wells, oil yield increased by an order of magnitude, water yield increased three times, and one of the dry wells reactivated.

According to regime observations (over 100 observation wells, observation periods exceeding 1 year), earthquakes in Sakhalin were accompanied by changes in the composition and yield of hydrocarbons with time above the Mukhta field and in near-surface sediments. The observation period was marked by 12 shocks with magnitude of 1 and one earthquake with magnitude of 9.5. It is established that weak earthquakes result in notable increase in vertical fluid migration to near-surface sediments.

Sh.Kh. Amirkhanov established similar facts based on the study of the gas composition in near-surface sediments prior to and after the Tashkent earthquake. This area was characterized by intense migration of hydrocarbons from a depth of approximately 800 m up to the surface. The number of points with high hydrocarbon contents increased gradually, which was justly interpreted as indicating distortion of rock continuity due to the earthquake. The abnormally high formation pressure values close to the geostatic pressure or sometimes exceeding the latter may also be explained by influence of tectonic processes.

Most of the researchers share the opinion that tectonic forces are one of the main causes responsible for development of abnormally high formation pressures. At the same time, the influence of seismic activity on the field of formation pressures is a short process. After sometime, pressures are restored. In addition, their notable influence on the field of formation pressures is possible only for the systems adjacent to seismically active regions (Ciscaucasia, Central Asia, and others), while abnormally high formation pressures are observable in areas located far from them (West Iberia, Timan-Pechora petroliferous province, and others).

During the last 20–25 years, stationary geophysical test areas were arranged in several areas of Russia. Among others, for example, high-accuracy repeated alignment, long-term high-accuracy gravimetric observations were carried out. These observations revealed changes in the gravity field two to three orders of magnitude higher than limiting accuracy of observations. Anomalous changes in the gravity field amount to 250–300 mGal. They defined also instability of these changes of the quasi-periodical character. The observations with periodicity of 2 months revealed short-period variations in the gravity field [25, 26].

V.A. Sidorov established quasi-periodical patterns of anomalous vertical displacements with the amplitude of 30–40 mm/year (locally up to 50 mm/year), which occur in very narrow extended zones (1–3 km, 5–10 km long). Anomalies appear in the same areas above fault zones with the period of 2–4 years. Duration of the fault activation period (“life period” of anomalies) ranges from several months to years. Anomalies in the gravity field with the amplitude up to  $(1-2) \cdot 10^{-6} \text{ m/s}^2/\text{year}$  are also observable above faults being also quasi-periodical with shorter period as compared with that characteristic of recent vertical movement [4]. The model of parametric deformations of the geophysical medium, proposed by the last author, was used for predicting zones with elevated fissuring.

Figure 5.3 illustrates variations in the gravity field in the zone of the Rechinskii Fault (Dnieper-Donets Depression) with quasi-periodical patterns. Non-tidal changes in the gravity and other fields are established in the northern Caucasus, Pripyat Depression, and other areas.

The long-term studies of earthquakes revealed “sinusoid” patterns of these changes, which “characterize the pulsating seismic regime of the Earth...The pulsating regime determines trend and periodicity in activation of geodynamic processes...which influence, in turn, intensity of tectonic movements, seismicity, and fluidodynamic” (N.A. Kas’yanova). The maximal oil yield is determined by the seismic regime.

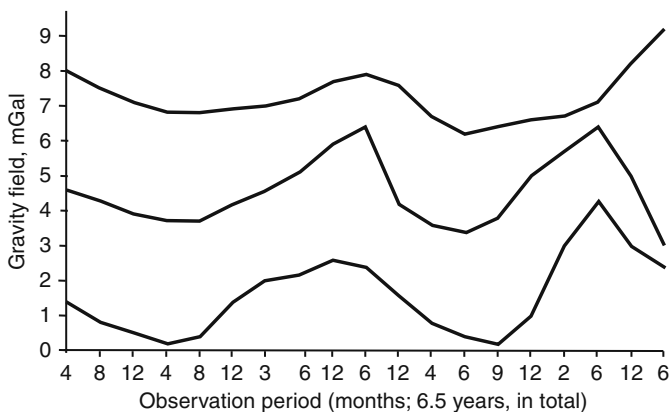


**Fig. 5.3** Variations in the gravity field in the Rechinskii Fault zone (Dnieper-Donets Depression)

Changes in the gravity field indicate density variations in the water-rock system in response to stress transformations under influence of external forces. Let us estimate this process quantitatively.

The equation of liquid movement with account for the influence of external forces is recorded as

$$a\nabla^2 P + \alpha \partial P_0 / \partial t = \partial P / \partial t, \quad (5.7)$$

where  $P$  is fluid pressure,  $P_0$  is external pressure,  $a$  is piezoconductivity,  $t$  is time, and  $\alpha$  is a coefficient depending on water compressibility, framework of the rock and its porosity, and water density.

It should be emphasized that the second member in the left part of equation (5.7) imitates development of internal recharge sources. Its sign determines the growth of pressures in the point influenced by the external pressure (compression results in the growth of system density and gravity field) or reduction (extension leads to lower system density and gravity field).

Let us estimate influence of tectonic stresses on changes in formation pressures with account for elastostrained properties of rocks. Let us imagine a geological body in the form of a sphere. Equation (5.7) in radial coordinates is recorded as

$$a \frac{d^2(r,P)}{dr^2} + \alpha \frac{dP_0}{dt} = \frac{d(r,P)}{dt}; \quad 0 \leq r \leq R. \quad (5.8)$$

Let us assume that the sphere experiences uniform pressure with the constant velocity, i.e.,  $P_0 = \beta t$ , and is completely isolated from surrounding rocks. In this case, the second member in the left part of the equation will be  $\alpha\beta$ . The task is solved in pressure increments ( $P(r,0) = P(r,t) = \Delta P$ ). Consider that  $P(r,0) = 0$  and receive  $P(r,t) = \Delta P$ . In this case, initial and boundary conditions are recorded as

$$P(r,0) = 0; \quad \frac{dP(0,t)}{dt} = 0; \quad \frac{dP(R,t)}{dt} = 0 \quad (5.9)$$

Solution of equation (5.8) with boundary conditions (5.9) acquires the following form (A.V. Lykov, 1967):

$$P = \frac{\beta t}{\frac{L_0}{E_0} + 1}; \quad L_0 = n_0 / (1 - n_0);$$

where  $E_0$  is the Young's modulus for water.

This obvious solution indicates that the pressure in the sphere grows proportionally to duration of the external stress (within elastic deformations, which do not exceed the ultimate stress limit of rocks). It can be used for the analysis of changes in the formation pressure depending on the coefficient of rock compressibility. Figure 5.4a demonstrates the growth of formation pressures for some lithologies (with  $\beta = 0.1$  mPa/day and the Young modulus for water being  $2.3 \cdot 10^3$  mPa). It is seen that the higher is compressibility of rocks, the faster is growth of formation

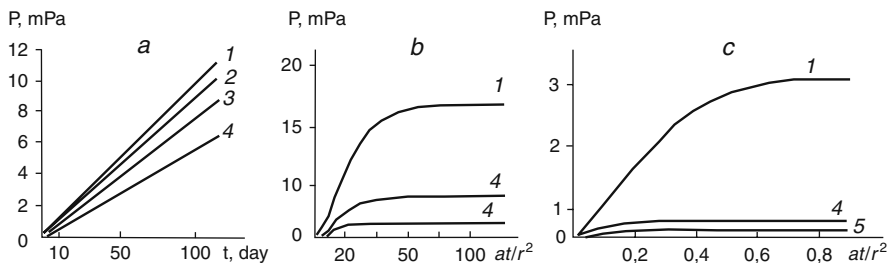


**Fig. 5.4** Variations in the pressure increment in the sphere. (a) Without interaction with the surrounding medium; (b, c) with different intensity of interactions: (1) in clayey-silty sediments; (2) in argillites; (3) in clayey sandstones; (4) in limestones; (5) in quartzites

pressures. This process is most intense in sandy-clayey formation and less intense in limestones.

Let us consider the same task under conditions of hydrodynamic interaction with surrounding rocks. In this case under the same initial conditions, boundary conditions are recorded as

$$dP(0,t) = 0,$$

$$\frac{dP(R,t)}{dr} + \frac{k_0}{m_0k} [P^0 - P(R,t)] = 0, \quad (5.10)$$

where  $P^0$  is the formation pressure in surrounding rocks,  $k_0$  and  $m_0$  are, respectively permeability and thickness of the near-boundary layer of the sphere, and  $k$  is a filtration coefficient for surrounding rocks.

The solution of equation (5.8) with boundary conditions (5.10) and  $P^0 = 0$  is recorded as (A.V. Lykov, 1967)

$$P(r,t) = \alpha\beta R^2 [1/6(1 + (2m_0k)/(k_0R) - r^2/R^2)] - f(r,t), \quad (5.11)$$

$$f(r,t) = \sum_{n=1}^{\infty} \frac{A_n}{\mu_n^2} \frac{R \sin(\mu_n r/R)}{r\mu_n} \exp\left(-\mu_n^2 \frac{at}{r^2}\right), \quad (5.12)$$

$$A_n = \psi\left(\frac{k_0R}{km_0}\right); \mu_n = \varphi\left(\frac{k_0R}{km_0}\right).$$

Let us consider the situation, when  $k_0 \ll k$  and assume that  $k_0 = 10^{-7}$  m/day and  $k = 10^{-3}$  m/day. In this case

$$f(r,t) = \sum_{n=1}^{\infty} \frac{A_n}{\mu_n^2} \exp\left(-\mu_n^2 \frac{at}{r^2}\right). \quad (5.13)$$

From (5.13), it is seen that sometime after the commencement of the external impact, the process becomes stationary since under high values of  $at/r^2$ , a series in equation (5.13) converges rapidly and the pressure in the domain is described by the following equation:

$$P(r,t) = \alpha\beta R^2 [1/6(1 + (2m_0k)/(k_0R) - r^2/R^2)]. \quad (5.14)$$

From (5.14), it follows that under external impact that does not exceed the ultimate stress limit of rocks, changes of pressures in the system are independent of time being directly proportional to intensity of this impact (in the given case,  $\beta$  is the external stress per unit of area, mPa/m<sup>2</sup>) all the other factors being the same. The onset of the stationary regime depends on parameters of the boundary layer, i.e., on intensity of hydrodynamic interaction with surrounding rocks. The absolute value of the formation pressure increment is determined by deformation properties of rocks with all other things being the same (Fig. 5.4b).

If it is accepted that  $k_0 = 10^{-4}$  m/day and  $k = 10^{-3}$  m/day, pressure increase and its temporal change are described by curves presented in Fig. 5.4c. The comparison between fig. 5.4b and 5.4c plotted with  $r/R = 0.1$ ,  $R = 200$  m, and  $\beta = 0.1$  mPa shows that increase in intensity of hydrodynamic interaction between the area in question and external factors (increase in the permeability coefficient of the boundary layer is four orders of magnitude) results in the lower pressure increment and faster onset of the stationary regime. This is confirmed by the fact that development of abnormally high formation pressures requires impermeable or low-permeability boundaries bordering a segment of the formation system.

In presented solutions, the external impact is accepted to be uniform along the surface of the body under consideration and of permanent intensity. In natural conditions, it is irregularly variable and characterized by different signs (compression, extension). In this connection, it is of interest to estimate the relaxation rate of formation pressures under short-term external impact.

Keeping this in mind, let us consider the pressure increment in a semi-isolated body under an instantaneous tectonic pulse with intensity  $\beta$ . Let us assume that the pressure at the body boundary at the initial moment equals zero. In this situation, initial and boundary conditions are recorded as

$$P(x,0) = 0; P(\infty,t) = 0; P(0,t) = 0. \quad (5.15)$$

Solution of equation (5.7) with  $dP_0/dt = 0$  and boundary conditions (5.15) is the following (A.V. Lykov, 1967):

$$P(x,t) = \frac{\beta}{2\sqrt{at}} \left\{ \exp \left[ -\frac{(x-x_1)^2}{4at} \right] + \exp \left[ -\frac{(x-x_1)^2}{4at} \right] \right\}. \quad (5.16)$$

It follows from equation (5.16) that the redistribution of the pressure increment under the instantaneous pulse is reversely proportional to the square root from the

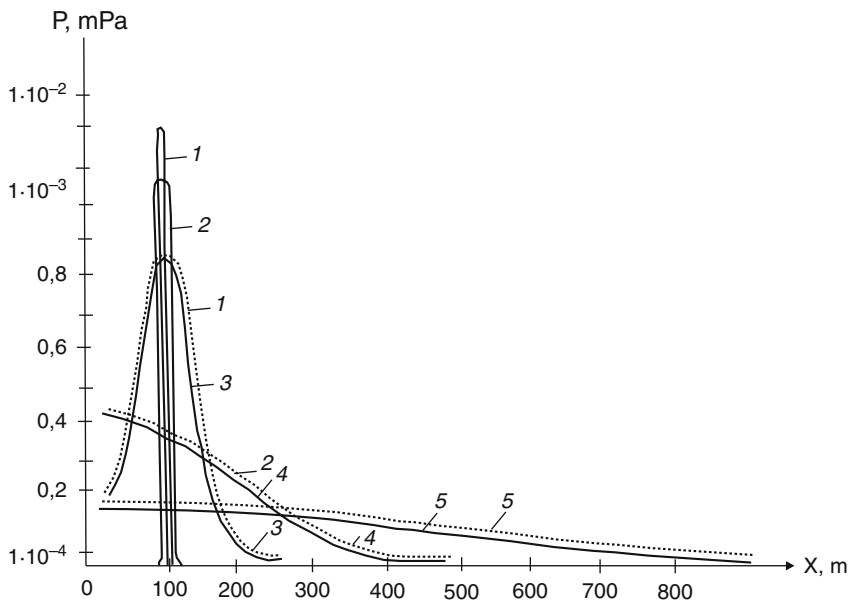


**Fig. 5.5.** Relaxation of formation pressures under instantaneous tectonic pulse. (1) Distribution of pressures  $t = 0.001$  day after the event; (2) the same with  $t = 0.01$  day; (3) the same with  $t = 0.1$  day; (4) the same with  $t = 1.0$  day; (5) the same with  $t = 10$  days. The dotted line corresponds to piezoconductivity  $a = 10^{-4}$  m<sup>2</sup>/day and the solid line to piezoconductivity  $a = 10^6$  m<sup>2</sup>/day

product of piezoconductivity and time. Figure 5.5 illustrates pressure relaxation under the instantaneous pulse ( $\beta = 1$  mPa) and different piezoconductivity values. Under  $a = 10^6$  m<sup>2</sup>/day pressure decreases practically up to the initial value during 0.1 day, while under  $a = 10^4$  m<sup>2</sup>/day this occurs during 10 days.

In stratified systems, piezoconductivity ranges from  $10^{-(1-2)}$  for clayey rocks [23] to  $10^{5-6}$  m/day for reservoirs. Consequently, the relaxation period of formation pressures that appear under tectonic stresses should also change in wide limits in different stratified systems. For example, the relaxation period for clayey rocks with  $a = 10^{-4}$  m/day should be approximately 200 kyr.

Thus, the present-day distribution of formation pressures in the elastically deformed medium can result from permanently changed stresses in the stratified system under influence of tectonic forces. It represents as if a photograph of the redistribution of formation pressures.

Figure 5.6 illustrates the distribution of pressures for the same time (0.01 day) under piezoconductivity of  $10^6$  m<sup>2</sup>/day and several instantaneous sources placed in different points and characterized by different sign: + (compression) or - (extension). It shows alternating piezomaximums and piezominimums as well as different gradients (with respect to both amplitude and direction).

Development of gradients of subsurface fluids implies their migration. Nevertheless, the stratified system demonstrates only the redistribution of pressures

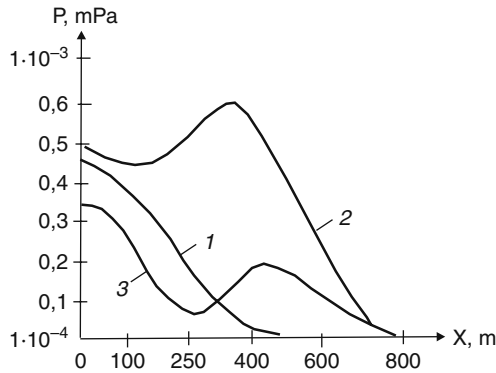


**Fig. 5.6.** The distribution of pressures in a semi-isolated body with piezoconductivity of  $10^6$   $\text{m}^2/\text{day}$  and  $t = 0.01$  day. (1) Positive instantaneous source of unit intensity  $W$  at point  $x_1 = 100$  m (compression of rocks); (2) two sources at points  $x_1 = 100$  m and  $x_2 = 400$  m, source intensity at point  $x_2 = 2W$ ; (3) source with intensity of  $W_3 = -W_1$  (extension of rocks) is located at point  $x_1 = 250$  m relative to Curve 2

related to irregular compression or extension of the elastically deformed mass if characterized by different properties (filtration, capacity, and compressibility coefficient) and isolated from its neighboring areas, not migration of fluids.

Thus, the following arguments in favor of the significant influence of geodynamics on development of abnormally high formation pressures are suggested:

- (1) Velocities of tectonic processes are comparable with velocities of relaxation of formation pressures or frequently exceed them.
- (2) Recurrence and quasi-periodicity of tectonic processes.
- (3) Natural observations confirming influence of tectonics on development of formation pressures.

### 5.3.4 Additional Recharge

The influx of liquid from deeper formations under pressures characteristic of lower layers should undoubtedly lead to the growth of the pressure in the relatively isolated system. The influx of fluids leads to the effect similar to that produced by the system compression (impact of external forces). For example, in the system with the base  $10^4$   $\text{m}^2$  in size and 10 m thick, the influx of only  $100$   $\text{m}^3$  of water should result in the pressure growth by 10 mPa.

Fluids from lower formations may migrate through weakened zones, tectonic fractures, and areas with filtration properties better than that in neighboring layers.

It can be presented in the following form. Let us assume a channel through which fluids migrate to the overlying relatively isolated block. At some moment, the influx reaches the expenditure  $Q_1$ , which should result in the growth of pressure in the block and, consequently, the vertical gradient of filtration through the

overlying sequence. This should lead to the outflow from the block with the expenditure  $Q_2$  (fluid movement may be lateral, not necessary vertical). The expenditure  $Q_2$  should grow until dynamic equilibrium is established between inflowing and outflowing expenditures. The pressure, which should be reached in the block, would be anomalous for its occurrence depth.

The anomaly coefficient depends only on the hydrodynamic isolation degree (permeability of the boundary layer) and pressure in the lower layer. This model is not the only one and is correct only with existence of a permanent recharge source in a partly open system.

The possible participation of local ascending flows in development of abnormally high formation pressures can be exemplified by particular areas [2].

In one of the water deposits located in western Pakistan, the sudden increase in the pressure up to the value exceeding the geostatic one resulted in hydraulic fracturing and water breakthrough from a depth of 600 m to the surface to discharge in the form of springs, which functioned during several months. In the Apsheron Peninsula, oil started to discharge from the fissure that appeared close to the well after its stopcocking. In Borneo, gas and water broke through along the wellbore from gas condensate fields, which are characterized by pressures close to geostatic values, to overlying sequences with oil pool to form abnormally high formation pressures in the latter. Gas and water migrated, together with oil, upward along the fault zone to discharge at the surface and form large craters. One of such craters sucked down the cement plant.

In the Dagadzhik oil field, pressure drawdown led to disruption and liquid break through the 350-m-thick clayey sequence, which resulted in the growth of formation pressures by 2.1 mPa and increase in the yield of production wells.

The list of examples is far from being exhausted. The question arises as to where the matter (oil, water, gas) originates from in lower formations? The elastic component is insufficient, which is confirmed by simple calculations. In order to answer this question, we should unavoidably admit the significant role of the basement, which represents a connecting link between the sedimentary cover of negative stratified structures and crust and mantle (Chapter 11). The study of palynomorphs from supra- and subsalt sediments in some oil fields of the Caspian region [5] revealed that older microfossil taxa occur in younger sediments. For example, Carboniferous and Devonian forms are observed in Permian–Triassic strata.

These finds are a direct indication of vertical fluid migration during past and, probably, recent geological epochs.

In the opinion of A.A. Smyslov, by large energy reserves sedimentary basins conquer active volcanic zones. According to V.B. Porfir'ev and other researchers, 210 oil and gas fields are discovered in volcanic and metamorphic rocks of the crystalline basement: North America (28), South America (5), Africa (109), Europe (8), Asia (60). They include many giant fields: Hugoton Panhandle ( $2 \cdot 10^{12}$  m<sup>3</sup> of gas and  $223 \cdot 10^6$  t of oil), Wilmington ( $330 \cdot 10^6$  t of oil), and Kern River ( $205 \cdot 10^6$  t of oil) in the United States); Audjila Nafora Amal ( $512 \cdot 10^6$  t of oil) in Libya; La Pas ( $222 \cdot 10^6$  t of oil) and Mara ( $104 \cdot 10^6$  t of oil) in Venezuela. Hydrocarbon accumulations in the basement are discovered in the Turan Plate, where the oil- and gas-saturated basement sequence is tens to, locally, hundreds of meters thick (to



450–900 m and even 900–1,000 m, for example in the Totuma oil field). Recent data on petroleum resource potential and hydrothermal activity in basement rocks are summarized in [24, 27].

Based on the study of water-soluble salts in largely clayey sediments of the Bazhenovka Formation in some areas of central West Siberia, it is shown that such salts (Ca and Mg sulfates) in argillites could originate only in formation conditions from hydrothermal sulfate solutions with temperatures of 250–300°C. According to these authors, hydrothermal vents existed in fault zones. In such zones up to 1 km wide, rocks are characterized by elevated porosity. Abnormally high formation pressures in central areas of West Siberia associate with argillites of the Bazhenovka Formation (Chapter 7). Anikeev [3], who summarized data on the abnormally high formation pressures distribution in many regions of the world, proposes relatively convincing model (theory, in his terminology) for explaining the formation of super-high pressures. This theory develops the concept of endogenic abnormally high formation pressure's origin. According to the latter, during periods of tectonic and seismic activation, fluids from the presumed gasogeodynamic system in the deep crust intrude the sedimentary cover to form "main superhead deposits and aureoles of intrusion." It is assumed that the sedimentary cover encloses thick screening sequences that "suppress energy of ascending fluids and preserve abnormally high formation pressures during long geological periods." In the opinion of this author, "additional pressure provided by gas is a remarkable feature of all the provinces and fields with abnormally high formation pressures. . .oil and water deposits with such pressures are everywhere anomalously gas saturated, except for extremely rare examples."

### 5.3.5 *Catagenetic Processes*

Under catagenesis we understand combination of processes that result in changes of the system volume and, consequently, growth of the formation pressure in the latter under its isolation.

The catagenetic processes are widespread. It is impossible to provide their comprehensive characteristic and estimate them quantitatively here; some of them are described in Chapter 6.

The catagenetic processes start immediately after deposition of sediments and are in progress during their entire life. Intensity of rock transformation increases with their subsidence. Velocities of these processes in normal thermodynamic conditions never exceed subsidence rates of sedimentary sequences, which are always substantially lower as compared with velocities of the pressure redistribution as is shown above. In this connection, it can be stated that catagenetic processes cannot be responsible for development of abnormally high formation pressures. Rock transformation occurs only in areas with intense subsidence of the sedimentary cover in negative structures or intrusion of liquids that disturb the thermodynamic equilibrium. In such a situation, they are, however, secondary relative to tectonics and hydrothermal activity.

### 5.3.6 *Chemical Processes*

Depolymerization of compounds is one of such processes [2 and others]. This process represents, however, the consequence, not the cause of abnormally high formation pressures, as follows from equation (5.1). This statement is confirmed also by the Le Chatelier principle: if the equilibrium system is subjected to the external impact, equilibrium shifts in direction indicated by this impact until counteraction in the system is equal to the latter.

With regard to depolymerization of complex hydrocarbons, the Le Chatelier principle has the following form: the pressure increase or decrease displaces equilibrium toward the formation of lesser or greater quantities of molecules, respectively. Thus, transformation of complex hydrocarbons into their simpler phases is possible only under reduced pressures in the system (for example, due to development of the oil field) and this process proceeds in the opposite direction, when pressures increase. Transformation itself cannot stimulate pressure changes in a system. The sole exception is the process, which is accompanied by the release of large volumes of gas. In this situation, we are dealing with the gasogeodynamic model of superhigh pressure formation by Anikeev (see above).

### 5.3.7 *Temperature Changes*

It follows from equation (5.1) that changes in internal energy of the closed system are proportional to the heat provided by the external source with all other factors being equal. The temperature increase in the system with the constant volume results in the pressure growth in the latter (particularly when the system contains gaseous phase). Being probably insignificant in terms of absolute values, this pressure increment may contribute substantially to the general pressure increase stimulated by other processes (for example, simultaneous increase in temperature and decrease in the system volume). The following potential heat sources are distinguishable:

(1) The regional heat influx from deep crustal levels. At the same time, the heat influx under development of the temperature gradient cannot stimulate development of abnormally high formation pressures, since the temperature gradient is a universal phenomenon, which is characterized by low values and insignificant variations.

(2) The heat release during compaction of sandy–clayey sediments due to the geostatic load. For assessing the role of this process, it is necessary to compare velocity of the temperature growth in response to sediment compacting except for the share, which is redistributed (in contrast to the filtration field, the thermal one cannot be isolated from the surrounding medium), and that of formation pressure relaxation.

In our opinion, the heat increment value should be insignificant since the velocity of the external pressure increment is extremely low (Chapter 6). For example, under the approximate sedimentation rate of 0.1 mm/year and average rock density of 2,300 kg/m<sup>3</sup>, approximately 10,000 years are needed for the pressure increase

by 0.1 mPa. Consequently, generated heat should also be insignificant and it will undoubtedly be redistributed.

This assumption is confirmed by geothermal observations in the eastern Ciscaucasia region (I.G. Kissin, 1967), according to which the temperature of sediments occurring under high geostatic pressure appears to be lower as compared with that of rocks under lower pressures. Such examples are available from any region.

Thus, even with some heat release during sediment compacting, which itself needs to be proven, it cannot be responsible for development of abnormally high formation pressures.

(3) The heat release during tectonic movements. N.A. Ogil'vi believes that they result in the formation of the anomalous thermal field. In his opinion, thermal anomalies are caused by neotectonic movements, since temperature fields of past geological epochs should be destroyed.

The last assumption is undoubtedly being confirmed by many examples. The temperature fields associated with tectonic movements are local, characterized by low values, and, consequently, cannot serve as an only factor responsible for development of abnormally high formation pressures.

(4) The temperature growth in response to thermodynamic processes related to phase transformations in the fluid-rock system. The phenomenon was first discovered in gas condensate fields with abnormally high formation pressures in the United States. The phase transformation of matter is, however, a consequence, not a cause of distortion in the formation pressure distribution during field exploitation. Two-thirds of oil wells demonstrate precipitation of the solid phase.

The heat influx into isolated parts of the stratified system may be provided only by the convective heat transfer from deep crustal layers along tectonic fractures, fissures, and weakened zones.

In order to estimate influence of the temperature on pressures, we used the van der Waals' equation that describes relations between pressure, volume, and temperature. This equation for a closed isolated system, where changes in the volume are excluded, is as follows:

$$P_2 = \left( P_1 - \frac{a}{v^2} \right) \frac{T_2}{T_1} - \frac{a}{v^2}, \quad (5.17)$$

where  $P_1$  and  $P_2$  are pressures under the temperatures of  $T_1$  and  $T_2$ , respectively,  $v$  is the volume of the system, and  $a$  is the van der Waals' correction to the Clapeyron–Mendeleev equation.

Let us assume that the initial pressure  $P_1$  is 0.1 mPa, volume is 1 l, and initial temperature is 27°C. The van der Waals' correction for water is 5.47°C. With these parameters, the temperature growth by 50°C should result in the 2.07 times pressure increase in the system. With larger volumes, the member  $a/v^2$  becomes very small so that it can be neglected. In this case, equation (5.17) turns into the Clapeyron–Mendeleev equation, according to which the pressure should increase by 17% under the same conditions.

These calculations are, however, very approximate since equation (5.17) is correct only for gases, where the coefficient  $a$  remains constant in the significant temperature interval. Liquids are characterized by variable values of this coefficient. Moreover, dependence of the latter on the temperature changes is relatively complicated and its determination requires special studies.

Thus, it is impossible to establish correlation between pressures and temperature. The curve of this correlation should, probably, be located between two curves which are separately compiled in line with the van der Waals and Clapeyron–Mendeleev equations.

Many researchers noted the important role of hot solutions, which migrate from deep crustal layers and transport large amounts of heat, in development of abnormally high formation pressures [2, 19, 20]. These works demonstrate that temperature anomalies result in the decreased isolation degree of the reservoirs since filtration of hot liquids through clayey sequences is accompanied by the substantial growth in the filtration capacity of clays. Consequently, the temperature influence on development of abnormally high formation pressures is dual. Its growth leads to the increase in pressure in the formation, on the one hand, and permeability of isolating clayey sequences, which accelerates relaxation of anomalous pressures and shortens their existence, on the other.

Having considered all the members of the thermodynamics equation (the work of external forces was not considered especially since this problem was touched during the analysis of processes that result in the increased volume of the system), the following conclusions can be drawn.

The following processes are responsible for development of abnormally high formation pressures:

- (1) tectonic forces, primarily those among them, which occur instantly;
- (2) hydrothermal activity and migration of gas–liquid mixture from deep layers;
- (3) powerful local heat flows substantially exceeding the temperature in the field. Processes (1) and (2) are usually consequences of tectonic forces.
- (4) All the three processes may take part in development of abnormally high formation pressures either together or separately.
- (5) Inasmuch as the velocity of the redistribution of formation pressures is higher even in clayey sediments than that of many geological processes (crust subsidence, sedimentation, denudation, and others), inherited pressures cannot be preserved during reservoir displacement to new hypsometric levels (one of the hypotheses explaining development of abnormally high formation pressures).
- (6) Changes in geostatic pressure are so slow that they may result in development of abnormally high formation pressures only under ideal conditions of complete isolation of a bed segment, which is practically unreal.
- (7) By velocities, epigenetic processes that change the volume of the system are similar to geostatic compression and, therefore, cannot substantially increase the pressure in the layer.

## References

1. Aliev F Sh, Bairamov T A (1993) On geological structure and hydrogeological conditions of the Apsheron Peninsula. *Otechestvennaya geologiya* 3:73–78
2. Anikeev V A (1964) Abnormally high formation pressures in oil and gas fields. Nedra, Leningrad
3. Anikeev V A (1980) Geodynamic theory of superhigh formation energy of drilled oil- and gas-bearing Earth interior. In: *Earth degassing and geotectonics*. Nauka, Moscow
4. Bondarenko S S, Barevskii L V, Dzyuba A A (1983) Migration peculiarities of deep groundwater. In: *Basics of hydrogeology*. Hydrogeodynamics. Nauka, Moscow
5. Dal'yan I B, Bulekbaev Z E, Medvedeva A M et al. (1994) Direct indications of vertical migration in the eastern Caspian region. *Geologiya nefi i gaza* 12:40–43
6. Durmish'yan A G (1977) On the problem of abnormally high formation pressures and its role in oil and gas prospecting. *Trudy VNIGRI* 397:55–69
7. Djunin V I (1981) Investigation methods and principles of deep formation hydrodynamics. VIEMS, Moscow
8. Djunin V I (1985) Investigation methods of the deep subsurface flow. Nedra, Moscow
9. Djunin V I (2000) Hydrodynamics of deep formations in petroliferous basins. *Nauchnyi mir*, Moscow
10. Florin V A (1994) *Sediment mechanics*. Nauka, Moscow
11. Gurevich A E (1969) *Groundwater, oil, and gas migration*. Nedra, Leningrad
12. Kartsev A A (1980) Hydrogeological prerequisites for manifestation of superhydrostatic pressures in petroliferous areas. *Geologiya nefi i gaza* 4:40–43
13. Kartsev A A (1992) *Oil and gas hydrogeology*. Nedra, Moscow
14. Kartsev A A, Vagin S B, Baskov E A (1969) *Paleohydrogeology*. Nedra, Moscow
15. Kartsev A A, Vagin S B, Serebryakova L K (1980) Paleohydrogeological reconstructions for revealing petroliferous zones (exemplified by western Ciscaucasia). *Byul MOIP* 1: 132–140
16. Kartsev A A, Lopatin N V, Sokolov B A, Chakhmakhchev V A (2001) Triumph of the organic (sedimentary-migratory) theory of oil genesis by the end of the 20th century. *Geologiya nefi i gaza* 3:2–5
17. Kissin I G (1964) *The East Ciscaucasia artesian basin*. Nauka, Moscow
18. Kissin I G, Belikov V M, Ishankuliev G A (1990) Extreme variations in the groundwater level in seismoactive areas. *DAN SSSR* 314:1099–1103
19. Kropotkin P N (1986) Earth degassing and genesis of hydrocarbons. *Zhurn Vsesoyuz Mendeleev ob-va* 31:540–547
20. Kropotkin P N, Valyaev G M (1979) Concealed faults and Earth degassing. In: *Tectonic evolution of the crust and faults*. Nauka, Moscow
21. Mukhin Yu. V (1965) *Compaction of clayey sediments*. Nedra, Moscow
22. Pavlovskaya L N (1967) The study of accuracy in modeling unstable filtration at the grid of ohmic resistances (in line with the Libman's method). In: *Proceedings of the coordinative meeting on hydraulic engineering*. Energiya, Leningrad
23. Perozio G N (1970) Epigenetic alterations in oil reservoirs of the Severo-Pokur and Vatin fields. In: *Problems of lithology and paleogeography of Siberia*. Novosibirsk
24. Shakhnovskii I M (1994) Once more on the petroleum resource potential of the basement. *Geologiya nefi i gaza* 9:29–34
25. Sidorov B A, Doldyreva V A, Gaipov B N et al (1988) Non-tidal variations of the gravity force in oil- and gas-bearing domains. In: *Abstracts of the 1st All-Union conference "Geodynamic basics of predicting petroleum resource potential of the Earth's interior."* Moscow
26. Sidorov V A, Kuz'min Yu. O, Bagdasarov M V et al (1994) Geodynamic methods for prospecting and exploration of oil and gas fields. *Geologiya nefi i gaza* 6:47–50
27. Veselov K E, Mikhailov I N (1994) Oil and gas at deep levels of the crystalline basement. *Geologiya nefi i gaza* 2:17–21

## Chapter 6

# Development of Filtration Properties in Deep Formations of Petroliferous Basins

The regional aspects concerning capacity and filtration properties are least studied among others in the general problem of deep fluid formation in stratified systems of negative structures. They are poorly covered in special works dedicated to the formation of deep fluids. Practically all the available information on capacity and filtration properties of rocks at deep levels occurs in publications dealing with oil and gas problems.

According to traditional views among hydrogeologists, sandy-silty and carbonate rocks of deep formations in negative stratified structures are considered a priori as permeable, while clays and salts as lithologies of very low permeability or impermeable.

In some local structures, capacity and filtration properties of sedimentary rocks are well studied. Numerous works on the structure and formation of reservoir rock properties characterizing productive formations of some exploration areas and structures need systematization and generalization.

“The only purpose of this chapter consists in summarizing numerous published materials describing the spatial distribution of capacity and filtration rock properties through separate areas and structures in order to reveal most general regularities in changes of reservoir rock at deep levels. Regional aspects of the geoinfiltration problem, which represent an autonomous practical task, are excluded from this analysis.”

Only sometimes, when the knowledge degree is sufficient, information on reservoir properties of rocks is analyzed for solving particular scientific tasks (by modeling and analytical calculations) with the West Siberian, Pechora, and eastern Ciscaucasia petroliferous basins taken as examples. The results of these studies may be useful in solving practical tasks such as, for example, regional assessment of petroleum resource potential.

The study of regularities in the formation of capacity and filtration properties of sedimentary rocks is a difficult task since they are controlled by many independent time- and space-variable factors and processes.

At the same time, it is clear that the analysis of hydrodynamic parameters without due account for the structure of the geoinfiltration field is unable to elucidate any of the aspects in the problem of the deep fluid formation. This is explained by two necessary and sufficient conditions needed for gravitational movement of liquid: the

pressure gradient and permeability of the medium exceeding zero. While the first condition receives relatively much attention in the hydrogeological literature (compilation of potentiometric maps, analysis of formation pressure field), the second one is poorly covered by special studies. Therefore, it is reasonable to pay more attention to this aspect with due account for recent information on the structure of reservoirs and caprocks.

The available information on capacity and filtration properties of sedimentary rocks constituting the platform cover that is based on rare and irregularly spaced exploration and exploitation wells is insufficient for the adequate coverage of large regions. The values of filtration parameters obtained by hydrodynamic or analytical laboratory methods characterize very small areas and narrow stratigraphic intervals. It would be unreasonable to interpolate these data directly on spacious petroliferous basins and entire thickness of petroliferous complexes. At the same time, it is very important to know values of filtration parameters at any point of these complexes and their spatial variations.

In this connection, *general geological concepts*, which allow the most adequate interpretation of experimental filtration data, represent the only possible basis for obtaining information on regional regularities in changes of sediment filtration properties through petroliferous basins. In this connection, of importance are data on the crust structure and its development, sedimentary formations and facies, geological and tectonic history of particular regions, spatial regularities in porosity variations as well as their responsible factors, and other materials from relatively well-studied intervals of platform sections in petroliferous basins [9, 39, 41, and others].

The following factors determine filtration properties of fluid-hosting rocks: sedimentation conditions and paleogeographic settings, position of regional and local provenances of detrital material, its lateral and vertical distribution, peculiarities in the spatial distribution of facies (marine, continental, channel, deltaic, coastal marine, bar, reefal, and others), diagenetic and catagenetic processes that determine transformation of incoherent sediments into rocks during their subsidence, and changes in thermodynamic conditions [27].

Thus, it is necessary to trace the temporal and spatial evolution of petroliferous complexes for obtaining adequate knowledge of regional changes in capacity and filtration properties of rocks.

## **6.1 Development of Reservoir Properties in Terrigenous Formations**

### ***6.1.1 Sedimentation Settings***

The reservoir properties of terrigenous rocks commence forming at the initial development stage of negative stratified structures and corresponding sedimentation process. Their lateral changes depend on differentiation of detrital material that is determined by the position of regional and local denudation areas and variations in

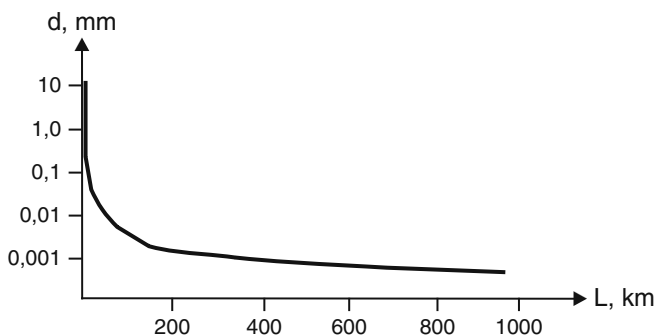


**Fig. 6.1** Differentiation of detrital material away from the provenance under water flow velocity of 24 cm/c (according to A.I. Zhivotovskaya)

sedimentation conditions (depth of the sedimentation basin, its size, water temperature and salinity, and others). Differentiation of detrital material, which is governed by hydrodynamics of particulate particles in the water column, provides conditions for formation of different facies and their spatial localization in the sedimentation basin.

There are theoretical calculations that prove the regular differentiation patterns of detrital material and, thus, regular distribution of facies (macroheterogeneity) through negative stratified structures (Fig. 6.1).

The coarse detrital continental and marine sediments are deposited along the periphery of negative stratified structures. Away from provenances, terrigenous poorly rounded and sorted detrital material gives way to marine sediments: lagoonal, coastal marine, shallow water, and pelagic. Such changes in sedimentation conditions form a continuous succession of facies with boundaries marked by transitions from more sandy to more clayey sediments [10, 41] (Fig. 6.2). In the absence of high-amplitude faults and, correspondingly, differently oriented vertical movements of blocks along them, lateral variations in the grain-size composition of sediments can be described by the monotone empirical function.

Marginal areas of negative stratified structures located close to regional sources of detrital material accumulate largely sands with insignificant share of silty and clayey particles. Clayey intercalations, if there are any, are thin and isolated in both vertical and horizontal directions. The terrigenous portion of the sedimentary section in the peripheral parts of negative stratified structures is usually composed of sandy rocks with isolated lenticular clay bodies.

Away from marginal parts of the basin, the share of clayey material in the section gradually increases. The isolated clay bodies join each other to form continuous layers, the thickness of which increases toward central areas of negative stratified structures. The same is true of clayey rocks (Figs. 6.3 and 6.4). Along the periphery of negative structures, clayey sediments are enriched in silty and, frequently, sandy material, while in their inner areas the share of clayey particles increases up to 90% and higher when local sources of detrital material are lacking.



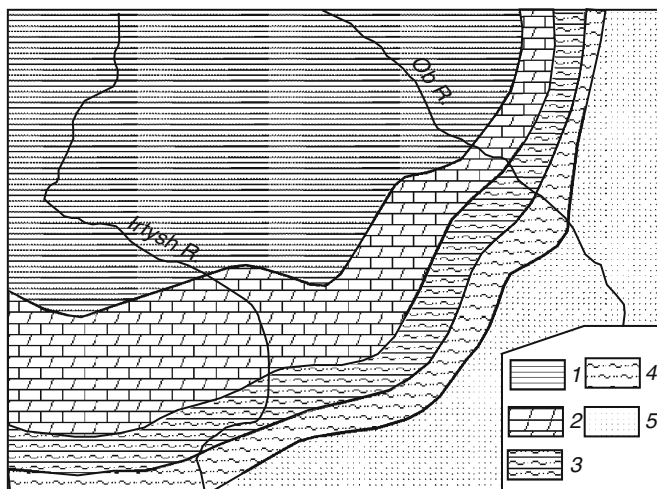


**Fig. 6.2** Schematic lithological-facies map of Lower Cretaceous sediments of West Siberia (after L.Ya. Trushkova). Sediments: (1) relatively deepwater (substantially clayey), (2) shallow-water marine, (3) coastal marine (substantially sandy, productive bed is lithologically variable), (4) coastal-marine and brackish-water lagoonal, (5) lagoonal and continental

For example, the Lyulinvor Formation, which represents an element of the Upper Cretaceous–Paleogene sequence through the entire West Siberian petroliferous basin, is characterized by the following changes in the grain-size composition. In the marginal southeastern part (Tym River upper reaches), the content of fraction 0.01 mm is 14%, while 200 km away from the basin coast it increases up to 87%. The content of fraction 0.25–0.10 mm decreases in the same direction and at the same distance from 86 to 2%. Thus, the Lyulinvor Formation is represented by rich and compact clays only in central parts of the petroliferous basin: toward its periphery, this unit is substantially enriched in sand. Similar changes are also observed in the Gan’kino Formation (Figs. 6.3 and 6.4).

In the Eastern Kuban Depression, Callovian coarse-grained sandstones are developed along its northeastern periphery. Grain size of sediments decreases gradually toward the axial part of the depression, where fine-grained sandstones appear.

In the Timan-Pechora petroliferous basin located between the Timan Range and Urals, the grain-size composition of Middle Devonian terrigenous sediments becomes gradually finer, which is accompanied by their better sorting. The share of marine clayey and carbonate–clayey sediments increases as well toward the deep part of the paleosea.

The similar situation is also characteristic of other sedimentary complexes of the West Siberia, eastern Ciscaucasia, and other regions. The scale of these changes is variable and depends on particular paleogeographic and paleogeologic settings.

Regional regularities in the variable grain-size composition of terrigenous sediments are superimposed by local structural–tectonic features of the sedimentation basin such as its bottom topography formed under the influence of tectonic

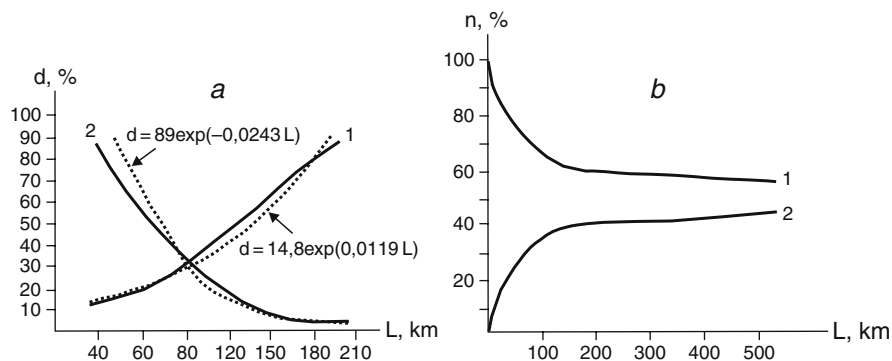


**Fig. 6.3** Changes in grain-size parameters and lithological composition of terrigenous sediments of West Siberia. (a) Differentiation of detrital material in the Gan'kino Formation of the southeastern part of the basin: (1–2) grain size: (1) <math><0.01</math> mm, (2) 0.25–0.1 mm; *dashed lines* correspond to empirical curves; (b) changes in the integral thickness of individual beds in the Pokur Formation in the southern part of the basin: (1) sandy, (2) clayey

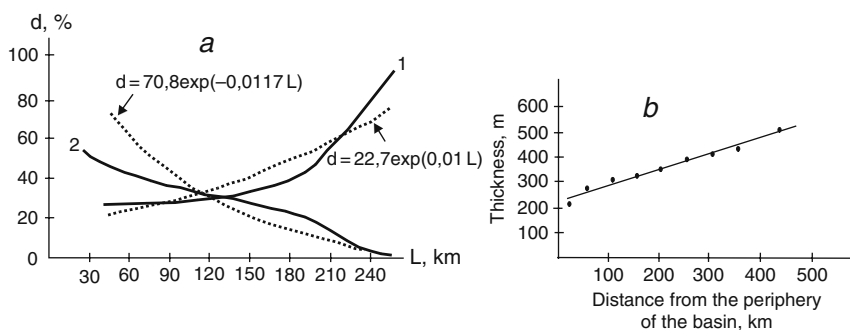


**Fig. 6.4** Changes in grain-size parameters and lithological composition of terrigenous sediments of West Siberia. (a) Differentiation of detrital material in the Lyulinvor Formation (for legend, see Fig. 6.3); (b) changes in the thickness of the Pokur Formation away from the periphery of the basin

processes. Uplifted shallow bottom areas are characterized by high-energy hydrodynamics due to sea waves, transgressions, and regressions. These areas receive no sedimentary material, while roiling of sediments results in removal and redeposition of clayey and fine-grained materials with simultaneous increase in their sand content and reduction in the thickness of some stratigraphic units on paleouplifts. This is observable on many positive structures in most of the petroliferous basins of Russia and adjacent regions.

For example, in the Taz field of West Siberia, the average thickness of Cenomanian sediments in the structure arch is 12 m and their sand content amounts to 83%, while in its limbs, these parameters are 22 m and 60%, respectively. As a whole, the section of the Taz Uplift is characterized by the high share of siltstones

and sandstones (up to 70%) and their elevated thickness. In limb areas of the structure, the integral share of coarse-grained rocks is reduced up to 40% and thicknesses of individual beds decrease up to 2–4 m. This regularity is so distinct that increase in the share of sandstones in the sedimentary section of the West Siberian petroliferous basin serves sometimes as a criterion for defining internal uplifts.

Regional changes in the grain-size composition are complicated by internal sources of sedimentary material related to paleoerosion areas. For example, in the Lower–Middle Jurassic fluid-hosting sediments of West Siberia, above-mentioned spatial distribution regularities are largely disguised by material transported from numerous inner denudation areas, which existed at that time along with regional provenances. The development of inner sources determined the mosaic compositional patterns and abrupt facies changes of sediments accumulated in continental settings at relatively insignificant distances. The schematic lithology-facies map in Fig. 6.2 demonstrates substantially more complicated distribution patterns for these sediments [32, 35, and others].

### ***6.1.2 Catagenetic Rock Transformations***

The sediments constituting sedimentary sections of negative stratified structures (petroliferous basins, inter- and intramontane depressions) are characterized (to certain depths) by directed downward changes in rock porosity related to post-sedimentary transformation. Chemical and physicochemical alterations of sediments are accompanied by their mechanical compacting under the load of accumulating sediments (geostatic compacting). The combined effect of these processes determines changes in capacity and filtration properties of rocks.

By the scale and intensity of sedimentary rock transformations, catagenetic processes are subdivided into regional and local. First of them is manifested universally and its intensity is determined by regional changes in lithology and mineralogical composition of rocks, their occurrence depths, chemical and gas composition of fluids, gradients in geostatic pressures, and regional tectonic movements. The regional processes of sediment transformation are superimposed by local factors such as the temperature and pressure growth, which is responsible for certain chaotic patterns in catagenetic transformation of sedimentary rocks and, correspondingly, distinct anisotropy of capacity and filtration properties. Of significance in the formation of filtration heterogeneity are also hydrothermal processes, owing to which rocks experience drastic transformation characterized by mosaic patterns. The transformation degree of capacity properties is largely dependent on thermodynamic conditions at each point of the system.

### ***6.1.3 Compaction***

Compositionally and genetically different sedimentary rocks react in a different manner to the geostatic pressure. Coarse-grained incoherent sediments may

decrease their porosity by 20–30%. At the same time, they are characterized by high porosity at deep levels. This is explained by better sorting and roundness of sand grains, mineralogical composition, and other factors.

For example, sands composed of angular clasts suffer from the geostatic pressure more than sands consisting of well-rounded grains since the pressure is proportional to the contact area with all other things being the same.

The number of contact points in angular rock fragments is significant. V. Engel'gardt established that the number of point contacts decreases downward while that of long, convex–concave, and sutural contacts increases, i.e., the interstitial space in sediments becomes reduced (Fig. 6.5).

The dissolved matter of primary minerals forms, partly or entirely, the basis for the formation of secondary cement, which reduces further the free interstitial space and porous permeability.

The significant role in compacting belongs to the mineralogical composition of rocks. Many studies carried out in different areas show that quartz- and carbonate-bearing sandy sediments are more susceptible to compacting than feldspar rocks. This is explained by elevated solubility of carbonates and quartz under the geostatic pressure [8].

The Jurassic and Neocomian sediments of West Siberia show frequently that feldspars, biotite, and crystalline schists intrude into quartz grains (Fig. 6.5). According to [33], in Jurassic and Cretaceous sediments intrusion contacts in quartz and feldspar grains amount to 40 and 36% of the total intergranular space. Moreover, well-sorted varieties of sandy–silty rocks show decrease in their initial thickness by 2.3–2.5, 3, 6.5, and 8.0% at depths of 1,500–1,600, 2,100–2,300, 2,300–2,400, and 2,800–3,000 m, respectively (Fig. 6.6).

Theoretical aspects of rock compacting are discussed in many works [e.g., 9], which demonstrate that changes in porosity ( $\varepsilon$ ) and permeability ( $K$ ) depending on

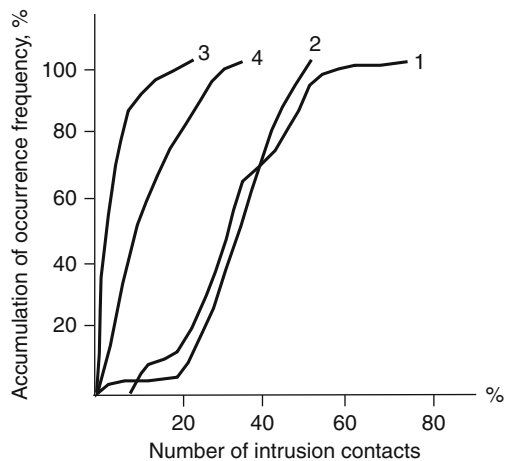
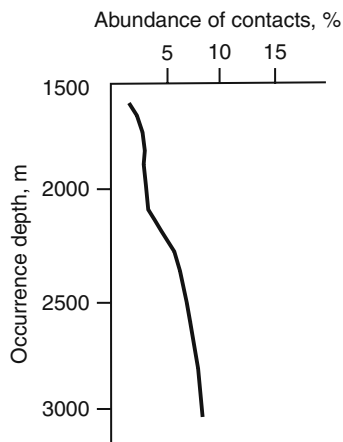


**Fig. 6.5** Integral number of intrusions of different rock-forming minerals into quartz (after [33]). (1) Quartz; (2) feldspar; (3) mica; (4) rock fragments

**Fig. 6.6** Correlation between abundance of convex–concave intergranular contacts and occurrence depth of sandy–silty sediments in West Siberia (after [33])



their occurrence depths are described in the following way:

$$\varepsilon_H = \varepsilon_0 \exp [-1.14\beta_n(t, \tau)H], \quad (6.1)$$

$$K_H = K_0[\varepsilon_H/\varepsilon_0]^{2(3+\alpha)/(2+\alpha)}, \quad (6.2)$$

where  $\varepsilon_0$  and  $K_0$  are coefficients of porosity and permeability near the surface,  $\varepsilon_H$  and  $K_H$  are the same parameters at depth  $H$ ,  $\beta_n(t, \tau)$  is the coefficient of irreversible compaction that takes into account time  $\tau$  and temperature  $t$  (for different rocks, this coefficient varies from  $25 \cdot 10^4$  to  $48 \cdot 10^{-1} \text{ m}^2/\text{kg}$ ), and  $\alpha$  is a structural parameter dependent on geometry of the interstitial space and ranging in different rocks from  $-2.4$  to  $-1.8$ . If equation (6.2) is given in the form

$$K_H = K_0 \exp(\gamma H),$$

$$\gamma = 0.28 \cdot \beta_n(t, \tau) \cdot [(3 + \alpha)/(2 + \alpha)], \quad (6.3)$$

one can see that changes in the coefficient of permeability due to irreversible deformations under influence of geostatic compaction (as well as changes in the grain-size composition of rocks) are described as a decreasing exponential function. Subsequently, they are superimposed by other different processes that change this regularity at deep levels.

It should be noted that such a correlation is in good consistency with empirical data obtained from other regions, although the latter represent a particular case of equations (6.1) and (6.3).

For example, L.V. Zalazaeva, who studied Jurassic and Cretaceous productive strata in central areas of the West Siberian petroliferous basin, established the following empirical logarithmical correlation between porosity ( $n$ ) and permeability ( $K$ ) based on 482 samples:

$$n = 2.95 \cdot \lg K + 18.95.$$

In the transformed form, the latter can be presented as

$$K = \exp [ - (18.95 - n)/6.78].$$

This means that the permeability coefficient depends exponentially on porosity. Similar regularities are cited in [24] for the following regions: Switzerland, Black Sea, central Pacific, West Siberia, Timan-Pechora province, northern Caspian region, Western Kuban Depression, and East Siberia.

Thus, present-day filtration properties of rocks resulted from long and complex transformation of former sediments into rocks.

Regional transformation of sedimentary rocks leads to significant decrease in the initial porosity at deep levels and reduction of interstitial permeability of sedimentary rocks (fissuring-related permeability deserves special consideration). This is confirmed by downward changes in rock porosity, which are characterized by general regular patterns being described to certain depths by the logarithmic or exponential correlation regardless of the region.

For example, transmissibility changes in zones of the intense and slow water exchange (where endogenic processes show no or insignificant influence on the subsurface fluid formation) are described for the Aptian–Cenomanian complex of the Ob-Irtysh interfluvium by empirical correlation [9]:

$$Km = 2,500 \cdot \exp ( - 5 \cdot 103L).$$

In this equation,  $L$  is the distance (km) from the marginal zone of the petroliferous basin toward the complex dip, which accords well with sampling results.

Most intense catagenetic transformation of rocks (compacting, dissolution, redeposition of dissolved material, and others) occurs within a relatively narrow depth interval (1,000–2,500 m). In this zone characterized by intense interactions in the fluid-rock system, capacity and reservoir properties of rocks are changeable under variable thermobaric conditions in any direction (increase or decrease).

### 6.1.4 Dissolution

Changes in rock porosity related to dissolution are frequently observed in different rocks regardless of their lithology. For example, the porosity growth established for sandstones of Dzungaria [25] is best manifested beginning from a depth of 1,200 m. The porosity increases due to dissolution of primary carbonate cement, which becomes unstable in new thermodynamic conditions. Moreover, porosity decreases regularly to depths of 1,000–1,500 m in response to geostatic compaction and cementation of interstitial spaces. Downward, carbonate (sometimes, sulfate) cement shows intense dissolution.

The similar process is established in sandstones of the Podkirmakin Formation of the Apsheron Peninsula. These sandstones are characterized by the uniform grain-size composition up to depth of 1,000 m and represent monolith with carbonate cement. Porosity in these sandstones below 1,700 m increases up to 22%, their carbonate cement is almost entirely dissolved, and the rock turns into incoherent sand.

Similar transformations are reported from Central Asia, the Volga-Urals province, Baltic Syncline, and other regions, which allow an inference that calcite dissolution (calcite cement) to certain depths and formation of induced porosity represent regular and widespread phenomenon [25].

Sometimes, separate intervals of sections composed of chemogenic and biogenic carbonate rocks are subjected to dissolution, in addition to primary cement of calcite-bearing terrigenous rocks (see below). In this case, conditions most favorable for calcite dissolution are observed in zones of local stresses, particularly in fissures, which are developed up to depths exceeding 1,500 m. In the depth interval of 1,500–2,500 m, abundance of healed fissures in carbonate rocks decreases, while their permeability and capacity become higher [25].

At the same time, rocks contain healed fissures and cement-filled interstices. The complete dissolution and removal of material is possible, when this process is accompanied by migration of subsurface fluids, which are able to both dissolve calcite and remove it from the system. It is not incidental that the highest induced porosity is characteristic of subsurface fluid discharge areas. This is frequently observed in fault-line zones with ascending migration of solutions undersaturated with calcite relative to host rocks. The areas lacking possibilities for such a migration could retain carbonate- and calcite-bearing terrigenous rocks with the high cementation degree.

Dissolution of carbonate cement and secondary carbonate minerals filling fissures and cavities is most intense in acid environments with high contents of carbon dioxide. The elevated content of the latter in the gaseous phase is characteristic of terminal stages of hydrothermal activity that takes place in fault and fault-line zones. Variations in pH of solutions through the sedimentary section are responsible for alternating calcite dissolution and precipitation zones, i.e., readily and poorly permeable zones.

For example, Devonian sandstones of the Kolva Megaswell in the Timan-Pechora petroliferous province demonstrate the “unambiguously” induced porosity related to dissolution of carbonate minerals in cement [20].

Based on widespread dissolution of cement in terrigenous rocks as well as chemogenic and biogenic carbonate varieties in the relatively narrow interval of the section (1,500–2,000 m), which is accompanied by increase in porosity and permeability of rocks (from 5 to 25% and from 0.001 to  $0.5 \mu\text{m}^2$ , respectively), Minskii [25] introduced notion of the calcite stability depth and defined area and zones of optimal reservoirs in certain intervals of the sedimentary section in petroliferous basins. The optimal reservoirs are those with high capacity at certain depths that are able to keep mineral resources, primarily hydrocarbon accumulations included.

Despite wide development of dissolution processes in both terrigenous (cement) and carbonate rocks proper, they are not regional in scale and associate with tectonically weakened zones (i.e., are of local distribution) and open present-day or past hydrodynamic systems.

### **6.1.5 Cementation**

Secondary transformation of sediments accompanied by porosity and permeability decrease is also reflected in cementation of interstitial spaces. For example, the sedimentary cover of the West Siberian petroliferous basin is lacking incoherent sands except for its uppermost part and marginal zones. This is evident from regeneration fringes in Jurassic and Neocomian terrigenous rocks, the share of which ranges from 0 to 14% with maximal values at depths of 2,000–2,200 m.

The thickness of fringes ranges from 0.01 to 0.14 mm, which is comparable with size of pores. Regional changes in porosity depend on the type, chemical and mineral composition of cement, and regional variations in the last parameters. At the same time, the cement type itself depends on the mineral composition of infilling material with all other things being equal.

For example, Callovian–Oxfordian medium- to fine-grained sandstones of the Ob-Irtysh interfluvium in West Siberia are characterized by the contact and interstitial types of cement in case of clayey hydromica–kaolinite and chlorite–hydromica–kaolinite filling material and basal and interstitial–basal type in case of its calcite composition. Secondary calcite cement fills usually interstices in sedimentary rocks of the basin to make them practically impermeable. For example, permeability of Callovian–Oxfordian sandstones in the Ob-Irtysh interfluvium is significantly reduced in samples with carbonate cement that grade into compact impermeable rocks.

The interstitial space in terrigenous rocks is frequently reduced due to transformation of clay material into cement. The first stage of such transformation is marked by the formation of montmorillonite cement. Depending on the composition of its exchange complex, porosity may partly or entirely be eliminated, when the latter contains calcium or sodium ions. During the section subsidence, montmorillonite becomes unstable in new thermodynamic conditions and grades into mixed-layer hydromicaceous and other clay mineral phases with the insignificant content of crystallization water.

For example, cement in Lower Cretaceous (Aptian) sandstones of the Terek–Caspian Trough occurring at depths exceeding 3,000 m is composed only of chlorite and glauconite. Deeper (up to 3,500 m), the glauconite share in cement decreases up to 1% and is transformed into chlorite.

The formation of new phases in sedimentary rocks is distinctly reflected in the composition of authigenic minerals in cement. Terrigenous sediments of the Dnieper–Donets Depression demonstrate regular downward increase in the glauconite content accompanied by crystal perfection with simultaneous (partial or complete) disappearance of less perfect forms. The ordering degree in mixed-layer phases increases in the same direction, while content of swelling packets, which



are replaced by hydromica and chlorite layers, decreases. Contacts between grains also change downward. This is particularly characteristic of depths of 3,700–4,300, where dissolution textures appear.

The sedimentary section of the West Siberian petroliferous basin demonstrates wide development of clayey cement represented by different minerals: kaolinite, chlorite, hydromica, and montmorillonite. In the lower part of the section, cement is dominated by epigenetic kaolinite and, less commonly, chlorite; the content of these minerals decreases upward the section and toward peripheral parts of the basin, where they are replaced by mixed-layer (montmorillonite–hydromica) and montmorillonite phases (Fig. 6.7).

The formation of new minerals may be connected with past and recent hydrothermal activities.

For example, pre-Jurassic terrigenous sediments of the West Siberian petroliferous basin are universally characterized by low filtration and capacity properties [15]. Their substantial improvement “results only from superimposed secondary processes determined by neotectonics and hydrothermal activity. These processes stimulate development of brecciation zones (tectonic fissuring) with *secondary hydrothermal alterations* caused ... by deep fluids” [42, p. 5]. The Paleozoic quartzite sandstones show several stages in the formation of new minerals. Based on their composition, it is assumed that hydrothermal solutions were first alkaline, hot (450–550°C), and characterized by the elevated oxidizing potential. Subsequently, the oxidizing potential of solutions decreased and they became colder (up to 150–200°C).

The different-age rocks of fault-line zones that separate the Pechora Depression from the Urals are characterized by secondary alterations reflected in their silicification “with the formation of chalcedony veinlets and lenses. . . , which cross bedding surfaces.” Observable are also several mineral associations (bitumens included) that fill fissures (“subsequent processes”). Calcite of younger generation encloses vapor–liquid inclusions with water–salt solution and hydrocarbons. These alterations are thought to be related to the influx of additional matter and fluids from lower intervals of the section [5].

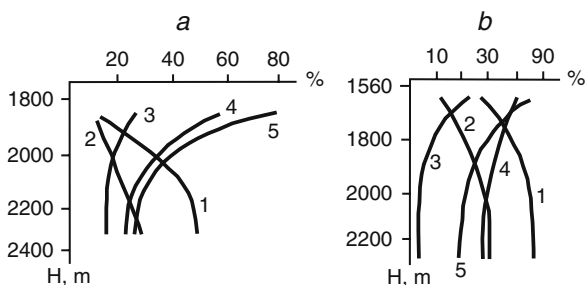


**Fig. 6.7** Changes in the mineral composition with depths (after G.V. Lebedeva and K.A. Chernyshev). (a) In the Surgut area; (b) in the Nizhnevartovsk arch: (1) hydromica, (2) chlorites, (3) kaolinite, (4) mixed-layer hydromica–montmorillonite aggregates, (5) swelling component in mixed-layer aggregates, %

The reduction of the interstitial space in terrigenous rocks is usually determined by secondary mineral formation. For example, boundaries with interstices in Jurassic and Neocomian sediments of the Middle Ob region are marked by hydration, splitting into fibers, and swelling of biotite. The volume of newly formed minerals increases several times, and depending on the transformation degree (chloritization, sideritization, kaolinization) they can fill completely the interstitial space in different-age terrigenous rocks.

In Cenomanian sediments of the Urengoi field, the share of sideritized biotite is 80–90%. Pellitization and kaolinization of feldspars are accompanied by an increase in their initial volume, which results, in the absence of possibilities for increasing the system volume, in filling the interstitial space by decomposition products. In addition, newly formed feldspar phases form regeneration fringes of albite around detrital feldspar grains or, less commonly, euhedral crystals.

In sandy–silty sediments of the West Siberian petroliferous basin, newly formed quartz constitutes regeneration fringes or occurs in the interstitial space, where it completely or partly fills free interstices. There are also newly formed anatase, leucoxene, rutile, siderite, and other minerals, some of which (calcite, siderite, pyrite, barite, and others) precipitates forming cement of the interstitial type.

Despite the selective character of some processes resulting in transformations of terrigenous sedimentary rocks (carbonate or clayey cement, significant or insignificant increase in porosity), they are characterized by regional and local scales.

As a whole, the West Siberian petroliferous basin demonstrates a distinct tendency for downward reduction of the interstitial space in terrigenous rocks from its periphery toward central areas. The integral effect of catagenetic transformations results in porosity and permeability changes in line with the exponential or logarithmic laws. In lower parts of the section, capacity and filtration properties of fluid-hosting rocks are largely yielded by fissuring in substantially compacted and cemented terrigenous rocks.

The downward decrease in the primary porosity and interstitial permeability of terrigenous rocks is universal and regular process established for most petroliferous basins [8, 11, 10]. In lower parts of sedimentary sections, the interstitial permeability is replaced by the fissure one.

Argillites of the Bazhenovka Formation are characterized exclusively by fissure permeability. Its detailed study in the interval of 2,870–2,894 m indicates that the middle part of the section is characterized by maximal values of open induced porosity (jointing), which decreases toward the roof and base of the section. Moreover, such a distribution demonstrates a trend close to the exponential one [26].

In the Terek-Caspian Trough open porosity in Aptian sandstones drilled in the depth interval of 2,000–4,000 m decreases up to 40%. Regeneration textures in these rocks are formed prior to the formation of dissolution textures; the latter are observed in strongly compacted and cemented varieties. The compaction is superimposed by cementation, silicification, calcitization, and other processes, owing to which coarse detrital terrigenous rocks become in some areas impermeable to play role opposite to reservoir properties (interstitial permeability). The subsequent fissuring and dissolution processes may yield fissure capacity and permeability.

In the western Ciscaucasia region, porosity in Lower Cretaceous sandy-silty rocks decreases from 22 to 7% in the depth interval from 1,300 to 4,100 m. Its most notable decrease is observed beginning from the depth of 3,500 m, which is reflected in development of amorphous silica and interstices of sandstones, regeneration of quartz, and replacement of clayey cement by secondary calcite and dolomite. The similar regularity is also established for silty rocks of the Kuma Formation in the same region, where porosity decreases from 35% at depth of 700 m to 2% at 5,000 m. The porosity decrease in silty-sandy rocks is observed against the background of their increasing occurrence depth.

These processes result in transformation of reservoirs into impermeable rocks (lack of interstitial permeability) in absence of tectonic or other fissuring.

For example, in the Levka area (Ciscaucasia), interstitial reservoirs are practically missing at depths exceeding 4,200 m; only fissuring-formed reservoirs with fissure openness of 3–56  $\mu\text{m}$  are developed.

Compaction of sedimentary rock and redistribution of material in them due to dissolution and redeposition are likely unable to eliminate completely interstitial permeability and capacity. For complete filling of pores, additional influx of material by solutions (hydrothermal fluids) is needed. Moreover, these solutions should be non-equilibrium relative to host rocks or, more exactly, oversaturated with different elements, which may serve as a source for newly formed minerals. In such a situation, combined action of the geostatic pressure, dissolution textures at grain contacts, and precipitation of secondary minerals is able to transform interstitial reservoirs into impermeable rocks.

Most favorable conditions for the influx of additional matter exist in tectonically active areas of fault-line zones, where the system of feathering fractures and fissures provides necessary conditions for interconnection between different parts of the sedimentary section in petroliferous basins during intrusion of hydrothermal solutions. In the absence of additional matter sources, interstitial reservoirs may exist also at deep levels. For example, in the Severskaya structure located close to the Levka area in the domain with the calm tectonic regime, interstitial reservoirs in siltstones of the Kuma Formation occur at depths exceeding 4,500 m.

Intense rock transformation took place in Devonian sandstones of the Volgograd region. At the initial stage, compaction of rocks was accompanied by dissolution and regeneration of quartz grains. Subsequent stages were marked by intense dissolution and redeposition of quartz with formation of quartzite sandstones. The content of clayey cement in sandstones decreased from 15 to 5%. At the same time, rocks with the relatively high porosity (up to 15%) were recovered in the depth interval of 4,000–4,200 m. This implies dissolution of older cement, which is possible due to migration of solutions undersaturated with certain elements relative to host rocks. It is also conceivable that this cement became unstable in new thermobaric conditions due to rock subsidence, changes in formation pressures, temperatures, chemical and gas composition of ascending fluids. As was mentioned, primary carbonate cement of terrigenous rocks may partly or completely be dissolved by subsurface fluids enriched in carbon dioxide.

Compaction, cementation, dissolution, and redeposition depend on the sorting degree of material that constitutes terrigenous rocks. For example, in terrigenous rocks of the Uralian and Verkhoyansk foredeeps, effective porosity in poorly sorted polymictic sandstones at depths up to 4,000 m is completely missing. At the same time, deeper well-sorted sandstones retain their high porosity.

Complex and diverse catagenetic processes at large depths resulted in repeated dissolution and redeposition of mineral matter during the long geological history. Changes in thermobaric conditions in the course of subsidence and intrusion of hydrothermal solutions lead to dissolution of some and formation of other minerals more stable in new conditions. The eventual result of these processes is practically complete reduction of the interstitial space and significant decrease (sometimes up to zero) of interstitial permeability at large depths.

Sometimes, several stages are distinguishable in the formation of authigenic minerals indicating repeated migration of subsurface fluids different in the chemical and gas compositions [36].

According to [8], Aptian and Albian sandstones and siltstones in the Kuma petroliferous area occurring at depths of approximately 3,000 m contain early and late diagenetic minerals. The early diagenetic minerals include Fe hydroxides, calcite of the first generation, anatase, calcium phosphates, glauconite, ferruginous chlorites, siderite, and kaolinite. The late diagenetic minerals are calcite of the second generation, quartz, pyrite, and ankerite. Catagenetic minerals are represented by calcite of the third generation and quartz. It is remarkable that calcite of the third generation occurs in variably silicified sandstones and incorporates fragments of regenerated quartz belonging to the earlier generation. This means that calcite of the third generation originated after authigenic quartz. The authors also note that distinct anisotropy in filtration properties of terrigenous rocks is manifested in location of reservoirs with high capacity and permeability properties in the immediate proximity with practically impermeable rocks.

The study of reservoir properties of sandy-silty rocks in some areas of the Azov-Kuban petroliferous basin revealed that they are “almost independent from their occurrence depths” [32]. In the Maikop field, the uppermost and basal parts of well-permeable sequence are composed of poorly permeable rocks. In the opinion of these researchers, sandy members of the East Kuban Depression were subjected to intense transformation by carbonic acid solutions prior to accumulation of hydrocarbons. Locally, rocks with low and high reservoir properties “multiply and intricately replace each other in the section” [32, p. 15]. The authors believe that “abundant bitumen veinlets are evidently determined by catagenetic redistribution of material and superimposed on earlier mineralization” [32, pp. 16–17]. This situation implies vertical migration of matter and confirms development of impermeable or low-permeability boundaries that separate well-permeable zones in the vertical section, i.e., *the stratum-block structure of deep formations*.

Similar regularity is also established for the Dnieper-Donets Depression, where the uppermost and basal layers of the thick sandstone sequence demonstrate more intense transformation as compared with its middle part (Table 6.1).

G.N. Dolenko and A.E. Kiselev showed that in the northwestern part of the Dnieper-Donets Depression, “Middle Paleozoic silty–sandy reservoirs characterized by regular downward deterioration of properties. . .enclose numerous members with high values of parameters” such as porosity, permeability, and others. These researchers established similar structure also for the Black Sea-Crimean and Carpathian petroliferous provinces.

Variations in intensity of transformation of terrigenous rocks at relatively short distances (tens to a few hundreds of meters) provide distinct filtration heterogeneity in all directions and stratum-block structure of deep formations isolated hydrodynamically from each other.

**Table 6.1** Changes in porosity and permeability of terrigenous rocks in the Dnieper-Donets Depression (N.E. Kanskii)

Area	Borehole	Sampling interval, m	Open porosity, %	Permeability, $10^{-3} \mu\text{m}^2$
Chizhevsk	10	3,826–3,875	3.3	0.01
			14.3	5.8
			2.1	0.0
	20	4,150–4,169	11.7	13
			12.9	16
			8.9	1.7
Khar'kov	1	3,855–3,871	13.6	–
			19.2	537.7
			7.0	3.5
			12	37
			19.8	327
Glinsko-Rozbyshevsk	126	3,823–3,875	9.1	1.6
			7.2	2.0
			14.4	87.5
	131	3,800–3,818	5.5	0.1
			9	2.5
			15.2	168.3
			13.5	18

In a closed system which receives no additional material, solutions oversaturated in new thermodynamic conditions with calcite included, such situation was impossible. Consequently, hydrothermal solutions that migrated through this part of the Azov-Kuban petroliferous basin were enriched in calcium at some stage of its development.

Similar regularities in vertical migration of fluids are established also in West Siberia [17–19] and Kamchatka. In the last region, pebbles in alluvium of the Pazhetka River are cemented by opal, chalcedony, and other minerals precipitated from recent hydrothermal solutions [23].

All these facts show that capacity and filtration properties of terrigenous rocks in negative stratified structures are forming under the influence of several factors

(sedimentation, diagenetic and catagenetic transformations). The latter determine downward (to certain depths) decrease in interstitial permeability, strengthening structural–crystalline bonds, deterioration of plasticity properties, and increase in ability to fissuring.

The rocks constituting deep members of sedimentary sections in such structures are largely characterized by fissure capacity and permeability and distinct anisotropy reflected in irregular alternation of well-permeable and practically impermeable rocks, which is determined by tectonic processes, influx of hydrothermal solutions from lower parts of the sedimentary section and basement, and phase transformations in the fluid-rock system.

Thus, at depths exceeding 3,000 m, well-permeable rocks alternate with practically impermeable varieties. The same rocks may serve as reservoirs in some geological epochs and as screening caprocks during others.

For example, oil and gas fields associated with the Pasha and Staryi Oskol formations in the North Caspian Depression occur at depths of 4,800–5,300 m. They are screened by entirely silicified sandstones (accumulations of the Kudinov-Korobkov Swell). In this region, intense jointing is established in both sandy–silty and clayey rocks at depth exceeding 5,000 m. Commercial oil accumulations in the Bazhenovka clays of West Siberia are overlain by clayey–silty rocks.

Interstitial reservoirs in the Chernolesk Depression, platform slope of the Terek-Caspian Trough, and East Manych Trough are observable to depths of 4,000 m, where they are replaced by their fissure counterparts. In the Carpathian foredeep, low porosity and intense jointing in sandy–silty rocks accompanied by widespread silicification and calcitization are established in the depth interval of 4,000–5,000 m.

Khanin [16], who studied in detail reservoir properties of rocks, arrived at the logical conclusion that owing to dissolution, compaction, and fissuring in sandy–silty rocks of deep formations, they may serve as both reservoir and caprock.

### **6.1.6 Tectonics**

The influence of tectonic stresses on the formation of filtration properties is well known. Tectonic movements result in fissuring in all lithologies, clayey varieties included. This reflected, in particular, in the growth of filtration capacity of carbonate and clayey rocks under valleys of different-order rivers. Moreover, the difference between filtration capacity in watershed and valley areas amounts to one to two orders of magnitude and higher, which is established by many groundwater-prospecting works. For example, R.S. Shtengelov (1974) revealed such a difference for the Iset River valley. Precisely elevated jointing in river valleys, which are confined to tectonically weakened zones, controls drainage of deep petroliferous formations at depths of 2,000–3,000 m (Ob, Volga, Kuma, Volkhov, and other rivers).

Tectonic processes determine elevated jointing at arches, limbs, and periclinal positive structures. The study of oil and condensate microfossils in some oil and gas fields of West Siberia and the Urals-Volga region shows that migrating microfossils

are confined to steep limbs of structures and tectonic zones. Most favorable filtration properties in weakened zones are marked at the surface by gas, thermal, and others anomalies, discharge of salt springs, oil seeps, and other phenomena. There are numerous facts confirming development of elevated permeability that involves the entire sedimentary section of petroliferous basins.

### 6.1.7 Hydraulic Fracturing

Tectonic movements accompanied by horizontal and vertical displacements of sedimentary cover blocks stimulate formation of differently oriented fissures in zones of tectonic stress relaxation. The formed tectonic fractures continue developing with formation of additional fissures due to intrusion of high-pressure fluids. Formation and development of fissures in such situations are determined by hydraulic fracturing.

Hydraulic fracturing is a well-known phenomenon in petroleum geology, where it is used for increasing permeability around wells and yield of productive formations (Yu.P. Zheltov, 1975). It is among the most effective similar methods. The method consists in providing the formation pressure in liquid, which should overcome the geostatic load and cementation of rocks to stimulate their rapture with formation of vertical and horizontal fissures from a few to tens of meters long and from a few millimeters to a few centimeters wide. It is established by drilling that fissures resulting from hydraulic fracturing amount to 15 cm across. The special photographic equipment registers development of fracturing after natural fissures under influence of high-pressure fluids. Sometimes, hydraulic fracturing accompanies drilling with high-density clay mud, which results in its consumption by fissures.

Let us consider formation conditions of hydraulic fracturing. The vertical stress ( $\sigma$ ) is determined from equation (Yu.P. Zheltov, 1975)

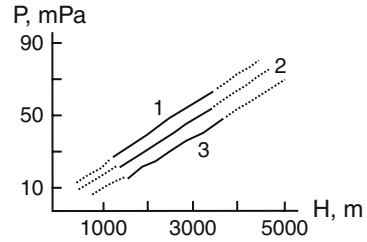
$$q_z = (q_g - nP)/(1 - n), \quad (6.4)$$

where  $q_z$  is the total geostatic load,  $\rho$  is density of overlying rocks,  $z$  is occurrence depth,  $n$  is porosity, and  $P$  is liquid pressure.

During hydraulic fracturing  $\sigma_\tau = \alpha q_g$  or  $\sigma_\tau = q_z$ . Lateral pressure  $q_\infty = \alpha q_g$ . The coefficient  $\sigma$  that is determined conditionally is accepted to range from 0.3 to 0.7 for brittle rocks, equal to 1.0 for soft rocks, and  $\alpha = \nu(1-\nu)n$  ( $\nu$  is the Poisson's ratio) for elastic rocks in the absence of tectonic stresses. For increasing the engineering strength of calculations, it can likely be accepted that  $q_\infty = q_g$ .

Figure 6.8 presents data on fissure opening pressures measured in 276 wells in the eastern coast of the United States. It is seen that hydraulic fracturing in the examined interval of the section (depths up to 3,500 m) occurs under variable liquid pressures below the geostatic one. At a depth of 3,000 m, it takes place under pressures ranging from 42 to 61 mPa. The formation of such fissures under pressures lower as

**Fig. 6.8** Correlation between fissure opening pressure and occurrence depths of beds (after P.P. Scott and V.I. Berlen). (1) Maximal; (2) medium; (3) minimal



compared with the geostatic one is explained by development of older tectonic and lithological-facies fractures.

The study of hydraulic fracturing revealed the following regularity: the higher is fluid saturation of rocks, the more favorable are conditions for development of vertical (primarily) fissures. The latter is explained by the fact that in the absence of horizontal tectonic compression the lateral pressure is always lower than the vertical geostatic load that prevents the formation of horizontal fissures. Their formation occurs under the ratio between the geostatic and formation pressures derived from the following equation:

$$q_g = P(1 - \sqrt{1 - \alpha^2}).$$

It follows that energy of ascending fluids required for the formation of horizontal fissures should exceed the geostatic load several times. For example, under  $\alpha = 0.8$ , the pressure on the surface of the horizontal fissure should be  $2.5 q_g$ .

The maximal width of fissure  $W$  (Yu.P. Zheltov, 1975) in its central part is derived from the equation

$$W = \frac{8(1 - \nu^2)PR}{\pi E} \arccos \alpha, \tag{6.5}$$

where  $R$  is radius of fissure and  $E$  is the Young modulus.

This equation was obtained under the condition that elastic material encloses a ring-shaped horizontal fissure with radius  $R$ , the surface of which is subjected to the permanent pressure  $P$ , and material located at infinitely large distance from fissure ends experiences the geostatic load  $q_g$ .

This equation shows that the width of fissure is directly proportional to its initial width and the formation fluid pressure on its surface, with all other factors being the same. When there is no opportunity for the fluid to outflow (healing of fissure ends), formation pressures are preserved for any long period. The above-mentioned solutions describe development of hydraulic fracturing without accounting for the hydraulic factor itself, primarily changes in the formation pressure in the fissure.

The origination and development of fissures with participation of the hydraulic factor can be described in the following way. Liquid pumped, naturally or artificially, into the formation changes parameters of fissures (width and length) and



pressure along fissures. It is assumed that liquid penetrates only into the fissure, while the rock matrix remains impermeable (non-filterable liquid). In this situation, the integral solution for the maximal widths of the horizontal fissure should be as follows:

$$W = \frac{8(1 - \nu^2)(P_c - q_g)R}{\pi E}, \quad (6.6)$$

where  $P_c$  is the liquid pressure in the conduit (tectonic fracture or borehole). Let us consider parameters of the vertical fissure resulting from filtration of absolutely non-filterable liquid. The pressure in the conduit (borehole) under the formation pressure tending to the geostatic one depends on the volume of pumped liquid ( $V_1$ ) and other parameters in line with the following equation (Yu.P. Zheltov, 1975):

$$\frac{P_c}{q_\infty} \left( \frac{P_c}{q_\infty} - 1 \right)^3 = 5.25 \frac{1}{(1 - \nu^2)^2} \left( \frac{E}{q_\infty} \right)^2 \frac{Q\mu}{q_\infty V_c}. \quad (6.7)$$

In this case, maximal parameters of fissures depend on

$$W = \frac{4(1 - \nu^2)L}{E}(P_c - q_\infty);$$

$$L = \sqrt{\frac{V_c E}{5.6(1 - \nu^2)h(P_c - q_c)}}, \quad (6.8)$$

where  $h$  is the bed thickness and  $L$  is a half-length of the fissure.

Hydraulic fracturing is frequently a spontaneous process. For example, during exploitation of the Nal'chik deposit of mineral waters, the latter flushed from Lower Cretaceous strata into Upper Cretaceous rocks separated from each other by Albian clays approximately 100 m thick. Simultaneously, the Cl content, mineralization, and temperature of groundwater in Upper Cretaceous rocks increased from 0.4 to 1.0 g/l, from 1.2 to 2.5 g/l, and from 34 to 38°C, respectively.

## 6.2 Development of Reservoir Properties in Carbonate Rocks

The more complicated task is the study of regional changes in permeability of carbonate and sulfate rocks at different catagenesis stages (some aspects of this problem are considered in the previous section). These rocks are also usually characterized by downward changes in porosity and permeability. Deterioration in filtration properties of carbonate rocks may be explained by negligible influence of surface factors (leaching, fossil, and recent karst), partial or complete healing of fissures, and compaction under the geostatic load.

Similar to terrigenous rocks, carbonate and sulfate varieties are subjected to diagenetic and catagenetic transformations, which is reflected in compaction, recrystallization of primary calcite, dolomitization, sulfatization, calcitization, silicification, and redeposition of material.

Carbonate rocks demonstrate cyclic formation patterns related to sedimentation. This is evident primarily from larger capacity of upper parts of carbonate cycles [20, 25, 35], i.e., heterogeneity is formed at the sedimentation stage (Pripyat and North Caspian depressions, Nep-Botuoba anticline). Main factors responsible for transformation of carbonate rocks are geostatic compaction, recrystallization, fissuring, leaching (karst processes), dolomitization, and mineral formation.

In the Timan-Pechora petroliferous basin, Ordovician–Lower Devonian “interstitial–cavernous–fissured” reservoirs were largely formed by tectonic processes, erosion, and leaching. Filtration–capacity properties of the Upper Devonian–Tournaisian complex are thought to be related mainly to reefogenic buildups, which crossed “all the large tectonic elements” and isolated carbonate banks that existed during sedimentation. The Upper Viséan–Lower Permian carbonate complex demonstrates facies diversity in its upper part (combination of reef–bank sediments and depression facies). Thus, filtration heterogeneity was forming simultaneously with sedimentation.

### **6.2.1 Compaction**

Contrary to crystallization, gravitational compaction plays a significant role in clayey parts of the section (clayey limestones) [31]. Calculations show that the spherical cavity (formed, for example, by karst leaching) in monolithic rocks resists to significant loads, i.e., survives at great depths. When there is an opportunity for liquid to flow out of the cavity, the latter is destroyed under the geostatic pressure of 60 mPa, which corresponds to depths of 2,400–2,500 m.

Depending on changes in thermobaric conditions, influx rates, and chemical composition of migrating solutions, capacity of carbonate rocks changes in all the directions and with time. Carbonate and sulfate minerals as well as rock-forming minerals of terrigenous varieties are unstable under changeable thermobaric conditions, which depend on the occurrence depth, tectonic settings, and hydrothermal activity. Due to changes in these processes, less stable minerals are replaced by more stable, although frequently of the same chemical composition. This is well evident from the successive formation of different calcite generations at different occurrence depths of carbonate rocks and terrigenous varieties with carbonate cement.

Filling of interstices and fissures in different lithologies by newly formed calcite, which is stable at great depths, is a well-known fact. Downward changes in carbonate rocks are poorly studied so far. It is conceivable, however, that their capacity and filtration properties should change in this direction similar to these parameters in terrigenous rocks.

The share of secondary calcite filling the interstices and fissures in carbonate rocks of the Osa Horizon in the Irkutsk Amphitheater decreases upward the section

from 8–13 to 4–6%. These rocks are characterized also by precipitation of secondary sulfate in the interstices and fissures, the content of which amount to 7.2%. The content of secondary salts (halite) in dolomites and limestones is as high as 13–17 and 6.5–10%, respectively. The interstices and cavities filled with halite range from 0.05 to 7 mm in size. Some of them are connected by short fissures (20–200  $\mu\text{m}$ ), which are also filled with halite. In addition to short fissures, these rocks contain long halite veins that cross the entire sequence. The fissures are usually perpendicular or inclined relative to bedding surfaces. Their development implies that the formation of the interstices and fissures during recrystallization and dolomitization in carbonate rocks of the Osa Horizon was followed by the influx of brines. These brines filled interstices, cavities, and connecting fissures to form halite under decreased temperatures and formation pressures.

In addition to the healed fractures, there are open fissures with the volumetric density of 3–66  $\text{m}^{-1}$ . It should be noted that the fissure permeability is two to three orders of magnitude higher as compared with the intergranular interstitial one ( $<10^{-5}$  versus  $10^{-2}$   $\mu\text{m}^2$ ) [23, 31, 34].

Catagenetic recrystallization, dolomitization, leaching, and tectonic fissuring are positive processes responsible for the formation of secondary porosity in rocks of the Osa Horizon. Oil and gas occurrences in the latter are confined to granular secondary dolomites that originated from dolomitized primary limestones. In these rocks, newly formed interstices are subsequently healed by mineral or clayey-organic matter as well. Intensity of rock transformation varies through the section due to leaching, sulfatization, silicification, and calcitization. The integral action of these processes results in variations of porosity (from 4 to 40%), which grows downward up to depths of 800 m and in the interval of 1,250–1,250 m and decreases at 800–1,000 m and below 1,250 m [23, 31, 34].

The upper Cretaceous section of the Terek-Sunzha region (eastern Ciscaucasia) is composed of limestones up to 400 m thick with marl interbeds. The limestones are slightly altered by post-sedimentary processes: dominant recrystallization and leaching. The integral porosity does not exceed 7%. Main capacity and filtration properties are determined by rock jointing that amounts to 36.6/ $\text{m}^{-4}$  and higher. It should be emphasized that the secondary porosity and permeability coefficient of limestones change upward the section (Fig. 6.9).

The section is characterized by abrupt reduction of filtration properties toward its roof and base up to complete impermeability. This indicates more intense healing of primary interstices and fissures in the basal part of the limestones section, i.e., near the boundary between different lithologies: limestones and Aptian clays. It is conceivable that similar situation is characteristic also of the boundary with the overlying sequence, which is shown by the dotted line in Fig. 6.9b.

Thus, all these processes combined with development of impermeable faults that separate the Malgobek–Voznesensk–Aliyurt structure from surrounding structures yielded prerequisites for preserving abnormally high formation pressures in limestones. The fields in question are characterized by relatively high (exceeding unit) vertical gradients of formation pressures. Such a distribution of capacity and filtration properties confirms the block structure with impermeable boundaries of variable origin.

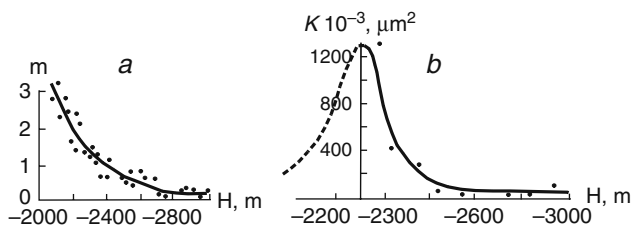


**Fig. 6.9** Changes in the coefficients of general secondary voidage (a) and permeability (b) (after N.P. Lebedev and A.L. Tagunova). The *solid line* is based on factual data, *dashed line* is hypothetical based on the height of the Malgobek–Voznesensk structure (eastern Ciscaucasia)

In 1994, S.A. Denk established substantial heterogeneity in capacity and filtration properties for carbonate deposits in the Perm region of the Urals. He noted the wide distribution of cavernous–fissured reservoirs with fissures (10–20 m wide and 2.2–2.4 m long) filled with clay, calcite, anhydrite, and solid bituminous matter as well as alternation of productive and “dry” elements in the section. This researcher argues against significance of the rock matrix in the formation of capacity properties.

Compaction and post-sedimentary transformation of carbonate rocks result in downward deterioration of their capacity and filtration properties. At the same time, leaching, recrystallization, dolomitization, and other processes lead to the formation of their both abnormally high and abnormally low parameters (up to complete impermeability) in particular intervals of the section. Natural hydraulic fracturing and tectonic processes that disturb rock continuity result in the formation of zones with elevated jointing and permeability. “Fissures play the role of conduits between porous and cavernous parts of the section. Tectonic processes and hydrothermal activity occur permanently or intermittently. In this connection, zones with elevated permeability are healed from time to time to become reactivated due to resumed tectonic and hydrothermal activities.”

The formation of capacity and filtration properties in the Semiluki Horizon of the Pripyat Depression is determined by tectonics. Changes in these properties occur along local linear zones with “long axes being parallel to the strike of a regional tectonic fracture” [30, p. 8]. Near the fracture, reservoir properties are deteriorated. This zone is accompanied by a wide band with maximal filtration values, which decrease again away from the fault. In our opinion, such patterns are explainable by migration of hydrothermal solutions upward the section, formation of the fluid intrusion in the Semiluki Horizon, and subsequent precipitation of secondary minerals along the periphery of this intrusion (partial or complete healing of interstices and fissures). Most notable changes in thermobaric conditions, formation pressures included, occur precisely along its boundaries, where fluids discharge into neighboring elements of the section. Similar situation is likely characteristic also of over- and underlying reservoirs.

The subsided parts of petroliferous basins (below 2.0–2.5 km) show no regional regularities in changes of filtration properties due to dominant influence of endogenic processes, which are manifested locally and play an important role in the formation of medium permeability.

Thus, both near-surface and deeply occurring carbonate rocks are characterized by high lateral and vertical variability in filtration and capacity properties, which change, in addition, through geological time. These changes are frequently determined by past and recent hydrothermal activities [4].

### 6.3 Formation of Clayey Reservoirs

Clayey sediments and clays constitute up to 70% of sedimentary sections in artesian basins, intermontane depressions, and marginal troughs (Fergana, Issyk-Kul, and Tajik depressions, Uralian and Caucasian foredeeps). This is particularly true of young basins (eastern Ciscaucasia, Turan Plate, West Siberia, and others).

It means that the role of clayey sediments in the formation of deep fluids is significant. Similar to hydrodynamics, many aspects of their participation in this process remain ambiguous. First of all, the following questions are unanswered: (1) Are clayey sediments permeable for water and hydrocarbons or not? (2) To what extent can they serve as a caprock for oil and gas accumulations? (3) Do hydrodynamic relationships exist between petroliferous formations separated by clayey members? (4) Is it possible to describe migration of subsurface fluids by linear filtration law? (5) How is the formation pressure distributed in compacting clayey sediments? and (6) What is the role of clays in development of formation pressures and chemical composition of subsurface fluids?

Let us consider one of the least known aspects concerning the formation of permeability of clayey rocks in order to estimate vertical hydrodynamic interaction between separate parts of sections in petroliferous basins.

Practically complete unavailability of summarizing works is one of the causes responsible for ambiguous interpretations of the role of clayey sediments in the formation of deep fluids.

Another cause responsible for such a situation is the complex nature of sediments in question. Individual clay minerals constituting corresponding sediments represent a complex natural system interacting with water solutions. Many experimental and theoretical studies fail to reveal in full and unambiguously interpret relationships of mineral matter with solutions. Physical properties and behavior of water in the bonded and crystalline states as well as physical and physicochemical processes occurring in this complex natural system are insufficiently studied. At the same time available empirical material needs generalization and comprehensive analysis aimed at revealing main regularities that govern fluid migration in clayey formations.

Variations in permeability of clayey sediments are determined by sedimentation settings, geostatic compaction, thermal impact, and post-diagenetic processes that form macro- and microheterogeneities.

As was mentioned, sedimentation settings determine regional variations in lithology of clayey sediments (macroheterogeneity). For example, clayey caprocks can largely (90% and more) be composed of finely dispersed clay particles in central parts of petroliferous basins and largely sandy-silty to sandy sediments in their marginal areas. Such lithological changes are usually accompanied by increase

in thicknesses of sedimentary sections. The growth of clay content in sediments and their thickness should result in significant deterioration of filtration properties toward central parts of petroliferous basins.

In syngenetic positive structures of the higher order, this regional (background) regularity is superimposed by local heterogeneities related to the individual structures. This is particularly true of areas with internal sources of detrital material. Many researchers reported on such facts.

### 6.3.1 Geostatic Compaction

Geostatic compaction is one of the most significant processes in catagenetic transformation of clayey sediments. Under the geostatic pressure, clays reduce their initial thickness by 10%, while for sandy varieties, this parameter is only a few percent. Figure 6.10 demonstrate curves of natural compaction compiled for clayey rocks from West Siberia and downward changes in compaction coefficients  $d\varepsilon/d\sigma$  and porosity  $\varepsilon$ . They are described by empirical exponential functions.

Figure 6.10 shows that the porosity and compaction coefficients decrease from 0.7 and 0.5, respectively, to  $<0.05$  at depths exceeding 4,000 m. Such a substantial downward decrease in absolute porosity should result undoubtedly in appearance of isolated subcapillary interstices and, accordingly, significant reduction of interstitial permeability of clays.

The figure demonstrates also a curve of theoretical changes in the interstitial permeability coefficient. Curve 1 was calculated using equation (6.2). It is seen that the permeability coefficient is an order of magnitude lower at depths exceeding 4,000 m as compared with its value at shallower levels.

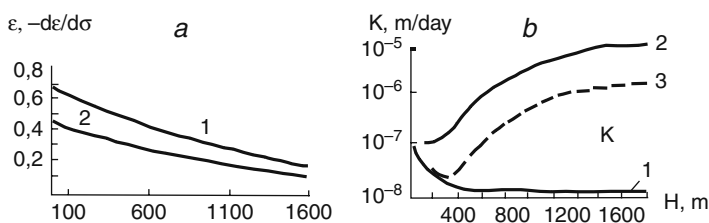


**Fig. 6.10** Changes in physico-mechanical properties of clayey rocks. (a) Compaction (1) and porosity (2) coefficients; (b) permeability coefficient: (1) depending on depths, (2) depending on temperature, (3) depending on depth and temperature (initial permeability  $K$  of  $10^{-7}$  m/day)

### 6.3.2 Temperature and Mineralization

The temperature of sedimentary rocks and subsurface fluids and their mineralization increase downward the section. Due to changes in the thermal field, interstitial permeability of clayey sediments should increase in particular stratigraphic units both

downward the section and from the petroliferous basin periphery toward its central areas. The temperature increase reduces viscosity of filtering liquid, which leads to drastic decrease in capillary interaction between liquid and mineral framework of rocks, which is equivalent to the increase in effective porosity and interstitial permeability of sediments. Even for sandy rocks, the temperature growth increases permeability several times. In clayey varieties, capillary forces become incomparably stronger as compared with coarse-grained sediments; therefore, changes in their permeability are substantially more significant.

According to I.A. Brillings (1977), permeability of montmorillonite under heating from 20 to 80°C increases more than two orders of magnitude as compared with its initial value (Fig. 6.10, Curve 2).

Z.A. Vodovatova established that in low-porosity sandstones with the clay content of 13–37 wt.%, the permeability coefficient increases by 200–300% in the temperature interval of 20–90°C. The heating effect is higher in rocks with the higher clay content. Substantial influence of heating on rock permeability during filtration of liquids with different chemical compositions is established by laboratory studies (V.M. Gol'dberg, 1980). It is shown that during heating of the sample from 20 to 90°C, the permeability coefficient increases three to five times for kaolin and an order of magnitude and more for montmorillonite. The most rapid growth of interstitial permeability is observed in the temperature interval of 60–90°C. This is accompanied by the growth of the molecular diffusion coefficient as well as thermal and electric parameters of clayey sediments.

In addition, permeability of montmorillonite and kaolinite clays changes with the growth of mineralization in filtering liquid. Many experiments demonstrate that permeability of clays during filtration of distilled water is always lower as compared with that for solutions. This is a well-known fact. Solutions with mineralization ranging from 1 to 30 g/dm<sup>2</sup> provide approximately 70% of the permeability growth. In some experiments, the permeability increased more than an order of magnitude. The influence of solution mineralization on interstitial permeability is more notable in montmorillonite clays than in kaolinite varieties. Moreover, the growth of interstitial permeability is higher or lower, when the exchange complex of montmorillonite includes Na and Ca, respectively.

The simultaneous increase in temperature and mineralization results in more substantial growth of the permeability coefficient than under influence of one of these factors. Thus, the studies of correlation between permeability of fine-grained sediments, on the one hand, and temperature and mineralization, on the other, provide grounds for the inference that the interstitial permeability of clays should substantially increase downward.

Figure 6.10 (Curve 3) illustrates the integral influence of compaction and heating on permeability of clayey rocks. The curve was compiled with assumption that temperature is characterized by the normal vertical distribution. The heating influence on permeability of clayey sediments was taken into account beginning from the depth, where temperature exceeds 20°C (available experimental data exceed this level). The figure shows that the interstitial permeability of clayey sediments first rapidly decreases (in limits of an order of magnitude) with depths due to

compaction and then grows gradually downward under influence of heating. The combined effect of these factors below 800–1,000 m results in increased *interstitial* porosity (leaving aside other factors responsible for the formation of reservoir properties). Figure 6.10 presents only a model curve based on limited experimental data. In natural conditions, deviations from the latter cannot be ruled out.

### 6.3.3 Mineralogical Composition of Clayey Rocks

The mineralogical composition of clayey rocks influences notably their permeability as well. Many researchers [1, 36, 37, and others] note that in the montmorillonite–kaolinite succession the minimal permeability is characteristic of montmorillonite clays, which contain swelling packets and large quantity of fixed water. Kaolinite clays demonstrate the maximal permeability. It is undoubted that permeability of clays increases several times with decrease in the ability of clay minerals to swelling (kaolinite, chlorite, illite). According to M.A. Tsvetkova, addition of 2% of hydrobiotite, kaolinite, and montmorillonite to quartz sand reduces its permeability from an initial 60.3 to 27.5, 17.4, and 5.8  $\mu\text{m}^2$ , respectively. The addition of 20% of these minerals decreases permeability of sands to respective 0.54, 0.12, and 0.02  $\mu\text{m}^2$  or one to two orders of magnitude.

At the same time, it is established for many regions of Russia and adjacent countries (West Siberia, Turan Plate, Fergana Depression, Ciscaucasia, and others) that different-age clayey rocks demonstrate changes in their mineralogical compositions down the section. While minerals of the montmorillonite groups prevail at shallow depths, they are successively replaced downward by mixed-layer varieties, hydromicas, kaolinite, and chlorite.

For example, Paleogene clays of the Fergana Depression show significant decrease in the content of the swelling phase among mixed-layer minerals from 80 to 20% through the depth interval of 1,800–2,000 m. Similar changes are observable also in the temperature interval of 70–100°C corresponding to these depths (Fig. 6.11). This is explained by the fact that the successive downward replacement

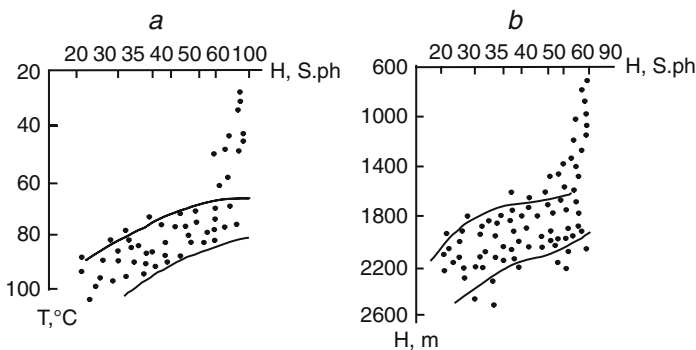


**Fig. 6.11** Correlation between contents of the swelling phase in clayey rocks of the Fergana Depression and changes in temperature (a) and subsidence depth (b)



of minerals is accompanied by decrease in the content of bonded and crystallization water, which reduces plasticity of clays and increases their rigidity (consequently, ability to fissuring).

The Jurassic sediments of the Fergana Depression experienced as well substantial catagenetic transformations reflected in changes of their mineralogical compositions [1]. Below 2,200 m, montmorillonite is practically missing; chlorite replaces hydrobiotite, while trioctahedral hydromica and montmorillonite give way to vermiculite. The study of over 800 samples revealed that Cretaceous sediments are characterized by regular downward decrease in the content of swelling phases. Paleogene clays are plastic up to depths of 1,800 m, compacted in the interval of 1,800–3,400 m, and argillite-like below this level. At depths of 1,400 m, mixed-layer phases of the hydromica–montmorillonite composition appear, in addition to montmorillonite; their content increases significantly from depths of 1,800 to 1,900 m. Montmorillonite is registered to depths of 2,800–2,900 m. Downward, swelling clay minerals are represented by mixed-layer phases and hydromicas prevail below 3,600 m. At depths of 5,630–5,790 m, montmorillonite and mixed layer are missing, being replaced by hydromica and chlorite.

Montmorillonite hydration becomes notable under relatively low temperatures (55°C). Under temperatures of 80–85°C, mixed-layer phases with low contents (up to 30%) of swelling packets prevail among clay minerals. Consequently, with regard to clayey rocks of the Fergana Depression we can speak about the thermodynamic (geochemical) threshold (combination of pressure and temperature) marked by significant changes in the mineral composition of clayey rocks (Fig. 6.12) and, accordingly, sharp increase in their interstitial permeability.

Clayey components of sediments and cement in West Siberia are represented by different minerals: kaolinite, chlorite, hydromicas, and montmorillonite. The lower part of the section is dominated by kaolinite and, less commonly,

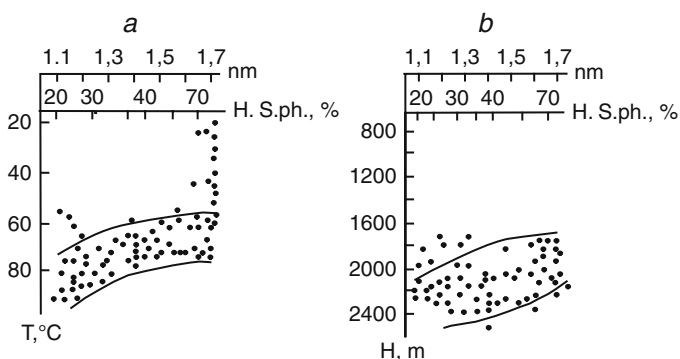


**Fig. 6.12** Correlation between contents of labile packets and mixed-layer montmorillonite phase in clayey sediments of West Siberia and changes in temperature (a) and subsidence depth (b) (after B.A. Lebedev and others)

chlorite, contents of which decrease upward the section, where they are replaced by mixed-layer phases and montmorillonite (Figs. 6.7, 6.11, and 6.12). In addition, recrystallization of clay minerals results in transition of finely dispersed kaolinite into its well-crystallized variety.

A.K. Dorofeeva established that the lower boundary of the montmorillonite distribution in the lower Sarmatian section of the Vil'ge-Volitsa zone (Carpathian foredeep) is located at 2,900–3,200 m with temperatures of 90–102°C. Mixed-layer minerals occur up to depths with temperatures of 120–160°C.

In the Terek-Sunzha area, Chokrakian clayey sediments are lacking montmorillonite, which is replaced by mixed-layer phases. The latter are transformed downward into hydromica. In the same direction, plasticity of clays decreases, while their fissuring decreases and they are transformed into argillites and shales [27].

Thus, clayey sediments of the Fergana Depression, West Siberia, Ciscaucasia, and other regions are characterized by the regularity in common: the mineral composition changes both through the entire section and within individual stratigraphic units, i.e., clay minerals reflect vertical catagenetic zoning. This universal phenomenon allows three catagenesis zones with different clay minerals to be defined in the sedimentary section of the crust: early, middle, and late catagenesis [27].

The *upper zone* (early catagenesis) is characterized by unfinished catagenesis, i.e., sediments are un lithified and diagenetically unaltered. The dominant process in this zone is water release from sediment interstices and interplane spaces of three-stage structures. No authigenic clay minerals of dioctahedral type are formed in this zone regardless of the initial composition of sediments, which is explained by low pressures and temperatures.

The *middle zone* (middle catagenesis) is characterized by authigenic formation of clay minerals with the dioctahedral structure. This zone retains volcanogenic minerals of the montmorillonite group and mixed-layer phases related to dehydration of hydromicas and containing molecular water layers (over 40% of swelling packets). The zone is characterized by development of chamosite, kaolinite, elongated and scaled montmorillonite, and glauconite.

In the *lower zone* (late catagenesis), authigenic formation of clay minerals terminates. The main feature of this zone is transformation of most volcanogenic montmorillonite and mixed-layer minerals containing over 40% of swelling packets into varieties with the monomolecular water layer. Clayey rocks are largely represented by argillites.

Among clay minerals, chlorite becomes more abundant and better crystallized. Kaolinite in basal layers of this zone is unstable and subjected to decomposition.

In marine sediments, intense transformation of primary minerals and formation of their authigenic varieties are characteristic of all three zones. Figures 6.7, 6.11, and 6.12 demonstrate that most intense dehydration and transformation of clayey matter occur in the depth interval of 1,800–2,200 m under temperatures of 60–90°C.

Dehydration proceeds under combined influence of many factors. Relatively narrow depth and temperature intervals imply the thermobaric threshold of geochemical transformation of clay minerals in these conditions. Transformation of clay minerals

at different stages of catagenesis is confirmed by modeling [37] in conditions close to natural with high pressures and temperatures. For example, after experiments lasting less than 4 days, the five-component association of clay minerals (kaolinite, hydromica, dioctahedral montmorillonite, and morite) from Paleogene clayey rocks of the Suzak field in the Fergana Depression became two component (hydromica–chlorite) in the medium containing K and Mg ions. The composition of clay minerals after the experiment was similar to that of the Turkestan Beds occurring at depths of 5.0–5.5 km.

The directed (under increasing depths and temperature) transformation of the mineral composition of clayey sediments should result in the growth of their interstitial permeability by several orders of magnitude as compared with upper parts of the section with dominant montmorillonite among clay minerals. The temperature and mineralization of migrating solutions change this parameter in the same direction and with the same intensity.

Nevertheless, other factors, not interstitial permeability, determine possibilities and scales of deep fluid migration in clayey sediments. It is not incidental that thousands of measurements of permeability in clayey rocks demonstrate their either zero or extremely low values, which determined eventually relation to them as to a fluid-confining formation. The interstitial space of clayey rocks at deep levels may be partly or entirely filled with secondary cement and newly formed minerals, which explains low or zero interstitial permeability observed in experimental conditions.

Mineral transformations of clayey rocks determine, along with other factors, their macro- and microheterogeneities, primarily jointing included. At different stages of their transformation (diagenesis, catagenesis), clays turn from highly porous muds into rocks with strong structural bonds (mud–argillite–shale succession) and capable of fissuring.

Jointing of clayey rocks is of great significance and should be taken into consideration in studies of their permeability. It is sufficient to say that expenditures of water through the clay rock surface of 1 km<sup>2</sup> and their fissures filled with sandy or silty material with the integral surface area of 1 m<sup>2</sup> are equal (under equal vertical pressure gradients and permeability coefficients of clayey and coarse-grained rocks differing from each other by six orders of magnitude). Even greater contrast is observed in the case of open fissures.

This is explained by the fact that owing to abundant differently oriented fissures (Fig. 6.13) the largest share of fluid expenditure is provided through fissures, which represent main filtration channels in clay rocks. Availability of fissures explains large discrepancy between estimates obtained for permeability by different methods: at samples in laboratory conditions, in natural conditions based on hydrodynamic sampling, and others. This discrepancy amounts to two to three orders of magnitude. Understated values obtained from samples are explained by the lower scale of sampling as compared with that of micro- and macroheterogeneities, i.e., probability of fissure or sandy interbed occurrence in the clay sample is low. Moreover, fissure-enclosing samples are usually ignored since it is difficult to impart them shapes required for the study at the special equipment.

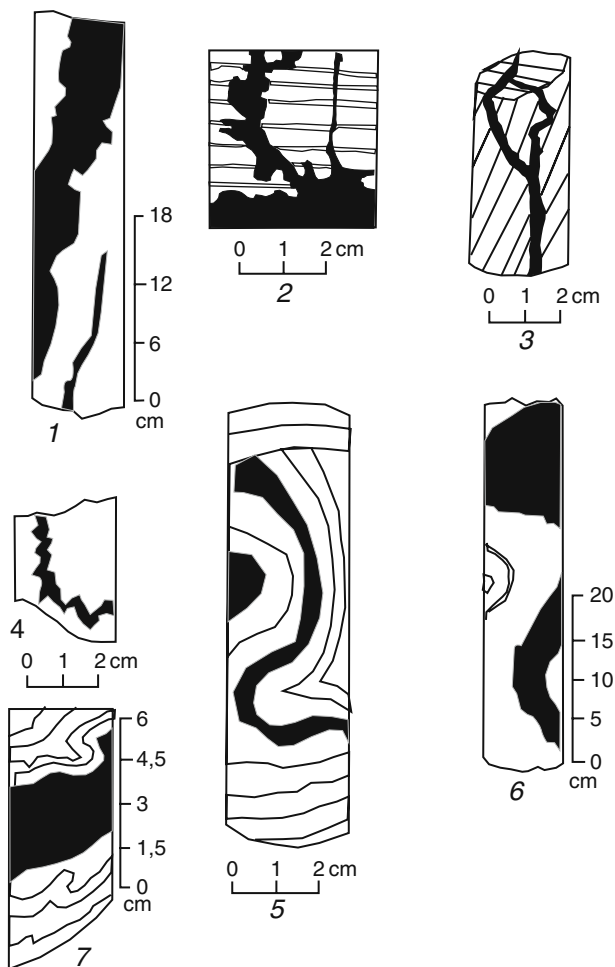


**Fig. 6.13** Microheterogeneity (jointing) in Jurassic clays and argillites of West Siberia. *Black* are fissures filled with sandy-silty material, *light* are clays and argillites

The study of aquifers and low-permeability beds by hydrodynamic sampling and other methods involves substantially larger areas, which increases the probability of macroheterogeneity registration. According to these studies, the permeability coefficient tends to its average value in the excitation zone.

Development of macroheterogeneity explains migration of liquids in natural (undisturbed) conditions through thick clayey sequences, when gradients are below initial values observed in laboratory experiments.

The clayey sequences over 30-m thick are usually accepted by hydrogeologists, who study deep formations, for reliable fluid-confining beds [37]. In addition, it is

assumed that there is an initial gradient value, which separates filtering and non-filtering settings [3]. This provides grounds for neglecting fluid migration in clayey rocks under influence of gradients observed in petroliferous basins (frequently, fractions of unit). This aspect is particularly important and needs special consideration. The laboratory experiments and observations of specially prepared beds reveal such an initial gradient value that separates filtering and non-filtering settings.

Exploitation of fresh groundwaters from upper parts of sedimentary sequences in platforms (Moscow, Dnieper-Donets, and other artesian basins) shows that the flow through clayey sediments represents a main source for groundwater reserves regardless of the thickness of overlying and underlying clayey sediments (from 10 to 400 m/day and more) and water intake (from a few tens to hundreds of thousands of cubic meters per day and more), i.e., 80–90% of the total water intake is provided by water from adjacent aquifers.

The reliability of these calculations is high, which is confirmed by correspondence in estimates obtained by different methods: analytical calculations, analog and digital modeling, isotopic studies, analysis and processing of the regime observations. Despite insignificant discrepancies between different estimates obtained by these methods, all of them indicate unambiguously such a flow even in situations when the thickness of clayey sediments amounts to a few hundreds of meters.

Intense flows and interaction between aquifers and rock complexes established during the water intake occur in slightly lithified and compacted clays, where interstitial filtration probably retained its significance. Nevertheless, filtration heterogeneity and jointing determine the significant role of these processes in hydrodynamic interaction between aquifers. Clayey rocks should be considered as constituting formations with double porosity (interstitial and fissure) [29 and many others]. Precisely macroheterogeneity (jointing) determines the block structure of clayey sediments and intense filtration of subsurface fluids in clays under gradients lower as compared with their initial values. This is evident from the data on permeability of clayey rocks obtained by different methods (Table 6.2).

The table shows that permeability determined in laboratory conditions is two to three orders of magnitude lower as compared with its values obtained by other methods. At the same time, permeability coefficient values determined by the field studies (hydrochemical, thermometric, and isotopic methods) and modeling for the disturbed regime are similar. Discrepancy between values determined by experimental and all remaining methods is explainable by fissuring-induced heterogeneity of clayey rocks, the scale of which is larger as compared with sizes of laboratory samples.

Thus, long-term exploitation of aquifers demonstrates that clayey sediments even up to 400 m thick are permeable under gradients substantially lower than a unit (initial gradients established experimentally in monoliths). This permeability is largely yielded by rock jointing. For example, clays and argillites sampled from the Maikopian sequence of Ciscaucasia in the depth interval of 700–3,934 m contain leaching cavities and abundant microfissures. Leaching interstices indicating former migration of fluids and fissures are filled with geochemically different bitumoids.

**Table 6.2** Permeability of clayey sediments [29]

Study area	Permeability coefficient (m/day) obtained by different methods			
	Laboratory	Analog simulation	Hydrochemical	Thermometric
Kiev	$(0.3-4.0)10^{-5}$	$(2-4)10^{-4}$	—	$(0.5-1.0)10^{-3}$
	$(0.6-2.0)10^{-6}$	$(2-4)10^{-4}$	—	$(0.5-1.0)10^{-3}$
Moldova	$(3-5)10^{-7}$	—	—	$2 \cdot 10^{-4}$
	$(3-5)10^{-7}$	—	—	$1 \cdot 10^{-4}$
	$(0.2-9.0)10^{-7}$	$(0.1-1.0)10^{-4}$	$4 \cdot 10^{-4}$	—
	$(0.2-8.0)10^{-7}$	—	—	$3 \cdot 10^{-3}$
	$(0.2-8.0)10^{-7}$	—	—	$(0.3-6.0)10^{-4}$
Iset River valley	$(3-6)10^{-6}$	—	$7 \cdot 10^{-5}$	—
	$1 \cdot 10^{-6}$	—	$6 \cdot 10^{-4}$	—
	$1 \cdot 10^{-7}$	—	$2 \cdot 10^{-6}$	—
East Siberia	—	$(1-3)10^{-3}$	$1 \cdot 10^{-3}$	—
	$(0.01-1.0)10^{-4}$	$(3-5)10^{-4}$	$5 \cdot 10^{-3}$	—

The vertical migration in clayey rocks is established in the Khayan-Kort and Starogroznenskoe fields (eastern Ciscaucasia). The content of epigenetic bitumen in clayey sediments in near-arch parts of structures in the Khayan-Kort field is as high as 0.16–0.18%, while permeability of clays is estimated to be  $(20-38) \cdot 10^{-3} \mu\text{m}^2$ .

Signs of hydrocarbon migration are established also in argillites of the Dnieper-Donets Depression, Jurassic, Cretaceous, and Paleogene sediments of the Fergana Depression, and Miocene argillites of the Spraberry Formation in Texas (United States). Open fissures filled with oil are discovered in Upper Cretaceous argillites of the Borislov oil mine. In the Perm region of the Uralian foredeep, Sakmarian argillites yield gas flow rate of 1,46,500  $\text{m}^3/\text{day}$ .

The clayey sequence of the Khassi-Mesaud (Algeria) separates productive Cambrian gravelstones and sandstones from saliferous sediments. Clays contain secondary anhydrite, gypsum, and bitumen. According to M. Ulmey, Cambrian terrigenous rocks enclose up to 40% of secondary anhydrite and gypsum.

G.A. Miropol'skaya (1972) established for Devonian sediments of the East European Platform correlation between sulfide deposition and magmatic processes (likely post-volcanic hydrothermal activity) in the crust. Sphalerite, chalcopyrite, and arsenopyrite are found in fissures of Devonian terrigenous different-lithology rocks, the Kynov clays included. It is evident that the formation of these minerals is possible only under the additional influx of material, which means that the clays were formerly well permeable.

According to [13], Jurassic argillites of the Zhetybai field (southern Mangyshlak) host four systems of tectonic fissures, of which only 5% are healed by calcite, subordinate barite, and other minerals. The fracturing degree of argillites is three to four times higher as compared with sandstones and siltstones. Upper Cretaceous argillites of the eastern Stavropol region recovered at depths of 2,480–2,680 m are hard, platy, and characterized by vertical open fissures filled locally with oil.

Oil migration in clayey sediments is established also in the Shurasan field (western Uzbekistan), where oil discharges to the surface, which indicates its present-day ascending flow, not paleomigration.

Thus, it can be stated that clayey rocks are permeable for both subsurface solutions and hydrocarbons with high viscosity. The assertion that clays are impermeable is valid only with regard to the interstitial permeability. If clays are considered as rocks with double porosity (interstitial and fissure dominant at deep levels), observed facts of fluid, gas, and liquid hydrocarbon migration are quite logical.

Fissures occur frequently in clayey rocks, particularly in argillites and argillite-like varieties. For example, clayey sediments of the West Siberian Lowland host abundant fissures of different genesis both open and filled with coarse-grained material. Fissures filled with sandy and silty materials are from 0.01 to 3 mm wide (Fig. 6.13) to, locally, 7 cm and from 0.05 to 1.5 m to, sometimes, a few tens of meters long. Long fissures are feathered by second-order jointing. The maximal jointing degree is characteristic of argillites. For example, open fissures in argillites of the Tyumen Formation are from 0.01 to 5.0 mm and the width of fissured zones amounts to 1.5 m. According to K.I. Mikulenko, background values of the specific surface of tectonic and post-diagenetic fissures are 0.7 and 1.8  $\text{m}^{-1}$ , respectively, with the anomalous value of 14  $\text{m}^{-1}$ .

High reservoir properties of the clayey Bazhenovka Formation of West Siberia are evident from commercial oil yields in several fields (Pravda, Salym, and others). The formation is characterized by the lenticular structure, which hampers correlation of sections even at distances between boreholes of 0.6 and 3.0 km, which means that lenses are shorter. The hydrological acoustic survey shows very weak to zero interaction between individual boreholes that penetrate different lenses, which implies absence of horizontal fracturing or its insignificant development and prevalence of vertical and inclined fissures. According to thin-section studies, microfissures 0.01–0.03 mm wide and 0.1–0.3 mm long are characterized by density of 50–70 per meter of the section thickness. It is undoubted that the formation is characterized by the high openness degree of micro- and macrofissures as well as by their significant lengths and distribution density.

Jointing in clayey rocks of the Bazhenovka Formation is distinctly related to tectonics and hydrothermal activity. This is confirmed by location of high-yield wells in the Salym field along two meridional faults that cross the arch of the structure. Away from faults toward limbs and periclinal, yields successively decrease up to zero values. The Salym structure itself is located immediately near the Ob-Pur system of faults, i.e., in the tectonically active zone of the West Siberian Plate.

Argillites and argillite-like clays of the Kuma Formation (Ciscaucasia) are practically lacking primary porosity being characterized by volumetric jointing ranging from 80 to 1,000  $\text{m}^{-1}$  and permeability of 0.001 to 0.01–0.02 and, less commonly, 0.1  $\mu\text{m}^2$ , which is peculiar of fissure reservoirs [27].

Clayey caprocks of the Dnieper-Donets Depression represented by argillites and siltstones with subordinate marls are characterized by intense jointing [38]. The fissure permeability of argillites (in samples) varies from 0.0018 to 0.023  $\mu\text{m}^2$ , average

volumetric density of microfissures ranges from 24 to 300  $\text{m}^{-1}$ , and permeability of fissures in argillites amounts to 15–20  $\mu\text{m}^2$ . Fissures in argillites show signs of migrating hydrocarbons in the form of light bitumens.

The laboratory study of clayey rocks from the Dnieper-Donets Depression reveals that under tectonic stress they demonstrate capability to thinning related likely to development of microfissures due to reorganization of clayey microaggregates during deformation beyond the fluidity limit and secondary leaching of carbonate cement along the system of microfissures by fluids with abnormally high pressures [27]. This is inferred from the study of clayey caprocks under uniform and non-uniform compression, variable pressures (up to abnormally high) and temperatures. It is established that lithified clayey rocks are also characterized by capability of substantial reorganization of the texture and structure and formation of micro- and macrofissures.

The non-uniform compression results frequently in irreversible deformations and distortion of the texture in clayey rocks under influence of the interstitial pressure [14]. The higher the pressure, the greater the thinning and increase in the interstitial (fissure) space. Under the interstitial pressure of 49 and 71 mPa, the volume increases by 0.4 and 11.8%, respectively. These laboratory data confirm the universally observed effect of thinning of clayey rocks in areas with development of abnormally high formation pressures.

Physical modeling in laboratory conditions demonstrates that under effective uniform pressures of 51 mPa and temperature of 20°C, clayey particles become flatter and lose their fine texture, which is accompanied by ordering of the structure [21].

Under non-uniform compression, which is characteristic of tectonically active areas, resulting in separation of microblocks and their reorganization, this tendency becomes more distinct under temperature growth up to 200°C, which is typical of deep formations. Three groups of rocks are recognizable based on their ability to fissuring [27].

The first group includes pure clays of different compositions with low admixture of non-clayey material. This group is characterized by high values of the plasticity coefficient ( $3.0\text{--}3.5 \leq K < \infty$  and fracturing values  $\leq 10 \text{ m}^{-1}$ ).

The second group is represented by compacted clayey rocks with contents of non-clay minerals ranging from 10 to 15%. Their ability to fissuring is estimated to be 25–30  $\text{m}^{-1}$ .

The third group consists of clay rocks (siltstones, clayey argillites) with the high content of non-clayey minerals. They are characterized by high capability to fissuring (from 25–30 to hundreds of reverse meters) and low plasticity coefficient ( $K \leq 1.8\text{--}2.0$ ).

All the samples taken from different oil- and gas-bearing areas of Volga-Urals region, West Siberia, Central Asia, Ciscaucasia, and Dnieper-Donets Depression (>1,500 samples in total) belong to the second and third groups, i.e., show capability to fissuring to a variable degree. It is undoubted that the clay-argillites succession is characterized by continuous series of qualitative alterations that transform high-plasticity clays into rocks with rigid structural–crystalline bonds and capable to fissuring, which form, in fact, reservoirs with interstitial permeability at depths exceeding 1,800–2,200 m.



High interstitial pressures in clayey rocks stimulate also the formation of microfissures and growth of permeability due to local hydraulic fracturing, opening of available microfissures, and increased volume of the interstitial space resulting from elastic and irreversible deformations of the clay rock framework. In all situations, permeability (confining properties) of clayey caprocks depends on thermodynamic conditions in every point [40].

Using clayey rocks of the Kuma Formation (Ciscaucasia) practically lacking primary porosity and characterized by abnormally high pressures as an example, A.A. Fomin studied the influence of effective stresses, anomalous interstitial pressures, and temperatures on the compressibility coefficient, porosity, and permeability. For comparison, he analyzed also the same parameters obtained under ordinary (equal to hydrostatic) values of the interstitial pressure. This author established distortion of the rock texture under high interstitial pressures: local hydraulic fracturing, opening of available fissures, and increase in the volume of the interstitial space, on the one hand, and increased compressibility in formation conditions, on the other. High interstitial pressures result in irreversible deformations. The data confirm the shift of the elasticity boundary toward lower effective stresses established during the study of the abnormally high formation pressure influence on deformation and reservoir properties of rocks under different volumetric stresses [27].

V.K. Fedorov, who studied hydraulic fracturing in deep boreholes of West Siberia, noted that under the release of the geostatic pressure during drilling, hydraulic fracturing occurs at contacts between different lithologies such as, for example, sandstones and clays.

Hydraulic fracturing in clayey rocks is confirmed by exploitation of oil and gas fields, where the hydraulic fracturing method is widely applied. There are also examples of the spontaneous formation of fissures due to hydraulic fracturing under high pressures on the bed, which results in the redistribution of formation pressures. The latter is explained by the formation of fissures, which provide hydrodynamic interaction between different previously isolated parts of the section. For example, in the Dagadzhik oil field (Cheleken), the drop of formation pressures in the course of its exploitation stimulated intense upward flow through the sequence 350 m thick. The formation pressure and temperature in the upper pool increased by 2.3 mPa and from 37 to 43°C, respectively. The yield of exploitation wells increased as well. Such an intense migration is possible only under availability of local well-permeable zones.

The study of clayey rocks sampled in the Carpathian foredeep, Dnieper-Donets, and Amudar'ya depressions revealed that increase in the pressure gradient by 30–50% as compared with the initial (formation) one results in distortion of rock continuity due to hydraulic fracturing [28]. The last authors established the following empirical correlation between the hydraulic fracturing pressure  $\Delta P$  and permeability coefficient  $K$  of clayey rocks:

$$\Delta P = 10/7 K^{-0.33}.$$

Based on >1,000 samples collected in different areas of Russia and adjacent countries, it was established that the more complex is composition of clayey rocks (higher content of admixtures), the lower is their capability to plastic deformations and higher are elastic and mechanical properties and capability to fissuring [27].

Modeling of the fissure formation based on samples from the Levka oil field located in the southern slope of the West Kuban Trough yielded similar results [27]. Core samples were obtained from depths exceeding 4,500 m. The Eocene sediments in this area are represented by siltstones with marl intercalations, argillites, and argillite-like rocks. The rocks are characterized by fissure permeability ranging from 0.001 to  $34 \cdot 10^{-3} \mu\text{m}$ , volumetric fissure density of  $4\text{--}780 \text{ m}^{-1}$ , and integral macro- and microfissure volumes of 0.3%.

The experiment was conducted at compact samples under irregular compression, interstitial pressures up to 82 mPa and temperatures up to 135°C. Under the stress exceeding the elasticity limit, argillites and siltstones experienced irreversible deformations accompanied by their thinning. The latter (increase in the interstitial space) was reflected in development of deformation-related microfissures. Moreover, the interstitial space in argillites grew on account of opening of microfissures, which increased their parameters 2.5–3.0 times. For example, the fissure capacity exceeded 10% of the integral porosity, not 0.1–0.01% characteristic of initial samples. Newly formed fissures crossing mineral grains of the matrix appeared as well. Recrystallization of carbonates, quartz, and clay minerals was accompanied by the formation of new well-developed crystals.

It is logical to assume that distortion of rock continuity (formation of new and opening of available fissures) should be confined to most weakened zones such as boundaries between microaggregates in clayey rocks. The latter are forming first in areas with the lithological and mineral heterogeneities.

The study of the mineral composition, physicochemical, physicochemical, and textural–structural peculiarities, and post-sedimentary transformations of Carboniferous clayey rocks from the Volga-Urals region showed that carbonate material regularly distributed in calcareous clays increases their strength and capability to fissuring [7, 6]. For example, pure clays consisting of dehydrated mica are characterized by the plasticity coefficient exceeding 6.0. The 10% content of regularly distributed pelitomorph calcite in these clays decreases their plasticity coefficient up to 1.9 or more than three times. Carbonate material dehydrates clayey rocks, which results in structural changes reflected in transformation of chaotic mesotextures into vaguely bedded or lenticular. Such a transformation leads to the formation of anisotropy along and across bedding surfaces. Development of secondary dolomite results in the formation of areas with the elevated permeability due to interaction of minerals with different absorption capacity.

Similar to carbonates, terrigenous admixtures influence dehydration. The experiments show that alien bodies always concentrate strains, which results in reorientation of clay minerals located in the immediate proximity to inclusions and aggregates. In the presence of large crystals or their groups, single small crystals behave as clay particles, i.e., change their spatial orientation.

Compaction of clayey rocks leads to the formation first of meso- and then micro-textures. Junction zones between different textures of clayey-carbonate rocks in the Volga-Urals region are characterized by elevated strains, porosity, and permeability representing migration paths for hydrocarbons [18, 19].

Such areas are established in clayey rocks of the Bazhenovka Formation with hydromicas and kaolinite being rock-forming minerals. Junction of microblocks composed of these minerals forms weakened zones. Organic matter absorbed by some clay minerals at the their boundary with absorbing components provides even more weakened zones as compared with junction zones of different textures. Development of different-origin zones during tectonic movements stimulated microfissuring along them.

Many experimental studies of deformation properties of clayey rocks [18, 22, 27] demonstrate that distortion of their continuity under high interstitial pressure results from thinning.

Based on the fact that clayey rocks are usually thinned in areas with abnormally high formation pressures, A.G Durmish'yan [12] proposed a hypothesis that the latter result from the thickening process. As was mentioned, elision represents a practically stationary process. Thinning of clayey rocks and distortion of their continuity in areas with abnormally high formation pressures are logical to explain by intrusion of hydrothermal solutions, hydraulic fracturing, and distortion of rock continuity with subsequent formation of new minerals and partial sealing of the section at lithological and hydrogeochemical boundaries.

Thus, due to action of complex and diverse processes, clayey rocks are transformed in lower parts of the section from fine sediments with dominant interstitial permeability into solid rigid rocks with high capability to fissuring and, correspondingly, very high permeability under favorable conditions. In deep parts of the section, clays should be considered as rocks with tight structural-crystalline bonds. This is also true of rocks of other lithologies and mineralogical compositions: limestones, dolomites, sandstones, siltstones.

## 6.4 Permeability of Saliferous Rocks

In conclusion, let us dwell on permeability of salts, which are widespread in sedimentary sections of platforms, aulacogens, and marginal troughs.

The aspects related to salt permeability are least studied. At the same time there are indications that salt may be permeable under certain geological development of artesian basins.

It is established that vertical migration of fluids is possible also in saliferous formations, which are usually considered to be impermeable due to their plastic properties. Nevertheless, the tectonic activity during some periods results in fissuring, which forms vertical well-permeable zones that serve as paths for ascending fluids and provide intermittent hydrodynamic interaction between different parts of the section in petroliferous basins.

Antsifirov [2] established such a migration in saliferous sediments of the Irkutsk Amphitheater, where the Lower Cambrian Usol'e Formation is composed of rock salt with anhydrite and dolomite beds. The integral thickness of salt members exceeds frequently 1,000 m. The total thickness of the formation exceeds 1,400 m. Structural-prospecting works in the Balykhta field revealed oil and gas occurrences, most intense of which associate with the middle and upper parts of the formation. One of the boreholes yielded a gas blowout with output of 1,70,000 m<sup>3</sup>/day that was preceded by gas and drilling mud outburst. Gas accumulation is located in the anhydrite–dolomite member 24 m thick (Balykhta structure). This member is traceable through the entire structure, although gas was obtained from a single borehole, which indicates impermeable vertical boundaries. Drilling revealed small gas accumulations in salt domes, drilling of which is accompanied by oil and gas blowouts. Similar oil and gas occurrences are observable also in the Atov, Parfenov, Osa, and other areas of the Irkutsk Amphitheater.

Oil and gas occurrences are also established in Jurassic saliferous sediments of the Amudar'ya petroliferous basin. The Kirpichli field of this basin contains dispersed hydrocarbons and bitumens. Direct indications of oil and gas occurrences are discovered in Gaurdak, Southern Iolotan, and other structures.

Occurrence of hydrocarbons in thick saliferous sequences can be explained by intermittent ascending migration of gas–water mixture with hydrocarbons with its subsequent differentiation into constituents (gas, solution, and liquid hydrocarbons) and phase transitions that provide fissure healing.

## 6.5 Conclusions

- (1) Lithologically analogous and coeval rocks, clayey varieties included, at large depths may be solid (impermeable) and well permeable under influence of different processes. The heterogeneity scale (junction of permeable and impermeable rocks) is variable: from a few tens to a few hundreds of meters.
- (2) Rocks at deep levels are largely characterized by fissure permeability.
- (3) Clayey rocks as well as rocks of any other lithology acquire at large depths rigid structural–crystalline bonds and capability to fissuring; therefore, they may be characterized by permeability comparable with that in other lithologies or be impermeable.
- (4) The substantial heterogeneity in filtration and capacity properties results in the formation of differently oriented impermeable (or poorly permeable) boundaries and stratum-block structure of deep formations in petroliferous basins.
- (5) In the geological time scale, filtration and capacity properties of the same stratigraphic interval demonstrate temporal and spatial changes due to activation of tectonic processes, concealed hydrothermal activity, and post-hydrothermal formation of new minerals that form distinct spatial anisotropy of filtration and capacity properties of rocks, i.e., deep reservoirs are always secondary [42].
- (6) The substantial role in the formation of reservoir properties of rocks belongs to vertical migration of fluids, primarily paleohydrothermal solutions included,

which is evident from newly formed minerals sometimes of several generations, healed free capacity or, to the contrary, anomalous secondary porosity (fissuring).

- (7) In most cases, uppermost and basal parts of hydrocarbon fields as well as their flanks should comprise fluid-containing formations with interstices and fissures completely healed by newly formed minerals. Precisely this explains why hydrocarbon fields are surrounded by less mineralized waters as compared with background values since dissolved salts in groundwater precipitated in the form of solid phase to fill almost entirely free interstices and fissures. This phenomenon is characteristic of all the lithologies.

## References

1. Akramkhodzhaev A M, Simonenko A M, Zindel L A et al. (1977) Clayey confining beds of oil and gas in Mesozoic and Paleogene formations of the Fergana Depression. Fan, Tashkent
2. Antsifirov A S (1963) On migration of hydrocarbons through rock salt. *Neftegazovaya geologiya i geofizika* 10:25–36
3. Arie A G (1984) Physical basics of groundwater filtration. Nedra, Moscow
4. Bagdasarova M V (2001) Interaction between carbonate rocks and hydrothermal systems during formation of oil and gas reservoirs. In: *Lithology and petroleum resource potential. Materials of the 2nd All-Russian Lithological Meeting and 8th All-Russian Symposium on Fossil Corals and Reefs*. Syktyvkar
5. Bashilov V I, Kuprin V F, Gottikh R P et al (1991) Hydrocarbon degassing of fault zones in the western slope of North Urals. *Geologiya nefi i gaza* 11:17–21
6. Bochkarev V S, Boyarskikh G K, Nesterov I I (1980) *Trudy VNIGNI* 218:133–157
7. Bondarenko S S, Barenkii L V, Dzyuba A A (1983) Migration peculiarities of deep groundwater. In: *Basics of hydrogeology. Hydrogeodynamics*. Nauka, Moscow
8. Chepikov K. R, Ermolova E. P (1980) Authigenic minerals from Lower Cretaceous sediments of the Prikumsk oil- and gas-bearing area as indicators of oil accumulation age. In: *Rock reservoirs of oil and gas*. Nedra, Moscow
9. Djunin V I (1981) Investigation methods and principles of deep formation hydrodynamics. VIEMS, Moscow
10. Djunin V I (1985) Investigation methods of the deep subsurface flow. Nedra, Moscow
11. Dobrynin V M (1970) Deformation and change of physical properties in oil and gas reservoirs. Nedra, Moscow
12. Durmish'yan A G (1977) On the problem of abnormally high formation pressures and its role in oil and gas prospecting. *Trudy VNIGRI* 397:55–69
13. Gaas G Ya (1974) Influence of jointing on screening properties of confining beds (exemplified by southern Mangyshlak fields). *Trudy VNIGRI* 351:136–141
14. Ignatovich N K (1947) Hydrogeological structure as a basis for hydrogeological zoning of the USSR territory. *Sov Geol* 19:24–33
15. Ivanov M K, Limonov A F (1995) Mud volcanism and clay diapirism of the Black and Mediterranean seas. In: *Materials of the annual scientific conference "Lomonosov's Readings."* MGU, Moscow
16. Khanin V A (1979) Terrigenous rocks: Oil and gas reservoirs at deep levels. Nedra, Moscow
17. Klubova T T (1971) Some peculiarities in the study of clay minerals in petroleum geology. In: *Proceedings of the 5th Plenum of All-Union Commission on Investigation and Use of Clays*. Ashkhabad
18. Klubova T T (1979) Migration of oil through clayey-carbonate rocks. In: *Physical properties of oil and gas reservoir under high pressures and temperatures*. Nauka, Moscow

19. Klubova T T, Klimushina L P (1980) Some regularities in migration of hydrocarbons in Bazhenovka clays of the Salym field. In: Rock reservoirs and oil migration. Nauka, Moscow
20. Korzun A V (1996) Hydrodynamics of deep formations in the northern Pechora artesian basin. Candidate dissertation (Geol-Mineral) MGU, Moscow
21. Kruglikov N M, Nelyubin V V, Yakovlev O N (1985) Hydrogeology of the West Siberian petroliferous megabasin and peculiarities in hydrocarbon formation. Nedra, Leningrad
22. Kushnarev M V, Pashkovskii V N, Begmetov E Yu et al. (1972) Projection of brine occurrence in the Bukhara-Khiva region. In: Geology of oil and gas fields in western and southern Uzbekistan. Tashkent
23. Lebedev L M (1979) Minerals of recent hydrothermal solutions. Nauka, Moscow
24. Makhnach A A (1989) Catagenesis and groundwaters. Nauka, Minsk
25. Minskii N A (1979) Regularities in the formation of optimal reservoirs. Nedra, Moscow
26. Nazina L A, Sklyar Yu G (1995) Correlation between contents of physically fixed water and capacity properties of massive rock samples from the Bazhenov Formation. *Geologiya nefii i gaza* 8:15–18
27. Physical properties of oil reservoirs under high pressures and temperatures (1979) Nauka, Moscow
28. Pilip Ya A, Danilenko V A (1979) Quantitative assessment of screening properties of hydrocarbon accumulation confining beds. *Neftegazivaya geologiya i geofizika* 5:19–20
29. Plugina T A (1978) Determination of geofiltration parameters of permeable rocks by working methods. In: Review: Hydrogeology and engineering geology. VIEMS, Moscow
30. Pokhil'chuk A A, Ur'ev I I, Tsalko P B (1991) The formation mechanism of carbonate reservoirs in the Semiluki Horizon of the Pripyat Trough. *Geologiya nefii i gaza* 8:6–11
31. Postnikov E V, Andryushchenko A I (1991) Assessing-genetic classification of carbonate reservoirs. *Geologiya nefii i gaza* 10:24–29
32. Proshlyakov B K, Kholodov V N (eds) (1985) Reservoir rock properties at deep levels. Nauka, Moscow
33. Prozorovich G E, Zaripov O G, Valyuzhenich Z L (1970) Problems of lithology of petroliferous sediments in central and northern West Siberia. *Trudy ZapSibNIGNI* 26:1–188
34. Reservoir properties of rocks in deep formations (1985) Nauka, Moscow
35. Rock reservoirs and oil migration (1980) Nauka, Moscow
36. Sarkisyan S G (1977) Influence of fluid and gas "breath" on post-sedimentary transformations of sedimentary sequences. *Trudy IGIRGI* 21:85–95
37. Sarkisyan S G, Kotel'nikov D D (1980) Clay minerals and problems of petroleum geology. Nedra, Moscow
38. Sokolov B A, Konyukhov A I (1995) Injection geology of sedimentary basins and petroleum resource potential. In: Materials of the annual scientific conference "Lomonosov's Readings." MGU, Moscow
39. Stetyukha E I (1964) Equations of correlation between physical properties of rocks and their occurrence depth. Nedra, Moscow
40. Vvedenskaya A Ya, Bakhtin V V (1977) Influence of thermobaric formation conditions on screening properties of clayey confining beds above accumulations with abnormally high formation pressures. *Trudy VNIGNI* 397:85–91
41. Vsevolozhskii V A (1991) Basics of hydrogeology. MGU, Moscow
42. Zubkov M. Yu, Sitdikov A Sh (1994) Secondary reservoirs in the pre-Jurassic complex of the Ur'ev field. *Geologiya nefii i gaza* 4:5–9

## Chapter 7

# Fluidodynamics in Deep Formations of the West Siberian Petroliferous Basin

The geological structure, general hydrogeological conditions, and tectonics of this petroliferous basin are discussed in numerous publications. Therefore, we present only the data necessary for solving the main task of this study: interpretation of hydrodynamics in deep formations.

### 7.1 Geological and Tectonic Structure

The West Siberian petroliferous basin is characterized by the two-stage structure: the lower stage corresponds to the basement and the upper one to sedimentary cover. The basement is composed of metamorphosed and deformed Precambrian, Paleozoic, and Lower Mesozoic (Triassic, Lower Lias) rocks. The upper part of the basement is represented by the weathering crust locally up to several tens of meters thick. The crust overlies schists, gneisses, volcanic, and intrusive rocks of different lithology and ages.

The folded basement is overlain by the Mesozoic–Cenozoic platform cover composed of Jurassic, Cretaceous, Paleogene, Neogene, and Quaternary sediments (Figs. 7.1 and 7.2). The thickness of the sedimentary cover consisting exclusively of terrigenous facies exceeds 3,500 m. The following sedimentary complexes are defined in the basin: Lower–Middle Jurassic ( $J_{1-2}$ ), Upper Jurassic–Lower Valanginian ( $J_3$ – $K_{1v}$ ), Lower Cretaceous–Cenomanian ( $K_{1a}$ – $K_{2sm}$ ), Upper Cretaceous–Paleogene ( $K_2$ – $P$ ), and Paleogene–Quaternary ( $P$ – $Q$ ).

#### 7.1.1 Lower–Middle Jurassic Complex ( $J_{1-2}$ )

The complex was deposited in the spacious accumulation basin that comprises two-thirds of the present-day one. The sea occupied only the northern part of the basin. Its remainder was characterized by continental settings. Continental sediments cover the basement missing only its highest parts (Aleksandrovsk Megaswell, Mezhev and Parabel arches, and other uplifts). The thickness and the lithology of the complex are highly variable, which is explained by several factors: basement topography, sedimentation settings and ages, subsequent erosion, and others.

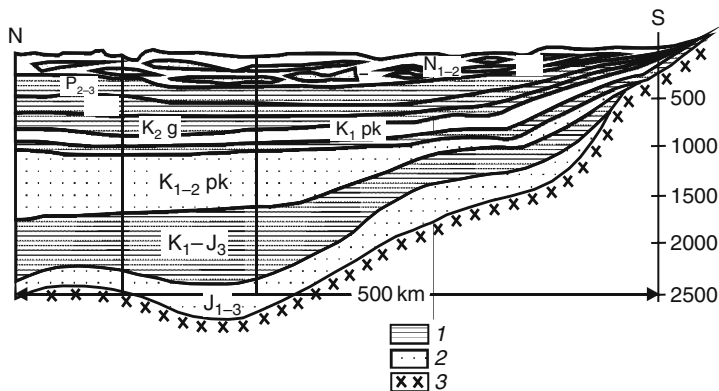
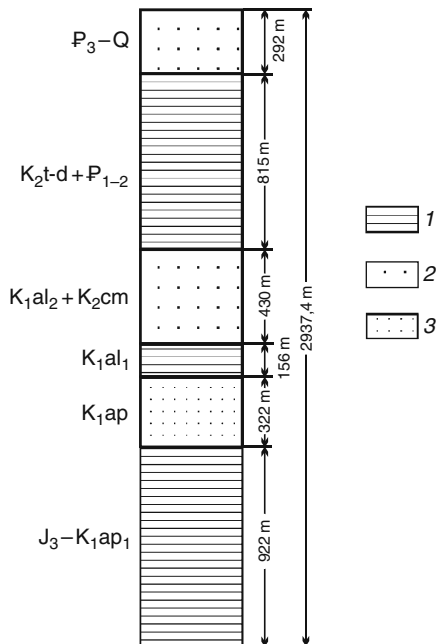


**Fig. 7.1** The section of the southern Ob-Irtys interfluvium. (1) Clayey rocks; (2) sandy rocks; (3) basement

**Fig. 7.2** The general section of the Frolovo field. (1) Clayey rocks; (2, 3) sandstones: (2) fine-grained, (3) coarse-grained



Maximal thicknesses of the complex are confined to negative structures, where it is 400–700 m thick amounting to 1,500 m in the northeastern part of the basin. In some positive structures (Chebach'e, Sen'kin, and others), the basement is represented by igneous rocks. In the remainder of the basin, it is composed of terrigenous sediments accumulated in river channels, large (largely sandy facies) and small



lakes, floodplains, and bogs (largely fine-grained facies). The sediments are united into the Pokrov and Tyumen formations. The Pokrov Formation is composed of tuffaceous sedimentary rocks, sandstones, and argillites up to 240 m thick. The Tyumen Formation is characterized by frequent facies replacements and distinct bedding consisting of sandstones, siltstones, and argillites.

### ***7.1.2 Upper Jurassic–Lower Valanginian Complex ( $J_3$ – $K_{1v}$ )***

The Callovian transgression was accompanied by general subsidence of the lowland, which was compensated by sediments only in some areas. In the Khanty-Mansi Depression, Callovian–Kimmeridgian sediments are only a few tens of meters thick, which indicates uncompensated subsidence. In the eastern part of the basin (shallow sea), where silty and sandy sediments accumulated, the thickness of this complex amounts to 300–400 m. Westward, the share of clays in the section and its thickness increase up to 80–90% and 500–600 m, respectively. The northern part of the basin was characterized by significant differentiation of the bottom topography due to intense tectonic movements: deep basins alternated with archipelagoes, which served as sources of detrital material and intermittently subsided below the sea level.

The complex comprises several formations composed largely of clayey sediments (clays, siltstones), which contain some sand admixture only in peripheral parts of the complex distribution area. The integral thickness of the complex exceeds 200 m.

### ***7.1.3 Lower Cretaceous–Cenomanian Complex ( $K_{1a}$ – $K_{2sm}$ )***

Lower Cretaceous sediments are united into the Frolov, Tar, Ilek, and Vartovsk formations. The Frolov Formation (Valanginian, Hauterivian, Barremian, Aptian) is represented by marine clayey facies distributed in the western part of the basin and replaced southward by the red-colored clayey Kiyala Formation (facies of desalinated lagoons and lakes) from 60 to 680 m thick. The Tar Formation (Upper Valanginian) is composed of medium-grained compact calcareous or incoherent to slightly cemented sandstones, the integral thickness of which increases from south northward and from west eastward from 40–50 to 250–270 m. The Ilek Formation (Valanginian, Hauterivian, Barremian) consisting of continental sandy–clayey sediments up to 600 m thick is developed in the southeastern part of the basin. The Vartovsk Formation (Hauterivian, Barremian) is distributed in the Pokur-Elogui area, where it is represented by sandstones, siltstones, and clays 300–600 m thick in total.

The Aptian marine (sandy–clayey) sediments form the Vikulovo Formation 150–190 m thick. Its analogue in the eastern slope of the Polar Urals represented by the Severnaya Sos'va Formation is composed of continental sands and siltstones up to 100 m thick.

The Albian marine clays constitute the Khanty-Mansi Formation up to 220 m thick. Marine sediments of Cenomanian age are united into the Uvat Formation consisting of siltstones and sandstones with limy intercalations.

Beyond the basin, thick sandy-silty and clayey sediments >1,000 m thick, which constitute the Pokur Formation and its analogues, accumulated in continental settings.

#### ***7.1.4 Upper Cretaceous–Paleogene Complex ( $K_2$ –P)***

During the Late Cretaceous and Paleogene, the basin accumulated in most of its areas deepwater substantially clayey sediments represented by the Kuznetsov (Turonian), Gan'kino (Maastrichtian–Danian), Ipatov (Upper Turonian–Lower Santonian), Slavgorod (Upper Santonian–Campanian), Talitsa (Paleocene), Lyulinvor (Eocene), and Chegan (Lower Oligocene) formations. Thickness of individual formations varies from several to hundreds of meters. The integral thickness of the complex exceeds 800 m. The sediments are represented by fat compact plastic to, locally, opoka-like clays and opokas, which become enriched in sandy-silty material and are replaced by coarse detrital facies in the peripheral part of the basin.

#### ***7.1.5 Paleogene–Quaternary Complex (P–Q)***

The complex is composed of continental and subordinate marine (in the northern part of the basin) sediments represented by fluvial, fluvial–lacustrine, glaciofluvial, and talus–proluvial facies.

The complex unites the Atlym, Novomikhailovsk, and Znamensk horizons (Upper Oligocene) up to 150 m in total represented by sandy and sandy–clayey sediments, Tavolga (Lower Miocene), Pavlodar (Middle Miocene–Middle Pliocene), and Kustanai (Upper Pliocene) formations that are distributed in the southern part of the basin, where they are composed of silty clays and sands. The integral thickness of the formations varies from 20 to 80 m.

The Quaternary sediments are represented by clays, loams, sandy loams, sands, and moraine facies or their irregular alternations. Their integral thickness ranges from several to 200 m.

#### ***7.1.6 Tectonics***

Two belts are distinguishable in the structure of the West Siberian basin: outer with dominant (up to 80%) positive and “neutral” structural forms and inner with different-order negative forms (up to 67%). Uplifting rates of individual structures were usually  $<2 \cdot 10^{-5}$  m/year; the maximal subsidence rate of  $6 \cdot 10^{-5}$  m/year was characteristic of the Ust-Yenisei Depression. According to S.B. Ershova, the Ob–Irtysh interfluvium was dominated in the Oligocene by subsidence with the velocity of  $2.8 \cdot 10^{-5}$  m/year, which decreased up to 0.008– $0.7 \cdot 10^{-5}$  m/year in the

Neogene (slight uplifting in the north and subsidence in the south) and increased slightly in the Late Pliocene–Quaternary to reach  $(50\text{--}70) \cdot 10^{-5}$  m/year nowadays.

Thus the velocity of “secular” tectonic movements varied from 0 to maximal values of  $70 \cdot 10^{-5}$  m/year in the Quaternary (Ob–Irtys interfluvium). Approximately similar variations were characteristic of sedimentation rates (Fig. 7.3).

The following tectonic fractures are defined in the sedimentary cover of the basin [1, 20, 28, 33]: (1) basement faults that cross the uppermost part of the basement and basal Lower–Middle Jurassic layers of the cover; (2) faults initiating in the basal part of the Upper Jurassic sequence (Mar’yanov Formation); (3) faults initiating in the lower part of the lower Aptian sequence (Pokur Formation) and disappearing higher in the section below Pliocene sediments. The amplitude of these fractures amounts to 60–70 m. The faults crossing the basal part of the Oligocene sequence

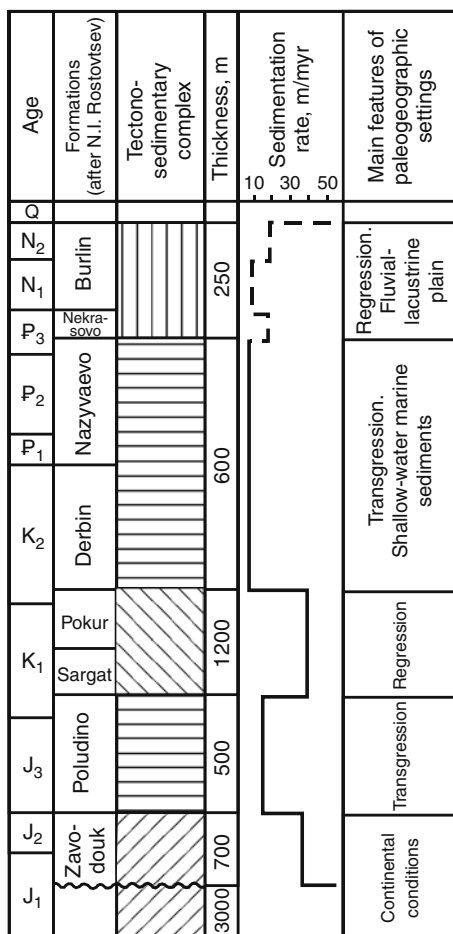


**Fig. 7.3** Changes in sedimentation rates through the West Siberian petroliferous basin during the Mesozoic (after A.V. Gol'dberg)

**Fig. 7.4** Schematic map of different-age and different-depth fractures in the West Siberian Plate (after E.V. German and A.N. Lastochkin, simplified). (1) Boundaries of the basin; (2) basement fractures dying off at different levels of the sedimentary cover; (3) fractures crossing the entire sedimentary section



are Paleocene in age and characterized by the amplitude of 300 m at the basement surface and 40–50 m at the base of the Paleocene sequence (Fig. 7.4).

Tectonic fractures are established in the Middle Ob region, Ob–Irtysh interfluve, eastern slope of the Ust-Yenisei Depression (with displacements of blocks for 1,000 m, for example, in the Malaya Kheta Swell), and Severnaya Sos’va area (Cenozoic faults with the amplitude of 100–800 m).

Most of the faults extend for several tens of kilometers and are accompanied by wide (up to 250–300 m) fracturing zones. Such fracturing zones associate usually with young faults. The fracturing increases downward the section. Inner areas of the basin are marked by normal faults with amplitudes of 100–150 m and length of 10–15 km. They become extinguished in the Lower–Middle Jurassic or Aptian (Pokur Formation) or Paleogene sequences; some of them cross all these sequences. The Pokur and Ipatovo formations in the Demin, Mezhov, Myl’dzhin, and other fields are characterized by *intense fracturing, fluid paleomigration along which is confirmed by the development of calcite and bitumens*.

The fractures are represented by dominant gliding, subordinate extension (filled with mineral aggregates), and open fissures. The most intense jointing is characteristic of the Tymen, Vasyugan, Vartovsk, and Pokur formations. Productivity of structures increases toward mobile zones, graben-shaped rifts included [1].

As a whole, the West Siberian petroliferous basin was characterized by the intense tectonic activity during its entire development history and in opinion of [20] “represents a classical example of a young geosynclinal domain.” This is evident from wide development of deep faults, long-lasting and stable subsidence regime, thick sedimentary cover, dominant marine sedimentation, high (up to 100°C) temperatures, volcanism along faults, and occurrence of carbonic acid in gases of oil fields.

The following peculiarities are notable in the geological structure of the West Siberian petroliferous basin:

- (1) The basin experienced long-lasting and stable subsidence accompanied by extension of accumulation areas. The latter provided to a variable degree of isolation of Jurassic and Cretaceous sediments from the influence of surface factors. The outcrops of these sediments are insignificant as compared with corresponding distribution areas. The exception is the southeastern part of the basin.
- (2) Away from the periphery of the basin, the thickness of all the stratigraphic units increases (Fig. 7.1) to be reduced at arches of positive structures.
- (3) Toward central areas of the basin, the share of clayey material in sediments increases (Figs. 6.3 and 6.4). The regional distribution of facies is complicated by local factors, the structural plane included. For example, the share of sandy material in sediments increases at arches of positive structures.
- (4) The sediments demonstrate signs of paleomigration of hydrothermal solutions and volcanic activity along faults.

## 7.2 Hydrogeological Conditions of the Basin

The thick Turonian–Lower Oligocene sequence of clayey rocks developed through the significant part of the basin determines different formation conditions of subsurface fluids in overlying and underlying formations. The upper part of the section is lacking regionally sustained low-permeability formations and forms, therefore, a single hydraulic system closely connected with the surface and characterized by autonomous hydrodynamic and hydrochemical regimes in the most part of the basin. In the book, these aquifers are omitted from consideration.

The complexes underlying the Turonian–Lower Oligocene clayey sequence that are usually subsided to significant depths (except for marginal parts of the basin) are characterized by restricted connections and referred to the lower hydrogeological stage. The Aptian–Cenomanian, Neocomian, and Lower–Middle Jurassic aquifers served as main study objects.

### 7.2.1 Aptian–Cenomanian Aquifer ( $K_{1a}$ – $K_{2sm}$ )

The aquifer is spread practically through the entire basin, except only for its marginal areas. It is represented by a sequence of sandy–silty and sandy–clayey sediments with the thickness increasing successively from the marginal area of the basin toward its centralmost subsided part up to 80–1,000 m.

The continental and coastal-marine facies of the aquifer are composed of fine-grained sands, sandstones, and siltstones intercalated by sandy and silty clays. The integral effective thickness of the complex amounts to 200–300 and 550 m in the peripheral and internal parts of the basin, respectively. The occurrence depth of its roof varies from 0 in marginal areas to 900–120 m in the central part of the basin. The occurrence depth of the base ranges from tens to 1,600–1,000 m (Middle Ob region).

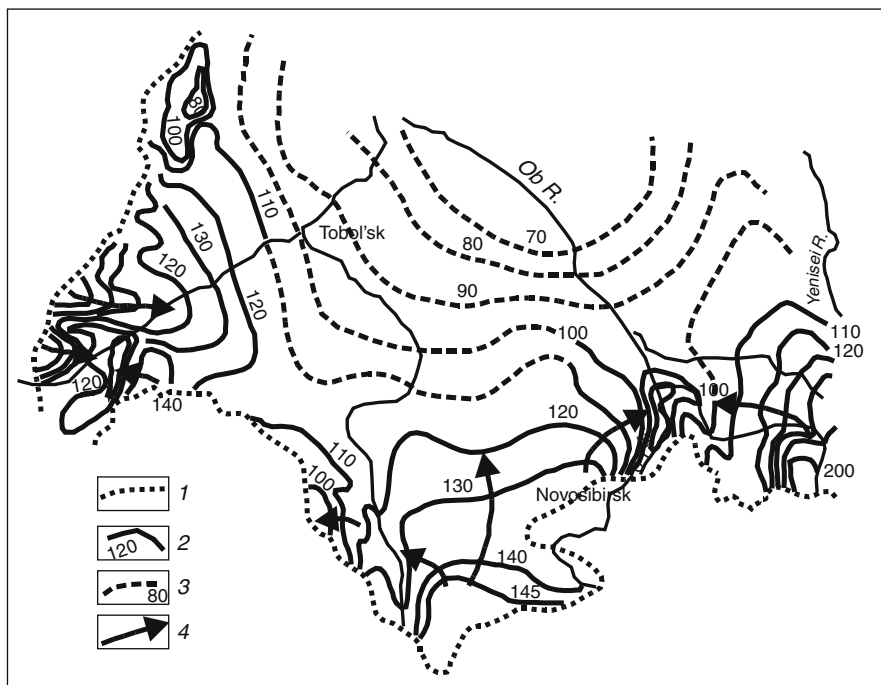


**Fig. 7.5** Schematic map of the Aptian–Cenomanian aquifer potentiometric surface in the marginal (southern) part of the petroliferous basin (after V.A. Vsevolozhskii). (1) Boundaries of the aquifer distribution area; (2) isolines of the water head, m (altitude); (3) the same based on limited data; (4) direction of the subsurface fluid flow

The sediments contain overall head waters (Fig. 7.5), the potentiometric level of which is sometimes located above the surface. Its patterns indicate that subsurface fluids migrate from the periphery of the basin surrounded by regional provenances toward its central areas. Specific yields vary regularly from 1 l/s along the periphery of the basin to  $1 \cdot 10^{-4}$ – $5 \cdot 10^{-5}$  l/s in the area of the latitudinal Ob River segment. The chemical cation composition and the mineralization change regularly from the periphery to the center of the basin from hydrocarbonate mixed to chloride-sodium and from 1 to 10–20 g/dm<sup>3</sup>, respectively. Central areas are overall characterized by anomalous mineralization values.

### 7.2.2 Neocomian Petroliferous Complex ( $K_{1v-b}$ )

The complex unites sediments of the Hauterivian–Barremian and Valanginian stages represented by terrigenous marine, coastal-marine, and continental lithologically heterogeneous and thickness-variable facies. Largely, sandy sediments are spread in the Chulym–Yenisei area and westernmost part of the basin, while dominant clayey facies are characteristic of central and southern areas. Westward, the thickness and

share of sandy interbeds decreases up to complete transition of sediments into clays of the Frolov Formation. In the western part of the lowland, Neocomian sediments may be considered, along with the Upper Jurassic sequence separating the Lower–Middle Jurassic and Aptian–Cenomanian aquifers, as representing a relatively confining formation. The integral thickness of sediments increases toward central areas of the basin, where it amounts to 900 m and higher. Individual sand layers are as thick as 60–75 m. The clay content varies from 70–80% in the Kiyalin Formation to 30–60% in the Vartovsk Formation, and to 80–90% in the upper part of the complex. The latter occurs at shallow depths only in the Chulym-Yenisei area, being subsided up to 2,500 m and deeper in the central part of the basin.

In marginal parts of the basin, the Neocomian complex is characterized by the elevated water content (specific yield amounts to 0.3–0.4 l/s), which decreases gradually toward central areas of the artesian structure, where maximal specific yields of boreholes are as high as 0.07 l/s, being usually thousandths fractions of the liter per second. In most of the basin, Neocomian sediments contain high-pressure fluids. In some areas, they are characterized by abnormally high formation pressures (Tyumen and other areas).

The potentiometric surface [31, 32] of the basin shows that subsurface fluids migrate from its marginal zones (regional recharge sources located along the boundaries with surrounding folded structures) toward central areas. The chemical composition of subsurface fluids changes in the same direction, being accompanied by increase in their mineralization: hydrocarbonate waters with mineralization of 0.5–2.0 g/dm<sup>3</sup> dominating in peripheral areas of the basin are gradually replaced by chloride–sodium water with mineralization up to 25 g/dm<sup>3</sup> with simultaneous increase in the elasticity of dissolved gas.

### ***7.2.3 Lower–Middle Jurassic Petroliferous Complex ( $J_{1-2}$ )***

The complex is represented by continental sediments, which form, along with the near-surface fissured part of the basement, a single petroliferous system. The complex outcrops only in the easternmost part of the basin and in some areas of the eastern slope of the Urals; in central areas, it is subsided up to depths of 3.0–3.5 km. The thickness of the complex varies from tens to 1,000 m and more.

The complex is composed of alternating sandstones, siltstones, and argillites with significant lateral variations in their proportions. The thickness of individual sand layers ranges from several to 50–80 m. The integral thickness of sand layers constitutes 30–80% of the total thickness of the complex; this proportion decreases toward central areas of the basin.

The lenticular structure and high share of clayey material determine the low water content; specific yields range from  $1 \cdot 10^{-4}$  to 0.1–0.3 l/s. Waters of the complex are largely of the head type with head values amounting to hundreds of meters. The potentiometric surface (Fig. 7.6) shows that groundwater migrates from the periphery of the basin, where regional recharge sources are located, toward its central and northern areas.

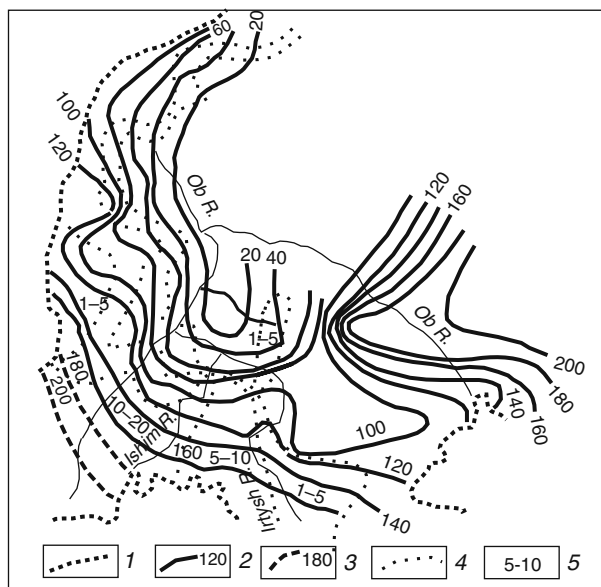


**Fig. 7.6** Schematic potentiometric map of the Lower–Middle Jurassic and Paleozoic sediment surface in the marginal (southern) part of the petroliferous basin (after S.S. Bondarenko). (1) Boundaries of the basin; (2) isolines of the reduced head (m) (altitude); (3) the same, assumed; (4) boundaries of areas with different transmissibility; (5) transmissibility ( $\text{m}^2/\text{day}$ )

The chemical composition of subsurface fluids changes from the hydrocarbonate to chloride–sodium one away from the marginal parts of the basin toward its centralmost subsided areas. These changes are accompanied by increase in salt contents from 0.7–3.0 to 50  $\text{g}/\text{dm}^3$ . Hydrocarbonate fresh or low-salinity waters are observable in the form of a narrow band along the eastern margin of the basin, where the complex in question is outcropping at the surface. The remainder of the basin is occupied by chloride–sodium waters with dominant salt contents of 20–30  $\text{g}/\text{dm}^3$ . Only in the Kolpashevo–Narym area, brines with mineralization of 50–80  $\text{g}/\text{dm}^3$  are recorded.

Of importance is the occurrence of heavy metals in subsurface fluids in the lower part of the basin section, where their content exceeds that in the World Ocean (Table 7.1). Judging from the local distribution of heavy metals through the basin, they originate from the basement.

**Table 7.1** Contents of heavy metals in groundwater from the lower parts of petroliferous basins

Metals	Content (mg/l)						
	Zinc	Copper	Lead	Nickel	Cobalt	Silver	Mercury
In groundwater	502	11.7	6.4	44.9	8.4	6.2	2.2
In seawater, after D. Griin	5.14	1.4	0.1–0.5	0.1	0.15–0.3	0.03	0.03



Thus, the following peculiarities are characteristic of the lower hydrogeological stage:

- (1) Increase in depths and distance from the periphery of the basin is accompanied by (a) decrease in specific yields and heads of subsurface fluids; (b) growth of their salt contents an order of magnitude; (c) gradual replacement of the hydrocarbonate composition of waters by the chloride one; and (d) increase in gas saturation and elasticity of dissolved gases.
- (2) The potentiometric surface of subsurface fluids as well as regularities in changes of water contents, chemical composition, and mineralization indicates that regional recharge sources are located along the periphery of the basin. Subsurface fluids are fed by either the water influx from surrounding folded structures or surface waters in aquifer outcropping areas [8, 19, 28, and others]. In addition, recharge is provided by infiltration of atmospheric waters in watershed areas or flows from surrounding folded structures may be intercepted by rivers and faults [17, 19, and others], or both these processes may act together depending on the geological structure of marginal parts of the basin [32].
- (3) Peripheral parts of the basin are largely composed of sandy rocks intercalated by thin sand-rich clay layers, which are locally missing. In these areas, all the sediments (from Jurassic to Quaternary) may be considered as representing a single aquifer, which is exemplified by the Chulym-Yenisei region.
- (4) In addition to gradual changes in hydrodynamic and hydrochemical parameters, inner areas of the basin are characterized by different anomalies in the chemical composition of fluids. There are also other anomalies, which are discussed below.

### 7.3 Some Peculiarities in Filtration Properties of Rocks

The available data on filtration properties of rocks are insufficient for regional studies of deep fluid hydrodynamics. As was mentioned, establishment of correlation between filtration properties, their genesis, and entire development history may contribute to solving this problem.

*Along the periphery of the basin*, the most significant role in the formation of filtration properties belongs to lithological-facies composition and geostatic compaction (changing toward central areas of the basin). Changes in capacity and filtration properties in these areas are gradual, being characterized by the exponential dependence (Chapter 6). In inner areas [3], dominant catagenetic transformations result in mosaic variations of capacity and filtration properties (from practically impermeable to well permeable). Regardless of lithology, rocks in these areas are dominated by fissure capacity and permeability.

Using the technique of least squares, empirical equations that describe changes in transmissibility along individual profiles across the artesian basin were obtained for

**Table 7.2** Calculation of permanent coefficients ( $K_0$  and  $\alpha$ ) in different areas of the basin

Profile	Permanent coefficients			
	$X$ (km)	$K(x), D$	$K_0$	$\alpha$
Turinsk-Uvat	50	0.7		
	365	0.02	1.22	$1.1 \cdot 10^{-2}$
Eremenskaya-Trekhozernaya-Komsomol'skaya	80	0.16	1.5	$3.1 \cdot 10^{-2}$
	180	0.01		
Komsomol'skaya Malyi Atlym	125	0.4	4.8	$1.98 \cdot 10^{-2}$
	306	0.01		
Berezino-Kasym	120	0.6	2.2	$1.1 \cdot 10^{-2}$
	220	0.2		
Pudino-Katal'gin-Chermshan	270	3.0		
	480	1.5	7.8	$3.5 \cdot 10^{-3}$
Kalpashevo-Parabel-Narym	350	1.0	3.25	$2.75 \cdot 10^{-3}$
	450	0.75		
Kalpashevo-Narym	350	1.0	3.46	$3.5 \cdot 10^{-3}$
	612	0.4		
Parabel-Narym-Ambar	450	0.75	3.4	$3.9 \cdot 10^{-3}$
	612	0.4		

well-known filtration properties of the Pokur Formation. Table 7.2 presents information for calculating empirical functions  $K(x) = K_0 \exp(-\alpha x)$  available for other areas.

Comparison of coefficients reveals substantial differences in changes in filtration properties of these sediments in different areas of the basin, which is consistent with geological conditions and development history.

For example, the following empirical equation  $T = 2,500 \exp(-5 \cdot 10^{-3} X)$  was obtained for the Ob-Irtys interfluvium. In this equation,  $T$  is the transmissibility in peripheral areas of the basin and  $X$  is the distance from the marginal part of the basin.

This equation accords well with natural measurements. For example, the transmissibility value calculated for the area located 1,000 km north of Pavlodar is 20 m<sup>2</sup>/day, while this parameter determined by experimental-filtration studies is 20–40 m<sup>2</sup>/day.

Similar regularities (although with other empirical coefficients) in changes in transmissibility are obtained for the near-Urals and eastern parts of the basin (Table 7.3) [4]. These regularities made it possible to develop the regional transmissibility model for the Aptian–Cenomanian aquifer, which was subsequently used for calculating lateral unit expenditures of fluids along their flows.

The Lower–Middle Jurassic sediments occurring always at depths of 3.0–3.5 km are characterized by worse filtration properties. Maximal transmissibility values (10–20 m<sup>2</sup>/day) are recorded in peripheral areas (near-Urals region, southern part of the basin). Toward central areas, it decreases rapidly up to 1 m<sup>2</sup>/day to show similar values through most of the basin. In opinion of S.S. Bondarenko (1961),

**Table 7.3** Average permeability values ( $K_0$ ) in clayey sediments of West Siberia

Area	Lithology	Age	Occurrence depth (m)	Determination method	$K_0$ (m/day)
Middle Transurals region, interfluve	Clays, dolomites	Eocene–Oligocene	100–200	Calculation	$4.3 \cdot 10^{-5}$
	–	–	–	–	$2.6 \cdot 10^{-5}$
	–	–	–	–	$1.3 \cdot 10^{-1}$
Middle Transurals region, Iset River valley	Clayey dolomites	Eocene	25–40	Laboratory	$1.7 \cdot 10^{-3}$
	–	–	13–17	–	$0.8 \cdot 10^{-3}$
	–	–	21–25	–	–
	–	–	29–32	Calculation	$1.1 \cdot 10^{-3}$
	Clay	Paleocene	25–30	–	$3.2 \cdot 10^{-3}$
	–	–	–	–	$6.9 \cdot 10^{-3}$
Omsk Irtysh region	Clay	Late Cretaceous–Paleocene	600–650	Calculation	$1.7 \cdot 10^{-5}$
			–	–	$4.3 \cdot 10^{-5}$
			–	–	$6.4 \cdot 10^{-5}$
Pavlodar Irtysh region	Clay	Late Cretaceous–Paleocene	Up to 500	Calculation	$4.5 \cdot 10^{-5}$
Ishim–Irtysh interfluve	Clay	Late Cretaceous	250–300	Modeling	$1.3 \cdot 10^{-5}$
			250–300		$2.2 \cdot 10^{-5}$
Southern Transurals region	Clay	Late Cretaceous–Paleocene	100–200	Modeling	$0.6 \cdot 10^{-5}$
			–		$1.2 \cdot 10^{-7}$
	–	Late Cretaceous	150–180	Modeling	$8 \cdot 10^{-5}$
Ob–Irtysh interfluve	Argillite	Early Cretaceous	2,400–2,800	Laboratory	$10^{-4}–10^{-5}$
Nizhnevartovsk Arch	Argillite	Early Cretaceous	2,050–2,250	Laboratory	$10^{-4}–10^{-5}$
			2,100–2,300		$10^{-5}$

zones with elevated transmissibility (up to 20–50 m<sup>2</sup>/day) definable in southern areas of the basin associate with fractures. Substantially higher (1–2 orders of magnitude) transmissibility values are characteristic of the Aptian–Cenomanian aquifer. In the near-Urals part of the basin, they amount to 200 m<sup>2</sup>/day to be maximal (2,000 m<sup>2</sup>/day and higher) in its southern and southeastern parts. At short distance from the periphery of the basin, they decrease, however, to 200–250 m<sup>2</sup>/day to remain lower at 50 m<sup>2</sup>/day in its inner areas.

*In inner areas*, capacity and filtration properties of rocks are determined by the following factors and processes.

*Lithological–mineralogical composition.* Mesozoic sediments of the basin are largely uniform with respect to their lithology being represented by carbonate-free

sandy-clayey varieties. Therefore, their filtration properties are determined by the share of clayey material in particular aquifers. Terrigenous sediments of the basin are largely characterized by clayey cement (Chapter 6), which reduces their permeability substantially. In sandy sediments, the share of syndimentary clayey particles increases gradually from the periphery of the basin toward its center to reach 30–50% and more in inner areas. Consequently, filtration properties should decrease in this direction as well.

At arches of positive structures of the second and higher orders, sediments contain the higher share of sandy material, owing to which their permeability in these areas is several times higher than at limbs [29, 30].

*Elastic deformations.* Their role is exemplified by Lower Cretaceous sediments of the Samotlor field [13], where the growth of pressure from the normal to the formation one results in porosity and permeability reduction by 12 and 300%, respectively (Fig. 7.7). These results confirm theoretical calculations [6] and confidently demonstrate as to what errors the laboratory study of permeability may lead. The role of elastic deformations is notable during exploitation of oil fields, where

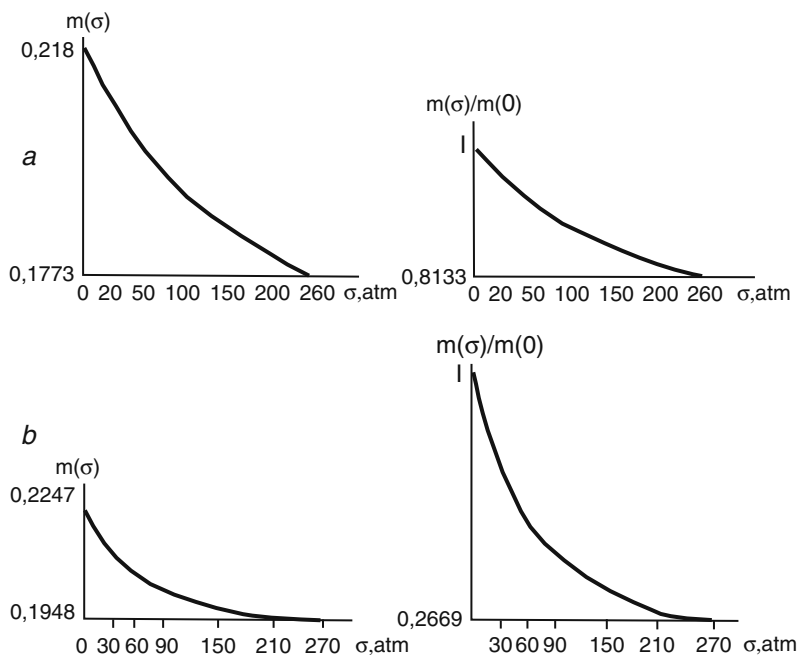


**Fig. 7.7** Correlation between permeability and effective pressure (after M.V. Kas'yanov and Yu.A. Afinogenov). Samotlor fields: (a) Borehole 2,011, sampled interval of 2,092.4–2,096.9 m, initial porosity 0.218; (b) Borehole 1,544, sampled interval of 1,647.6–1,653.6 m, initial porosity 0.2247

it is seen in closure of fissures under reduced formation pressure (Salym and other fields).

*Secondary mineral formation* is widespread in central areas of the basin. Calcitization that sharply reduces transmissibility is characterized by the local distribution.

Rozin [26] describes different anomalies, mineralogical included, which are determined, in his opinion, by “local mosaic” hydrothermal activity. The author considers significant decrease in contents of feldspars, micas, sphene, and epidote, intense kaolinization (Surgut and Vartovsk arches and other areas), development of epigenetic carbonates, origin of which is related to deep carbon dioxide and calcium, as resulting from secondary transformation of sediments (mineralogical anomalies). Epigenetic carbonates are “contaminated by isomorphic admixtures and characterized by lower decomposition temperatures as compared. . . with their sedimentary counterparts.” The evolution of epigenetic processes consists in kaolinization, carbonatization, and quartz regeneration [26]. The author confirms relations between vertical migration of deep solutions and catagenetic transformations of primary sediments by the following facts: (1) Neighboring areas differ in character and scale of epigenetic transformations. Kaolinization is characteristic of some areas and missing in others. The sections with anomalous and background transformations are sometimes located in the immediate proximity to each other. (2) The vertical constituent of epigenetic transformations is distinct. (3) Many epigenetic transformations cross facies boundaries. In lithologically anomalous sections, intervals with intensely transformed rocks include sediments with different facies and lithological characteristics. “Epigenetic zoning crosses the facies one.” (4) Epigenetic transformations are frequently rooted in the basement. “Rocks of the latter. . . bear in zones of mineralogical–petrological anomalies signs of secondary alterations characteristic also of rocks constituting the sedimentary cover.”

Many researchers note secondary jointing in the lower part of the section. This phenomenon is particularly distinct in argillites of the Bazhenovka Formation well studied in the Salym oil field. The following jointing types are definable based on the study of argillites [34]. (1) Interstices associated with substantially clayey rocks. Their density is determined by the thickness of laminae from fractions to 1.0–1.5 mm. (2) Fissures associated substantially with massive carbonate rocks with carbonate microconcretions. Their density is proportional to abundance of the latter. Fissures are developed 0.5–1.5 to 1.0–1.25 cm away from each other. (3) Caverns (lower part of the section) developed in rocks characterized by high lithological microheterogeneity, intense deformations, and brecciation. Numerous intercrossing fissures are frequently filled with calcite. Walls of caverns and open fissures are covered by crystalline quartz and dolomite.

The structure of clays, which consist of hydromica and kaolinite microblocks with weakened zones at their contacts, stimulates their fracturing. Such a block structure resulted from catagenetic silicification of the Bazhenovka clays [14, 16].

The capability of fracturing is determined by catagenetic transformations of clayey rocks and clayey cement as well as by admixtures of carbonate and silty material (Chapter 6). Catagenetic transformations are reflected in the successive transition of montmorillonite into mixed-layer phases, hydromicas, and kaolinite.

Based on the study of water-soluble organic matter in clays of the Bazhenovka Formation in the Salym field [7], it is inferred that clayey rocks experienced thinning to “host epigenetic migrating fluids.” Moreover, it is assumed that ascending migration occurred discretely and terminated in the Vartovsk Formation. Two migration stages are definable: Jurassic and Neocomian.

In the Shaim area, sediments of the productive formation (Vogulkin Formation) are overlain by clayey facies of the Voyanian regional stage composed of kaolinite and subordinate mixed-layer phases with admixture of chlorite and montmorillonite. Fissures are 1–2 mm wide, 5–15 cm long, and characterized by rectilinear and sinuous shapes.

In the Kaimys, Mezhev, and other areas, the integral thickness of clayey sediments constituting the Georgievsk and Bazhenovka formations and lower Kulomzin Subformation is as high as 150 m (locally up to 270 m). The clayey rocks are characterized by uniform lithology: sandy–silty layers constitute 5–25% averaging 10%. Most of the argillites are composed of kaolinites, hydromicas, and chlorites. They are locally fractured. The specific surface of open fissures varies from 0.3 to 6.5  $\text{m}^2/\text{m}^3$ . It is assumed that oil pools in Valanginian sediments (Mezhov field) resulted from ascending migration, since clays are characterized by elevated jointing (2.8  $\text{m}^2/\text{m}^3$ ) and high sand contents.

Similar changes in the mineralogical composition of clays and their jointing degree are noted in the Berezovo, Aleksandrovsk, Nadym-Pur, and Put-Taz areas also [16, 29, 30]. The enrichment of subsurface fluids with silica and juvenile carbonic acid stimulates, along with other factors, the formation of authigenic kaolinite. For the formation of authigenic quartz, the content of which amounts to 64% of total  $\text{SiO}_2$ , subsurface fluids should be enriched with silica. The formation of these minerals increases capability of clayey rocks to fracturing (Chapter 6) and increases, correspondingly, their permeability. Tables 7.3 and 7.4 present information on permeability of clayey rocks and their fissure permeability determined for different areas of the artesian basin by different methods, respectively.

Thus, the most significant role in the formation of filtration properties of rocks in peripheral areas of the basin belongs to their lithological-facies composition and geostatic compaction (successively changing toward its central areas).

The innermost subsided areas of the petroliferous basin are characterized by intense catagenetic rock transformations. Changes in capacity and filtration properties of rocks are mosaic (practically impermeable rocks alternate with well-permeable varieties); the rocks are characterized by dominant fissure capacity and permeability *regardless of their lithology*.

The secondary mineral formation in fissures is related to the past (and, probably, recent) hydrothermal activity. All these processes form the block structure of the geofiltration field.

**Table 7.4** Filtration properties of fissures

Area	Sampling interval (m)	Lithology	Fissure permeability (mD)
Loptyn-Yakh	2,157–2,164	Argillite	1.2
Sovetsk	2,212–2,215		40.0
Sosnino	2,764–2,778		0.24
Medvedev	2,537–2,577		0.08
Sen'kino	2,343–2,346		0.08
Alenkino	2,155–2,199	Argillite+siltstone	0.3
Srednii Vasyugan	2,273–2,289		17.0
Medvedev	2,286–2,290		0.04
Ust-Balyk	2,096–2,095		2.0
Ust-Sil'ga	2,278–2,285		14.0
Sen'kino	2,291–2,301		0.15
Nizhnevartovsk	2,237–2,247	Siltstone	0.14
Novo-Vasyugan	2,854–2,859		0.6
Sosnino	2,061–2,085		2.0
Medvedev	2,537–2,577		0.11
Novovartovsk	2,237–2,245		0.14

## 7.4 Influence of Peripheral Areas of the Basin on Fluidodynamics in Petroliferous Formations

### 7.4.1 Characteristic of Areas Providing Recent Infiltration Recharge of Deep Fluids

Let us briefly dwell on regional and local recharge sources of deep fluids, since they are sufficiently well studied [5, 31, 19, and others].

The distribution of potentiometric water heads (Figs. 7.5 and 7.6) and regional regularities in changes in the composition of subsurface fluids demonstrate confidently that main recharge sources (both external and internal) of deep formations are largely localized in marginal parts of basins. The results of water balance and hydrodynamic calculations performed for peripheral areas of the southern part of the basin in [31] as well as original hydrodynamic calculations show that the recharge value of deep fluids and their distribution through the region depend on particular natural factors. Specific recharge values (flow modules, unit expenditures) are mostly controlled by physico-geographical conditions of the region and filtration properties of rocks. The distribution of recharge values through the region and proportions between local discharge and external influx are determined by structural peculiarities of particular areas, their sedimentary sections, and hydrographic system of the basin periphery.

The *near-Urals segment of the basin* is characterized by the transgressive position of the platform cover, which determines specific recharge conditions of subsurface fluids. In most of the region except for the northern Transurals part, Upper

Cretaceous–, Oligocene clayey sediments (upper relatively confining sequence) rest immediately upon different-age rock of the Urals. In this connection, infiltration recharge of complexes is hampered to a significant extent. The main recharge source of subsurface fluids in Jurassic and Cretaceous formations is represented by the influx from the Urals.

For the Jurassic aquifer, unit expenditures of subsurface fluids (per unit of the flow width) along the flow vary from 700 to 2,000 m<sup>3</sup>/day. In the northwestern part of the basin, where outcropping Jurassic sediments provide opportunity for their immediate infiltration by atmospheric precipitation, unit expenditures increase up to 3,500 m<sup>3</sup>/day.

According to water balance calculations [31], the integral deep water recharge of the Aptian–Cenomanian aquifer that is formed on the eastern slope of the Middle and South Urals (up to the Ivdel latitude) is 3.2 km<sup>3</sup>/year and unit expenditures for the same areas vary from  $36.5 \cdot 10^3$  to  $100 \cdot 10^3$  m<sup>3</sup>/day. In the Polar Urals and southern Yamal Peninsula, Cretaceous sediments are outcropping to provide conditions for infiltration recharge of subsurface fluids of the complex, although no sufficient data are available for its quantitative assessment.

In the *near-Kazakhstan segment of the basin*, sediments of the lower hydrogeological stage are also overlain almost everywhere by thick relatively low-permeability sequences. Climatic conditions and filtration properties of pre-Mesozoic rocks developed in the Kazakh Hills are unfavorable for the formation of the substantial lateral influx. Water balance assessments yield values of deep infiltration recharge at the calculation accuracy level. This means that the near-Kazakhstan segment of the basin yields practically zero recharge of deep subsurface fluids. The approximate estimates of the unit expenditure obtained for the Jurassic and Cretaceous aquifers in the Lake Chagly–Ishim River valley are 3 and 150 m<sup>3</sup>/day, respectively.

The Fore-Altai Plain is characterized by the highest (altitude up to 145 m) position of the potentiometric surface and wide development of fresh groundwater in Aptian–Cenomanian sediments (depths of up to 500–600 m and deeper). In this connection, the southeastern periphery of the basin and Gornyi (Mountainous) Altai are anonymously considered as representing one of the main regions of present-day recharge of deep fluids. At the same time, the role of individual areas of this region in the formation of deep fluid recharge is different.

The Biisk-Barnaul area (Ob–Chulym interfluvium) cannot be considered as a recharge source of the West Siberian petroliferous basin at all, since the entire subsurface flow from slopes of the Altai-Sayany region is drained by the Ob River valley. In interfluvium of the Ob Plateau, infiltration recharge of deep formation is hampered by the thick sequence of poorly permeable loams. At the same time, the vertical distribution of groundwater heads indicates that the Ob Plateau may be considered as a recharge source for deep fluids. Of greatest interest is a relatively small area corresponding to the Alei River middle reaches and Irtysh–Alei–Charysh interfluvium. Very favorable conditions for infiltration recharge in this region are determined by the stratigraphic position and high permeability of Cretaceous sediments, pinching out and facies replacement of upper clayey sequences, and wide development of sands in the absence of the surface drainage.



According to water balance calculations [26], the infiltration recharge value in this region varies from <10 to 20–35 mm/year. In case of favorable structural conditions, this value amounts to 70 mm/year and higher (Semipalatinsk Irtysh area).

The integral recharge value of deep subsurface fluids that are forming in the Alei–Irtysh region after deduction of the discharge into the Irtysh River valley is as high as  $2 \cdot 10^6 \text{ m}^3/\text{day}$  [31].

The *Ob–Yenisei interfluve*. The present-day infiltration recharge of this region differs from the above-mentioned areas by widely outcropping Cretaceous and Jurassic sediments. The facies replacement of sandy sediments by clayey varieties is observed at significant distance from surrounding folded structures. This fact allows the interfluve to be considered as a main recharge area for deep subsurface fluids of the eastern part of the artesian basin. The deeply incised Yenisei River valley that initiates at the transition between the Siberian Platform and the West Siberian Plate should both catch the groundwater flow from the platform and drain groundwaters of the eastern slope of the artesian basin. This implies the existence of the subsurface watershed in the Ob–Yenisei interfluve that separates the deep subsurface flow of the near-Yenisei part of the West Siberian artesian basin from its remainder. The position of this watershed is indefinable because of the unavailability of data on deep fluid heads. Most likely, it coincides approximately with the present-day watershed between the Ob and Yenisei river tributaries. The existence of deep undersurface watersheds in interfluves of large rivers that represent, in fact, hydraulic boundaries between artesian basins is confirmed by many studies.

Favorable geological and physico-geographic conditions provide opportunity for deep ascending filtration through practically entire sedimentary section of the interfluve. This is evident from the distribution of temperatures through the section of the Maksimkin Yar borehole located approximately in the middle of the Ob–Yenisei watershed. The deep recharge value for this borehole was calculated using the technique from [5, 31]. The calculations show that the deep recharge value received by Jurassic and Neocomian sediments occurring at depths of 1,650–2,470 m is 0.42 l/s per  $1 \text{ km}^2$ , which constitutes 25% of the total infiltration and approximately 3% of the annual sum of atmospheric precipitation in this area.

According to water balance calculations, the infiltration recharge value obtained for deep subsurface fluids of main areas of the Ob–Yenisei interfluve (inner recharge area) ranges from 20 to 54 mm/year.

The integral deep subsurface flow that is formed in the southern part of the Ob–Yenisei interfluve (up to Tym River upper reaches) without basins of Yenisei River left tributaries approximates  $200 \text{ m}^3/\text{s}$  ( $6.3 \text{ km}^3/\text{year}$ ).

Thus, the main volume of present-day recharge of deep fluids in the eastern areas of the West Siberian artesian basin is largely formed within the lowland in basins of the Ob River right tributaries (Chulym, Ket, Tym, and others) (inner recharge areas). The lateral influx from the Altai–Sayany folded region is substantially lower as compared with infiltration recharge in inner recharge areas.

The insufficient knowledge prevents the quantitative assessment of the deep flow for the northern part of the Ob–Yenisei interfluve. It is conceivable that the latter is substantially lower than in its southern part due to permafrost development.

In addition to the above-mentioned areas, the Vasyugan and Turgai plateaus, East Urals and Siberian ridges, Lyulin-Vor Uplift, Irtysh–Ishim watershed, and watershed between the Irtysh River as well as a group of saline lakes, where subsurface fluid heads decrease downward, represent potential inner domains of infiltration recharge. This provides prerequisites for downward filtration, although water balance calculations do not confirm these assumptions.

The analysis of the temperature distribution through the vertical section in several fields of the central part of the basin reveals conditions favorable for descending filtration of subsurface fluids downward to depths of 600 m. Unavailability of data on changes in subsurface fluid heads through the vertical section for the same fields prevents the quantitative assessment of this recharge.

Noteworthy is the distribution of temperatures in lower parts of the section in inner areas of the basin reflected in upward convex shape of the curve. This indicates that some areas of the basin are potentially favorable for ascending filtration from the basement.

Some researchers assumed such a possibility based on other features [5, 22, 26]: occurrence of dry carbon dioxide accumulations in the basement–sedimentary cover transition, hydrochemical, mineralogical, hydrodynamic, and geochemical (presence of heavy metals) anomalies in lower parts of the sedimentary section, which disappear gradually from older to younger sediments. Assumed flows from the basement are, however, strictly localized [5, 26] and of low intensity.

The presented data on recharge areas allow the following conclusions:

- (1) Main recharge areas of deep fluids are located along the periphery of the basin. The recharge is provided by both lateral influx of subsurface fluids from the surrounding folded structures and infiltration of atmospheric precipitation at watershed areas with the favorable geological structure and climatic conditions.
- (2) The transgressive structure of sedimentary cover in peripheral areas of the basin, where the recharge value appears to be minimal (Urals, near-Kazakhstan part of the region), significantly affects the deep fluid recharge value. Maximal infiltration recharge values are characteristic of the southeastern part of the basin (Altai–Sayany folded region, Ob–Yenisei watershed), where the outcropping Mesozoic sedimentary cover is largely composed of sandy sediments. The deep infiltration value in the southeastern part of the basin is 5–10 times higher than that in its near-Urals segment, which was previously noted by some researchers.

Noteworthy is the difference between recharge values in the peripheral and inner parts of the basin. For example, in the southeastern and inner areas, this parameter is 2.0 and 0.012 l/s per km<sup>2</sup> and lower, respectively.

#### ***7.4.2 Characteristic of Present-Day Deep Fluid Discharge Areas***

The position of deep fluid discharge areas and the mechanism of this process are the most important and, simultaneously, least known and debatable aspects of their dynamics.

The following types of fluid discharge are known: stimulated by recovery of aquifers due to erosion; discharge in areas of facies replacement and pinching out of regional relative confining unit (“lithological windows”); along tectonic fractures and brecciation zones; in the form of ascending filtration of subsurface fluids through poorly permeable rocks; into marine and oceanic basins.

All the researchers who studied the formation of deep subsurface fluids in the West Siberian petroliferous basin believe that all these types of the subsurface fluid discharge take place in this region.

Before going to discussion of the above-mentioned types of fluid discharge, several principal remarks should be made.

The large size of the basin significantly influences hydrodynamics of deep fluids. The basin is over 1,000 and 2,000 km across in latitudinal and longitudinal directions, respectively. Its area exceeds  $3.5 \cdot 10^6$  km<sup>2</sup>. The filtration resistance along beds increases gradually from the periphery of the basin toward its central areas, while the vertical resistance of rocks decreases (Chapter 3). F. M. Bochever demonstrated that calculations in line with the Myatiev-Girinskii method yield good results under the ratio of coefficients of reservoir filtration ( $K$ ) to caprock permeability ( $K_0$ ), which is as follows:

$$K/K_0 \geq 150, \quad (7.1)$$

$$Kmm_0/K_0\Delta L < 0.05, \quad (7.2)$$

where  $m$  and  $m_0$  are thicknesses of readily and poorly permeable rocks, respectively.

Inequality (7.1) is executed practically always, while inequality (7.2) is executed only under the flow length of tens to hundreds of kilometers, which is true of the West Siberian petroliferous basin. Thus, away from the periphery of the basin, ascending vertical discharge through clayey sediments and, accordingly, reduction of lateral expenditures in the absence of river drainage are possible.

The head gradients of lateral flows decrease from the periphery of the basin toward its central areas from  $n \cdot 10^{-3}$  to  $n \cdot 10^{-(4-5)}$  and lower. Vertical gradients vary in the same direction from 0 to  $n \cdot 10^{-(1-3)}$  and higher and the area of the vertical discharge increases from 0 to  $n \cdot 10^5$  m<sup>2</sup> and more. Neglecting changes of filtration properties of reservoirs and taking the average permeability value of clayey rocks equal to  $10^{-5}$  m/day (Table 7.2), we obtain the following parameters for the basin recharge area:

$$m = n \cdot 10^1 \text{ m}; K = n \cdot 10^1 \text{ m/day}; \Delta H/\Delta x = 10^{-3},$$

$$\Delta H = n \cdot 10^2 \text{ m}; K_0 = 10^{-5} \text{ m/day}; \Delta H/\Delta z = 0;$$

the ratio of unit (per 1 m of the flow length) expenditures should be equal to

$$\frac{Q_x}{Q_z} = \frac{mK\Delta H/\Delta X}{m_0K_0\Delta H/\Delta X} \rightarrow \infty,$$

i.e., marginal zones of the basin should be dominated by horizontal migration of subsurface fluids.

For areas remote from the basin periphery, these parameters should be

$$m = n \cdot 10^1 \text{ m}; \quad K = n \cdot 10^1 \text{ m/day}; \quad \Delta H / \Delta x = 10^{-5},$$

$$\Delta H = n \cdot 10^5 \text{ m}; \quad K_0 = 10^{-5} \text{ m/day}; \quad \Delta H / \Delta z = 10^{-2}.$$

Consequently,  $Q_x/Q_z = n \cdot 10^{-1}$ , i.e., this ratio indicates that vertical and lateral expenditures in central areas of the basin are comparable between each other.

The integral horizontal resistance ( $R_1$ ) increases several orders of magnitude away from marginal zones of the basin and is described by the following equation:

$$R_L = \frac{\Delta L}{\beta e^{-\alpha x}},$$

where the coefficient  $\beta$  takes into account both the linear increment of the filtration area and the initial (for the extreme periphery of the basin) transmissibility value.

### ***7.4.3 Discharge Stimulated by Recovery of the Lower Hydrogeological Stage Due to Erosion***

Such a groundwater discharge is reflected in the potentiometric surface along the periphery of the basin, where recovery of the aquifer by the river network is accompanied by pinching out of the regional relative confining unit.

In the near-Urals and southwestern parts of the basin, Aptian–Cenomanian strata are recovered by most of the largest rivers (Tobol, Ui, Ayat, Iset, Pyshma, and others). The potentiometric surface indicates that subsurface fluids in these areas flow from watersheds toward river valleys (Fig. 7.5). Subsurface fluids that are formed in the peripheral parts of the basin discharge partly or completely into river valleys. The influence of the river network is particularly well seen in the hydrodynamic behavior of the groundwater flow of the Aptian–Cenomanian aquifer in the near-Urals and southwestern parts of the basin (Fig. 7.8). The figure demonstrates the spatial position of closed domains of groundwater formation along the periphery of the basin.

Under the closed domains, we understand areas with the complete hydrogeological cycle (recharge, migration, discharge) of subsurface fluids.

The dynamically closed domains of the deep fluid formation are separated from central subsided areas of the basin by a subsurface hydraulic barrier, from which forming groundwater flows toward inner areas of the basin.

In the southeastern part of the basin, a wide and deep (up to 120 m and deeper) valley of the Ob River and its tributaries is a main discharge area for subsurface fluids forming in upper and middle reaches of the Ob River valley. The Ob River drains all the aquifers, Paleozoic petroliferous complexes included.

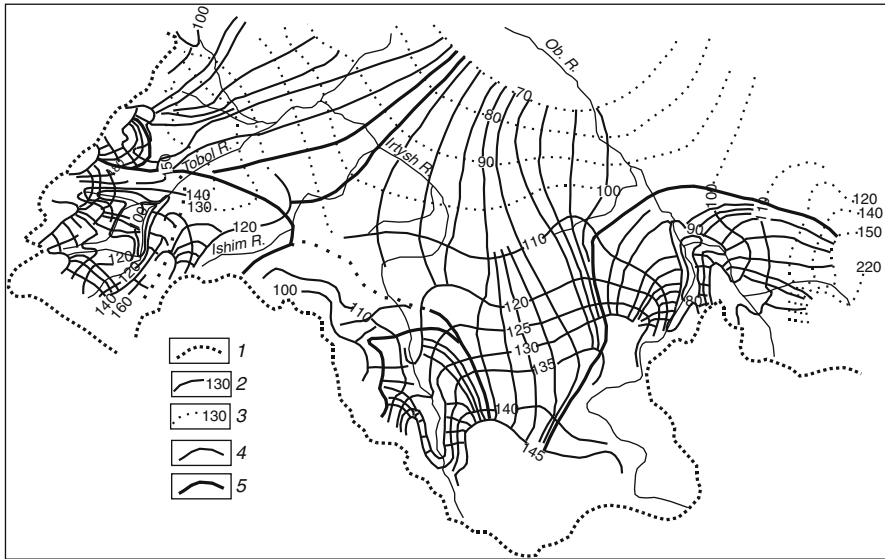


**Fig. 7.8** Hydrodynamic scheme of the groundwater flow in the Aptian–Cenomanian complex. (1) Boundaries of the basin; (2) piezoisohypses (m) (altitude); (3) the same, assumed; (4) flow lines; (5) boundaries of closed flow areas

In the Biisk–Barnaul area, the Mesozoic–Cenozoic sedimentary cover is composed of relatively thin (up to 300 m) facies-variable, sandy–clayey sediments. The potentiometric surface of subsurface fluids indicates that the Ob River drains all the aquifers (petroliferous complexes), Paleozoic formations included. The integral discharge value estimated for groundwater reserves of the Biisk–Barnaul Ob region ranges from 0.6 to 2.2 l/s per 1 km<sup>2</sup> [31].

In the Tomsk–Kolpashevo area characterized by the peculiar geological structure (regional Turonian–Paleocene relative confining unit is missing since Upper Cretaceous–Paleogene marine facies are replaced by continental and coastal-marine, coarse-grained sediments), the Ob River valley from its mountainous fringing to the Kolpashevo Village represents an area of local intense groundwater discharge from the Aptian–Cenomanian and, probably, Lower–Middle Jurassic aquifers [24]. This type of groundwater discharge is readily evident from the potentiometric surface and changes in lateral unit expenditures of subsurface fluids in peripheral areas of the basin, where recovery of aquifers by the river network is accompanied by facies replacements and pinching out of regional relative confining beds.

The peculiar geological structure of the southeastern part of the basin and the position of the Ob River valley allow inference that the entire right side of the latter cannot be considered as representing the deep fluid recharge source for the inner part of the basin. This inference is confirmed by hydrodynamics of the Aptian–Cenomanian aquifer (Fig. 7.8).

#### 7.4.4 Discharge Along Tectonic Fractures and Brecciation Zones

It is difficult to substantiate the hydrogeological role of fractures. The defined zones of the intense discharge associated with faults are confined to the periphery of the basin. One of such zones is established in the Sos'va-Kashai area of the Transurals region [19 and others], where it associates with tectonic fractures along the western boundary of the Kuznetsov group of uplifts. The second discharge zone of deep fluids related to tectonic fractures is located in the eastern part of the Taz Peninsula, where the spring of bromine and iodine headwaters is observed in the Sambur structure area.

#### 7.4.5 Discharge in the Form of Ascending Migration of Deep Fluids Through Low-Permeability Rocks

As was mentioned (Chapter 2), in order to answer unambiguously the question of why pressures of subsurface fluids decrease toward central areas of the basin, we should compile both potentiometric maps and hydrodynamic schemes, illustrating the orthogonal network of heads and flows as well as changes in lateral expenditures of fluids along flows. In addition, modeling of these processes is appropriate.

In order to understand the discharge mechanism and changes in lateral expenditures of subsurface fluids from the peripheral toward central parts of the basin, the hydrogeological situation in the Pavlodar Ob–Irtys area located in the southern segment of the basin was modeled (two-dimensional task) (Fig. 7.1).

In the model, transmissibility of sediments was accepted as changing exponentially (see above) and permeability of overlying Upper Cretaceous–Paleogene strata was considered to be constant and equal to  $10^{-5}$  m/day (Table 7.2).

First-type boundary conditions were specified for outer boundaries of the section (distance of 460 km). The water head in the overlying aquifer was prescribed for the roof of the clayey sequence.

The modeling results presented in Fig. 7.9 and Table 7.5 indicate that 95% of the fluid expenditure are discharged at a distance of 460 km from the southern margin

**Fig. 7.9** Changes in expenditures and duration of the water renewal period in Aptian–Cenomanian sediments of the Ob–Irtys interfluvium. (1) Lateral expenditure (%); (2) integral vertical load (%); (3) water renewal period (kyr)

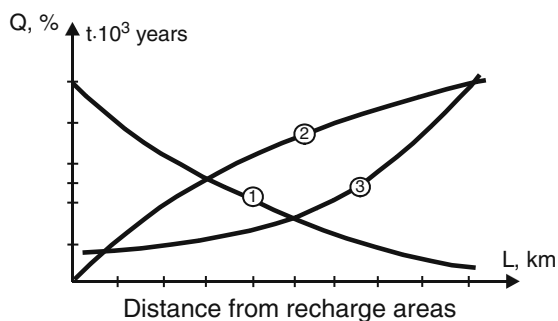


**Table 7.5** Balance of the subsurface flow along the flow line, Ob–Irtys interfluvium (based on modeling results)

Distance from the recharge area (km)	Influx (m <sup>3</sup> /day)	Outflow (m <sup>3</sup> /day)	Vertical outflow (m <sup>3</sup> /day)	Module of the vertical discharge (m <sup>3</sup> /day)	Water-exchange period (kyr)
46	200	175	25	0.006	38
69	175	145	30	0.007	42
115	145	123	22	0.005	52
161	123	114	9	0.002	62
207	114	80	34	0.008	66
253	80	68	12	0.003	95
299	68	52	16	0.004	111
345	52	39	13	0.003	145
391	39	31	8	0.002	195
437	31	18	13	0.003	242

of the basin with the most notable gradient at a distance of 150 km. The decrease in the lateral expenditure is gradual due to the absence of river network drainage.

Comparison between modeling results and hydrogeological calculations shows that modeling based on flow bands reveals no principal differences. Therefore, in further interpretations, hydrodynamic calculations based on fluid flow lines were used.

The schemes reflecting general changes in expenditures of subsurface fluids along flow lines in the Lower–Middle Jurassic and Aptian–Cenomanian complexes (Figs. 7.10–7.13) distinctly demonstrate that reduction in subsurface fluid expenditures occurs from the periphery of the basin toward its center, which is well consistent with theoretical concepts (Chapter 3). This reduction in expenditures is, however, different in different areas, being most significant in the Jurassic and Cretaceous aquifers of the near-Urals part of the basin, which is characterized by maximal subsidence, maximal clay contents, and significant facies variations.

At the same time, changes in expenditures of subsurface fluids depend largely on the occurrence depth of water-bearing rocks. This is particularly well evident from comparison of curves illustrating expenditure changes in the Lower–Middle Jurassic and Aptian–Cenomanian complexes (Figs. 7.12 and 7.13). They demonstrate that in the deeper Lower–Middle Jurassic complex overlain by thick (up to >1,000 m) different-age clayey sediments, reduction in the lateral fluid expenditure of up to 10% occurs in a relatively narrow band of 50–100 km width. In the Aptian–Cenomanian complex of the same area, similar reduction takes place at a distance of at least 150–200 km from the boundary of its distribution area, i.e., increase in the occurrence depths is accompanied by more rapid reduction of subsurface fluid expenditures.

The change in expenditures of subsurface fluids within the same petroliferous complex is, however, variable. This is evident from plots illustrating changes in lateral expenditures (Fig. 7.12). The eastern slope of the Urals (Fig. 7.12,

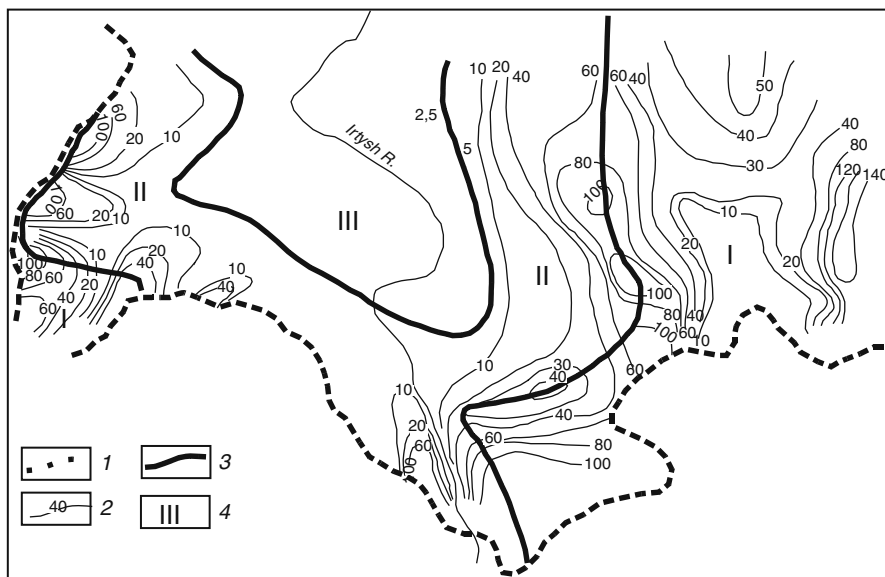


**Fig. 7.10** Changes in lateral unit expenditures of groundwater in the Aptian–Cenomanian complex of West Siberia. (I) Boundaries of the aquifer; (2) isolines of lateral unit expenditures (percentage of the expenditure at the boundary of the aquifer distribution area); (3) boundaries of hydrodynamic zones with: (I) intense water exchange, (II) hampered water exchange, (III) very low water exchange

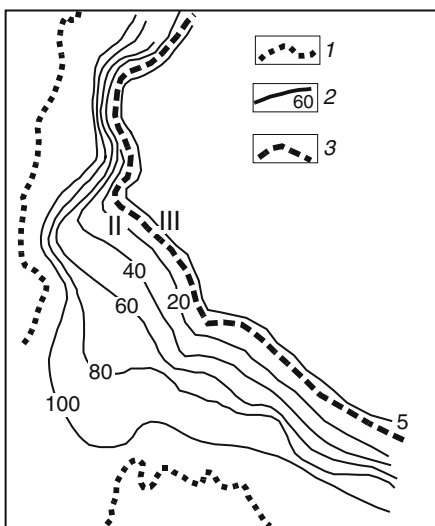


**Fig. 7.11** Changes in lateral unit expenditures of groundwater in the Lower–Middle Jurassic complex of West Siberia. (I) Boundaries of the aquifer; (2) isolines of lateral unit expenditures (percentage of the expenditure at the boundary of the aquifer distribution area); (3) boundaries of hydrodynamic zones with: (I) intense water exchange, (II) hampered water exchange, (III) very low water exchange



**Fig. 7.12** Changes in lateral unit expenditures of groundwater in the Lower–Middle Jurassic complex of West Siberia. (1) Southern part of the basin; (2) southwestern part of the basin, profile 450 km long; (3) Trans-Middle Urals, profile 150 km long

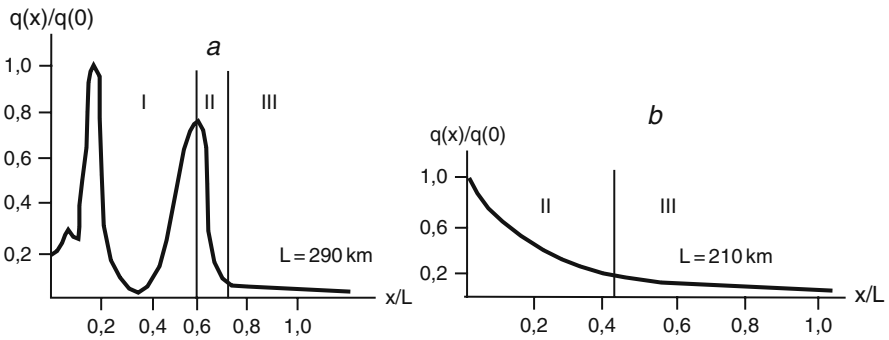
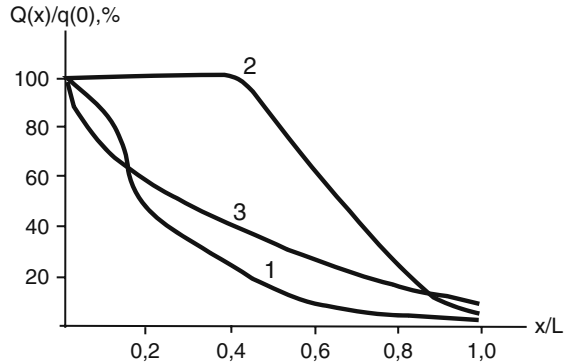


**Fig. 7.13** Changes in lateral unit expenditures of groundwaters along flow lines in the Aptian–Cenomanian aquifer. (a) Southeastern part of the basin, profile 290 km long; (b) Trans-Middle Urals, profile 210 km long. Zones with: intense water exchange, (II) hampered water exchange, (III) very low water exchange

Curve 3) characterized by rapid subsidence of Jurassic largely marine clayey sediments demonstrates the most significant reduction in subsurface fluid expenditures. In this area, 90% of the forming fluid expenditure discharge in the band of 150 km width. A similar situation is characteristic of the southern part of the basin (Fig.7.12, Curve 1), where the discharge band is 160 km wide.

Slightly different situation is peculiar of the Turgai Trough and the area adjacent to the north. In this area, Jurassic sediments occurring at relatively shallow depths are uplifted, which results in a twice wider band (up to 400 km), where the subsurface fluid expenditures of the Lower–Middle Jurassic complex become reduced by the value (90%) similar to that in the near-Urals and southern parts of the basin (Fig. 7.12, Curve 2).

Similar changes in expenditures of subsurface fluids determined by the geological structure of the basin are also characteristic of the Aptian–Cenomanian complex. The minimal and maximal expenditure gradients are registered in the eastern and

western parts of the lowland, respectively, while its intermediate values are observed in the southern half of the basin (Fig. 7.13).

The above-mentioned regularities in general lowering of the potentiometric surface level with its simultaneous flattening toward central most subsided areas of the basin and deterioration of filtration properties as well as reduction in lateral expenditures of subsurface fluids are characteristic of other petroliferous basins as well (Chapters 9 and 10).

This indicates unambiguously the hampered discharge of subsurface fluids that diffuse through spacious areas. Such a reduction in lateral expenditures from maximal initial values in the peripheral part of the basin practically up to zero values in its central areas is explainable only by the increase in the *integral* vertical discharge through clayey sediments (Figs. 7.9–7.13). This indicates, in turn, hydraulic connection along the entire periphery of the basin between deep formations and surface through the upper hydrological stage.

The characteristic morphological feature reflected in wide development of bogs that form practically a single draining surface with surface flows provides the regular distribution of boundary conditions at the roof of the sedimentary cover in the petroliferous basin.

The hydrodynamic relations between aquifers (petroliferous complexes) are complicated by draining effect of river valleys and deeply incised lakes, which significantly intensifies the hydrodynamic exchange of aquifers between each other and with the surface and makes it more concentrated. The draining effect of large and small river valleys is maximal in marginal parts of the basin, which is explained by the reduced thickness of separating clayey sequences, their macro- and microheterogeneity, and immediate exchange between rivers and deep petroliferous complexes established in some areas of clay sequence pinching out. In such areas, the drainage depends to a significant extent on the position of the river relative to migration paths of deep fluids, in addition to depths of erosional incision and geological structure of its valley. When the river valley is transverse relative to the fluid flow, the discharge becomes local, concentrated, and closed (Ob–Tom–Chulym interfluve, rivers of the Turgai Trough, and others). To the contrary, when river valleys are parallel to the fluid flow, no concentrated discharge is observed and draining is gradual, which is evident only from insignificant changes in the potentiometric surface of groundwaters under river valleys (rivers draining the eastern slope of the Urals).

Away from marginal parts of the basin, where oil- and gas-bearing complexes are subsided to deeper levels and thickness of clayey sequences increases, relations between deep formations in its peripheral areas become different, with the draining effect of the river network being weaker and indistinguishable in the potentiometric surface.

In these conditions, the diffused ascending filtration of deep fluids, which results in gradual reduction of their lateral expenditures, migration velocities, and gradients as well as in longer renewal periods, becomes the dominant discharge mode (Tables 7.6 and 7.7).

**Table 7.6** Renewal periods of groundwaters in the Aptian–Cenomanian complex

Area or borehole	Distance (km)		Module of subsurface flow (l/s from 1 km <sup>2</sup> )	Thickness (m)	Porosity	Average renewal period (thousand years)
	From Chulym borehole	From Urals				
Chulym			2.56	540	0.293	93
Parabel	460		1.2	658	0.267	43
Lutinets	540		1.1	784	0.249	56
Moiseevo	700		0.208	760	0.219	253
Kogit		680	0.11	682	0.215	420
1		450	0.043	722	0.212	1,132
2		107	0.07	420	0.252	480
3		62	0.29	370	0.299	120
4		22	1.25	90	0.384	8.65

**Table 7.7** Groundwaters renewal periods in the Lower–Middle Jurassic complex

Area	Distance from the distribution area of the complex	Module of subsurface flow (l/s from 1 km <sup>2</sup> )	Average thickness (m)	Average porosity	Renewal period (thousand years)
Severnaya	160	0.045	200	0.2	29
Sos'va	200	0.037			340
	250	0.023			550
	280	0.046			29
	320	0.02			630
Near-Kazakhstan	25	0.148	300	0.2	132
	48	0.013			146
	80	0.0103			165
	100	0.01			190
	110	0.007			264
	142	0.006			330
	165	0.003			630
	170	0.001			1,350
310	0.0007	2,720			

The above-mentioned peculiarities in hydrodynamics of the deep subsurface flow in the lower hydrogeological stage of marginal zones in the petroliferous basin allow the following conclusions:

- (1) Hydrodynamic schemes of subsurface fluid flows combined with plots illustrating changes in relative unit expenditures yield comprehensive information on dynamics of the subsurface flow in the lower hydrological stage of marginal zones of the basin.

- (2) The deep subsurface flow in marginal zones of the basin forms in close relation with the surface; therefore, its dynamics demonstrates different spatial and temporal intensity depending on the relief and river network patterns.
- (3) Regional regularities in reduction of subsurface fluid expenditures indicate unambiguously that the *flow* represents the main fluid discharge type. Owing to diffused ascending filtration through clayey sediments, deep subsurface fluids enter successively overlying aquifers, groundwater flows, and river network to be transported to the Kara Sea representing a regional drainage basin.
- (4) Inasmuch as only a few percent of the integral subsurface flow formed along the periphery of the basin enter the Kara Sea, the latter cannot serve as a regional discharge area for deep subsurface fluids. It is conceivable that the Kara Sea represents a local discharge area for subsurface fluids that formed in the adjacent northern margin of the basin (Yamal and Taimyr peninsulas, Polar Urals).
- (5) The entire marginal parts of the basin located in the immediate proximity to regional recharge areas (or adjacent to the latter) should be considered as a regional discharge domain for deep subsurface fluids.
- (6) The most favorable conditions for hydrodynamic relations between aquifers and their discharge are peculiar of peripheral parts of the basin, which sometimes represent hydrodynamically closed formation areas for the deep subsurface flow (drainage of entire sections of petroliferous complexes). They provide no influence on hydrodynamics of subsurface fluids in central areas of the basin.
- (7) The main recharge domains for deep subsurface fluids are the Ob–Yenisei and Alei–Irtysh interfluves, some areas of the Urals, and, probably, watersheds of Ob River left tributaries (Vasyugan, Parabel, Parbig, and other rivers) and Irtysh River right tributaries (Tara, Om, and Tartas rivers).

## 7.5 Influence of the Elision Recharge on Formation Pressures at Deep Levels

The influence of the elision recharge on the deep fluid pressure formation is estimated for the southern margin of the basin in the Om Depression located in the Ob–Irtysh interfluve area (Fig. 7.1).

The upper, Oligocene–Quaternary aquifer was omitted from consideration, since it belongs to the first hydrogeological stage. The quantitative assessment of the additional elision recharge from clays was performed for the period beginning from the Cenomanian–Turonian transition when the Turonian–Oligocene sediments overlying the Aptian–Cenomanian complex started forming; prior to that time, all water released from clays entered the sedimentation basin.

Boundary conditions during target setting (two-layer flat model represented by Lower–Middle Jurassic and Aptian–Cenomanian complexes separated by a low-permeability sequence) were specified proceeding from the following considerations. According to the proposed schemes, most subsided domains of artesian basins represent recharge areas, from which deep fluids migrate toward reservoir outcrops.

Consequently, the central part of the basin should host a hydraulic barrier representing an impermeable boundary (Fig. 4.1). Boundary conditions of the first and second (permanent expenditure corresponding to the infiltration recharge value) types were specified for the reservoir outcropping area and upper boundary of the sedimentation basin, respectively. The base of the reservoir (Lower–Middle petroliferous complex) was considered as an impermeable boundary. The expenditure of released interstitial waters was preset immediately into reservoirs. Parameters required for the task solution were specified proceeding from the following assumptions.

The permeability coefficient of clayey sediments was accepted to be permanent corresponding to  $10^{-5}$  m/day (Table 7.2). Transmissibility changes in the Aptian–Cenomanian complex were accepted to be exponential from 2,500 m<sup>2</sup>/day in marginal parts of the basin to 250 m<sup>2</sup>/day at a distance of 500 km [5]. Transmissibility of the Lower–Middle Jurassic complex was preset in line with its changes presented in Fig. 7.7. It was assumed that filtration properties of the entire section under consideration remained constant at all the subsequent stages of the petroliferous basin evolution.

The present-day unit expenditure of the subsurface fluid flow in this area is 15 m<sup>3</sup>/day or  $5.5 \cdot 10^3$  m<sup>3</sup>/year. For the Lower–Middle Jurassic complex, the unit expenditure in the same area was accepted to be an order of magnitude lower (no information).

It should be noted that beginning from the time when the sedimentary cover started forming up to the Miocene, the southern margin of the basin was characterized by warm humid climate (contrary to the present-day continental one), which is evident from organic remains and weathering crust composition. Proceeding from these observations and assuming that reservoir permeability in the past was at least similar to its present-day values, one can infer that the expenditure of the subsurface flow in the recharge area of petroliferous complexes was also at least similar to the present-day one.

The following assumptions were made to increase the reliability of obtained results:

- (1) The thickness of the lower clayey sequence is permanent to be 900 m. Released waters migrate only upward to enter the Aptian–Cenomanian aquifer. Volumes of released interstitial waters were calculated only for areas of the basin with maximal clay thicknesses (Table 7.2).
- (2) Regional clayey caprocks and relatively thick clayey members are composed of exclusively clayey particles without admixture of silty and coarse-grained material.
- (3) Additional recharge from clays is of permanent intensity.
- (4) In line with the elision concept, elision recharge was considered to be minimal in the peripheral part of the basin and maximal in the Om Depression.

The volume of additional recharge was calculated for the Frolovo area (Fig. 7.2), where the thickness of clayey sediments is maximal throughout the entire section (Table 7.8). Figure 7.14 demonstrates dynamics of released interstitial solutions.

**Table 7.8** Volumes of waters released from clays during their compaction

Upper Jurassic–Cretaceous sequence (J <sub>3</sub> –K <sub>1ap</sub> )			Lower Albian sequence (K <sub>1al1</sub> )			Upper Cretaceous–Paleogene sequence (K <sub>2t</sub> –d–P <sub>1–2</sub> )		
Subsidence period (Myr)	Subsidence interval (m)	Expenditure (Q) (m <sup>3</sup> /m <sup>2</sup> )	Subsidence period (Myr)	Subsidence interval (m)	Expenditure (Q) (m <sup>3</sup> /m <sup>2</sup> )	Subsidence period (Myr)	Subsidence interval (m)	Expenditure (Q) (m <sup>3</sup> /m <sup>2</sup> )
46	0–20	250.2						
6	930–1,040	24.2						
5	1,040–1,140	16.2						
5	1,140–1,240	16.2						
8	1,240–1,400	24.2	8	0–160	10.8			
10	1,400–1,615	24.2	10	160–375	9.2			
10	1,615–1,830	24.2	10	375–590	9.2			
10	1,830–2,045	24.2	10	590–805	7.9			
10	3,045–2,245	16.2	10	805–1,005	6.6			
10	2,245–2,445	16.2	10	1,005–1,205	5.2			
10	2,445–2,645	16.2	10	1,205–1,405	5.2	40	0–815	162.4
14.5	2,645–2,935	16.2	14.5	1,405–1,695	5.2	14.5	815–1,105	14.5
Total for the entire period		468			59			176.9
Sedimentation basin		330 (70%)			29 (50%)			14.5 (91%)

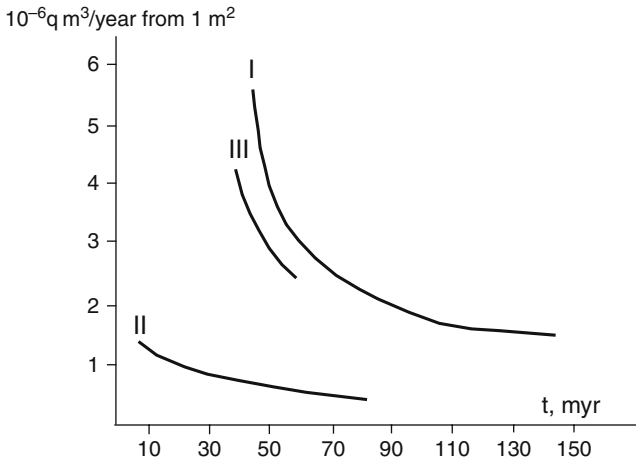


**Fig. 7.14** Changes in volumes of interstitial solutions released from clayey sequences of West Siberia. Sediments: (I) Upper Jurassic–Lower Cretaceous, (II) Lower Albian, (III) Upper Cretaceous–Paleogene

The volume of waters released from clay due to their compaction is determined from the equation [23]

$$V_k = \frac{m}{1 + e}(e_{k-1} - e_k),$$

where  $V_k$  is the volume of water released from rocks with the porosity coefficient  $e$  for the particular period and  $(e_{k-1} - e_k)$  is changes in the porosity coefficient for the same period.

Variations in the porosity coefficient were calculated using the curve of natural clay compaction constructed for West Siberia (Fig. 6.10).

During the entire development history of the West Siberian petroliferous basin (its most subsided part),  $704 \text{ m}^3/\text{m}^2$  of interstitial waters were released,  $373 \text{ m}^3/\text{m}^2$  released into the sedimentation basin and exposed low-permeability reservoirs included.

Consequently, relatively closed reservoirs received  $2.6 \cdot 10^{-6} \text{ m}^3/\text{year}$  on average (averaged for 144 Myr) from  $1 \text{ m}^2$  or  $1 \cdot 10^{-4} \text{ l/s}$  from  $1 \text{ km}^2$ . According to F.G. Gurari,  $800 \cdot 10^{12} \text{ m}^3$  of interstitial waters were released from clayey sediments for the entire history of the West Siberian basin or  $5 \cdot 10^{-6} \text{ m}^3/\text{year}$  from  $1 \text{ m}^2$ , or  $1.8 \cdot 10^{-4} \text{ l/s}$  from  $1 \text{ km}^2$ , which is very close to our calculated data.

V.A. Vsevolozhskii (1973) calculated approximately that the groundwater influx from the Aptian–Cenomanian complex toward inner areas of the basin limited by the isohypse of 90 m (radius of 400 km) is 400 l/s (according to our data derived from the unit expenditures, it is seven times higher). Comparison of this value with the volume of waters released from compacted clays for the same area ( $\sim 38 \text{ l/s}$  for the semicircle with the radius of 400 km) shows that the elision recharge is an order

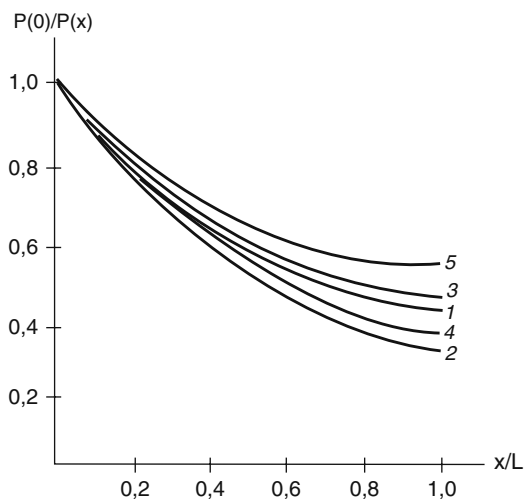
of magnitude lower than that related to the weakened lateral influx and incomparable with the subsurface flow that is forming in marginal areas of the present-day recharge.

Such a comparison demonstrates incommensurable volumes of these two recharge types. Indeed, the infiltration recharge value ( $5.5 \cdot 10^3 \text{ m}^3/\text{year}$ ) exceeds the elision recharge value ( $1.3 \cdot 10^3 \text{ m}^3/\text{year}$ ) more than 3,000 times. Therefore, the latter should increase 2,960 times to affect notably subsurface fluid heads. Thus, according to the model, the elision recharge is  $3,850 \text{ m}^3/\text{year}$  per 1 m of the width and 500 km of the length of the section, which exceeds five times the volume of all water released from clays for their entire geological history and more than an order of magnitude the volume of interstitial waters received by reservoirs.

The indicated parameters of aquifers (petroliferous complexes), expenditures of the present-day infiltration recharge, and volumes of released interstitial waters provided the distribution of fluid heads presented in Fig. 7.15. Curves 2 and 1 describe the distribution of fluid heads without account for additional recharge from clays (initial condition) and in the Aptian–Cenomanian and Lower–Middle Jurassic petroliferous complexes. Curves 3 and 4 characterize the distribution of fluid pressures in the same complexes for the situation when additional recharge was received only by the Aptian–Cenomanian complex and Curve 5 illustrates the distribution of heads in the Lower–Middle Jurassic complex when it received all the elision solutions.

The distribution of fluid pressures (Fig. 7.15) shows that even such a significant additional recharge from clays ( $3,850 \text{ m}^3/\text{year}$  per 1 m of the width of the cross section 500 km long) under given values of present-day infiltration recharge and selected parameters of the system (substantially overestimated expenditures of infiltration recharge smooth potential errors related to discrepancies between model and natural parameters) slightly influenced the distribution of subsurface fluid heads and left their migration vector unchanged in both the lower and upper complexes.

**Fig. 7.15** Schematic paleodistribution of subsurface fluid heads in the southern part of the Ob–Irtysh interfluvium. Initial distribution of heads: (1) in Jurassic sediments, (2) in Cretaceous sediments, (3) the same, with recharge from clays, (4) in Jurassic sediments, (5) in Aptian–Cenomanian sediments, (6) the same in the Jurassic aquifer, which received the entire volume of interstitial solutions squeezed during the entire development history of the basin





No reversed direction of the flow (from subsided parts of the basin toward its periphery) was observed also in the situation when the present-day infiltration recharge was assigned only for the Aptian–Cenomanian complex, i.e., its whole volume ( $5,500 \text{ m}^3/\text{year}$  per 1 m of the width) entered only the latter, while all the elision recharge was received by the Lower–Middle Jurassic complex. In such a situation, the ratio of infiltration recharge of subsurface fluids to the influx from clays was 1.43, not 1.57, which is observed in two previous situations.

The modeling (performed with a large reserve of engineering reliability) unambiguously demonstrates groundless overestimation of the role of elision waters in the formation of fluid pressures during past and, in particular, recent geological epochs: *the latter is determined by the decrease in the geostatic load due to denudation.*

Thus, it is evident that the complex approach, when all the factors responsible for the development of formation pressures in petroliferous basins, the West Siberian and East Ciscaucasia (see below) basins included, are taken into consideration, is needed in studies of every natural process.

The elision concepts of subsurface fluid migration in deep formations are based on the only physical process (compaction) that determines the recharge source and their spatial distribution. In this situation, when the geological structure, filtration properties of permeable rocks and separating low-permeability sequences, outer and inner boundary conditions, and others features are ignored, the role of this source increases to acquire decisive significance in the formation of deep fluid pressures and, consequently, their migration.

Elision should be considered in evolutionary succession and together with other processes such as present-day infiltration recharge, spatial and temporal relaxation rates of formation pressures in different lithologies, clayey sediments included, and others with quantitative assessments of these processes.

Thus, the following points should be emphasized:

- (1) The influx rate of waters released during catagenetic transformations of clayey rocks is incommensurably low (observable at the background of the geological timescale) as compared with that peculiar of the pressure redistribution even in similar sediments (Chapter 4).
- (2) It is principally incorrect to study migration of subsurface fluids and draw conclusions on the petroleum reserve potential of the basin and its separate parts based only on elision concepts as it happens now [9–12 and others].

## **7.6 Fluidodynamics of Deep Formations in Central Areas of the Basin**

Fluidodynamics is studied mainly in the Surgut Arch located in the central part of the basin, which hosts over 30 discovered hydrocarbon fields and is sufficiently well known, as well as in separate well-studied fields in central and northern areas of the basin. Brief information on some of them is given below.

### 7.6.1 *Salym Field*

This field is one of the most interesting and best studied. It is the first field in the basin where oil pool is discovered in argillites.

The Salym field is located at the transition between two large structures: Khanty-Mansi Depression and Surgut Arch separated, likely, from each other by faults. The sedimentary cover in this area is approximately 3 km thick. Its basal part is represented by the Lower–Middle Jurassic Tyumen Formation overlain successively by the Abalak and Bazhenovka formations. The latter is composed of fractured argillites 30–40 m thick.

In the opinion of most researchers, the *Tyumen Formation* is lacking abnormally high formation pressures, although reliable data are insufficient. In most boreholes, which recovered the upper part of the Tyumen Formation, the latter was sampled together with the Bazhenovka Formation, which is penetrated through its entire thickness. Only in two boreholes, it was sampled separately. One of them (184) appeared to be dry. Another borehole (49) yielded the normal pressure (similar to that in the Bazhenovka Formation). Drilling of the Tyumen Formation in Borehole 312 required drilling mud to be weighed up to  $2,000 \text{ kg/m}^3$ , which indicates the high formation pressure. Borehole 123 drilled in the neighboring Sredne-Shapkinsk field recovered abnormally high formation pressure (52 mPa at a depth of 2,800 m with the anomaly coefficient of 1.9). Thus, limited samples imply development of both normal (hydrostatic) and abnormally high formation pressures in the Tyumen Formation.

Inasmuch as the *Bazhenovka Formation* encloses oil accumulations and is characterized by abnormally high formation pressures, it is sufficiently well studied. The formation exemplifies the block structure of the lower part of the sedimentary section, which is reflected in both natural and distorted settings.

The complex tectonic structure is determined by a system of faults established by seismic and magnetometric methods and compression-induced deformations, which are reflected in vertical fractures and slickensides. The block movements were in progress during the entire history of the basin, the recent epoch included.

In natural conditions, the pressure in the Bazhenovka Formation at a depth of 2,700 m varies from 20.3 (Borehole 10) to 48.1 mPa (Borehole 101), i.e., the anomaly coefficient is 1.73 [25]. Fifty of 152 samples revealed abnormally high formation pressure, with the anomaly coefficient exceeding 1.4 and 20 of them showed normal hydrostatic or lower hydrostatic pressure. In 52 boreholes, the oil yield was very low or they were dry. In some boreholes (12, 13, 17, 20, and 21), abnormally high formation pressures resulted in emergency situations. Table 7.9 presents formation pressure values obtained for some boreholes.

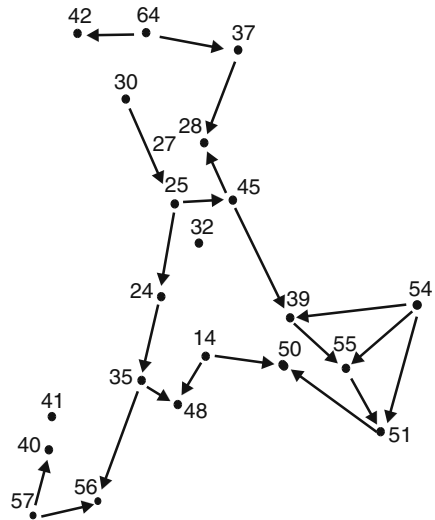
The horizontal gradients of formation pressures are differently oriented (Fig. 7.16) and range from  $n \cdot 10^{-3}$  to  $n \cdot 10^{-2}$  to reach  $n \cdot 10^{-1}$  in some areas. The horizontal gradients between boreholes 12-31, 12-68, 169-127, and 150-127 exceed a unit.

The filtration experiments conducted in some paired boreholes (27-25, 24-18, 107-28, 107-112, 127-150, 169-150) revealed no hydrodynamic interaction even

**Table 7.9** Formation pressures in the Bazhenovka Formation measured at 2,700 m

Borehole	$P_{form}$ (mPa)	Borehole	$P_{form}$ (mPa)	Borehole	$P_{form}$ (mPa)	Borehole	$P_{form}$ (mPa)
14	43.36	30	43.5	40	31.1	51	29.6
18	43.09	31	26.6	41	36.6	54	42.09
24	42.1	32	45.1	42	43.0	55	34.75
25	43.1	35	35.65	46	42.97	56	28.0
27	42.65	37	42.96	48	31.78	57	41.72
28	42.3	39	36.79	50	27.46	64	44.4

**Fig. 7.16** The Salym field. Direction of lateral gradients (Bazhenovka Formation)

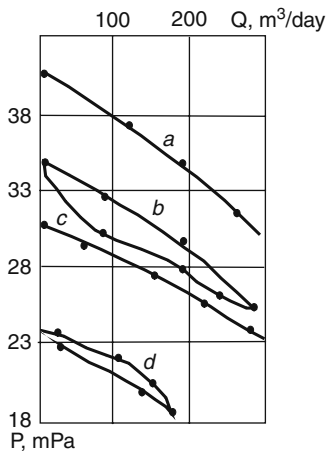


between closely spaced pairs. In boreholes 169 and 127 located 500 m away from each other, hydrolocation established such relations. At the same time, Borehole 150 located at a distance of 300 m demonstrated no response to flow disturbance and the difference between formation pressures remained significant.

Interaction between boreholes 27 and 28 (distance of 2.8 km) exploited during the long period was noted only in 1974 and 1975. After long-lasting exploitation, no such relations were established between them. During the exploitation period of 10 years, the difference between current pressures demonstrated tendency for gradual increase. This implies undoubted development of the impermeable boundary between these boreholes during exploitation (closure or healing of fissures) due to changes in the strain state in response to decreased formation pressures.

After commercial exploitation initiated in 1974 (wells 24, 27, 28, 68, and others), the pressure in some new tested boreholes appeared to be higher than that in old boreholes: 44 mPa in Borehole 92 (1976); 47 mPa in Borehole 124 (1982). In 1979,

**Fig. 7.17** Indicator diagrams for the well of the Salym field (after V.K. Fedorov and V.N. Nesterov). (a) After exploitation; (b–d) test exploitation: (b) 1974, (c) 1975, (d) 1976



the initial formation pressure in Borehole 73 was 42 mPa, while in exploitation Well 54 located 3.2 km away from the latter, it was 24.6 mPa. These data indicate that the Bazhenovka Formation is characterized by the stratum-block structure with impermeable boundaries between separate blocks both in natural and disturbed conditions. Exploitation of the Salym oil field was accompanied by gradual decrease in pressures, which remained low after termination of well exploitation. The curve illustrating the correlation between the formation pressures retains its patterns at each new level (Fig. 7.17), i.e., the single block is exploited, which indicates the elastic-closed response to disturbance and impermeable boundaries on all its sides. Beyond these boundaries, no exploitation effect and influx of the fluid into a closed system are observed.

Absence of hydrodynamic interaction between blocks of the structure under consideration and development of impermeable boundaries are also evident from sharp gradients of formation pressures between closely spaced wells. For example, wells 54 and 55 located 6.5 km away from each other were characterized by the formation pressure gradient of 11.8 mPa after exploitation beginning in the first of them and test beginning in another. The gradient between wells 64 and 93 located 6 km away from each other was 16.8 mPa under the same conditions. Similar significant gradients of formation pressures are observed between wells 18-24, 72-27, and other pairs.

According to hydrodynamic testing data, the piezoconductivity coefficient of productive sediments is  $5 \cdot 10^7$  m<sup>2</sup>/day. With such a value, the disturbance at a distance of 6 km should be notable in wells 1.6 days after the beginning of well exploitation. At the same time, no interaction between them is observable even after an year of exploitation.

Commercial exploitation of observation hole 81 during the period from the terminal 1979 to the middle of 1981 was accompanied by the continuous increase

in the formation pressure by 20 mPa. At the same time, exploitation wells (24, 27, 28, 84, and 141), some of which are located at a distance of approximately 6 km from each other, demonstrated significant decrease in formation pressures.

The significant increase in formation pressures was also observed in some other observation boreholes (10, 18, 50, 71, 85, 92, 93). Their such behavior cannot be explained by technical errors during hole testing. This is explainable by two factors: either by fluid influx from the underlying sediments or by changes in the strain state (compression) in some areas of the section.

Other observation boreholes (25, 39, 44, 46, and 54) demonstrated the fall in the formation pressure. After 9 years of exploitation, the pressure in observation Borehole 35 remained practically unchanged.

*Temperature anomalies.* The Salym field is characterized by temperature anomalies and its temperature field differs significantly from the regional background. Its geothermal gradients (4.4–4.6°C per 100 m) are among highest values in the central part of the basin. The temperature field of the field is highly differentiated. In the Bazhenovka Formation, temperature variations amount to 60°C (from 91 to 150°C in boreholes 156 and 312, respectively). Sometimes, such differences are observed at short distances. For example, the temperature difference between boreholes 312 and 154 located 5 km away from each other is 30°C. The formation temperature increases from limbs of the structure toward its arch. Zones of elevated temperatures are characterized by the linear strike close to the meridional one, which emphasizes their relations with tectonic fractures.

*Hydrogeochemical anomalies.* The composition of subsurface fluids in Jurassic sediments is characterized by significant lateral variations: from hard chloride-calcic (after V.A. Sulin) to hydrocarbonate-sodium one. The water mineralization ranges from 1.7 to 17 g/l. The salt composition demonstrates inversion: mineralization decreases slightly downward the section, while the share of hydrocarbonates increases. The zones with high-alkali groundwaters (pH up to 8) usually cross the entire section and are characterized by elevated contents of microcomponents. Such a situation is probably explained by ascending migration of deep fluids from lower parts of the section.

This assumption is confirmed by palynological data, which indicate the occurrence of Lower–Middle Jurassic and Paleozoic microfossils in oils from the Bazhenovka Formation [15, 16]. The ascending fluid migration is also confirmed by the fact that the content of Paleozoic microfossils in oils increases during field exploitation. According to studies carried out by specialists from the Institute of Geology and Exploration of Combustible Mineral Resources, Paleozoic forms constitute up to 45% of the assemblage in oils from the Bazhenovka Formation. In Well 32, such alien forms constitute up to 24%. Their minimal content is recorded in oils from wells 38 and 56 confined to limbs of the structure. Additional palynological studies carried out in 1986 (after 10 years of exploitation) revealed significant increase in the share of older microfossils (up to 85–100%) in oils from production wells 24, 27, 28, 32, 72, 117-p, and 153-p.

In some wells, dissolved gas is characterized by the anomalously high content of carbon dioxide (up to 17%), nitrogen (up to 42%), and hydrogen (up to 28%), which evidence ascending migration as well.

*Mineralogical anomalies.* Fractures with slickensides are filled with vein minerals of several generations: calcite, rhodochrosite, pyrite, dolomite, and quartz. Vein minerals constitute up to 30–40% of the rock volume. Early generations are readily soluble. Later minerals are represented by quartz and dolomite, regular crystals of which indicate their free growth. There are situations when all the vein minerals appear to be intensely corroded and fragmented with spaces between rock fragments filled with oil, which indicates repeated movements along fractures and migration of oil. Development of several generations of secondary minerals emphasizes pulse patterns of hydrothermal processes.

In Well 554 with the yield of 250 t/day located in the seismically active zone, vein minerals that constitute approximately 50% of the rock volume were leached (by >50%) and destroyed up to the detritus state. In Well 142 located beyond the seismically active zone at a distance of 600 m from the previous one, thin fissures are filled with calcite lacking leaching signs.

*Oil anomalies.* Such anomalies are established in wells 13, 40, 61, 71, 76, 91, and others. Geochemical properties of oils (presence of benzol, asphaltene, paraffin, and others) mark oil anomalies, which are interpreted as resulting from vertical migration of oil from underlying Paleozoic strata.

The ascending migration is stimulated by a system of fractures and fault zones defined by gravimetric, magnetometric, seismic, and repeated leveling data. The faults activated during different epochs, the Neogene–Quaternary included. The study of current vertical movements based on *repeated leveling* data made it possible to define areas of recent uplifting and subsidence separated by zones with maximal gradients of current vertical movements, which associate locally with faults [27].

The distribution of formation pressures in natural conditions, hydrolocation measurements, exploitation, spatially close positions of “dry” and productive wells, the distribution patterns of the temperature field, and hydrochemical and palynological data demonstrate that the Salym field consists of several hydrodynamically isolated blocks with impermeable, differently oriented boundaries between them. Moreover, impermeable boundaries are formed during exploitation of the field. Thus, the Salym field represents a stratum-block system.

### **7.6.2 Western Surgut Field**

The hydrodynamic situation in Lower Cretaceous rocks of the western Surgut field is studied in many boreholes. The sampled interval is approximately 200 m thick (from 1,984 to 2,200 m). No anomalous pressures are registered in the Lower Cretaceous sequence of the field (Table 7.10).

**Table 7.10** Measured and reduced formation pressures in the western Surgut field

Borehole	$P_{mes}$	$P_{mes}$ (mPa)	Measured altitude (m)	Density (kg/m <sup>3</sup> )	$P_{red}$ (mPa)	Indef I	
						(mPa)	(mPa)
						-2,400 m	-3,000 m
157	217.4	21.74	1,984.5		25.90	0.05	0.13
45	205.3	20.53	2,003		24.50	0.05	0.12
48	222.4	22.24	2,010		26.14	0.05	0.12
49	224.0	22.4	2,012		26.28	0.05	0.12
50	211.2	21.12	2,030		24.82	0.05	0.12
185	210.9	21.09	2,216	1,010	22.93	0.02	0.10
45	226.3	22.63	2,219	1,009	24.44	0.02	0.10
49	247.2	24.72	2,221	1,008	26.51	0.02	0.10
157	226.0	22.6	2222.5	1,012	24.38	0.02	0.10
180	227.7	22.27	2,223		24.54	0.02	0.10
183	231.7	23.17	2,224		24.93	0.02	0.10
48	173.6	17.36	2,227		19.09	0.02	0.10
45	247.7	24.77	2,229	1,009	26.48	0.02	0.10
196	229.3	22.93	2,235		24.58	0.02	0.10
161	224.3	22.43	2,242	1,011	24.01	0.02	0.09
302	223.3	22.33	2,253		23.80	0.02	0.09
161	223.6	22.36	2,256		23.80	0.02	0.09
187	226.0	22.6	2,256	1,011	24.04	0.02	0.09
159	231.5	23.15	2,258		24.57	0.02	0.09
160	248.0	24.8	2,259		26.21	0.02	0.09
182	231.7	23.17	2,259		24.58	0.02	0.09
300	227.0	22.7	2,280	1,008	23.90	0.02	0.09
44	234.2	23.42	2,283	1,011.5	24.59	0.01	0.09
194	226.5	22.65	2,295		23.70	0.01	0.09

Mineralization of subsurface fluids in this interval is insignificant varying from 14.4 to 16.4 g/dm<sup>3</sup> with their density ranging from 1,009 to 1,015 kg/m<sup>3</sup> (Table 7.11). In connection with density changes in the interval of 200 m, formation pressures were reduced to depths of -2,400 and -3,000 m. Table 7.10 presents calculation results, which demonstrate that the reduction error does not exceed 0.05 mPa, being usually 0.02 mPa.

Gradients of formation pressures measured practically at the same depth vary from 1.47 to 7.41 mPa (Fig. 7.18). This makes it possible to determine directions of lateral gradients of reduced pressures between individual boreholes (indef not more than 0.05 mPa at -2,400 m). Figure 7.19 illustrates directions of horizontal gradients of reduced pressures. It shows that horizontal gradients are oriented in different directions even in the relatively small area of the structure, which indicates its stratum-block structure and development of vertical and near-vertical, low-permeability or impermeable boundaries along bedding of Lower Cretaceous strata. The similar situation is observed in the southern Surgut field also (Fig. 7.20).

**Table 7.11** The groundwater chemical composition and mineralization in Lower Cretaceous sediments of the western Surgut field

Borehole	Sampling depth (m)	Mineralization (g/l)	Content of macro- (g/l) and microcomponents (mg/l)													
			Cl	SO <sub>4</sub>	HCO <sub>3</sub>	Na+K	Ca	Mg	SiO <sub>2</sub>	CO <sub>2</sub>	Br	J	H <sub>2</sub> BO <sub>3</sub>	pH		
157	2,273		9.4		0.4	5.8			0.092	0.052	0.026	60.6	31.2			7.4
185	2,280	16.0	9.6		0.17	5.8	0.33	0.03	0.022			57.0	24.0	42.0		7.4
49	2,285	16.0	9.4		0.24				0.03	0.04				26.0		7.6
45	2,286	16.2	9.2		0.658	5.85	0.286	0.025	0.015	0.035	52.1			14.1		7.2
183	2,286	16.2	9.2		0.58	5.85	0.29	0.023	0.028	0.035	56.1		36.8	18.0		7.4
180	2,288	16.4	8.01		0.073	5.0	0.3	0.005	0.21				19.2	45.2		9.0
187	2,317	16.4	9.2		0.008	0.829	0.3	0.012	0.02	0.026	70.1		13.7	18.0		7.4
159	2,323	15.5	8.2		0.03	1.42	0.28	0.03	0.025	0.005	61.7		21.8	27.0		7.4
161	2,326	15.8	9.0		0.793	5.79	0.254	0.025			50.6		20.3	50.0		7.2
30	2,344	15.48	8.16		0.004	1.39	0.2	0.46	0.01	0.26	57.2		24.8	25.4		7.4
44	2,348	14.9	8.9		0.008	0.07	0.24		0.04		61.6		25.7	25.3		7.0



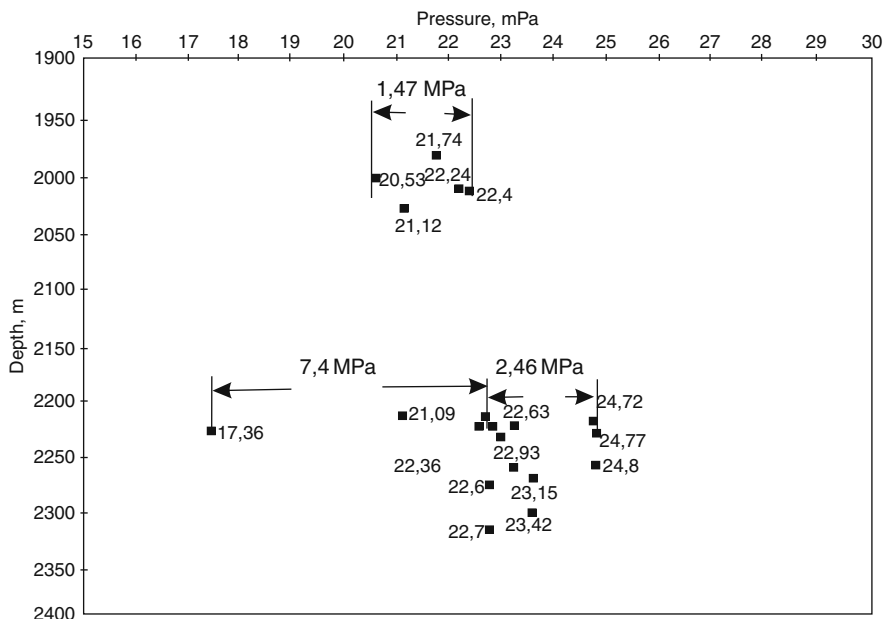


Fig. 7.18 The western Surgut field. Lateral pressure difference ( $K_1$ )

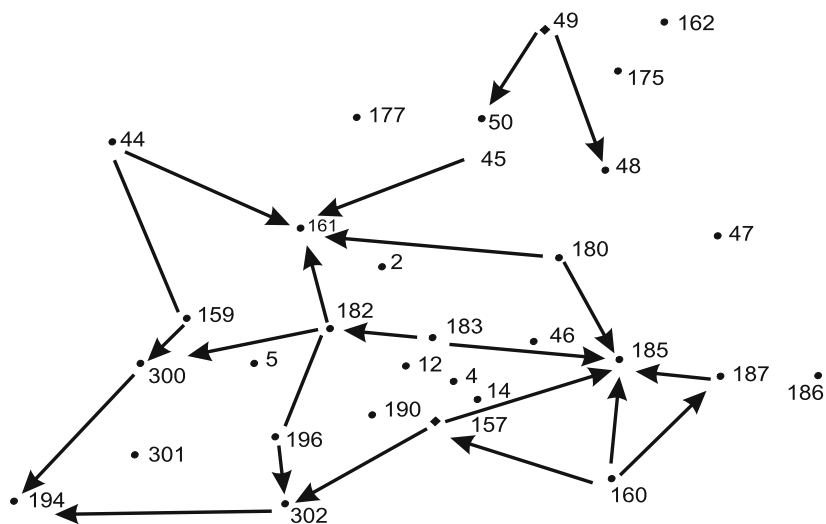
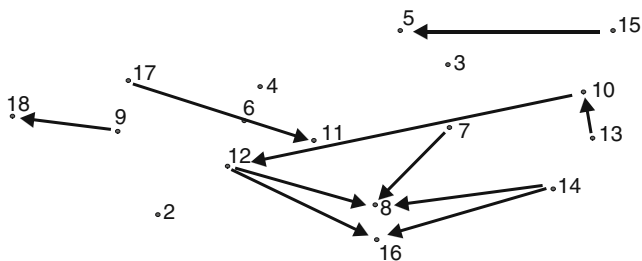


Fig. 7.19 The western Surgut field. Direction of reduced formation pressure gradients (comparison surface  $-2,400$  m)



**Fig. 7.20** The western Surgut field. Directions of horizontal reduced formation pressure gradients in groundwaters of Lower Cretaceous sediments

### 7.6.3 Kharasavei Field

In Lower Cretaceous sediments, formation pressures vary in wide limits through the relatively small area of the field (Fig. 7.21) (Table 7.12).

The formation pressures range from normal (anomaly coefficient of 1.06) to abnormally high with the anomaly coefficient amounting to 1.89 (Table 7.12). The difference between formation pressures measured at the same depth ranges from 4.4 to 7.4 mPa (Fig. 7.21) and horizontal gradients of reduced formation pressures are

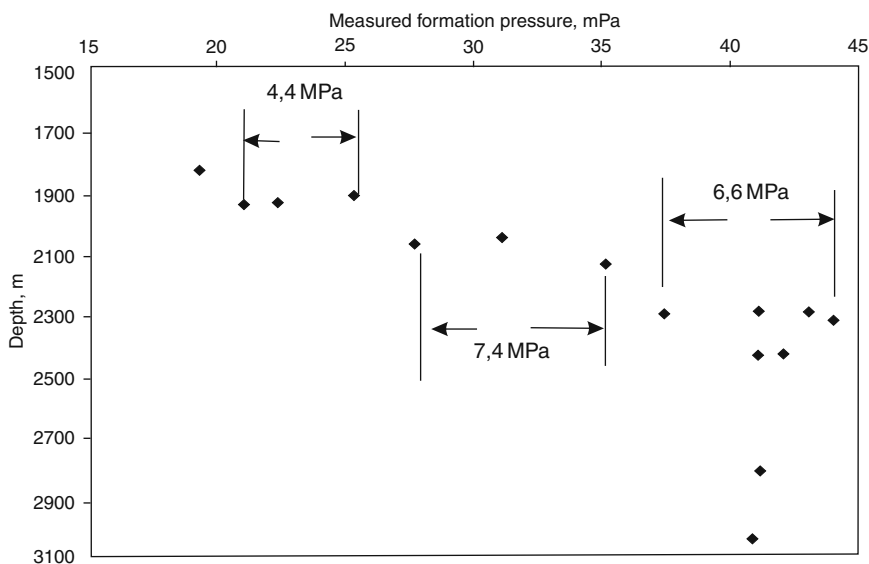


**Fig. 7.21** The Kharasavei structure. Lateral differences in measured formation pressures ( $K_1$ )

**Table 7.12** Measured and reduced formation pressures in the Kharasavei field

Borehole	$P_{mes}$ (mPa)	Middle of the sampling interval (m)	$P_{red}$ (mPa)	Anomaly coefficient
4	41.05	2,435	41.1	1.69
4	21.0	1,937	25.03	1.08
4	19.3	1,827	25.03	1.06
4	25.4	1,904	30.36	1.33
4	35.1	2,136	37.74	1.64
12	22.3	1,928	27.02	1.16
12	37.7	2,067	31.03	1.34
19	41.1	2,815	37.39	1.46
19	40.8	3,040	34.4	1.34
20	41.1	2,297	42.13	1.79
20	44.0	2,325	44.75	1.89
35	42.0	2,427	43.27	1.73
31	43.0	2,299	44.01	1.87
36	37.4	2,302	38.38	1.62
34	31.1	2,047	34.63	1.52

differently oriented (Fig. 7.22). The possible reduction error is substantially less as compared with the difference between measured and reduced formation pressures.

The abnormally high formation pressure itself indicates development of impermeable or poorly permeable, differently oriented boundaries and stratum-block structure of the Kharasavei field.

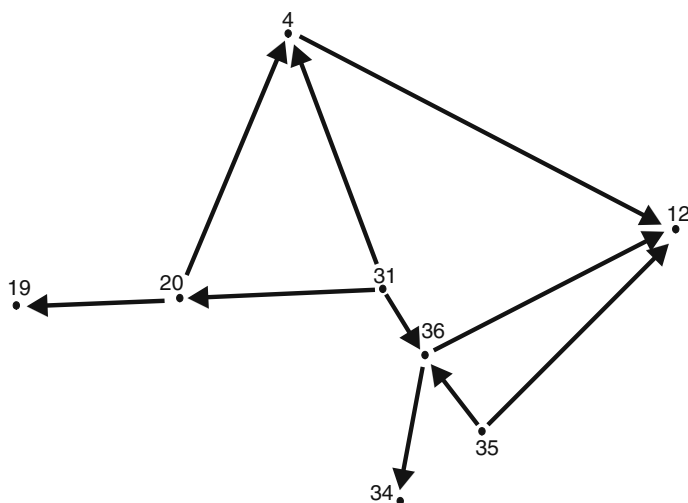


**Fig. 7.22** The Kharasavei structure. Directions of horizontal reduced formation pressure gradients in groundwater of Lower Cretaceous sediments

### 7.6.4 Ust-Balyk Field

In the Ust-Balyk field, Lower Cretaceous sediments are cored by many boreholes in a relatively narrow interval of the section (Table 7.13). Their remarkable features are low mineralization of subsurface fluids, which varies from 3.0 to 17.8 g/l, and low density practically through the entire examined interval, which makes reduction of pressures optional (Table 7.14).

Nevertheless, for increasing the reliability of interpretations, the formation pressures were reduced with the assessments of a reduction error (Table 7.13). The reduction error (indef) does not exceed 0.04 mPa (for the comparison plane of  $-2,400$  m), which corresponds to 4 m of the water column; accordingly, it is higher for the comparison surface of  $-3,000$  m (Table 7.13). As was mentioned, the higher error is determined by larger distance of the comparison plane from sampling depths of maximal quantity of intervals. The low reduction error explained by low density of subsurface fluids allows formation pressures to be reduced ignoring density changes.

Under such conditions, the gradient of formation pressures at close depths varies from 1.84 to 3.28 mPa (Fig. 7.23), which indicates the development of horizontal pressure gradients (measurement results are given for natural conditions that existed prior to the testing or the commercial exploitation). When constructing schemes illustrating directions of horizontal gradients of reduced formation pressures (Fig. 7.24), we used values of the reduced formation pressure (if there are several of them) located most closely to the comparison plane ( $-2,400$  m). Development of horizontal gradients implies poorly permeable or impermeable differently oriented boundaries and blocks within the field.

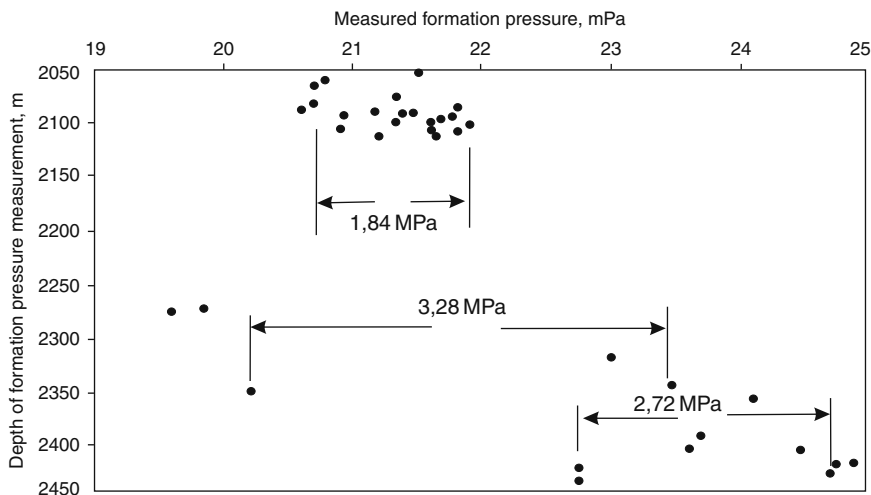


Fig. 7.23 The Ust-Balyk structure. Lateral differences in measured formation pressures ( $K_1$ )

**Table 7.13** Measured and reduced formation pressures in the Ust-Balyk field

Borehole	$P_{mes}$ (mPa)	Sampling altitude (m)	$P_{red}$ (mPa)	Indef-2,400 m	Indef-3,000 m
66	21.62	2,110.5	24.52	0.04	0.37
69	21.33	2,078	24.55	0.04	0.37
71	21.8	2,111	24.69	0.04	0.37
76	21.5	2,056.5	24.94	0.04	0.37
82	21.43	2,092.5	24.51	0.04	0.37
83	21.9	2,105	24.85	0.04	0.37
84	21.45	2,093	24.52	0.04	0.37
87	21.8	2,088.5	24.92	0.04	0.37
119	21.16	2,091.5	24.25	0.04	0.37
203	21.37	2,095	24.42	0.04	0.37
204	20.93	2,094.5	24.99	0.04	0.37
63	20.71	2,067	24.04	0.04	0.37
65	21.62	2,101.5	24.61	0.04	0.37
67	21.66	2,100.5	24.66	0.04	0.37
68	21.2	2,114.5	24.06	0.04	0.37
74	21.75	2,097	24.78	0.04	0.37
75	20.6	2,089	24.71	0.04	0.37
80	20.77	2,062.5	24.15	0.04	0.37
214	21.33	2,100	24.33	0.04	0.37
236	20.9	2,107.5	24.83	0.04	0.37
72	21.6	2,109	24.51	0.04	0.37
80	20.7	2,084.5	23.86	0.04	0.37
65	<i>19.6</i>	<i>2,277</i>	<i>20.83</i>	<i>0.02</i>	<i>0.37</i>
79	<i>24.07</i>	<i>2363.5</i>	<i>24.44</i>	<i>0.0</i>	<i>0.37</i>
88	<i>20.16</i>	<i>2,354</i>	<i>20.62</i>	<i>0.01</i>	<i>0.37</i>
221	<i>23.44</i>	<i>2350.5</i>	<i>23.94</i>	<i>0.01</i>	<i>0.37</i>
<b>63</b>	<b>19.83</b>	<b>2,273</b>	<b>21.10</b>	<b>0.02</b>	<b>0.37</b>
<b>79</b>	<b>24.07</b>	<b>2,364</b>	<b>24.43</b>	<b>0.0</b>	<b>0.37</b>
<b>116</b>	<b>23.66</b>	<b>2,397</b>	<b>23.69</b>	<b>0.0</b>	<b>0.37</b>
<b>117</b>	<b>24.43</b>	<b>2,432</b>	<b>24.34</b>	<b>0.0</b>	<b>0.37</b>
<b>221</b>	<b>23.44</b>	<b>2350.5</b>	<b>23.94</b>	<b>0.01</b>	<b>0.37</b>
<b>547</b>	<b>22.97</b>	<b>2,323</b>	<b>23.74</b>	<b>0.01</b>	<b>0.37</b>
<b>1,103</b>	<b>23.57</b>	<b>2,409</b>	<b>23.48</b>	<b>0.0</b>	<b>0.37</b>
<b>36</b>	<b>24.66</b>	<b>2,432</b>	<b>24.34</b>	<b>0.0</b>	<b>0.37</b>
<b>39</b>	<b>24.83</b>	<b>2424.5</b>	<b>24.59</b>	<b>0.0</b>	<b>0.37</b>
<b>58</b>	<b>24.7</b>	<b>2,426</b>	<b>24.44</b>	<b>0.0</b>	<b>0.37</b>
<b>1,204</b>	<b>22.71</b>	<b>2438.5</b>	<b>22.33</b>	<b>0.0</b>	<b>0.37</b>
<b>1,205</b>	<b>22.72</b>	<b>2427.5</b>	<b>22.45</b>	<b>0.0</b>	<b>0.37</b>

Ordinary, italic, and bold fonts correspond to the Hauterivian, Valanginian, and Neocomian sediments, respectively.

Vertical gradients are relatively high. For example, the pressure differences are 1.4 mPa ( $\Delta z=206$  m) in Well 63, 2.2 mPa ( $\Delta z=175.5$  m) in Well 65, and 1.3 mPa ( $\Delta z=22$  m) in Well 80. Consequently, respective gradients are 0.068, 1.25, and 0.6. Such high values of this parameter indicate development of poorly permeable horizontal boundaries.

**Table 7.14** Groundwater chemical composition and mineralization in Lower Cretaceous sediments of the Ust-Balyk field

Borehole	Depth (m)	Br (mg/l)	<i>J</i> (mg/l)	HCO <sub>3</sub> (mg/l)	SiO <sub>2</sub> (mg/l)	Mineralization (g/l)	Density (kg/m <sup>3</sup> )
69	1,905	50.64	19.46	378.2	10.2	16.1	
69	1,943	63.27	24.69	378.2	13.0	17.6	
69	1,945	56.05	20.3	402.0	13.0	16.3	1,010
70	1,929.5	53.8	17.9	384.0	32.0	16.0	1,010
61	2,091	13.4	6.0	359.0	9.0	5.4	
64	2,116	55.0	20.1	219.0	21.0	16.15	1,011
78	2,111	62.9	24.5	378.2	18.0	15.44	1,010
86	2,112	49.0	19.5	390.4	26.0	14.5	1,010
89	2,123	59.7	22.0	305.0	8.0	14.8	1,009
202	2,120	60.8	23.5	500.2	10.2	15.2	1,010
215	2,128	58.1	22.0	329.0	22.0	16.2	1,010
218	2,105	60.7	22.0	402.6	26.0	15.9	1,009
75	2,108	58.6	23.4	578.2	14.0	16.3	1,011
201	2,113	55.4	22.4	353.8	14.0	16.7	1,011
75	2,120	56.1	24.3	390.4	15.8	16.5	1,011
64	2,180	32.5	13.4	305.0	18.2	10.3	1,007
69	2,134	10.1	2.6	97.6	9.4	3.9	1,002
72	2,131	54.1	21.4	426.6	17.3	16.1	1,011
75	2,141	56.9	24.3	244.0	13.5	16.4	1,011
76	2,113	50.0	22.9	451.4	13.5	15.8	1,010
80	2,102	62.9	23.7	475.8	3.5	14.9	1,010
214	2,142	63.4	74.5	353.8	11.3	15.4	1,010
63	2,133	54.4	20.1	610.0	21.0	16.4	1,011
64	2,112	33.7	12.6	250.1	14.3	10.2	1,007
69	2,162	13.3	5.9	183.0	10.2	5.0	1,002
80	2,135	9.44	7.1	170.8	11.2	3.3	1,002
61	2,117	14.0	6.8	414.8	9.0	4.9	1,002
62	2,175	29.1	11.1	561.2	24.0	9.4	1,001
63	2,191	52.8	20.1	799.1	26.0	16.4	1,011
69	2,125	48.5	48.5	976.0	15.0	16.1	1,011
70	2,229	17.7	6.0	324.4	3.5	5.6	1,002
72	2,227	40.2	19.7	854.0	21.0	12.7	1,008
80	2,193	56.5	23.8	805.0	14.0	16.2	1,011
65	2,267	53.8	21.1	939.4	13.5	17.5	1,012
66	2,350	50.1	20.2	902.8	5.3	16.2	1,011
68	2,337	6.1	3.4	414.8	3.6	10.9	1,002
72	2,301	52.0	21.4	451.4	9.5	15.2	1,010
87	2,340	46.6	22.3	915.0	20.6	15.01	1,010
61	2,469	17.8	3.4	829.6	3.0	5.9	1,002
<b>234</b>	<b>2,887</b>			<b>1830.0</b>		<b>18.0</b>	

Bold font designates Jurassic sediments

The stratum-block structure of formations is confirmed by hydrogeochemical data (Table 7.14). Mineralization (Fig. 7.25) and contents of ions are variable in lateral and vertical directions. Horizontal gradients of subsurface fluid mineralization in Lower Cretaceous sediments of the field as well as gradients of reduced

**Fig. 7.24** The Ust-Balyk structure. Directions of horizontal reduced formation pressure gradients in groundwater of Lower Cretaceous sediments

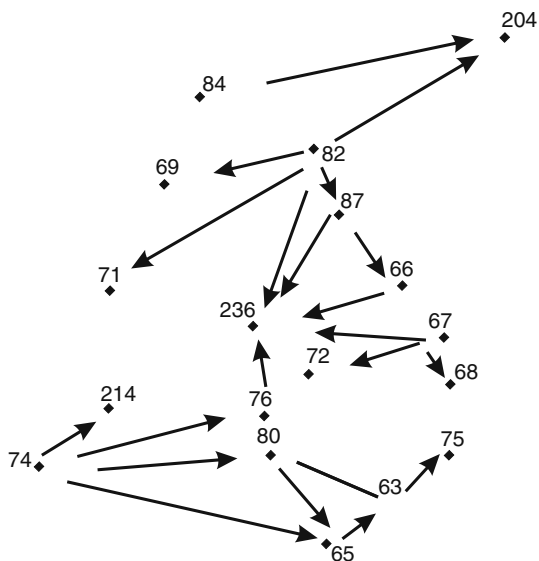
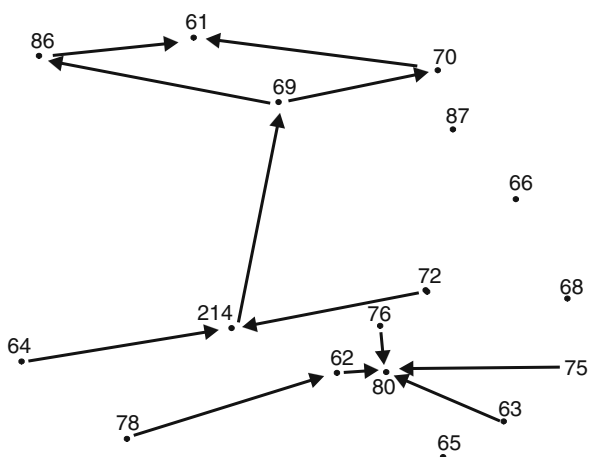


**Fig. 7.25** The Ust-Balyk structure. Gradients of groundwater mineralization in Lower Cretaceous sediments. Sampling interval of 2,100–2,200 m



formation pressures are oriented in different directions. Of particular interest is the downward increase in contents of hydrocarbonates.

The block structure of formations is also characteristic of the Malaya Rechka field in the southeastern part of the Nizhnevartovsk Arch, where the 3-year-long exploitation revealed three blocks.

The list of structures mentioned in the book, for which the similar analysis was carried out, is far from being complete. The defined regularities are characteristic of all the oil fields discovered in the Surgut Arch and other areas of West Siberia.

**Table 7.15** Abnormally high and elevated formation pressures (after [18])

Field	Age	Interval (m)	$P_{mes}$ (mPa)	$K_{an}$
Frolovo	R-PR	3,193–3,198	Bottom pressure 8.8	1.28
Festival'naya	PZ	Above 3,100	37.0	1.2
Khanty-Mansi	PZ	3,062–3,152	37.5–39.4	1.24
Novyi Port	PZ	2,542–2,548	27.5	1.08
Novyi Port	PZ	2,600–2,607	29.2	1.12
Yuzhno-Russkaya	PZ	4,208	33.0	1.26
Salym	T-J	2,930–3,041	35.0	1.17
Salym	T-J	2,970–3,000	43.5–44.6	1.47
Gubkin	T-J	2,900–2,980	36.0–37.0	1.24
Zapadno-Tarkasalinskaya	T-J	3,153	48.0	1.52
Urengoi	T-J	3,644–3,704	62.0	1.69
Urengoi	T-J	3,000	35.3	1.18
Pestsovaya	$K_{1v-nc}$	2,890–3,080	32.2–34.2	1.11
Pestsovaya	$K_{1a}$	3,220	35.0	1.09
Severo-Lubkinskaya		2,720–2,900	31.5–35.5	1.18
Zapolyarnaya	Bazhenovka Fm.	3,350–3,363	44.2	1.32
Vostochno-Tazovskaya	Achimov Fm.	Above 3,410	54.0	1.58
Yamburg	$K_{1a}$	2,890–3,080	32.2–34.3	1.11
Bovanenkovo	$K_{1h-b}$	2,150	25.2	1.17
Kharasavei	$K_{1h-b}$	1,930	23.0	1.19

In addition, the stratum-block structure of formations is confirmed by the wide distribution of elevated and abnormally high formation pressures (Table 7.15).

## 7.7 Vertical Paleomigration of Deep Fluids

In the West Siberian petroliferous basin, general mineralization patterns of subsurface fluids are disturbed by their local maximums and minimums. Hydrochemical anomalies are strictly localized, which confirms past and recent migration of fluids. In some areas, their migration is significant to involve the entire Jurassic–Lower Cretaceous section. Depending on intensity, periodicity, and composition of subsurface fluids, different types of vertical hydrochemical zoning are established in the basin. Anomalies are reflected in changes in both total mineralization and contents of many heavy metals and other microcomponents (P, S, V, Cr, Mn, Co, Ni, and others). Some of them are characterized by values two to three orders of magnitude higher than in seawater (Table 7.1), which excludes their syngenetic formation. The relationship between microcomponents and vertical migration is evident from the following facts: lateral changes in the component distribution and its vertical compositional stability; lack of correlation between fluids and lithology of host rocks; local development of anomalies in contents of heavy metals, which vary at short distances an order of magnitude and more; confinement of elevated contents of microcomponents to fractures and tectonically active zones. Anomalous  $CO_2$  and



H<sub>2</sub> contents are established in several areas of the West Siberian basin. Similar to microcomponents, gas saturation is characterized by lateral and vertical variations.

Intrusion of deep fluids with elevated temperatures, mineralization, chemical and gas compositions disturbs the physicochemical equilibrium of the fluid-rock system. This results in physicochemical processes that are accompanied by phase transitions, substantial changes in the composition of host rocks and fluids, and formation of mineralogical anomalies.

The catagenetic transformation of aquifers and its relation with vertical migration of deep fluids along tectonic fractures and weakened zones are confirmed by lateral differentiation of these changes through the basin, immediate proximity of sections with anomalous and background mineralogical compositions to each other, distinct vertical trend of epigenetic processes, and other features [26 and others].

The hydrochemical and other anomalies established in West Siberia are correlative with thermal anomalies, which are also highly differentiated through both the basin and its separate structures. For example, temperature geothermal gradient variations in some third-order structures amount to 20°C and 1°/100 m within a single bed. Thermal anomalies are confined to active faults (Fig. 7.26) to form a narrow band along the latter. They resulted undoubtedly from vertical filtration of hot fluids since sharp anisotropy of thermophysical properties in lithologically uniform rocks is hardly possible.

A. A. Rozin noted hydrochemical, geochemical, mineralogical, thermal, and, locally, hydrodynamic anomalies, which coincide spatially between each other, fractures, and tectonically weakened zones. This allows an inference on widespread vertical filtration of deep fluids that involves the significant portion of the sedimentary section in the West Siberian petroliferous basin. Fluids migrate(d) in the form of numerous autonomous ascending flows along weakened zones. Some of them are characterized by higher intensity or select most suitable conduits for migration. It should be emphasized that according to [28], local structures of West Siberia are crossed by numerous normal faults, which determine their small-scale block patterns. Among them, faults associated with crustal extension are dominant. Some of these fractures cross the entire sedimentary section and are reflected in the present-day topography. Markevich [21] considers West Siberia as representing a classical example of young developing geosyncline. This is evident from wide development of deep-seated faults, in addition to other features. Some of these faults are permeable and serve as conduits for deep fluids from the crust and upper mantle that form numerous and different-pattern anomalies.

The wide development of vertical migration in West Siberia is confirmed by palynological data also [2]. The Jurassic productive complex of many fields (Danilov, Upin, Yakhlin, Lukashkin Yar, Em-Egov, Saly, and others) encloses Early Paleozoic microflora. Oils from the Jurassic complex contain pollen and spores from host and underlying Paleozoic (sometimes, Triassic) rocks. The share of the alien microflora exceeds 50% of its integral content to reach sometimes 100%. Its maximal concentrations are characteristic of slope parts of the lowland in the Berezovo, Shaim, and Aleksandrovska areas adjacent to the folded Urals.

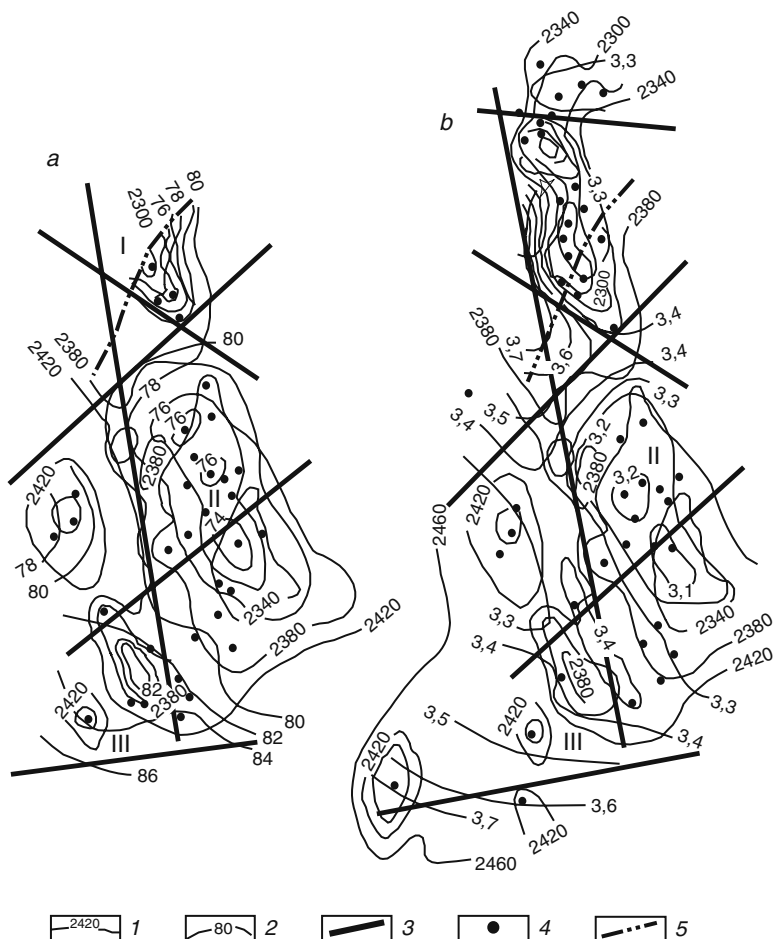


**Fig. 7.26** Schematic map of temperatures in layer BS<sub>10</sub> (a) and geothermal gradients (b) in Neocomian sediments of the southern Surgut Arch [19]. (1) Isohypses of the layer BS<sub>10</sub> surface (m); (2) isotherms (°C) (a) and gradient isolines (°C/100 m) (b); (3) fractures defined by geophysical methods; (4) boreholes with measured temperatures; (5) boundary of the productive layer. (I–III) Uplifts: (I) Ust-Balyk, (II) Mamontov, (III) Srednii Balyk

In the Neocomian petroliferous complex of the Malyi Atlym field located in the immediate proximity to Atlym dislocations, spores and pollen are represented by Lower Cretaceous (50%), Jurassic and Triassic (30%), Upper Paleozoic (10%), and Lower Paleozoic (7%) forms. In the Malyi Balyk field, spores and pollen are Cretaceous (dominant), Jurassic (12–15%), and Early Paleozoic (10–15%) in age. In the Megion field, Lower Paleozoic and Cretaceous forms constitute 75 and 20%, respectively. The palynological assemblage from the Albian–Cenomanian complex of the Eremino oil field includes Cretaceous (80%), Jurassic (5–7%), and Upper

Paleozoic (2%) taxa. In the Em-Egov field, 39% of pollen and spores are Cretaceous and approximately 50% of them are older in age.

General regularities in the distribution of alien microfossils noted in [2] are the following: (1) different-age sediments (from Paleozoic weathering crust to Aptian–Cenomanian complexes) contain coeval and alien microfossils; (2) “condensates of gas fields, Cenomanian included, separated from Jurassic sediments by the sequence >3–4 km thick, contain the notable share of Early Paleozoic forms as well;” (3) assemblages of alien microfossils in West Siberia are confined to steep limbs of structures located close to fractures, i.e., weakened vertical zones with potentially better filtration properties; (4) the share of alien forms decreases upward the section.

## 7.8 Main Conclusions

- (1) In central areas of the West Siberian petroliferous basin, deep formations are characterized by the stratum-block structure, which is reflected in both natural and disturbed conditions. This is evident from heterogeneities in the field of formation pressure reflected frequently in their differently oriented gradients, mineralization, hydrochemical, thermal, and other parameters.
- (2) Many facts indicate intense vertical paleomigration (probably, recent as well), which evidence for the significant role of the basement in the formation of deep fluids.
- (3) The stratum-block structure is possible only in formations with impermeable or poorly permeable, differently oriented boundaries between individual blocks.
- (4) The stratum-block structure of formations becomes less contrasting upward the section, being practically indistinct in the Aptian–Cenomanian sediments.
- (5) The stratum-block structure of formations excludes regional flows in central most subsided parts of the basin. Lateral flows are local in scale and exist only within individual blocks. Deep parts of the section are largely characterized by intermittent vertical migration, which is fed by fluids from the basement and, probably, crust and upper mantle.
- (6) Elision provides no influence on the development of formation pressures in the basin.

## References

1. Bochkarev V S, Boyarskikh G K, Nesterov I I (1980) *Trudy VNIGNI* 218:133–157
2. Chepikov K. R, Medvedeva A M, Klimushkina L P (1980) On autonomous position of the Paleozoic complex in West Siberia based on palynological analysis of oils. In: *Rock reservoirs of oil and gas*. Nedra, Moscow
3. Chistyakova N F, Rudkevich M Ya (1993) Hydrochemical indicators of formation conditions of hydrocarbon accumulations (exemplified by the West Siberian petroliferous basin). *Geologiya nefi i gaza* 5:29–33
4. Djunin V I (1985) *Investigation methods of the deep subsurface flow*. Nedra, Moscow

5. Djunin V I (2000) Hydrodynamics of deep formations in petroliferous basins. Nauchnyi mir, Moscow
6. Dobrynin V M (1970) Deformation and change of physical properties in oil and gas reservoirs. Nedra, Moscow
7. Fedorova T A, Bochko R A (1991) water-soluble salts of the Bazhenovka Formation as a criterion for defining reservoir zones. *Geologiya nefi i gaza* 2:23–26
8. Garmonov I V (1961) Groundwaters of the southern West Siberian Lowland and their formation conditions. AN SSSR, Moscow
9. Kartsev A A (1980) Hydrogeological prerequisites for manifestation of superhydrostatic pressures in petroliferous areas. *Geologiya nefi i gaza* 4:40–43
10. Kartsev A A (1992) Oil and gas hydrogeology. Nedra, Moscow
11. Kartsev A A, Vagin S B, Baskov E A (1969) Paleohydrogeology. Nedra, Moscow
12. Kartsev A A, Vagin S B, Serebryakova L K (1980) Paleohydrogeological reconstructions for revealing petroliferous zones (exemplified by western Ciscaucasia). *Byul. MOIP* 1:132–140
13. Kas'yanov M V, Afinogenov Yu A (1972) Determination of physical properties of rocks in productive formations of the Samotlor oil field in conditions close to natural. *Trudy SNIIGGIMS* 148:48–53
14. Klubova T T (1971) Some peculiarities in the study of clay minerals in petroleum geology. In: Proceedings of the 5th Plenum of All-Union Commission on Investigation and Use of Clays. Ashkhabad
15. Klubova T T, Klimushina L P (1980) Some regularities in migration of hydrocarbons in Bazhenov clays of the Salym field. In: Rock reservoirs and oil migration. Nauka, Moscow
16. Klubova T T, Klimushina L P, Medvedeva A M (1980) Formation of oil pools in clays of the Bazhenovka Formation. In: Petroleum resource potential of the Bazhenovka Formation in West Siberia. IGIRGI, Moscow
17. Kovalev V F (1960) Groundwaters of the Central and North Transurals region and problems of the petroleum resource potential. *Trudy gorno-geol in-ta AN SSSR, Uralian filial* 47:60–61
18. Krayushkin V A (2002) On oil and gas origin. In: Earth degassing: Geodynamics, geofluids, oil, and gas. Geos, Moscow
19. Kruglikov N M, Nelyubin V V, Yakovlev O N (1985) Hydrogeology of the West Siberian petroliferous megabasin and peculiarities in hydrocarbon formation. Nedra, Leningrad
20. Markevich V P (1966) Geological development and petroleum resource potential of the West Siberian Lowland. Nauka, Moscow
21. Markevich V P (2001) Tectonic formation conditions of oil and gas fields in platform structures. In: Abstracts of the International Conference “Oil and gas genesis and formation of their accumulations in Ukraine as a scientific basis for predicting and prospecting new fields. Chernigov
22. Mavritskii B F (1962) the West Siberian artesian basin (hydrogeology, geothermy, and paleohydrogeology). *Trudy LGGP AN SSSR* 39:1–150
23. Mukhin Yu. V (1965) Compaction of clayey sediments. Nedra, Moscow
24. Nelyubin V V, Smolentsev Yu K (1966) On a new groundwater discharge area in the West Siberian basin. *Sov Geol* 7:114–117
25. Plavnin A G, Stavitskii B P (1985) Initial formation pressure in reservoir of the Bazhenov Formation in the Salym field. *Trudy ZapSibNIGNI* 193:122–133
26. Razin A A (1977) Groundwaters of the West Siberian artesian basin and their formation. Nauka, Novosibirsk
27. Sidorov B A, Doldyreva V A, Gaipov B N et al. (1988) Non-tidal variations of the gravity force in petroliferous domains. In: Abstracts of the 1st All-Union conference “Geodynamic basics of predicting petroleum resource potential of the Earth's interior.” Moscow
28. Umperovich N V, Bgatova G F, Pashutina S R, Semenova E F (1966) New data on disjunctive dislocations in the platform cover of the West Siberian Plate obtained by the method of reflected waves (Ob–Irtys interfluvium). *Geologiya i geofizika* 1:76–84

29. Ushatinskii I N, Zaripov O G (1976) Mineralogical and geochemical indicators of the petroleum resource potential in the Mesozoic sediments of the West Siberian Plate. *Trudy ZapSibNIGNI* 96:1–207
30. Ushatinskii I N, Zaripov O G (1970) Post-sedimentary alterations in mineralogy and filtration properties of oil and gas reservoir in West Siberia. *Trudy ZapSibNIGNI* 35:1–312
31. Vsevolozhskii V A (1991) Basics of hydrogeology. MGU, Moscow
32. Vsevolozhskii V A, Djunin V I (1972) On some regularities in formation of hydrodynamic zoning in artesian basins. *Vestnik MGU. Ser geol* 4:58–65
33. Zapivalov N P, Polkanova V V (1979) Neotectonics and petroleum resource potential of southern West Siberia. *Geologiya nefi i gaza* 12:48–57
34. Zubkov M. Yu, Sonich V P, Zaripov O G (1986) Geological and lithological criteria for estimating petroleum resource potential of the Bazhenoka Formation in West Siberia. In: *Problems of the petroleum resource potential of the Bazhenovka Formation in West Siberia*. Moscow

# Chapter 8

## Fluidodynamics in Hydrocarbon-Bearing Formations of the Northern Pechora Petroliferous Basin

### 8.1 Geological Structure

We consider here only the northern part of the Pechora petroliferous basin belonging to the Timan-Pechora Province. The basin is bordered by the Kolva Megaswell, Sorokin Swell, Pechora Sea, and Chernyshev Range in the west, east, north, and south, respectively.

The Upper Proterozoic basement of the Pechora Syncline is overlain by the Paleozoic–Cenozoic sedimentary cover. The work is dedicated to deep petroliferous formations. Therefore, main attention is paid to the lower part of the section, while its upper portion is considered briefly.

The basement is composed of metamorphosed schists, quartzite sandstones, quartzites, dolomites, and limestones of Riphean age. They are locally intruded by magmatic bodies of the acid, intermediate, and basic compositions. The basement rocks are exposed in the Timan and Uralian ranges.

The sedimentary cover in the region under consideration is composed of Vendian–Lower Cambrian (?), Ordovician, Silurian, Devonian, Carboniferous, Permian, Triassic, Jurassic, Cretaceous, and Cenozoic rocks (Fig. 8.1) [17, 20].

#### 8.1.1 Paleozoic Group (PZ)

The Paleozoic group is represented by all its systems. It is largely composed of carbonate rocks (Silurian–Lower Permian); terrigenous rocks are subordinate (Cambrian System (?), Middle Devonian, Upper Permian).

#### 8.1.2 Cambrian System (€)

The Vendian–Lower Cambrian rocks are studied in the Timan and Uralian ranges. In the region under consideration, these rocks are defined conditionally by geophysical methods. They are presumably developed in some areas of the Pechora

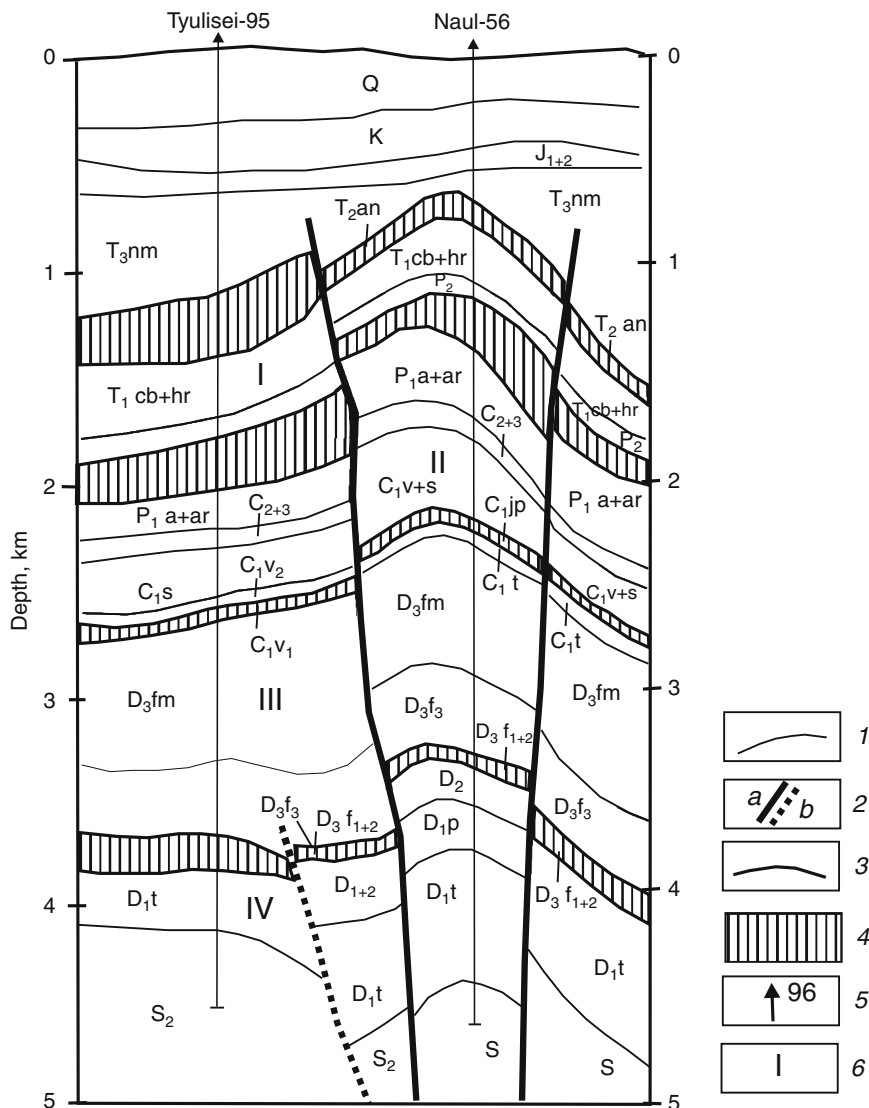


**Fig. 8.1** The transverse geological–hydrogeological section across the Sorokin Swell (after [10]). (1) Stratigraphic boundaries; (2) tectonic dislocations: (a) proven, (b) assumed; (3) boundaries of aquifers; (4) low-permeability sequences (confining beds); (5) borehole and its number; (6) aquifers: (I) Upper Triassic, (II) upper Viséan–Artinskian, (III) upper Frasnian–Tournaisian, (IV) Silurian–Lower Devonian

artesian basin, which rest unconformably upon the Riphean basement. The thickness of these rocks ranges from 50 to 450 m being maximal in relatively deep areas of the basement.

### **8.1.3 Ordovician System (O)**

The Ordovician rocks overlying unconformably Cambrian or Riphean strata are represented by sandy-clayey and carbonate to carbonate-clayey varieties with evaporate interbeds in the lower (Lower-lower Middle Ordovician) and upper (upper Middle-Upper Ordovician) parts of the section.

### **8.1.4 Silurian System (S)**

The Silurian rocks are spread through the entire Pechora Syncline outcropping in the Urals, Pai-Khoi, Chernyshev, and Chernov ridges, where they are represented by both series. The Lower Silurian ( $S_1$ ) rocks are represented by massive dolomites, clayey and dolomitized limestones intercalated by sulfate, argillite, and marl beds. They are 300–600 m thick in the Khoreiver Depression and up to 1,000 m thick in the Varandei-Adz'va structural zone. The Upper Silurian ( $S_2$ ) section is composed of alternating limestones, dolomites, marls, and sandstones. In the Khoreiver Depression, most of the Upper Silurian rocks are missing. The integral thickness of Silurian rocks is approximately 1,000 m.

### **8.1.5 Devonian System (D)**

The Devonian System is represented by all three series. Its rocks rest with angular and stratigraphic unconformity upon different strata of the Ordovician and Silurian systems. The Devonian rocks are characterized by significant variations in lithology, thickness, and stratigraphic completeness of sections. They are represented by both terrigenous (Pragian Stage of the Lower Devonian and lower Frasnian Substage of the Upper Devonian) and carbonate (Lower and Upper Devonian) facies. The integral thickness exceeds 2,000 m.

#### **8.1.5.1 Lower Series ( $D_1$ )**

The Lower Devonian rocks are characterized by the limited distribution in the Pechora Syncline, where they outcrop in the Southern Lai Swell, Pechora-Kozhva Megawell, and Varandei-Adz'va structural zone. The rocks belong to the Lochkovian ( $D_{1l}$ ) and Pragian ( $D_{1p}$ ) stages. The Lochkovian Stage is composed of three lithologically different sequences: carbonate, terrigenous-carbonate, and anhydrite-dolomite. The Pragian Stage overlies conformably the Lochkovian strata



and is represented by a sequence (>1,000 m) of alternating marls, argillites, clayey limestones, and anhydrites.

#### **8.1.5.2 Middle Series (D<sub>2</sub>)**

The Middle Devonian rock overlies transgressively (with angular and stratigraphic unconformity) pre-Devonian or Lower Devonian strata differing substantially from them in lithological-facies features. They are characterized by highly irregular distribution in the Pechora Syncline missing in the Southern Timan Range, Northern Izhma-Pechora and Khoreiver depressions, Varandei-Adz'va structural zone, and inliers of the Kolva Megaswell basement. The Middle Devonian rocks are represented by alternating sandstones, siltstones, and argillites. Their characteristic feature is development of relatively thick (up to 20–40 m) monomineral quartz clay- and, usually, carbonate-free sandstones. Maximal thicknesses of the Middle Devonian section are characteristic of the Pechora–Kozhva Megaswell.

#### **8.1.5.3 Upper Series (D<sub>3</sub>)**

The Upper Devonian strata are distributed throughout the entire Pechora Syncline overlying Middle Devonian and older rocks with stratigraphic and angular unconformity. They constitute the Famennian (D<sub>3</sub>fm) and Frasnian (D<sub>3</sub>f) stages. Based on lithology, the Upper Devonian sediments are divisible in two sequences: lower thin terrigenous–carbonate and upper carbonate up to 1,000 m thick. The individual stratigraphic units are characterized by the variable thickness and heterogeneous facies composition.

#### **8.1.5.4 Frasnian Stage (D<sub>3</sub>f)**

The stage comprises three substages, which are divisible in turn into several horizons. It is characterized by significant facies variability both in lateral directions and through the section. The lower part of the section corresponds (from the base upward) to the Pashiiskii, Kynov, and Sargaevo horizons (D<sub>3</sub>p+kn-sr) composed of argillites (clays) with thin siltstone and sandstone interbeds. The overlying Semiluki Horizon (D<sub>3</sub>sm) is represented by either the Domanik Formation (D<sub>3</sub>dm) composed of bituminous siliceous–clayey limestones and dolomites with clayey–silty interbeds or shallow shelf and reefal sediments. The thickness of the horizon is 10–20 m in the former situation and 100–200 m in the latter one. The successively overlying Vetlosyan, Sirachoi, Evlanovo, and Livny horizons (D<sub>3</sub>vt+sr+ev+lv) form a sequence consisting of alternating different-origin limestones, dolomites, anhydrite and argillite beds, sandy–clayey sediments, and clayey limestones with general prevalence of carbonate varieties. The Semiluki sequence encloses numerous reefal bodies, which determine significant facies variability reflecting development of isometric depressions, linear aulacogens, shallow shelf, and isolated banks at that time. Such a structure of the section determines, in turn, highly variable capacity and filtration properties of sediments. The integral thickness of the stage is 300–600 m.

### **8.1.5.5 Famennian Stage (D<sub>3</sub>fm)**

The Famennian sediments developed in the northwestern part of the basin rest with stratigraphic unconformity upon the Frasnian Stage. They are largely represented by carbonate varieties intercalated by rare anhydrites and argillites. The Famennian Age was presumably characterized by development of reefs as well. The thickness amounts to 500–800 m.

## **8.1.6 Carboniferous System (C)**

The Carboniferous sediments overlie conformably the Famennian strata and characterize all its three series.

### **8.1.6.1 Lower Series (C<sub>1</sub>)**

The Lower Carboniferous comprises three stages: Tournaisian (C<sub>1t</sub>), Viséan (C<sub>1v</sub>), and Serpukhovian (C<sub>1s</sub>). The Tournaisian Stage is composed of limestones and dolomites with argillite and rare siltstone and sandstone beds. They are spread irregularly missing, for example, in the Khoreiver Depression. The Viséan Stage consists of two members: lower argillaceous with clayey limestone and sandstone intercalations (Yasnaya Polana Superhorizon, C<sub>1jp</sub>) and upper carbonate (Oka Superhorizon, C<sub>1ok</sub>). The Serpukhovian Stage (C<sub>1s</sub>) is characterized by development of anhydrites and dolomites constituting the undivided Tarusa and Steshev horizons (C<sub>1tr+st</sub>) 40–150 m thick and limestones of the Protvino Horizon (C<sub>1pr</sub>) 40–80 m thick. The integral thickness of the Lower Carboniferous sediments is 400–600 m.

### **8.1.6.2 Middle Series (C<sub>2</sub>)**

The Middle Carboniferous strata comprising the Bashkirian (C<sub>2b</sub>) and Moskovian (C<sub>2m</sub>) stages overlie conformably sediments of the lower series. They are composed of limestones and dolomites with marly and argillaceous interbeds in the lower part of the section. The thickness ranges from 30–50 to, locally, 100 m.

### **8.1.6.3 Upper Series (C<sub>3</sub>)**

The Upper Carboniferous sediments are characterized by the highly irregular distribution missing in large negative tectonic structures and, partly, on swells. They are represented by organogenic–detrital frequently silicified limestones with maximal thicknesses (up to 200 m) in the western part of the Pechora Syncline.

## **8.1.7 Permian System (P)**

The Permian sediments characterizing the lower and upper series of the system in question rest upon different-age Carboniferous strata. They constitute universally stratigraphically complete sections except for the Varandei-Adz'va structural

zone. The lower part of the Permian section is composed of carbonate–terrigenous facies, while its upper part consists of terrigenous material originating from orogenic structures that formed during the closure of the Uralian paleocean.

#### **8.1.7.1 Lower Series ( $P_1$ )**

The series is represented by all the stages of the standard stratigraphic scale: Asselian ( $P_{1as}$ ), Sakmarian ( $P_{1s}$ ), Artinskian ( $P_{1a}$ ), and Kungurian ( $P_{1k}$ ).

The first three stages form a single undivided carbonate–terrigenous sequence composed of gray limestones with admixture of clayey and subordinate silty material. The share of terrigenous material increases upward the section to form in its Artinskian portion clay and sandstone layers. The integral thickness of the Lower Permian sediments is approximately 300–400 m.

The Kungurian sediments were deposited in the intracontinental sea basin. They are terrigenous largely gray pyritized argillites and siltstones with rare limestone and dolomite interbeds. The integral thickness is 170–200 m.

#### **8.1.7.2 Upper Series ( $P_2$ )**

The Upper Permian sediments resting upon Kungurian strata without apparent unconformity characterize all three stages: Ufimian ( $P_{2uf}$ ), Kazanian ( $P_{2kz}$ ), and Tatarian ( $P_{2t}$ ). In the Pechora Syncline, the Upper Permian section is composed of continental and continental–lagoonal terrigenous sediments. Two types of sections are distinguishable: gray-colored terrigenous in the north and grayish red in the south and Uralian Foredeep.

The Ufimian Stage ( $P_{2uf}$ ) is largely represented by sandstones with plant remains as well as with marine, coastal-marine, and terrestrial faunal fossils. The Kazanian ( $P_{2kz}$ ) and Tatarian ( $P_{2t}$ ) stages are represented by the undivided section of sandy–silty–clayey sediments. The thickness of Upper Permian sediments decreases northward due to disappearance of Kazanian and Tatarian layers. Their integral thickness is 400–500 m.

### **8.1.8 Mesozoic Group ( $MZ$ )**

The sediments of the Mesozoic group overlie with stratigraphic and, locally, angular unconformity in the Permian section. According to organic remains, they are represented by Triassic, Jurassic, and Cretaceous strata approximately 700 m in total.

#### **8.1.9 Triassic System ( $T$ )**

The Triassic sediments are widespread in the Pechora Syncline, which characterize all three series. In the Pechora petroliferous basin, the Triassic section is divided

into four formations (from the base upward): Charkabozh ( $T_{1cb}$ ), Kharalei ( $T_{1hr}$ ), Anguran ( $T_{2an}$ ), and Nar'yán-Mar ( $T_{3nm}$ ). The section is composed of alternating sandstones, siltstones, and clays with the proportion of the latter variety increasing northward. The share of clayey sediments decreases upward the section: lower two stages are composed of clays 450–500 m thick, the Anguran Formation is represented by variegated siltstones and sandstones 130–170 m thick, while the Upper Triassic portion of the section corresponds to the gray-colored sequence of alternating sandstones, siltstones, and clays 300–750 m thick.

### ***8.1.10 Jurassic System (J)***

The Jurassic sediments rest with stratigraphic and angular unconformity upon Triassic terrigenous sequences. The system consists of two lithologic–stratigraphic complexes. The lower complex is composed of silty–sandy sediments accumulated in lacustrine–fluvial and continental plain settings intermittently flooded by sea (undivided Lower–Middle Jurassic,  $J_{1-2}$ ). The upper complex ( $J_3$ ) is represented by marine facies: largely clayey sediments with rare sandstone and siltstone interbeds approximately 100 m thick in total.

### ***8.1.11 Cretaceous System (K)***

In the northern part of the Pechora Syncline, the Cretaceous System is represented only by sediments of its lower series, which overlie conformably the Jurassic sequence.

The lower part of the Lower Cretaceous section is largely composed of gray clays with intercalations of fine-grained siltstones and rare coal seams. Higher in the section, they are successively replaced by a sequence of alternating sandstones and siltstones and by pure sandstones. The uppermost part of the section consists of continental sands and clays. The thickness of Cretaceous sediments is 200–250 m.

### ***8.1.12 Cenozoic Group (KZ)***

The Cenozoic sediments occur throughout the entire Pechora Syncline. The remarkable feature of their section is alternation of glacial loams with boulders and members of siltstones, sands, and gravel formed in marine and lacustrine–glacial settings in the north and south of the basin, respectively [15].

The oldest Early Pleistocene boulder–gravel sediments are localized in erosional incisions and characterized by high density and intense hypergenetic alteration of rock fragments [15]. Higher in the section, they are replaced by clays and siltstones with marine fossils, which are crowned by Lower Pleistocene moraine sediments. The overlying Middle Pleistocene sediments are represented by different

glacial facies. The Upper Pleistocene sequence begins with marine sediments and is terminated by sediments of the boreal transgression, which are preserved in large river valleys. Post-glacial (Holocene) sediments constitute marine terraces and fluvial sequences in the northern part of the basin. They are represented by gray-yellow quartz sands and subordinate sandy loams with gravel interbeds. The thickness of Quaternary sediments ranges from a few meters in the Timan Range to 250–300 m in some depressions of the syncline. Average thicknesses are 100–125 m in the maritime part of the syncline and 25–30 m in its southern areas.

The Pechora petroliferous basin is characterized by wide development of permafrost rocks with the continuous, discontinuous, massive-island, and island distribution. The study area falls into the continuous distribution domain. Through tabetisols (or areas completely lacking permafrost) are missing, except for the Malyi and Bol'shoi Toravei lakes and Chernaya River areas. Three domains differing in the vertical structure and permafrost thickness are defined: Izhma-Pechora, Bol'shezemel'skii, and Pechora–Cisuralian. The area under consideration is confined to the Bol'shezemel'skii domain comprising its northern and central parts. The northern part of the domain is characterized by one-layer permafrost rocks 150–300 m thick on average (400–500 m in the watershed area of the Kolva River upper reaches). In its central part, permafrost rocks are characterized by the two-layer structure extending in the form of a band approximately 100 km wide from the Pechora River in the west to the Chernyshev Range in the east. The upper permafrost layer is 50–100 m thick. It joins locally the lower (buried) permafrost layer 500–600 m thick. The surface of the relict permafrost layer is located at depths of 80–150 m to 150–200 m in watersheds. The thickness of the relict layer exceeds 250–500 m.

## 8.2 Tectonics

Tectonic zoning of the Pechora Syncline is performed for the middle structural stage, which constitutes 70% of the integral thickness of sedimentary cover comprising several first-order structures [8].

The *Kolva Megaswell* that represents a large (300 km long and 30–40 km wide) complicated linear inverted NW-trending aulacogen is located in the central part of the Pechora Syncline. It is bordered by continuous faults with the amplitude up to 800 m that initiated in the Riphean. In the upper part of the sedimentary cover, they grade into flexures.

The *Khoreiver Depression* is defined in the northeastern part of the Pechora Syncline. It is termed as depression conditionally because of bordering well-developed positive structures separated by high-amplitude tectonic fractures. These are the Kolva Megaswell in the west, Sorokin Swell in the east and northeast, and Chernyshev Range in the southeast and south.

The *Sorokin Swell* represents a narrow NW-extending horst >200 km long and 8–10 km wide that is developed at the roof of the Permian carbonate sequence [8]. It is separated from the Khoreiver Depression by the NW-trending Varandei Fault

(Fig. 8.1). The basement is uplifted along this fault for 0.5–0.8 km and the roof of the Carboniferous sequence for 0.3–0.4 km. The western limb of the swell is bordered by the fracture along its entire length, while the eastern one only between the Naul and Yareiyag structures.

All the fractures of the Pechora Plate are oriented in four directions: northwestern, northeastern, near-meridional, and near-latitudinal. By age, they are divided into Riphean, Early Paleozoic, Late Paleozoic–Early Mesozoic, and Cenozoic.

The Riphean faults are usually oriented in the northwestern direction. The amplitude of vertical displacements along the faults ranges from 200–300 to 1,000–1,500 m. The peculiar feature of these fractures is their activity during the entire geological history of the region. Current movements along the faults are reflected in rectilinear boundaries of structures [10].

The Early Paleozoic faults are NE trending. Maximal amplitudes of horizontal movements along them are 15–20 km. Most of these faults were active only in the Early Mesozoic.

The Late Paleozoic–Early Mesozoic fractures are differently oriented. They are usually arcuate or twisting in plane and have amplitudes of horizontal displacements approximating 0.5–2.0 km.

The Cenozoic tectonic fractures are divided into two groups. The first group is represented by faults that resulted from activation of older deep fractures and are correspondingly oriented in the northwestern or northeastern directions. Development of fractures belonging to the second group is determined by the growth of neotectonic structures [10].

The neotectonic stage in the evolution of the Pechora Syncline was characterized by movements of several types. When the syncline was reactivated in the Oligocene, uplifting was dominant. The minimal amplitude of neotectonic uplifting in the northern Pechora Syncline during the Miocene and Early Pliocene was 1,200 m. In the Late Pliocene, uplifting was replaced by subsidence with accumulation of clayey sediments. The Quaternary was marked by alternating uplifting and subsidence phases with the general uplifting trend. The integral neotectonic uplifting of the region is estimated to be 1,000–1,200 m.

### 8.3 Hydrogeological Conditions

The Pechora artesian basin is an element of the Timan-Pechora petroliferous province. It occupies the inner areas of the latter, which prevents from estimating marginal zones as regional recharge sources (Urals, Timan) for inner areas of the basin, which are poorly studied. In this book, we consider only lower parts of the basin section, which is necessary for solving corresponding problems. Hydrogeological characteristic and hydrogeological stratification of the section are based on data from [10, 19].

The following hydrogeological domains and systems of artesian basins are defined in the Pechora Plate: the Pechora system of artesian basins, Kanin–Timan folded basin of fissure and artesian waters, Uralian folded region of fissure,

fissure–karst, and fissure–vein waters. According to schematic hydrogeological zoning by I.S. Gabovich, the Pechora system of artesian basins or Pechora artesian basin or the Bol'shezemel'skii-Pechora artesian basin (I.S. Zaitsev, M.K. Tolstikhin, B.N. Lyubomirov, and others) is defined in limits of the Pechora Syncline contacting with the Kanin–Timan basin of fissure waters in the west and the Cisuralian artesian basin in the east. In the south, the Pechora artesian basin is bordered by the transitional zone between the Uralian Foredeep and Timan range.

Two second-order basins are definable within the Pechora artesian basin: Izhma-Pechora and Bol'shezemel'skii. Based on structural and tectonic features, they are divisible into hydrogeological units of the higher order. For example, the Bol'shezemel'skii artesian basin comprises three different petroliferous regions: Pechora–Kozhva, Khoreiver, and Varandei-Adz'va.

In line with principles of defining hydrodynamic stages [19], all four stages are distinguishable in the northern part of the Pechora artesian basin.

The first hydrodynamic stage corresponds to the upper part of the section up to the upper regional surface of permafrost rocks, which play the role of an impermeable sequence (Mesozoic–Cenozoic hydrodynamic stage).

The second hydrodynamic stage comprises the most part of the section composed of Mesozoic, Upper Devonian, Carboniferous, and Permian rocks outcropping on slopes of the Urals and Timan Range; its lower boundary corresponds to the surface of regionally distributed Kynov–Sargaevy clays (Upper Devonian–Triassic hydrodynamic stage).

The third hydrodynamic stage includes sediments occurring between the Kynov–Sargaevy confining sequence and basement (Ordovician–lower Frasnian hydrodynamic stage).

The metamorphic deformed rocks of the Riphean–Lower Cambrian basement can be considered as representing the fourth hydrodynamic stage (Riphean–Lower Cambrian hydrodynamic stage).

### ***8.3.1 Upper Jurassic–Cretaceous Confining Sequence ( $J_3-K$ )***

The sequence developed practically through the entire petroliferous basin comprises the Upper Jurassic Raznin and Poromes formations and Neocomian sediments. It is largely composed of clayey sediments with sandy and silty rocks constituting approximately 20%. Their share increases in the southern, eastern, and western directions. The integral thickness of the sequence amounts to 350 m.

### ***8.3.2 Jurassic Aquifer ( $J$ )***

The aquifer is largely developed in the northern part of the Pechora petroliferous basin, where it is composed of terrigenous rocks. The thickness is 200–300 m. The aquifer is poorly studied.

### **8.3.3 Upper Permian–Triassic Aquifer ( $P_2-T$ )**

This aquifer is developed continuously through the entire Pechora artesian basin being largely composed of sandy–clayey sediments accumulated under the regressive regime. The Upper Permian sequence is represented by alternating sandstones and clayey varieties. The Triassic sediments are terrigenous, of continental genesis. The stratigraphic completeness of the aquifer is highly variable: the northern part of the Sorokin Swell is lacking Upper Permian sediments, while Middle and Upper Triassic strata are missing in the south. The thickness is also highly variable: from 200 m in the south to >1,500 m in the north. The petroliferous complex is characterized by the lenticular structure and irregular distribution of permeable zones. This determines variations in porosity (10–20%) and permeability (100–600 fm<sup>2</sup>). The Upper Triassic clayey–silty sediments 20–50 m thick serve as an upper discontinuous confining sequence. Mineralization of formation waters ranges from 5 g/dm<sup>3</sup> in areas adjacent to the Urals to 100 m g/dm<sup>3</sup> in the Shapkino-Yur'yakh Swell area.

In the north, the upper part of this complex a few hundreds of meters thick is located in the permafrost zone and represents a relative confining sequence.

### **8.3.4 Lower Permian (Kungurian) Confining Sequence ( $P_2kg$ )**

The sequence is spread through the entire Pechora petroliferous basin and includes lower to upper Artinskian terrigenous and Kungurian clayey–halogenic rocks. By lithology, its two types are distinguished as follows: dominant clayey and clayey–silty northeast of the Pechora–Kozhva Megaswell and carbonate–terrigenous–halogenic–sulfate in southern and southeastern areas of the Pechora basin. The thickness of the confining sequence is highly variable through the basin being determined by its stratigraphic completeness [16]. In the Northern Sorokin Swell, Southern Khoreiver Depression, and Southern Kolva Megaswell, the sequence is enriched in sand material, which results in deterioration of its screening properties.

### **8.3.5 Upper Visean–Artinskian Aquifer ( $C_{1v3}-P_{1ar}$ )**

This complex is one of the thickest and most widespread aquifers in the Pechora basin. It is largely carbonate consisting of limestones and dolomites. Its thickness varies from a few tens of meters to >2,000 m. The lower part of the aquifer encloses thick members (up to 300 m) of high-porosity leached and karst-affected limestones. The basal part of the Permian portion includes organogenic–detrital limestones with reefal buildups. Recrystallization, leaching, dolomitization, and other processes determined the mosaic distribution of filtration–capacity properties with porosity ranging from 10 to 34% and permeability of 50–700 fm<sup>2</sup> controlled by fracturing and cavernosity of rocks. Formation fluids are largely chloride-sodium brines with mineralization of 40–170 g/dm<sup>3</sup>.



### 8.3.6 Visean Confining Sequence ( $C_{1v1}$ )

This relative confining sequence corresponding to the Malinovskii and Yasnaya Polyana superhorizons is continuously spread in the Varandei-Adz'va structural zone and Pechora-Kolva Aulacogen, while in the Khoreiver Depression it is characterized by the local distribution. The sequence is only 50–70 m thick. It is composed of clayey-sandy sediments and serves locally as a reservoir with hydrocarbon accumulations (Naul, Yugid, Vuktyl, and other fields).

### 8.3.7 Upper Frasnian-Tournaisian Complex ( $D_3f_3-C_{1t}$ )

The complex includes Upper Devonian (Frasnian and Famennian stages) and Lower Carboniferous (Tournaisian Stage) sediments; the latter is characterized by the discontinuous distribution. The Tournaisian and upper Famennian rocks are missing from the Khoreiver Depression. The remarkable feature of this complex is high lithological diversity of constituting rocks and highly variable thicknesses in different lithotectonic zones. It is composed of carbonate, carbonate-clayey, sandy-silty, sulfate, and siliceous-clayey-carbonate rocks.

Of interest are widespread reefal buildups (South Bagan, Sandivei, Musyurshor, Verkhnyaya Kolva, Central Khoreiver Uplift, Syrkhara, and others), which determine high variations in lithology and, correspondingly, changes in the thickness of the most permeable part of the complex (from 1,000 to 500 m).

The maximal thickness of the complex (up to 2,700 m) is recorded in the Middle Pechora Uplift. In the region under consideration, its thickness is relatively permanent varying from 1,000 to 1,500 m. Dolomites and limestones are characterized by best filtration-capacity properties: porosity up to 17–20%, permeability up to  $80-130 \cdot 10^{-15} \text{ m}^2$ . Waters are chloride-sodium with mineralization of  $100-200 \text{ g/dm}^3$ . Water-soluble gases are methane, nitrogen-methane, and, less commonly, methane-nitrogen in composition.

### 8.3.8 Kynov-Sargaievo (Lower Frasnian) Confining Sequence ( $D_3kn-sr$ )

The relative lower Frasnian confining sequence is usually defined as comprising the Upper Devonian Kynov and Sargaievo horizons and serves as the upper regional confining unit for the Middle Devonian-lower Frasnian complex or for older aquifers if the latter is missing. The sequence is spread practically through the entire Pechora basin. Its maximal thickness (up to 1,000 m) and stratigraphic completeness are observed in the central and northern parts of the Pechora-Kozhva Aulacogen. In southeastern and southern directions, regular decrease in the thickness of the sequence up to 10–50 m is accompanied by abrupt reduction of its stratigraphic completeness due to almost complete pinching out of the Kynov Horizon. The

sequence is composed of dominant clayey sediments with sandy–silty and carbonate interbeds, which deteriorate notably its screening properties in the southern and eastern parts of the Pechora basin.

### ***8.3.9 Middle Devonian–Lower Frasnian Aquifer (D2-D3f1)***

The Middle Devonian–lower Frasnian terrigenous aquifer comprises sediments of the Eifelian and Givetian stages of the Middle Devonian and Pashiiskii Horizon of the Upper Devonian. Its present-day distribution area, stratigraphic completeness, and thicknesses are determined by the scale and amplitude of the pre-Kynov erosion. The aquifer is missing in the Khoreiver Depression, southern part of the Usa Swell, and Varandei-Adz'va zone. In the region under consideration, it occurs in the Kolva Megaswell (without the Eifelian Stage). Maximal thicknesses of the aquifer are registered in the Pechora–Kozhva Aulacogen (up to 1,000 m). Fluid-enclosing rocks are represented by sandstones with clay, argillite, and carbonate interbeds. Sandy beds are composed of well-rounded quartz grains, which provide their good filtration–capacity properties: porosity 16–27%, permeability up to 2,000 fm<sup>2</sup>. The Upper Devonian Kynov–Sargaevo clays, marls, and clayey limestones serve as an upper regional relative confining sequence for the aquifer in question.

Formation fluids are chloride-sodium with mineralization of 100–250 g/dm<sup>3</sup>. Water-soluble gases are methane and, less commonly, nitrogen–methane in composition.

### ***8.3.10 Ordovician (Silurian)–Lower Devonian Aquifer (O–D<sub>1</sub>)***

The complex is developed through the entire Pechora basin. The composition of the complex is variable with notable prevalence of carbonate varieties. Its section demonstrates upward succession of different rocks from continental terrigenous (O<sub>1</sub>–O<sub>2</sub>) to lagoonal–marine terrigenous–carbonate–halogenic (O<sub>2</sub>–O<sub>3</sub>) to marine carbonate (S–D<sub>1</sub>) in origin. The Ordovician, Silurian, and Lower Devonian sequences are outcropping only in the western slope of the Urals and in the Uralian Foredeep. Their maximal integral thickness of 1,500–2,000 m is recorded in the latter area. The complex is characterized by low filtration–capacity properties: porosity up to 16% and permeability 15 fm<sup>2</sup>.

In the Kolva Megaswell area, the complex is recovered at depths of 3,000–4,000 m. Lower Devonian clayey–carbonate, clayey, and sulfate sediments serve as its upper relative confining unit. In the Khoreiver Depression, where these sediments are missing, the relative confining unit is represented by the Kynov–Sargaevo clayey sequence.

Waters of the aquifer in the Khoreiver Depression are chloride-sodium brines with mineralization of 130–190 g/dm<sup>3</sup> and high contents of bromine (up to 360–600 mg/dm<sup>3</sup>). Water-soluble gases are of the nitrogen–methane type with the

methane content of 60–75% and high concentrations of hydrocarbons (up to 8.3%). The gas–oil ratio ranges from 0.8 to 1.1 m<sup>3</sup>/m<sup>3</sup>.

### **8.3.11 Vendian–Lower Cambrian Aquifer (V–Є)**

The aquifer is composed of alternating terrigenous sandstones, siltstones, argillites, and clays. The upper confining sequence is represented by the Padun clayey formation. By chemical composition, formation waters are chloride-sodium with mineralization amounting to 200–250 g/dm<sup>3</sup>. Waters are strongly metamorphosed ( $r_{Na}/r_{Cl} = 0.55–0.79$ ). Their characteristic feature is the relatively high Br content (up to 1,200 mg/dm<sup>3</sup>).

### **8.3.12 Riphean Aquifer (R)**

The aquifer is largely composed of sandy and subordinate carbonate rocks of the Dorogor and Uftyug formations. The lower and upper confining units are represented by the Piz clayey formation and basal Vendian strata, respectively [18]. Mineralization of formation waters from this complex ranges from 117 to 150 g/dm<sup>3</sup>.

Thus, the formation of deep fluids is undoubtedly influenced by the following main factors: (1) development of large and small structural elements separated from each other by tectonic fractures frequently with the significant displacement amplitude (up to 800 m), which is comparable with or exceeds the thickness of large stratigraphic units; (2) extensive system of differently oriented and different-age fractures that divide the region into blocks; (3) significant neotectonic movements characterized by the oscillatory, undulatory, and disjunctive patterns that affect the rock strain; (4) largely carbonate section (90% of the sedimentary cover thickness) and lack of thick clayey sequences, which prevent significant influence of elision processes; (5) development of permafrost rocks, which diminish the role of peripheral parts of the basin as source of present-day infiltration recharge and excludes internal sources of infiltration recharge.

## **8.4 Methods Used for the Analysis of Fluid Geodynamics in Deep Formations of the Pechora Petroliferous Basin**

Dissimilar to the West Siberian petroliferous basin, density of deep fluids in the basin under consideration demonstrates substantial lateral and vertical variations, which makes it necessary to reduce formation pressures through the entire examined section to the single comparison plane. With this purpose, plots  $\rho(H)$  and  $P_{form}(H)$  were constructed *separately for each structure* with the assessment of the reducing error. Further, the reducing error with account for the selected comparison plane

and possibility of using pressure reduction for each structure were assessed. The field of points in plots  $\rho(H)$  was bounded by straight lines to simplify calculations and increase “engineering reliability margin.”

The single comparison surface for all the complexes under consideration was selected at a depth of  $-2,400$  m (the middle part of the well-studied interval).

This may be illustrated by several fields of the Sorokin Swell. Figure 8.2 demonstrates plots of downward changes in density; Table 8.1 presents coefficients of empirical straight lines and reducing error values for all the structures in the study region and Table 8.2 selectively for some structures with account of all the boreholes drilled in each of them.

The reducing error was assessed for two planes:  $-2,400$  and  $-4,000$  m. As was expected, the position of the comparison plane relative to sampling points influences substantially the formation pressure reducing error (Chapter 2). For the comparison plane of  $-4,000$  m, the reducing error was, as it should be, substantially higher, since most of the sampling depths fall into the interval of  $1,500$ – $2,400$  m.

It is well evident from Table 8.2 that the error of reducing to depth of  $-2,400$  m is below  $0.5$  mPa, while that of reducing to depth of  $-4,000$  varies from  $2.0$  to  $3.9$  mPa. As is expected, the error becomes substantially lower in intervals located close to the comparison plane of  $-4,000$  m. For example, in the sampling point located at a depth of  $4,068$  (Borehole Naul-56), the error of reducing to depth of  $2,400$  m is  $1.48$  mPa (calculated value of the formation pressure), while that of reducing to the comparison plane of  $-4,000$  becomes close to zero ( $0.01$  mPa). Similar values are obtained for Borehole Varandei-2 ( $1.63$  and  $0.4$  mPa, respectively). In other cases, the reducing error varies from  $0.02$  to  $0.5$  mPa. The sole exception is the

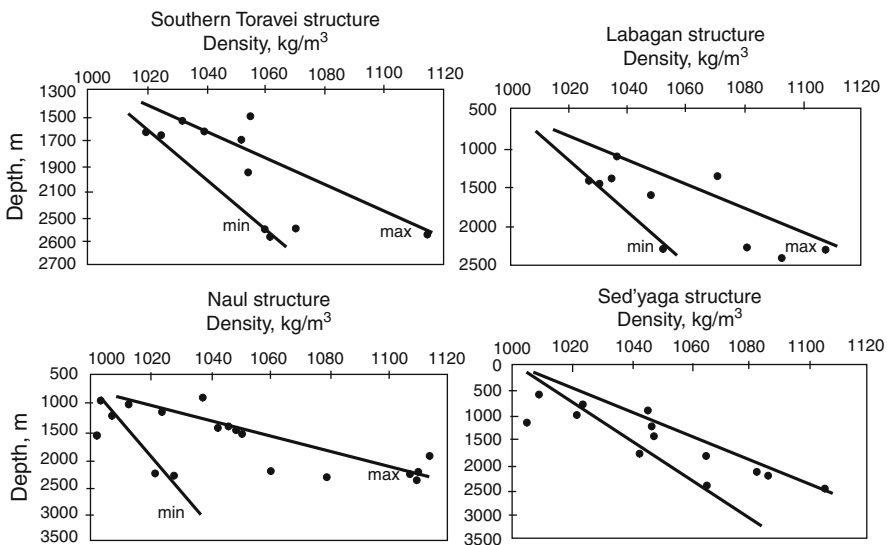


Fig. 8.2 Downward changes of water density in some structures of the Sorokin Swell

**Table 8.1** Angular coefficients of empirical equations of straights  $\rho$ - $Z$  and errors of reduced pressures

Area	Equation coefficient $1 \cdot 10^{-5}$		Reducing error, mPa
	minimum	maximum	
Sorokin Swell			
Varandei	2.4	4.2	0.2–3.6
Southern Toravei	3.2	3.5	0.02–0.3
Naul	2.8	4.45	0.03–0.5
Labagan	4.8	5.0	0.01–0.2
Sed'yaga	3.5	4.1	<0.1
Northern Sorokin	2.2	3.4	<0.1
Average	3.15	4.11	<0.17
Kolva Megaswell			
Chyl'chuyu	2.2	3.5	0.1–0.4
Southern Chyl'chuyu	2.2	3.2	0.05–0.2
Khar'yaga	2.8	4.5	0.07–0.6
Khancharga	2.0	4.0	0.04–0.07
Yareiyu	2.3	4.4	0.1–1.0
Vozei	2.2	3.8	0.1–0.5
Sarutayu	1.2	4.2	0.1–0.4
Inzyrei	2.5	3.7	0.1–0.6
Average	2.1	3.9	0.28
Khoreiver Depression			
Namyurkhit	2.3	3.2	0.2–0.6
Ardala	2.1	4.2	0.4–0.8
Oshkotyn	2.4	4.0	0.06–0.6
Northern Chernaya Rechka	2.9	4.5	0.2–0.6
Yanemdei	1.2	3.0	0.3–0.5
Dusyushev	2.5	4.3	0.5–1.0
Syurkharata	2.8	3.5	0.2–0.3
Southern Syurkharata	2.5	3.4	0.3–0.4
Tedin	2.0	3.6	0.3–0.6
Western Khosedayu	2.4	4.1	0.4–0.5
Sandivei	5.8	6.1	<0.1
Salyuka	3.5	5.6	0.4–0.6
Bagan	2.6	3.1	0.03–0.2
Ole'nya	2.0	3.5	0.1–1.0
Sadayagun	2.6	4.0	0.01–0.7
Verkhnyaya Kolva	2.4	4.0	0.4–0.7
Varktnav	2.5	4.2	0.07–1.2
Average	2.3	3.7	0–4.2

point at depth of 1,160 m (Borehole Toravei-23), which is explained, however, by incompletely renewed formation pressure (10.7 mPa) in this area.

For determining difference between formation pressures in individual structures, plots illustrating their correlation with depths were constructed for each structure (Fig. 8.3), when initial information was sufficient. As follows from plots, the difference between formation pressures ranges from 1.0 to 2.8 mPa, which exceeds the

**Table 8.2** Reduced formation pressures for individual structures with the assessment of reducing error under different comparison planes

Borehole	Formation pressure, mPa	Altitude of formation pressure measurement	$P_n$ , mPa $K=-2,400$	Reducing error $K=-2,400$	$P_n$ , mPa $K=-4,000$	Reducing error $K=-4,000$
<b>Southern Toravei</b>						
31	17.64	1,667	25.66	0.20	43.35	2.78
31	15.6	1,510.5	25.29	0.25	42.97	2.82
32	18.3	1,538	27.7	0.24	45.38	2.82
32	27.3	2,467	26.55	0.02	44.22	2.56
32	28.2	2,559	26.41	0.04	44.08	2.53
33	14.97	1,335	26.51	0.31	44.20	2.88
33	25.7	2,114	25.54	0.00	43.21	2.57
35	16.6	1,519	26.2	0.25	43.88	2.82
35	26.2	2,406	26.13	0.0	43.80	2.57
36	16.11	1,530	25.59	0.25	43.28	2.82
<b>Varandei</b>						
1	17.0	1,699.1	24.68	0.29	42.78	3.76
2	57.9	4,250.9	36.07	-1.63	54.41	0.4
3	16.95	1,678.5	24.85	0.3	42.96	3.77
3	17.66	1,643.5	25.93	0.31	44.04	3.79
3	12.7	1,463.0	22.89	0.35	41.01	3.89
4	19.0	1,789.1	25.71	0.27	43.81	3.71
5	12.7	1,444.8	23.05	0.36	41.17	3.90
7	28.44	2,573.8	26.49	-0.10	44.60	3.02
8	19.42	1,758.9	26.45	0.28	44.56	3.73
9	17.65	1,640.4	25.95	0.31	44.06	3.8
10	16.59	1,654.3	24.75	0.31	42.86	3.79
10	18.64	1,677.3	26.55	0.30	44.66	3.78
<b>Naul</b>						
51	18.8	1,607	27.46	0.38	45.0	3.58
52	24.5	2,235	26.34	0.10	43.99	3.29
52	15.4	1,374	26.27	0.45	43.76	3.65
52	23.92	2,244	25.66	0.09	43.31	3.29
53	25.0	2,281	26.33	0.07	43.99	3.26
53	15.47	1,422	26.09	0.44	43.59	3.63
54	12.6	1,234	25.19	0.49	42.65	3.68
54	25.4	2,337	26.20	0.04	43.77	3.23
55	11.1	1,169.5	24.36	0.5	41.80	3.70
56	46.9	4,068	27.33	-1.48	45.17	0.01
56	46.9	4,110	26.81	-1.53	44.66	0.01
57	25.5	2,250	27.17	0.09	44.83	3.28
58	15.8	1,464	25.98	0.43	43.49	3.62
59	15.1	1,430	25.64	0.44	43.14	3.63
59	23.7	2,345	24.31	0.03	41.99	3.23
61	20.6	1,962	25.44	0.24	43.04	3.43

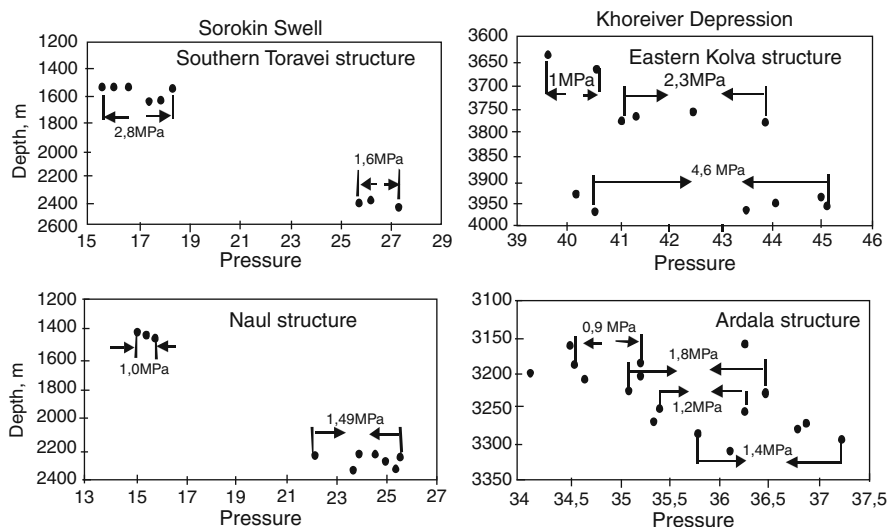


**Fig. 8.3** Differences in measured formation pressures at similar depth

reducing error. This provides grounds for applying the pressure-reducing method in the Sorokin Swell area.

Similar calculations and analysis were performed for all the structures of the Kolva Megaswell and Khoreiver Depression (Tables 8.1, 8.2, 8.3).

**Table 8.3** Reduced formation pressures for structures of the central Khoreiver Depression

Borehole	Age	Formation pressure, mPa	Depth, m	$P_{red}$ , mPa
Western Khosedayu				
1	D <sub>3</sub> f <sub>2</sub>	34.2	3,024	26.88
3		32.65	2,950	26.21
5		31.8	2,938.5	25.5
7		32.45	2,979.6	25.66
9	D <sub>3</sub>	32.95	2,973.4	26.23
10		33.1	2,924.5	26.96
11		33.68	2,980.6	26.87
12	D <sub>3</sub> f <sub>2</sub>	33.15	2,941.5	26.81
12		31.67	2,927.5	25.5
13		32.23	2,946.3	25.83
21	D <sub>3</sub>	32.85	3,000	25.81
22		33.41	3,011.3	26.24
41		32.27	2,954.3	25.78
42	D <sub>3</sub> f <sub>2</sub>	32.26	2,909.1	26.3
43		32.32	2,961	25.75

**Table 8.3** (continued)

Borehole	Age	Formation pressure, mPa	Depth, m	$P_{red}$ , mPa
44		32.15	2,978.4	25.37
Sikhorei				
1	D <sub>3</sub> f <sub>2</sub>	36.2	3,149	27.38
1		34.2	3,151	25.36
50		33.8	3,090	25.69
Sikhorei				
51	D <sub>3</sub> f <sub>2</sub>	33.2	3,152	24.34
52		32.7	3,061	24.93
Eastern Sikhorei				
8	D <sub>3</sub> f <sub>2</sub>	33.11	3,008.4	25.97
16		33.4	3,116	24.98
Northern Sikhorei				
20	D <sub>3</sub> f <sub>2</sub>	34.46	2,989.3	27.55
20		33.9	3,014.3	26.69
Eastern Kolva				
50	D <sub>3</sub> f <sub>2</sub>	37.73	3,314.2	27.18
50	C <sub>1</sub> s	31.7	2,891.2	26.09
51	D <sub>3</sub> f	42.45	3,759.1	26.6
52	D <sub>3</sub> f <sub>2</sub>	43.88	3,777.5	27.81
100		35.2	3,248.3	25.42
101	D <sub>3</sub> f <sub>1</sub>	45.0	3,946.4	26.89
Ardala				
21	C <sub>1</sub> s	32.05	2,880.2	26.42
22	D <sub>3</sub> f <sub>2</sub>	35.93	3,283.8	25.46
45	D <sub>3</sub> fm	35.92	3,132.7	27.28
46	P <sub>1</sub> kg-ar	36.25	3,159.7	27.28
47	D <sub>3</sub> f <sub>2</sub>	25.07	2,323	25.96
47		35.2	3,222	25.48
48		37.2	3,287	26.69
49		36.46	3,227.9	26.67
Oshkotyn				
1	C <sub>3</sub>	27.2	2474.2	26.34
1	C <sub>1</sub>	35.05	3150.2	26.21
42	C <sub>3</sub>	27.17	2,487	26.16
42	D <sub>3</sub> fm	34.6	3,078	26.63
42	D <sub>3</sub> f <sub>1</sub>	39.35	3,429	27.14
44	D <sub>3</sub> f <sub>2</sub>	34.23	3119.2	25.77
Yanemdei				
1	D <sub>3</sub> f <sub>1</sub>	36.45	3,366	25.43
2	D <sub>3</sub> f <sub>2</sub>	35.8	3,169	27.06
Sredne-Yanemdei				
1	D <sub>3</sub> fm	35.8	3,296.9	25.58
Syurkharata				



**Table 8.3** (continued)

Borehole	Age	Formation pressure, mPa	Depth, m	$P_{red}$ , mPa
1	C <sub>2</sub>	25.95	2,451.1	25.39
2	D <sub>3</sub> fm	34.56	3,103.4	26.73
4	D <sub>3</sub> f <sub>2</sub>	35.66	3,201.8	26.72
Southern Syurkharata				
10	D <sub>3</sub> fm	34.4	3,118.8	26.03
12	D <sub>3</sub> f <sub>2</sub>	34.42	3,143.1	25.76
Tedin				
1	P <sub>2</sub>	18.04	1,830.4	24.43
1	D <sub>3</sub> f <sub>2</sub>	35.0	3,153.4	26.25
40		35.0	3,200.9	25.69
41		33.74	3,100.7	25.62
43	P <sub>2</sub>	18.0	1,781	24.94
Pyusei				
22	D <sub>3</sub> f <sub>2</sub>	35.85	3,165.2	27.05
22		35.72	3,250.2	25.92
Uremyd				
30	D <sub>3</sub> fm	34.1	3,102.4	25.84
31	D <sub>3</sub> f <sub>2</sub>	43.92	3,191.5	25.59
Northern Khosedayu				
1		37.9	3,534	24.31
2		31.4	2,880	25.75
3		33.3	2,987	26.37
4		31.78	3,000	24.69
5		32.64	3,072	24.69
7		31.18	2,980	24.33
10		36.2	3,354	24.82
10		35.49	3,230.8	25.61
14	D <sub>3</sub> f <sub>2</sub>	34.88	3,292	24.26
19		31.43	2,936	25.11
21		32.12	3,073	24.16
22		30.39	2,891	24.61
23		31.47	2,990	24.5
24		32.86	3,020	25.53
26		32.61	3,050	24.92
33		33.1	3,062	25.27

The reduced formation pressures were used for the study of hydrodynamic condition in individual structures and modeling the hydrodynamic regime. For the Pechora basin, hydrodynamic conditions were modeled in the form of the four-layer sequence (Silurian–Lower Devonian, upper Frasnian–Tournaisian, upper Viséan–Artinskian, and Upper Permian–Triassic layers) with three low-permeability confining units (Kynov–Sargaevo, Viséan, and Lower Permian (Kungurian) overlain by permafrost rocks).

Inasmuch as the fluid density changes substantially in all the directions, the “direct” method (based on measured formation pressures at analogous or close depths) was widely applied in the Pechora petroliferous basin. Its application is naturally possible only for well-studied structures, which are located in the central part of the Khoreiver Depression (upper Frasnian–Tournaisian aquifer, Table 8.4).

**Table 8.4** Formation pressures measured at close depths in individual areas of the central Khoreiver Depression

Borehole	$P_{form}$ , mPa	Measurement attitude, m	Borehole	$P_{form}$ , mPa	Measurement attitude, m
Eastern Kolva			Northern Khosedayu		
100	35.2	3,248	1	31.4	3,040
101	35.34	3,253	2	31.4	2,880
50	36.23	3,284	3	33.3	2,987
50	39.6	3,634	4	31.78	3,000
51	4.06	3,667	5	31.67	3,030
Ardala			7	31.18	2,980
21	35.21	3,203	10	31.33	3,030
47	35.33	3,268	14	31.6	3,034
48	36.86	3,274	18	30.43	3,021
45	36.78	3,277	19	31.63	3,010
22	35.93	3,283	21	31.45	3,050
49	35.78	3,285	22	31.01	3,006
46	37.32	3,293	23	31.52	3,000
Oshkotyn			24	32.86	3,020
44	34.23	3,103.2	26	32.09	3,030
1	35.04	3,108	33	33.6	3,068
42	36.8	3,114	Western Khosedayu		
Yanemdeï			1	33.4	3,005
2	35.8	3,169	3	32.38	2,975
Seinorogoyakha			5	32.24	2,981
1	35.45	3,273.3	7	32.45	2,979
Syurkharata			9	33.0	2,973
10	34.4	3,119	10	33.54	2,979
12	34.42	3,143.17	11	33.7	3,003
Southern Syurkharata			12	32.69	3,026
2	43.5	3,185.4	13	32.23	2,976
4	35.2	3,183.8	22	33.12	2,989
Tedin			40	33.6	2,972
1	34.0	3,114	41	32.4	2,974
40	33.8	3,104	43	32.25	2,972
41	33.74	3,100	44	32.15	2,978
42	34.0	3,120	Sikhorei		
Pyusei			1	36.2	3,149
22	33.9	3,104	50	33.8	3,090
Uremyd			51	32.8	3,127
30	34.1	3,1.02	52	32.21	3,087
			8	31.1	3,008
			16	32.2	3,075
			20	34.3	3,041

With this purpose, the best-studied intervals of the section were defined. Such intervals are 3,000–3,030, 2,970–3,000, 3,270–3,290, and 3,100–3,120 m in the Northern Khosedayu, Western Khosedayu, Ardalin, and Tedin fields, respectively (Table 8.4). The pressure difference at the same depths ranges from 0.5 to 4.0 mPa.

Similar approach was used also for the study of concentration and temperature fields in well-studied structures of the Khoreiver Depression. For these structures, schemes illustrating directions of formation pressure lateral gradients, concentrations, and temperatures for the best-studied upper Frasnian–Tournaisian petroliferous complex were constructed.

## 8.5 Fluid Dynamics in Deep Formations of Individual Well-Studied Structures

The detailed study of local regularities is based on the complex analysis and comparison of hydrodynamic, hydrogeochemical, and thermal fields in all the structures known to different extent [5, 10]. We present here information only on best-studied structures located in the central part of the Khoreiver Depression and well-studied upper Frasnian–Tournaisian aquifer. Tables 8.3, 8.4, and Figures 8.3–8.5 present results of these studies.

Tables 8.3 and 8.4 contain information for constructing schemes illustrating lateral gradients. The latter show also gradients of reduced pressures (Fig. 8.5). In most cases, gradients of the potential obtained by different methods are consistent with each other.

The description, characteristics, and classification of blocks with account of all the available information on formation pressures, temperatures, and concentrations are given in [10]. We consider here only the Northern Khosedayu structure based on the information from last work.

The analysis of the distribution of lateral gradients determined by different methods allows three blocks to be defined (Fig. 8.4).

The first block is located in the southwestern part of the Northern Khosedayu area (Boreholes 7, 14, 19, 22, 23). The reduced pressures in this structure vary from 24.0 to 24.5 mPa, while pressures measured at the same depth range from 31.0 to 31.5 mPa, i.e., the difference is 0.5 mPa (substantiated error value); therefore, this block may be characterized as gradient free. Northward, 4 km away from the latter (Boreholes 2, 3, 10, 24, 33), measured and reduced formation pressures increase rapidly up to 33.0 and 26.5 mPa, respectively, i.e., the pressure difference is as high as 2.0–2.5 mPa. This indicates undoubtedly existence of hydrodynamically impermeable or poorly permeable boundary between these blocks. In the third block, insignificant piezomaximums and piezominimums alternate between each other.

The block structure is confirmed by the temperature field, where two blocks are distinguishable. The first of them characterized by elevated temperatures (up to 70°C) corresponds spatially to the block with maximal pressures. The second temperature block is characterized by low-gradient field with temperatures of

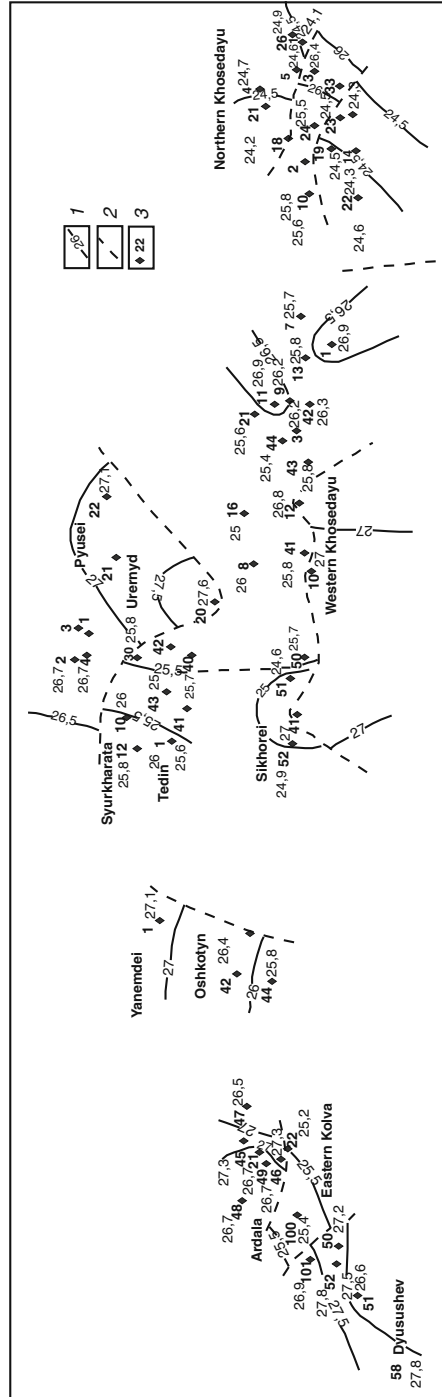


**Fig. 8.4** The stratum-block structure of some areas in the Khoreiver Depression. (1) Lines of reduced pressures; (2) assumed impermeable or poorly permeable hydrodynamic boundaries; (3) borehole and its number

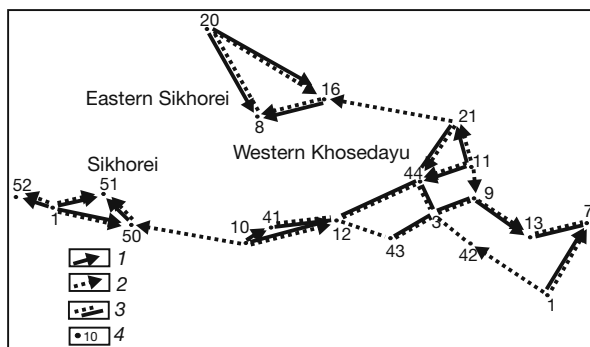


**Fig. 8.5** Directions of lateral gradients of reduced formation pressures. (1) Directions of gradients measured at close depths; (2) the same for reduced pressures; (3) gradient-free zones; (4) borehole and its number

65–68°C and gradient of 2–3°C. This block comprises the most part of the Northern Khosedayu structure corresponding to the first and third hydrodynamic blocks.

The stratum-block structure of the structure is also evident from hydrochemical data. The hydrochemical field is very complicated. Nevertheless, it shows correlation between distributions of mineralization, pressure, and temperature. Maximal mineralization values (204 g/dm<sup>3</sup>) are confined to the block with maximal temperatures and pressures. The remainder of the structure demonstrates no significant changes in mineralization, which varies around 170 g/dm<sup>3</sup>.

The spatial coincidence of pressure, temperature, and mineralization maximums is explainable by ascending near-vertical filtration of hot and highly mineralized fluids.

T.A. Kiryukhina [9] defines in the upper Frasnian–Tournaisian aquifer of the Northern Khosedayu structure three geochemical types of oils, which are characterized by different genetic parameters and geochemical properties originating from different source rocks. N.N. Kosenkova assumes three different oil pools in this structure. The spatial distribution of different oil types and pools coincides with blocks definable by the hydrodynamic, hydrochemical, and thermal data.

## 8.6 Regional Peculiarities of Fluidodynamics in the Pechora Petroliferous Basin

Regional peculiarities of fluid dynamics are derived from modeling [6, 10]. The modeling technique is discussed in Chapter 2.

The solution of the inverse problem yielded pressure values for the entire study region and Ordovician–Triassic section, which were used for constructing schematic hydrodynamic maps and profiles for all the aquifers. In addition, modeling results

made it possible to assess the value and direction of the vertical gradient, i.e., estimate interactions between formations [3, 10]. The analysis of these results provided information on peculiarities in fluid hydrodynamics of deep formations in the northern part of the Pechora basin.

The distribution of formation pressures through the region in question derived from modeling is consistent with directions of lateral gradients obtained by the pressure reducing and direct methods.

The analysis of modeling results allowed general concepts of regional fluid dynamics in Paleozoic sediments of the Khoreiver Depression (Fig. 8.6), Sorokin Swell, and Kolva Megawell to be obtained. These concepts are discussed in sufficient detail in [10]. We consider here only two of four aquifers: Silurian–Lower

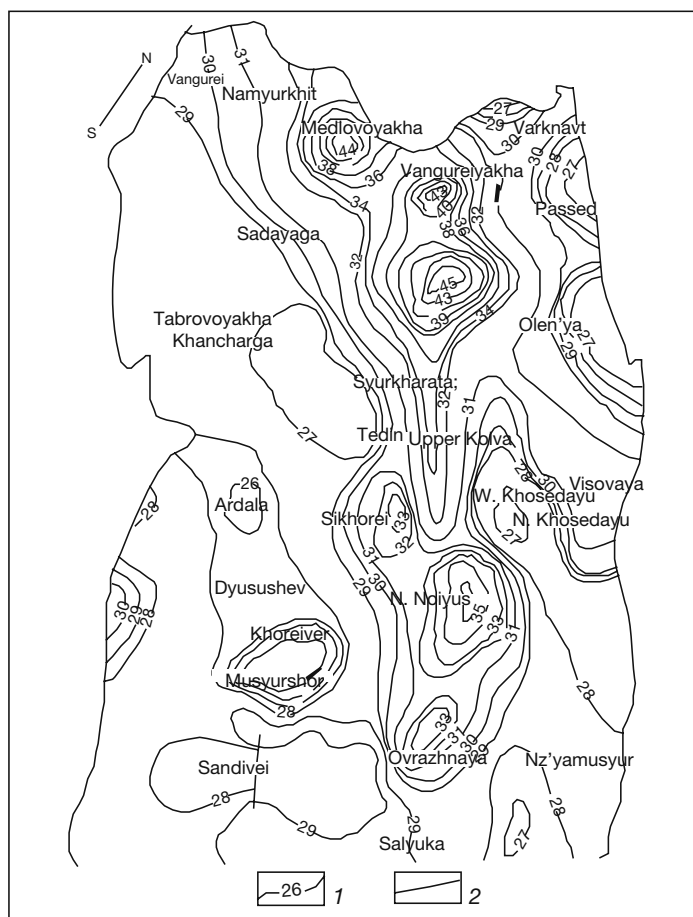


**Fig. 8.6** Schematic hydrodynamic map of the Silurian–Lower Devonian aquifer in the Khoreiver Depression (after A.V. Korzun). (1) Isolines of formation pressures based on modeling, mPa; (2) tectonic fractures and related relatively impermeable boundaries

Devonian and Permian–Triassic occurring correspondingly in the lower and upper parts of the sedimentary cover.

### 8.6.1 Silurian–Lower Devonian Petroliferous Complex

*Sorokin Swell.* In most parts of this structure, the petroliferous complex is characterized by high values of the pressure gradient, which vary from 28 to 43 mPa. Lateral gradients range from  $10^{-3}$  to  $10^{-1}$  to reach locally a unit. The zone with the highest gradients comprises northern areas (Varandei, Southern and Northern Toravei, Naul, Labagan fields). The southern part of the Sorokin Swell demonstrates high values of the reduced pressure (up to 32 mPa) being characterized, however, by insignificant gradients of reduced pressures in local structures (0.5–1.0 mPa).

Such a distribution of pressure in the Silurian–Lower Devonian petroliferous complex implies lack of interaction between the high-gradient and practically gradient-free zones and development of relatively impermeable boundaries. Thus, we can speak about two blocks in this complex: the northern with high gradients (up to  $10^{-1}$ ) and maximal pressures of 43 mPa and southern one with low gradients (up to  $10^{-3}$ ) and pressure values up to 32 mPa. For solving the inverse problem, these blocks were separated by the zone with low permeability values up to  $10^{-4}$  m/day, which spatially coincided with the tectonic fracture.

The detailed analysis of the fluidodynamics in the first block revealed smaller relatively isolated fluidodynamic blocks reflected in three local piezomaximums and two local piezominimums. The Varandei block is marked by the piezominimum with pressures decreased up to 36 mPa. The lateral gradient between this minimum and neighboring areas is as high as  $10^{-2}$ . This points to lack of fluidodynamic interaction between the block with piezominimum and neighboring areas.

The pressure values maximal for the entire Silurian–Lower Devonian petroliferous complex are observed in the Toravei (up to 41 mPa) and Southern Toravei (up to 43 mPa) areas that are confined to the Varandei Fault zone. South of these areas (at a distance of 10 km), reduced pressures rapidly decrease up to 28 mPa (central part of the Naul structure). In order to provide the pressure decrease during modeling, the impermeable boundary was preset between the Southern Toravei and Naul fields with respective maximal and minimal pressure values; otherwise, the task convergence was impossible. Farther south of the block with the piezominimum, pressure increases rapidly again up to 34 mPa. The third piezominimum located at the transition between the Labagan and Naul areas is also confined to the Varandei Fault.

Comparison between locations of fluidodynamic boundaries in the petroliferous complex revealed by solving the inverse problem shows that they are probably related to fractures in the Sorokin Swell. For example, the piezominimum zone is separated from the northerly located high-gradient block (pressure difference between them is 10 mPa) by the tectonic fracture. This fault is traceable only up to lower Frasnian sediments. The fault zone in the overlying upper Frasnian–Tournaisian petroliferous complex is marked by the piezomaximum. Such

a distribution of reduced pressures through the section may result from near-vertical ascending filtration along the zone with elevated fracturing, which could be formed in poorly permeable clayey sediments above the tectonic fracture. In addition, the vertical discharge from the underlying petroliferous complex is evident from data on oil geochemistry. Oil pools located in Lower and Upper Devonian sediments are characterized by similar geochemical properties, which indicate that both of them originate from the same Lower Devonian source rocks [9].

The near-latitudinal fault that separates the northern subsided area from the southern uplifted one coincides with the hydrodynamic boundary dividing the swell into two blocks: high gradient with maximal pressure values and practically gradient free [10].

The formation of piezomaximums and their localization in the tectonic fracture zone (Varandei Fault) is explainable by ascending subsurface fluids along the latter. This agrees with the present-day view of the formation of narrow fault-line feathering fractures in the zone of tectonic dislocations. Moreover, jointing in these zones is characterized by cyclic patterns being determined by geological development of the region. Recent tectonic movements result usually in activation of large faults and, correspondingly, intensified fracturing. Malyshev [11] classifies the Varandei regional fault as a fracture of continuous action, which implies its current activity.

*Khoreiver Depression.* Pressure values derived for the Silurian–Lower Devonian petroliferous complex by modeling range from 25 to 45 mPa. Several large zones with high pressures (up to abnormally high) are defined. The first largest zone extends in the form of a relatively narrow band (15–20 km wide) in the near-meridional direction via the Sadayaga and Southern Sadayaga structures farther southeastward with pressure values of 45 and 41 mPa in the former and latter, respectively (Fig. 8.6). Values of the lateral gradient relative to piezominimums amount to 0.1–0.5.

The second piezominimum with pressures up to 44 mPa is confined to the Northern Chernaya Rechka structure. It occupies an area approximately 100 km<sup>2</sup> in size. The lateral gradient is as high as 0.2–0.3 and decreases rapidly in all the directions up to 0.01 and lower in areas with lower pressures (up to 38 mPa) (Fig. 8.6). Such high-gradient values suggest development of poorly permeable boundaries, which prevent lateral relaxation of pressures.

The Northern Noiyyu and Pian structures are characterized by pressures up to 35 mPa and irregular variations in their gradients. The central part of the piezomaximum demonstrates minimal lateral gradient values, which grow rapidly in the southwestern direction and remain practically unchanged in the northeastern one. Approximately 30 km south of the last maximum, pressures in the Ovrazhnaya structure area reach 33 mPa (Fig. 8.6). This piezomaximum zone neighbors two areas with minimal pressure values (up to 27 mPa). The difference in pressures between piezomaximums and piezominimums is 8 mPa and lateral gradient is 0.02. This piezominimum is approximately 500 km<sup>2</sup> in size and involves the entire Northern Khosedayu and partly (by one of its tongues) the Visovaya areas (Fig. 8.6).



The large piezominimum of formation pressures is confined to the Varandei Fault to occupy the Varknavt, Passed, and Olen'ya areas, where their values decrease up to 27 mPa.

Another minimum with pressures of 28 mPa coincides with the Northern Kolva and Iz'yamusyur areas. It is bordered by last two piezomaximums and extends southeastward to reach values of 26 mPa at the transition between the Khoreiver Depression and Chernyshev Range.

A small (approximately 10 km<sup>2</sup>) oval piezomaximum with formation pressures of 33 mPa is located between the Western Khosedayu and Sikhorei structures, where it complicates the high-gradient zone (Fig. 8.6).

The triangular area with pressures up to 41 mPa is revealed in the southern part of the Khoreiver Depression in the junction zone of the Kolva Megaswell, Khoreiver, and Bol'shaya Synya depressions, and Chernyshev Range.

The seventh large piezomaximum (1,200 km<sup>2</sup>) with formation pressures of 31 mPa is recorded between the Musyurshor, Dysushev, and Central Khoreiver structures. This zone with high pressures extends toward the Kolva Megaswell (Fig. 8.6).

Three small maximums with pressures of 29–30 mPa form a chain along the Eastern Kolva Fault.

The western part of the Khoreiver Depression is characterized by low-gradient pressures (lateral gradients of 10<sup>-3</sup>–10<sup>-4</sup>). This is probably explained by both hydrodynamic conditions in this area and insufficient information, which prevent from interpreting the structure of the fluid flow.

The zone with maximal values of the lateral gradient crosses from the southeast northwestward practically the entire Khoreiver Depression in its central part (Fig. 8.6). The zone is 4–6 km wide and 130–150 km long. It encloses presumably the relatively impermeable boundary.

*Development of hydrodynamically isolated blocks and relatively impermeable boundaries in the northern part of the Pechora basin prevents from the formation of the regional deep fluid flow in its structural elements.*

### **8.6.2 Upper Permian–Triassic Petroliferous Complex**

*Sorokin Swell.* The Upper Permian–Triassic petroliferous complex is the uppermost one among all the considered complexes. The main feature of its fluidodynamics is practically gradient-free distribution of formation pressures: differences between pressure values do not exceed 0.5–0.75 mPa. Nevertheless, two blocks with different values of the reduced pressure are distinguishable. The first of them extending from the northern part of the Sorokin Swell to the Labagan structure is characterized by minimal formation pressures ranging from 24.5 to 25.0 mPa.

The second block is confined to the southern part of the swell, where the pressure increases up to 26.5 mPa. For solving the inverse problem, the impermeable boundary between these blocks should be preset. The hydrodynamic boundary coincides

spatially with the tectonic fracture that divides the Sorokin Swell and continues into lower petroliferous complexes.

Thus, all the petroliferous complexes of the Sorokin Swell are characterized by the complicated distribution of reduced formation pressures and their lateral gradients. The near-latitudinal fault that divides the swell into the northern subsided and southern uplifted parts is reflected in all the complexes as an impermeable barrier. Other hydrodynamic boundaries, probably, of different geneses defined in other complexes may be displaced relative to each other.

Comparison between localization of hydrocarbon accumulations in petroliferous complexes of the Sorokin Swell area shows that most of them correspond to piezominimums or coincide with low-gradient zones.

No hydrocarbon accumulations are discovered in the Silurian–Lower Devonian petroliferous complex of the Toravei and Southern Toravei structures, which are marked by distinct piezomaximums.

The Varandei and Naul structures characterized by piezominimums enclose oil pools.

Similar spatial coincidence between piezominimums and hydrocarbon accumulations is also recorded for overlying petroliferous complexes: upper Frasnian–Tournaisian complex in the Southern Toravei, Naul, Labagan, and Sed'yaga structures; upper Visean–Artinskian complex in the Varandei, Southern Toravei, and Labagan areas. The last complex in the Naul and Toravei areas is lacking oil and gas pools.

The Upper Permian–Triassic complex characterized by low-gradient fluidodynamics regardless of constituting structures encloses a single oil pool that extends from the Varandei area in the north to the Labagan structure in the south. It is conceivable that this is explained by low lateral gradients of formation pressures in this complex.

## **8.7 Abnormally High Formation Pressures in the Northern Pechora Petroliferous Basin**

The Pechora petroliferous basin is characterized by development of abnormally high formation pressures. This implies impermeable boundaries and stratum-block structure of different portions of the section. The most distinct zone with abnormally high formation pressures is confined to the Inzyrei structure located at the transition between the Khoreiver Depression and Kolva Megaswell. The structure is bordered in the west and east by regional faults: Central Kolva and Eastern Kolva, respectively (Fig. 8.7). These faults intersect in the southern part of the structure to isolate the block. The displacement amplitude of Ordovician–Lower Devonian sediments is 1.0–1.2 km. The faults are distinguishable, although with lower amplitude, also in overlying formations passing into flexures in Mesozoic sediments. This implies lateral isolation of the Inzyrei structure. In addition to main faults, the structure is crossed by a system of smaller gently dipping feathering fractures [15].

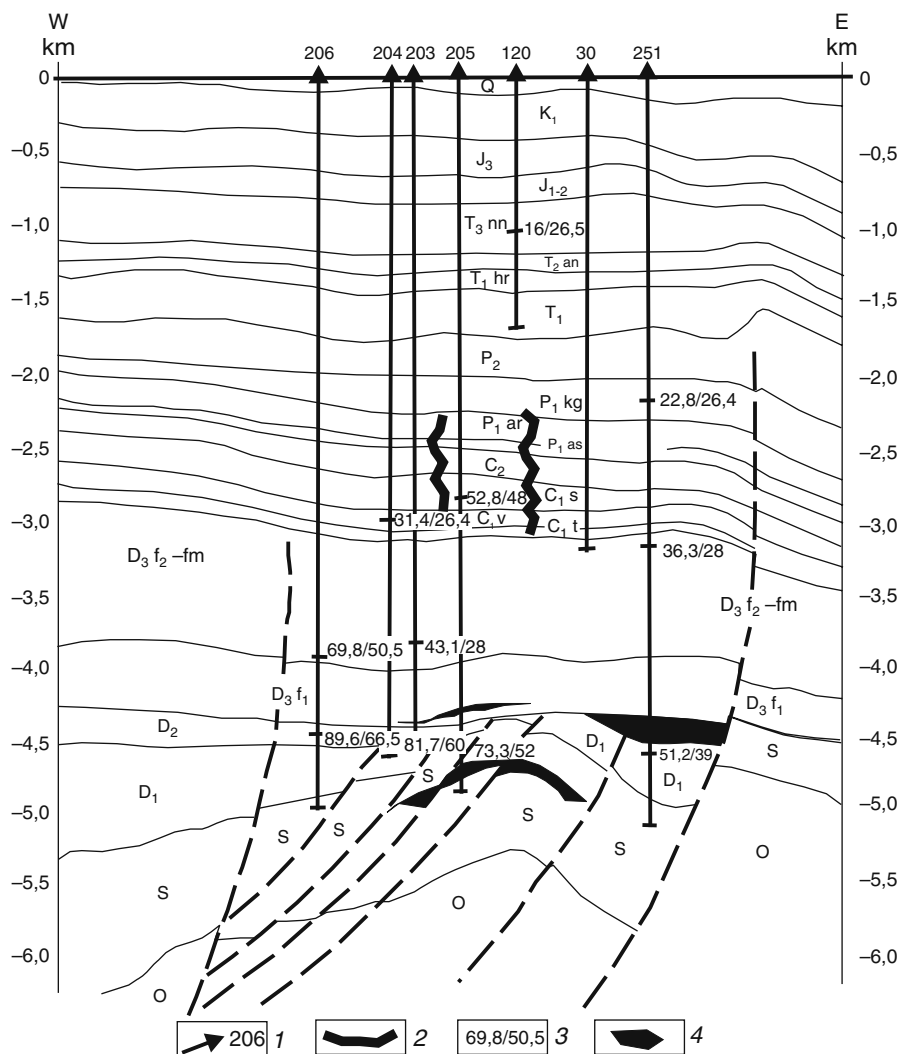


**Fig. 8.7** The latitudinal geological–hydrogeological section across the Inzyrei area (after I.A. Malyshev with additions by A.V. Korzun). (1) Borehole and its number; (2) boundaries based on hydrodynamic data; (3) formation pressure (numerator and denominator are measured and reduced values, respectively); (4) oil pool

The development of regional confining units in the section of the Inzyrei structure (Fig. 8.7) suggests much hampered hydrodynamic interaction between its neighboring elements of the section in both vertical and horizontal directions, which favors preservation of abnormally high formation pressures. Thus, the geological structure of the Inzyrei area provides conditions favorable for lateral hydrodynamic isolation of some blocks in the section and, consequently, long-term preservation of abnormally high formation pressures.

The Inzyrei structure was drilled by seven boreholes, which penetrated all the petroliferous complexes. Four of these boreholes revealed abnormally high formation pressures. Maximal anomaly coefficients (1.86–1.99) are characteristic of Boreholes 204–206 (Table 8.5).

The analysis of the lateral and vertical distributions of reduced pressures through the Inzyrei area revealed development of significant lateral gradients both within this structure and relative to neighboring areas. In the Silurian–Lower Devonian petroliferous complex, the pressure difference is 22 mPa between Boreholes 205 and 251 and 8 mPa between Boreholes 204 and 205 located 4 km away from each other. Such a situation is possible in the absence of the hydraulic interaction (existence of impermeable boundaries) between these boreholes. Significant differences in formation and reduced pressures are also characteristic of overlying petroliferous complexes (Tables 8.5, 8.6; Fig. 8.7). In the upper Frasnian–Tournaisian petroliferous complex, pressure difference in Boreholes 204 and 203 is significant, while pressures in Boreholes 203 and 251 are similar.

In Borehole 205, abnormally high formation pressures are registered throughout the entire section in question from Silurian to Permian sediments. In Boreholes 204 and 251, they are observed only in Lower Devonian sediments below the Kynov–Sargaevo confining sequence. Elevated formation pressures in Triassic (Borehole 120) and Lower Carboniferous (Borehole 30) formations with the respective anomaly coefficients of 11.15 and 1.11 imply their development in lower parts of the section as well.

The development of abnormally high formation pressures in the Inzyrei structure area is likely related to recent tectonic movements. According to [15], the most part

**Table 8.5** Measured formation pressures and anomaly coefficients in the Inzyrei structure

Borehole	Age	Formation pressure, mPa	Depth, m	$K_{\text{anom}}$
120	T <sub>1–2</sub>	16.0	1,391.5	1.15
203	D <sub>3f</sub>	43.1	3,783.6	1.14
204	C <sub>1s</sub>	31.38	2,867.2	1.09
204	D <sub>3s ps</sub>	81.7	4,352.2	1.88
205	P <sub>2</sub>	33.2	1,914	1.73
205	C <sub>1s</sub>	52.78	2,842	1.86
205	S	73.28	4,677	1.57
206	D <sub>1f2</sub>	54.41	4,018.6	1.35
206		69.8	4,172.6	1.67
206	S	89.6	4,512.6	1.99
Southern Inzyrei				
251	D <sub>3fm1</sub>	36.3	3,203.9	1.13
251	P <sub>1ar</sub>	22.8	2,045.9	1.11
251	S	51.21	3,868.9	1.32
Northern Inzyrei				
30	C <sub>1s</sub>	27.78	2,498.9	1.11

**Table 8.6** Reduced pressures and lateral gradients in the Inzyrei structure

Borehole	Reduced pressure, mPa	Depth, m	Density, kg/m <sup>3</sup>	Reduced pressure, mPa	Depth, m	Density, kg/m <sup>3</sup>	Distance between boreholes, m	Gradient
203/204	44.1	3896.6	10.53	31.38	2,867.2	1,133	2,000	0.5632
203/205	44.1	3896.6	10.53	36.3	3,213	1,110	2,600	0.2847
203/205	44.1	3896.6	10.53	52.8	2,842	1,134	2,600	0.4432
203/251	44.1	3896.6	10.53	36.3	3,203.9	1,110	11,400	0.0658
204/205	31.38	2867.2	11.33	36.3	3,213	1,110	3,600	-0.1079
204/205	31.38	2867.2	11.33	52.8	2,842	1,134	3,600	0.0073
204/251	31.38	2867.2	11.33	36.3	3,203.9	1,110	11,400	-0.0332
205/251	36.3	3,213	11.10	36.3	3,203.9	1,110	13,800	0.0007

of the Pechora petroliferous basin experiences moderate subsidence and consists of intricately shaped triangular blocks, which move in different directions (uplifting and subsiding) with different velocities. Ryzhov [15] defines five large blocks in the Kolva Megaswell, Khoreiver Depression, and Sorokin Swell, which differ in directions and velocities of movements from the generally subsiding Pechora basin. Such neotectonic conditions stimulate undoubtedly the formation of blocks with strains of different intensities and directions. In terms of neotectonics, the Inzyrei structure falls into the domain characterized by intense uplifting (Fig. 8.7). The block uplifting is accompanied by strong lateral compression, which could result, being combined with hydrodynamic isolation of the block, in development of abnormally high formation pressures in the Inzyrei structure area.

Subsurface fluids in the Inzyrei structure are characterized by lowered temperatures and higher mineralization as compared with these parameters at the same depths in neighboring structures. It is conceivable that the growth of formation pressures stimulated dissolution of minerals [10].

This assumption is confirmed by Mityushova [12], who considered the state in the fluid-rock system of the Middle Devonian petroliferous complex relative to aragonite, calcite, dolomite, magnesite, anhydrite, gypsum, halite, and mirabilite, as well as correlation between concentrations of these minerals, fluid mineralization, and occurrence depths of the complex [10].

Most of abnormally high formation pressure values are recorded below the Kynov-Sargaevy confining sequence, which indicates its perfect screening properties. In addition, the complicated structure and numerous tectonic fractures in Ordovician-Lower Devonian sediments prevent relaxation of formation pressures and favor preservation of abnormally high formation pressures in them.

## 8.8 The Temperature Field in Deep Formations

The region under consideration is characterized by extremely irregular studies of the lateral and vertical distributions of temperatures. Therefore, the distribution of temperatures in narrow intervals of the section (20–30 m) and their lateral gradients

were analyzed in the structures, for which most complete information on temperatures, formation pressures, and fluid mineralization is available. Table 8.7 presents such initial information.

The plots illustrating the temperature distribution through the entire section made it possible to reveal the best-studied intervals (Fig. 8.8), for which similar plots were subsequently constructed (Fig. 8.9). The presumed measurement error was preset to be 1°C (0.1°C measurement error and 1.0°C is error on account of the natural gradient 1°C per 20–30 m of the thickness). Such an analysis was conducted for several structures of the Khoreiver Depression, Kolva Megaswell, and Sorokin Swell.

*Eastern Kolva structure.* Figure 8.8 demonstrates the temperature distribution in the depth interval of 2,500–4,100 m. It is evident that the vertical temperature gradient below 3,400 m increases rapidly to reach 10°C/100 m. In the upper part of the examined section, the gradient is 3.3°C/100 m. The interval of 4,030–4,060 m, which was recovered by most boreholes, was selected for the study. The lateral distribution of the temperature in the form of gradients is shown in Fig. 8.10.

This figure shows that the maximal temperature difference in the selected depth interval is 14°C between Boreholes 52 and 100 and 12°C between Boreholes 52 and 101. The maximal temperature value for this interval is noted in Borehole 52 located near the arch of the structure, where it is as high as 102°C (no data are available for the arch proper).

Thus, similar to the formation pressure field, the temperature field of the Upper Devonian–Tournaisian petroliferous complex in the Eastern Kolva structure is characterized by significant lateral heterogeneity, differently oriented gradients, and substantial vertical variations in the temperature gradient, which is explainable by thermodynamic processes that proceed with either consumption or release of heat in different parts of the section.

*Ardala area.* The plot in Fig. 8.1 demonstrates temperature changes in the interval of 900–3,600 m. The interval of 3,250–3,450 m shows, in addition, its lateral changes. The analysis of plots illustrating correlation between temperature and depth constructed only for the last interval in particular boreholes reveals that the vertical gradient remains practically stable, although the plots appear to be displaced along the temperature axis (Fig. 8.10). This is explainable (if technical measurement errors are excluded) by different intensities of heat flows through the area in question.

The distribution of lateral temperature gradients through the area and temperature differences between boreholes are shown in Fig. 8.10. The maximal temperature difference in the Ardala area is 11°C (between Boreholes 21–49 and 21–47). The maximal temperature value is confined to the structure arch, while the temperature distribution isolines in the area are generally inconsistent with its structural patterns.

In the *Western Khosedayu* and neighboring structures, most of the temperature measurements in boreholes fall in the interval of 3,000–3,120 m (Table 8.7). Figure 8.9 illustrating the distribution of temperatures in this interval shows similar patterns with the shift of plots along the temperature axis against the background of the constant vertical temperature gradient. The exception is a high value of the vertical gradient obtained for Boreholes 9 and 12. Most of the data obtained for

**Table 8.7** Temperatures measured at close depths of individual areas in the central part of the Khoreiver Depression

Borehole	Age	Temperature, °C	Depth, m
Eastern Kolva			
51	D <sub>3</sub> f <sub>1</sub>	97	4,036
52	D <sub>3</sub> f <sub>1s</sub>	102	4,050
100	D <sub>3</sub> f <sub>1</sub>	88	4,062
101		90	4,056
Ardala			
21	D <sub>3</sub> f <sub>2</sub>	89	3,290
22		80	3,300
45		84	3,280
46		86	3,280
47		78	3,304
49	D <sub>3</sub>	78	3,283
Western Khosedayu			
1	D <sub>3</sub> f <sub>2</sub>	72	3,100
3		70	3,065
5		70	3,100
7		57	3,084
8		71.5	3,130
9	D <sub>3</sub>	70	3,100
10	D <sub>3</sub> f <sub>2</sub>	69	3,119
12		73.2	3,030
13		66	3,106
20		70	3,158
21	D <sub>3</sub>	63	3,132
40	D <sub>3</sub> f <sub>2</sub>	71	3,081
41		71	3,100
42		66	3,100
44		68	3,050
Eastern Sikhorei			
1	D <sub>3</sub> f <sub>2</sub>	72	3,100
50		71	3,095
51		70	
Tedin			
1	D <sub>3</sub> f <sub>2</sub>	75	3,210
40		75	3,205
41		78	3,170
42		74	3,185
43		66.5	3,162
Syurkharata			
1	D <sub>3</sub> f <sub>2</sub>	75	3,200
2		77	3,260
Southern Syurkharata			
10	D <sub>3</sub> f <sub>2</sub>	76	3,255
12		78	3,240

**Table 8.7** (continued)

Borehole	Age	Temperature, °C	Depth, m
Urernyd 30	D <sub>3</sub> f <sub>2</sub>	75	3,210
Northern Khosedayu			
Borehole	Age	Temperature, °C	Depth, m
1	D <sub>3</sub> f <sub>2</sub>	68	3,040
4		68	3,000
5		65	3,030
7		67	2,980
10		67	3,030
14		65	3,000
19		65	3,020
21		66	3,000
22		68	3,006
23		65	3,000
24		70	3,001
25		67	3,030

the maximal number of boreholes fall in the interval of 3,080–3,100 m, where temperatures vary from 57 to 71°C (Fig. 8.9). This best-studied interval is illustrated by the scheme reflecting the distribution of lateral temperature gradients (Fig. 8.10). Maximal temperature values are 73 and 71°C in boreholes Western Khosedayu-12 and Sikhorei-1, respectively, drilled in arch areas of the structures. The maximal difference (9°C) is noted between Boreholes 13 and 7 in the Western Khosedayu structure. It should be noted that the latter is characterized by relatively low differences in temperatures (2–5°C) and development of gradient-free zones.

In the *Northern Khosedayu* area, the lateral temperature distribution is studied in the interval of 3,000–3,030 m. The plots illustrating correlation between temperature distribution and depths in this interval (Fig. 8.9) show that they shift along the temperature axis, which indicates heterogeneity in the temperature field. Similar to previous areas, the maximal temperature value (70°C) is confined to the central part of the structure. According to the analysis of the distribution of lateral temperature gradients, most of the Northern Khosedayu area is characterized by the gradient-free thermal field (Fig. 8.10). This implies lack of the convective heat transfer within the last area.

The analysis of the lateral and vertical distributions of temperatures in structures of the *Syurkharata* group of uplifts (Syurkharata, Southern Syurkharata, Tedin, Pyusei, and Yanemdei) reveals heterogeneity of their thermal fields (Figs. 8.9, 8.10). It shows that the Tedin area is characterized by the shift of plots illustrating the vertical thermal gradient along the temperature axis. The maximal temperature value (78°C) is registered in Boreholes Tedin-43 and Southern Syurkharata-12.

Thermal anomalies and their distribution through the Pechora petroliferous basin are considered in [13, 14]. Geothermal anomalies are thought to be related to



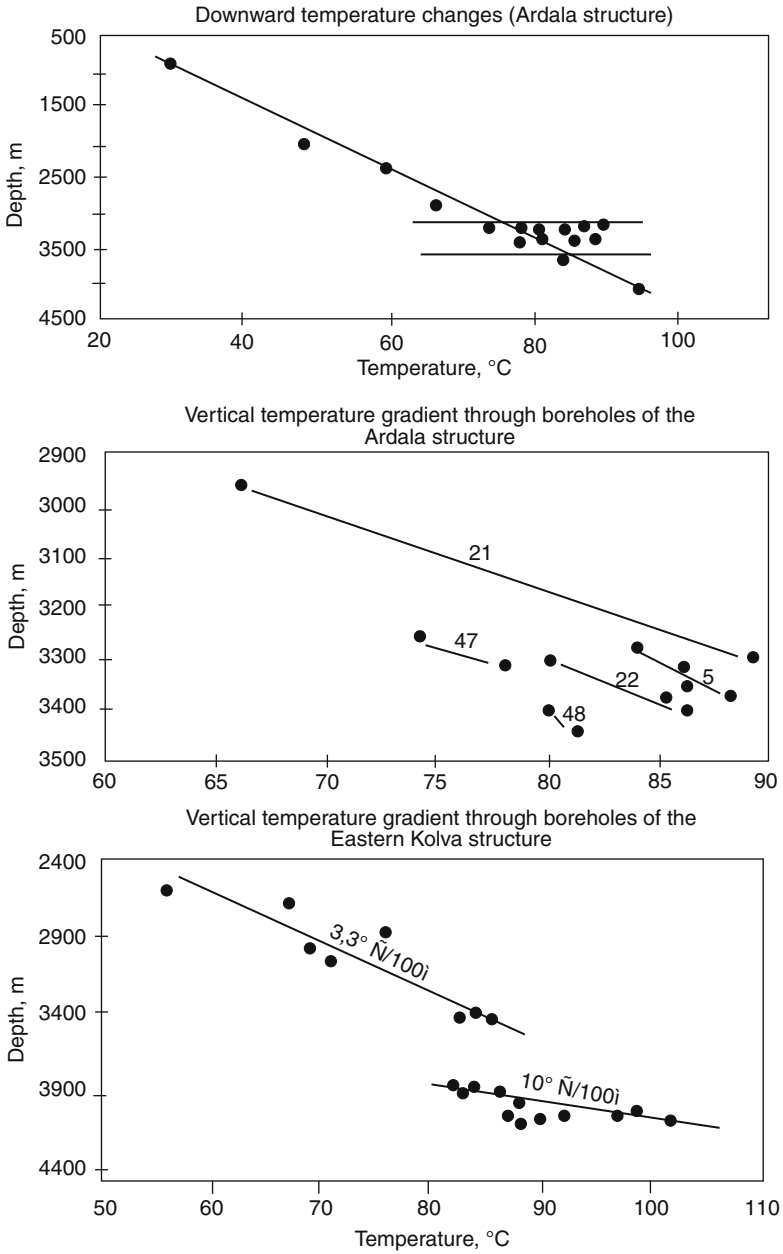


**Fig. 8.8** Downward temperature changes in the central part of the Khoreiver Depression

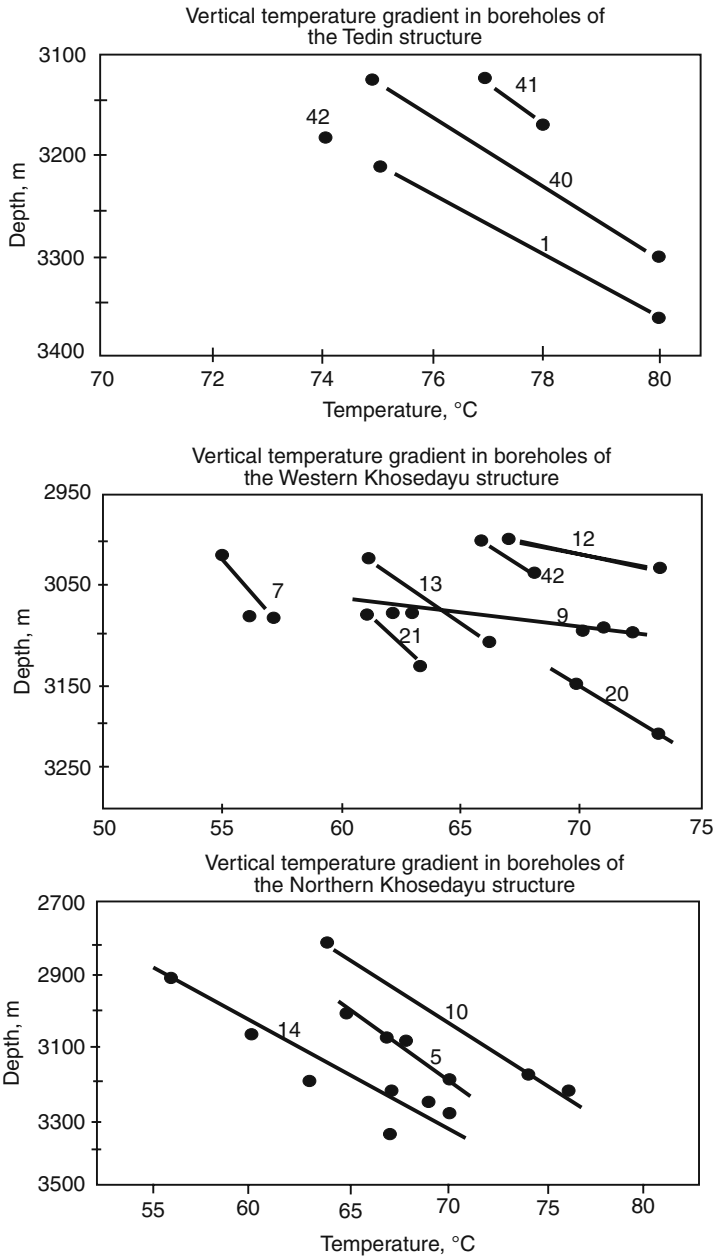


**Fig. 8.9** Downward temperature changes. Numerals near straight lines designate borehole numbers

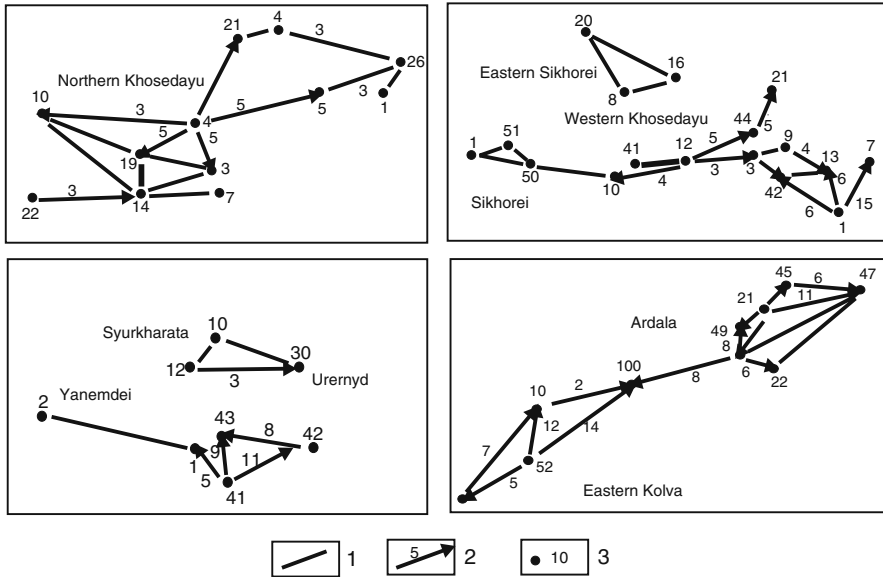


**Fig. 8.10** Directions of lateral gradients and temperature difference in the central Khoreiver Depression

intrusions of presumably Permian–Triassic age that are established by drilling and geophysical methods and confirmed by the post-magmatic hydrothermal activity. According to these authors, geothermal gradients in anomalous areas are as high as 6.1–7.64°C/100 m. Moreover, “they may increase downward (Western Tebuk, Dzh’er).” The authors note also coincidence between geothermal and hydrochemical anomalies in waters of the Middle Devonian and lower Frasnian sediments at depths of 1,000 and 2,000 m.

The defined anomalies associate with both young faults and zones of recently activated deep-seated faults (western slope of the Chernyshev Range). This is confirmed by development of thermal springs with temperatures up to 30°C in the Pymva-Shor, Edzhid-Yu, and “thermal” Lake Syv-Yu areas [13].

Thus, all the studied areas are characterized by lateral and vertical heterogeneities of thermal fields. This is explainable by several factors:

- (1) Intense thermodynamic processes resulting from changes in thermodynamic equilibrium and proceeding with consumption or release of heat. This is evident from substantial changes in temperature gradients at different depths and different boreholes within the same area. For example, in the Eastern Kolva field the vertical temperature gradient in the depth interval of 3,800–4,000 m is 10°C/100 m being equal to the normal value (3.3°C/100 m) in the depth interval of 2,600–3,400 m.
- (2) Different-intensity heat flows migrating from the lower boundary (basement). This is indicated by shifts of plots constructed for different boreholes along

the temperature axis, which is established in the Tedin, Western Khosedayu, Northern Khosedayu, and other structures.

- (3) The heterogeneous thermal field confirming lack of lateral migration (convective heat transfer) of deep fluids and supporting the known hypothesis of the stratum-block structure of deep formations and influence of the lower boundary [2–4].

## 8.9 Distribution of Deep Fluid Mineralization

The mineralization field was studied, when possible, in the same limited areas with well-known baric and thermal fields. For determining values and directions of mineralization gradients between points (boreholes), the mineralization values measured practically at the same depths (within the interval of 50 m) were selected. The distribution of mineralization values in narrow well-studied intervals of the section is considered in Table 8.8.

**Table 8.8** Fluid mineralization measured as close depths in some areas of the Khoreiver Depression

Borehole	Sampling depth	Mineralization, g/dm <sup>3</sup>
Eastern Kolva		
50	3,398	196
100	3,406	174
50	3,462	187
52	3,471	177
50	3,714	175
51	3,772	135
52	3,828	150
Dysushev		
160	3,443	189
57	3,480	129
55	3,491	146
Ardala		
47	3,326	175
21	3,344	197
22	3,384	184
49	3,386	198
45	3,394	163
Oshkotyn		
42	3,274	172
44	3,278	130
Syurkharata		
2	3,310	202
4	3,310	199
3	3,354	197

**Table 8.8** (continued)

Borehole	Sampling depth	Mineralization, g/dm <sup>3</sup>
Southern Syurkharata		
12	3,249	152
10	3,270	194
Visovaya		
2	3,180	176
3	3,250	167
5	3,197	181
6	3,230	152
Northern Khosedayu		
2	2,998	177
22	3,024	168
19	3,028	177
Northern Khosedayu		
10	3,031	174
14	3,036	175
18	3,053	169
21	3,072	158
4	3,072	143
26	3,085	175
5	3,119	182
Northern Khosedayu		
7	3,242	177
24	3,250	176
3	3,231	204
Sikhorei		
1	3,148	137
8	3,175	177
16	3,130	193
51	3,156	199
Tedin		
43	3,186	178
40	3,228	154
41	3,293	152
42	3,332	197
Pyusei		
1	3,660	147
Ureynyd		
30	3,228	152

The *Eastern Kolva*, *Ardala*, and *Oshkotyn* structures are located close to each other; therefore, they are considered together. This is important for establishing values and directions of formation pressure gradient between structures, although main attention was paid to the study of fluid mineralization within each of them.

In the Eastern Kolva and Ardala structures, mineralization values vary from 135 to 196 and from 163 to 198 g/dm<sup>3</sup>, respectively (Table 8.8). Schemes of mineralization gradient directions (Fig. 8.11) show that the central part of the Eastern Kolva structure (Boreholes 50, 52) is marked by distinct mineralization maximum (up to 1,986 g/dm<sup>3</sup>), away from which its values decrease toward limbs of the latter. Similar situation is also observed in the Ardala structure: its central part corresponds to the gradient-free zone with maximal mineralization values up to 198 g/dm<sup>3</sup>,

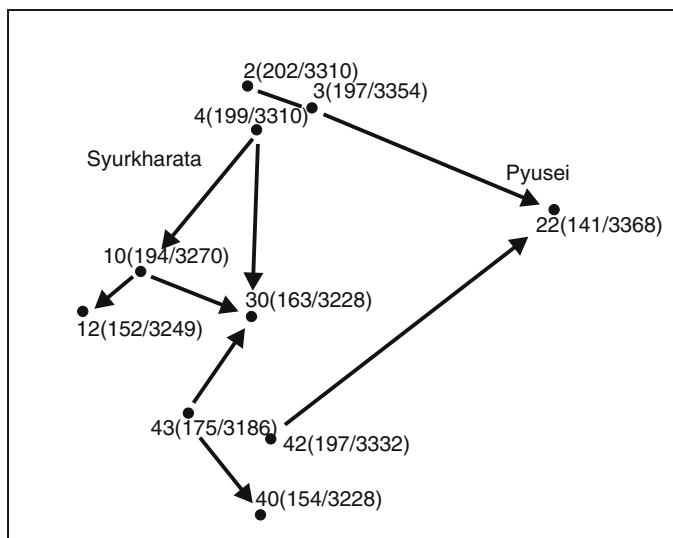
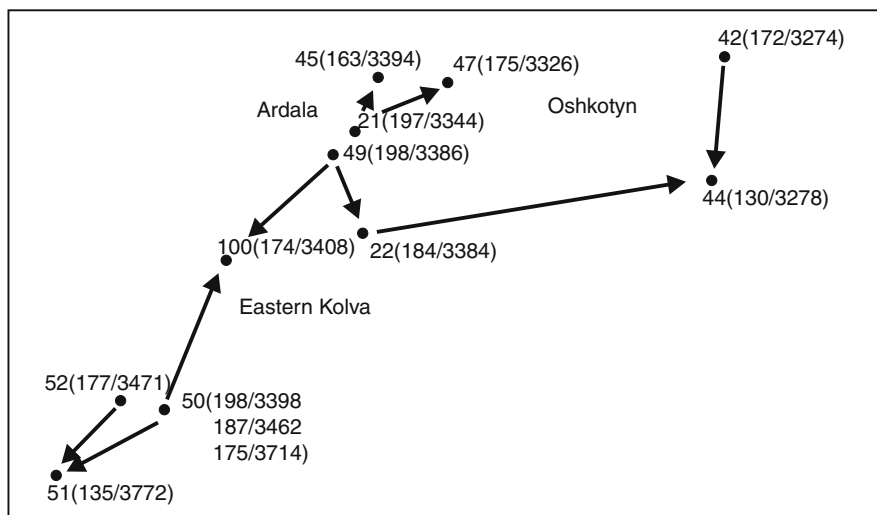


**Fig. 8.11** Directions of mineralization gradients in individual areas of the central Khoreiver Depression

which decrease toward peripheral areas of the structure. The maximal difference in mineralization through the Oshkotyn structure is  $42 \text{ g/dm}^3$ .

The comparison of mineralization values in the same interval between boreholes drilled in these structures reveals the significant gradient toward the junction zone between the Ardala and Eastern Kolva structures (Borehole 100). It is 24 and  $22 \text{ g/dm}^3$  near the Ardala and Eastern Kolva structures, respectively.

The *Western Khosedayu structure* is located in the central part of the Khoreiver Depression being slightly elongated in the latitudinal direction. Its mineralization distribution was analyzed together with that in the Sikhorei, Eastern Sikhorei, and Northern Sikhorei structures. Mineralization values in all these structures vary from 122 to  $199 \text{ g/dm}^3$  indicating substantial heterogeneity of their field. The analysis of the distribution of mineralization gradients (Fig. 8.12) displayed several maximums within the latter, with the highest mineralization values of  $190\text{--}191 \text{ g/dm}^3$  (Boreholes 12 and 43, Western Khosedayu structure) and  $193 \text{ g/dm}^3$  (Borehole 16, Eastern Sikhorei structure) also confined to their central parts. Maximal mineralization values in the Sikhorei structure are registered in its western marginal part. In general, this area is characterized by mosaic distribution of fluid mineralization values, which indicates lack of their lateral migration.

The *Northern Khosedayu structure* is the largest and best-studied element of the Khoreiver Depression. Mineralization values in its limits range from 143 to  $204 \text{ g/dm}^3$ . The Visovaya structure located nearby is characterized by values of  $152\text{--}181 \text{ g/dm}^3$ . The lateral distribution of mineralization gradients (Fig. 8.12) shows that the southwestern part of the structure corresponds to the relatively large gradient-free zone with values varying from 174 to  $177 \text{ g/dm}^3$ . It is noteworthy that similar gradient-free zone was defined in this structure based on the study of thermal and baric fields. Such a situation is characteristic also of most studied structures of the region in question.

Thus, the mineralization field is characterized by both lateral and vertical heterogeneities with the complicated distribution of mineralization and temperature values in the narrow depth interval of 30–50 m.

For testing the inference on the block structure of the Khoreiver Depression, independent geochemical studies of the hydrocarbon fluid composition were conducted [7, 9].

Oil fields are established in the Eastern Kolva, Western Oshkotyn, Sikhorei, Western and Northern Khosedayu, Yanemdei, Tedin, Syurkharata, Southern Syurkharata, Pyusei, and other areas. All the pools are confined to the Upper Devonian carbonate reservoirs. These structures and petroliferous complex were studied in detail with respect to their hydrodynamics (Fig. 8.4).

As a whole, oils are characterized by substantial variations in their physicochemical parameters and hydrocarbon composition. Several groups of oils with different characteristics are definable.

The first group includes oils from the Eastern Kolva and Western Oshkotyn fields. They are characterized by average density values ( $0.848\text{--}0.856 \text{ g/cm}^3$ ). The content of light fractions (boiling point  $200^\circ\text{C}$ ) and tarry-asphaltene components varies from 21 to 23 and from 7.6 to 10.1%, respectively. In contents of solid paraffins, these

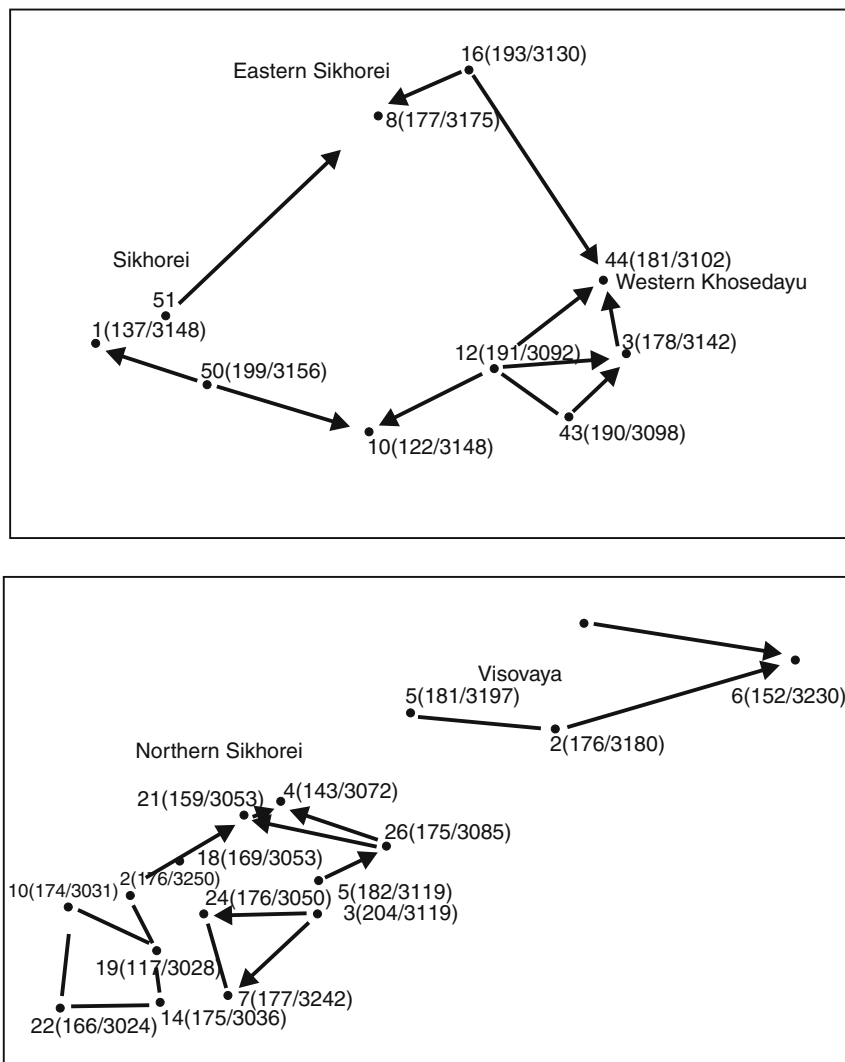


**Fig. 8.12** Directions of mineralization gradients in individual areas of the Khoreiver Depression

oils differ slightly from each other: they are several times higher in the Western Oshkotyn fields as compared with the Eastern Kolva field (13.4 versus 2.4%).

The hydrocarbon composition of saturated fractions (200–430°C) shows the complete succession of normal alkanes (from  $C_{12}$  to  $C_{34}$ ) and isoprenanes (from  $C_{14}$  to  $C_{20}$ ). The latter are dominated by pristane. The pristane/phytane value is 1.1.

The second group unites oils of the Central Khoreiver structures (Sikhorei, Upper Sikhorei, Western Khosedayu, Yanemdei, and Tedin fields). They are heavy to very heavy (0.874–0.930 g/cm<sup>3</sup>), sulfurous to highly sulfurous (2.2–3.7%) oils with the



high content of asphaltene–tar components (13.8–24.4%). Of the latter, asphaltenes occur in higher proportions as compared with tar. The oils are characterized by the high content of solid paraffins (8.7–17.9%) and insignificant concentration of light fractions ranging from 3 to 9%; only in the Sikhorei area, it amounts to 19%. Similar to the previous group, oils contain complete succession of normal alkanes and isoprenanes, although in contrast to the former they demonstrate two maximums in the distribution of normal alkanes corresponding to low-molecular ( $C_{15}$  and  $C_{17}$ ) and high-molecular ( $C_{24}$  to  $C_{27}$ ) varieties. Isoprenanes are dominated by phytane. The pristane/phytane value is approximately 0.5. In addition, chromatograms of these oils show peaks corresponding to hydrocarbons of the triterpane type.

The third group comprises oils from fields of the Syurkharata zone of uplifts (Syurkharata, Southern Syurkharata, Uerneyd, and Pyusei). By their physicochemical parameters, these oils are similar to their counterparts from the Central Khoreiver Uplift differing only in higher contents of light fractions (16–21%) and lower concentrations of solid paraffins (2.5–8.2%).

Similar to oils from the previous group, they are characterized by the complete succession of normal alkanes and isoprenanes with maximum corresponding to  $C_{14}$ . The pristane/phytane value is 0.3–0.4. Contrary to the above-mentioned oils, their counterparts from the third group are characterized by higher contents of hydrocarbons of the triterpane type.

Thus, three types defined among oils from the central part of the Khoreiver Depression differ in physicochemical parameters and hydrocarbon composition. They were formed under peculiar thermobaric conditions. From the genetic point of view, it may be stated confidently that oils of the above-mentioned groups differ from each other.

For example, oils of the Eastern Kolva and Ardala fields were generating in relatively “hard” thermobaric conditions from mixed humic–sapropelic organic matter. Oils from the Central Khoreiver Uplift are likely of mixed origin. Main components of the system are probably oils generated from humic and sapropelic organic matter, which could be mixed immediately in pools. This means that formed pools of one type could receive additional portions of hydrocarbons with different origins. The latter could migrate from lower formations of the sedimentary cover along weakened zones (fault or fracturing zones). Such a scenario is confirmed by palynological data. At the same time, oils from the Syurkharata structures enriched in triterpane hydrocarbons could originate from organic matter that accumulated under conditions of rapid lithification of sediments, which prevent it from decomposition.

Development of different thermobaric conditions during oil formation is consistent with previous inferences (see above), i.e., substantially heterogeneous temperature and pressure fields exist now and existed in past geological epochs. This confirms the concept of the stratum-block structure of deep formations and development of boundaries between blocks.

Thus, according to the complex analysis, the Central Khoreiver Uplift located in the northern part of the Pechora petroliferous basin is characterized by heterogeneous baric, thermal, and hydrochemical fields as well as by different oil

geochemistries. This is also evident from characteristics of similar fields in the upper Frasnian–Tournaisian complex of the Northern Khosedayu structure.

The analysis of the hydrodynamic profile along the structure and lateral gradients (Fig. 8.4) makes it possible to define three blocks with different hydrodynamic, thermal, and hydrochemical conditions and specific geochemical properties of oils.

The first block 25–30 km<sup>2</sup> in size is located in the southwestern part of the structure (Boreholes 10, 19, 23, 7, 14, 22). Its reduced pressure varies from 24 to 24.5 mPa, while pressures measured in the same depth interval (3,000–3,070 m) range from 31.0 to 31.5 mPa, i.e., the pressure gradient is 0.5 mPa and the block may be considered as gradient free. The block is characterized by maximal temperature and fluid mineralization values. Similar to pressures, no gradients in concentration of salts are registered.

Oil enclosed in this block is characterized by several maximums. The first maximum is formed by odd low-molecular *n*-alkanes C<sub>15, 17, 19</sub> and the second one is observed in the high-molecular area (C<sub>22–28</sub>). Isoprenanes are dominated by phytane. It is assumed that oil of such a composition resulted from multiple influxes of different-generation hydrocarbons into the pool [7, 9]. For example, prevalence of odd low-molecular homologues is noted in oil from the Ordovician–Lower Devonian complex. The block under consideration was most likely connected hydrodynamically with underlying sequences at some development stage.

The second block is located 4 km northeast of the previous one. Its formation pressures are as high as 33 mPa (Boreholes 2, 3, 24, 33). The block is approximately 10 km<sup>2</sup> in size. It is characterized by insignificant pressure and temperature gradients (the temperature variations are 2–3°C). The block demonstrates maximal fluid concentrations. The confinement of pressure, temperature, and fluid concentration maximums to this block is explainable by the current influx of hot and highly mineralized fluids from underlying formations.

In contrast to previous oils, their counterparts from block under consideration show no maximum in the spectrum of odd low-molecular *n*-alkanes C<sub>15, 17, 19</sub>.

The third conditionally defined block located northeastward of the second one (Fig. 8.4) demonstrates alternating piezominimums and piezomaximums within the formation pressure field. The temperature distribution pattern resembles that in the first block.

By hydrocarbon proportions in the saturated fraction, oils from this block are attributed to varieties generated from organic matter of the mixed humic–sapropel composition. The maximum is formed by of *n*-alkanes C<sub>21, 22, 23</sub> with pristine prevailing over phytane among isoprenanes. The oil composition indicates confidently that no hydrodynamic exchange existed between this block and underlying formations.

Thus, the stratum-block structure of deep formations is confirmed by four measured parameters: formation pressure, temperature, concentration of oils, and their geochemistry. Similar inferences are derived also from modeling for the Khoreiver Depression, Kolva Megaswell, and Sorokin Swell. It should be emphasized that boundaries between blocks are conditional to a significant extent due to incomplete information and irregular knowledge of the region.

## 8.10 Typification of Hydrodynamic Blocks

A fragment of the formation system bordered on all sides by relatively impermeable boundaries and characterized by uniform formation conditions of deep fluids is considered as a relatively isolated hydrodynamic block.

Modeling conducted for the region as a whole and detailed analysis of hydrogeological conditions in individual structures by different methods offer opportunity to define blocks, which differ in hydrodynamic, thermal, and hydrogeochemical fields. The characteristic of these blocks and their typification are considered below.

The relationships between three basic hydrogeological parameters in all the defined hydrodynamic blocks serve as a main criterion for their typification. These parameters are the formation pressure, temperature, and mineralization.

The comparison and complex analysis of the pressure, temperature, and mineralization fields made it possible to characterize hydrodynamics and formation of deep fluids in some blocks and to outline their types. The data on oil geochemistry were also used for this purpose as well. Two main types of hydrodynamic blocks and their subtypes were defined.

The analysis of obtained results reveals that blocks belonging to these two types are characterized by elevated and lowered formation pressures.

The lateral and vertical sizes of individual blocks are determined by both the geological–hydrogeological situation and the knowledge state of the region. Each block comprises one or several petroliferous formations; sometimes it corresponds to some part of the formation.

Blocks vary from 10–25 to 1,000–5,000 km<sup>2</sup> in size. The largest blocks are defined in the Khoreiver Depression, where they are usually characterized by isometric configuration, which is explained by different types (geneses) of their boundaries. In the Sorokin Swell and Kolva Megaswell, blocks are usually smaller and increase upward the section, i.e., blocks degenerate in this direction.

The blocks are of complicated shapes, which are also determined by the type of boundaries and their geometry. The genetic nature of boundaries and their reflection in the hydrodynamic field are spatially variable.

The entire Ordovician–Triassic section approximately 4,000 m thick is characterized by differently oriented lateral gradients of deep fluid pressures, which reflect the complicated structure of their field. Maximal gradients (up to 1) are observed in the Silurian–Lower Devonian petroliferous complex. They decrease upward the section to reach zero values in the Upper Permian–Triassic complex. Values of vertical gradients decrease in the same direction as well. In addition to the complicated field of pressure gradients, the region under consideration is characterized by irregular distribution of temperature and mineralization gradients. All these features combined with development of zones with abnormally high formation pressures confirm the stratum-block structure of deep formations in the northern Pechora petroliferous basin.

Development of relatively isolated blocks in the northern Pechora basin is responsible for lack of regional flows in deep parts of the sedimentary section in

both relatively large structural elements such as the Khoreiver Depression, Kolva Megaswell, and Sorokin Swell and structures of the third and higher orders.

The pressure difference between blocks averages 2–3 mPa. In zones with abnormally high formation pressures, it amounts to 10–14 mPa, which exceeds the reduction error. In the Khoreiver Depression, this difference between blocks is usually 2–5 mPa reaching maximal values of 10 mPa only in some local zones of the Silurian–Lower Devonian petroliferous complex in the northern part of the depression. The most contrasting pressure field is observed in the central and southern parts of the Kolva Megaswell ( $\Delta P$  2–14 mPa) particularly in areas adjacent to the abnormally high formation pressure zone.

The Sorokin Swell, where difference in formation pressures between blocks in the lower petroliferous complex amounts to 6 mPa and is practically indistinguishable in the upper (Upper Permian–Triassic) one, occupies the intermediate position.

The formation pressure in blocks and its variations depend on purely hydrodynamic and, probably, some other factors, which is evident from its correlation with temperature and mineralization. The comparison and complex analysis of the fluid pressure, temperature, and mineralization fields make it possible to characterize hydrodynamics and its formation conditions in some blocks and outline their main types. When necessary information on oil geochemistry is available, it is also used to substantiate their classification. Based on all these features, two main types of hydrodynamic blocks and their subtypes are distinguished.

### ***8.10.1 Blocks of the First Type***

These are usually large blocks with practically gradient-free distribution of the hydrodynamic potential between several measured boreholes ( $\Delta P \leq 0$ ) and temperature gradient of 2–3°C. The upper Frasnian–Tournaisian petroliferous complex of the Khoreiver Depression comprises several such blocks: Northern Khosedayu (Boreholes 10, 19, 23, 7, 14, 22), Southern Syurkharata, Pyusei, Tedin, and Western Khosedayu (Boreholes 12, 44, 3, 43, 13).

The similar large block is defined in the Silurian–Lower Devonian petroliferous complex of the northwestern Khoreiver Depression. All the petroliferous complexes of the Sorokin Swell include several blocks that are characterized by low-gradient formation pressures, while its Upper Permian–Triassic complex is divided into two practically gradient-free blocks.

Such a situation in the distribution of pressure, temperature, and mineralization fields implies no significant current migration of deep fluids within these blocks. In addition, stable thermobaric conditions provide now no prerequisites for intense physicochemical processes, which could result in the complicated structure of the formation pressure field. In addition, no changes in the strain state of rocks, which destabilize usually the hydrogeological situation, occur likely now.

### ***8.10.2 Blocks of the Second Type***

The Northern Khosedayu (Boreholes 2, 3, 24, 33), Eastern Kolva (Borehole 52), Ardala (Borehole 46), Western Khosedayu (Boreholes 9, 11), and Sikhorei (Borehole 1 area) blocks referred to this type are characterized by the highest formation pressures, temperatures, and mineralization relative to surrounding areas. This is explainable by the current ascending flow of fluids with such parameters.

It is impossible to estimate the scale of such migration since both filtration parameters of formations and quantitative characteristics of processes are variable in space and time. Nevertheless, it is confirmed by palynological spectra (older taxa occur in younger sediments), geochemical composition of oils [7, 9], and other indirect evidence.

The inference of vertical migration within limited areas is consistent with recent concepts of permeability of the geological medium at deep levels. As is known, the near-vertical flow of subsurface fluids is usually determined by rock permeability (jointing at deep levels) and pressure gradients.

In addition, the local heat influx can be yielded by convective heat transfer, which is confirmed by elevated temperatures in blocks with high values of formation pressures (Borehole 24 of the Northern Khosedayu area).

It is clear that lithological windows related to facies transitions and old erosion play important role in the vertical flow of subsurface fluids through poorly permeable rocks. Nevertheless, the main role in this process belongs to jointing (Chapter 6). According to current views, the fissure permeability is characterized by the irregular distribution. It is considered that maximal fissure density is confined to zones of tectonic dislocations. For example, it is noted that hydrocarbon accumulations in the Pechora petroliferous basin are localized in such zones [10]. This is determined by development of a system of feathering fissures and narrow weakened zones along faults, which provide the main migration flow of subsurface fluids and hydrocarbons.

In the Sorokin Swell area, some of the formation pressure piezomaximums are confined to zones of tectonic fractures (for example, the Varandei Fault), which is likely explained by the ascending flow of subsurface fluids along them.

The quantity and openness degree of fractures are subjected to temporal variations. Their activation (openness or closeness) may be caused by cyclic tectonic strains or other factors. Although periods of intense changes in strains can be very brief, they are very important for fluid migration. Activation of old and formation of new fissures increase rock permeability during such episodes by several orders. Neotectonic movements result usually in displacements and jointing degree growth in zones of major faults. Malyshev [11] classed the Varandei regional fault with fractures of continuous activity, the current stage included.

In addition, vertical migration influences also characteristics of the hydrochemical fields. Its anomalies determined by migration of subsurface fluids are local, which was shown for the Mangyshlak Peninsula (A.I. Timurziev), West Siberia (A.A. Rozin), and other regions. They are usually confined to zones of tectonic dislocations or their intersections.

The distribution of jointing in rocks beyond tectonic dislocation zones is debatable. In the opinion of some researchers, maximal jointing is developed in both arch and periclinal parts of structures. For example, V.N. Kirkinskaya and E.M. Smekhov note, "In local uplifts, their periclinal parts are usually characterized by relatively elevated jointing. The distribution of other such zones through the structure is controlled by its morphological peculiarities (narrow steep arch, steep limbs)." In the Sorokin Swell area, several piezomaximums observable in the upper Frasnian–Tournaisian petroliferous complex are also confined to arches of structures (Varandei, Sed'yaga, and others).

Changes in the fissure permeability may be caused by hydraulic fracturing related to the fluid flow proper. Chekalyuk [1] was the first to pay attention to this phenomenon: "During migration of liquid and transfer of the pressure by the latter from underlying formation with the high compression components, such a phenomenon is local. Hydraulic fracturing occurs owing to decrease in the volume of the mineral rock mass under additional compression. Taking into consideration heterogeneity in mechanical properties of rocks even within limited areas (for example, within a single anticlinal structure), the additional pressure of a few mPa should cause hydraulic fracturing in some places. In this connection, vertical migration becomes a self-activating process."

The aforesaid confirms probability of vertical ascending migration within blocks of the second type and possibility of the formation of their peculiar hydrodynamic features.

### ***8.10.3 Blocks of the Third Type***

Such blocks with minimal values of formation pressures and maximal temperature and mineralization of subsurface fluids are established in the Ardala (Borehole 21) and Labagan areas. Such a distribution of hydrogeological parameters is possible, when the block is characterized by permeable lower and upper boundaries, which yields prerequisites for relaxation of pressures upward the section, i.e., such conditions provide possibilities for through vertical migration of fluids. Similar to blocks of the second type, the blocks in question are characterized by geological prerequisites for such a migration, which is confirmed by indirect evidence. In this case, the formation pressure in the block should be lowered and the flow from the underlying formation should provide elevated temperatures and mineralization of subsurface fluids.

### ***8.10.4 Blocks of the Fourth Type***

This type includes blocks with minimal formation pressures, temperatures, and mineralization of fluids. They are usually confined to junction zones between structures (for example, Ardala, Eastern Kolva, and Sikhorei (Borehole 51) areas). The formation of such hydrodynamic blocks is determined primarily by continuous decrease

in formation pressures in the latter due the fluid discharge into the overlying petroliferous complex or due to relaxation of strain in the fluid-rock system. Relatively prolonged decrease in the pressure may activate processes stimulating restoration of the physicochemical equilibrium with the block (for example, precipitation of carbonates from solution). Such processes reduce, in turn, fluid mineralization and temperature. The temperature fall may also result from the Joule–Thompson effect during transition of dissolved gas into the free phase under formation pressure reduction in the block.

### ***8.10.5 Blocks of the Fifth Type***

The type unites blocks with maximal values of the fluid potential and its concentration and minimal temperatures (Inzyrei area). The last area is characterized by development of abnormally high formation pressures and intense neotectonic movements, which result in changes of the strain state in the fluid-rock system. These processes were likely responsible for increased solubility of minerals and, consequently, mineralization of subsurface fluids.

The lowered fluid temperatures in this block are explainable by cooling due to transition of dissolved gas into free phase (similar to the previous block). At the same time dissimilar to this orificing mechanism related to the natural pressure fall, in this block it was caused by the technogenic impact. Drilling and well test in the Inzyrei area were accompanied by intense gas flows and such a degassing of subsurface fluids could cause local temperature decrease in the near-hole zone.

### ***8.10.6 Blocks of the Sixth Type***

These blocks are characterized by maximal formation pressures and low-gradient temperature field with difference of 2–3°C (Syurkharata and Tedin areas). Their mineralization field is unknown because of data deficiency. It is conceivable that no ascending fluid migration is characteristic of the blocks, which is evident from lack of the temperature maximum. The elevated formation pressure is most likely related to lateral compression.

## **8.11 Conclusions**

- (1) Differently oriented horizontal gradients of formation pressures are developed both through the region under consideration and its separate structures; well-studied structures are also characterized by differently oriented temperature and mineralization gradients. This indicates the stratum-block structure of deep formations in the Pechora petroliferous basin.

- (2) Anomalous values of formation pressures as well as horizontal and vertical gradients decrease upward the section; block sizes increase in the same direction as well. The blocks with lateral sizes ranging from 25 to 5,000 km<sup>2</sup> comprise either a single petroliferous complex (or its separate segment) or several of them. Maximal gradients (up to 1.0) of formation pressures are recorded in the Silurian–Lower Devonian petroliferous complex, from where it decreases upward to reach zero values in the Upper Permian–Triassic one. Values of vertical gradients decrease in the same direction.
- (3) The stratum-block structure of deep formations prevents the regional flow of subsurface fluids within the Pechora petroliferous basin.
- (4) Development of zones with abnormally high formation pressures evidences in favor of the stratum-block structure of deep formations in the northern part of the basin.
- (5) The stratum-block structure of deep formations degenerates upward the section.

## References

1. Chekalyuk E D (1977) Water-oil solutions. Naukova Dumka, Kiev
2. Djunin V I (1981) Investigation methods and principles of deep formation hydrodynamics. VIEMS, Moscow
3. Djunin V I (1985) Investigation methods of the deep subsurface flow. Nedra, Moscow
4. Djunin V I (2000) Hydrodynamics of deep formations in petroliferous basins. Nauchnyi mir, Moscow
5. Djunin V I, Korzun A V (2001a) Fluidodynamics and formation of hydrocarbon accumulations. Mineral resource base of Russia in 21st century. In: Materials of the scientific-practical conference. Arkhangel'sk
6. Djunin V I, Korzun A V (2001b) Geological formation model of deep groundwaters and origin of hydrocarbon accumulations. In: Proceedings of the 5th International conference "New ideas in geosciences." Moscow
7. Djunin V I, Korzun A V, Kiryukhina (1999) Hydrodynamics of deep formations and petroleum resource potential (exemplified by the northern Pechora Depression). In: Abstracts of the 13th geological meeting of the Komi Republic "Geology and mineral resources of northwestern European Russia." Syktyvkar
8. Gafarov R A (1963) Structure of the Precambrian basement of northern East European Platform. Nauka, Moscow
9. Kiryukhina T A (1995) Oil types in the Timan-Pechora basin. Vestnik MGU Ser geol 2:39–49.
10. Korzun A V (1996) Hydrodynamics of deep formations in the northern Pechora artesian basin. Candidate dissertation (Geol-Mineral) MGU, Moscow
11. Malyshev N A, Pinchuk A V (1992) Past buried local uplifts: New oil and gas prospecting objects in the Kolva Megaswell. Trudy Inst Geol Komi NTs UrO RAN 76: 103–110
12. Mityushova T P (1994) Interaction of the water-rock system exemplified by the Middle Devonian-lower Frasnian aquifer in the Pechora Syncline. In: Materials of the 3rd scientific conference of the Institute of Geology, Komi Scientific Center, Uralian Division, Russian Academy of Sciences. Syktyvkar
13. Nevskaya N M, Dedeev V A (1973) Geothermal and hydrodynamic peculiarities in the sedimentary cover of the Pechora Syncline and their relation with endogenic processes. Trudy VNIGRI 338:63–70
14. Nevskaya N M et al. (1979) Influence of epigenetic rock alterations on the regime of deep aquifers in the Timan-Pechora Province. Sov. Geol 10:100–105



15. Ryzhov N I (1988) Neotectonics of the European northern USSR. Nauka, Leningrad
16. Scientific basics of development of prospecting-exploration works for oil and gas in the Timan-Pechora Province (1987) Syktyvkar
17. Tectonics of the northeastern European Platform (1988) Inst Geol, Syktyvkar
18. The Riphean and Vendian of the European northern USSR (1987) Syktyvkar
19. Vsevolozhskii V A (1991) Basics of hydrogeology. MGU, Moscow
20. Zaporozhtseva I V, Kuril'chik V A, Biron R I (1977) Geological development of western and central parts of the Bol'shezemel'skaya Tundra and its petroleum resource potential. In: Proceeding of the 8th geological conference of the Komi ASSR "Petroleum resource potential of the European northeastern USSR and northern Urals." Syktyvkar

# Chapter 9

## Fluidodynamics in Deep Formations of the Eastern Ciscaucasia Petroliferous Basin

### 9.1 Geological Structure

The geological, hydrogeological, and tectonic settings of the eastern Ciscaucasia petroliferous basin are described in [4, 8]. Figure 9.1 presents the schematic geological and tectonic structure of the basin (Terek-Sunzha area included).

The platform part of the eastern Ciscaucasia petroliferous basin consists of the basement and the sedimentary cover [4]. The basement is composed of metamorphosed and deformed different-lithology rocks (shales, sandstones, volcanics, and igneous varieties) ranging in age from the Paleozoic to the Early Mesozoic (Triassic). The basement rocks are intensely deformed. They are recovered at a depth up to 4,000 m and penetrated for 400 m.

The folded basement is overlain by the Mesozoic–Cenozoic platform sedimentary cover composed of Jurassic, Cretaceous, Paleogene, Neogene, and Quaternary sediments (Fig. 9.1). The thickness of the sedimentary cover in most subsided basement areas exceeds 4,000 m.

#### 9.1.1 The Jurassic System

The Jurassic sediments are universally spread and represented by all three series.

##### 9.1.1.1 The Lower Jurassic Series (J<sub>1</sub>)

The Lower Jurassic Series is characterized by sediments of the Lotharingian, Pliensbachian, Domerian, and Toarcian stages. The sediments are represented by sandstones, conglomerates, siltstones, argillites, and shale enclosing locally (northern Osetiya) dolerite dikes and tuffs. The thickness of sediments of different stages varies from 800 to 3,000 m.

##### 9.1.1.2 The Middle Jurassic Series (J<sub>2</sub>)

The Middle Jurassic section includes sediments of the Aalenian, Bajocian, and Bathonian stages that range in thickness from 200 to 1,200 m. They are represented by sandstones, siltstones, argillites, and porphyrites (Bajocian Stage).

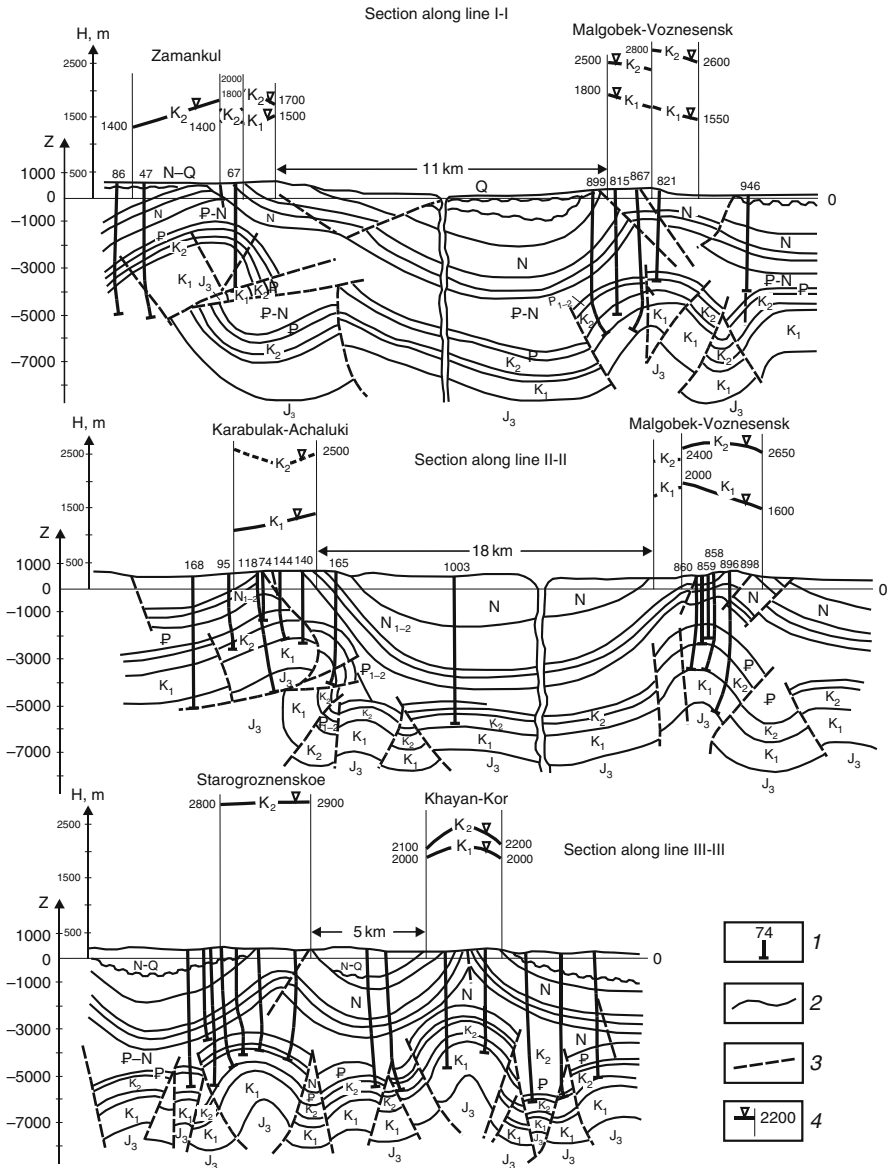


**Fig. 9.1** Geological-hydrogeological sections across the Terek-Sunzha Uplift. (1) Borehole and its number; (2) stratigraphic boundaries; (3) faults; (4) altitude of the groundwater reduced level

### **9.1.1.3 The Upper Jurassic Series (J<sub>3</sub>)**

The Upper Jurassic section comprises the Callovian, Oxfordian, Lusitanian, Kimmeridgian, and Tithonian stages. The Callovian Stage, 50–60 m thick, consists of sandstones and sandy ferruginous limestones in its lower and upper parts, respectively. The Oxfordian Stage, 400–500 m thick, is composed of bituminous limestones and dolomites. The Lusitanian Stage, 80–500 m thick, is characterized by massive dolomites and limestones. The Kimmeridgian Stage comprises limestones up to 600 m thick. The Tithonian Stage includes different-facies limestones (reefal included), dolomites, and sandstones up to 2,000 m thick.

## **9.1.2 The Cretaceous System**

The universally distributed Cretaceous sediments are represented by two series.

### **9.1.2.1 The Lower Cretaceous Series (K<sub>1</sub>)**

The Lower Cretaceous section includes sediments of the Valanginian, Hauterivian, Barremian, Aptian, and Albian stages with the integral thickness ranging from 500 to 1,150 m. The Valanginian Stage consists of locally dolomitized limestones and marls. The Hauterivian Stage is represented by marly sandstones and limestones. The Barremian Stage is composed of marly limestones and calcareous sandstones with clay interbeds in the lower and upper parts, respectively. The Aptian Stage is characterized by marly and clayey sandstones up to 200 m thick. The Albian Stage up to 120 m thick includes marly sandstones in the lower part of the section and carbonate clays in its upper portion.

### **9.1.2.2 The Upper Cretaceous Series (K<sub>2</sub>)**

The Upper Cretaceous sediments are distributed through the entire basin and characterize all the stages. They are represented by uniform limestones with marls and rare sandstone interbeds. Their thickness varies from 30 to 800 m.

## **9.1.3 The Cenozoic Group**

The Paleogene–Neogene (P–N)

### **9.1.3.1 The Paleocene Series (P<sub>1</sub>)**

The Paleocene sediments are attributed to three formations: El'burgan (siliceous marls up to 180 m thick), Goryachii Klyuch (argillites with sand and sandstone interbeds in the middle part up to 180 m thick), and Abaza (siliceous marls with opoka interbeds).

### 9.1.3.2 The Eocene Series (P<sub>2</sub>)

The Eocene comprises three formations: Cherkessk (sandy and clayey marls up to 170 m thick), Kuma (foliated marls up to 100 m thick), and Belaya Glina (clayey marls 70–200 m thick).

### 9.1.3.3 The Maikop Group (Oligocene – Lower Miocene, P<sub>3</sub>– N<sub>1</sub>)

The universally developed Maikop sediments up to 1,000 m thick in most subsided areas of the basin are represented by sandy clays with sand intercalations along the periphery of their distribution area. The thickness of the group and the clay content in the section increase toward the Caspian Sea.

### 9.1.3.4 The Miocene Series (N<sub>1</sub>)

The Tortonian Stage includes the following units: Chokrakian (clays with sandstone interbeds up to 700 m thick) and Karaganian (clays with marl, sand, and sandstone interbeds 200–450 m thick) regional stages.

The lower part of the Sarmatian regional stage is composed of deepwater clays up to 300 m thick. The lower Sarmatian is represented by a thick (up to 800 m) clayey sequence with rare sand and sandstone beds in the upper part. The upper Sarmatian section consists of sandy-clayey sediments 200–400 m thick. The Meotian regional stage is characterized by sands and clays 500–1,000 m thick.

### 9.1.3.5 The Pliocene Series (N<sub>2</sub>)

In the eastern Ciscaucasia region, the Pliocene is represented by widespread Akchagylian clays with sand interbeds (300–400 m thick) and Apsheronian sandy-clayey and shallow-water marine sediments 300–900 m thick.

## 9.1.4 The Quaternary System (Q)

The Quaternary sandy-clayey section is largely composed of sediments belonging to the Bakuan (up to 200 m thick), Khazarian (up to 220 m thick), and Khvalynian (up to 100 m thick) regional stages.

## 9.2 Tectonics

For the eastern Ciscaucasia petroliferous basin, tectonics is of particular importance because of its proximity to the Alpine fold belt.

The region includes the following tectonic elements: the homocline of the northern Caucasus slope (Mineral'nye Vody Uplift, Chernogorsk Homocline), Terek-Caspian marginal trough (platform slope of the Terek-Caspian Trough, Terek-Sunzha zone of uplifts), and Ciscaucasia epi-Hercynian platform (Stavropol

Arch, Chernyi Les Depression, Arzgir-Prikumsk zone of uplifts, Eastern Manych Depression, Karpinsky Ridge).

The homocline of the northern Caucasus slope with universally developed Jurassic and Cretaceous sediments is complicated by second-order folding, transverse uplifts, and concealed faults. Among the largest of these structures in the homocline are the Mineral'nye Vody, Argudan, Korin, and Sulak uplifts, Datykh, Korilam, Varandei, and Benoi brachyantoclines.

The Terek-Caspian marginal trough is a near-latitudinal structure extending east and southeastward from the Mineral'nye Vody Uplift. The trough is divided into two parts: zone of frontal folding and platform slope. The frontal folding zone is composed of a thick Mesozoic sequence and divided by the Sulak meridional uplift into three areas with different hydrodynamic conditions: Terek-Sunzha zone of uplifts, Dagestan Wedge, and southern Dagestan.

The Terek-Sunzha zone of uplifts comprises the Sunzha and Terek anticlinal structures representing two largest Mesozoic and Middle Miocene petroliferous zones of the North Caucasus. Both these structures consist of linear echelon-arranged anticlines complicated by systems of longitudinal and diagonal fractures with amplitudes of several hundreds of meters (Fig. 9.1). These are the Zamankul, Zmeisk, Malaya Kabarda, Karabulak-Achaluki, Starogroznenskaya, and Oktyabr'skaya anticlines in the Sunzha structure and Arak-Dalatar, Malgobek-Voznesensk, El'darav, Khayan-Khortov, and Gudermes anticlines in the Terek structure.

The peculiar features of the Terek-Sunzha structure are disharmonic folding with several structural stages, narrow arches, very steep limbs of uplifts, and intervenient faults with displacement amplitudes of several hundreds of meters (Fig. 9.1).

The Dagestan Wedge represents a complicated tectonic uplift characterized by highly variable strikes of fold structures from the latitudinal (Terek-Sunzha) to near-meridional (southern Dagestan) one.

The platform slope of the Terek-Caspian Trough is studied to lesser extent. The structure is generally characterized by the development of intermediate folding resembling that of the discontinuous platform type. This segment of the trough comprises the near-Terek anticlinal zone and the Terek-Sulak superimposed trough composed of thick Mesozoic-Cenozoic sediments.

The Ciscaucasia epi-Hercynian platform is relatively well studied in its eastern part, where the following structural elements are defined: the Arzgir-Prikumsk zone of uplifts, the Chernyi Les Depression, the Eastern Manych Depression, and the Karpinsky Ridge.

The Chernyi Les Depression represents a deeply subsided zone, which grades eastward into the platform slope.

The Arzgir-Prikumsk zone of uplifts is complicated by a system of dome-shaped structures, which are linear near-latitudinal in its southern part: Chkalovsk, Proskavei, Pravaya Kuma, Achikulak, and others. In the northern part, structures are largely dome shaped and separated by faults with amplitudes of several tens

of meters. The Eastern Manych Depression separates the Arzgir-Prikumsk zone of uplifts from the buried Karpinsky Ridge.

Observations of the regime in the stationary geophysical test area revealed rapid vertical movements along tectonic fractures. For example, the velocity of differently oriented vertical movements in the Terek-Sunzha area is estimated to reach 5 mm/km and higher. The area is composed of alternating uplifting and subsiding blocks. In addition, southern areas of the basin are characterized by high seismicity reflected in >1,000 different-magnitude earthquakes per year.

Thus, the eastern Ciscaucasia petroliferous basin adjacent to the Alpine fold belt is characterized by intense tectonic activity, the recent one included the development of long-leaving faults with displacement amplitudes amounting to several hundreds of meters, and high seismicity. All these factors naturally influence the formation of deep subsurface fluids.

### 9.3 Hydrogeological Conditions

The southern boundary of the eastern Ciscaucasia petroliferous basin coincides with the axis of the Glavnyi (Main) Caucasian Ridge. The basin also includes partly the folded massif. It is considered that the latter represents a regional infiltration recharge system, i.e., a formation zone of deep subsurface fluids in the Mesozoic–Cenozoic complexes.

The western boundary of the basin is drawn along the Stavropol Arch up to the Bezopasnoe Uplift. Further, it passes along the Sal'sk Swell to the Karpinsky Ridge to follow its central part eastward up to the Caspian Sea (via Buzga and Promyslovoe uplifts). In the east, the basin is covered by the sea.

The basin comprises second-order negative structures: Terek-Kuma, Alkhanchurt, Sunzha, and others. According to A.M. Ovchinnikov, these are “superimposed basins.”

The Mesozoic petroliferous complexes are recognizable based on low-permeability regional confining beds, stratigraphic, lithological facies, and other features.

In this work, the main emphasis is made on the hydrogeodynamic characteristic of Mesozoic aquifers (petroliferous complexes); less attention is paid to Quaternary and Neogene complexes when estimating the influence of marginal zones of the basin on Mesozoic deep fluid recharge.

The Mesozoic section is practically missing reliable confining beds and its aquifers are connected between each other. One of the most reliable confining beds is represented by saliferous facies of the Tithonian Stage separating Upper Jurassic and Lower Cretaceous sediments in the southeastern Stavropol region. In the Prikumsk area, saliferous sediments are missing.

The second relative confining bed in the Mesozoic section is a clayey member at the base of the Aptian sequence, which separates the Neocomian and Jurassic petroliferous complexes in most of the Prikumsk area. In the northwestern part of the latter (Maksimokumskii, Priozerskii, and adjacent areas), this relative confining bed is poorly developed.

The clay member crowning the Albian Stage separates the Upper and Lower Cretaceous sediments in the significant part of the eastern Ciscaucasia region. In some areas (Yamongoi, South Achikulak, and others), no clayey caprock is observed in the uppermost part of the Upper Cretaceous section. Thus, the Mesozoic section is practically missing regional relative confining beds [7].

The Maikop sediments that separate Upper Cretaceous and Cenozoic complexes represent relative regionally sustained and thick (up to several hundreds of meters) confining bed.

The following aquifers (petroliferous complexes) are recognizable in the sedimentary cover of the basin based on stratigraphic features: Permian–Triassic, Lower–Middle Jurassic, Upper Jurassic, Lower Cretaceous, Upper Cretaceous, and Paleocene–Miocene. Similar complexes are distinguished in sediments overlying the Maikop Group (aquifers of Maikop sediments are also not considered here): Khazarian ( $Q_2hz$ ), Khvalynian ( $Q_2hv$ ), Bakuan ( $Q_1b$ ), Apsheronian ( $N_2^3ap$ ), Akchaglyian ( $N_2^3ak$ ), Sarmatian ( $N_1^3s$ ), and Karaganian ( $N_1^2k$ ).

### 9.3.1 The Maikop Aquifer

The Maikop section is highly variable both laterally and through the section. Three areas with relatively uniform structure of the section are distinguishable: Peredovye Ranges, eastern, and western parts of the basin.

Outcrops of Maikop sediments are accompanied by discharges of fresh and slightly mineralized waters of the sulfate and, less commonly, chloride-sodium composition. Downward, waters become successively hydrocarbonate-sodium, chloride-magnesian, and chloride-calcic in composition and acquire additional pressure. Particularly high (anomalous) formation pressures are recorded in the Terek-Sunzha zone (up to 210 and 258.6 mPa in the Karabulak-Achaluki field and the Malgobek-Voznesensk area, respectively). Fluid mineralization in these areas varies from 400 to 1,200 mg-equiv/l increasing downward from 521.1 mg-equiv/l at depths of 295–300 m to 1,036 mg-equiv/l at depths of 477–485 m.

The Maikop sequence is most saturated with fluids in the eastern part of the basin, where their mineralization is as high as 803–1,183 mg-equiv/l and they are hydrocarbonate-sodium in composition.

### 9.3.2 The Paleocene–Eocene Aquifer

The aquifer is represented by carbonate and sandy-clayey sediments characterized by significant lateral and vertical lithological-facies variations.

In the Stavropol Arch, the aquifer is largely sandy, while southeastward, it becomes more clayey. The aquifer is saturated with water due to intense fracturing in some intervals of the section. Its outcrops in the Chernye Mountains are accompanied by numerous freshwater springs. The Nal'chik area is marked by springs of mineralized waters. North of outcrops, mineralization increases. In the Mineral'nye



Vody Uplift area, waters with mineralization of 1–25 g/dm<sup>3</sup> are highly variable in composition.

Groundwaters from this aquifer are best studied in the Prikumsk area, where water yield is low and mineralization ranges from 972 to 1,203 mg-equiv/l. In the Karpinsky Ridge area, their mineralization varies from 787 to 1,774 mg-equiv/l.

### ***9.3.3 The Upper Cretaceous Petroliferous Complex***

The Upper Cretaceous petroliferous complex is distributed through the entire basin and is composed of fissured limestones. The Upper Cretaceous sediments outcropping in piedmonts provide numerous springs frequently with the high yield.

Hydrogeodynamics of the complex is influenced by numerous fault zones. For example, fracture waters in the Caucasian Mineral'nye Vody area are confined to such NE-trending fault zones.

The Prikumsk zone of uplifts includes areas of anomalous formation pressures distinguished against the background of the generally dipping potentiometric surface away from the outcropping aquifer.

In the Upper Cretaceous complex, the area of abnormally high formation pressures is substantially larger as compared with that in Lower Cretaceous sediments, being comparable with similar zone in the Jurassic aquifer.

Along the periphery of the petroliferous basin, the Upper Cretaceous sediments contain fresh groundwaters used for economic and drinking purposes. Downward, mineralization of waters increases rapidly to reach 1,382.7, 2,062.5, 1,725.5, and 4,528.5 mg-equiv/l in the Argudan, Zmeisk, Datykh, and Benoi areas, respectively, at a insignificant distance away from outcrop areas.

In most of the eastern Ciscaucasia region, groundwaters from Upper Cretaceous sediments are notably desalinated as compared with their counterparts from Lower Cretaceous formations. In some of its areas (Mineral'nye Vody Uplift, Zol'sk, Argudan, Sovetsks, Otkaznensk, and others), mineralization of subsurface fluids in Upper Cretaceous sediments is higher as compared with that in the Lower Cretaceous aquifer. In other areas, groundwaters in Upper Cretaceous sediments are highly desalinated, which may be explained by the transition of dissolved matter into the solid phase or the influx of solutions with lower mineralization or different chemical composition as compared with in situ fluids. East of the Mineral'nye Vody Uplift, mineralization of groundwaters increases rapidly up to 2,694 mg-equiv/l (Georgievsk area).

The southern part of the eastern Ciscaucasia region is characterized by the wide distribution of chloride-calcic brines with mineralization exceeding 2,000–2,500 mg-equiv/l in Upper Cretaceous sediments. The chemical composition of groundwater is best studied in the Terek-Sunzha area, where mineralization is usually as high as 1,200–1,600 mg-equiv/l, with anomalous concentrations up to 2,930 mg-equiv/l. Subsurface fluids are enriched in iodine (30–40 mg/l) and brome (100–150 mg/l).

In the Prikumsk zone of uplifts, mineralization of subsurface fluids in Upper Cretaceous sediments ranges from 1,050–1,200 to 2,800–2,964 mg-equiv/l in the Zakumsk and Arbala areas, respectively.

### ***9.3.4 The Lower Cretaceous Petroliferous Complex***

The Lower Cretaceous complex is almost universally represented by terrigenous rocks, which are replaced by limestones only in some outcropping members (Valanginian). Famous Narzan springs in the Caucasian Mineral'nye Vody area associate precisely with these limestones. Groundwater in this area is characterized by low mineralization usually up to 0.5 g/dm<sup>3</sup> reaching 1.4–3.1 g/dm<sup>3</sup> in Kislovodsk and 6.2 g/dm<sup>3</sup> in Nal'chik.

In the remainder of the basin, Lower Cretaceous sediments enclose highly mineralized subsurface fluids.

In the Stavropol Arch, most wells are characterized by low yields. Mineralization of subsurface fluids in this area ranges from 1,950 to 2,820 mg-equiv/l. North of the Mineral'nye Vody Uplift, mineralization of fluids from Aptian–Albian sediments increases rapidly up to 2,306 mg-equiv/l (North Nagut area).

In the Prikumsk area, Lower Cretaceous sediments are recovered at depths of 2,400–2,800 m. They contain up to 13 sandy beds separated by thin (3–15) clay members. The elevated formation pressure is recorded only in some wells. Mineralization of subsurface chloride-calcium-sodium fluids varies from 2,316 to 2,868 mg-equiv/l. Microcomponents are represented by Sr, J, Br, Ba, Al, Fe, Mn, and Cu.

In the northern part of the petroliferous basin, fluids of the Lower Cretaceous complex are recovered in the Karpinsky Ridge at a depth of 50 m (Buzga Uplift). The water content in the complex is laterally variable. Fluids are usually highly mineralized (from 2,433 to 4,825 mg-equiv/l), being chloride-calcium-sodium by the composition with the bromine content of 200–300 mg/dm<sup>3</sup>.

### ***9.3.5 The Upper Jurassic Petroliferous Complex***

The Upper Jurassic petroliferous complex is best studied in the Prikumsk area and in the zone of homoclinal dipping of the Caucasian northern slope, where it is largely composed of fractured limestones.

In the southern part of the eastern Ciscaucasia basin, except for the Mineral'nye Vody Uplift, this complex is characterized by wide development of abnormally high formation pressures, which are recorded in the Zhuravsk, Mar'insk, Solomensk, Zamankul, Karabulak-Achaluki, and other areas. In the Prikumsk area, hydrogeodynamic settings are similar to conditions in the Lower–Middle Jurassic petroliferous complex.

Hydrochemical conditions are diverse. In the southern part of the region, subsurface fluids are characterized by highly variable chemical composition and mineralization ranging from 54 to 113 mg-equiv/l. They are distributed in a narrow zone where Upper Jurassic sediments occur relatively close to the surface (Zol'sk, Baksan, Tserikh-Gel, and other areas). Downward, mineralization of fluids in the complex increases rapidly up to 1,155 and 1,978 mg-equiv/l in the Nal'chik and Mar'insk areas, respectively; in the latter area, it reaches even 14,218 mg-equiv/l.

Most part of the eastern Ciscaucasia basin is characterized by chloride-sodium-calcic brines with mineralization exceeding 3,500 mg-equiv/l. Slightly lower mineralization (up to 2,800–3,000 mg-equiv/l) is observed in the Peredovye Ranges, southern Prikumsk area, and between Kayasula, Mekteb, Granichnyi areas, and Kizlyar.

In the Terek-Sunzha anticlinal zone, mineralization of subsurface fluids in the Upper Jurassic sediments ranges from 2,811 to 3,097 mg-equiv/l to increase up to 4279.7 mg-equiv/l in the Karabulak-Achaluki area. The large hydrochemical anomaly is traceable through the Solomensk, Otkaznensk, and Mar'insk areas, where mineralization is maximal, being as high as 10,000–14,218 mg-equiv/l.

Similar to Middle Jurassic sediments, the Upper Jurassic complex of the Prikumsk area is characterized by desalinated fluids.

Thus, against general downward increase in mineralization, subsurface fluids demonstrate different-order hydrogeochemical anomalies (see below).

### ***9.3.6 The Lower–Middle Jurassic Petroliferous Complex***

The complex is best studied in the Prikumsk area, where its sandy varieties contain commercial oil and gas accumulations.

In the southern part of the eastern Ciscaucasia basin, the complex was sampled in western Kabardino-Balkaria, where it is relatively well studied with respect to its hydrogeodynamics. In the remainder of the basin, Lower–Middle Jurassic sediments dip to depths of 4,000–5,000 m and are recovered by occasional deep boreholes.

The practically entire distribution area of the complex in the southern part of the eastern Ciscaucasia basin is referred to as the zone of ascending sedimentary and elision waters [6].

The hydrochemical data available for western Kabardino-Balkaria demonstrate that desalinated composition-variable fluids with mineralization of 100–125 mg-equiv/l are distributed in the Middle Jurassic aquifer in immediate proximity to its outcrops. Downward, mineralization increases rapidly to reach 4,436 mg-equiv/l in the Nal'chik area. By composition, fluids are chloride-sodium-calcic and are attributed to the chlorine-calcic type.

In the Prikumsk and adjacent northern Dagestan areas, hydrochemical conditions in the petroliferous complex are best studied. Mineralization of fluids varies from 2,550–2,663 mg-equiv/l in the Andrei-Kurgan and Zarmut areas to 5,948 mg-equiv/l

in the Nadezhdinskoe area. Local desalination of fluids is registered between the Andrei-Kurgan and Pavlensk areas.

Fluids represent chloride-sodium-calcic, substantially metamorphosed ( $\text{Na/Cl} = 0.75\text{--}0.89$ ) brines of the chlorine-calcic type. They are enriched in iodine ( $5\text{--}23.5 \text{ g/dm}^3$ ), bromine ( $170\text{--}510 \text{ g/dm}^3$ ), boric acid ( $105\text{--}718 \text{ g/dm}^3$ ), and other microcomponents.

In the Prikumsk petroliferous area, mineralization of fluids is locally variable through the section (Novo-Kolodeznaya and other wells). Similar to the Pechora petroliferous basin, older aquifers are characterized by lower mineralization of waters.

### ***9.3.7 The Permian–Triassic Petroliferous Complex***

The aquifer rocks are represented by fractured limestones with different fluid content. No water influx was obtained from some wells. “Dry” wells are frequently located in the immediate proximity to productive wells that yield oil, water, and gas. The highest fluid yield is recorded for wells located in eroded arch areas of anticlines. Toward limbs, the latter decreases. Fluids of Permian–Triassic formations are recovered in the Velichaevsk, Zimnyaya Stavka, Vostochnyi, Russkii Khutor Severnyi, and Russkii Khutor Tsentral’nyi areas.

Locally developed permeable zones are isolated from each other with respect to fluid geodynamics both laterally and through the section. It is conceivable that the vertical fluid exchange between different members exists, nevertheless, via presumable tectonic fractures, which were not crossed by boreholes. Fluids with abnormally high formation pressures, high mineralization, and yield of  $2,500\text{--}3,000 \text{ m}^3/\text{day}$  in Paleocene sediments drilled by Borehole Kulsulin-1 provide probable evidence for such an exchange.

The geological structure influences the distribution of mineralization and formation pressures, in addition to water-bearing zones. Single measurements of formation pressures in the Upper and Lower Triassic sediments of the Velichaevsk and Vostochnyi areas imply hydrodynamic isolation of individual structures from each other.

The characteristic feature of fluids in the Permian petroliferous complex is their slightly lowered mineralization ( $1,238\text{--}3,000 \text{ mg-equiv/l}$ ) as compared with overlying Jurassic and Cretaceous sediments. Moreover, the zone of maximal fluid desalination corresponds substantially with areas of elevated formation pressures (Urozhai, Velichaevsk, and other structures). In these areas, mineralization of subsurface fluids in Permian sediments is 1.5 times lower as compared with that in Triassic and Jurassic sediments.

Thus, (1) main recharge sources for subsurface fluids of petroliferous complexes in the eastern Ciscaucasia basin associate with uplifted areas located along its periphery (Caucasus, Stavropol Arch); (2) the problem of the position of regional and local discharge areas has now no unambiguous solution; and (3) away from

regional recharge areas, decrease in formation pressures (heads) and mineralization of deep fluids are accompanied by changes in their chemical composition. In lower parts of the section, decrease in fluid mineralization associates with the formation of hydrodynamic anomalies.

### 9.4 Influence of Peripheral Parts of the Basin on Fluidodynamics in Deep Petroliferous Complexes

When developing hydrodynamic models of fluid flows, there is no need of taking into consideration density changes through the sedimentary section for most of the aquifers overlying the Maikop Group (Bakuan, Apsheronian, and Akchagylian) since their density varies insignificantly around the value of 1,000 kg/m<sup>3</sup>. For Mesozoic petroliferous complexes, the situation is different.

Within the petroliferous basin, the fluid density varies substantially in all the directions (for example, the Karabulak-Achaluki field, Fig. 9.2), which makes it necessary to calculate reduced formation pressures for Mesozoic petroliferous complexes with the assessment of the reduction error (Chapter 2). In the considered situation, the sea level (altitude) is taken for the reduction (comparison) plane. Table 9.1 presents partial information on measured and reduced formation pressures for some areas of the eastern Ciscaucasia petroliferous basin. It demonstrates substantial variations in measured formation pressures within all the Mesozoic aquifers, which indicates both lateral and vertical heterogeneities of their fields. Therefore, hydrodynamic models were developed with account for the variable density. Flow lines for Mesozoic petroliferous complexes differ slightly from each other depending on their potentiometric surfaces.

S.G. Shagoyants, who studied aquifers overlying the Maikop Group (Bakuan, Apsheronian, Akchagylian, and others), arrived at the conclusion that deep fluids

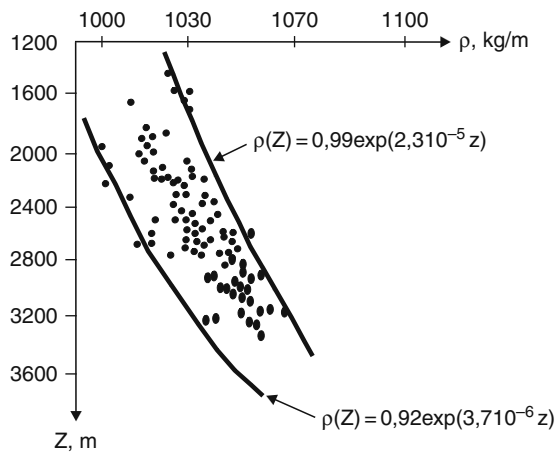


**Fig. 9.2** Correlation between groundwater density and depth in the Karabulak-Achaluki fields (eastern Ciscaucasia) and empirical equations of curves limiting the field of data points

**Table 9.1** Measured formation pressures and reduced heads for some areas of the eastern Ciscaucasia petroliferous basin

Area	Well	Age	Middle of the sampling interval (m)	Altitude of the middle of sampling interval (m)	Formation pressure (mPa)	Reduced pressure (mPa)
1	2	3	4	5	6	7
Andrei-Kurgan	1	K <sub>1</sub>	3,355	3,295	34.9	190
	1	J <sub>2</sub>	3,680	3,620	38.5	225
Arbala	1	K <sub>1</sub>	3,034	30,122	31.4	54
	1	K <sub>2</sub>	2,423	2,422	26.0	140
Aleksandrovskii	1	K <sub>1</sub>	3,340	3,089	36.5	499
	2		3,314	3,063	35.6	436
Arzgir	3	K <sub>1</sub>	2,540	2,436	26.4	165
Arkhangel'skii	1	K <sub>1</sub>	3,923	3,802	38.7	650
Bezvodnyi	29	K <sub>1</sub>	3,132	3,111	30.0	-190
Belaya Mechet	1	K <sub>1</sub>	2,329	1,934	24.9	532
Bezozerskii	1	K <sub>1</sub>	3,357	3,310	33.6	-76
	2		3,368	3,321	39.0	-113
	3		3,370	3,323	34.3	-29
	4		3,374	3,223	34.6	4
	5		2,727	2,678	27.7	-14
	6		2,755	2,682	28.8	100
	4	K <sub>2</sub>	2,544	2,495	28.1	233
Bazhigan	5		2,527	2,478	29.1	319
	3	J <sub>2</sub>	3,550	3,500	35.3	-70
	2	K <sub>1</sub>	3,450	3,400	36.4	145
Vostochno-Sukhokumsk	3	J <sub>2</sub>	3,691	3,686	38.7	43
	4	J <sub>3</sub>	3,573	3,569	37.6	62
Georgievsk	1	K <sub>1</sub>	3,371	3,363	35.8	97
	3	K <sub>1</sub>	3,025	2,967	42.5	1,506
Gaevsk	2	K <sub>1</sub>	2,719	2,590	27.0	66
	2	K <sub>2</sub>	2,550	2,422	24.6	0
Dubovaya Balka	1	K <sub>1</sub>	2,028	1,617	17.1	76
Golubinyi	1	K <sub>1</sub>	2,623	2,465	25.9	86
Dem'yanovka	2	K <sub>1</sub>	3,202	3,017	33.4	264
Essentuki	1-	K <sub>1</sub> -J	1,403	1,403		815
	KMV					
Zimnyaya Stavka	55	K <sub>1</sub>	1,050			803
	6	J	3,436	3,409	35.9	89
Stavka	38		3,235	3,207	34.9	202
	28		3,097	3,068	31.6	22
	10		3,129	3,070	33.2	143
	12		3,080	3,053	30.7	-58
	9		3,107	3,021	32.1	58
	18	K <sub>1</sub>	3,050	3,022	31.5	57
	50		3,097		27.5	182
	19		3,085	3,058	32.4	109
	23		2,837	3,812	22.9	-89
	29		3,063	3,037	31.0	-9

**Table 9.1** (continued)

Area	Well	Age	Middle of the sampling interval (m)	Altitude of the middle of sampling interval (m)	Formation pressure (mPa)	Reduced pressure (mPa)
Zakumsk	1	K <sub>1</sub>	2,242	2,807	39.3	59
Golubinyi	1		2,862	2,613	27.2	63
	2	J	2,900	2,752	29.0	99
	3		2,942	2,793	30.5	216
	2	K <sub>1</sub>	2,565	2,432	26.0	130
	2	K <sub>2</sub>	2,300	1,994	23.3	310
Kolodeznyi	3	K <sub>1</sub>	2,292	1,994	23.3	310
	2	J <sub>2</sub>	3,450	3,405	38.0	265
	5		3,166	3,133	33.4	97
	13		3,164	3,126	35.7	335
	1		3,085	3,085	33.0	120
	2		3,133	3,089	33.4	145
	12		3,125	3,083	33.9	201
	3	K <sub>1</sub>	3,114	3,072	32.9	113
	4		3,112	3,075	32.9	106
	7		2,849	2,809	29.9	92
Kultai	1	J <sub>2</sub>	3,462	3,438	37.3	-109
	5		3,359	3,335	36.0	156
	4	K <sub>1</sub>	3,293	3,268	34.4	71
Kovyl'nyi	5		3,771	3,146	33.6	121
	1		3,370	3,346	34.3	-28
	2	K <sub>1</sub>	3,296	3,271	33.6	-14
Kapievka	4		3,187	3,162	32.7	9
	1		3,644	3,614	37.0	15
	3	K <sub>1</sub>	3,869	3,838	41.5	226
	6		3,873	3,842	40.6	122
Kamyshovyi	9		3,873	3,845	38.8	-61
	1		3,306	297	34.3	34
	3		3,300	3,287	33.7	-20
	5		3,311	3,296	35.1	111
	7	J	3,291	3,276	34.0	21
	8		3,266	3,552	34.9	136
	21		3,283	3,269	34.8	109
	34		3,290	3,271	38.9	51.6
Kumsk	1	J	3,730	3,690	39.1	3
	1	K <sub>1</sub>	2,942	2,901	31.9	160
Kurgan-Amur	2		3,510	3,475	37.1	245
	7		3,520	3,485	35.3	-43
	9	J	3,393	3,360	33.5	-91
	16		3,558	3,502	37.7	180
	1		3,300	3,276	36.0	256
	2	K <sub>1</sub>	3,300	3,265	33.0	-51
	6		3,298	3,263	34.0	61
Kayasulin	3		3,350	3,315	35.5	156
	1	K <sub>1</sub>	3,826	3,676	39.8	209
	1		2,750	2,464	26.8	63

**Table 9.1** (continued)

Area	Well	Age	Middle of the sampling interval (m)	Altitude of the middle of sampling interval (m)	Formation pressure (mPa)	Reduced pressure (mPa)	
Mekteb	2	K <sub>1</sub>	2,889	2,809	28.7	-102	
	3		2,753	2,668	26.3	-197	
	4		2,768	2,690	26.8	-165	
	1	K <sub>2</sub>	2,521	2,440	26.0	11	
	2		2,524	2,440	27.3	179	
	7	J	3,452	3,387	36.3	160	
	10		3,436	3,372	36.1	155	
	6		2,928	2,855	29.6	43	
	7		2,026	2,968	32.5	116	
	8		2,922	2,854	29.9	79	
	9		2,929	2,852	29.8	68	
	Marysh	2	K <sub>1</sub>	2,908	2,845	32.2	32
		4		3,124	3,058	32.6	132
		10		2,884	2,882	30.2	142
18		2,893		2,828	30.0	113	
19		2,896		2,832	30.4	148	
13		2,900		2,838	30.2	122	
14		2,908		2,845	30.0	95	
28		2,881			30.1	102	
1		3,785		3,335	65.5	3,043	
2		3,818		3,368	74.0	3,958	
Nadezhdinsk	3	J	4,253	3,803	77.4	3,843	
	4		4,560	4,010	62.5	2,135	
	5		3,966	3,510	90.5	5,460	
	7		3,832	3,396	67.5	3,279	
	6		3,269	3,247	34.0	71	
Netekum	229	K <sub>1</sub>	3,269	3,247	31.5	-203	
	218		3,270	3,249	35.1	175	
	6		3,157	3,136	30.0	-215	
	7		3,157	3,136	29.5	-276	
	229		3,155	3,135	33.4	120	
	230		3,153	3,132	30.1	198	
	2		3,409	3,359	34.1	-45	
Ozek-Suat	4	K <sub>1</sub>	3,410	3,360	34.1	-46	
	5		3,408	3,359	34.1	-45	
	6		3,423	3,371	35.5	81	
	13		3,364	3,013	31.4	51	
	32		3,447	3,413	35.5	45	
	5		3,402	3,370	mouth, 60	92	
Otkaznensk	29	J	3,224	3,189	mouth, 9	124	
	30		3,189	3,160	mouth, 9.1	119	
	43		3,209	3,179	mouth, 8.2	112	
	3		2,325	2,593	mouth, 3	62	
	37		3,149	3,115	mouth, 15	182	
	4		3,223	3,188	33.1	45	
	5		3,495	3,299	36.7	300	



**Table 9.1** (continued)

Area	Well	Age	Middle of the sampling interval (m)	Altitude of the middle of sampling interval (m)	Formation pressure (mPa)	Reduced pressure (mPa)
Praskovei	16	K <sub>1</sub>	3,540	3,326	35.5	144
	6		3,460	3,302	36.3	249
	20		3,100	2,950	32.7	257
	23		3,650	3,436	37.9	268
	26		3,100	2,950	31.5	137
	5		2,850	2,367	30.8	666
	3		2,474	2,323	29.8	616
	4		2,485	2,392	32.0	766
	10		2,412	2,267	30.3	723
	13		2,445	2,323	26.7	306
	14	2,664	2,570	39.2	302	
	21	J	2,668	2,449	30.9	593
	27		2,517	2,419	32.0	738
	22		2,572	2,437	30.0	517
	40		2,484	2,358	30.3	634
	44		2,555	2,379	31.3	706
39	2,580		2,430	27.2	247	
Plavensk	69	K <sub>1</sub>	3,088	3,074	32.5	86
Primanych	1	K <sub>1</sub>	2,961	2,973	31.9	183
Pravokumsk	10	K <sub>1</sub>	2,961	2,973	31.9	183
	1		2,754	2,467	32.3	529

discharge “by gradual secular migration of confined waters upward through the clayey roof of the aquifer.”

The groundwater level serves as a drainage basis for all the confined waters of aquifers. “Closer to the sea basin, its level becomes a drainage basis instead of groundwaters.”

This inference is based on the analysis of the potentiometric surface, which is characterized by gradual changes in the groundwater head within aquifers overlying Maikop sediments and gradual replacement of hydrocarbonate solution by the chloride one with the simultaneous increase of its mineralization. It is difficult to argue against this inference on the discharge type. It is supported by our original and published data based on the quantitative analysis of changes in unit groundwater expenditures along the flow line and modeling.

It is established that deep fluids of the Upper Cretaceous petroliferous complex discharge both at the surface (into the river and erosion networks) and in the zone of their dipping in development areas of laccoliths and along tectonic fractures, i.e., it is affirmed and confirmed that deep fluid may partially discharge in the immediate proximity to regional recharge centers of Mesozoic sediments.

With respect to the formation mechanism and position of regional discharge centers of confined fluids of the Lower Quaternary and Apsheronian aquifers,

the subsequent work [2] is of undoubted interest. Based on modeling, this author quantitatively assessed the discharge of confined waters.

According to these studies, 92–97% of the total fluids formed in regional recharge areas (marginal parts of the basin) discharge on land through the entire distribution area of aquifers by migrating first into overlying and then groundwater aquifers. Moreover, this work also demonstrates that the most intense discharge occurs in the immediate proximity to regional recharge centers of deep subsurface fluids.

Kortsenshtein [9] admits hydrogeological role of tectonic dislocations, “which disrupt partly or completely continuity of the groundwater flow and may unite different-age aquifers.” He precisely explains some hydrochemical anomalies in Lower Paleogene sediments by development of faults. He defines regional recharge (Greater Caucasus ranges, which is accepted by most researchers), flow, and discharge centers. The flow area begins at the northern boundary marking submergence of Mesozoic strata under the Cenozoic cover and extends through the entire basin. The regional discharge corresponds to the fault zone along the Caspian Sea bottom, while the local discharge occurs through facies windows and tectonic fractures located north of the Manych Trough.

Thus, Kortsenshtein’s views reflect classical concepts of the regional movement of deep fluids, spatial position of regional recharge and discharge centers, presumable lateral movement of deep fluids over long distances, and difficult water exchange between petroliferous complexes. In his opinion, only the Jurassic petroliferous complex is reliably isolated, in terms of fluidodynamics, from overlying aquifers.

This standpoint is shared, sometimes with significant reservations, by many researchers who were dealing with the eastern Ciscaucasia hydrogeology (e.g., [7, 12]).

The Karpinsky Ridge is unanimously considered to represent the discharge area of Mesozoic fluids. Some researchers assume that brines migrating from the North Caspian depression also discharge in this area. Both viewpoints are based on the quantitative analysis of hydrochemical data on groundwater from Pleistocene and Upper Pliocene sediments, which demonstrate well-developed hydrochemical anomalies in the Buzga Uplift of the buried Karpinsky Ridge.

To assess the influence of the current infiltration recharge, the hydrodynamic maps (orthogonal grid of flow lines and hydroisohypses) were compiled for the following aquifers: Bakuan, Apsheronian, Akchagylian, Lower Cretaceous, and Upper Cretaceous.

Let us consider some of them to exemplify the role of regional recharge and discharge centers in the formation of underground fluids in inner areas of petroliferous basins.

This procedure was realized through the analysis of changes in lateral unit expenditures, reduced pressures (levels), or gradients of deep fluids along flow lines (Chapter 2).

Such an analysis is difficult for Mesozoic petroliferous complexes due to insufficient reliability or lack of initial information on areas adjacent to regional recharge

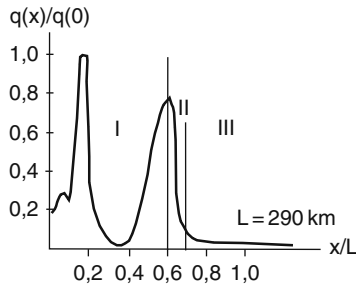


**Fig. 9.3** Variations in the lateral groundwater unit expenditure along the flow line in the Baku aquifer of the eastern Ciscaucasia petroliferous basin.  $L$ , Integral length of the flow line;  $q(0)$ , unit expenditure in the infiltration recharge area;  $q(x)$ , the same at a distance  $x$  from the recharge area; (I, II, III) hydrodynamic zones of intense, slow, and very slow water exchange, respectively

centers (for example, no information is available on filtration properties of rocks). Therefore, it was performed for all the aquifers provided with necessary data, the deepest aquifers overlying Maikop sediments included.

Figure 9.3 illustrates reduction of unit expenditures along one of the flow lines in the *Bakuan aquifer*, which represents the uppermost confined bed of the regional distribution.

The figure shows that the latter varies significantly, due to local drainage and recharge bases, in the band adjacent to the regional recharge center. The expenditure either decreases (discharge) or increases (local recharge). Such a situation is observed at a distance of approximately 170 km (intense water-exchange zone). This is followed by directed reduction of lateral expenditures, which results in the complete discharge of groundwaters from the Baku Horizon into overlying sediments by the flow (head in overlying groundwater and low-head aquifers is lower as compared with that in underlying formations) for a distance of 30–40 km (approximately 210 km away from rock outcrops). This is a zone of slow water exchange, which is practically lacking the solution influx from the external boundary.

Figure 9.4 illustrating changes in the lateral unit expenditure (a) and groundwater gradients (b) along the same flow line shows that the *Akchagylian aquifer* is characterized by practically coinciding boundaries between hydrodynamic zones and different extreme values of gradients and expenditures. Therefore, plots illustrating changes in lateral gradients along flow lines may be used for assessing the role of the basin periphery as an area of infiltration recharge and defining boundaries of hydrodynamic zones.

Three hydrodynamic zones are distinguishable in this complex. The first zone (I) with distinct changes in the expenditure (recharge and discharge along the flow line) is up to 100 km wide. Its potentiometric surface is formed under the influence of surface factors (relief, infiltration, river network). In the plot, the segment corresponding to this zone is characterized by significant variations in lateral gradients and expenditures of groundwaters.

The second zone is approximately 60 m wide. In this zone, groundwater formed in regional and local recharge centers discharges in the form of areal flow into

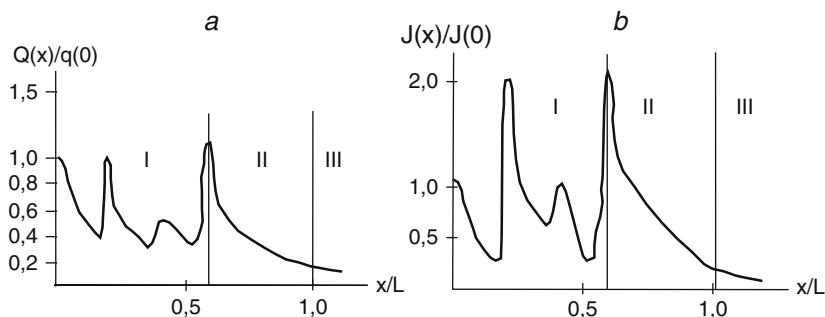


**Fig. 9.4** Variations in the lateral groundwater unit expenditure (a) and gradients of reduced pressures (b) along the flow line in the Akchagylian aquifer of the eastern Ciscaucasia petroliferous basin. For legend, see Fig. 9.3

overlying formations almost entirely at a distance of 160 km. The zone of very slow water exchange receives no infiltration recharge from any studied petroliferous complexes of the Greater Caucasus piedmonts, i.e., the formation of groundwater is independent of surface factors (intensity of infiltration recharge, draining influence of the river network).

The gradual decrease in lateral gradients and fluid expenditures occurs in the zone of slow water exchange (Fig. 9.4, zone II) 60–70 km wide. This zone shows no significant variations in gradients and expenditures, which is explained by decelerated underground migration into overlying formations.

Zone III (Fig. 9.4) is characterized by  $q(x)/q(0) < 10\%$ . For comparison of data on sedimentary sections, flow bands in compiled potentiometric maps of Mesozoic sediments are outlined in the same areas of the basin (three flow lines for each petroliferous ring complex).

The analysis of changes in gradients of the reduced level along the flow line reveals three hydrodynamic zones in the *Upper Cretaceous petroliferous complex* (Fig. 9.5, Profile I–I). The flow line is confined to the Chernyi Les Trough and the Stavropol Arch.

The conditionally defined zone of intense water exchange is reflected vaguely at the working scale (1:5,00,000). Nevertheless, in the area approximately 200 km long, where the Upper Cretaceous petroliferous complex is exposed, its potentiometric levels are formed under the influence of surface factors. Beyond this area, the complex dips rapidly. The zone of slow water exchange is defined in the relatively small area of width 15 km, where groundwater pressures in the Upper Cretaceous petroliferous complex decrease in parallel with its dipping (Fig. 9.5, Profile I–I).

The zone of slow water exchange occupies most of the Upper Cretaceous aquifer distribution area. Inasmuch as the complex dips quickly, the influence of peripheral areas on the formation of groundwaters in deep formations is negligible. In this zone, they are formed under the influence of inner processes, primarily geodynamics included. The zone is characterized by various anomalies: hydrodynamic, hydrochemical, gas, thermal, and others.

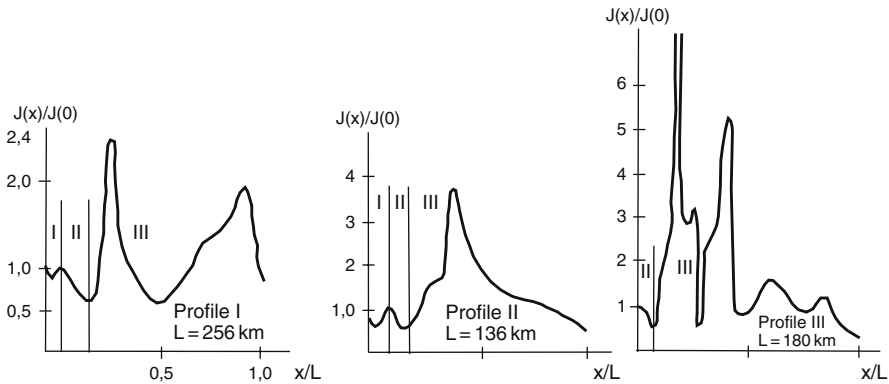


**Fig. 9.5** Variations in gradients of reduced pressures along the flow line in the Upper Cretaceous aquifer of the eastern Ciscaucasia petroliferous basin. For legend, see Fig. 9.3

Along the flow line (Fig. 9.5, Profile II–II) that crosses the Mineral'nye Vody Uplift in the Caucasian Mineral Waters (CMW) area to follow further across the Chernyi Les Trough, the zone of intense water exchange is also vaguely outlined. This is explained by the large-scale studies and insufficient measurements of formation pressures in the area adjacent to the discharge area. The zone is approximately 26 km wide. The zone of slow water exchange is defined in the CMW area, where the groundwater flow is highly variable under the influence of surface factors due to the shallow position of the Upper Cretaceous petroliferous complex.

The zone of very slow water exchange is developed almost universally and corresponds to rapidly dipping Upper Cretaceous rocks.

The flow that crosses anomalous hydrodynamic zones such as the Terek-Sunzha zone of uplifts, the Terek-Caspian Trough, and the Arzgir-Prikumsk zone of uplifts (Fig. 9.5, Profile III–III) demonstrates some peculiarities in changes of fluid pressure gradients.

This area is characterized by the most rapid subsidence of the petroliferous complex, abnormally high formation pressures, and other anomalies. With respect to tectonics, this is the most active area of the eastern Ciscaucasia basin with recent tectonic movements (Terek-Sunzha region) [1].

Even zone of slow water exchange in this area extending for approximately 12 km is indistinct in the plot. The zone of intense water exchange is developed practically through the entire region. It is characterized by most abrupt changes in gradients of reduced pressures. Their measured values are so high that curves in the plot should be broken. As was mentioned, this is explained by the block tectonic structure of the Terek-Sunzha region and the isolation of blocks from each other (Fig. 9.1).

In the Prikumsk zone of uplifts, extreme values of pressures decrease due to larger scale of tectonic heterogeneity in platform environments.

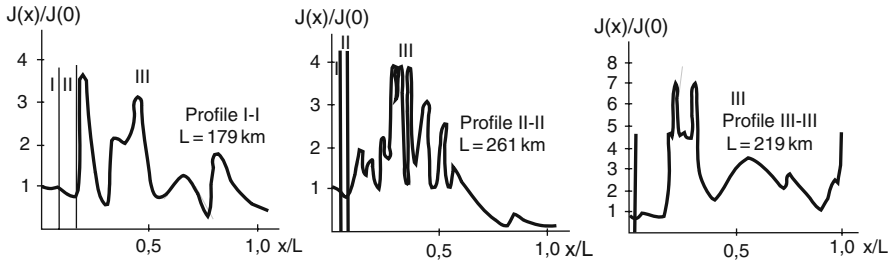


**Fig. 9.6** Variations in gradients of reduced pressures along the flow line in the Lower Cretaceous aquifer of the eastern Ciscaucasia petroliferous basin. For legend, see Fig. 9.3

For the *Lower Cretaceous petroliferous complex*, the analysis was based on changes in gradients of reduced values along flow lines (Fig. 9.6).

All three zones are defined along Profile I–I which crosses the western Mineral'nye Vody Uplift. Similar to the Upper Cretaceous petroliferous complexes, the first and second zones are defined conditionally due to insufficient information on piedmonts and elevated areas of the basin. The zones of intense and slow water exchange extend for 15 and 20 km away from the Glavnii Caucasian Range, respectively. The remainder of the basin is occupied by the zone of very slow water exchange.

As compared with the Upper Cretaceous complex, the Lower Cretaceous one is characterized in the area under consideration by higher measured values of extreme gradients as well as their higher contrast and recurrence (occurrence frequency).

Along Profile II–II (Fig. 9.6), the zone of very slow water exchange (III) is definable at a distance of 18 km away from the regional development center of formation pressures (recharge center) and characterized by very frequent extreme values of its gradients. Spatially, this zone corresponds to the Terek-Caspian Trough with abnormally high formation pressures and Mineral'nye Vody Uplift. In the Arzgir-Prikumsk zone of uplifts, the gradient values decrease and the curve is characterized by gentler patterns. Zones I and II are defined conditionally along this profile, which is explained by rapid subsidence of the petroliferous complex under the Terek-Caspian Trough.

Practically a single zone of slow water exchange is definable along Profile III–III (Fig. 9.6) that crosses the Terek-Sunzha and eastern Prikumsk areas, which is also explained by rapid subsidence of the complex. As compared with the Upper Cretaceous aquifer, absolute extremum values in this zone are lower and less contrasting.

*The Jurassic petroliferous complex.* Inasmuch as this petroliferous complex is less studied in the lower part of the basin as compared with overlying formations, it is difficult to estimate the role of peripheral parts of the basin in the formation of groundwaters. In addition, the complex dips most rapidly in piedmonts.

The zone of intense water exchange (I) is indefinable at all in plots (Fig. 9.7). The zone of slow water exchange 3–7 km wide is also established conditionally along profiles II–II and III–III. In Profile I–I that crosses the East Kuban Depression,

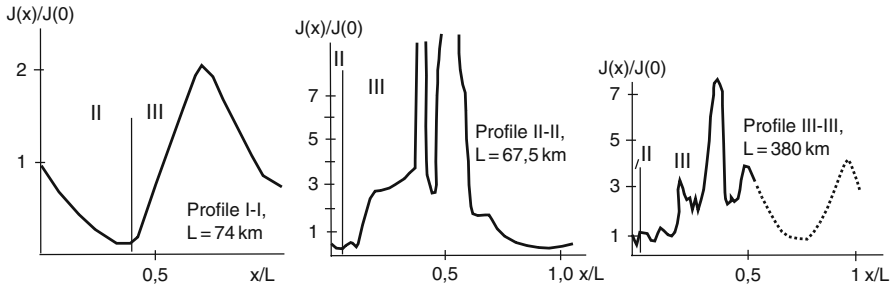


**Fig. 9.7** Variations in gradients of reduced pressures along the flow band in the Jurassic aquifer of the eastern Ciscaucasia petroliferous basin. For legend, see Fig. 9.3

zone II is distinguished at a distance of 30 km, which is explained by insufficient measurements of potentiometric levels (formation pressures).

The zone of very slow water exchange (III) is best developed along Profile III–III, which crosses the Terek-Sunzha and Prikumsk areas. The Terek-Caspian Trough, which is characterized by highest values of formation pressures in the Jurassic petroliferous complex, is readily recognizable along Profile II–II.

Based on the above-mentioned data, it should be noted that the width of the zone, where groundwater that is formed in regional recharge centers discharges completely, depends largely on the geological structure of petroliferous basin margins. It is narrower in areas with the transgressive occurrence of sediments, where water-bearing formations are overlain by other, particularly clayey rocks. The deeper the petroliferous complexes, the less developed the zone, which is influenced by surface factors, such as, primarily, infiltration recharge. Similar situation is observed in the West Siberian petroliferous basin as well.

Practically the entire territory of the eastern Ciscaucasia petroliferous basin occupied by Mesozoic sediments (except for a narrow band along piedmonts) represents a hydrodynamic zone of very slow water exchange characteristic of its subsided and uplifted areas. The influence of marginal parts of the basin or so-called regional recharge centers is lacking. In these areas, recharge and migration of deep fluids are determined by tectonics, geodynamics, internal structure of the region, and basement waters.

The more detailed the study and the more wider the information on both the basin as a whole and its separate parts, the better definable the blocks that make petroliferous complexes (horizons) autonomous. In the block limits, the flow is local. Ascending filtration represents a main migration path of deep fluids and the lower boundary of the sedimentary cover serves as the recharge source.

This zone is characterized by different anomalies: hydrochemical, hydrodynamic, gas, mineralogical, geochemical, and others.

The analysis of changes in both expenditures and gradients of reduced pressures is most suitable and reliable for assessing the influence of peripheral areas of petroliferous basins, the eastern Ciscaucasia one included, on the formation of

deep fluids. The comparison of data on the Akchagylian aquifer (Fig. 9.4) shows that hydrodynamic zones almost correspond to each other in both cases; only their absolute extreme values are different.

The small scale of studies and the lack of quantitative data on potentiometric level in the Mesozoic complexes of petroliferous basin mountainous and piedmont parts are responsible for conditional character of zones of intense and slow water exchange defined along all the flow bands.

## 9.5 Influence of Elision Recharge on the Formation of Deep Fluid Pressures

A.A. Kartsev, S. B. Vagin, and many other researchers believe that elision processes play significant role in the development of formation pressures. Paleohydrological maps are compiled for the Lower–Middle Jurassic, Lower, and Upper Cretaceous petroliferous complexes of this region with outlining sedimentation (elision) and infiltration stages. In these maps, deep fluids are shown migrating from most subsided areas of the petroliferous basin toward its peripheral parts. This scenario is shared by all the researchers.

I.G. Kissin notes also important role of clayey rocks in the origin of formation pressures. In his work [7], this author explains abnormally high formation pressures in the Terek-Sunzha area by gravitational compaction of clayey sediments. In this connection, he considers the last area as a hydraulic barrier, which is rounded by the flow of deep fluids that move from the south north- and northeastward to discharge in the Karpinsky Ridge area and presumably along faults at the boundary between the Precambrian and the epi-Hercynian platforms.

Some researchers (A.A. Klimenko, A.S. Panchenko, A.S. Danov, A.I. Polivanova, M.A. Miroshnikov, and others) believe that the true elision water exchange or its residual processes are now “observable close to present-day infiltration areas being expressed in the form of ‘domes’ of the potentiometric surface, zones with elevated pressures, and local changes in directions of deep flow movement.”

Later, many other researchers (I.N. Egorova, N.I. Popov, G.P. Yakobson, V.I. Ryabenko, P.I. Bloschitsyn, K.I. Vorob’eva, M.V. Miroshnikov, and many others) arrived at the same conclusion.

Taking into consideration the attention that is paid to elision processes, which are considered to determine formation pressures and development of hydrocarbon accumulations in most subsided parts of the eastern Ciscaucasia petroliferous basin (in the zone of very slow water exchange), we carried out the quantitative assessment of their influence on the formation pressures using modeling with solution of the flat surface task.

Hydrogeological conditions were schematized in the following manner. The substantially clayey Maikop sequence is overlain by alternating clayey and sandy



sediments of Neogene and Quaternary ages. This complex sequence encloses several aquifers and water-bearing horizons separated from each other by clayey sediments of different thickness and distribution.

In connection with the purpose of these studies, only the Apsheronian aquifer was examined. All the over- and underlying formations [aquifers (petroliferous complexes) included] were considered as clayey sediments, which isolated to some extent the Apsheronian aquifer from the surface, on the one hand, and represented an additional elision recharge source of subsurface fluids, on the other hand. Such a problem statement increases the probability of revealing anomalous formation pressures and the reversed movement of subsurface fluids (toward outcrop areas), i.e., the results should confirm important role of the elision component in the recharge of deep fluids.

The assessment of released interstitial solutions was performed for the most subsided portion of the section, where the thickness of sediments is maximal. Moreover, the latitudinal cross section (from the Stavropol Uplift to the Caspian Sea) was extrapolated to the middle of the sea; therefore, the thickness of all the pre-Apsheronian (Maikopian sequence included) and post-Apsheronian sediments increased to 4.6 km and 900 m, respectively, with respective bases located at depths of 6.4 and 0.9 km.

The quantity of released interstitial solutions was calculated using the curve of natural clayey rock compacting in the eastern Ciscaucasia region [11] and the dependence proposed in [10].

According to calculations, 2,300, 488, and 300 m<sup>3</sup>/m<sup>2</sup> of interstitial solutions were released from pre-Apsheronian sediments during the periods corresponding to the Maikopian Clay accumulation, Apsheronian Age, and post-Apsheronian time, respectively.

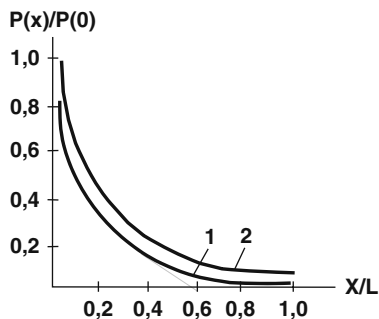
The post-Apsheronian sediments released 200 m<sup>3</sup>/m<sup>2</sup> of interstitial solutions.

Thus, the integral volume of released interstitial solutions amounts to 3,300 m<sup>3</sup>/m<sup>2</sup> or  $1.32 \cdot 10^{-4}$  m<sup>3</sup>/year per m<sup>2</sup> or 5.6 m<sup>3</sup>/year for the entire length of the examined section (425 km).

Of the integral volume of interstitial solutions, 2,800 m<sup>3</sup>/m<sup>2</sup> returned back to the sedimentary basin and into outcropping Apsheronian sediments. To account for this fact, the volume of released interstitial solution returned into the Apsheronian aquifer should be as high as 0.85 m<sup>3</sup>/year (it is accepted that released interstitial waters from underlying and overlying sediments migrate only upward and downward, respectively).

The current groundwater expenditure in the recharge area of the Apsheronian aquifer was quantified proceeding from the following. According to minimal estimates, the transmissibility of the aquifer varies from 400 to 600 m<sup>2</sup>/day in areas adjacent to regional recharge centers decreasing gradually toward the plain part of the basin, where it amounts to 100–200 m<sup>2</sup>/day. The groundwater head gradients in recharge areas range from 0.03 to 0.04 [2]. The expenditure of the subsurface flow per 1 m of its width is 15 m<sup>3</sup>/day under average transmissibility of 500 m<sup>2</sup>/day and gradient of 0.03.

**Fig. 9.8** The modeled distribution of groundwater formation pressures in the Apsheronian aquifer. (1) With account for infiltration recharge; (2) with account for infiltration and elision recharge



Thus, the ratio of the expenditure of the natural (infiltration) groundwater flow to that of the elision recharge is 980 and 6,500 with the elision recharge volume being equal to 5.6 and 0.85 m<sup>3</sup>/year, respectively (or 0.015 and 0.02 m<sup>3</sup>/day).

In the model, transmissibility of Apsheronian sediments was accepted as linearly changing from 500 to 30 m<sup>2</sup>/day in the most remote point (Caspian Sea). The additional recharge from clayey sediments was provided when accumulation of recent sediments terminated (i.e., for 25 Ma). Moreover, the entire additional recharge and its part that entered the Apsheronian aquifer were increased 100 and 650 times, respectively, for their reflection in changes of heads (pressures). Figure 9.8 presents the results of modeling.

As follows from the figure, such a high voluntary increased recharge from clays (550 m<sup>3</sup>/year for the entire length of the section or 3,24,000 m<sup>3</sup>/m<sup>2</sup> for the entire period since the formation of Maikopian sediments) resulted in insignificant changes in heads (pressures) of groundwater (Curve 2) relative to the distribution of heads without the elision recharge (Curve 1).

Thus, similar to the West Siberian petroliferous basin, the contribution of elision the formation pressures at deep levels is negligible. The role of these processes may be notable only under complete isolation of the particular part of the section.

## 9.6 Local Fluidodynamics in Individual Structures of the Basin

Let us consider local fluidodynamic peculiarities in well-studied structures of the Terek-Sunzha Uplift in the eastern Ciscaucasia region characterized by the development of abnormally high formation pressures. Variations in the reduced levels (hereinafter, the sea level is accepted as the comparison plane) between separate parts of structures amount to hundreds and thousands of meters (Fig. 9.1). In the Malgobek-Voznesensk, Goryachii Istochnik, and Khayan-Kote structures, reduced levels vary from 270 to 540, in the range of 2,000, and from 200 to 500 m, respectively.

Even more contrasting patterns are observed in disturbed conditions, where the isolated position of some blocks and structures proper is more distinct.

The long exploitation of wells in the Malgobek-Voznesensk structure demonstrated that wells in different blocks separated by tectonic fractures (wells are located 0.8–2.0 km away from each other) are hydrodynamically autonomous. At the same time, wells located along the fault at larger distances from each other are interconnected with respect to hydrodynamics. It is noteworthy that faults crossing this structure are active; according to high-accuracy repeated leveling, they are marked by the vertical displacement of blocks, which amounts to 13–20 mm during 8 months (A.T. Donabedov).

Figures 9.1 and 9.9 illustrate the distinct block structure of the Terek-Sunzha Uplift.

The Prikumsk zone of uplifts with relatively calm tectonic settings and low-amplitude fractures (lower as compared with the thickness of productive formations) is characterized by similar situation: lack of dynamic interaction between fluids of individual uplifts, i.e., their hydrodynamic isolation (Fig. 9.9). Gradients of reduced levels between individual structures average 100–200 m reaching >100 m in the Kolodeznaya-Velichavskaya and >500 m in the Velichavskaya-Pravoberezhnaya structures. In the relatively small Prikumsk zone of uplifts, gradients of reduced levels exceed 700 m.

In addition, hydrodynamic sampling reveals no interaction between seven pairs of wells in the Achaluki structure, between two pairs of wells in the Velichavskaya and Pravoberezhnaya structures, and between three pairs of wells in the Vostochno-Bezvodnaya and Pravoberezhnaya structures.

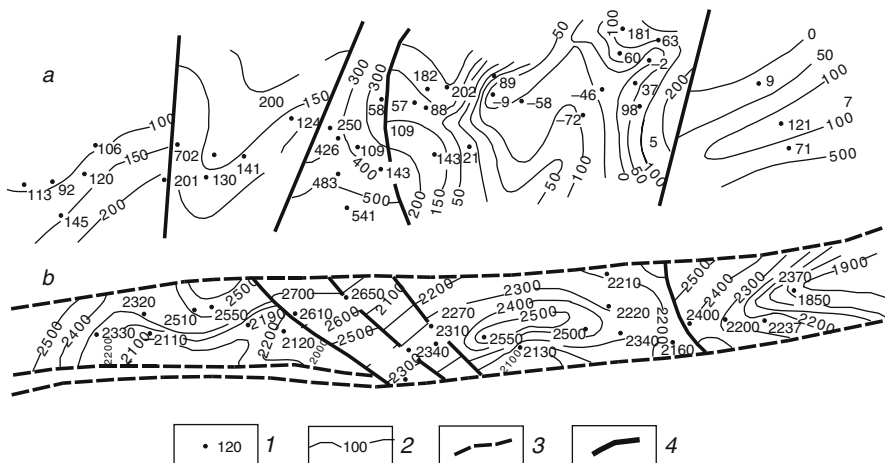


**Fig. 9.9** Schematic maps of the potentiometric surface. (a) Lower Cretaceous sediments of the Prikumsk zone of uplifts; (b) Upper Cretaceous sediments of the Terek-Sunzha zone of uplifts; (1) borehole and altitude of the reduced level (m); (2) piezoisohypses (altitude) (m); (3) tectonic fractures established by geophysical methods; (4) the same established by the hydrodynamic method

The exploitation of wells in the Russkii Khutor (Tsentral'nyi) field demonstrated that even low-amplitude faults might sometimes serve as reliable screens and influence development of fields (Yu.A. Sterlenko). This inference is derived from the following observations. Well 26 exploited Bed VIII<sub>1</sub> that contacts Bed VIII<sub>2</sub> along the normal fault. After the exploitation commencement (1968), the content of oil decreased gradually, while that of gas and water increased from 70 t/day, 450 m<sup>3</sup>/day, and 7% to 8 t/day, 2,600 m<sup>3</sup>/day, and 50%, respectively. In March 1978 (63 months later), concentration of oil and condensate increased abruptly to 28 t/day, while that of water decreased up to 4%. Long exploitation resulted in the development of the critical gradient in formation pressures, the hydraulic fracturing in the fault zone, and the migration of fluids from Bed VIII<sub>2</sub> into Bed VIII<sub>1</sub>.

The hydrodynamic isolation of separate blocks is also observed sometimes through the section. For example, in Upper Cretaceous sections, formation pressures in natural and distorted conditions are by several mPa lower as compared with that in terrigenous Lower Cretaceous sediments. Relative to overlying Lower Paleocene strata, reduced formation pressures differ (sometimes substantially) as well. The vertical gradients between blocks are also high amounting locally to 4.

Thus, the area relatively calm with respect to tectonics is also characterized by significant differences in potentiometric levels (pressures) between strictures and their separate parts, which indicate their hydrodynamic isolation from each other in the horizontal plane and block structure of deep horizons.

Let us consider the results of interval-by-interval sampling through the Lower and Upper Cretaceous aquifer of the Sovetskii area, which reflect the distribution of formation pressures in the vertical section.

In this area, Upper Cretaceous sediments recovered by Borehole 1 are sampled through the entire section. It is established that potentiometric heads (formation) of groundwater decrease gradually upward from +1,323.5 m at a depth of 3,074 m to 623.5 m at a depth of 3,262 m. At the base of the section, the pressure becomes practically equal to that observed at the roof of Lower Cretaceous strata and then grows gradually upward to reach +2,298 m in Neocomian sediments, i.e., substantially exceeds values characteristic of uppermost Cretaceous layers. This indicates the development of the piezominimum in these sediments.

Figure 9.10 illustrating the distribution of reduced heads (pressures) through sections shows that the latter is irregular with distinct anomalies in some of them. It should be noted, however, that it is not quite correct to compile maps for deep horizons in isolines without accounting for different genesis of boundaries when they are characterized by the stratum-block structure. Inasmuch as many researchers are skeptical relative to the method of formation pressure reducing, we used the method of the filtration force calculation proposed in [3] for assessing probable movement directions of deep fluids in the Upper Cretaceous petroliferous complex. The calculation was performed for both entire petroliferous basin and its separate areas. Figure 9.11 demonstrates the horizontal component of the filtration force calculated for the Terek-Sunzha region. It is evident that the distribution of filtration force horizontal vectors is characterized by chaotic patterns, implying possible lateral movement of deep fluids through the entire region under consideration

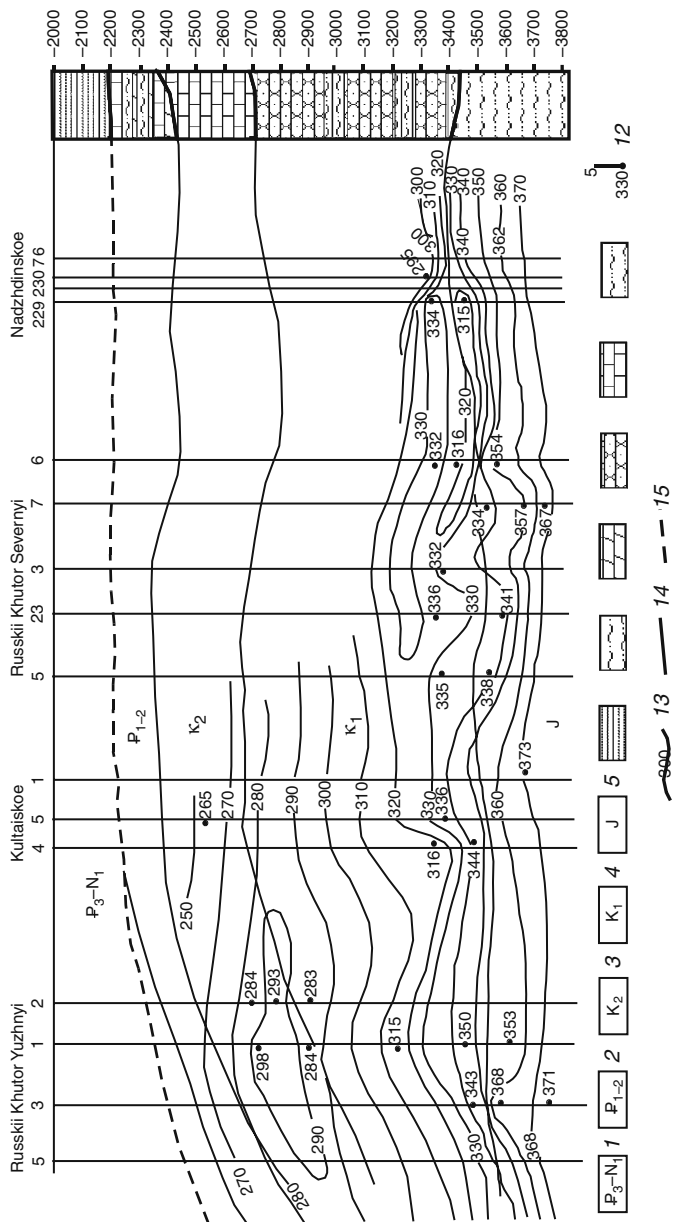


**Fig. 9.10** Schematic hydrogeological cross section along the profile Russkii Khutor Nadzhinskoe (eastern Ciscaucasia petroliferous basin). (1) Upper Cretaceous–Lower Neogene aquifer; (2–5) aquifers; (2) Lower–Middle Paleogene, (3) Upper Cretaceous, (4) Lower Cretaceous, (5) Jurassic; (6) clay; (7) siltstone; (8) marl; (9) sandstone; (10) limestone; (11) sandy-siltstone; (12) borehole number (5) and measured formation pressure, atm (330); (13) isolines of equal formation pressures; (14) boundaries of aquifers; (15) conditional boundary of the aquifer

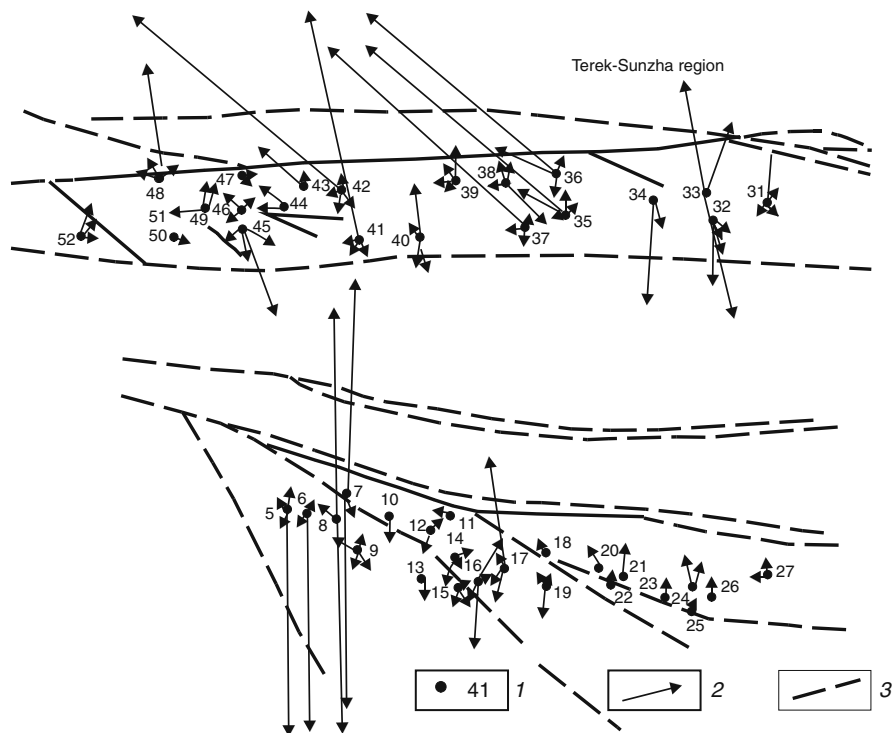


**Fig. 9.11** Vectors of the horizontal component of the filtration force measured for eastern Ciscaucasia structures. (1) Borehole and its number; (2) vector of the horizontal component of the filtration force; (3) tectonic fracture

(the length of vectors corresponds approximately to the filtration force value). This picture has nothing to do with real situation (Fig. 9.9), since it ignores numerous high-amplitude tectonic fractures comparable with the thickness of petroliferous complexes (Fig. 9.1). In addition, automatic calculation by this method selects for the point in question several combinations of three nearest points, which introduce substantial uncertainty into the calculated filtration force. At the same time, calculations of the filtration force also show lack of regional flows and development of local flows in small areas.

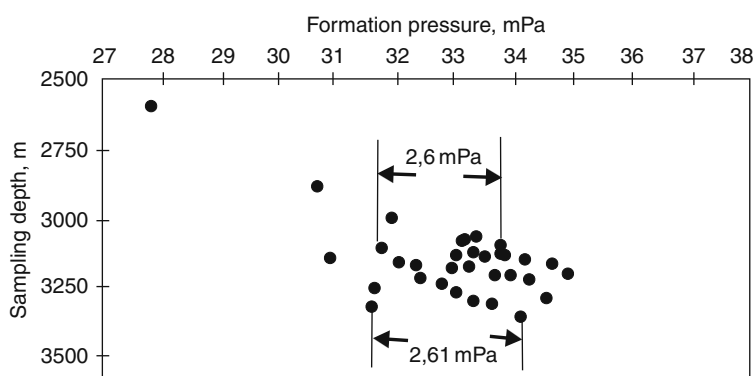
The distribution of measured formation pressures and reduced levels may be exemplified by several well-studied structures.

### 9.6.1 The *Russkii Khutor Severnyi* Settlement

Table 9.2 presents formation and reduced pressures in this area. Figure 9.12 illustrating the distribution of measured formation pressures at deep levels shows that they vary from 2.35 to 2.61 mPa. Figure 9.13 demonstrates directions of horizontal gradients between reduced formation pressures and pressures measured at equal

**Table 9.2** Measured and reduced formation pressures in Lower Cretaceous sediments (Russkii Khutor Severnyi)

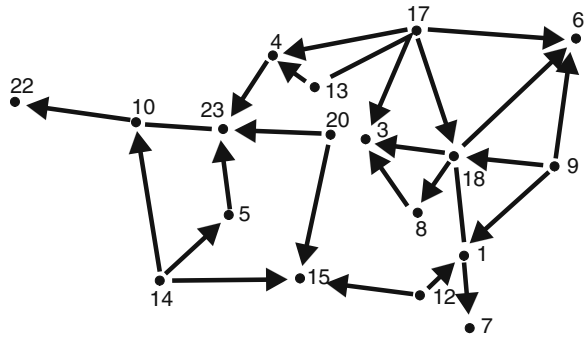
Borehole	Middle of the sampling interval (m)	Altitude of the middle of the sampling interval (m)	Measured pressure (mPa)	Reduced pressure (mPa)
1	3,173	3,156	33.3	74
3	3,163	3,144	33.2	33
4	3,264	3,245	34.16	66
5	3,163	3,150	33.5	101
6	3,184	3,168	33.24	56
7	3,277	3,259	36.0	234
8	3,180	3,162	33.39	76
9	3,211	3,193	34.9	195
10	3,180	3,160	34.2	160
12	3,200	3,181	33.65	83
13	3,191	3,173	34.03	129
14	3,196	3,173	34.66	192
15	3,207	3,187	33.62	73
16	3,123	3,110	33.65	158
17	3,178	3,159	34.1	151
18	3,207	3,190	34.1	118
20	2,610	2,590	27.83	126
22	3,161	3,139	33.82	144
23	3,193	3,183	33.12	28
24	3,129	3,105	33.12	110

**Fig. 9.12** Difference between formation pressures measured at similar depths. Russkii Khutor Severnyi, eastern Ciscaucasia

depths. It follows from the latter that the area under consideration is characterized by differently directed lateral gradients of formation pressures.

Similar to formation pressures, the hydrochemical field is also heterogeneous. Table 9.3 presents analytical results of the hydrochemical study in this area prior

**Fig. 9.13** Lateral gradients of reduced pressures. Russkii Khutor Severnyi, eastern Ciscaucasia



to its exploitation. Horizontal gradients between Cl and Br contents at close depths are shown in Figs. 9.14 and 9.15. Both figures and tables demonstrate significant heterogeneity of the hydrochemical field. For example, Ca, sulfate ion, and hydrocarbonate ion contents range between 0.49 and 7.7, 0.025 and 0.47, and 0.13 and 8.1 g/dm<sup>3</sup>, respectively. The difference between minimal and maximal Br contents is more than two times: 145 and 351 mg/dm<sup>3</sup>.

### 9.6.2 The Zapadno-Mekteb Field

This field is characterized by the development of a practically gradient-free zone of formation pressures in the Lower Cretaceous sediments (Table 9.4). The observable differences in reduced levels are comparable with the reducing error, which is as high as 57 m for this area. Mineralization of fluids in this area is also uniform varying from 62.8 to 68.3 g/dm<sup>3</sup>, i.e., the hydrochemical field is gradient free. Thus, the field represents a single block lacking notable filtration heterogeneity and boundaries of different genesis in limits of the block (field).

### 9.6.3 The Velichaevsk Area

In this area, reduced levels (pressures) exceed the reducing error, which permits the use of the pressure-reducing method. Figures 9.16 and 9.17 illustrate directions of horizontal gradients for reduced levels and mineralization, respectively. The chemical composition of groundwaters is relatively uniform (Table 9.5).

### 9.6.4 The Achikulak Area

Table 9.6 presents measured formation pressures and reduced levels for this area. The difference between measured formation pressures is 1.9 mPa (Fig. 9.18), which substantially exceeds the reducing error. Lateral gradients of reduced pressures are



**Table 9.3** Chemical composition of groundwater in Lower Cretaceous sediments (Russkii Khutor Severnyi)

Hole	Middle of sampling interval (m)	Density (kg/m <sup>3</sup> )	Na+K (g/dm <sup>3</sup> )	Ca (g/dm <sup>3</sup> )	Mg (g/dm <sup>3</sup> )	Cl (g/dm <sup>3</sup> )	SO <sub>4</sub> (g/dm <sup>3</sup> )	HCO <sub>3</sub> (g/dm <sup>3</sup> )	J (g/dm <sup>3</sup> )	Br (mg/dm <sup>3</sup> )
1	3,287	1,084.6	34.2	6.2	0.64	76.5	0.34	0.48	12.9	271.3
5	3,288	1,076.4	36.5	5.6	0.74	67.4	0.41	0.32	8.8	200.0
6	3,174	1,076.5	32.5	6.6	0.47	63.1	0.12	0.30	10.6	295.0
6	3,198	1,077.8	34.9	7.6	0.72	68.4	0.21	0.49	11.2	297.0
7	3,254	1,090.1	40.0	7.7	0.72	77.1	0.34	8.1	42.2	
8	2,637	1,037.0	21.0	0.49	0.15	32.6	0.1	1.16	19.3	145.8
8	3,191	1,081.0	41.6	7.0	0.52	77.0	0.29	0.23	13.3	308.6
9	3,194	1,079.0	34.3	6.2	0.54	65.3	0.16	0.24	12.3	
10	3,189	1,086.6	39.3	7.5	0.76	75.2	0.23	0.16	8.0	319.2
10	3,159	1,066.0	36.0	5.1	0.55	65.2	0.13	0.71	7.81	266
10	3,180	1,076.0	32.1	5.5	0.42	60.4	0.025	0.31	11.8	
12	3,211	1,083.6	42.1	7.4	0.79	78.8	0.4	0.63	19.4	324.5
13	3,196	1,078.6	36.7	6.9	0.67	69.8	0.2	0.49	11.8	271.8
14	3,215	1,067.0	39.1	6.3	0.77	72.7	0.26	0.43	10.4	224.0
14	3,197	1,062.3	36.4	4.3	0.57	64.5	0.73	0.73	11.8	244.7
14	3,175	1,066.9	34.6	4.24	0.55	61.7	0.04	0.67	11.5	260.7
15	3,181	1,066.0	39.4	5.4	0.44	71.1	0.06	0.39	12.5	282.0
15	3,202	1,083.4	37.2	6.9	0.79	71.7	0.22	0.21	12.7	282.4
17	3,178		33.6	6.7	0.54	65.1	0.18	0.13	12.5	269.7
18	3,190	1,070.0	36.6	6.5	0.69	69.3	0.31	0.22	12.7	361.8
18	3,208	1,084.6	42.2	7.5	0.89	79.8	20.36	0.22	14.9	303.2
18	3,281	1,075.5	38.8	5.7	0.67	7.9	0.47	0.56	11.9	308.6
23	3,161	1,063.4	34.8	3.8	0.51	61.6	0.6	0.6	12.6	244.7

**Fig. 9.14** Lateral gradients of chlorine contents. Russkii Khutor Severnyi, eastern Ciscaucasia. Absence of the arrow means lack of the gradient

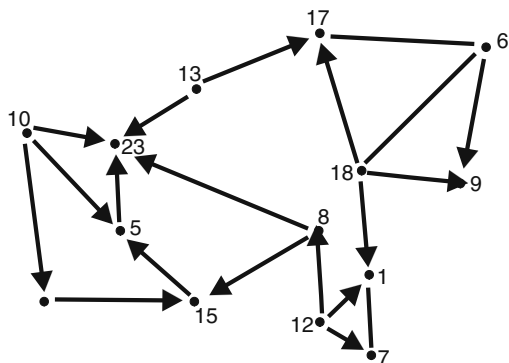


**Fig. 9.15** Lateral gradients of bromine contents. Russkii Khutor Severnyi, eastern Ciscaucasia. Absence of the arrow means lack of the gradient

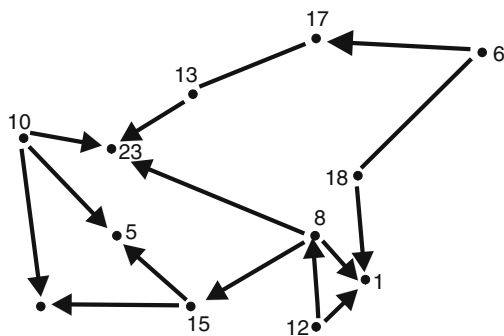


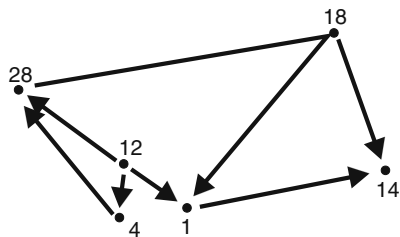
**Table 9.4** Measured and reduced formation pressures and chemical composition of fluids in the Zapadno-Mekteb field

Borehole	Middle of the sampling interval	Measured pressure (mPa)	Reduced pressure (mPa)	Altitude of the middle of the sampling interval
10	2,821	30.2	141	3,015
10	2,847	30.5	150	
13	2,838	30.2	125	
14	2,845	30.0	97	3,153
18	2,828	30.0	115	2,865
18	2,846	30.0	96	
19	2,832	30.4	150	2,914
21				2,911
28	2,847	30.1	104	2,894

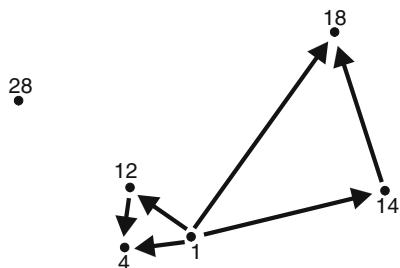
  

Density (kg/m <sup>3</sup> )	Mineralization (g/dm <sup>3</sup> )	Ca (g/dm <sup>3</sup> )	Mg (g/dm <sup>3</sup> )	Cl (g/dm <sup>3</sup> )	SO <sub>4</sub> (g/dm <sup>3</sup> )	Br (g/dm <sup>3</sup> )
1,047	68	1.2	0.3	39.7	0.05	149.0
1,047	68.8	1.7	0.4	39.4	0.07	316.8
1,034						
1,042	67.2	0.8	0.15	35.8	0.13	154.3
1,043	62.8	0.8	0.7	37.2	0.1	164.9
1,045	63.9	3.9	0.32	37.0	0.2	149.0

**Fig. 9.16** Lateral gradients of reduced pressures. Velichaevsk area, eastern Ciscaucasia



**Fig. 9.17** Lateral gradients of mineralization. Velichaevsk area, eastern Ciscaucasia



**Table 9.5** Chemical composition of fluids in Lower Cretaceous sediments of the Velichaevsk area of the eastern Ciscaucasia

Hole	Middle of sampling interval (m)	Ca (g/dm <sup>3</sup> )	Mg (g/dm <sup>3</sup> )	Cl (g/dm <sup>3</sup> )	SO <sub>4</sub> (g/dm <sup>3</sup> )	HCO <sub>3</sub> (g/dm <sup>3</sup> )	Mineralization J (g/dm <sup>3</sup> )	Br (mg/dm <sup>3</sup> )
1	3,139	5.0	0.3	53	0.2	0.4	97	8
1	3,138	5.0	0.3	53	0.2		97	
1	3,085	5.8	0.5	70	0.07	0.3	115	
4	3,112	6.0	0.4	60			108	
4	3,131	1.2	0.4	69	0.2		104	
12	3,095	5.7	0.5	67	0.06		109	
14	3,096	5.8	0.8	63	0.05	0.6	104	20
18	3,101	3.5	0.4	56	0.02	0.4	91	11 186

oriented in different directions. Minimal values of reduced heads associate with periclinal and arches of structures corresponding, probably, with draining boundaries, while their maximal values are characteristic of the structure arch.

### 9.6.5 The Ozek-Suat Area

In this area, reduced levels vary from 45 to 182 m. The difference between them exceeds the reducing error, which offers opportunity for assessing directions of fluid

**Table 9.6** Measured and reduced formation pressures in the Achikulak area of the eastern Ciscaucasia

Borehole	Middle of the sampling interval (m)	Altitude of the middle of the sampling interval (m)	Measured pressure (mPa)	Reduced pressure, altitude (m)
<i>Lower Cretaceous sediments</i>				
38	2,530	3,425	35.6	78
27	2,615	2,523	28.6	334
26	2,786	2,718	29.3	186
45	2,813	2,744	28.1	32
30	2,816	2,746	28.1	39
80	2,818	2,747	29.8	205
29	2,826	2,734	28.0	42
41	2,830	2,759	28.6	75
25	2,834	2,749	28.8	105
40	2,839	2,772	29.0	102
71	2,839	2,752	28.2	42
32	2,842	2,753	28.6	64
36	2,850	2,760	28.4	54
67	2,857	2,750	28.1	25
34	2,858	2,791	28.1	16
33	2,863	2,748	28.2	46
39	2,863	2,787	29.7	153
44	2,868	2,793	30.0	176
43	2,874	2,707	30.1	169
47	2,888	2,725	29.3	76
42	2,893	2,735	28.9	129
<i>Upper Cretaceous sediments</i>				
25	2,573	2,489	29.8	470
30	2,576	2,506	28,4	317
35	2,594	2,499	28.6	342
41	2,594	2,522	29.4	398
29	2,600	2,507	29.7	441
36	2,624	2,534	29.3	373
32	2,625	2,536	29.6	408
40	2,628	2,561	30.1	424
27	2,631	2,539	29.4	378
33	2,635	2,520	29.2	379
38	2,637	2,531	29.0	348
88	2,650	2,550	29.2	389
44	2,655	2,581	29.6	357
42	2,656	2,579	28.8	280
34	2,664	2,597	29.8	359
47	2,667	2,604	29.7	343
37	2,688	2,544	29.2	352
46	2,949	2,761	28.8	71

**Fig. 9.18** Changes in groundwater formation pressures measured at similar depths in Lower Cretaceous sediments of the Achikulak area

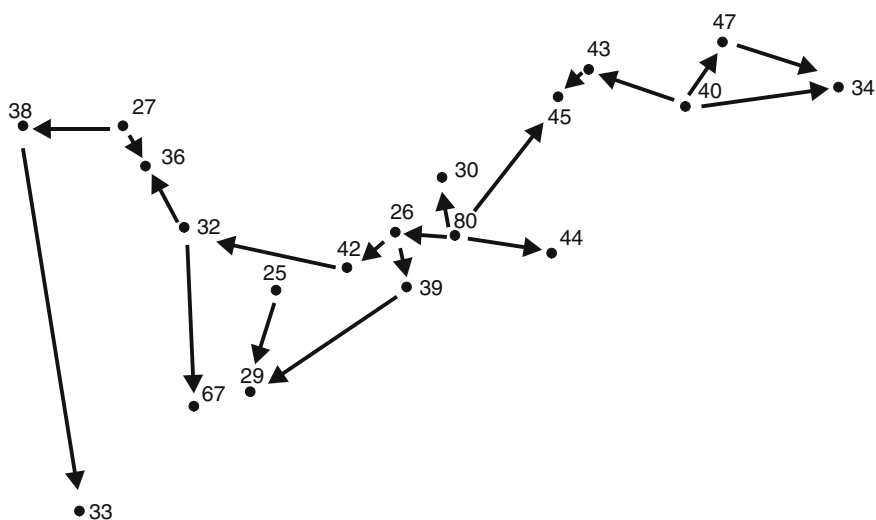
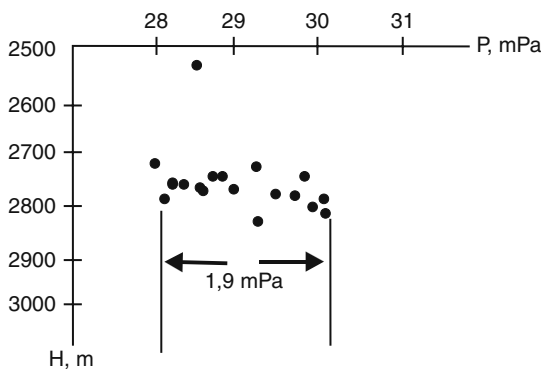


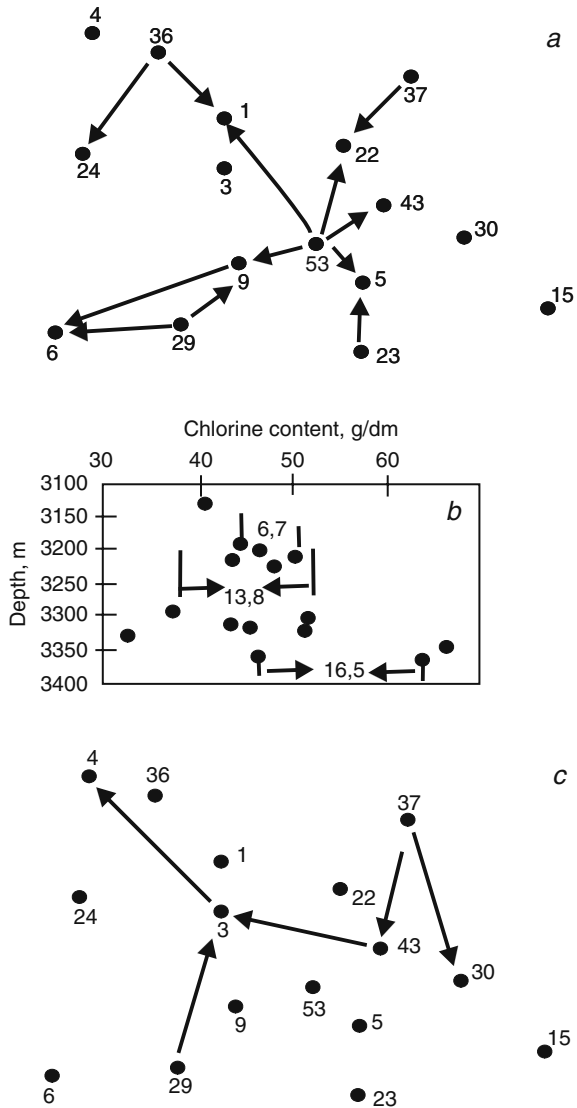
**Fig. 9.19** Lateral gradient of reduced groundwater pressures in the Lower Cretaceous complex of the Achikulak area

migration between separate points (Fig. 9.20c). Groundwaters in Lower Cretaceous sediments demonstrate substantial variations in the Cl content (Fig. 9.20a, b).

## 9.7 Abnormally High Formation Pressures

Several fields are characterized by abnormally high and elevated formation pressures (Table 9.7, which are possible only under their reliable isolation, i.e., under stratum-block structure of the sedimentary cover (petroliferous complexes).

**Fig. 9.20** The Ozek-Suat area. Lower Cretaceous sediments: (a) lateral gradients of the chlorine content, (b) downward changes in the chlorine content, (c) lateral gradients of reduced pressures



### 9.8 Regional Fluidodynamics in the Eastern Ciscaucasia Petroliferous Basin

Potentiometric maps (scale 1:5,00,000) were compiled to study regional formation peculiarities of deep fluids. For this purpose, available information was processed in line with the technique described in Chapter 2, i.e., the regional generalization was preceded by the analysis of hydrodynamic situation in separate structures with the assessment of data reliability.

**Table 9.7** Anomalous and elevated formation pressures of fluids in the eastern Ciscaucasia petroliferous basin

Hole	Age	Middle of sampling interval (m)	Formation pressure (mPa)	Anomaly coefficient
<i>Akhlovsk</i>				
813	K <sub>2</sub>	3,255	36.2	1.11
905	K <sub>2</sub>	3,056	32.8	1.07
799	K <sub>2</sub>	3,092	47.5	1.54
801	K <sub>2</sub>	3,209	46.8	1.46
<i>Bragunsk</i>				
35	K <sub>2</sub>	4,600	72.0	1.68
39	K <sub>2</sub>	3,000	56.0	1.87
40	K <sub>2</sub>	4,150	62.9	1.52
43	K <sub>2</sub>	4,450	56.1	1.26
46	K <sub>2</sub>	4,000	61.0	1.53
48	K <sub>2</sub>	2,317	34.4	1.48
49	K <sub>2</sub>	4,450	56.4	1.27
52	K <sub>2</sub>	4,200	61.7	1.47
178	K <sub>2</sub>	4,450	35.3	1.56
<i>Vostochnaya</i>				
1	J <sub>2</sub>	3,227	35.3	1.09
2	J <sub>2</sub>	3,380	36.4	1.08
3	J <sub>2</sub>	3,379	36.1	1.07
4	J <sub>2</sub>	3,243	34.9	1.08
7	J <sub>2</sub>	3,411	36.7	1.08
<i>Veselovsk</i>				
17	K <sub>1</sub>	1,091	24.2	2.22
<i>Granichnaya</i>				
5	K <sub>1</sub>	3,578	34.4	0.96
2	K <sub>1</sub>	3,564	37.7	1.06
<i>Yastrebinoe</i>				
97	K <sub>2</sub>	4,027	63.1	1.56
98	K <sub>2</sub>	4,067	58.0	1.43
99	K <sub>2</sub>	3,791	46.9	1.24
100	K <sub>2</sub>	4,349	57.7	1.33
102	K <sub>2</sub>	2,919	45.2	1.55
103	K <sub>2</sub>	4,066	43.6	1.07
104	K <sub>2</sub>	3,940	43.0	1.09
105	K <sub>2</sub>	4,140	66.0	1.59
107	K <sub>2</sub>	4,240	42.4	1.0
111	K <sub>2</sub>	4,179	41.1	1.0
109	K <sub>2</sub>	4,489	66.6	1.48
<i>Karabulak-Achaluki</i>				
18-A	K <sub>1</sub>	2,390	34.9	1.46
26-A	K <sub>1</sub>	2,163	31.6	1.46
37-A	K <sub>1</sub>	2,310	34.0	1.47
45-A	K <sub>1</sub>	2,498	34.2	1.37
39-A	K <sub>1</sub>	2,400	33.2	1.38
83	K <sub>1</sub>	2,480	32.7	1.32

**Table 9.7** (continued)

Hole	Age	Middle of sampling interval (m)	Formation pressure (mPa)	Anomaly coefficient
100	K <sub>1</sub>	2,500	33.1	1.32
23-A	K <sub>1</sub>	2,306	33.1	1.44
42	K <sub>1</sub>	2,500	33.4	1.34
82	K <sub>1</sub>	2,600	34.2	1.32
81	K <sub>1</sub>	2,450	31.9	1.3
41	K <sub>1</sub>	2,300	31.7	1.38
106	K <sub>1</sub>	2,400	32.8	1.37
50	K <sub>1</sub>	2,550	35.1	1.38
16-K	K <sub>1</sub>	2,800	37.0	1.32
73	K <sub>1</sub>	2,900	35.9	1.24
108	K <sub>1</sub>	2,861	37.0	1.29
117	K <sub>1</sub>	3,040	38.7	1.27
112	K <sub>1</sub>	2,725	35.3	1.3
<i>Gudermes</i>				
183	K <sub>2</sub>	4,874	71.0	1.46
184	K <sub>2</sub>	5,378	66.1	1.29
188	K <sub>2</sub>	5,161	56.8	1.1
181	K <sub>2</sub>	5,015	69.6	1.4
190	K <sub>2</sub>	5,391	75.0	1.39
197	K <sub>2</sub>	5,257	56.0	1.07
203	K <sub>2</sub>	5,259	67.3	1.18
<i>Gorokhovskaya</i>				
4	J	3,180	33.5	1.05
2	J	3,330	35.3	1.06
8	K <sub>1</sub>	2,599	26.8	1.03
4	K <sub>1</sub>	3,011	31.2	1.03
5	K <sub>1</sub>	3,096	31.7	1.02
4	K <sub>2</sub>	2,573	25.	0.97
6	K <sub>2</sub>	2,620	26.1	1.0
<i>Zhuravskaya</i>				
13	K <sub>1</sub>	3,294	37.2	1.13
<i>Zamankul</i>				
46	J <sub>3</sub>	3,950	46.1	1.17
58	J <sub>3</sub>	4,000	47.0	1.18
60	J <sub>3</sub>	2,300	33.4	1.45
61	J <sub>3</sub>	3,940	44.9	1.14
66	K <sub>1</sub>	3,763	32.2	0.86
61	K <sub>1</sub>	3,775	33.0	0.87
64	K <sub>1</sub>	3,777	31.0	0.82
60	K <sub>1</sub>	3,729	32.3	0.87
21	K <sub>2</sub>	2,140	33.4	1.56
32	K <sub>2</sub>	2,030	31.4	1.55
18	K <sub>2</sub>	2,150	33.5	1.56
20	K <sub>2</sub>	2,150	33.7	1.57
23	K <sub>2</sub>	2,180	33.2	1.52
26	K <sub>2</sub>	1,945	30.6	1.57
41	K <sub>2</sub>	2,200	29.4	1.34



**Table 9.7** (continued)

Hole	Age	Middle of sampling interval (m)	Formation pressure (mPa)	Anomaly coefficient
37	K <sub>2</sub>	2,111	33.0	1.56
44	K <sub>2</sub>	2,150	31.3	1.46
<i>Kurskaya</i>				
1	K <sub>1</sub>	3,815	48.6	1.27
2	K <sub>1</sub>	3,585	50.8	1.34
5	K <sub>1</sub>	3,530	43.8	1.56
1	K <sub>2</sub>	3,420	47.6	1.46
<i>Levokumskaya</i>				
50	K <sub>1</sub>	3,252	35.2	1.08
<i>Malgobek-Voznesensk</i>				
802	K <sub>1</sub>	2,000	34.1	1.71
842	K <sub>1</sub>	2,500	37.5	1.5
840	K <sub>1</sub>	3,245	42.5	1.31
841	K <sub>1</sub>	3,600	46.9	1.3
819	K <sub>1</sub>	3,500	51.1	1.46
846	K <sub>1</sub>	2,000	31.4	1.57
817	K <sub>1</sub>	2,000	34.5	1.73
863	K <sub>1</sub>	3,250	47.0	1.45
824	K <sub>1</sub>	3,449	47.3	1.37
817	K <sub>1</sub>	3,536	50.2	1.42
825	K <sub>1</sub>	2,554	46.3	1.3
826	K <sub>1</sub>	3,308	45.5	1.38
862	K <sub>1</sub>	3,358	45.8	1.36
130	K <sub>1</sub>	3,161	39.8	1.26

As is noted (Chapter 2), regional potentiometric charts were compiled in line with the particular-to-general principle, i.e., from the study of hydrodynamics in individual structures to their subsequent generalization. It should be noted that maps for individual structures were compiled at scales 1:10,000 and 1:25,000, which lost some hydrodynamic features during their transformation into scales of 1:5,00,000 and larger. Therefore, the potentiometric maps compiled for the eastern Ciscaucasia region and the Bukhara-Karshi petroliferous basin reflect only basic (regional) features of the distribution of reduced heads (pressures). Values of reduced levels are averaged for individual structures. That is why these maps have nothing to do with the previously compiled charts and reflect only principal possible directions of deep fluid migration.

The used factual material is partly shown in Table 9.1. The eastern Ciscaucasia region is irregularly studied with respect to the lateral and vertical fluid hydrodynamics.

The best studied is the Arzgir-Prikumsk zone of uplifts, where the petroliferous complexes under consideration occur at relatively shallow depths and are subjected to drilling in connection with exploration and exploitation of hydrocarbon fields. The Mineral'nye Vody Uplift, where hydrodynamic studies were and are conducted

at deposits of mineral waters, is also sufficiently well known. In the Terek-Sunzha petroliferous area, detailed hydrodynamic information is available only for the Cretaceous petroliferous complexes. Each of total over 100 structures was drilled by one to 30–40 boreholes.

Remaining areas of the basin (Stavropol Arch, Karpinsky Ridge, and others) are insufficiently studied because of different reasons: very deep occurrence of Mesozoic petroliferous complexes (Terek-Caspian Trough), low productivity of Cretaceous and Jurassic sediments with respect to oil and gas.

The analysis of available materials revealed that many structures are lacking sufficient information on measured formation pressures (many data on formation pressures were omitted from consideration as unreliable).

Most confident data are obtained only on structures of the Prikumsk and Terek-Sunzha uplift zones, which have been studied in detail; the results are discussed in this section. In the remaining territory of the basin, only single measurements of fluid formation pressures and densities are available for individual structures and fields, which prevented from establishing correlation  $\rho(z)$  and assessing the reducing accuracy for particular structures. In such a situation, the dependence  $\rho(z)$  established for entire large tectonic structures (Stavropol Arch, Karpinsky Ridge) was used as the reduced formation pressure. Thus, factual material used for compiling potentiometric maps is far from being equivalent at the regional scale.

Figures 9.9, 9.13, 9.14, 9.17, 9.19, and 9.20 illustrate, as examples, potentiometric maps compiled for individual structures at scale 1:50,000.

For the eastern Ciscaucasia petroliferous basin, regional hydrodynamic schematic maps are compiled at scale 1:50,000 for the Upper Cretaceous (Fig. 9.21), Lower Cretaceous (Fig. 9.22), and Jurassic (Fig. 9.23) petroliferous complexes. They also show single or average values of the reduced potentiometric level for individual areas (fields). The peculiarities in fluid dynamics are characterized below separately for individual petroliferous complexes.

The *Upper Cretaceous petroliferous complex* is best studied in the Terek-Sunzha zone of uplifts. This zone is characterized by abnormally high formation pressures (Table 9.7) in all the Mesozoic petroliferous complexes. The Upper Mesozoic complex demonstrates higher values of measured and reduced formation pressures as compared with underlying sediments. The abnormality coefficient is locally as high as  $>2$ . Differences in formation pressures both through individual structures and between them indicate the stratum-block structure of this area. Differences between reduced levels amount through the entire Terek-Sunzha area to 2,300 m (23 mPa).

For the Arzgir-Prikumsk zone of uplifts, the available material is less representative as compared with that for underlying petroliferous complexes and for the Terek-Sunzha area. In the Arzgir-Prikumsk area, the detailed potentiometric maps can be compiled only for some structures. Differences in the potentiometric levels recorded for the Achikulak, Praskovei, and Podsolnechnaya structures are 400, 500, and 200 m, respectively.

For the Mineral'nye Vody Uplift, unreduced measured formation pressures were used because of low mineralization. For the remaining territory, we used heterogeneous published and unpublished materials.

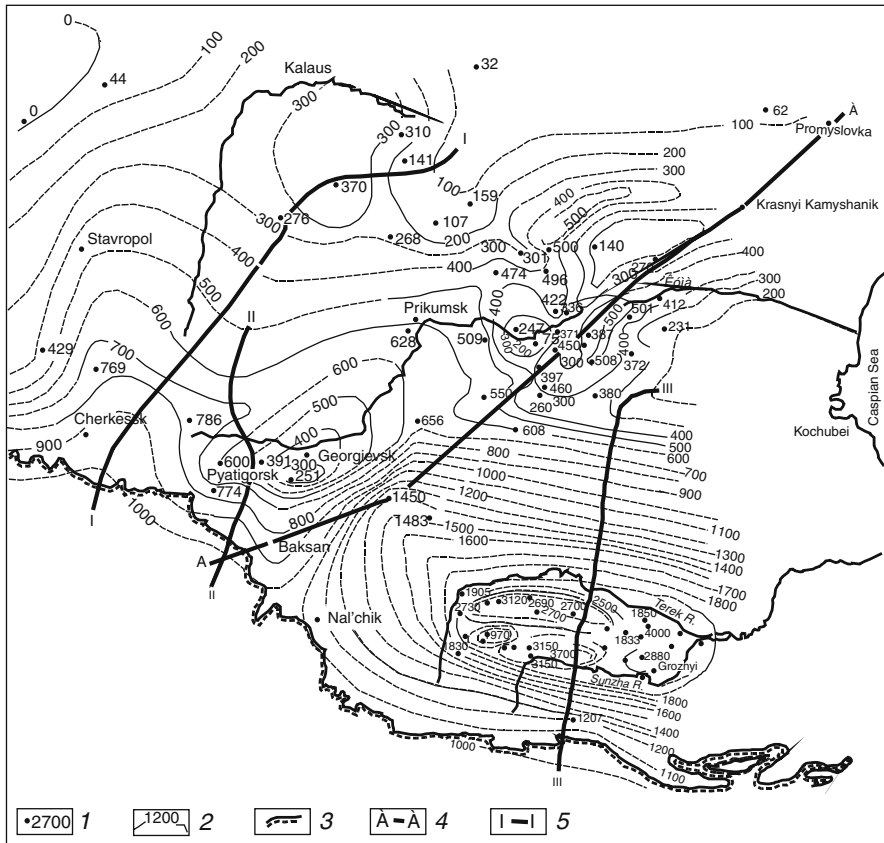


**Fig. 9.21** The schematic map of the groundwater potentiometric surface in Upper Cretaceous sediments, eastern Ciscaucasia. (1) Average altitude of the reduced level; (2) isolines of the reduced level, (3) boundary of Mesozoic outcrops; (4) line of the cross section; (5) groundwater flows (direction of movement)

Similar to the above-mentioned petroliferous complexes, the region under consideration is characterized by general lowering of the potentiometric surface from areas of formation outcrops (Caucasus) in the northern and northeastern directions. Because of low reliability and incompleteness of factual material, no distinct block structure is defined in large structural elements (probably is missing). Nevertheless, the potentiometric surface is characterized by closed contour, extreme values, and large differences between reduced levels in the Terek-Sunzha and Arzgir-Prikumsk zones of uplifts. The abnormally high values of the reduced level are also characteristic of the platform slope of the Terek-Caspian Trough: 1,450 and 1,483 m in the Sovetskaya and Kurskaya structures, respectively.

This characteristic of fluid dynamics in the eastern Ciscaucasia petroliferous basin is incomplete without the analysis of changes in formation pressures through



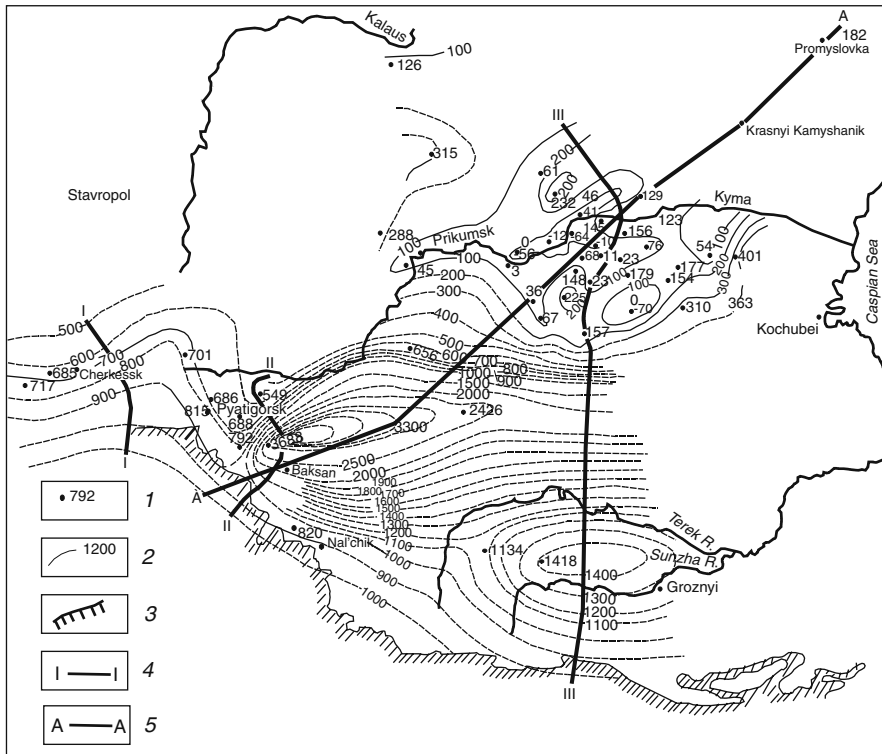


**Fig. 9.23** The schematic map of the groundwater potentiometric surface in the Jurassic aquifer, eastern Ciscaucasia. (1) Borehole and reduced level value (altitude, m); (2) isolines of the reduced level, (3) groundwater flows (direction of movement); (4) boundary of Jurassic outcrops; (5) line of the cross section

zone of uplifts, relations between potentiometric levels change. In the Jurassic petroliferous complex, their values vary from 3,600 to <100 m.

Through the entire Prikumsk zone of uplifts, potentiometric levels are higher in the Upper Cretaceous petroliferous complex than in the Lower Cretaceous and Jurassic complexes. Relationships between last complexes are permanently variable through the entire Prikumsk zone. In the Kuma River valley, potentiometric levels in them are characterized by abnormally low values, which are probably explained by draining (paleodrainage) of deep fluids by the river. At the same time, the Upper Cretaceous complex shows no such variations in the potentiometric surface, which is inconsistent with the general draining model. It is conceivable that groundwaters drain(ed) along interblock planes in the Upper Cretaceous complex.

In the Eastern Manych Depression and the Karpinsky Ridge, the relationship between potentiometric levels is as follows: their highest values are characteristic of Upper Cretaceous sediments and they become successively lower in the Jurassic and lower Cretaceous petroliferous complexes.

Such a situation undoubtedly indicates hydrodynamic isolation of separate parts of the section. Only in the Promyslovoe field area, the relation between potentiometric levels changes again; they become lower downward. It should be remembered that the Eastern Manych Depression and the Karpinsky Ridge are characterized by the limited quantity of formation pressure measurements. Therefore, these inferences are conditional to significant extent.

Figures 9.1 and 9.9 demonstrate fluidodynamics across the best studied Prikumsk and Terek-Sunzha zones of uplifts. The difference between potentiometric levels in the Zamankul and Malgobek-Voznesensk structures located 11 km away from each other amounts in different blocks to 700–1,000 m for the Lower and Upper Cretaceous petroliferous complexes and 400–500 m for a single aquifer (Fig. 9.1). It is remarkable that highest values of potentiometric levels are observed in the Upper Cretaceous complex. These observations support the above inference on the stratum-block structure of deep horizons.

In the Prikumsk petroliferous area, the schematic hydrodynamic profile crosses fields covered by maximal quantity of measurements (Russkii Khutor Yuzhnyi, Russkii Khutor Severnyi, Kultai, Nadezhdinskoe). The profile unites values of formation pressures measured in particular boreholes. The analysis of the distribution of formation pressures reveals in some fields anomalous values at different section levels against the background of their regular downward increase. The particularly mosaic patterns are recorded for the distribution of formation pressures in fields adjacent to the Kuma River valley (Russkii Khutor Severnyi, Nadezhdinskoe), where pressures demonstrate significant lateral and vertical differences.

In the Nadezhdinskoe field, pressure values in the same intervals of closely spaced boreholes (0.5 km) differ by 3.4 mPa, while in boreholes 229 and 6 located 1.6 km away from each other, this difference is 2.54 mPa. In the Russkii Khutor Severnyi field, two distinct hydrodynamic anomalies are defined against the background of upward decrease of formation pressures: positive and negative.

The *Lower Cretaceous petroliferous complex* is distributed through the entire basin (Fig. 9.22) and is best studied with respect to its fluidodynamics.

Dissimilar to the Jurassic complex, factual material available for its lower Cretaceous counterpart made it possible to compile potentiometric maps for all the structures of the Arzgir-Prikumsk and Terek-Kuma zones of uplifts. For the remaining part of the basin, single measured values of formation pressures are taken from earlier works [5 and others].

Altitudes of levels are approximately 1,000 m in areas of outcropping sediments, 500–800 m in the Mineral'nye Vody Uplift, and –100 m in the Stavropol Arch.

The Terek-Sunzha area is characterized by anomalous levels (1,500–2,200 m), which is higher as compared with that in the Jurassic complex. Differences in the level positions for the Lower Cretaceous petroliferous complex are 700, 600, and 400 m in the Malgobek-Voznesensk, Karabulak-Achaluki, and Zamankul structures, respectively. This indicates lack or very hampered relations between both individual structures located in the relatively small areas and their parts.

In contrast, the platform slope of the Terek-Caspian Trough is characterized by anomalous levels (up to 1,500 m), which are lower than that in the Jurassic petroliferous complex.

The Chernyi Les Trough is located between the zone with anomalously low (Stavropol Arch) and anomalously high (Terek-Caspian Trough) potentiometric levels. This structure is characterized by level altitudes of 300–600 m.

The Arzgir-Prikumsk zone of uplifts demonstrates significant variation in level altitudes: from –100 m (Kurtinskaya structure) to +337 m (Yuzhno-Sukhokumskaya structure).

Negative level altitudes are registered in the following structures: Podsolnechnaya, Neftekumskaya, Ostrogorskaya, Kovyl'naya, and Bezvodnaya located along the Kuma River valley. At the same time, the zone of lowered level values is displaced toward the left slope of the valley relative to the Jurassic petroliferous complex.

Eastward, variations in level altitudes are most contrasting at close distances. For example, altitudes of the potentiometric level are 97, 330, 310, and 165 m in the Vostochno-Sukhokumskaya, Stepnaya (15 km away from the previous one), Perekrestnaya, and Maiskaya (approximately 7 km away from the previous one) structures, respectively.

As was noted, respective differences in potentiometric levels amount to 200, 500, and 300 m for the Vladimirsкая, Podsolnechnaya, and Achikulak structures. Each of them is characterized by individual distribution of reduced levels and gradients, which implies their hydrodynamic isolation.

The *Jurassic petroliferous complex* includes sediments of all three series, which are irregularly distributed through the basin. Because of such distribution patterns and insufficient information, they are considered together (Fig. 9.23).

With respect to its fluidodynamics, the complex is best studied in the Arzgir-Prikumsk zone of uplifts, where sufficient data are available to compile potentiometric maps for some structures (Vostochnaya, Kamyshovaya, Maiskaya, Sukhokumskaya, and Yuzhno-Sukhokumskaya) at scale 1:1,00,000. Other structures (Andrei-Kurgan, Bazhigansk, Velichaevsk, Sukhokumskaya, Gorokhovskaya, Zimnestavkinskaya, Zapadno-Golubinskaya, Kolodeznaya, Kutaiskaya, and others) are characterized only by one to three measurements.

Practically no measurements are available for the Terek-Caspian Trough, which is explained by the deep occurrence of the petroliferous complex. Single measurements of formation pressures were made only in the Terek-Sunzha zone of uplifts (Zamankul, Karabulak-Achaluki structures). In the Mineral'nye Vody Uplift, immediate measurements of potentiometric level altitudes were used since groundwaters are characterized in this area by low mineralization.

In the remainder of the basin, formation pressures were calculated in line with the technique described in Chapter 2. Thus, when compiling maps of the potentiometric surface for the Jurassic petroliferous complex, we used different and irregularly distributed factual material.

In the area of complex outcrops, the potentiometric level is located at 900–1,000 m. This area hosts springs of both fresh and mineralized waters. In the Mineral'nye Vody Uplift, the level is lowered up to 700–800 m.

The most subsided part of the complex is characterized by abnormally high values of the reduced level: 2,400–3,700 m in the platform slope of the Terek-Caspian Trough (Kurskaya, Sovetskaya, and Mar'inskaya structures).

In the Terek-Sunzha zone, anomalous values become lower, although potentiometric levels remain higher (1,100–1,400 m) as compared with areas adjacent to regional recharge areas.

The Prikumsk petroliferous area is characterized by different fluidodynamics. In this area, altitudes of potentiometric levels do not exceed usually 100 m. In some structures (Urozhainenskaya, Podsolnechnaya, Pravoberezhnaya, Polevaya, Ozek-Suat), the potentiometric level is located below the sea level (–12 m, –64 m). These structures are distributed along the Kuma River valley, which drains(ed), likely, deep formations. Away from the river valley, groundwater potentiometric levels raise up to 300 m (Georgievskaya structure) and even 400 m (Stepnaya structure). In the Arzgir-Prikumsk zone of uplifts, reduced potentiometric levels are highly variable at short distances: 54, 401, 23, and 179 m in the Vostochno-Sukhokumskaya, Stepnaya (12 km away from the previous one), Kultaiskaya, and Russkii Khutor Severnyi (9 km away from the previous one) structures, respectively. The list of such examples is far from being exhausted. Such variations influence the potentiometric surface (Fig. 9.23).

Through the basin as a whole, the potentiometric surface of the Jurassic petroliferous complex becomes lower (if extreme values are ignored) from areas of its outcropping toward the Karpinsky Ridge. Extreme values of the potentiometric level are characterized by different signs (higher or lower as compared with their background distribution). The last values are characteristic of both small areas and large structural elements (blocks): the Terek-Sunzha area is characterized by anomalous level values, the platform slope of the Terek-Caspian Trough is an area with maximal anomaly coefficients, while the adjacent Arzgir-Prikumsk zone demonstrates lowered level values.

Such a scatter in reduced levels measured in different tectonic blocks implies their hydrodynamic isolation and stratum-block structure of deep parts of the section. It should be emphasized that these patterns are also confirmed by immediate measurements of formation pressures along a single plane, which excludes errors related to reduction of formation pressures.

Thus, the substantial heterogeneity in the field of formation pressures is notable both in local structures and at the regional scale. Despite the fact that the potentiometric surface demonstrates tendency for lowering through the region from areas of complex outcropping (presumed regional recharge area) toward the Stavropol Arch and the Karpinsky Ridge, there are many structures with anomalous levels, which excludes the formation of regional flows. The areas with abnormally high levels are characterized by deep occurrence of aquifers; deep fluid drainage is possible in areas with low potentiometric levels along the Kuma River valley.



## 9.9 Conclusions

Thus, the analysis of the distribution of formation pressures in the eastern Ciscaucasia petroliferous basin reveals the following features: (1) formation pressures are subjected to rapid lateral and vertical variations through the sedimentary section; (2) most significant changes in formation pressures associate with tectonically active areas particularly marked by recent tectonic and seismic movements (Terek-Sunzha structure); (3) the Mesozoic sediments of the basin represent a system of blocks partly to completely isolated with respect to fluidodynamics, sizes of which vary from several hundreds of meters to a few tens of kilometers and are likely controlled by recent tectonic movements; (4) the block structure of sedimentary cover prevents the formation of regional deep fluid flows; (5) investigation of processes responsible for the formation of blocks isolated with respect to fluidodynamics in the vertical section should be accompanied by the study of filtration rock properties with differently oriented impermeable (or poorly permeable) boundaries; their development is confirmed by single samples; (6) hydrochemical fields are also heterogeneous with differently oriented gradients; (7) most of the anomalies are unexplainable without the complex analysis, which should take into consideration information on hydrochemistry, gas composition, temperature, mineralogy (secondary mineral formation), palynology, and geochemistry. These properties represent a task for future studies.

## References

1. Djunin V I (1985) Investigation methods of the deep subsurface flow. Nedra, Moscow
2. Dzhamalov R G (1971) Hydrogeology of Pliocene sediments and regularities in the formation of subsurface flow in the Terek-Kuma artisan basin Candidate dissertation (Geol-Mineral). MGU, Moscow
3. Gurevich A E (1985) Practical manual for the study of groundwater migration during exploration of mineral resources. Nedra, Leningrad
4. Hydrogeology of the USSR. North Caucasus. Volume 9 (1970) Nedra, Moscow
5. Kartashev A M et al. (1969) Analysis of hydrodynamic parameters of petroliferous formations (for calculations) and study of their hydrogeological characteristics in areas of the trust "Stavropol'burneft." Stavropol
6. Kartsev A A, Vagin S B, Serebryakova L K (1980) Paleohydrogeological reconstructions for revealing petroliferous zones (exemplified by western Ciscaucasia). Byul. MOIP 1: 132–140
7. Kissin I G (1964) The East Ciscaucasia artesian basin. Nauka, Moscow
8. Kolodii V V (1966) Hydrodynamic and paleohydrodynamic conditions in Pliocene sediments of the West Turkmen Depression. Sov Geol 12:50–62.
9. Kortsenshtein V N (1977) Water-pressure systems of largest gas and gas condensate fields. Nedra, Moscow
10. Mukhin Yu. V (1965) Compaction of clayey sediments. Nedra, Moscow
11. Stetyukha E I (1964) Equations of correlation between physical properties of rocks and their occurrence depth. Nedra, Moscow
12. Sukharev G M (1979) Hydrogeology of oil and gas fields. Nedra, Moscow

# Chapter 10

## Fluidodynamics in Deep Formations of the Bukhara–Karshi Petroliferous Basin

### 10.1 Stratigraphy

The second-order Bukhara–Karshi petroliferous basin represents an element of the more complex Amudar'ya (Karakumy) basin. It consists of the Paleozoic basement and Mesozoic–Cenozoic sedimentary cover. Figure 10.1 yields some ideas about the geological structure and tectonics of the basin.

The basement is composed of metamorphosed different-age and different-lithology rocks: granites, amphibolites, schists, quartzites, and others. All of them are strongly dislocated and folded.

The basement is overlain with distinct unconformity by the sedimentary cover composed of Jurassic, Cretaceous, Paleogene–Neogene, and Quaternary sediments of different geneses. The integral thickness of sedimentary sequence varies from a few hundreds of meters in piedmonts to 3,000–4,000 m in innermost subsided parts of the basin.

#### 10.1.1 Mesozoic Group (MZ)

##### 10.1.1.1 Jurassic System (J)

The Jurassic sediments are practically unexposed. Their outcrops are observable only in mountainous structures surrounding the basin. They are recovered by almost all the prospecting boreholes missing only in arches of the Gazli and Kurbanola uplifts. Their maximal thickness is 1,850 m (Kugitangtau) averaging 160–310 m in the Bukhara flexure (Setalan-Tepe, Dzharkak, Karaul-Bazar, and others).

In the lower part, the Jurassic section is largely composed of terrigenous rocks: alternating continental sandy–clayey facies, which retain their appearance through the entire basin varying only in the thickness.

In the upper part of the section, Jurassic sediments are represented by marine facies, carbonate in the lower part of the sequence (Callovian–Oxfordian), and saliferous gypsum (Kimmeridgian–Tithonian) in its upper portion. The thicknesses of carbonate and saliferous-gypsum sediments exceed 350 and 700 m, respectively.

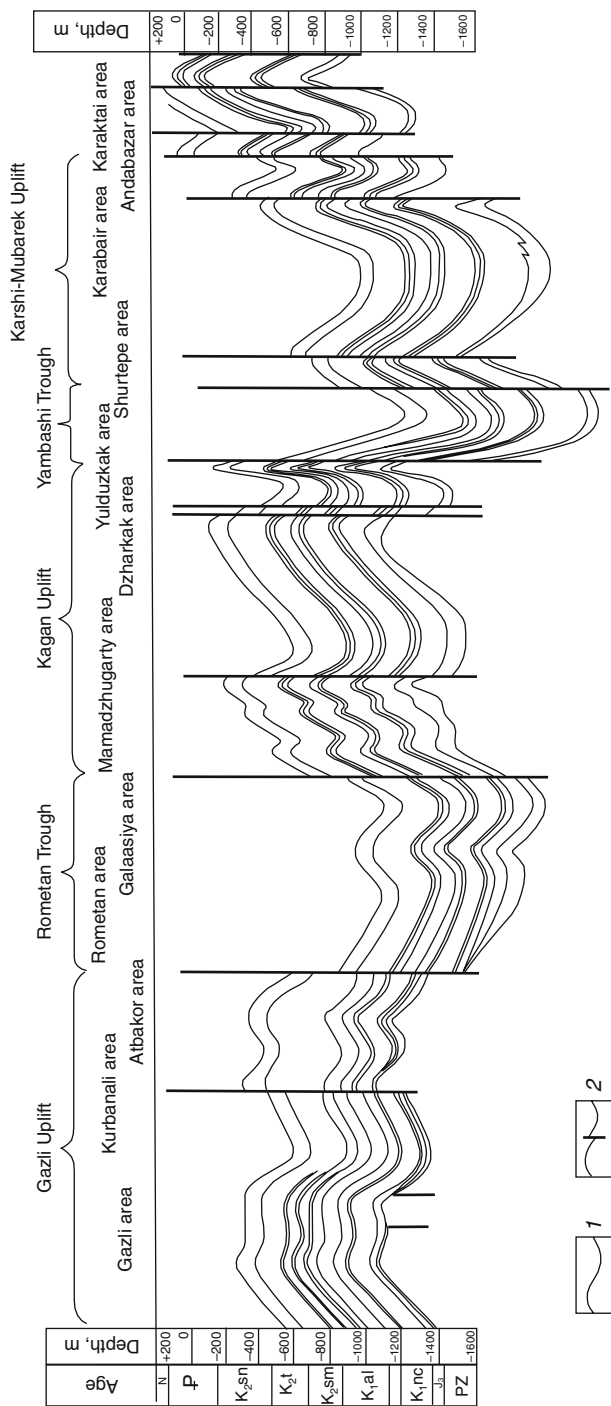


**Fig. 10.1** Geological cross section of the Bukhara Step (after S.A. Korsakov and E.V. Ivanov, simplified). (1) Stratigraphic boundaries; (2) tectonic fractures

### **10.1.1.2 Cretaceous System (K)**

The Cretaceous sediments are characterized by the universal distribution. Prospecting boreholes recovered both lower and upper series of the system. They are represented by marine, lagoonal, and continental facies.

#### *Lower Series (K<sub>1</sub>)*

The lower series is represented by the Neocomian, Aptian, and Albian sediments. The Neocomian is composed of clays, sandstones, siltstones, and rare conglomerate beds. The thickness of these rocks varies from 120 to 650 m (Kasan Anticline) decreasing (up to complete pinching-out) from the south northward. They are largely continental in origin. The Albian is represented by basal fine- to medium-grained sandstones with clay, marl, and limestone beds.

#### *Upper Series (K<sub>2</sub>)*

The series is represented by Cenomanian, Turonian, Senonian, and Danian sediments.

The Cenomanian sequence is composed of fine-grained sandstones with a clayey member 20–30 m thick in its middle part. The share of clays and coquina layers increases west- and southwestward. The thickness of Cenomanian sediments increases in the same direction from 150 (Dzhakrak) to 335 m (Farab).

The Turonian Stage consists of clays with thin beds of sandstones and subordinate coquina and marl. The thickness of Turonian sediments increases from 150 to 450 m in southwestern and western directions.

The Senonian sequence consists of two parts: detrital rocks (lower) and platy limestones (upper). The thickness ranges from 50 to >400 m.

The Danian sediments are represented by compact (less commonly incoherent) fine-grained gypsum. They are usually thin (from 2 to 20 m) and missing from sections.

### **10.1.2 Cenozoic Group (KZ)**

#### **10.1.2.1 Paleogene (P)**

The Paleogene sediments of the basin are represented by dolomites, limestones, gypsum clays with siltstone, marl, and coquina interbeds. The thickness ranges from 30 to 270 m.

#### **10.1.2.2 Neogene (N)**

In the basin, the Neogene section is composed of sands, loam, clay, and gravel usually less than a few tens of meters thick.

The basin is characterized by the following main geological features: (1) directed thickness increase in southern and southwestern directions; (2) appearance of additional stratigraphic units to form a complete section in the same directions; (3) development of the thick of salt–anhydrite sequence (up to >700 m thick) in the uppermost Jurassic sequence and largely clayey rocks (up to >200 m thick) in the uppermost Neocomian and lower Albian, which play the role of confining beds.

## 10.2 Tectonics

During the Paleozoic, the Bukhara–Karshi petroliferous basin experienced geosynclinal development with accumulation of thick sequences of sedimentary and igneous rocks. In the Permian–Triassic epoch, the geosynclinal regime was replaced by the platform one. The basin was completely formed during the Alpine orogenic epoch, when the Paleozoic basement was subdivided into blocks and Mesozoic sediments appeared to be deformed into gentle folds. In the Quaternary, neotectonic movements were in progress, which is evident from development of recent river terraces and intense seismicity.

The Bukhara–Karshi region is characterized by the basement subsided in the stepwise manner in the southwestern direction. It is penetrated at depths of 1,250–1,350, 3,000, and 400 m under the Kagan Uplift, Chardzhou, and Bairam-Ali areas, respectively. Two steps are defined in the basin: Bukhara and Chardzhou.

### 10.2.1 Bukhara Step

The step is located south of the Kuldzhuk-Tau and Zirabulak-Ziaetdin ranges. In the southeast and southwest, the step is bordered by different-order regional faults. The Hercynian and Alpine faults are of the northwestern and northeastern strikes, respectively.

The Bukhara Step comprises a system of complex NW–SE-trending uplifts and intervenient troughs separated from each other by different-age and different-depth faults.

The faults are usually the Hercynian and Alpine in age. Some troughs (Rometan, Yambashi, and others) were formed in the Neogene.

Several uplifts complicated in turn by structures and faults of higher orders are defined in the Bukhara Step: Meshekli, Yangikazgan, Gazli, Kagan, and Mubarek.

The Gazli and Yangikazgan uplifts are separated from each other by the wide (approximately 30 km) Tuzgoi graben-shaped trough complicated by a system of anticlinal folds. In the northeast, the Yangikazgan Uplift is bordered by the Alpine Dzhusan-Tepe Fault. In the Gazli block, the basement is divided by local fractures into a system of smaller blocks, many of which are uplifted to form salients in the present-day structure. There are local anticlines developed in the Gazli Uplift: Gazli, Tashkuduk, Karakyr, Atbakor, Kukhnagumbas, and others. Most of the fractures are recorded in the Tashkuduk Anticline adjacent to the flexure–fracture zone in the

southern part of the Gazli Uplift. North of Tashkuduk, abundance and amplitude of fractures decrease. In the central part of the uplift, they are practically missing; closer to the Fore-Kyzylkum regional fault (Yangikuduk structure), they appear again.

The Rometan post-Paleogene trough separates the Kagan Uplift from the Gazli one. In the basement, the trough is reflected in the form of block bordered by the North Romestan, South Romestan, and Bukhara (in the south) regional faults.

The Kagan Uplift is bordered on all sides by different-age regional faults. It comprises 15 uplifts (Mamadzhugargaty, Akdzhar, Shurchi, Sarytash, Karaul-Bazar, and others) well manifested in the topography. Almost all of them are complicated in limbs by fractures with amplitudes ranging from 20–30 to 150–300 m. In the southeast, the Kagan Uplift contacts with the Yambashi Trough adjacent to the most complex Mubarek Uplift. The latter is established to comprise 14 folds located in three tectonic zones.

The Shurtepe and Shursai folds are characterized by development of faults in the northern near-arch parts or northwestern limbs (the first line of fractures). The North Mubarek, Shumak, Kyzylrvat, and Maidadzhoi folds with distinctly steeper southeastern limbs complicated by faults form the second line of fractures. The third line of fractures represented by the South Mubarek, Aktepe, Karabair, and Baiburak folds is characterized by two-dome structures and strong tectonic dislocations. The block structure is evident both in the basement and in the sedimentary cover. Fractures are usually represented by normal faults with amplitudes ranging from 20–30 to 100–150 m.

The formation of structures in the Mubarek Uplift terminated in the Pliocene–Quaternary. They were subjected to substantial reorganization by the terminal Eocene–initial Neogene. Deep structural drilling revealed a system of near-latitudinal and NE-trending faults. Tectonic dislocations in the sedimentary cover are related to movements in the basement, which are developing in the inherited manner. Some of the fractures degrade in the upper parts of the section. The arched parts of the North Mubarek, South Mubarek, and Shurtepe structures are complicated by shear grabens traceable below the base of the Upper Cretaceous sequence.

### ***10.2.2 Chardzhou Step***

The Chardzhou Step is separated from the previous one by the Bukhara regional fault. It comprises three large structural elements: the Amudar'ya zone of uplifts, Karakul, and Beshkent troughs. The Amudar'ya zone includes the Pitpak-Darganata, Kabakli, Chardzhou, Dengizkul, and other uplifts, each complicated by systems of complex local positive structures crossed by numerous tectonic fractures.

The Beshkent Trough is located in the immediate proximity to the Tien Shan; therefore, tectonic movements in this area are more intense as compared with other parts of the Amudar'ya Depression.

Thus, the sedimentary cover of the Bukhara–Karshi petroliferous basin represents a system of blocks (similar to blocks of ice in the river during ice motion) bordered by different-age and different-depth faults, which determine the stratum-block structure of the fluidodynamic field in Mesozoic–Cenozoic sediments. Such a complex tectonic structure of the sedimentary cover in the basin determines, in turn, differently oriented gradients of formation pressures, which vary at short distances. In addition, the region is characterized by elevated seismic activity, which influences undoubtedly the field of formation pressures [2].

### 10.3 Hydrogeological Conditions

The sedimentary cover of the Bukhara–Karshi petroliferous basin comprises several petroliferous complexes. In this section, we characterize only three of them: Jurassic, Albian–Cenomanian, and Turonian–Paleocene.

#### 10.3.1 Turonian–Paleocene Petroliferous Complex

The complex is characterized by the universal distribution. Fluid-bearing rocks outcrop along slopes of mountainous structures and in the central part of the basin. Boreholes recovered brackish and saline frequently self-discharging fluids with the head value up to 650 m. The rocks are represented by sands, sandstones, limestones, and marls. Groundwater mineralization varies from 1.5 g/dm<sup>3</sup> near recharge areas to 32 g/dm<sup>3</sup> closer to discharge areas. Fluids are usually of the mixed cation composition: hydrocarbonate–chloride–sulfate. Northwestward in the flow direction, the chloride content grows, while that of hydrocarbonates decreases.

#### 10.3.2 Albian–Cenomanian Petroliferous Complex

The complex is widespread. It is separated from underlying formations by a regional relative confining bed represented by lower Albian clays.

The groundwater mineralization in the complex varies from 1 to 100 g/dm<sup>3</sup>. The northeastern part of the basin is characterized by hydrocarbonate, sulfate, and sulfate–hydrocarbonate calcic-sodic fluids with mineralization of 1–3 g/dm<sup>3</sup>. The area dominated by fluids of such type is 50–80 km wide. West- and southwestward, mineralization increases up to 50–100 g/dm<sup>3</sup> and fluids become chloride sodic in composition.

#### 10.3.3 Jurassic Petroliferous Complex

Despite lithological variations in fluid-bearing rocks, the entire Jurassic section is united into a single petroliferous complex, which is sufficiently well studied

in the basin. The occurrence depths of the complex vary from 650 to >2,100 m. Groundwaters are confined to terrigenous and carbonate–anhydrite rocks. By composition, they are chloride-sodic and chloride-calcic brines with mineralization of 70 to >340 g/dm<sup>3</sup> and high bromine content. Their temperature amounts to >100°C.

## 10.4 Influence of Peripheral Basin Areas on Fluidodynamics in Petroliferous Complexes

The role of the basin periphery that is traditionally attributed to regional recharge areas and hydrodynamic zoning is considered separately for each petroliferous complex based on the analysis of changes in reduced potentiometric levels and their gradients along the flow (Chapter 2). It would be more correct to assess groundwater expenditures, but lack of information on filtration properties of fluid-bearing rocks excludes such an approach.

### 10.4.1 Turonian–Paleocene Groundwater Complex

Figure 10.3 demonstrates changes in lateral gradients and hydrodynamic zones that are analyzed for this complex along two flow lines in the potentiometric map (Fig. 10.2). The plots are compiled in relative coordinates, which initiate in

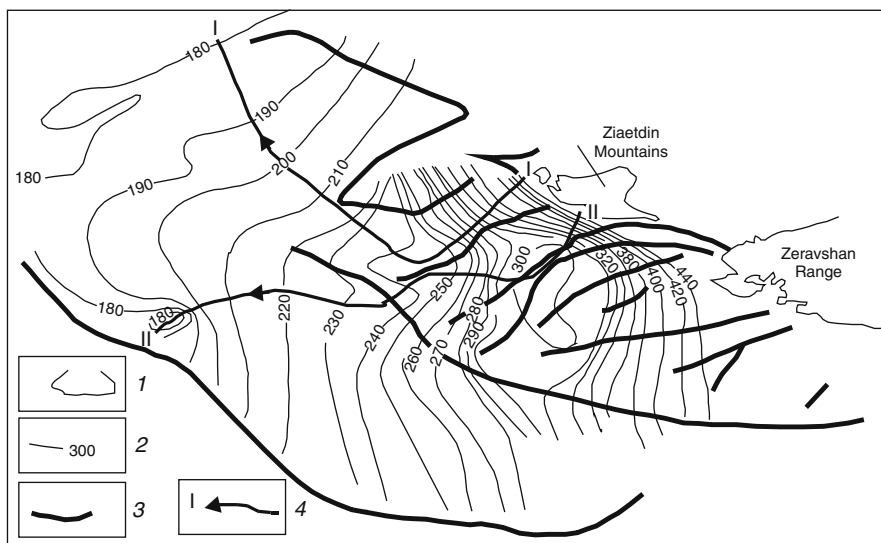


**Fig. 10.2** Schematic map of the potentiometric surface of the Turonian–Paleocene petroliferous complex, Bukhara–Karshi petroliferous basin. (1) Contour of outcropping Mesozoic sediments; (2) isolines of the reduced level; (3) faults; (4) flow lines



piedmont areas. Three zones are defined along Profile I-I. The zone with the intense water exchange (Zone I) is characterized by variations of gradients determined by surface factors: climate, river network, inner recharge, and discharge areas. This zone is only 30 km wide. Along the dip of the groundwater complex toward inner areas of the basin, the zone of intense water exchange is replaced by the zone of slow water exchange (Zone II, Fig. 10.3), where gradients and, consequently, velocities and expenditures decrease gradually, which is explained by the ascending diffused groundwater discharge through overlying clayey sequences. The zone is approximately 20 km wide, i.e., practically complete groundwater discharge is realized in a very narrow band.

Thus, the zone of the very slow water exchange (Zone III, Fig. 10.3) begins approximately 50 km away from regional present-day infiltration recharge areas. It should be emphasized that regional recharge zones occupy a band of only 50 km wide. Therefore, the Ziaetdin Mountains cannot be attributed to the regional zone of infiltration recharge and deep fluid pressure formation in the Turonian–Paleocene petroliferous complex.

Along Profile II-II (Fig. 10.3), the zone of the intense water exchange is too small to be shown at the study scale. Due to the steeper dip of layers constituting the complex, the zone of the slow water exchange is practically adjacent to surrounding orogenic structures. The zone is 30–33 km wide. Groundwaters of the Turonian–Paleocene petroliferous complex that were formed in mountainous and piedmont areas discharge almost entirely within this zone. In the inner subsided part of the complex (the zone of the very slow water exchange), gradients are characterized by extreme values (0.3 and 1.0 in point  $x/L$ , Fig. 10.3), which are related only to inner processes in deep formation, e.g., to local ascending discharge along weakened faults zones (other internal processes are also possible). The extreme gradient values are variable, although lower as compared with their counterparts in deeper petroliferous formations.

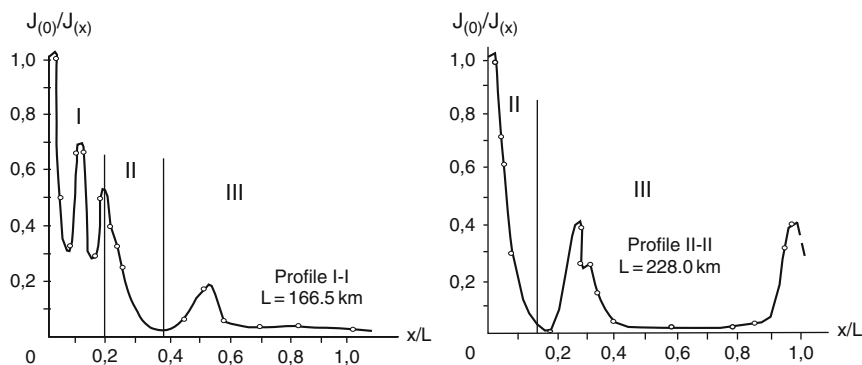


**Fig. 10.3** Changes in lateral gradients along groundwater flows in the Turonian–Paleocene petroliferous complex, Bukhara–Karshi petroliferous basin. For legend, see Fig. 9.3

### 10.4.2 Albian–Cenomanian Petroliferous Complex

Figure 10.4 demonstrates the potentiometric surface of this complex. Figure 10.5 illustrates changes in lateral gradients along the flow in the Albian–Cenomanian complex. The zone of the intense water exchange in the complex under consideration is out of the study scale. The zone of the slow water exchange, the boundary of which is drawn based on minimal gradient values along the flow line ( $x/L = 0.3$ ), occupies a band 55 km wide. The zone is marked by the practically complete ascending discharge owing to the flow (along faults as well), which determines rapid reduction of groundwater horizontal gradients in the complex at the relatively short distance.

The zone of the very slow water exchange occupies the largest remaining part of the Albian–Cenomanian petroliferous complex distribution area. This zone is also characterized by extreme values of groundwater lateral gradients amounting to 0.8 (Fig. 10.5), which is more than twice higher as compared with extreme values in the Turonian–Paleocene complex (Fig. 10.3). The growth of horizontal gradients and their extreme values can be explained by additional recharge source (all other things being the same) related probably to recent or present-day ascending migration along faults.

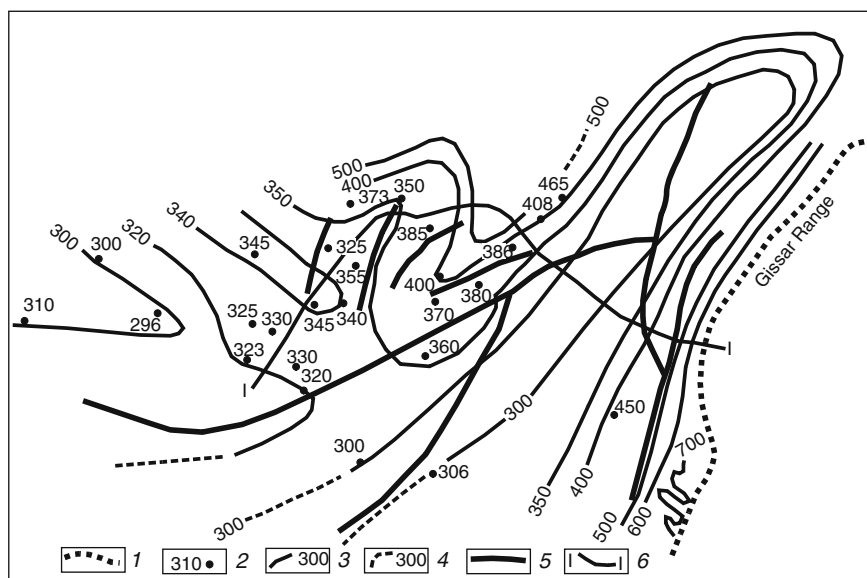
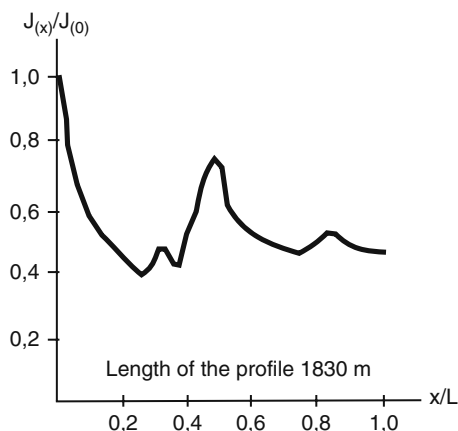


**Fig. 10.4** Schematic map of the potentiometric surface of the Albian–Cenomanian petroliferous complex, Bukhara–Karshi petroliferous basin. (1) Contour of outcropping Mesozoic sediments; (2) average altitude of the reduced level; (3) isolines of the reduced level; (4) the same, assumed; (5) faults; (6) flow lines

**Fig. 10.5** Changes in lateral gradients along groundwater flows in the Albian–Cenomanian petroliferous complex, Bukhara–Karshi petroliferous basin



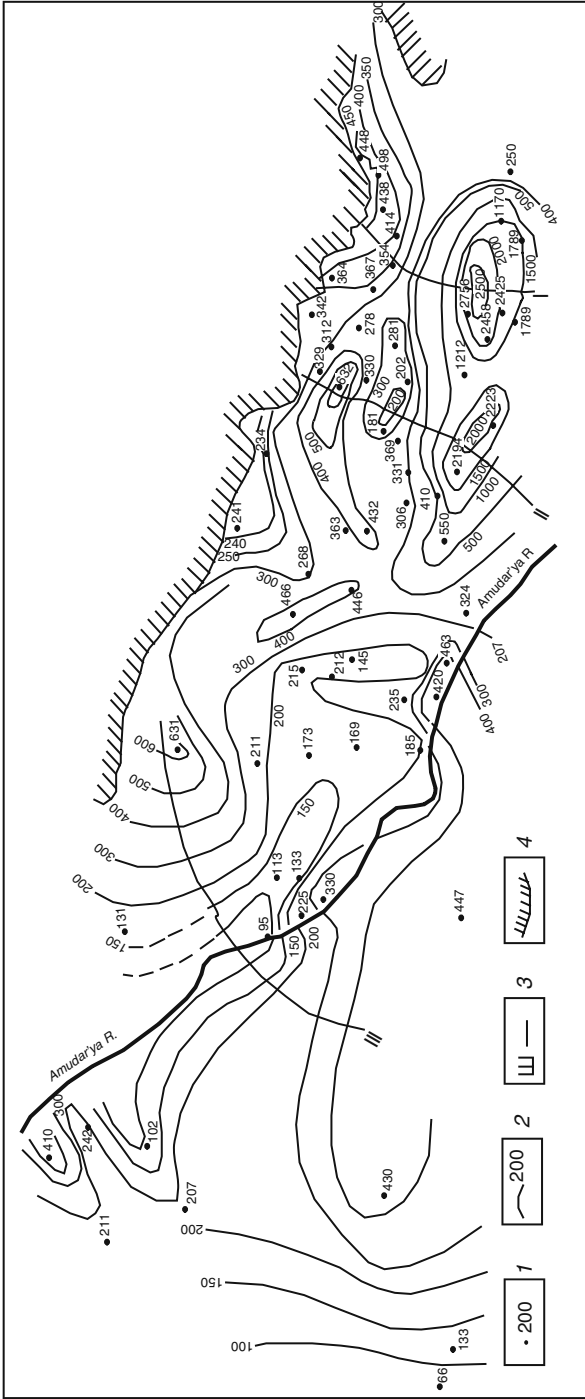
### 10.4.3 Jurassic Petroliferous Complex

Figures 10.6 and 10.7 demonstrate the schematic map of the potentiometric surface and changes in groundwater lateral gradients along the flow in the Jurassic petroliferous complex, respectively. It is seen that both intense and slow water exchange zones are poorly definable at the accepted study scale; the last zone is also located close to the basin periphery. At the same time, extreme values of horizontal gradients are so high in this complex that they cannot be shown sometimes in corresponding plots (Fig. 10.6). While extreme values of lateral gradients for groundwaters of the Turonian–Paleocene and Albian–Cenomanian petroliferous complexes are rare, deviations from the normal distribution of lateral gradients in the Jurassic complex are usual.

Thus, the deeper the petroliferous complex, the greater the contribution of internal processes to the formation of deep fluids and fields of formation pressures. In other words, deeper petroliferous complexes are characterized by reduced zones of the intense and slow water exchange as compared with overlying complexes and increased hydrodynamic anomalies down the section.

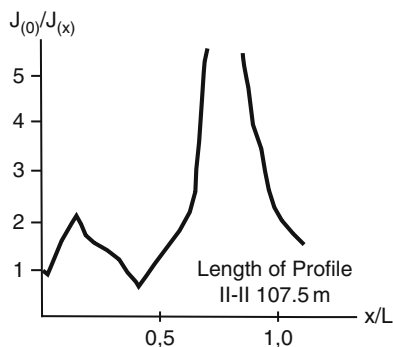
## 10.5 Local Fluidodynamics in Particular Basin Structures

Figure 2.2 demonstrates downward changes in the groundwater density for the entire petroliferous basin. These changes are highly variable through the basin: in some structures (particularly with brine occurrences) the lateral scatter of data points is so great that it prevents from using the method of pressure reducing (error exceeds scatter in measured and reduced formation pressures), in other structures the reducing error is too low or low groundwater mineralization (up to  $10 \text{ g/dm}^3$ ) makes pressure reducing unnecessary.



**Fig. 10.6** Schematic map of the potentiometric surface of the Jurassic petroliferous complex, Bukhara-Karshi petroliferous basin. (1) Average altitude of the reduced level; (2) isolines of the reduced level; (3) flow lines; (4) contour of outcropping Mesozoic sediments

**Fig. 10.7** Changes in lateral gradients along groundwater flows in the Jurassic petroliferous complex, Bukhara–Karshi petroliferous basin



Let us consider hydrogeodynamic features of individual well-studied structures.

According to hydrodynamic studies, three boreholes that penetrated Neocomian sediments in the Uchkyr field of the Bukhara–Karshi petroliferous basin show no interaction. The formation pressure in these boreholes was estimated to be 13.2 mPa or 1,320 m of the water column. Exploitation revealed also hydrodynamic independence of the Tashkuduk, Uchkyr, Yangikuduk, Gazli, Kurbanali, and Atbakor structures, i.e., deep formations are characterized by the stratum-block structure.

The difference in formation pressures measured at similar depths is highly variable (Figs. 10.8 and 10.9): the Gazli field is characterized by the normal distribution of formation pressures (although sampling depths there are insignificant ranging from 800 to 1,400 m); in the Kandym and North Mubarek fields, the pressure difference at similar depths varies from 1 to 4 mPa; in the Shartan field, it does not exceed 0.3 mPa. Such a difference in formation pressures (gradient development) at close depths in some fields confirms their stratum-block structure.

It should be emphasized that changes in the groundwater density in some fields of the basin (e.g., Mubarek field) are insignificant (mineralization  $<10 \text{ g/dm}^3$ ), which exclude errors related to formation pressure reducing. Nevertheless, they demonstrate local peculiarities in the distribution of formation pressures (Fig. 10.10), significant role of faults, and hydrodynamic isolation of structures as well. Moreover, some faults are hydrodynamically active with ascending fluid discharge, while others are impermeable (healed).

## 10.6 Abnormally High Formation Pressures

The Bukhara–Karshi petroliferous basin is characterized by relatively wide development of abnormally high formation pressures, particularly in lower parts of sections. This is primarily explained by position of the basin: it contacts the Alpine fold zone with present-day intense tectonic movements and high seismicity.

The abnormally high formation pressures are recorded in the Chardzhou Step (southern part of the Bukhara–Karshi region and areas adjacent to southwestern

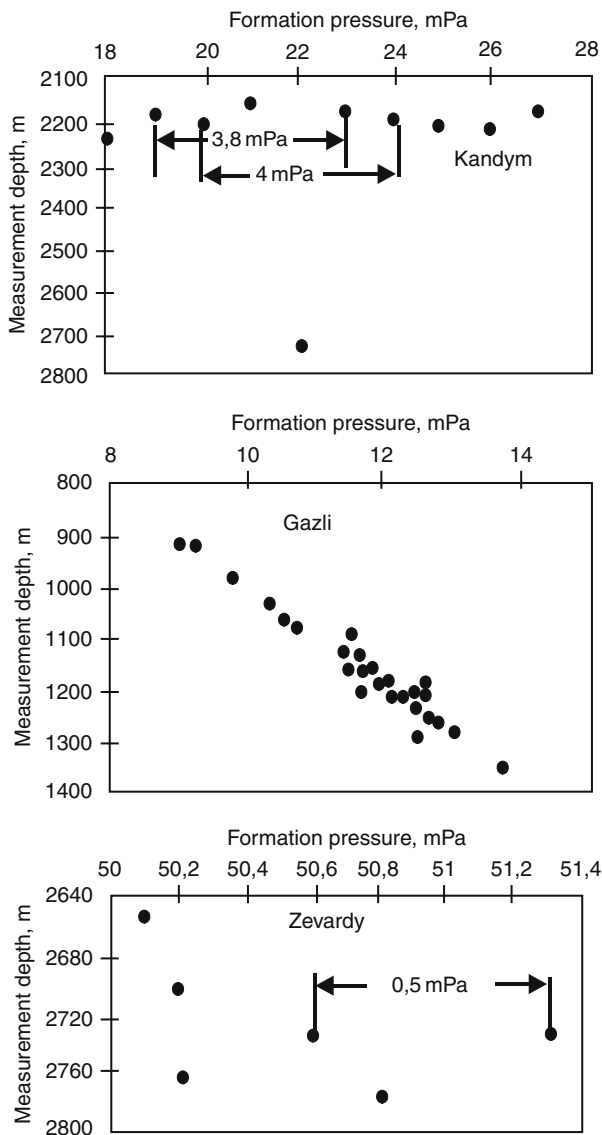


**Fig. 10.8** Changes in formation pressures measured at similar depths, Bukhara–Karshi petroliferous basin

spurs of the Gissar Range), near tectonic fractures in the Beshkent Trough, and in some areas of the Dengizkul Uplift. In these areas, drilling was accompanied by the loss of riser stability and drilling assembly sticking. They are also characterized by different-scale brine occurrences with densities amounting to  $1,330 \text{ kg/m}^3$  (Kamashi area, Borehole 3) and averaging  $1,220 \text{ kg/m}^3$ . Their mineralization is as high as 670–

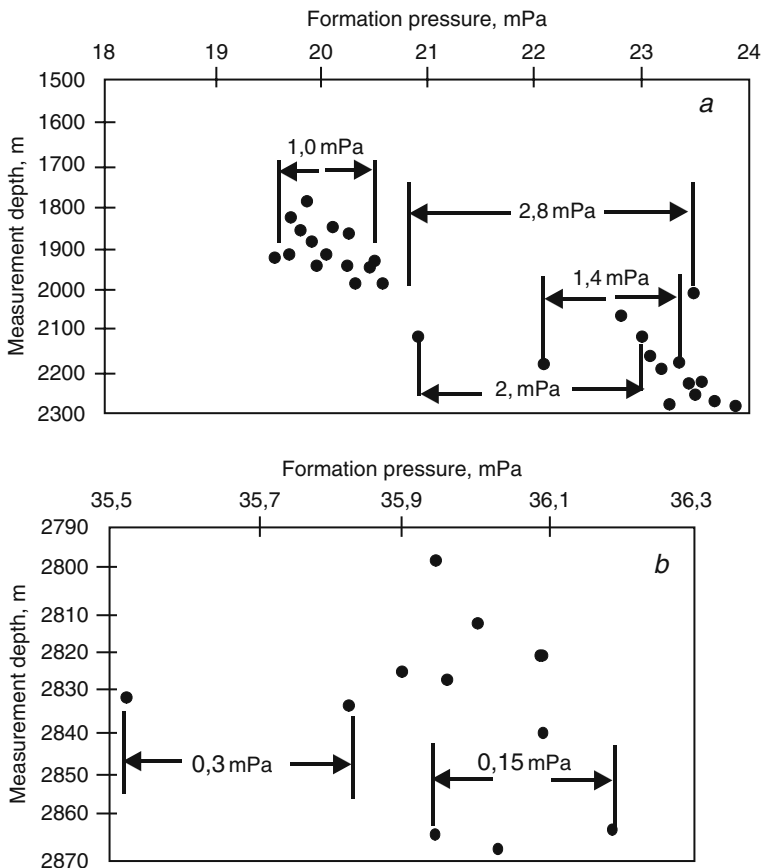


**Fig. 10.9** Changes in formation pressures measured at similar depths, Bukhara–Karshi petroliferous basin. (a) North Mubarek; (b) Shurtan

735 g/dm<sup>3</sup> (Nishan and Zevardy areas). The brine yield decreases gradually due to borehole overgrowing with salt crystals and exhaustion of reserves. The chemical composition of brines differs substantially from that of enclosing rocks and is similar in many characteristics to low-temperature hydrothermal solutions [1].

Similar to structures with abnormally high formation pressures, brine occurrences are confined to zones of deep-seated faults and their intersections. V.S. Beskrovnyi arrived at the conclusion that brines are epigenetic relative to enclosing saliferous sediments in southwestern spurs of the Gissar Range. V. Ya. Sokolov confirmed subsequently the conclusion. The last author cites data on occurrence of dissolved organic matter and hydrocarbon gases in brines as evidence supporting this inference. In all the boreholes that recovered brines, the content of hydrocarbon gases is an order of magnitude (and more) higher as compared with background values. It is of interest that anomalous gas contents as compared with

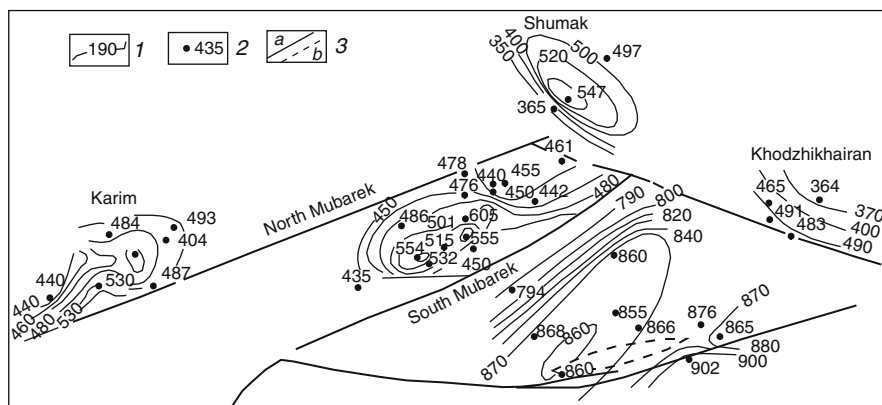


**Fig. 10.10** Schematic map of the groundwater piezometric surface in the Jurassic complex of the Mubarek group of uplifts, Bukhara–Karshi petroliferous basin. (1) Peizoisohypses of the reduced level; (2) well and reduced level value, m; (3) faults: (a) proven, (b) assumed

its background values are observable in several boreholes in salt sections 50–100 m above the brine-saturated interval (V.A. Kudyakov and T.N. Avazov) and their distribution area is strictly localized to form a linear zone. This indicates undoubtedly that vertical migration of hydrocarbon gases is realized in some geological epochs (tectonically active) through salts, which were previously considered as being completely impermeable. The vertical ascending gas flow “sometimes terminates in the salt sequence, although being always rooted at its base” (V.A. Kudyakov and T.N. Avazov). When the salt–anhydrite sequence is crossed by faults for its entire thickness, brines migrated to Lower Cretaceous sediments (Sharapli and Mary areas).

The data on hydrodynamic sampling of sub-salt sediments and intervals with brines in the salt–anhydrite sequences given below are taken from the work by I. Sh. Strelko with colleagues (Table 10.1).

**Table 10.1** Measured formation pressures and abnormality coefficients

Area	Borehole	Depth of the bed roof, m	Formation pressure at the bed roof, mPa	Abnormality coefficient
Kultakh	19	2,876	56.9	1.98
Zevardy	19	2,597	49.9	1.92
Pamuk	24	2,718	49.63	1.82
Alan	2	2,717	56.5	2.08
Kamashi	1	3,257	57.1	1.75
Beshkent	3	3,098	56.83	1.83
Nishan	3	3528	56.11	1.59



The table shows that anomaly coefficients (ratio between formation and conditional hydrostatic pressures) are high, particularly in the Alan area. Abnormally high formation pressures in Upper Jurassic sediments are of certain interest for the characteristic of the zone with the very slow water exchange. Accidents during drilling under abnormally high formation pressures in areas shown in Table 10.1 prevented from reaching planned penetration depths by 58 of 123 drilled boreholes.

It is clear that occurrence of epigenetic organic matter within saliferous sediments indicated undoubtedly that abnormally high formation pressures in the Bukhara–Karshi petroliferous basin were formed on account of alien solutions from underlying deposits during the single-stage (in geological terms) formation of vertical tectonic fractures with their subsequent healing by newly formed minerals under changed thermodynamic conditions.

Development of abnormally high formation pressures in many structures indicates hydrodynamic isolation of separate parts of the section (lateral and vertical), i.e., the stratum-block structure of fluid-hosting rocks.

At the same time, it should be emphasized that fluidodynamic isolation may be provided by some other factors, in addition to salt development in the section. The hydrodynamic study in the Gazli Uplift reveals that all the fractures (Fig. 10.1) represent screens, which is explainable by the fact that movements along them occur under compression. For example, flexure-fractured zones bordering the Gazli Uplift serve as such screens.

Exploitation and analysis of data on the regime reveal different interaction mode between separate parts of the Gazli structure in the lateral direction. The pressure difference between them amounts to 0.9 and 1.22 mPa in horizons IX and X of the Upper Cretaceous sequence.

All the wells in the Gazli structure except for those located in the flexure-fractured zones responded to the emergency flowing of Well 108 during 20 months. Formation pressures became restored after accident elimination, although this process was partial: in Well 102, the pressure decreased by 0.46 mPa to be restored by 0.1 mPa during 30 months; in Well 38, the pressure decreased during 14 months by 0.2 mPa and became restored during 10 months by 0.05 mPa; in Well 108 (emergency), the pressure lowered by 0.49 mPa and became restored only by 0.092 mPa.

The analysis of data on restored pressures demonstrates undoubtedly that accident elimination was followed only by the redistribution of formation pressures in the structure (drawdown of only elastic reserves), which implies lack of hydrodynamic connection with both recharge areas and conjugate structural uplifts. This is also evident from the neutral response of Well 5 in the Mamadzhugargaty structure located in the neighboring Kagan Uplift. All these observations confirm the stratum-block structure of deep formations in petroliferous basins.

Another example is provided by Well 3 in the Yulduzkak field. Despite the long exploitation of the Dzharak field, this well located 10 km away does not show any reaction to the disturbance. This is explained by development of two faults between these fields that play the role of screens (Fig. 10.1).

The hydrogeological role of faults is not always unambiguous. For example, the draining role of the North Rometan and Bukhara faults is established only for the southern part of the Gazli Uplift (V.N. Pashkovskii and N.L. Andreev), i.e., the same fault may be either impermeable or permeable in its different parts.

It should be emphasized that even small low-amplitude fractures can play the screening role. For example, in the South Mubarek field the pressure in the gas accumulation decreased by middle of 1969 by 2.3 mPa, while in Well 9 it remained practically unchanged. The amplitude of small fractures in this structure amounts to 10–40 m.

The list of examples of hydrodynamically isolated blocks in the Bukhara–Karshi petroliferous basin is far from being exhausted.

## **10.7 Regional Fluidodynamic Features of the Basin**

### ***10.7.1 Jurassic Petroliferous Complex***

Figure 10.7 illustrating the potentiometric surface of this complex demonstrates the tendency for its deepening from the Gissar and Zeravshan ranges along dipping fluid-bearing strata. For example, altitudes of the potentiometric level decrease from 300–600 m near orogenic structures to 100–150 m and shallower in the Khazarli and Berdeush structures. The Gissar and Zeravshan ranges are considered serving areas of regional infiltration recharge for all petroliferous complexes, the Jurassic one included.

Against such a background in inner areas of the Bukhara–Karshi basin, there are many structures with elevated formation pressures up to their abnormally high values.

### ***10.7.2 Albian–Cenomanian Petroliferous Complex***

The schematic map of the groundwater potentiometric surface in the Albian–Cenomanian complex (Fig. 10.4) reflects regional changes in its position and direction of the potential (possible) movement of fluids. Maximal values of reduced levels (altitudes 600–700 m) are confined to outcropping areas of the complex in the Gissar Range. From this area, values of reduced levels decrease along the dipping complex up to 300 m and shallower. This decrease is, however, irregular: in some areas gradients of levels are higher and in others, lower. The change in gradients may be related to both changes in filtration properties of rocks and inner processes.

### ***10.7.3 Turonian–Paleocene Petroliferous Complex***

The potentiometric groundwater surface in this complex (Fig. 10.2) demonstrates the same regularities established for the above-mentioned complexes: (1) maximal

values of levels (pressures) are confined to areas adjacent to orogenic structures (Zeravshan Range, Ziaetdin Mountains), while their minimal values are observed in inner parts of the petroliferous complex; (2) maximal gradients are characteristic of areas adjacent to regional infiltration recharge zones and decrease along the groundwater flow.

#### ***10.7.4 Main Inferences***

Differences in formation pressures measured along the same surface in natural conditions, lack of hydrodynamic interaction between structures and their individual wells, and development of abnormally high formation pressures indicate the stratum-block structure of the Mesozoic petroliferous complex.

The influence of the basin periphery traditionally referred to present-day regional infiltration recharge zones is observable only in a narrow band a few tens of kilometers wide.

The block structure restricts or, sometimes, prevents from development of regional groundwater flows in inner areas of the basin influenced substantially by internal processes, primarily tectonics, and both recent and past hydrothermal activities.

The intensity of hydrodynamic anomalies and heterogeneity in the stratum-block structure of deep formations become stronger downward.

## **References**

1. Vakin E A, Kutuyev F Sh (1979) Deep generation of the fluid component in recent hydrothermal solutions. In: Study and use of geothermal resources in volcanic domains. Nauka, Moscow
2. Vartanyan G S, Kulikov V G, Yazvin L S (1984) Groundwater system. Byul. MOIP, Ser Geol 1. 59:115–126

# Chapter 11

## Heat and Mass Transfer in Deep Formations of Petroliferous Basins

Both lateral and vertical deep fluid hydrodynamics are irregularly studied; the available data concern largely productive formations, while the remainder of the section remains unknown or poorly known with respect to its hydrogeology. Therefore, the vertical distribution of formation pressures and filtration properties is insufficiently studied.

In order to fill this gap and estimate somehow vertical hydrodynamic relationships between petroliferous complexes, some researchers compare information obtained from different boreholes (for assessing vertical gradients). Such an approach is not always justified and may lead to confusion and incorrect conclusions because of the stratum-block structure of deep formations in petroliferous basins.

Hydrochemical, geochemical, mineralogical, and other data allow us at least to understand trends in migration processes and develop new or use traditional methods for obtaining their quantitative estimates. In this connection, it is of interest to generalize available information that indicates large-scale vertical migration of groundwaters in deep formations of petroliferous basins (Chapter 14).

### 11.1 Palynological Analysis: Evidence for Vertical Migration of Deep Fluids

The study of palynomorphs indicates in most cases unambiguous direction for migration of deep fluids.

The palynological analysis conducted for several petroliferous basins (Urals-Volga, Timan-Pechora, West Siberian, Ciscaucasia, Dnieper-Donets Depression, Mangyshlak, and others) revealed wide development of vertical fluid migration. It is established [5–7] that microfossil assemblages occurring in oils, gases, and condensates from these basins differ from their counterparts in host rocks. The average share of migratory components in oils, condensates, and gases is as high as 50–80, up to 90, and >95%, respectively. “High resistance of microfossils to external impacts, their high migratory ability, and possibility for defining stratigraphic position make them reliable indicator of oil migration paths. . .” [7, p. 84].

The established fact that hydrocarbon accumulations in the Paleozoic basement formed in situ, not migrated from young sediments filling depressions to fractured rocks of positive structures, is one of the most important inferences derived from these studies.

Based on palynological data, large-scale vertical migration of hydrocarbons is established in the West Siberian petroliferous basin [7]. For example, the Jurassic productive complex in several fields (Danilovskoe, Yakhliinskoe, Pakhrom, Yashkin Yar, Salym, Em-Egovskoe, and others) yielded the Early Paleozoic microflora. Oils of the Jurassic complex contain palynological remains originating either from host or Paleozoic to, rarely, Triassic rocks. The share of migratory microfloral remains exceeds frequently 50% of their total content to reach sometimes 100%. The latter is characteristic of flank parts of the depression in the Berezovo, Shaim, and Aleksandrov districts, i.e., platform areas adjacent to the folded Urals.

In the Neocomian petroliferous complex of the Malyi Atlym field located in the immediate proximity to Atlym dislocations, the spores-and-pollen spectrum includes Lower Cretaceous (50%), Jurassic and Triassic (30%), Upper Paleozoic (10%), and Lower Paleozoic (7%) forms. In the Malyi Balyk field, microfossils are largely Cretaceous (12–15%) and Early Paleozoic (10–15%) in age. In the Megion field, their assemblage consists of dominant Early Paleozoic (75%) and Cretaceous (20%) forms. In the Albian–Cenomanian complex of the Eremenskoe area, the assemblage is represented by Cretaceous, Jurassic, and Upper Paleozoic forms (80, 5–7, and 2%, respectively). In the Em-Egovskoe area, 39 and ~50% of the palynological spectra are Cretaceous and older migratory forms, respectively.

According to [7], general regularities in the distribution of migratory microfossils are as follows:

- (1) Both autochthonous and allochthonous (migratory) components are defined in sediments from the weathering crust developed after Paleozoic to Aptian–Cenomanian rocks.
- (2) “Condensates of gas fields, Cenomanian accumulations included, that are located 3–4 km above Jurassic formations contain as well the notable share of Lower Paleozoic forms.”
- (3) Migratory elements of microfossil assemblages in West Siberia are confined to steep limbs of structures close to tectonic fractures, i.e., weakened zones with potentially better vertical filtration properties.
- (4) Abundance of migratory forms decreases upward the section.

The Middle Carboniferous strata in the Osa oil field (East Siberia) yielded palynological remains of Late Precambrian to Early Cambrian age. In this field, vertical migration involved the most part of the section.

The vertical migration confirmed by palynological data is also established for Carboniferous sediments of the Dnieper-Donets Depression, which contain Devonian forms. Hydrochemical anomalies in this area are most spread in the lower part of the sedimentary sequence becoming narrower upward the section.

It is justly noted in [22] that tectonic and seismic activity in some periods stimulates opening of vertical filtration paths, which can subsequently be filled with mineral aggregates or even by asphalt and ozokerite. The recent vertical migration of deep fluids is evident from temperature anomalies. Geothermal anomalies are manifested even at the surface (several tens of fractions of the degree). They are mapped by the IR survey and may serve as a criterion for prospecting hydrocarbon accumulations or, to some extent, defining vertical deep fluid discharge areas.

## 11.2 Anomalies in Deep Formations and Vertical Ascending Migration of Deep Fluids

When studying the distribution of hydrochemical, gas, and geothermal anomalies in several exploration areas of the Dnieper-Donets Depression, L.G. Karetnikov related them to the ascending discharge of deep fluids. Maximal values of vertical flows confined to zones of tectonic fractures are established largely in near-arch parts of positive structures, where they result in the formation of many anomalies in local structures: abnormally high mineralization, temperature, gas saturation and composition, and formation pressures.

The maximal content of water-soluble gases is observed in the fault-line zones; away from them, it decreases rapidly. For example, the content of water-soluble gas near tectonic fractures and away from them in the Novogireevsk area (Dnieper-Donets Depression) is 1857 and 60 cm<sup>3</sup>/l, respectively. Similar regularity is also characteristic of several other fields of the Dnieper-Donets Depression. Temperature is highly variable as well. In the Zachepilov, Glinsko-Rozbysh, Shebelev, and Priluki areas, temperature near tectonic fractures is 58°C, while at the same depths away from the latter, it drops to 52°C.

The southern part of East Siberia demonstrates spatial correlation between centers of brine discharge, geothermal anomalies, and faults. The vertical migration component is established for the entire sedimentary sequence and confirmed by hydrogeological and geochemical anomalies [10]. For example, migratory bitumoids are noted in salts, halogen-carbonate sediments, traps, and kimberlites. Helium of radiogenic origin occurs in carbonate rocks in concentrations close to its contents in lower formation; in surface waters, its concentrations exceed background values. Mineral anomalies are evident from the transformation of the Upper Cambrian red-colored sequence in fault zones and arches of positive structures as well as from the occurrence of epigenetic bitumen in halogen-carbonate rocks.

In East Siberia, salt is established to fill voids, caverns, and fissures in carbonate and sulfate-carbonate rocks of the Verkhne-Bel'sk Formation in the Kan-Tassev Depression and in sandstones of the lower Mot Subformation in the Nep Arch. In these areas, three stages are defined for oil migration, which left traces in the form of newly formed minerals.

The first stage is recognizable based on small bitumen inclusions in fragments of second-generation quartz, where they appear to be sealed. In addition, development

of oil corresponding to the first migration stage is evident from its occurrence in slit-like voids in completely silicified sandstones.

Oil of the second migration stage that occurs in connected voids and fissures differs by its physical properties from the previous one. The oldest pre-Vendian migration stage is established based on the occurrence of bitumoids in sandstones of the lower Mot Subformation [6]. Similar migration stages are recognized for Cambrian carbonate rocks. In northern Siberia, three oil migration stages are distinguished: pretrap, posttrap, and recent.

In fault zones and depressions of the Baikal rift zone, the heat flow exceeds 2–3 times its background values. Thermal anomalies in these areas associate with numerous springs of largely nitrogen or, locally, carbonaceous thermal springs with temperatures up to 70°C. The areas are also characterized by correlation between seismic activity and heat flow intensity. The recent stage in the formation of polymetallic (mostly Zn) ores is observable in the Transbaikal region. I.S. Lomonosov relates their formation to the present-day hydrothermal activity (ascending migration of thermal brines).

In the Nizhnyaya Kura region, some areas (Kyurovdag, Mishovdag, and others) are crossed by numerous faults of the variable strike. These areas are characterized by rapid changes in the salt composition (carbonates, sulfates, alkaline-earth metals) and mineralization. The characteristic feature of hydrochemical anomalies is their spatial localization. The areas also host mud volcanoes confined to intersections of faults. Sh.A. Panakhi explains rapid hydrochemical changes by both facies variations and stagnation of fluids in some blocks conceding, however, their vertical migration along faults.

The geochemical study of groundwater in the Fergana Depression [27] revealed that similar to West Siberia, the chemical composition of deep highly mineralized fluids in local centers of their vertical discharge is characterized by mosaic patterns.

The geochemical study of mercury and other microcomponents demonstrated that their anomalous concentrations are confined to faults being frequently associated with hydrocarbon accumulations and representing sometimes accompanying component during exploitation of oil fields (California). In areas of surface fluid discharge, mercury precipitates from solutions. Some mineral springs in the United States deliver daily to the surface 60–100, 0.2–0.3, 40–60, and 3,000–10,000 kg of B, Ge, J, and Br, respectively [26].

N.A. Filippovskii and M.R. Khamraev recorded anomalous Hg contents (up to 42–47 cm<sup>3</sup>/kg) relative to background values at depths of 15–20 m under the zone of the West Almalyk and Burdzhart faults in Central Asia. Anomalous concentrations of rare alkaline metals (Sr, B) are registered at the intersection of the regional Bukhara and local Kasan faults [4]. Anomalous Hg contents (three to seven times higher as compared with background values) are established in near-surface soil layers near Tashkent. These anomalies are spatially connected with old deep faults and their intersections with young fractures indicating vertical migration of fluids.

In the Chardzhou Step (Bukhara-Karshi petroliferous basin), grains of rock-forming minerals in sandstones and siltstones are covered by relict cement with regenerated quartz and feldspars. In this case, three stages in the migration of different-composition solutions are recognizable. The first stage was marked by

the migration of solutions enriched in Fe, which were responsible for the formation of ferrous cement. This was followed by the migration of chemically different solutions, which dissolved partly ferrous cement. At the terminal stage, migrated groundwater was enriched with silica. It should be noted that rocks contain microfissures that cross grains of rock-forming minerals and are locally displaced relative to each other. Microfissures in deformed grains are filled with secondary minerals. It seems that at some stage of the Bukhara-Karshi region development, rock-forming minerals and cement-filling voids were characterized by similar mechanical properties or even first of them were less resistant to breaking forces as compared with cement. Then, tectonic strains overcame the ultimate stress limit of rocks, which resulted in microfracturing and stimulated intense migration of solution to fill fissures.

Based on the geochemical study of Rb, Br, Ca, Sr, B, and Fe in the Samara region [13], it was inferred that origin of these elements cannot be explained in the traditional manner (by leaching, dissolution, exchange, and replacement reactions). In opinion of the last author, the only logical explanation is ascending migration of fluids from deeper crustal layers, i.e., from the basement in the situation under consideration. In the Shumovsk hydrocarbon field (Cis-Urals), the thermal, hydrodynamic, hydrochemical, gas (helium), microbiological, and palynological anomalies are localized in the same areas. This implies intense vertical migration of fluids from Devonian sediments into Permian formations.

V.I. Dvorov established that the red-colored sequence in the fault-line zones of the Cheleken Peninsula is composed of deformed sandy-clayey sediments, which were squeezed out along fractures, with secondary calcite, aragonite, pyrite, galena, sphalerite, chalcopyrite, barite, gypsum, and other minerals. The western Cheleken fault-line zone hosts travertine strata and blocks of carbonate sandstones. The fault-line zone of red-colored rocks is established to contain As, P, Mn, Pb, Sn, Ga, Mo, Sr, V, Cu, Zn, Ti, Mg, B, and other elements. Brines with anomalous concentrations of metals are localized along deep-seated faults and their feathering normal faults and brecciation zones.

Gold and sphalerite pan sampling and correlation of obtained results with the distribution of deep undercrust faults as well as thermal and hydrodynamic anomalies revealed spatial coincidence of all the anomalies (gold and sphalerite included) associated with the Carpathian Foredeep [12]. This provided grounds to the last author to conclude about the high potential of the region with respect to hydrothermal deposits of nonferrous and noble metals in the sedimentary cover of the trough.

Hydrocarbons (light oil, bitumen) are found in the form of inclusions in boulders of dolerite porphyrites from the middle Toarcian volcanic sequence (Crimea). They occur in cavities of amygdales and geodes as well as in quartz and calcite crystals. Hydrocarbons are also recorded in fluorine of endogenic origin (Mongolia).

Calcite crystals of hydrothermal origin found in the zone of the Chernye Gory Fault (northeastern Caucasus) that extends to the Moho discontinuity enclose solid bitumen, bituminous-vapor, and bituminous-vapor-liquid inclusions, which provided grounds to A.M. Nikanorov and E.O. Sainisyan to assume vertical migration, which involves the entire section, the basement included. In this connection, Nikanorov [21] emphasizes the necessity and importance of investigating



inclusions as witnesses of deep fluid migration for interpreting paleohydrogeological conditions, paleotemperatures, paleopressures, and paleohydrochemical settings.

The gas-bacterial survey allows gas composition anomalies to be defined in near-surface sediments. These anomalies are controlled by systems of tectonic fractures. The elevated or abnormally high concentrations of gases are registered in shallow boreholes located immediately above fracture zones. In opinion of V.F. Mokienko, differentiated patterns of these anomalies are explained by sizes and shapes of individual blocks. Geochemical anomalies in near-surface sediments of tectonic fracture zones in the southeastern part of the Carpathian Foredeep Inner Zone indicate their high oil-conducting properties (for example, near the Pokut Fault zone 3–4 km wide). According to the helium survey, near-surface sediments are characterized by highly variable He concentrations, which is explained by its vertical migration (Sh.Kh. Amir Khanov).

The Ukrainian crystalline massif demonstrates as well distinct and unambiguous correlation between faults, He contents in groundwater, and specific yields of wells. In areas with the thick sedimentary cover (for example, in the Galitsiya-Volyn Depression with sediments approximately 5 km thick), this correlation is less distinct.

Nevskaya and Dedeev [20] reported on numerous occurrences of spontaneous nitrogen–methane gases at the surface above hydrocarbon pools in the Timan-Pechora petroliferous province. For example, in the Layavozh field, the composition of gases at the surface is identical to that in the gas pool. Spontaneous gases discharge together with mineralized waters.

Frequent occurrences of near-surface gas anomalies and their association with faults and the latter with oil and gas fields provided a basis for developing methods (G.A. Mogilevskii and other researchers) for prospecting oil and gas accumulations using gas-bacterial data on near-surface sediments and, even, snow cover.

It is known that deep fluids, those from petroliferous formations included, discharge under different-order river valleys. The larger the river, the higher the draining potential and the deeper the parts of the section involved in its draining activity [30]. The draining effect of the river network is frequently evident from the potentiometric surface patterns of rivers such as Volga, Ob, Kuma, and others and distribution of saline water domes under their valleys. The discharge of deep fluids is sometimes so significant that mineralization of surface waters in the low water period becomes substantially higher (Nizhnyaya and Podkamennaya Tunguska, Sukhona, Volkhov, and other rivers).

The vertical ascending migration of deep fluids is also indicated by surface oil occurrences. In addition to above-mentioned occurrences (Chapter 5), they are known in the Surkhandar'ya River valley (Shakarlyk-Astana), where oil-saturated waters discharge in the form of springs. According to K.V. Babkov, the Tajik Depression hosts 21 oil occurrences in the form of seeps along fissures confined to deep-seated faults.

Surface signs of oil migration are established in the northern Aldan Shield characterized by numerous regional different-age faults. There, areas with elevated

hydrocarbon concentrations coincide with neotectonic fault zones in the basement that are also traceable in the sedimentary cover. Similar signs of surface hydrocarbon occurrences in the form of numerous deposits of asphalt-bearing rocks that indicate vertical migration are known in northwestern areas of the Samara region and western areas of the Tatar Republic [4].

E.I. Kudryavtsev found natural outcrops of dry hydrocarbon gas in the Savan hot spring area of western Kamchatka composed of Upper Neogene and Quaternary volcanogenic-sedimentary rocks 5–6 km thick. In areas of gas occurrences in prospect holes at a depth up to 2 m and excavations, water surface is usually covered by rainbow films or, less commonly, small drops of oil corresponding to its kerosene fraction. Surface oil occurrences are also reported from the eastern Ciscaucasia, Trans-Urals region, East and West Siberia, and other regions.

The borehole drilled near a large surface oil seep in the marginal zone of Lake Marakaib (Columbia) yielded an oil gusher from depth of 30 m. In this area, the entire sedimentary section is characterized by abnormally high formation pressures.

Sometimes, the vertical ascending discharge of mineralized metalliferous waters is observed in orogenic areas: in Pamirs, waters of raised lakes located at 3.8–4.2 km are characterized by mineralization up to  $>140 \text{ g/dm}^3$  being enriched in chlorine, sodium, carbonates, sulfates, and ore components of deep origin; in the South Urals, waters ascending from Riphean sediments contain many elements, hydrocarbons included, characteristic of hydrothermal deposits; saliferous sediments of the Cis-Urals contain (apart from hydrocarbons) Fe, Cu, Ni, Mn, and other metals, which are characteristic of hydrothermal solutions and recorded recently almost universally in subsurface brines [16, 17].

Intense vertical migration up to depths of 10 km is also evident from rock fragments delivered by mud volcanoes. Signs of volcanic and mud volcanism activity are established in the junction area between the Dnieper-Donets Depression and the Donets Ridge, in West Siberia, and other regions. The Azerbaijan territory hosts 52 gas-volcanic centers, which erupted 145 times since 1810.

Considering anomalies that accompany vertical migration, it is necessary to dwell on the sufficiently well-substantiated concept explaining the formation of brines, saliferous sediments, and related abnormally high formation pressures. According to this concept proposed by V.A. Krotova, brines represent derivatives of saliferous sediments, while the latter result from the intrusion of high-temperature brines from underlying formations, which appear to enter different thermodynamic conditions (lower pressure and temperature), when salt concentration in subsurface fluids exceeds the solubility limit (under changed thermodynamic conditions). In this situation, salts precipitate to cement host sediments and form inclusions, lenses, intercalations, and thick salt beds.

According to T.I. Gurova, salinization in the form of salt precipitation in voids, caverns, and fissures is widely developed in East Siberia to involve sulfate-carbonate rocks of the upper Bel'sk Subformation and Usol'e Formation in the Kan-Tassev Depression and sandstones of the lower Mot Subformation in the Nep Arch, where salt cements rock fragments to significantly reduce primary porosity of rocks.

In the North Caspian Depression, arches of salt domes are characterized by variable shapes. Along their peripheral parts, there are cornices with the under-cornice zones characterized by steep dip angles. These facts indicate indirectly powerful breakthrough of salts from below, which intrude similar to magma the sedimentary sequence to form variably shaped bodies and transform substantially host rocks.

In their numerous works, V.A. Krotova, V.F. Derpgolts, and N.A. Kudryavtsev note paragenetic relation between brines and saliferous sediments. The latter are characterized by the maximal thickness in zones of deep-seated faults widely developed near orogenic structures and in troughs (for example, in the Bukhara-Karshi petroliferous basin).

Areas complicated by the salt-dome tectonics adjacent to the rift zone (southern Siberian Platform) are characterized by the anomalous heat flow 1.5 times exceeding its background values. This may be explained by posthydrothermal activity. The Dnieper-Donets Depression hosts salt stocks that intrude Devonian to Upper Permian sediments. The salt stocks are developed along faults and weakened zones that determine their extremely capricious shapes. Locally, Devonian salts occur among younger sediments, for example, separating Upper and Lower Permian strata and resembling stratiform intrusions.

In the Bukhara-Karshi petroliferous basin, the Mesozoic anhydrite-gypsum sequence and related brines are developed in zones of deep-seated faults being controlled by them. Abnormally high formation pressures are also confined to lower parts of salt sequences in these zones. Anhydrite, calcite, dolomite, and other minerals are secondary. The halite behavior is lithology independent. It occurs in sandstones, secondary anhydrites, calcareous clays, although tending to the basal part of the red-colored sequence. Brines of the Jurassic saliferous sequence contain Pb, Zn, Fe, and Rb (up to 2.7, 15, 4, and 35 mg/dm<sup>3</sup>, respectively) as well as hydrocarbons.

The brine output amounts to 2,000 m<sup>3</sup>/day to be reduced rapidly and stops after 10–15 days [18], which indicates the block (lenticular) structure of brine-bearing formations of the section.

The sequence manifests also oil and gas occurrences in Jurassic saliferous sediments. For example, dispersed hydrocarbons and bitumens are found in the Kirpichli field. Direct signs of oil and gas are established in the Gaurdak, Southern Iolotan, and other structures. Thus, saliferous sediments may be permeable in some periods of geological history.

It is of interest that Lower, Middle, and Upper Jurassic terrigenous and carbonate rocks in brine-bearing structures contain brines as well. In some structures (Bairam Ali, Dzhimkumy, Mary, Keli), brines also occur in overlying Neocomian red-colored sediments, where their mineralization is as high as 337–443 g/dm<sup>3</sup>. Brines in Cretaceous formations are analogous to their counterparts in Jurassic sediments. They are also characterized by high concentrations of Rb, Zn, Pb, As, Ag, Sn, and other elements [25], which indicates undoubted genetic affinity of brines in the subsalt (Jurassic) and Neocomian sediments.

The salt thickness is variable even within a single structure, which excludes the possibility of their uniting into particular beds. The above-mentioned and other

features allowed D.S. Ibragimov and K.A. Sabirov to state that salts are derivatives of superconcentrated brines that intruded the Mesozoic sediments of the Bukhara-Karshi petroliferous basin from deeper formations. It is difficult to refute this inference.

Using the Hassi-Messaoud field (Algeria) as an example, M. Ulmi and other researchers argue for the possibility of deep fluid migration from the saliferous sequence occurring under the overburden load and characterized by abnormally high formation pressures. In opinion of M. Ulmi, migration involves the entire section, the basement included, to form hydrocarbon accumulations with abnormally high formation pressures in the basal part of the sedimentary sequence. The same process is responsible for the formation of oil pools confined to Jurassic bituminous clays and basement rocks in West Siberia. This inference is based on the following considerations. The content of secondary gypsum and anhydrite forming interbeds in Cambrian sediments resting upon basement rocks and composed of gravelstones and sandstones increases upward the section. The maximal abundance of interbeds and the quantity of these minerals are observed below the overlying sequence consisting of clays and halogen sediments (up to 40%). These facts may also be interpreted in the other manner, i.e., as influence of ascending migration.

Signs of vertical migration are established in saliferous sediments, which are traditionally considered to be impermeable due to their plastic properties. Periods of tectonic activity are accompanied by fracturing and formation of vertical well-permeable zones, which serve as paths for ascending fluids and temporal hydrodynamic connection between different parts of the section in petroliferous structures.

Antsifirov [3] reported on such a migration in saliferous sediments of the Irkutsk Amphitheater, where the Lower Cambrian Usol'e Formation is composed of rock salt with anhydrite and dolomite interbeds frequently >1,000 m thick in total. The thickness of the formation exceeds 1,400 m. Structural-prospecting boreholes drilled in the Balakhta area recovered oil and gas occurrences most intense in the middle and upper parts of the formation.

For example, one of the boreholes yielded the gas gusher at the rate of 1,70,000 m<sup>3</sup>/day preceded by gas and drilling mud blowouts. The gas pool is localized in the anhydrite–dolomite member 4 m thick. This member is traceable through the entire structure, although gas is obtained from the only borehole, which indicates impermeable vertical boundaries determined by secondary mineral formation and lack of lateral migration. Drilling in this area revealed small gas accumulations in salt domes, the recovery of which is accompanied by oil and gas blowouts. Similar oil and gas occurrences are registered in the Atov, Parfenov, Osa, and other areas of the Irkutsk Amphitheater. Their development in thick saliferous sequences is explainable only by intermittent ascending paleomigration of gas–water–hydrocarbon mixture with its subsequent differentiation (separation of constituents) and phase transitions that provide fissure self-healing.

The list of examples confirming relationships between faults, saliferous sediments, brines, hydrothermal mineralization, and oil and gas occurrences is far from being exhausted. Despite different interpretations of factual material, it is undoubted

that recent data indicate the possibility of vertical migration of deep fluids from the crust and upper mantle.

Until now, the hydrogeological role of faults remains unclear to significant extent. This is particularly true of areas with wide development of thick poorly permeable sequences. Nevertheless, recent studies demonstrate that faults are complex geological objects with different parameters. Brecciation zones are up to 40 km wide, 200–2,000 km long, and up to 50 km deep. These zones are complicated by fractures and folds and characterized by prolonged multistage development. Thicknesses and lithological-facies composition of rock within them experience substantial variations. This is particularly true of deep-seated faults.

Nowadays, active faults represent one of the prospecting criteria. For example, L.P. Dmitriev and other researchers relate hydrocarbon accumulation to regional faults. In addition, they consider large faults to be one of the oil and gas prospecting features, which narrow first-priority potential areas and increase efficiency of geological-prospecting works. This is also emphasized in [31], where petroleum recourse potential of individual structures, the Prirakovskii oil field included, was estimated based on the detailed neotectonic study of the area. These estimates were subsequently confirmed by drilling. A.A. Tereshchenkov and other authors proceed even further and argue that lack of information on fractures leads to delay (up to 5 years) in the development of fields, since significant share of financial resources is spent for structural drilling, which results in substantially lower efficiency of geological-prospecting works.

Recognition of active and abandoned fluid dynamic zones is an important task in prospecting brines, oil, gas, and other mineral resources related to ascending migration of hydrothermal solutions. Centers of internal hidden discharge of subsurface fluids point to such areas [11, 16, 17].

Thus, relations between hydrodynamic, hydrochemical, geochemical, and other anomalies confirming vertical ascending movement of deep fluids are noted for many areas in Russia and other countries [2, 9, 10, 17, 23, 31] and these observations should be taken into account when studying fluid dynamics of deep formations in petroliferous basins.

The past vertical migration left behind various signatures: secondary formation of various minerals; catagenetic (sometimes different-age) alteration of sedimentary rocks, which are characterized by local development and distinct vertical patterns frequently independent of lithology; older palynomorphs in younger sediments; hydrothermal mineralization; and hydrochemical and other anomalies.

The recent ascending migration of fluids is evident from different features: (1) domes of salt waters under large draining river valleys (Volga, Kama, Volkhov, East Siberia rivers); (2) surface oil occurrences (Timan, Tajik Depression, Transural region, eastern Ciscaucasia, Samara Volga region, Tatar Republic); (3) lowered potentiometric surface of deep fluids under valleys of first-order rivers (Ob, Kuma); (4) correlation between different anomalies (gas, thermal, hydrochemical) and spatial position of different-order faults; (5) near-surface gas anomalies above arches of positive structures; (6) changes in coloration of rocks occurring at the surface

above positive structures; (7) development of mud volcanism, which involves the significant portion of the sedimentary section; (8) some types of saline, mineral, and thermal springs with specific components of endogenic origin.

Such an extensive (far from being complete) empirical material is mentioned not incidentally but to emphasize that despite some references in publications, the vertical migration of deep fluids still receives insufficient attention. Some theoretical considerations and available extensive empirical materials imply that vertical migration of fluids (water, oil, gas) in deep formations of petroliferous basins prevails over the lateral one and at the regional scale represents, probably, the only movement trend. The role of lateral migration is insignificant being limited probably to separate structures or tectonic blocks [1, 8, 9, 12, 13–15, 19, 29, 31].

It is evident that the equilibrium fluid dynamic system is free of any changes. When such changes are observable, for example, in the form of mineralogical and other anomalies, the system was (is) open and received(es) additional matter. Inasmuch as the role of peripheral areas is negligible, matter could originate from the basement, which represents a connecting link between sedimentary cover, crust, and upper mantle. The influx of matter due to hydrothermal processes leads to distortion of the thermodynamic equilibrium in the solution–gas–rock system. This should result in either dissolution of the solid phase or precipitation of excessive matter from solutions, i.e., formation of new minerals. Registering newly formed minerals in rocks (particularly superimposed on each other), we may confidently state that alien geochemically unbalanced solutions intruded into the study section at some stages of its development. Superimposed newly formed minerals indicate several migration stages of fluids and multiple replacements of geochemical and thermodynamic conditions within the particular interval of the section, which allow inference on recurrent fracturing and fissure healing.

Depending on previous geochemical and thermodynamic condition, fissuring could be healed partly or completely through the entire thickness of the fractured zone or in some of its interval. Formation intensity of new minerals is determined by gradients of concentrations, pressures, and temperatures as well as by lithological–mineralogical properties of host rocks and their spatial changes, all other factors being equal.

It can be expected that under constant gradients of concentrations, pressures, and temperatures, insignificant changes in geochemical conditions and, consequently, formation of prerequisites for precipitation of the solid phase from solutions occur at transitions between different lithological and mineral varieties of host rocks (geochemical barriers). Since the composition of rocks in the vertical section is most variable (for example, replacement of limestones by siltstones, dominant quartz sandstones by feldspar varieties, and others), the geochemical setting and intensity of fissure healing is similarly highly variable at lithological-facies boundaries.

The same solution may form geochemical system equilibrium and nonequilibrium relative to host rocks, which determines the fissure healing degree (partial or complete). Sometimes, fissures may remain open. It means that the vertical section may comprise alternating well-permeable, poorly permeable, and impermeable intervals. Fracturing or tectonic strains exceeding the resistance limit of particular

lithological rock varieties in the alternating system of sedimentary cover is one of the main factors providing fissuring-induced permeability.

Migration of nonequilibrium solutions, which brings additional matter, is responsible for fissure healing. Wide development of healed fissures (similar to interstice capacity) and formation of new minerals particularly in the lower part of the section imply intense migration of alien solutions.

### 11.3 Main Inferences

The analysis of extensive factual material allows the following regularities to be defined in the formation of deep fluids: the stratum-block structure and hydrodynamic isolation of blocks in both lateral and vertical directions; lack of regional (lateral) deep fluid flows, which are expected only in separate parts of the basin (blocks, structures) at distances of a few kilometers.

In this connection, the use of the term “aquifer or petroliferous complex” in case of deep formations is not quite valid since a single aquifer (petroliferous complex) comprises numerous areas (blocks) with different formation conditions of deep fluids.

In inner subsided parts of sedimentary sequences, near-vertical ascending migration along faults and weakened zones is the only kind of deep fluid movement. This vertical ascending migration is realized along faults regardless of surrounding hydrodynamically isolated blocks or in fluid dynamic interaction with them. Both behavior types are determined by geological development, primarily by tectonics, lithological–mineralogical peculiarities of host and overlying rocks, properties of migrating hydrothermal solutions, and syngenetic subsurface fluids.

Vertical migration plays the main role in migratory processes of deep fluids. Most favorable paths for the vertical migration are faults, arches of positive structures, periclinal, steep folds, flexures, weakened zones, and other structures, which are accompanied by linear near-vertical zones with elevated fissuring. The “fluid and gas breath” [11, 24] of the crust and mantle [12, 14, 15, 28] represents a feeding source for the vertical migration.

Classical concepts of the lateral fluid dynamic unity of aquifers (petroliferous complexes) and the existence of regional deep fluid flows should likely be rejected. Efforts should be aimed, instead, at the study of fluidodynamic and hydrogeochemical regularities in individual structures and areas, which should be followed by regional generalizations. Only such an approach based on hydrogeological criteria is reliable and efficient for prospecting mineral resources, oil and gas fields included.

### References

1. Anikeev V A (1964) Abnormally high formation pressures in oil and gas fields. Nedra, Leningrad
2. Anikeev V A (1980) Geodynamic theory of superhigh formation energy of drilled oil- and gas-bearing Earth interior. In: Earth degassing and geotectonics. Nauka, Moscow

3. Antsifirov A S (1963) On migration of hydrocarbons through rock salt. *Neftegazovaya geologiya i geofizika* 10:25–36
4. Atamanyuk N I, Krupskii Yu Z, Ermakova V I (1979) Geochemical criteria of oil and gas permeability of fractures. *Neftegazovaya geologiya i geofizika* 8:25–28
5. Chepikov K R, Ermolova E P (1980) Authigenic minerals from Lower Cretaceous sediments of the Prikumsk petroliferous area as indicators of oil accumulation age. In: *Rock reservoirs of oil and gas*. Nedra, Moscow
6. Chepikov K R, Ermolova E P, Medvedeva A M (1980) On oil migration in Vendian and Cambrian sediments of the Nep-Botuoba Anticline. In: *Rock reservoirs of oil and gas*. Nedra, Moscow
7. Chepikov K R, Medvedeva A M, Klimushkina L P (1980) On autonomous position of the Paleozoic complex in West Siberia based on palynological analysis of oils. In: *Rock reservoirs of oil and gas*. Nedra, Moscow
8. Djunin V I (1985) Investigation methods of the deep subsurface flow. Nedra, Moscow
9. Dzyuba A A (1977) Recent hydrothermal activity on old platforms. In: *Hydrothermal process in regions of tectono-magmatic activity*. Nauka, Moscow
10. Isaev V P, Rukavishnikov I I (1977) Role of lateral and vertical migration during oil and gas formation in the southern Siberian Platform. *Trudy ZapSibNIGNI* 118:8–15
11. *Journal of the All-Union Mendeleev Society* (1986) 31:482–600
12. Kardash V T (1977) On relation of sedimentary ore genesis in the Ukrainian Carpathians and magmatism. *Dokl AN USSR* 7:596–600
13. Kozin A N (1978) Influence of the endogenic factor on formation of stratal chloride waters. *Geologiya i geokhimiya grouchokh iskopaemykh* 50:16–22
14. Kropotkin P N (1986) Earth degassing: and genesis of hydrocarbons. *Zhurn Vsesouz Mendeleev ob-va* 31:540–547
15. Kropotkin P N, Valyaev G M (1979) Concealed faults and Earth degassing. In: *Tectonic evolution of the crust and faults*. Nauka, Moscow
16. Krotova V A (1974) Interrelations between hydrogeological and tectonic factors and their influence on the formation and distribution of hydrocarbon accumulations. *Trudy VNIGRI* 348:8–17
17. Krotova V A (1978) Integrity of subsurface fluids and geotectogenesis. In: *Problems of hydrogeology and engineering geology*. Nauka i Tekhnika, Minsk
18. Kushnarev M V, Pashkovskii V N, Begmetov E Yu et al (1972) Projection of brine occurrence in the Bukhara-Khiva region. In: *Geology of petroliferous deposits in western and southern Uzbekistan*. Tashkent
19. Nesterov I I, Ryl'kov A V, Kulakhmetov N Kh et al. (1977) Scales of oil and gas migration in Mesozoic sediments of West Siberia. *Trudy ZapSibNIGNI* 118:3–8
20. Nevskaya N M, Dedeev V A (1973) Geothermal and hydrodynamic peculiarities in the sedimentary cover of the Pechora Syncline and their relation with endogenic processes. *Trudy VNIGRI* 338:63–70
21. Nikanorov A M (1977) Vapor-liquid inclusions in minerals as a basis for paleohydrogeological reconstructions. *Dokl AN BSSSR* 21:839–842
22. Romanyuk A F, Subbota M I, Kleimenov V F (1977) Migration distance of lateral and vertical hydrocarbon migration in the Dnieper-Donets Depression. *Trudy ZapSibNIGNI* 118:81–86
23. Rustamov R I (1993) Results of hydrodynamic studies obtained during exploration of oil fields in the Srednyaya Kura Depression. *Crucial problems of petroleum hydrogeology*. Nauka, Moscow
24. Sarkisyan S G (1977) Influence of fluid and gas “breath” on post-sedimentary transformations of sedimentary sequences. *Trudy IGIRGI* 21:85–95
25. Sokolovskii L G, Sedletskii V I (1970) Geochemical peculiarities in origin of highly mineralized brines in southern Central Asia. *Sov Geol* 7:101–112
26. Sukharev G M (1979) Hydrogeology of oil and gas fields. Nedra, Moscow
27. Taliev S D (1976) An example of seismicity influence on vertical migration of fluids and localization of hydrocarbon accumulations. *Trudy VNIGRI* 387:125–137



28. Vakin E A, Kutyev F Sh (1979) Deep generation of the fluid component in recent hydrothermal solutions. In: Study and use of geothermal resources in volcanic domains. Nauka, Moscow
29. Valyaev B M (1987) Geodynamic aspects of deep hydrocarbon degassing. Doctorate dissertation (Geol.-Mineral.). GIN RAN, Moscow
30. Vsevolozhskii V A (1991) Basics of hydrogeology. MGU, Moscow
31. Zapivalov N P, Polkanova V V (1979) Neotectonics and petroleum resource potential of southern West Siberia. *Geologiya nefi i gaza* 12:48–57

## Chapter 12

# Genesis of Boundaries Forming the Stratum-Block Structure of Deep Formations in Petroliferous Basins

The study of lateral and vertical fluid dynamics in stratified systems of petroliferous basins (eastern Ciscaucasia, West Siberia, Central Asia, Timan-Pechora Province) was accompanied by the analysis of formation pressures in over hundred hydrocarbon accumulations as well as mineral and industrial waters in several thousands of boreholes.

The main inferences derived from this analysis are the following:

(1) All the study regions and most oil and gas fields (structures) are characterized by differently oriented lateral gradients of formation pressures, which differ frequently by their values (in addition to direction). There are also structures free of such gradients such as the West Meketebe in eastern Ciscaucasia, Gazli in Central Asia, and other fields. Moreover, different orientations of gradients are registered for both reduced values and formation pressures measured at the same depths of some fields, which excludes probable errors related to pressure reducing to the single comparison surface under changed fluid density.

(2) Different orientations of gradients indicate the heterogeneous field of formation pressures and are inconsistent with concepts of the regional lateral movement of deep fluids over large distances. In addition, they point to lack of possibilities for relaxation of formation pressures in the fluid-saturated medium. Consequently, the field of capacity and filtration properties should include areas or differently oriented poorly permeable or impermeable zones.

(3) Deep formations of stratified systems in petroliferous basins should be considered as a system of relatively isolated blocks (stratum-block structure). The block is a fragment of the section partly or completely isolated with respect to its fluidodynamics from its adjacent parts [2, 3, 7]. This is particularly well illustrated by areas with abnormally high formation pressures, which are recorded in all the regions under consideration. The stratum-block structure of stratified systems degrades upward the section, which is reflected in the increase in block sizes.

Development of extremums (piezominimums and piezomaximums) in the field of formation pressures in deep stratified systems of negative structures associated with some of their blocks poses at least three questions:

(1) What processes are responsible for the formation of impermeable or poorly permeable boundaries in lithologically relatively uniform and coeval sediments of petroliferous complexes occurring at large depths?

(2) Are there internal recharge and discharge areas, which provide complex flow patterns and what is their nature?

(3) What processes hinder relaxation of formation pressures even within individual blocks with distinct boundaries (for example, tectonic boundaries with displacements, amplitude of which is comparable with the thickness of petroliferous complexes)?

The first and principally important question concerns factors responsible for relative isolation of blocks in the stratified system, i.e., nature of boundaries (the second and third questions are discussed to different extent in Chapters 11 and 13).

The analysis of materials on geology, tectonics, lithological–mineralogical properties of rocks, history of geological development, and hydrogeology allows the following types of boundaries to be defined at the current (initial) stage of the study: tectonic, lithological-facies, mineralogical–geochemical, and fluid dynamic. The existence of these boundary types is real for every region, although each of them is rare in its “pure” form. Of course, typification of these boundaries is incomplete, since it reflects only the initial stage of their study. Further investigation in this direction may help in more reliable determining and substantiating their genesis. The study of these boundaries is a crucial task since their knowledge will enhance efficiency of geological-prospecting works for oil and gas and contribute much to development of mathematical hydrodynamic models for exploitation of oil and gas, industrial, mineral, and thermal water deposits.

The *tectonic type* of boundaries is divisible into several subtypes.

The first subtype is represented by fractures with displacements, the amplitude of which amounts to tens and hundreds of meters being comparable with the thickness of a petroliferous complex. In this case, the displaced block may contact in plan with impermeable or poorly permeable rocks.

Boundaries of this subtype are most characteristic of marginal troughs and platform structures adjacent to the Alpine orogenic zone (eastern Ciscaucasia, Bukhara–Karshi petroliferous basin, Kura and Fergana depressions). In addition, they occur in junction zones between structures of the second and higher orders. For example, the East Kolva and Varandei faults separate the Khoreiver Depression from the Kolva Megaswell and Sorokin Swell (Pechora petroliferous basin) with the displacement amplitude up to 800 m. It is natural that blocks should be isolated from each other with respect to their hydrodynamics. In the Ciscaucasia and Bukhara–Karshi regions, displacement amplitudes are several hundreds of meters as well.

The second subtype of tectonic boundaries is observed in areas, where tectonic fractures with low displacement amplitudes or lacking them at all are formed under compression. In this case, brecciation of rocks is accompanied by squeezing out of rock fragments into the interstitial and fissure space, their dissolution, and transformation into cementing mass. Compression reduces point contacts and stimulates formation of their convex–concave varieties, which results in deteriorated capacity and filtration properties of rocks. In addition, compression reduces porosity and permeability by 12 and 300% relative to their initial values, not to mention physicochemical transformation of rocks. All these processes are well known and partly

described in Chapter 6. Thus, compression zones can be considered frequently as relatively impermeable boundaries.

The third subtype of tectonic boundaries associates with extension zones. Contrary to the second subtype, these zones are characterized by elevated values of capacity and filtration parameters and may serve as paths for deep fluid draining. Owing to such properties, the zone represents a peculiar hydrodynamic boundary similar to the boundary in the groundwater flow under the drain or in the watershed. At the same time, the formation of boundaries in extension zones may be related to other processes: for example, fissure interstitial space healing by newly formed minerals.

Near-vertical zones with anomalous physical properties termed as fracturing or brecciation or seismically strained zones are readily definable in most seismic records of many regions [10, 11, and others].

*Lithological-facies boundaries.* The sedimentary facies medium [3, 5, 15] is characterized by sharp anisotropy of filtration properties in lateral and vertical directions, which is determined by both sedimentation conditions and diagenetic (catagenetic) processes.

The zones with elevated capacity and permeability are largely connected with erosion of poorly permeable rocks and facies replacement of clayey sediments by coarse-grained material confined to peripheral parts of stratified systems in negative structures or arches of inner uplifts.

When structures of the second and higher orders are inherited, their features are traceable through the entire sedimentary cover determining their thorough character [14].

Positive synsedimentary local structures demonstrate regular changes in main lithological parameters: the median size of grains increases toward their arches, while the clay content increases toward their peripheral parts. Therefore, arches of positive structures and cores of folds are characterized by elevated porosity, which is frequently accompanied by increase in abundance of sandy beds in the section (Fig. 12.1).

In this connection, periclinal and negative structures may be considered as representing poorly permeable boundaries.

Local structures are also influenced by tectonics, which is reflected in more intense fissuring in arched parts of its positive varieties. In this case, the character

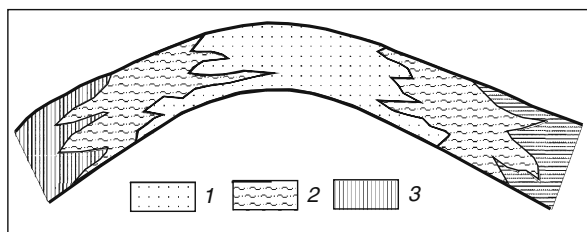


**Fig. 12.1.** Principal model demonstrating lithological changes in terrigenous sediments of positive structures. Sediments: (1) largely sandy, (2) sandy-clayey, (3) largely clayey

and intensity of fissuring should be considered as resulting from superposition of sedimentary and tectonic processes.

Coeval members of the Pechora petroliferous basin contain different-facies rocks replacing each other in the lateral direction. In carbonate sequences, they form either facies belts or isolated banks. Terrigenous complexes include different-lithology rocks related to coastal zones, channels of paleorivers, underwater fans, and other structures. The facies replacement in carbonate complexes occurs usually at distances of hundreds of meters to a few kilometers; the thickness of facies amounts to 1 km. In terrigenous complexes, facies up to a few hundreds of meters thick demonstrate changes at distances from a few meters to a few kilometers [8].

Particularly rapid facies variations are observable in the upper Frasnian–Tournaisian largely carbonate petroliferous complex of the Pechora basin. It comprises both wide belts of shallow-shelf sediments and narrow reefogenic zones (a few kilometers wide). Reef buildups are characterized by best filtration–capacity properties among carbonate formations and form highly permeable bodies up to several hundreds of meters thick, which grade into carbonate sediments of the rear part of the shelf, and are rapidly replaced by fore-reef complexes in their frontal parts [8].

The filtration–capacity properties of reef zones deteriorate rapidly seaward and in straits between reef buildups. No such rapid deterioration is observed in the zone of transition to ordinary shelf sediments.

The real situation with changes in filtration properties is even more complicated. Reefs may represent both linear structures extending along the shoreline (barrier reefs) or solitary buildups (reef banks). Reefogenic buildups in the Central Khoreiver Uplift area form chains consisting of separate structures separated by straits filled with poorly permeable sediments.

In addition, it is established recently that central and southern parts of the Khoreiver Depression host numerous solitary reefogenic banks (North Khosedayu, Bagan) with highly permeable complexes surrounded by low-filtration depression sediments. Reefogenic complexes are registered in Silurian, Upper Devonian, Carboniferous, and Permian sequences of the northern Pechora petroliferous basin.

In terrigenous complexes, significant changes in filtration properties are more rapid. Initially, zones with elevated capacity and filtration parameters associate with paleoerosion areas, belts of coastal sandstones extended along the shoreline and replaced seaward by clayey siltstones and argillites, and arch parts of paleouplifts.

The Pechora petroliferous basin hosts very narrow shoestring bodies of sandstones accumulated in former river channels as well as complex underwater fans formed at the transition from shallow to deep areas. In fans, best filtration properties are characteristic of rocks from their upper parts.

In some local structures, tectonic processes are frequently reflected in intense fracturing of fold arches. This is particularly evident in arches of local uplifts, where fissure-related permeability demonstrates variations of two to three orders of magnitude for both carbonate and terrigenous rocks.

The sedimentogenic lithological-facies heterogeneity is superimposed by processes of irregular geostatic compaction during rock subsidence. Elements of the section with elevated contents of clayey material (limbs, periclinal of positive

structures, and interstructural areas) experience maximal compaction, while arches of positive structures with dominant coarse-grained material that is characterized by the lower compaction coefficient are less subjected to such changes.

The aforesaid implies existence of numerous lithological-facies boundaries within petroliferous complexes. In addition, differences in lithology and grain size of material determine the degree and trend of secondary transformations of sedimentary rocks.

Thus, lithological-facies boundaries are observable in all the lithologies, carbonate rocks included: for example, in development zones of reefogenic buildups, which are characterized by sharp boundaries, local distribution, and high capacity and filtration parameters. This is a peculiar type of lithological-facies boundaries that separate zone with substantially different rock permeability.

*Mineralogical–geochemical boundaries.* These are differently oriented zones (horizontal, vertical, and others), where interstices and fissures are partly or completely filled with secondary minerals. Development of secondary minerals is evident from many features. The existence of such boundaries is confirmed by the following facts:

- (1) close location of “dry” and productive wells drilled in lithologically uniform and coeval rocks of narrow section intervals at a distance of a few hundreds of meters;
- (2) lack of fluidodynamic interaction between wells exploiting the same productive formation;
- (3) development of formation pressure gradient in natural conditions;
- (4) deterioration of capacity and filtration properties of rocks toward roofs and bases of productive formations under replacement of lithological–mineralogical rock varieties [2–4, 8].

New minerals are forming only under changed thermodynamic conditions, influx of solutions from underlying formations, and their vertical migration through the stratified section. The influx of solutions only from underlying formations is confirmed by impossibility of their migration along bedding surfaces from regional recharge centers (Chapter 3). This provides grounds for assumption of intense paleo-hydrothermal activity that left numerous traces in the form of secondary minerals in sedimentary rocks of negative structures.

Intense formation of secondary minerals is evident from overgrowing boreholes during exploitation of oil and gas fields.

In this connection, the formation of fluids in deep stratified systems may be presented in the form of *pulsation fluid thermodynamic* (pulsation fluid geothermodynamic) (Chapter 13) [52], or gas-geodynamic [1], or fluidodynamic [12, 13] models. According to these models, gas–water mixture intrudes under high pressures into the sedimentary cover during periods of tectonic activity, which results in distortion of the physicochemical and thermodynamic equilibria in the fluid-rock system. This activates physicochemical processes accompanied by phase transitions: dissolution of the solid phase or its precipitation from solutions.

The formation of secondary minerals is particularly intense at geochemical barriers that coincide both in plan and in section with lithological-facies boundaries and zones, where relaxation of formation pressures and temperatures is maximal. The latter is explained by the fact that reduction of pressures and temperatures decreases solubility of many groundwater components to distort a system and provide conditions favorable for precipitation of the solid phase from solutions.

These processes are observable in natural conditions during exploitation of oil (as well as mineral and thermal water) fields, where they are reflected in overgrowing of boreholes and near-hole space by newly formed minerals. Sometimes, boreholes fail and require repair after 2–3 years of exploitation. The relaxation rate of formation pressures and temperatures in natural conditions after intrusion of subsurface fluids may be slower, although sufficiently rapid in terms of geological time.

The near-vertical ascending migration of deep fluid is established for all the regions under considerations (Chapters 7–10), the Pechora petroliferous basin included [8].

The studies by Kushnareva [9] confirm the formation of such boundaries in the Pechora petroliferous basin. This author defines different fissures in Famennian carbonate rocks: “mineral fissures” up to 3-mm thick healed by crystalline quartz and sulfates that cross bedding; “clayey fissures” healed by clayey or clayey-bituminous matter, located parallel to bedding surfaces, and crossing “mineral fissures”; fissures of the “paracase” group occurring in zones of disjunctive dislocations “are characterized by significant thickness. . . , cross enclosing rocks in form of a dense network, and host hydrothermal aggregates and limestone clasts” [9, p. 93]. In some areas, these fissures are filled with vein calcite, chalcedony, sulfides (pyrite, sphalerite, and galena), and rare fluorine and sulfur.

Based on these features, Kushnareva [9] arrives at the following conclusion: “Comparison of results obtained by different methods allows at least one doubtless inference on widely developed oil migration within the sedimentary cover.” The author emphasized that oil migrated along faults, each area was characterized by its own fluid source, and migration occurred “repeatedly and, probably, with breaks.” The migrating fluid “filled all the voids that contacted with the main migration channel.” In reservoirs, lateral migration initiated.

In [6], it is shown that paleohydrothermal activity left its traces in the form of “numerous calcic and chalcedonic veins crossing Famennian and Tournaisian limestones with their peculiar association of sulfide minerals (sphalerite, galena), fluorine, sulfur, and tectonic breccia.”

It is undoubted that formation of secondary minerals described by several researchers results in substantial deterioration of capacity and filtration rock properties and, consequently, development of impermeable or poorly permeable boundaries (zones of different extension and thickness).

*Fluidodynamic boundaries.* They are represented by piezominimums and piezomaximums, toward which or from which fluids migrate. Such boundaries are well known in hydrogeology of upper formations (watersheds and river valleys). In deep formations, they may be represented by near-vertical faults or weakened zones, which serve as path for migrating fluids. In plan, discharge zones associate

with piezominimums, while zones with internal recharge sources are marked by piezomaximums.

Thus, boundaries of different genesis determine the formation of relatively isolated blocks within deep formation systems of the sedimentary cover. Nature of these boundaries is difficult for unambiguous interpreting (their typification proposed in this work is schematic to a significant extent and needs to be improved, which is a task of future studies).

The boundaries in stratified systems and their configuration are closely related to the structural plan of inner areas in petroliferous basins being determined largely by the position of tectonic fracturing zones and axial parts of different-order negative structures.

Thus, in all the fluidodynamic interpretations of any scale, regional or local assessments of petroleum resource potential, calculations of identified reserves in mineral deposits, hydrocarbons included, substantiation of geofiltration models for inner areas of stratified systems, and solution of any geological tasks, it would be correct to proceed a priori from the existence of internal hydrogeodynamic boundaries between blocks of stratified systems proving their lack for every particular situation.

## References

1. Anikeev V A (1980) Geodynamic theory of superhigh formation energy of drilled oil- and gas-bearing Earth interior. In: Earth degassing and geotectonics. Nauka, Moscow
2. Djunin V I (2000) Hydrodynamics of deep formations in petroliferous basins. Nauchnyi mir, Moscow
3. Djunin V I, Korzun A V (2001) Fluidodynamics and formation of hydrocarbon accumulations. Mineral recourse base of Russia in the 21st century. In: Materials of the scientific-practical conference. Arkhangel'sk
4. Djunin V I, Korzun A V (2001) Geological formation model of deep groundwaters and origin of hydrocarbon accumulations. In: Proceedings of the 5th international conference "New ideas in geosciences." Moscow
5. Djunin V I, Korzun A V, Kiryukhina T A (1999) Hydrodynamics of deep formations and petroleum resource potential (exemplified by the northern Pechora Depression). In: Abstracts of the 13th geological meeting of the Komi Republic "Geology and mineral resources of northwestern European Russia." Syktyvkar
6. Goncharov V S, Esikov A D, Il'chenko V P (2002) The distribution of carbon isotope composition in natural gases from fields of northern West Siberia. In: Earth degassing: Geodynamics, geofluids, oil, and gas. Geos, Moscow
7. Ibragimov D S, Akhmedov A G, Isamukhamedova T I et al. (1993) Block hydrogeological structure of the Cenomanian aquifer in the Tashkent artesian basin and peculiarities in the formation of its slightly mineralized waters. Tashkent
8. Korzun A V (1996) Hydrodynamics of deep formations in the northern Pechora artesian basin. Candidate dissertation (Geol-Mineral) MGU, Moscow
9. Kushnareva T I. (1972) Petroleum resource potential of Famennian sediments in the Timan-Pechora Province. In: Geology and petroleum resource potential of the European northeast USSR. Syktyvkar
10. Perozio G N (1970) Epigenetic alterations in oil reservoirs of the Severo-Pokur and Vatin fields. In: Problems of lithology and paleogeography of Siberia. Novosibirsk



11. Reservoir properties of rocks in deep formations (1985) Nauka, Moscow
12. Sokolov B A (2001) New ideas in petroleum geology. MGU, Moscow
13. Sokolov B A, Konyukhov A I (1995) Injection geology of sedimentary basins and petroleum resource potential. In: Materials of the annual scientific conference "Lomonosov's Readings." MGU, Moscow
14. Vsevolozhskii V A (1991) Basics of hydrogeology. MGU, Moscow
15. Vsevolozhskii V A, Dyunin V I (1996) Analysis of regularities in hydrodynamics of deep formation systems. Vestnik MGU. Ser geol 3:61–72

## Chapter 13

# Principal Formation Model of Deep Fluids in Petroliferous Basins

The main peculiarities in the formation of deep subsurface fluids in artesian basins of platform demonstrate that

- (1) peripheral parts of petroliferous basins (“regional recharge areas”) provide no influence on the formation of deep fluid in the zone of very slow water exchange (Chapters 7, 9, and 10);
- (2) fluidodynamic conditions in the zone of very slow water exchange are characterized by the stratum-block structure (even though the displacement of rocks along fractures is unobservable) with restricted or zero fluidodynamic relationships between each other (Chapters 7–10);
- (3) deep layers of the sedimentary cover in platforms and depressions are characterized by intermittent, largely vertical, ascending migration of fluids that leave traces in the form of secondary minerals and various anomalies and are responsible for distinct heterogeneity in filtration and capacity properties of reservoirs and intervenient sequences;
- (4) variability in the chemical and gas composition of fluids at relatively short distances indicates nonequilibrium state of hydrogeodynamic systems, which is evident from the development of abnormally high formation pressures and strong lateral and vertical differentiation of pressure fields;
- (5) released waters passing into the free state at all the catagenetic stages play insignificant role in the formation of fields of deep fluid formation pressures.

Thus, at first sight, there are paradoxical events. On the one hand, the role of peripheral parts of platform is insignificant, being notable only in a narrow band along their margins, i.e., peripheral areas provide no influence on the formation of deep groundwater in both quantitative (they discharge completely in the marginal zone) and qualitative (mineralization and chemical composition) respects. On the other hand, present-day manifestations of secular ascending fluid migration in central areas of petroliferous basins and depressions (subaqueous discharge in river valleys in the form of springs, surface oil and gas shows, and other facts) imply inner recharge sources in deep petroliferous complexes.

On the one hand, theoretical calculations and long exploitation of subsurface fluids in multilayer systems of the upper hydrodynamic zone demonstrate that clayey

rocks are permeable and cannot serve as reliable screens; on the other hand, abnormally high formation pressures are frequently registered under and inside clayey sediments. These facts indicate the existence of deep fluid recharge sources, the influence of which may be noticeable in different intervals of the section, the surface included, and strong heterogeneity in migratory (filtration) parameters of rocks in every direction.

Rocks themselves, which release interstitial and crystallization water at all the stages of diagenesis and catagenesis, are one of the potential sources of the deep fluid recharge (Chapters 4, 5).

As was shown, rates of elision processes are extremely low and incomparable with velocities in the redistribution of pressures in clayey rocks, not to mention reservoirs. These processes may play any significant role only under sedimentation rates exceeding  $10^{-3}$  m/year and permeability of clayey sediments  $<10^{-7}$  m/day. Examples of such high sedimentation rates are limited and, consequently, the role of clayey sediments in the formation of pressure fields is usually insignificant. In addition, elision process cannot explain superhigh formation pressures exceeding geostatic values as well as irregularity in their vertical distribution.

Transition of crystallization water into the free phase occurs largely at relatively shallow depths and in a relatively narrow temperature range (Chapter 6). Below 2,500 m, transformation of rocks constituting the sedimentary cover continues, although the influx of crystallization water becomes practically negligible. In this connection, any significant role of free and crystallization water in the formation of deep fluid formation pressures seems unlikely.

It is appropriate, evidently, to mention data on the quantity of released crystallization water during transformation of clay minerals, which is also thought to serve as an additional recharge source and form flows of deep fluids (Table 13.1, Fig. 13.1). Transformation of montmorillonite into biotite in  $1 \text{ m}^3$  of rocks is accompanied by the release of  $0.17916 \text{ m}^3$  of crystallization water or approximately 18% of the clay volume. If we assume that the clay thickness is 100 m and their distribution area is  $1 \text{ m}^2$ , the total volume of released water should be  $17.9 \text{ m}^3$  from  $1 \text{ m}^2$ . This value is obtained under relatively hard conditions; real natural mediums always contain different clay minerals in variable proportions.

**Table 13.1** Volumes of released crystallization water during transformation of clay minerals

Mineral	Most frequent density ( $\text{kg/m}^3$ ) <sup>a</sup>	Average density ( $\text{kg/m}^3$ ) <sup>a</sup>	Natural density interval ( $\text{kg/m}^3$ ) <sup>a</sup>	Volume of released water from $1 \text{ m}^3$ of clays ( $\text{m}^3$ )	Integral volume of released water from $1 \text{ m}^3$ of clays ( $\text{m}^3$ )
Montmorillonite	2,500	2,500	2,004–2,520		
Chlorite	2,600–2,840	2,720	2,600–3,000	0.08088	0.08088
Hydromica	2,830	2,830	2,500–3,120	0.03887	0.11975
Muscovite	2,760–3,100	2,930	2,500–3,120	0.03413	0.15388
Biotite	3,000–3,120	3,006	2,500–3,120	0.02528	0.17916

<sup>a</sup>Data from *Physical Properties of Rocks and Mineral Resources* (Nedra, Moscow, 1976).

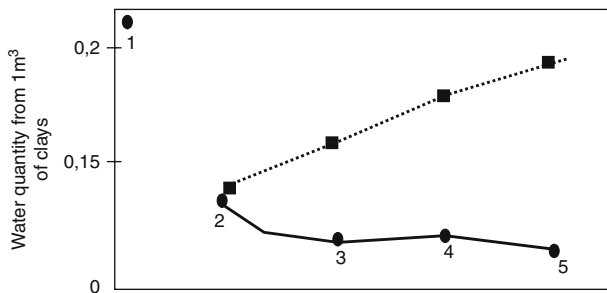


**Fig. 13.1** Quantity of crystallization water released from the montmorillonite–biotite succession. Minerals: (1) montmorillonite, (2) chlorite, (3) hydromica, (4) muscovite, (5) biotite. The *dotted line* designates the integral volume

Calculated tens and hundreds of millions of cubic meters of elision waters (compression compacting) reduced to the unit of area and time appear in most cases to be extremely small values and the elision process itself is substantially stationary in terms of geological time.

Let us consider, as an example, an approximate calculation. According to N.I. Zelentsova, the discharge of deep groundwater from Carboniferous sediments into the Volga River valley in the Samarskaya Luka area estimated by the gas dynamic and hydrochemical methods varies from 2 to 52 m<sup>3</sup>/day. Let us assume that the discharge takes place during 100 years. In this case, the integral discharge volume should be approximately 10<sup>6</sup> m<sup>3</sup>. Under the elastic water yield of deep formations being approximately 10<sup>-4</sup>, the groundwater level fall in Carboniferous sediments in the area of 1 km<sup>2</sup> should reach 10 km, which exceeds the thickness of the entire sedimentary cover. The East European Platform hosts tens of such sources, which discharge during the period longer than 100 years. It means that the entire secular discharge of deep fluids in the platform established in the Volga, Kama, Belaya, Pechora, Pizhma, Volkhov, Don, and other river valleys should be incomparably higher as compared with the volume of waters provided by rocks during catagenesis.

This approximate calculation of possible level falls due to deep groundwater discharge also demonstrates that the latter should be compensated on account of internal recharge sources since the real level fall does not exceed 10–20 m. Such a discharge cannot be provided by the elastic capacity. This inference is substantiated by the analysis of the distorted filtration regime in more than 100 groundwater intakes of the non-Chernozem area of Russia that exploits household groundwater. This analysis shows that the longer the period of the artificial load, the lower the share of the elastic capacity in the integral water intake and the higher the share of additional groundwater reserves. After 5–10 years of exploitation, the share of elastic capacity is only 3–5% of the water intake volume. Thus, rocks themselves cannot provide sufficient volume of water per unit of time.

In our opinion, the formation of deep fluids from the zone of very slow water exchange, primarily inner recharge sources and various anomalies in physical and geological fields included, can be explained in the context of thermodynamics.

The first law of thermodynamics is described as follows (Chapter 5):

$$dU - \delta Q + \delta A \text{ or } dU = \delta Q + P_{\text{inner}}dV + \delta A^*$$

or

$$dU - C dT + P_{\text{inner}}dV + \delta A^*,$$

where  $dU$  is the change in the inner energy of the system,  $Q$  is the quantity of heat received by the system,  $P_{\text{inner}}dV$  is the work against the external pressure,  $\delta A^*$  is the work performed by the system against other external forces,  $C$  is the thermal capacity, and  $T$  is the absolute temperature.

For irreversible processes (all geological processes are irreversible), the second law of thermodynamics is described as follows:

$$T dS > dU + \delta A,$$

where  $S$  is the entropy of the system (function of the system state), the differential of which in the elementary reversible process is equal to the ratio between finitely small quantity of heat received by the system and absolute temperature of the latter. Other designations are as in the previous equation. Entropy of the complex system is equal to the sum of all its uniform parts. Inasmuch as all natural processes are irreversible, entropy of the isolated system may increase to reach maximum at the state of system thermodynamic equilibrium.

For the system that experiences external pressure and is characterized by the mass and energy exchange with environments, physicochemical processes, and other kinds of work, the first thermodynamic law should be described as follows:

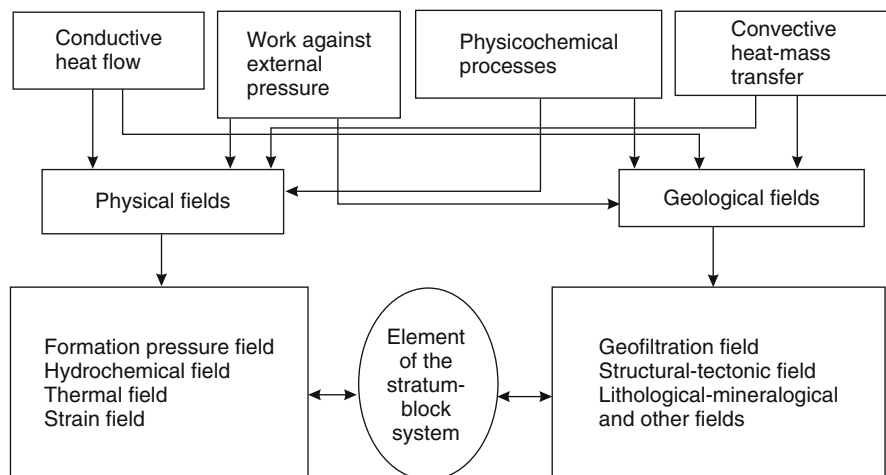
$$T dU > dQ - P_{\text{inner}}dV + \sum_{i=1}^N \mu_i dn_i \pm dW,$$

where  $U$  is the energy of the system,  $Q$  is the external heat obtained by the system,  $P_{\text{inner}}$  is the external pressure,  $dV$  is the change in the system volume,  $\mu_i$  is the chemical potential of the  $i$ th component,  $dn_i$  is the change in the  $i$ th component mole, and  $W$  is the mass exchange (heat–mass transfer) between the system and environments. The last three members of inequality describe processes under which the fluid-rock system makes positive or negative work.

This equation represents the most general mathematical model that describes the formation of physical and geological fields and their interaction. When applied to deep petroliferous formations, it works in the following way.

Let us consider relation of this equation with the formation of deep fluids. This relation may be presented as the following principal model.

$$dU = dQ - P_{\text{inner}}dV + \sum_{i=1}^N \mu_i dn_i \pm dW.$$



The first member of the equation designates conductive heat flows that change temperature in the element of the stratum-block system. The second member describes work of the system against the external pressure (impact). The third member of the equation reflects work of the system during physicochemical processes, phase transitions in the fluid-rock system included. The fourth member characterizes work of the system during the mass–energy exchange with environments.

All these processes form physical and geological fields, which are closely interrelated and changeable during geological development of the petroliferous basin.

Physical fields are fields of formation pressures, temperatures, concentrations and strains, and others, gravitational one included. Geological fields include geofiltration, lithological–mineralogical, structural–tectonic, and other fields, boundaries of the stratum-block system included.

It should be emphasized that all the physical and geological fields are interrelated. Changes in one of them provoke changes in others. For example, changes in the field of formation pressures lead to distortion of thermodynamic equilibrium and, consequently, physicochemical processes, which proceed with consumption or release of heat (changes in the thermal field) and dissolution or precipitation of minerals (changes in capacity and filtration properties, formation of inner boundaries).

The work of the block system against external impact, for example, tectonic strains (second member of the thermodynamics equation), results in the same consequences, primarily distortion of thermodynamic equilibrium, changes in physicochemical processes (dissolution or precipitation of various minerals), and temporal variations in the formation pressure field included. As was mentioned (Chapter 5), the time-variable formation pressure field characterized by quasiperiodical patterns is observable in all the regions being registered by observations in stationary geophysical testing areas. Precisely this provides grounds for the inference that the time-variable strain field (“hydrogeodeformation field”)

is responsible for nonstationarity of thermodynamic process and formation of time-variable physical and geological fields.

Let us pay more attention to the last member of the thermodynamic equation. In our opinion, the heat–mass exchange of the block system element with environments results in most significant changes in physical and geological fields, and formation of various anomalies (hydrodynamic, hydrochemical, thermal, mineralogical, palynological, and others), which represent characteristic features of deep aquifers (petroliferous complexes) and cannot be usually formed without additional (external) influx of matter and energy.

In periods of tectonic activation, gas–water mixture characterized by tremendous energy ascends from deep layers of the crust and, probably upper mantle and cuts, similar to intrusive magmatic bodies, the sedimentary cover to fill weakened fracture zones (Fig. 13.2). Ascending upward the section, the mixture gradually loses its energy for overcoming overburden pressure and cohesion forces, for rock deformation, hydraulic fracturing, and filling of different traps (i.e., it forms fluid intrusions, for example, in arches of positive structure adjacent to the main conduit), and, probably, formation of the microrelief at the Earth's surface.

Depending on the energy of ascending solutions, the scale of lateral migration (fluid intrusion) is variable. It is easier to penetrate along bedding surfaces for

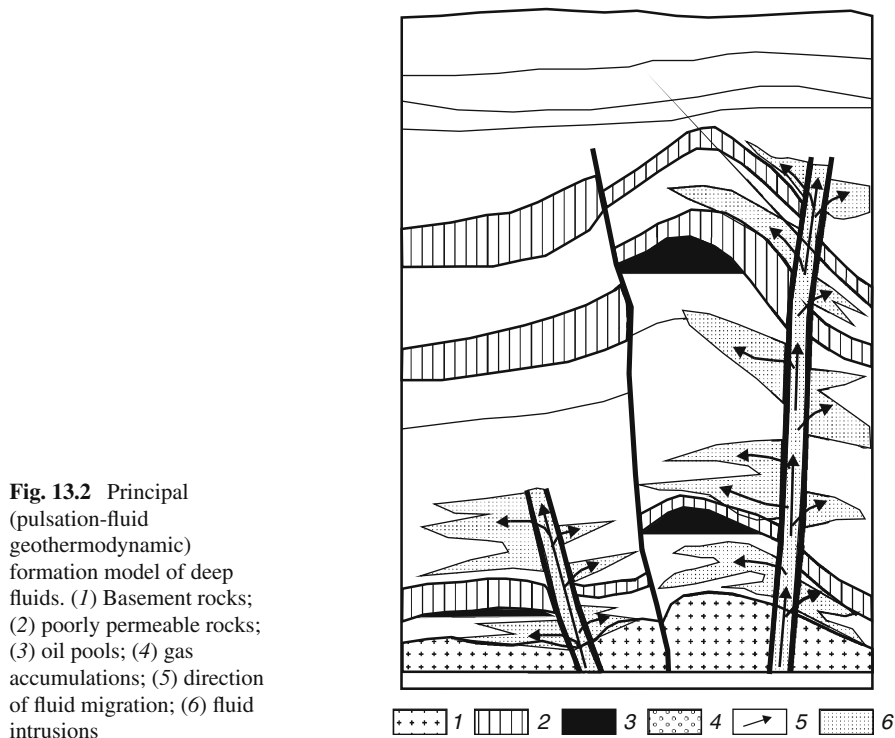


**Fig. 13.2** Principal (pulsation-fluid geothermodynamic) formation model of deep fluids. (1) Basement rocks; (2) poorly permeable rocks; (3) oil pools; (4) gas accumulations; (5) direction of fluid migration; (6) fluid intrusions

solutions than for stratiform intrusions, which are sometimes thousands of square kilometers in size and spread for a distance of tens of kilometers away from vertical or inclined conduits (in East Siberia, trap bodies are tens of thousands of square kilometers in size). It is logical to assume that lateral migration of endogenic fluids should be more significant.

The penetration depth (height from the basement, to be more exact) of ascending endogenic solutions is determined by both their energy and section structure: lithological and mineral composition of host rocks, their thickness, bedding patterns, development of plastic poorly consolidated sediments, their thickness and position in the section, geostatic pressure, and many others features. When energy of the gas–water mixture is relatively high and hydrothermal activity is durable or frequent during a relatively short geological period, gas-bearing mixture may discharge to the surface capturing rock fragments from brecciation zones, similar to traps or mud volcanoes at the cessation stages. It is possible to draw the analogy of the formation of traps and stratiform intrusions to deposition of saliferous sediments from oversaturated solutions.

The intense intrusion of gas–water mixture is likely followed by the period of slow and long gradually attenuating influx of insignificant volumes of water and gas with time-variable compositions and temperatures into the sedimentary cover. This process is accompanied by the redistribution of formation pressures, heat, and matter in all the directions. As was mentioned, such a redistribution may result under certain conditions (under geochemical incompatibility and time-variable thermodynamic conditions) in fissure healing due to overburden pressures, phase transitions in the fluid-rock system, and formation of partly or completely isolated hydrodynamic blocks. New tectonic movements accompanied by hydrothermal activity may change existing geological and physical fields; for example, to redistribute formation pressures in both vertical and horizontal directions and form, thus, their new field.

Such a model, which unites tectonics of regions, hydrothermal activity, and thermodynamic processes determining phase transitions in the deforming elastic medium, which are responsible, in turn, for strongly heterogeneous filtration properties of host rocks and impermeable boundaries (geofiltration field), may be termed as the *pulsating-fluid thermodynamic* (previously, *pulsating-fluid geothermodynamic*) model of the deep fluid formation in the zone of very slow water exchange (Fig. 13.2).

The proposed model eliminates inconsistencies in the problem of deep fluid formation such as, for example, existence of various anomalies, which are characteristic of fluid dynamics in deep formations of petroliferous basins. Apart from dynamic problems of deep fluid formation, the model also explains its hydrogeochemical, gas, thermal, and other aspects, formation of hydrocarbon accumulations included.

It is natural to assume that ascending gas–water mixture should be different in its chemical and gas composition as compared with solutions enclosed in sedimentary rocks (since these parameters are variable, sometimes significantly, through the vertical section). When this mixture enters overlying aquifers (petroliferous



complexes) and mixes with in situ water solutions within lithologically and mineralogically different host rocks, they disturb thermodynamic equilibrium in the rock-fluid system. This may lead to oversaturation of solution (or, more exactly, mixture of compositionally different solutions) with some components relative to host rocks under existing pressures and temperatures. The latter stimulates phase transitions and precipitation of different salts from solution, growth of crystals of secondary minerals, and complete or partial fissure healing. The redistribution of pressures and temperature decrease (the latter results usually in decreased solubility of mineral salts) in injected solutions promotes the formation of secondary minerals as well. This process should be more intense in areas with piezominimums, i.e., areas of natural discharge of subsurface fluids characterized by lowered formation pressures.

Intensity of all these processes is likely determined by rates of formation pressure fall and velocities of the temperature redistribution, all other things being equal (chemical and gas composition of alien solutions, lithology, and mineral composition of host rocks). It should be added that if hydrothermal solution intrudes under high pressures exceeding their values in the formation, this process is accompanied by hydraulic fracturing. Owing to this, tectonic fractures appear to be superimposed by additional fissures (which explain the development of anomalous secondary porosity and jointing). Of importance is that formation of vertical and horizontal fissures is accompanied by lateral migration along bedding surfaces, particularly along boundaries separating rocks with different lithological–mineralogical properties.

Hydraulic fracturing results in the increased capacity and permeability of the medium, on the one hand, and in intensified redistribution of formation pressures, their faster relaxation, and more rapid fissure healing, on the other hand.

The formation pressure fall in the medium subjected to elastic deformation should also be accompanied by additional closure of newly formed fissures due to the partial transfer of the overburden load on fluid-hosting rocks (as was observed in the Salym field of the West Siberian petroliferous basin).

These two parallel opposite processes result eventually in jointing reduction to, probably, its complete elimination and sealing of some segments of the section and formation of hydrodynamically isolated blocks. These blocks may preserve different formation pressures (abnormally high included) even under their similar initial values, which is determined by a combination of above-mentioned processes.

These assumptions are confirmed by groundwater exploitation, particularly under simultaneous drainage of two and more aquifers (petroliferous complexes) containing subsurface fluids with different chemical and gas compositions. Significant falls in formation pressures in aquifers (petroliferous complexes) and mixing in production wells stimulate precipitation of sulfates, calcium carbonates, and other minerals in them.

The formation of secondary minerals in distorted environments is a relatively rapid process. The complete fill of water-raising and distribution pipes and, correspondingly, the breakdown of production wells occur after several weeks to 3 or more years.

Similar processes are observed in developed oil and gas fields, where precipitation of gypsum, calcite barium and strontium sulfates, and other minerals complicated well exploitation, as well as in all the Moscow heat stations, which exploit brines of the Ryazhsk aquifer occurring at depths of 1,000–1,300 m. The formation scale of minerals in disturbed environments is so high that required development of special methods to fight salt formation in production well. Up to 60% of production wells in some fields of the Urals and Volga regions suffer from salt precipitation [10]. When pumping industrial wastes into deep formations, one of the main problems to be studied for predicting changes in well intake capacity due to potential salt precipitation is geochemical compatibility of pumped wastes with subsurface fluids in reservoirs and mineral properties of host rocks. In other words, geochemical barriers, which provoke mineral formation, versus equilibrium conditions should be revealed.

It is quite logical to assume that these processes occur in natural environments, although physicochemical reactions are substantially slower due to lower pressure and temperature gradients as compared with the parameters in distorted conditions. Therefore, complete healing of fissures in natural environments takes evidently decades to a few hundreds of years.

In tectonically active areas with frequent seismic events and tectonic movements, fissure formation and healing replace each other during relatively short periods. In calmer areas, tectonic fracturing and hydrothermal activity are relatively long processes separated by some periods. Fissure healing leads to hydrodynamic (horizontal and vertical) isolation of blocks in the sedimentary cover of petroliferous basins.

Similar to many other geological processes, tectonic movements with fracturing and hydrothermal (or low-temperature solution) activity are characterized by cyclic (periodical) patterns.

Tectonic movements accompanied by fracturing may result in temporal hydrodynamic interaction between blocks with its subsequent attenuation due to mineral formation, fissure healing, and their mechanical compression. If the younger jointing (width of fissures and openness degree) zone is larger than the older one, hydrodynamic isolation is sometimes preserved, when newly formed fissures appear to be shorter (with lesser penetration depth) as compared with the width of the older zone with healed jointing.

In zones with young tectonic movements, new fissures are forming in areas both with older healed jointing and lacking the latter. Ascending fluids may differ in their chemical, gas, and organic compositions from previous solutions, which should result in the precipitation of different authigenic minerals; the latter is frequently revealed in the form of several migration stages by the detailed mineralogical study of host rocks. Repeated tectonic movements, which provide prerequisites for interaction between older and younger petroliferous complexes, result in chaotic horizontal and regular vertical distribution patterns of newly formed minerals in sedimentary sequences of platforms.

The proposed formation model of capacity and filtration rock properties is consistent with observed phenomena and development of open porosity and permeability

(unhealed jointing). This implies that past- and present-day fluid-hosting rocks contain(ed) either inert (oil, gas) or undersaturated fluids under existing(ed) thermobaric conditions. In addition, depending on particular thermobaric conditions, phase transitions, and open jointing patterns, healing may be partial along fissures and complete across them. In other words, the same fissure (or their system) may be healed by secondary minerals in some of its segments and remain opened in the others, i.e., there is a perfect analogy with disturbed exploitation conditions when technological equipment overgrowing is faster in areas with more significant pressure and temperature falls.

Before giving evidence for interaction of platform and depression sedimentary covers with the basement and crust, let us dwell on the following point. The complex distribution patterns of formation pressures in separate structures (Chapters 7–10) may be explained, first, by filtration heterogeneity of host rocks. It is known that under high filtration properties of rocks, the potentiometric surface of subsurface fluids becomes flattened and gradients of potentiometric levels decrease. Under low filtration properties, the situation is reversed. Significant heterogeneity in capacity and filtration properties through local structures determines pressure gradients in the same formation through relatively small areas. Second, the temporal and spatial distributions of formation pressures are controlled by changes in the stressed state of host rocks, which is usually ignored in hydrogeodynamic calculations.

For deep formations of petroliferous basins, the influence of the strained state in host rocks should be taken into consideration, particularly in areas with the active tectonic regime. According to many researchers (G.S. Vartanyan, G.V. Kulikov, V.P. Petrenko, B.A. Tkhostov), accumulation of tectonic stresses leads in such areas to changes in the formation of pressure field, which is recorded in local structures isolated from each other in the fluid dynamic respect. If the increment rate of strains is higher as compared with the redistribution rate of formation pressures in the system, the pressure distribution should be irregular under changeable stresses. In such a situation, the gradient of formation pressures should always exist, which provides a conspicuity of the local or the regional fluid flow. In truth, only redistribution of formation pressures within different hydrodynamically isolated parts of the section in petroliferous structures can take place under permanent accumulation and relaxation of stresses in the fluid-rock system. For example, observable water–oil contacts in local structures can result from this process rather than from regional or local groundwater migration.

The correlation between tectonic stresses and changes in the field of formation pressures with account for elastic deformation properties of rocks is described in Chapter 5.

Thus, the observed present-day distribution of formation pressures in the elastically deformed medium may result from recent tectonic stresses. It represents a peculiar instant reflection of the formation pressure redistribution in the system that experiences tectonic stresses of different intensity and sign. Figure 5.6 illustrates the distribution of formation pressures at the same moment (0.01 day) under piezoconductivity of  $10^6 \text{ m}^2/\text{day}$  and several instant sources of tectonic stresses placed at points of 100, 250, and 400 m. It follows from the figure that tectonic perturbances

of different intensities and signs (in this case, the positive and negative sources are compression and extension of rocks, respectively) produce the complex distribution of formation pressures with piezominimums and piezomaximums as well as with gradients different in their values and directions. Nevertheless, no movement is registered in the situation under consideration. Instead, only redistribution of formation pressures related to irregular compression or extensions of the elastically deformed massif heterogeneous in its filtration, capacity, and mechanical properties is observed.

According to V.P. Petrenko and I.G. Kissin, the stress field may also influence the formation of the groundwater chemical composition, which is documented in areas of elevated seismic activity. The transition of the solid matter to solution and its precipitation from solution depend on the pressure in the solution-rock system. The heterogeneity of the stress and formation pressure fields and their temporal changes should result in differentiation of the hydrogeochemical field, which is, in fact, observed in reality. Chapters 7–9 demonstrate substantial changes in the composition of some chemical components and mineralization in relatively small areas, which are explainable by the irregular distribution of formation pressures and stresses. The similar (irregular) distribution of micro- and macrocomponents and fluid mineralization is also registered in other structures of West Siberia, Central Asia, Ciscaucasia, the Fergana, and Kura depressions. It is conceivable that such a distribution represents a general regularity characteristic of hydrogeochemical fields of deep formations in petroliferous basins as well as in intermontane and intramontane depressions.

Let us consider examples indicating that the basement is a connecting link between the sedimentary cover and the crust and, probably, upper mantle.

Recent summarizing information on petroleum resource potential and hydrothermal activity in basement rocks can be found in [3, 4, 6, 7, 9].

The Jurassic sediments separated from the basement by the 5-m-thick clay layer in the Naryn Monocline of the Fergana Depression yield hydrocarbon and carbon dioxide gases as well as highly mineralized waters. The overlying Cretaceous and Paleogene sediments demonstrate hydrodynamic and hydrochemical anomalies. In [8], it is noted that vertical migration is so intense that hydrocarbons are preserved and replenished even in the upper zone of intense accumulation destruction. In the Maimi-Su area, the recent oil pool in Paleogene Bed VIII is forming from water–oil mixture that migrates along faults in the basement and is responsible for the local positive anomaly of formation pressures in these rocks.

Some areas of the Baltic crystalline shield located hundreds of kilometers away from the sedimentary cover of the platform yield mineralized waters and brines. They are confined to fault zones in Archean and Proterozoic peridotites and pyroxenites. In the Soncha mine, mineralization of waters is as high as  $52 \text{ g/dm}^3$ . The Br and J concentrations in them are 288 and  $73 \text{ mg/dm}^3$ , respectively. Dissolved gas is characterized by the following composition (%): methane 60.35, nitrogen 31.87, helium 3.8, heavy hydrocarbons 2.32, and argon 1.84. Brines are also known in the Lovozero Massif. According to V.D. Bezrodnyi, washing fluid in the interval of 900–1,600 m in Well 1886 was enriched with helium, hydrogen, and methane up

to 3.5, 24.8, and 81.5%, respectively. This zone is confined to radial, near-vertical faults, and areas of tectonic brecciation along almost horizontal updip-thrusts. At a depth of 1,200 m, groundwater mineralization was  $51 \text{ g/dm}^3$ . By their chemical composition, waters are chloride calcic-sodic. The content of minor elements in them is as follows ( $\text{mg/dm}^3$ ): Sr 1,150, Br 272, I  $\sim 8$ , B 4, K 60, Rb  $\sim 0.15$ . Gas is composed of methane, hydrogen, and heavy hydrocarbons (63.3, 20, 16.7%, respectively). Downward, the content of As, Mn, and Al increases.

In the Kola super-deep hole, water-saturated, highly foliated Middle Proterozoic and Archean granitogneisses are recovered in intervals of 4,565–4,925 and 6,170–7,620 m.

In these intervals, the Cl concentration increased 10–40 times and clayey mud acquired the anomalous composition: mineralization  $6.8 \text{ g/dm}^3$ , chlorine 82 equiv%, hydrocarbonates 13 equiv%, and sodium 99 equiv%. These zones also contain newly formed high-water minerals (kaolinite and chlorite) forming in the presence of high-temperature chloride solutions. According to calculations by Bezrodnyi, during the Early Paleozoic volcanic stage, the Lovozero Massif (the studied depth interval) received over  $6 \cdot 10^{11}$  tons of matter from the upper mantle. Of this quantity, 0.3 and 0.8% are Cl and  $\text{H}_2\text{O}$ , respectively. Concentration of migrating solutions that took part in the mineral formation was close to saturation with respect to NaCl.

In the Tatar Arch, the borehole drilled in the basement is located in the tectonically active zone. Recovered rocks are characterized by intense jointing, particularly in the lower and middle parts of the section; the upper one is partly or completely healed since the lithological–mineralogical composition of rocks changes distinctly at the boundary between the basement and the sedimentary cover. Jointing in these zones is so intense that core recovery in some cases was equal to zero. Some intervals demonstrated gas emanations, intensity of which increased downward more than 100 times as compared with background values; this was accompanied by simultaneous increase in the methane content in gas. Some samples showed the occurrence of light oily bitumen. Microfissures were completely or partly healed by bituminous matter. The intervals of 4,140–4,401 and 4,876–5,006 m yielded the significant influx of gas-containing water. Formation pressures exceeded hydrostatic values. In the sampling interval of 4,073–5,099 m, the fluid yield was  $120 \text{ m}^3/\text{s}$ . Mineralization of water amounted to  $282.9 \text{ g/dm}^3$ , of which  $90 \text{ g/dm}^3$  was represented by calcium. Concentrations of minor elements J and Br are  $83 \text{ mg/dm}^3$  and  $1.9 \text{ g/m}^3$ , respectively. Gas consists of methane, volatile volcanic components (15–17%), and heavy hydrocarbons (5%). Basement rocks were subjected to intense metasomatic potassic-sodic transformation.

In the Dnieper-Donets Depression, depths of 200 m below the basement surface yielded the influx of aerated waters. Basal conglomerates in the Pannonian Depression enclose an oil and gas pool with abnormally high formation pressures. In the same structure, similar high-pressure fluids are recovered at a depth of 100 m below the basement surface (Aldje field). Igneous rocks and limestones of the basement in the Lake Maracaibo area provide oil and gas occurrences [1].

The West Siberian petroliferous basin hosts fields (Festival'noe, Urmanskoe) where abnormally high formation pressures occur at the boundary between the basement and the sedimentary cover, which indicates their connection.

In the Pripyat Depression, 160 boreholes drilled in the basement recovered sulfate waters with mineralization 1.5–2.0 g/dm<sup>3</sup> at a depth of 100 m and chloride-calcic and chloride-sodic waters with mineralization exceeding 100 g/dm<sup>3</sup> at depths of 200–400 m. In granite gneisses of the Canadian crystalline shield, many boreholes recovered groundwater with mineralization of 25–40 g/dm<sup>3</sup> at depths of 500–600 m and exceeding 100 g/dm<sup>3</sup> at a depth of 1000 m. G.V. and Yu.G. Bogomolovs explain these facts by squeezing of excess groundwater from depressions to neighboring crystalline massifs. It was mentioned that the work spent by groundwater to overcome filtration resistance is less when it moves upward for a few kilometers as compared with that spent for moving along bedding for tens and hundreds of kilometers. This is confirmed by studies of hydrocarbon migration. In addition, the idea of squeezing out excess fluids from depressions is inconsistent with palynological data and does not explain commercial accumulations of oil and gas in the basement up to depths of 1,000 m (Totuma field). By elision processes, it is also impossible to explain the occurrence of brines, hydrogen, and gases in deep fault zones and their accumulations at hydrochemical barriers under impermeable or poorly permeable horizontal boundaries with partly or completely healed jointing.

In the southern Siberian Platform, the area with occurrences of cinnabar, galenite, pyrite, and other hydrothermal minerals is larger as compared with the distribution area of traps. Hydrothermal mineralization involves the entire sedimentary section, Quaternary sediments included. This indicates that the terminal stage of hydrothermal activity took place after accumulation of Quaternary sediments. A.A. Dzyuba, who investigated hydrothermal activity in old platforms, arrived at the reasonable and undisputable conclusion on the significant role of hydrothermal solutions. In his opinion, hydrothermal fluids are likely mobilized from melted rocks, while volatile volcanic components are largely released from magma rather than from the simple capture of sea and filtration waters in the near-surface zone.

In anomalous zones of the Siberian Platform connected with faults, intense bitumen development is documented through the entire sedimentary section beginning from its base where accumulations of bitumen are maximal. In this case, their source is unambiguous.

According to [7], recent hydrothermal activity is also established in seas. Waters in depressions of the Red Sea are characterized by elevated density, salinity, and temperature. For example, temperature is 21°C in the near-surface layer, 56°C at a depth of 2,200 m, and 61°C in bottom waters. Mineralization at the bottom layer is as high as 310 g/dm<sup>3</sup>.

In mountainous regions (Caucasus, Carpathians, Pamirs, Tien Shan), relations of mineral and thermal waters containing specific distinctly endogenic components with hydrothermal solutions of crustal and subcrustal origin are undoubted. If the unity of Earth's development is accepted, it should also be admitted that these

processes may take place in platforms as well, although their consequences are buried under thick sedimentary sequences. Nevertheless, they leave traces in the form of various anomalies (hydrodynamic, hydrochemical, geothermal, gas) and widespread secondary mineral formation, which attenuate upward the section and are unambiguously correlated with faults.

These and many other facts concerning hydrogeological peculiarities of the basement indicate that the role of the latter, crust, and upper mantle in the formation of deep groundwaters should not be ignored or underestimated.

The proposed *pulsation-fluid thermodynamic model* follows from existing concepts. As was mentioned (Chapter 5), Anikeev [2] proposed a convincing gas geodynamic model (theory, in his terminology) of superhigh formation pressure development.

Ivanchuk [5] registered the discovery of the phenomenon of “hydrovolcanism in the sedimentary cover of the crust.” In his opinion, two conditions are needed for the development of hydrovolcanism, i.e., vertical movement of groundwaters: (1) “sealing” of interstitial solutions squeezed largely from clayey sequences and (2) possibility for the vertical breakthrough of accumulated energy under enhanced tectonic movements. The only recharge source is represented by additional released liquid from clayey sequences; the latter forms sandy pulp, which moves along faults capturing at its way rock fragments. This author reports on hydrovolcanism in Central Karakumy, southern Sweden, Azerbaijan, Nepal, California, Japan, Timan-Pechora region, southern Dagestan, and other regions of the world. For example, in the Timan-Pechora petroliferous province, signs of hydrovolcanism in the form of secondary minerals (calcite, chalcedony, sulfides, fluorine, sulfur) are found in the Vuktyl gas condensate field and Zapadno-Soplyas structure. In the Gaurdak field, secondary minerals include sulfur, calcite, and gypsum [5].

As was shown, elision processes are stable at the geological timescale and cannot result in abnormally high formation pressures, let alone provoke “hydrovolcanism.” Explanation of observed phenomena in the sedimentary cover of platforms by the hydrovolcanism theory does not stand up to elementary criticism, while the pulsation-fluid geothermodynamic model explains fact cited by Ivanchuk.

There are many known examples demonstrating intrusion of ductile igneous bodies into more rigid sedimentary rocks of platforms. In such situations, possibility and reality of magma intrusion with the formation of shape- and composition-variable geological bodies both along (stratiform intrusions) and across (laccoliths and others) rock bedding cast no doubts. The source of matter is also undoubted. When the crust and the upper mantle are mentioned as sources of periodical gas–water mixture influx along deep fault to the sedimentary cover of platforms, this runs into heavy opposition or role of these processes is underestimated since it is considered that platforms terminated the certain development stage and became tectonically inactive. Nevertheless, if we proceed from the unity of Earth’s development, we should admit geodynamic activity of lower parts of sedimentary sections in petroliferous basins, which is confirmed by observations in stationary geophysical testing areas.

Many scientists indicated significant role of the mantle in the formation of deep fluids: A.P. Vinogradov, V.F. Derpogol’ts, L.N. Kapchenko, V.A. Sulin,

V.A. Krotova, P.N. Kropotkin. It was assumed for the eastern Ciscaucasia petroliferous basin by I.G. Kissin, K.L. Anikeev, and other researchers.

Thus, the *pulsation-fluid thermogeodynamic model* explains (1) development of internal recharge sources; (2) stratum-block structure of deep formations and its degradation upward the section; (3) distinct heterogeneity in rock capacity and filtration properties at deep levels; and (4) anomalies in physical and geological fields.

## References

1. Anikeev V A (1964) Abnormally high formation pressures in oil and gas fields. Nedra, Leningrad
2. Anikeev V A (1980) Geodynamic theory of superhigh formation energy of drilled oil- and gas-bearing Earth interior. In: Earth degassing and geotectonics. Nauka, Moscow
3. Bashilov V I, Kuprin V F, Gottikh R P et al. (1991) Hydrocarbon degassing of fault zones in the western slope of North Urals. *Geologiya nefi i gaza* 11:17–21
4. Djunin V I, Korzun A V (2003) Fluid migration: Oil origin and formation of hydrocarbon accumulations. Nauchnyi mir, Moscow
5. Ivanchuk P P (1994) Hydrovolcanism in the sedimentary cover of the crust. Nedra, Moscow
6. Kropotkin P N (1986) Earth degassing and genesis of hydrocarbons. *Zhurn Vsesouz Mendeleev ob-va* 31:540–547
7. Krotova V A (1978) Integrity of subsurface fluids and geotectogenesis. In: Problems of hydrogeology and engineering geology. Nauka i Tekhnika, Minsk
8. Taliev S D (1976) An example of seismicity influence on vertical migration of fluids and localization of hydrocarbon accumulations. *Trudy VNIGRI* 387:125–137
9. Veselov K E, Mikhailov I N (1994) Oil and gas at deep levels of the crystalline basement. *Geologiya nefi i gaza* 2:17–21
10. Vitvitskii V V, Efstaf'ev V P, Fed'kushkov Yu I (1982) Gas formation from chloride brines of the Moscow artesian basin *DAN SSSR* 2264: 470–473



## Chapter 14

# Oil Origin and Formation of Hydrocarbon Accumulations

When substantiating the above-mentioned formation model of deep fluids in lower and middle parts of sections covering platforms and filling inter- and intramontane depressions, we should also consider the formation problem of hydrocarbon accumulations in stratified sedimentary systems with account for principal inferences derived from the analysis of hydrodynamics in deep formations of petroliferous basins.

Despite the voluminous literature (monographs, articles, and unpublished reports), no unified theory of oil and gas origin has been developed during more-than-a-century-long history of prospecting, exploration, and exploitation of oil and gas fields.

Therefore, it is premature to consider different views on oil origin and formation of hydrocarbon accumulations as a theory. Any theory should both explain all the facts observed in natural objects and serve as a basis for reliably predicting petroleum reserve potential and prospecting commercial oil and gas fields in different regions. Until recently, neither available “theories” nor their modifications meet these requirements. Therefore, we can speak now only about concepts or hypotheses of oil origin.

This problem is of importance for efficient geological-prospecting works for oil and gas based on estimates of their resource potential through the basin (lateral and vertical), which are substantiated, in turn, by theoretical postulates of different hypotheses of oil and gas origin. The problem is particularly important now when, first, it is realized that proven hydrocarbon reserves are limited and, second, expenditures for drilling are continuously growing due to increased depths of exploration and exploitation wells.

As was mentioned in the “Introduction” section, our approach to the problem of oil origin and formation of oil and gas accumulations is based on hydrogeological data.

In this chapter, we consider only the hydrogeological problems, which concern immediately the formation of oil and gas fields, since in our opinion, precisely groundwaters transport dissolved and free hydrocarbons, form, and destroy their accumulations.

## 14.1 Hydrogeological Aspects of Oil Origin and Formation of Hydrocarbon Fields

In previous chapters, we presented results of long-term studies dedicated to regional hydrogeological problems and quantitative estimates (by analytical calculations, modeling of particular natural objects, and factor-diapason modeling of natural processes), which concern immediately the problem of oil origin and formation of hydrocarbon accumulations. These studies yielded the following inferences:

(I) Classical views on regional flows in petroliferous basins, which are based on hydraulic principles and admit (a) significant role of orogenic structures and peripheral parts of the basin in the formation of deep fluids, (b) transfer of formation pressures over significant distances and to deep levels, (c) hydrodynamic relations within individual petroliferous complexes, and (d) regional flows of subsurface fluids, are inconsistent with observable facts, and need to be revised.

*Regional flows in deep formations of oil and gas basins cannot exist in principle.* The subsurface flow formed in peripheral areas of the basin discharges immediately close to regional infiltration recharge centers due to ascending diffused migration through poorly permeable rocks or locally under river valleys and through weakened zones of tectonic fractures. This is well illustrated by figures in Chapters 7–10, which reflect changes in formation pressures and gradients of groundwaters along beds of petroliferous complexes from peripheral areas of basins toward their centers.

Mass transfer in deep sedimentary sequences of negative structures results from activity of endogenic factors, regardless of processes in marginal parts of petroliferous basins.

The lack of regional lateral flows with infiltration recharge and the development of anomalies in physical fields pose the problem of the deep fluid recharge source beyond marginal zones of petroliferous basins. Only the crust–mantle boundary may serve such a recharge source, which acts indirectly through the basement. Internal recharge centers are local (deep-seated faults, their intersections, and others), not regional. These observations made it possible to substantiate “pulsation-fluid thermodynamic” formation model of deep fluids (Chapter 13), which allows the problem of oil origin and formation of hydrocarbon accumulations to be partially solved.

(II) In oil and gas hydrogeology, significant attention is paid to elision, which plays a substantial role in the development of formation pressures and supplies into reservoir products of buried organic matter transformation (phosphatized organic matter) that serves as primary material for hydrocarbon formation.

In our opinion, analytical calculations and modeling of rock compaction using equations of filtration consolidation under different sedimentation rates (increment of overburden pressure) and subsidence as well as under different compaction and permeability coefficients demonstrate the impossibility of abnormally high formation pressures within compacting rocks. Compression (elision) transformation of clayey rocks (water contained in the crystal lattice of clay minerals and becoming free during transformation included) cannot play a substantial role in the

development of a regional formation pressure field. Tens to hundreds of millions of cubic meters of elision (compression compacting) and crystallization waters (such values are cited in many publications) reduced to the area and time units appear to be extremely small values. In addition, the elision regime (dehydration of clay minerals included) proper is substantially stationary in terms of geological time since relaxation rates of formation pressures (based on modeling) are significantly higher as compared with increment rates of the overburden pressure and subsidence rates in the petroliferous basin. In the open system, these processes cannot result in anomalies of formation pressures. Their significant role is notable only under ideal isolation. The studies in the West Siberian and eastern Ciscaucasia petroliferous basins with sedimentary sections comprising clayey sediments up to >1,000 m thick revealed no influence of elision on development of formation pressure fields (Chapters 4, 7, and 9).

(III) Petroliferous formations represent *a stratum-block system lacking or characterized by weak hydrodynamic relationships between blocks in all the directions*. Such a situation results from combined action of many geodynamic and physico-chemical processes in the fluid-rock system. The important role in the formation of stratum-block structure of the section belongs to catagenesis. In [32], it is noted that the formation of oil pools and their subsequent evolution result in progressive catagenetic transformations and superimposed phenomena with the formation of “sedimentary lenses,” which represent a product of secondary structural–mineral associations (Chapter 6).

The stratum-block structure is an integral feature of petroliferous formations, i.e., regularity in common with changeable heterogeneity scale only. The blocks are variable in size from tens and hundreds of meters in tectonically active areas (junction areas between platforms and surrounding orogenic structures, marginal troughs, intraplatform aulacogens, recent geosynclines, and others) to a few tens of kilometers in areas with the calm tectonic regime. Upward the section, blocks increase in size to disappear in the upper part of the section, which results in restored fluidodynamic relations between individual (stratigraphic) elements of the section.

The surface that marks restoration of the fluidodynamic unity between all the elements of the section is usually located above the distribution boundary of oil and gas fields.

The stratum-block structure of deep formations in petroliferous basins and boundaries between blocks is recently confirmed by many researchers who study the exploitation regime of oil and gas fields and reservoir properties of rocks. Let us consider a few examples.

The complex structure of baric and thermal fields and vertical multistage zoning determined by undulatory oscillating movements is established for the Dnieper-Donets Depression [66]. “The latter property forms a system of horizontal permeable baric zones... and new genetic type of geothermobaric traps. The mosaic patterns of anomalous formation pressures are developed through the entire depression regardless of rock age *to form lenticular anomalies of high and low formation pressures.*” The depression is divided into small hydrogeodynamic

systems, i.e., the block structure is characteristic of section elements within thermal dehydration systems (according to the terminology of the last author).

During the detailed exploration and exploitation of oil and gas fields, their structure appears to be significantly more complex than it was thought at the initial stage [61].

For some oil and gas fields of West Siberia (Novopokur, Vyintoi, Kustovskoe), this is confirmed by the following observations.

*The Novopokur field.* Some boreholes drilled in Upper Jurassic sediments ( $Yu_1$ ) of the presumably oil-bearing portion of the section appeared to yield water–oil mixture or water. At the same time, boreholes drilled beyond the pool contour provided oil. During exploitation, some boreholes respond to pumping by the yield growth, while others remain neutral to an additional disturbance in the bed. All the exploitation wells are located around the pumping one, i.e., the exploitation wells respond in different manners to processes in the pumping one. Some boreholes demonstrate inconsistency between the distribution of oil and water through the section: groundwaters are located above oil within the same field. This required more detailed stratigraphic subdivision into individual blocks ( $Yu_1^1$ ,  $Yu_1^2$ , and others) separated by confining beds such as low-amplitude or amplitude-free tectonic fractures [61]. These authors also demonstrated the “high density of the network” formed by such fractures. More than 30 NE- and NW-trending fractures that complicate seemingly unified oil pool are defined and traced through the Novopokur field, owing to which nine pools and six promising objects are recorded in the Bed  $Yu_1$ .

*The Vyintoi field.* Three boreholes drilled 500 m away from the well that encountered multilayer pools and provides high oil yields appeared to be watered in the Bed  $BV_4$  and practically dry in Bed  $Yu_1$ . Borehole 290 drilled in the central part of the field appeared to be dry in the same Bed  $Yu_1$ . The field provides no indications confirming the anticlinal structure of the pool. Six pools and six promising objects are defined in the Bed  $Yu_1$  of this field. Five of pools are tectonically screened.

*The Kustovskoe field.* In this field, exploitation wells demonstrate rapid watering in the Bed  $BS_4$ . Most of the wells (75%) were watered during a year with the water content exceeding 50%. Exploitation wells also show different response to pumping. Screening in the field is provided by plastic deformation, cataclasis, carbonatization, ozokerization, and flowing of plastic rocks into weakened zones, not by the interface between permeable and impermeable rocks (fracture with displacement). These zones are tens to a few hundreds of meters wide [61]. The zones develop from the base upward to form the block structure of the section. Similar dislocations experienced repeated renewal.

These dislocations “could serve as migration paths and confining beds” during different geological periods. The fact that these zones could serve as migration channels is confirmed by geochemical properties of oils.

In the *East Pereval'noe field*, compositionally similar oil pools are divided by the 400-m-thick clay sequence [58, 61]. They are now characterized by jumps of the water–oil contact up to 15 m at a distance of 2–4 km, i.e., this migration

channel was permeable in the past and is impermeable now. The core and thin sections demonstrate jointing, cataclasis, slickensides, and volcanism signs. Thus, seemingly unified oil pools appear to be separated into isolated blocks. The estimated reserves of the East Pereval'noe and East Oleininskoe fields were not confirmed by the 3- to 5-year-long exploitation, which required an additional study of the geological structure and petroleum resource potential in these fields [34]. The thorough study revealed differences in structures of lower ( $J_3-K_1$ ) and upper ( $K_2-KZ$ ) portions of the sedimentary section and secondary origin of hydrocarbon pools, which resulted from the influx of oils from underlying Paleozoic sediments.

The stratum-block structure of oil fields is confirmed in many regions: Pripyat Depression, Ciscaucasia, Astrakhan, and others.

Thus, *the works [14–16] demonstrate inconsistency of infiltration and elision theories explaining the formation of deep fluids in petroliferous complexes and assume instead their stratum-block structure with the recharge at the lower boundary and additional internal sources. This inference is confirmed by recent investigations and regardless of the fact how different researchers term similar structure (cellular, zoned-block, lenticular, block structures, asedimentary lenses), its essence remains unchangeable; the stratum-block structure excludes lateral migration over any significant distances and, thus, transfer of dispersed hydrocarbons, and formation of their accumulations, medium and large pools included.*

## 14.2 Recent Hypotheses (Theories) of Oil Origin

No anonymous view exists on the problem of oil genesis, although industrial production of oil and gas lasts over 150 years. Similar to any other mineral resources, origin of oil and gas is a complex problem due to multifactor cause–effect relationships in the nature. Recently, two main concepts are popular: organic (sedimentary-migratory hypothesis and others) and inorganic (mineral, emanation, and other hypotheses). In addition to long-existing sedimentary-migratory and abiogenic oil and gas origin hypotheses, several new concepts having a claim on the role of a generalizing theory of oil genesis were published during last years: fluid dynamic (B.A. Sokolov and others), geosynenergetic (A.E. Lukin), sedimentary-inorganic (I.I. Chebanenko, N.I. Evdoshchuk, and others), sedimentary-fluidodynamic (B.P. Kabyshev, Yu.B. Kabyshev), and others. In this chapter, we consider only two main hypotheses: sedimentary-migratory and mineral (inorganic); others are discussed in [16].

### 14.2.1 Sedimentary-Migratory Hypothesis

The hypothesis of sedimentary-migratory oil origin was proposed in the United States and became widespread in the former Soviet Union. Owing to its simplicity, it was and is popular among both scientists and practical geologists all over

the world [73]. Vassoevich [68], who is justly considered to be a founder of the evolutionary-genetic studies in petroleum geology, as well as his apprentices and followers, developed it most comprehensively in their works.

The hypothesis is based on the postulate that organic matter buried in sediments passing during long geological history through all the stages of diagenesis and catagenesis is transformed due to abiogenic synthesis into oil, i.e., a separate phase of most stable liquid hydrophobic products resulting from routine fossilization of organic matter in subaqueous environments.

The following arguments are usually mentioned in favor of the sedimentary-migratory hypothesis:

(1) All the sedimentary rocks (Riphean to Recent) on continents contain carbonaceous organic matter in concentrations averaging  $12\text{--}15\text{ kg/m}^3$  calculated for  $C_{\text{org}}$ . By its composition, dispersed organic matter is close to kerogene of combustible shales and coals. Organic matter in sedimentary rocks is usually of the sapropelic or humic-sapropelic types. Some share of organic matter is usually represented by bitumoids or carbonaceous compounds soluble in organic solvents such as  $\text{CCl}_2$ ,  $\text{CHCl}_3$ ,  $\text{CS}_2$ ,  $\text{C}_6\text{H}_6$ , and others. They consist of oil and tarry-asphalt components. According to Vassoevich, the hydrocarbon content in sedimentary rocks averages  $250\text{--}300\text{ g/m}^3$ . Occurrence of bitumoids is considered to reflect living matter fossilization in the biosphere, where sediments are accumulated in all the basins. Organic matter occurs in all the lithologies. In clays, the content of organic matter is twice and four times higher as compared with that in silts and sands, respectively. Thus, "oil is a product of lithogenesis" (Vassoevich, 1982, p. 14). This postulate unites all the adherents of the biogenic theory of oil origin. "Presence of biomarkers in hydrocarbons indicates that hydrocarbon migration started with the appearance of life" [7].

(2) Correlation of the quantity and type of bitumoids with the hydrocarbon composition, on the one hand, and their insoluble residue in rocks, on the other hand, is established by both Russian and foreign researchers. In opinion of adherents of the organic hypothesis, such an origin of oil indicates undoubtedly that sedimentary rocks contain autochthonous bitumoid with inherent hydrocarbons that form the basis of microoils. In bitumoids and oils, carbon plays the main role, being accompanied by hydrogen, oxygen, nitrogen, sulfur, and, frequently, metals, nickel and vanadium included.

(3) Microoil, which may be represented by several generations, is the most reduced, migratory, and neutral component of autochthonous bitumoids (largely of their oil fraction) consisting largely of hydrocarbon mixture and dissolved low-molecular tars (definition by N.B. Vassoevich). It is established that certain phases and stages of lithogenesis are characterized by their own hydrocarbon generation. Processes which occur during one of the stages in the sedimentary section at depths of 2–4 km at temperatures of  $80\text{--}150^\circ\text{C}$  are responsible for the main phase of oil generation. This stage is marked by substantial activation of microoil formation, its accumulation, desorption, and separation from parental organic matter. Sometimes, microoil is separated as an autonomous phase to form oil proper, which is classed with allochthonous bitumoid. Sequences where these processes proceed are called

source formations. The possibility of such a process in the nature is substantiated by modeling of thermolysis of sapropelic matter, combustible shales, brown coals, bituminous clays, and others, which yielded bitumoids under heating. The heating time is of significance; i.e., the longer the heating, the lower the critical temperature of the main oil-generation phase required for microoil maturing. Microoil and oil represent links of the same chain. The microoil reserves are orders of magnitude higher as compared with oil reserves. In opinion of Vassoevich, "being objective, it is impossible to leave without answer a question concerning probable relationships between micro- and macrooils, i.e., dispersed and concentrated occurrence forms of oil hydrocarbons and accompanying compounds in natural environments."

(4) Similarity between chemical compounds in bitumoids, microoil, and oil, according to chromatographic, spectral studies, and extraction data.

(5) Occurrence of molecular structures characteristic of tissues of living organisms: plants and animals.

(6) The problem of initial oil migration from source rocks and its influx into a reservoir was solved by establishing the fact that bitumoids and microoil are dissolved by compressed  $\text{CO}_2$ ,  $\text{CH}_4$ , and their homologues as well as by salinity-variable waters. Experiments were conducted in thermodynamic conditions close to the formation environments. Microoil was dissolved and released from both crushed samples and cores. The fact that the interstitial pressure in clayey rocks is higher as compared with hydrostatic one being sometimes close to geostatic values (the last statement is unsubstantiated, not confirmed by calculations and incorrect in principle; see above) is considered as one of arguments favoring migration of oil from clays. On the one hand, this provides conditions for migration of microoil into neighboring reservoirs and on the other hand, this hampers the influx of abiogenic oil in line with the theory of its inorganic origin, i.e., "microoil migrates from source rocks in form of gas and water solutions. The role of these two migrations modes is likely different at different stages" (N.B. Vassoevich, 1982).

(7) The ratio of isotopes, carbon and helium included, is considered to indicate organic origin of oil. E.M. Prasolov (1990) established the ratios of helium isotopes ( $^3\text{He}/^4\text{He}$ ) for different geological media. These ratios are widely used by adherents of the organic oil origin hypothesis for its substantiation [7 and others]. In opinion of these scientists, the isotopic composition of gases (helium and carbon) is characteristic of sediments in most oil fields. At the same time, it is admitted that hydrocarbon gases in oil and gas fields may have "at least partly different genesis," which is explained by the wide distribution of methane in natural conditions [33]. For example, Bazhenova and Sokolov [7] note that the ratio between carbon and helium isotopes is indicative of sedimentary-migratory oil origin. Helium isotopes represent practically the only indicator of its mantle origin. The content of juvenile helium allows the share of mantle hydrocarbons to be estimated. The isotopic study of fumaroles in mid-oceanic ridges revealed that the  $\text{CH}_4/^3\text{He}$  value in mantle gases is as high as  $10^6$ . In gases of oil fields and emanations from mud volcanoes, this ratio is  $10^{11-12}$ , which indicates the insignificant share of mantle components in hydrocarbon accumulations [7].

(8) In 1985, Sokolov proposed the fluidodynamic concept, which explains some facts unexplainable by the sedimentary-migratory “theory.” In our opinion, this concept represents a rebate to the mineral hypothesis of oil origin and formation of hydrocarbon accumulations (increase in temperatures and depths of the main oil-generation phase). The concept gained wide recognition, since it explains many observed geological facts.

Most researchers understand fluidodynamics as pulsating (periodical) ascending migration of solutions, oils, and gases ( $\text{CH}_4$ ,  $\text{CO}_2$ ,  $\text{N}_2\text{S}$ ,  $\text{H}_2$ ,  $\text{N}_2$ , and others) with different temperatures, compositions, and pressures, which form various anomalies in physical and geological fields (field of formation pressures included) [14, 18, 62, 63, and others]. This usually ascending concentrated (local) discharge through deep-seated faults (or their intersections) frequently in the form of mud volcanism, subaqueous discharge, and others associates with recent active geodynamic crust zones.

The sedimentary-migratory “theory” combined with the fluidodynamic concept is very popular among scientists and practical geologists who use it for assessing the petroleum resource potential of different regions.

Let us consider some examples.

The formation of hydrocarbon accumulations in the Baikit Anticline and Katanga Saddle of the Siberian Platform is explained by fluidodynamic processes during the Neogene–Quaternary. This is substantiated by the following facts. Post-Cambrian trap magmatism and hydrothermal processes resulted in substantial metasomatic transformation of Riphean carbonate rocks. These processes should “unavoidably destruct hydrocarbon pools transforming liquid oil into graphites. . .if intrusion of magma and thermal solutions into sedimentary complexes followed the formation of hydrocarbon accumulations; i.e., when oil and gas were localized in the sedimentary sequence.” Consequently, age of hydrocarbon accumulations is constrained by the formation of neotectonic structures and “anomalous surface gas and lithochemical fields as well as fluidodynamic processes” [38].

The formation of hydrocarbon accumulations in the Dnieper-Donets aulacogen is also explained by fluidodynamic processes [31]. This work demonstrates widely developed vertical migration of hydrocarbons accompanied by additional convective heating of sedimentary sequences and intensified hydrocarbon development in source formations. Hydrocarbons migrate through both reservoirs and argillites being confined only by salts. Emphasizing the dominant role of the sedimentary-migratory mechanism in oil origin and formation of hydrocarbon accumulations, the last authors admit deep sources of oil generation also, which explains regularities in the distribution of oil fields in the region under consideration and offers opportunities for predicting hydrocarbon reserves.

The petroleum resource potential of the Pripyat paleorift, which was formed during the Hercynian orogenic stage (Late Famennian), is also understood in the context of the fluidodynamic concept [36]. The paleorift hosts five mantle-seated faults, which served as conduits for the conductive and convective heat transfer accompanied by intrusion of mafic and ultramafic magma into the crust and sedimentary cover that resulted in intensified hydrocarbon migration from source



formations. The main oil-generating center is confined to the eastern part of the Pripyat Depression with main oil fields (over 60), i.e., oil and gas generation from organic matter associates with rifting, vertical movement of hot magma, and heat flows that intensify hydrocarbon generation from organic matter dispersed in source rocks [36]. Hydrothermal processes are thought to be responsible for oil occurrences in volcanic domains [6].

Thus, the sedimentary-migratory hypothesis combined with data on fluidodynamic processes is widely used for explaining oil and gas generation in many regions.

### ***14.2.2 Shortcomings of the Sedimentary-Migratory Oil Origin “Theory”***

#### **14.2.2.1 General (Geological) Considerations**

The best-grounded criticism of the sedimentary-migratory oil origin “theory” by Yu. I. Pikovskii (1986, 2002) comes to the following: (1) lithogenesis stages responsible for oil generation, energy sources necessary for hydrocarbon generation from kerogene, formation mechanism of hydrocarbon accumulations from dispersed microoil, forms and moving forces of oil migration in sedimentary rocks are unknown; (2) occurrence of different geochemical types of oils even in the same field is unexplainable; (3) the spatial distribution of hydrocarbon accumulations within source formations is characterized by irregular patterns; (4) hydrocarbon pools as well as dispersed hydrocarbons and carbonaceous minerals frequently enclosed in mineral crystals (vapor–water and oil inclusions) occur in the lower part of the sedimentary cover and crystalline rocks of the basement; (5) the distribution of hydrocarbon accumulations is distinctly correlative with deep-seated faults; (6) the occurrence of medium, large, and giant hydrocarbon accumulations is unexplainable; (7) distinct criteria for defining source rocks, except dispersed oil by composition close to the ordinary one, are absent. All these points need to be clarified.

For comparing two main theories of oil origin and their substantiating arguments, Pikovskii [53] compiled the table that demonstrates consequences following from alternative oil-generation theories (organic and mineral) and their consistency with peculiarities of this process observed in natural environments (Table 14.1).

The author also notes that available arguments “favoring the sedimentary-mineral theory of oil origin” [53] are ambiguous and this problem is unsolved (and, probably, will never be solved) similar to problems of hydrocarbon migration and their concentration in fields. The mineral theory overcomes these problems much better. Sedimentary formations play main role only in accumulation and preservation of hydrocarbon reserves that formed owing to deep Earth degassing and due to confining beds of different origin.

There is also additional evidence calling into question the organic theory of oil origin. In opinion of [67], shortcomings of the sedimentary-migratory theory are

**Table 14.1** Oil and gas generation features (after Pikovskii, 2002, with additions)

Oil and gas accumulation features	Consistency of this phenomenon with the oil-generation concept without additional assumptions	
	Sedimentary concept	Endogenic concept
Confinement to sedimentary basins	Yes	Yes
Occurrence of dispersed oil compositionally close to that in accumulations	Yes	Yes
Secondary nature of oil and gas accumulations in natural reservoirs	Yes	Yes
Possibility for the formation of large hydrocarbon accumulations through the entire section of the sedimentary basin, crystalline basement included, regardless of host lithologies, content, and type of organic matter	No	Yes
Irregular oil and gas accumulation. High density of giant and unique oil and gas fields in relatively small areas	No	Yes
Abnormally high pressures in hydrocarbon accumulations	No	Yes
Relatively short geological period (close to the recent epoch) marked by the formation of all large fields of the world	No	Yes
Correlation of oil and gas fields with recent crust movements; currently continued oil and gas accumulation	No	Yes
Confinement of oil and gas accumulations to large activated deep-seated faults	No	Yes
Replenishment of exploitation reserves in oil and gas fields	No	Yes

as follow: (1) transformation of organic remains into oil is not substantiated by experiments; (2) source rocks are lacking organic matter incompletely transformed into oil (cellulose, chitin, bones, and others) as well as microoil residues or its traces (physical impossibility of completion of microoil migration without signs of its migration) and oil and gas fields.

It should also be noted that it is unclear how to explain the occurrence of untransformed macro- and microfloral remains aged from the Proterozoic to the Recent that migrated in past and migrate now upward the section. What prevents their transformation into microoil? For example, Paleozoic fossils in the Bazhenovka Formation increase from 24 to 85–100% during field exploitation. These plant remains occur in more favorable thermodynamic conditions as compared with sediments of the Bazhenovka Formation proper and should be transformed into microoil for the period lasting since the Paleozoic. Nevertheless, this did not happen. The similar situation is also observed in other regions.

At present, all the main arguments in favor of the sedimentary-migratory theory and against the mineral one are based on geochemical data, although some of them are interpreted in different manners.

The use of advanced geochemical methods for the study of oil and organic matter yields results that cast doubts on the sedimentary-migratory hypothesis of oil origin. Gorgadze [23, 24] established some properties of dispersed organic matter and oil inconsistent with the sedimentary-migratory "theory." These contradictions consist of the following:

"Organic matter from source rocks contain frequently compounds that are absent in oils (for example, phthalates). The latter are found neither in organic matter of rocks nor in products of kerogene thermolysis. . . . The remarkable feature of these compounds is their absence in oils, which offers opportunities for discriminating between productive and nonproductive formations."

"Organic matter in coeval sequences is characterized by different maturity degree even at distances of several centimeters."

"Mass chromatograms of bitumoids with  $m/z$  217 demonstrate frequently unidentified hydrocarbons (most likely, homological series), which are missing from oils."

"The sterane oil maturation coefficient is usually higher as compared with that of organic matter in source formations. Moreover, the similar situation is also observable in products of kerogene, asphaltene, and oil thermolysis."

"The organic matter maturity degree estimated using the value of thermolysate sterane parameter increases in the tar-kerogene-asphaltene-bitumoid-oil succession" [23].

In our opinion the above-mentioned facts are not systemic and do not refute the sedimentary-migratory hypothesis of hydrocarbon origin; they pose only the question as to all the source rocks are able to generate oil or not.

Based on the soft thermolysis study, it is established for the Salym (Bazhenovka Formation) and Samotlor (Bed BS<sub>8</sub>) fields that thermolysates of tars and asphaltenes (components of dispersed organic matter) contain oleanane, which is missing from oils and products of asphaltene thermolysis. This surprised the authors, although there are no causes for such a reaction, if we remember that, according to [5], dispersed organic matter differs from that in oil.

### ***14.2.3 Isotopic Composition of Gases***

The isotopic composition of gases is an autonomous aspect of the problem concerning hydrocarbon origin. In his work of 1990, which represents large generalization of data on the isotopic composition of gases, E.M. Prasolov demonstrated the table, which allows, in his opinion and in opinion of its followers, genesis of helium isotopes to be determined (Table 14.2).

As follows from the table, the helium isotope ratio in oil and gas pools is two to three orders of magnitude higher as compared with that in the mantle, which favors, at first sight, the sedimentary-migratory theory of hydrocarbon origin.

**Table 14.2**  $^3\text{He}/^4\text{He}$  value for different geological media

Geological medium	$^3\text{He}/^4\text{He}$ value
Mantle	$(1.2-0.3) \cdot 10^{-5}$
Crust, granites	$(0.8-1.2) \cdot 10^{-8}$
Sedimentary rocks	$(0.5-3.5) \cdot 10^{-8}$
Volcanic domains	$n \cdot 10^{-5}$
Oil and gas pools (dominant)	$n \cdot 10^{-(7-8)}$

In opinion of Prasolov, the “primary distribution of isotopes determined the isotopic composition of the crust. Various geochemical processes in the crust result, however, in the redistribution of isotopes between different substances and their fractions, particularly under low temperatures” (Prasolov, 1990, p. 27). The distribution of isotopes occurs during their migration due to their volatility and *their ratio is determined by many processes that are difficult for accounting, which casts doubts on unambiguity of main inferences.*

The author proposes geochemical classification that determines both their origin and ratios and includes different process (genetic, migratory) and their interaction.

In the above-mentioned and subsequent works [54, 55], Prasolov emphasizes ambiguity of conclusions on hydrocarbon genesis based on gas isotope ratios.

This is also confirmed by the study of this ratio in the Kola Peninsula, where the  $^3\text{He}/^4\text{He}$  value in intrusive ultramafic rocks ranges from  $1-2 \cdot 10^{-8}$  to  $3.3 \cdot 10^{-5}$  [48], i.e., includes all the diapasons of ratios presented in Table 14.2. Such high values of this ratio were never determined in igneous rocks. The authors note justly that no signatures exist now that would indicate unambiguously genesis of helium isotopes since their present-day composition results from many factors: melt degassing degree, content of radioactive minerals, concentration of migrating isotopes and their losses, preservation of isotopes, duration and intensity of postmagmatic process, and many others.

The same is true of carbon isotopes. The wide range of variations in the carbon isotope composition is established for carbonates from Black Sea mud volcanoes, where  $\delta^{13}\text{C}$  values range from  $-43.3$  to  $-10.5\%$ . The authors [54, 55] (Prasolov included) cannot interpret unambiguously this fact and propose its “temporary” explanation. The similar situation is characteristic of natural carbonate tubes in the underwater discharge area in the Cadiz Bay of the Atlantic Ocean [5], where explanation is also presumable.

In [57], Rodkina calls in question the inference by Prasolov on the negligible contribution of mantle gases based on the carbon and helium isotope composition defining two types of errors.

*The first error* is connected with the selection of characteristic ratio values (both toward over- and understatement). The traditionally used  $\text{CH}_4/{}^3\text{He} \equiv 10^6$  value characteristic of high-temperature fumarole and volcanic gases provides “0.1–0.5% estimate for contribution of mantle hydrocarbons even to fields of the Pacific ring most enriched in the mantle component” [57, p. 131].

In low-temperature zones (amagmatic domains), the situation is different. For example, the Okinawa back-arc basin is characterized by the  $\text{CH}_4/{}^3\text{He}$  value close

to  $10^9$ , lower  $^3\text{He}/^4\text{He}$  values, and lighter carbon isotope composition. In addition, geological data provide no grounds for assuming the enrichment of these gases with components from sedimentary rocks.

Away from the volcanic domain, the  $^3\text{He}/^4\text{He}$  value decreases. The concentration of  $\text{CO}_2$  decreases as well and its isotopic composition becomes heavier. This is accompanied by increase in the relative share of  $\text{H}_2$  and  $\text{CH}_4$ . The similar situation is observed in California, where the  $\text{CH}_4/^3\text{He}$  value is even higher reaching approximately  $10^{10}$  and  $^3\text{He}/^4\text{He}$  value is also elevated. In this area, gas is undoubtedly enriched in methane from sedimentary rocks.

*The second error* is connected with “ignoring the flow of matter presumably subducted into the mantle beneath back-arc basins” [57, p. 132]. This flow is of both mantle and biogenic origin, which results unavoidably in the depleted mantle component.

According to petrological data, the fluid from subduction zones is episodically (quasiperiodically) accumulated in the continental crust to form the corresponding regime. This is confirmed by modeling of this process and seismotomographic data. At the same time, there are indications of the substantial contribution of mantle gases to the formation of hydrocarbon accumulations: the isotope composition of accompanying components (Nd, Pb, Sr) in most oil and gas fields of the former USSR and China confirms their crustal or mantle origin, which is also evident from high  $^3\text{He}/^4\text{He}$  values.

In fields confined to active plate boundaries, this ratio is elevated. Nevertheless, this elevation is insignificant, which is interpreted as evidencing against participation of mantle fluids in the formation of hydrocarbon accumulations.

In opinion of M.V. Rodkina, of importance is both the average value of this ratio and isotope variations in closely spaced hydrocarbon accumulations. Using fields of California, West Siberia, and Japan (Green Tuff area) as examples, it is shown that despite significant scatter of data points, each area is characterized by good correlation (>99%) between  $^3\text{He}/^4\text{He}$  values and isotopic composition of hydrocarbons. In addition, empirical straight lines available for  $\text{Lg}(^3\text{He}/^4\text{He}/^{13}\text{C})$  values of all the areas are almost parallel. The increase in the  $^3\text{He}/^4\text{He}$  value results in heavier isotope composition of methane (up to 20–30%), which indicates the increased contribution of the mantle component. In our opinion, the regularity in variations of  $\text{Lg}(^3\text{He}/^4\text{He}/^{13}\text{C})$  values represented in figures [57] is not universal. For example, it is indistinct in central areas of America and latitudinal segment of the Ob River. The above-mentioned examples indicate substantial enrichment of continental margins with the recycled fluid and elimination of mantle isotopic signatures through the section.

Krayushkin [42] considers the  $\delta^{13}\text{C}$  content in different natural objects as indicating inorganic origin of hydrocarbons (Table 14.3)

Different contents of carbon isotopes indicate “different oil-saturation degree of the crust and mantle through the area and section and occurrence of giant solitary or cluster centers of natural non-biotic synthesis of oil and natural gas” [42].

The  $\delta^{13}\text{C}$  isotope composition values of –25 to –28‰ are considered as indicating biogenic origin of oil. Previously, the substantially higher content of this isotope

**Table 14.3**  $\delta^{13}\text{C}$  values (‰) in natural objects

Object	$\delta^{13}\text{C}$ values (‰)
Natural oil	From -20 to -30
Accompanying oil gas	From -30 to -55
Natural gas	From -20 to -62
Methane from fermentation in animal stomach	From -62
Sea methane hydrates	From -36.1 to -94.0
Fischer-Tropsch oil	From -14 to -65
Graphite of chondrites	-20
Kerogene of carbonaceous chondrites	From -17 to -27
Noncarbonate carbon of ultramafics and primary fluid inclusions in mantle peridotite xenoliths	From -22 to -29
Natural diamonds	From -0.5 to -33
Recent marine biota of the tropical and middle latitudes	From -8 to -34

(-2 to -7.2‰) was considered to indicate its mantle source. Recently, diamonds with  $\delta^{13}\text{C}$  values of -3.3‰ and lower are discovered, *i.e.*, the value range of mantle carbon became substantially wider, owing to which unambiguity of hydrocarbon biogenic origin in oil and gas fields casts certain doubts. The formation of hydrocarbon accumulations accompanied undoubtedly by their transformation, migration, and mass exchange results in the changed carbon isotope composition, which can be primarily of both biogenic and abiogenic origin [47]. This work also demonstrates that oxidizing hydrate disproportioning of polycarbon substances results in the formation of hydrocarbon molecules enriched in the light carbon isotope due to differences in rates of elementary processes of the bond rupture in the system of different  $^{12}\text{C}$ - $^{13}\text{C}$ ,  $^{12}\text{C}$ -H, and  $^{13}\text{C}$ -H combinations and the formation of  $\text{CO}_2$  containing largely  $^{13}\text{C}$ .

According to [45], the  $\delta^{13}\text{C}$  isotope content and its shift depend on recent tectono-magmatic activity (that measured by instrumental methods included): areas with the active and calm tectonic regimes are characterized by lighter (-20 to -21‰) and heavier (-8 to -10‰) carbon isotope compositions, respectively, which is explained by deeper magmatic chambers in former areas and shallower (near-surface at the cessation stage) in the latter.

In opinion of V.A. Krivoshei, "the high-temperature mineral synthesis that provides the thermodynamically regular distribution of carbon isotopes through all the components of hydrocarbon systems is a main process responsible for the formation of the entire spectrum of oil and gas compounds. Deep sources determine the directed undulatory evolution of hydrocarbon synthesis" [44]. The study of the carbon isotope composition in vapor-liquid inclusions (gas, oil, bitumen) reveals the previously unknown phenomenon of the quant distribution of the  $\delta^{13}\text{C}$  isotope shift.

The influx of deep hydrocarbons is characterized by the pulse pattern. Their phase state, as well as wide spectrum of physicochemical parameters and properties, reflects several migration cycles (Chapters 11 and 13).

This is confirmed by studies of carbon isotopes in northern West Siberia [20, 21]. Particular attention in these studies was paid to search of factors responsible

for lateral and vertical variations in  $\delta^{13}\text{C}$  values of free gases. In the giant Nadym-Medvezh'e gas pool, the  $\delta^{13}\text{C}$  value increases from the north southward from  $-52.9$  to  $-40.8\text{‰}$ , while in the Urengoi pool, this value increases from  $-43.6$  to  $-44.8\text{‰}$  at depths of 1,104–1,150 m to  $42.6\text{‰}$  at 30 m. In the Yamal petroliferous region,  $\delta^{13}\text{C}$  value demonstrates variations through the section as well being  $-32.4$ ,  $-40$ ,  $-39.2$ , and  $-47.6\text{‰}$  in the Valanginian, Aptian, Albian, and Cenomanian formations, respectively; in permafrost rocks of the upper portion of the section (K<sub>2</sub>m-b-Q) at depths of 15–150 m, this value ranges from  $-70.4$  to  $-76.8\text{‰}$ . These patterns in the  $\delta^{13}\text{C}$  distribution provided grounds for defining two types of the section: with carbon isotope becoming regularly heavier (migratory genetic type) and with its relatively stable composition (syngenetic type). Sections of the first type are characteristic of many gas fields in other regions.

Thus, the available data are insufficient for unambiguous discrimination between isotopes of different-composition and different-origin gases; therefore, it is premature to speak about the sedimentary-migratory theory [33] as the only one explaining oil origin and formation of hydrocarbon accumulations based on isotope ratios in gases.

#### ***14.2.4 Mineral (Inorganic) Theory***

This theory is based on two facts: widespread degassing of the Earth and experimental synthesis of hydrocarbons by catalysis under various pressures, temperatures, and catalysts (chemical basis of the hypothesis). This theory was first formulated in Russia owing to works by D.I. Mendeleev, who synthesized oil in laboratory conditions (carbide hypothesis), and other Russian scientists such as P.N. Kropotkin and his followers.

The following facts are thought to support this hypothesis of mineral oil origin:

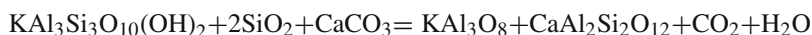
- (1) Occurrence of oil in basement rocks and hydrocarbon signs in crystalline, metamorphic, metasomatic, and igneous formations.
- (2) Occurrence of hydrocarbons in deepwater hydrothermal solutions of mid-oceanic and marginal-sea ridges.
- (3) Synthesis of many hydrocarbons in laboratory conditions.
- (4) Association of hydrocarbons with deep-seated faults and mud volcanoes serving as conduits for their near-vertical ascending migration.
- (5) Development of abnormally high formation pressures in different parts of sedimentary sections.
- (6) The hypothesis explains the occurrence of carbonaceous compounds in meteorites and vapor–liquid hydrocarbon inclusions in minerals and crystalline rocks.

The paleohydrothermal activity is reflected in vapor–liquid inclusions observed in minerals and different rocks. The study of fluid inclusions in minerals from

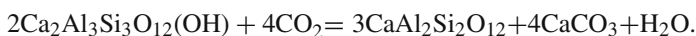
vein, metamorphic, and igneous rocks revealed that they could not appear without the influx of mantle fluids. Based on approximately 100 analyses of gas phases from diamonds and garnets from mafic and ultramafic xenoliths in kimberlite pipes, two groups of fluid inclusions are defined: (1)  $\text{H}_2\text{O}-\text{N}_2-\text{CO}-\text{CH}_4-\text{C}_2\text{H}_2-\text{C}_2\text{H}_6-\text{C}_2\text{H}_8$ ; (2)  $\text{CO}_2-\text{N}_2-\text{CO}-\text{CH}_4-\text{C}_2\text{H}_2-\text{C}_2\text{H}_6-\text{C}_2\text{H}_8$ . In diamonds formed at depths of approximately 400 km, the  $\text{H}_2/\text{H}_2\text{O}$  value is equal to 4.2, while at depths of about 120 km, this ratio is 0.03. Minerals “preserve relicts of (fluid) inclusions with high, intermediate, and low densities” reflecting “metamorphic” evolution. Fluid inclusions “are captured by growing minerals at different levels of the crust during the rock rise and cooling” [51]. In the presence of  $\text{CO}_2$ , wollastonite ( $\text{CaSi}_3\text{O}_8$ ) is transformed into calcite ( $\text{CaCO}_3$ ) and quartz ( $\text{SiO}_2$ ). In the presence of water, orthoclase ( $\text{KAlSi}_3\text{O}_8$ ) and rhombic pyroxene are transformed into biotite ( $\text{K}(\text{Fe}, \text{Mg})_3\text{AlSi}_3\text{O}_{10}(\text{OH})_2$ ) and quartz ( $\text{SiO}_2$ ).

Thus, fluids in ascending magma include carbon and hydrogen compounds, which form oil pools in the sedimentary cover due to complex reactions with organic matter. Hydrocarbon pools are forming in all the lithologies, crystalline rocks included.

At the same time, during metamorphism, rocks can release water and carbon dioxide. For example, the following reactions occur in low-temperature metapelites [51]:



or



Sometimes, inclusions represent crystallized brine, which could be impossible without admixture of  $\text{NaCl}$  in migrating solutions.

In opinion of A.A. Kichk (2002), juvenile solutions (hydrocarbons included) occur in basement rocks in insignificant quantities in crystal cavities. In tectonically mobile zones, transformation of their rocks, which constitute thousands of cubic kilometers, is accompanied by the release of “tremendous fluid volumes. Presence of large quantities of waters in rocks explains hydrochemical anomalies in form of desalinated solutions with the specific isotopic composition. Dynamics of fluid movements along fault zones is complex and hydrocarbon pools are formed in reservoirs with better capacity and filtration properties, not necessary located immediately above the basement. This explains absence of pools in the basal part of the petroliferous basin sedimentary cover.

Sign-variable fluctuations of tectonic strains determine slow secular ascending movement of fluids, which corresponds to the ‘cold’ degassing regime. Thus, fluid removal results directly from the regional tectonic activity.”

Concentration of *n*-alkanes  $\text{C}_1-\text{C}_4:\text{C}_{10}-\text{C}_{33}$  or  $\text{C}_1-\text{C}_6:\text{C}_{14}-\text{C}_{33}$  and isoprenes  $\text{C}_{11}-\text{C}_{20}$  (pristane, farnesane, phytane, and others) in inclusions in peridotite xenoliths (fragments of the upper mantle), basalts, granites, ophiolites, and ultramafics from different world regions (Australia, Antarctica, Indonesia, Japan, Italia, Canada,



Cyprus, China, Philippines, Russia, Turkey, the United States, Zimbabwe, and others) is estimated to vary from 0.1 to 500 ppm and that of  $\delta^{13}\text{C}$  isotopes from  $-20$  to  $28.9\%$ . All these rocks were formed at depths of 300–400 m under temperatures of 1,000–1,200°C and pressures amounting to 3–4 GPa. Primary inclusions of H, H<sub>2</sub>O, CO<sub>2</sub>, CO, and hydrocarbons with concentrations up to 30–35 ppm are found in natural diamond of Asia, Africa, North and South America. Kimberlites are also established to contain hydrocarbons and oil up to 1,154–7,087 ppm. Kimberlites and diamonds with  $\delta^{13}\text{C}$  concentrations of 0.5–31.9‰ were formed at depths of 400–500 m under temperatures of at least 1,100–1,250°C and pressures up to 4–5 GPa. All these facts indicate the existence of oil and gas under high temperatures and pressures at deep levels where biogenic material is missing [42].

The Earth degassing accompanied by vertical migration is established in many petroliferous basins. Let us consider some of recently established examples.

The sedimentary-migratory concept of oil origin can hardly explain spatial differentiation of commercial fields with hydrocarbons of different compositions and phase states exemplified by the Dnieper-Prityat aulacogen with the Prityat largely petroliferous province (30 oil fields) and Dnieper-Donets petroliferous province (over 200 oil and gas fields) [71]. The hypothesis of organic oil origin also cannot explain the petroleum resource potential of the Prityat Trough. The lack of gas pools in formations with saliferous deposits, which prevent from vertical migration, is difficult to understand. In the Dnieper-Donets province, commercial oil and gas pools are observable up to depth of 5,100 and 6,300 m, respectively. Gas pools are localized only in the southeastern part of the province, while its northwestern part is characterized by both gas and oil pools and areas located closer to the Prityat Trough host only oil fields. The thickness of the sedimentary section in the northwestern part of the province amounts to 6.0–6.5 km, which is sufficient for development of both main oil- and gas-formation phase, on the one hand, and only gas pools, on the other. In this area, hydrocarbon accumulations are screened by clays and argillites (dissimilar to saliferous members in the Prityat Depression), which may be permeable to some degree during certain geological epochs to permit vertical gas migration.

Thus, no correlation is observed between main stages of oil formation (depth exceeding 5 km and temperatures of 180–250°C) and catagenesis stages, on the one hand, and the spatial distribution of hydrocarbon pools, on the other. Remote lateral migration, which could promote concentration of hydrocarbons, is excluded in the situation under consideration. Their spatial differentiation is more readily explainable by the mineral (deep) hydrocarbon generation related to the Earth degassing (concept of ore and hydrocarbon formation unity or naftometallogeny by N.S. Bezrodnyi) [71].

Main arguments against abiogenic origin of oil are the following:

- (1) Lack of structures in common in oil compounds synthesized in laboratory conditions and organic compounds of living organisms;
- (2) Optical properties of synthesized hydrocarbons and natural oil of biogenic origin are different.

Let us consider these data with account for recent data.

### 14.2.5 Artificial Synthesis of Hydrocarbons

The mineral hypothesis includes two main aspects: endogenic+metasomatic genesis of hydrocarbons and their synthesis in laboratory conditions. The Fischer-Tropsch reaction is usually considered to confirm artificial synthesis of hydrocarbons. Depending on thermodynamic conditions, its products may be represented by *n*-alkanes, olefines, subordinate isoalkanes, and aromatic hydrocarbons; “neither isoprenes nor cyclanes were synthesized by this reaction.” In addition, this reaction requires high temperatures and normalized CO<sub>2</sub> and H ratio, “which is hardly observable in natural environments at the significant scale” [7].

During the last 30 years, researchers from different countries performed many studies concerning catalytic (inorganic) synthesis. At first, these were the Fischer-Tropsch catalytic systems and in the last 20 years, catalytic studies of hydrocarbons from CO, CO<sub>2</sub>, and H<sub>2</sub> using biofunction catalytic systems with metal-bearing (Fe, Ni, Co, Mo, and others) catalysts and metal oxide systems with clays, SiO<sub>2</sub>, Al<sub>2</sub>O<sub>3</sub>, and zeolites under temperatures of 220–450°C were carried out. The obtained hydrocarbons ranging largely from methane to mixture of liquid phases (C<sub>20</sub>+) with variable concentrations of olephanes, *n*-alkanes, isoparaffins, and aromatic compounds were compared with natural hydrocarbons from gas condensate fields [26, 46, and others]. According to [42], products of the catalytic synthesis are represented by normal, isoprenoid, and other hydrocarbons (in opinion of O.K. Bazhenova, no isoprenoids were synthesized in laboratory conditions). Oil synthesized from H<sub>2</sub> and CO<sub>2</sub> contains series C<sub>2</sub>+ and is characterized by the δ<sup>13</sup>C value ranging from –65‰ at 127°C to –20‰ and that from H<sub>2</sub> and CO is characterized by δ<sup>13</sup>C values of –25 and –14‰, respectively.

Thus, the wider spectrum of initial components and catalysts in different thermodynamic conditions allows more hydrocarbon varieties compositionally similar to natural phases to be synthesized.

### 14.2.6 Optical Properties of Oils

Inconsistency between optical properties of synthesized and natural oils is considered as one of the important arguments favoring the sedimentary-migratory theory of their origin and arguing against the mineral one. “Optical activity of oils reflecting the chiral purity of biological systems and limited number of hydrocarbon isomers in oil, which results from their selective accumulation by living organisms, represent undoubted evidence for its genetic relation with biogenic matter. Regardless of the carbon source (endogenic, cosmic, or biogenic), initial oil matter should be involved into the life cycle in its history” [7 and many others].

The optical activity of oil depends on triterpene, sterane, and gonane contents in fractions under temperatures exceeding 420–450°C. This confirms the biogenic theory of oil origin from living matter. Nevertheless, this correlation is not

obvious. The mechanism of migration of microfossils and relict structures to oil accumulations in “relative quantities and proportions of both molecular mass and chemical structure similar to these parameters in the dispersed organic matter” is not yet explained (Yu.P. Pikovskii, 1986). This geochemical correlation should be explained by migration mechanism. How does “the heavy residue containing the main share of steranes, triterpenes, and gonanes” that determine optical properties of oil as well as “tars, asphaltenes, and minor elements” migrate? How could geochemical properties of microoil remain unchanged during many millions of years required for oil generation with their subsequent preservation in different geological conditions that changed multiply during these millions of years as well? Similar to host rocks, oil experiences permanent quasiperiodical changes under the influence of many geological, primarily geodynamic, thermodynamic, catagenetic, and other processes; therefore, its physical and chemical properties should also change with time. This is probably responsible for the fact that geochemical properties of oil and gases vary within the same field that experiences differently oriented vertical movements of separate blocks (spatially variable stress field with alternating zones of extension and compression) [18].

Let us consider the results of the recent study dedicated to optical properties of oils. Yu.D. Pushkarev asserts that determination of optical properties of oils is senseless since the same sample “may contain simultaneously left-handed, right-handed, and optically inert components. . . The capability of oils to rotate the polarization plane clockwise is secondary and is determined by selective transformation of left-handed compounds by bacterial communities that live in oil and consume the latter, while left-handed components of oil are nothing else, but bacterial remains. It follows from assumption that presence of such remains in oils deprives biogenic markers in oils, which are similar to the latter in the isotopic composition, of genetic information value” [56].

Thus, the lack of optical anisotropy in synthesized oil is insufficient for an unambiguous inference on oil genesis, since optically active hydrocarbon compounds are transformed with time into inert varieties and their proportion is also changeable, while the widening spectrum of catalysts offers opportunities to obtain progressively widened spectrum of synthesized hydrocarbons.

The past and recent hydrothermal activity (obligatory element of the mineral oil origin hypothesis) associates with geodynamically active zones in petroliferous basins. The long-known confinement of oil and gas fields to tectonically active zones and recent geodynamic processes provides grounds for classifying territories using these features and defining hydrocarbon accumulations of the geodynamic type. Gorbachev [22] proposes their classification based on tectonic features with the assessment of the petroleum resource potential.

In platforms, most promising with respect to the petroleum resource potential are structures of the aulacogen type (paleorifts), which are characterized by the reduced thickness of the crust, inverse relief of the basement, thick sedimentary sequences, and development of diapirs. The latter may be formed during several rifting stages, each marked by own petroliferous complex generating and accumulating hydrocarbons. The best examples of such a structure are the Pechora-Kolva aulacogen

with three rifting stages (Baikalian, Caledonian, and Hercynian) and Donets-Pripyat aulacogen [69].

The studies of the deep structure in West Siberia revealed strain and compression zones as well as wide development of thrusts in the basement and basal part of the sedimentary cover in the latitudinal segment of the Ob River region.

The aforesaid determines criteria for the defining areas promising with respect to hydrocarbon accumulations. They are primarily tectonically active zones, areas adjacent to deep-seated faults, conjunction zones of major high-order structures, and others. This should be followed by defining reservoirs, where intense lateral migration from zones of deep-seated faults overlain by confining beds is possible. Sampling should be conducted through the entire section of the sedimentary cover. If hydrocarbon accumulations are discovered in upper parts of the section, they or their signs should also be certainly found in underlying formations.

Bagdasarova [3] described geodynamic types of hydrocarbon accumulations. Based on the study of geophysical fields in the stationary testing areas and the analysis of the available geological information, she established the following.

The *Rechitsa Fault (Pripyat Depression)* controls main oil fields and is characterized by the vertical zone of crust and upper mantle thinning and elevated temperatures. This fault serves as a conduit for fluid migration. The latter determines variations in geophysical fields (magnetic, gravitational).

The *Terek-Caspian Trough* is controlled by deep-seated faults. Main oil accumulation zones, also controlled by these faults, are characterized by thinning zones and higher permeability, elevated temperatures, and intense different-sign block movements. The zones of elevated jointing and permeability are mostly confined to intersections of differently oriented faults. The intense recent vertical ascending discharge of fluids is represented by thermal springs locally with oil films. Similar to the Pripyat Depression, the trough is accompanied by alternating thinning and compression zones.

The capacity of reservoirs confined to faults is connected at deep levels with secondary porosity, caverns, and fissures. The periphery of oil pools is marked by zones of secondary cementation and redeposition of silica, calcite, ankerite, siderites, anhydrite, and others, which serve frequently as confining beds. They are similar to zones of hydrothermal metasomatism of rocks. Oil fields are contoured by desalinated groundwater. In our opinion, this is explained by phase transitions caused by changes in thermodynamic conditions (see above). This fact indicates the influx of fluids from deep spheres and allows hydrocarbon accumulations to be considered as "hydrothermal postvolcanic emanations during Earth degassing" in both past and recent geological epochs [3]. The latter is confirmed, for example, by the occurrence of Cretaceous rock blocks and fragments among Maikopian sediments in the Terek-Caspian Trough. The Maikopian sequence is saturated with high-pressure fluids that stimulate clayey diapirism. Ascending fluids are characterized by the variable compositions, temperatures, pressures, and temporal dynamics against the background of different-intensity geodynamic processes.

The neglect of recent geodynamic processes decreases the effectiveness of hydrocarbon prospecting works and prevents from developing the formation model of

hydrocarbon accumulations, which would reflect adequately the real situation. This leads to substantial difficulties during their exploitation (usually reflected in discrepancy between estimated and factual reserves), which is noted by many researchers [41].

For example, in [52], such a discrepancy between identified and extractable reserves is explained by the neglect of recent geodynamic processes that result in decrease (compression zones) or increase (extension zones) of filtration-capacity properties of reservoirs and confining beds. In addition, filtration-capacity properties depend substantially on the strain-deformation state. "Along with sedimentary variation, superimposed heterogeneities affect to different extent hydrocarbon reserves," since compressibility of interstices ( $n \cdot 10^{-4}$  mPa) is substantially lower (approximately two orders of magnitude) as compared with that of fissures ( $n \cdot 10^{-2}$  mPa). The studies (using labeled atoms) revealed development of high drainage zones. Irregular volumetric compression results in the increased rock volume due to the opening of existing and formation of new fissures (dilatancy), which frequently leads to dissolution ("corrosion under pressure") with the formation of caverns and "cataclases" in all the rock lithotypes, particularly in carbonate varieties. Irreversible deformations increase permeability up to six orders of magnitude. When studying pressures in exploitation wells in the Bazhenovka Formation of the Salym field (fissure reservoirs), we established three deformation stages (elastic, plastic, and dilatancy type), which are reflected in indicator diagrams illustrating correlation between the integral oil recovery and current formation pressure and between productivity coefficient and bottom hole pressure. The oil production from extension zones exceeds 85%, while in compression areas wells are characterized by low and unstable yields, which decrease substantially as formation pressure falls up to 10–20 mPa. Wells located in areas of anomalous compression are characterized by non-commercial yields or are dry (Well 8,705 with the horizontal drift of approximately 300 m).

It was shown for the Astrakhan field that the pressure in zones of lateral compression combined with that of the lateral extension exceeds 65 mPa, and all the vertical fissures are closed. Wells drilled in this zone appear to be dry (Well 316E) or are with low yields (wells 55E, 717E, and others). These wells are located in the central part of the field with highest position of the complex and should be most productive, according to the traditional point of view. Similar situation is also characteristic of the Volodarskaya deep borehole drilled on the Astrakhan Arch. In this area, the compression zone represents an impermeable or poorly permeable boundary ("side screen"), which excludes lateral fluid migration within the field. Similar situations are also observed in the Tengiz (thickness of oil-bearing formation >1.5 km) and Salym oil fields [52]. The increase in the effective strain against the background of deep occurrence and anomalous compression particularly in peripheral parts of thinning zones stimulates fissure closing and healing. Reservoirs become transformed into confining beds, *side screens* (boundaries of blocks) for most rock lithotypes (anhydrites, dolomites, limestones, argillites, siltstones, and others), which results in the formation of zonal-block systems with different filtration-capacity properties (Chapter 6). The last authors believe justly that such a zonal-block structure of

fields, high lateral and vertical heterogeneity of reservoir, and confining beds should be taken into consideration during their exploitation [52].

In [70], it is proposed to use fluidodynamics for prospecting hydrocarbon accumulations. The fluidodynamics is unavoidably accompanied by physicochemical dissolution, leaching, and formation of secondary minerals; these processes are widespread in Paleozoic and Cretaceous sequences of West Siberia. They are responsible for a mineralogical and geochemical “mosaic” observable at different depths. The author proposes to organize monitoring in hydrocarbon accumulations for developing the theoretical basis of fluidodynamics. Development of seismic methods that would take into account consequences of fluidodynamic processes (geodynamic processes and strain zones included) should increase effectiveness of hydrocarbon prospecting.

Thus, at present there are no significant arguments against the hypothesis of mineral formation of liquid hydrocarbons.

### ***14.2.7 The Mineral–Organic Hypothesis***

In our opinion, oil origin can be explained by uniting all the arguments in favor of above-mentioned antagonistic (at first sight) concepts and proceeding from general laws of Earth’s evolution.

The global distribution of organic matter buried in the sedimentary cover of negative structures during sedimentation is an indisputable fact. Similarly indisputable is also the formation of dispersed microoil from buried organic matter in sediments under certain thermodynamic conditions (main phase or oil-generation zone included) and its migration. The Earth’s degassing is also an undoubted phenomenon confirmed by many observations.

The pulsation fluidodynamic formation model of deep fluids proposed in [14, 15, 17] explains driving forces, various anomalies in physical and geological fields in lower and middle parts of the petroliferous basin section, oil origin, and formation of hydrocarbon accumulations based on the following facts:

(1) High-temperature hydrothermal solutions stimulate the formation of microoil at all the levels of the sedimentary section in zones adjacent to their conduit (usually, fault zones), i.e., the main phase of oil generation may exist during the long period through the entire sedimentary section with optimal temperature conditions.

(2) Ascending through the section, the vapor–water mixture captures available microoil and organic matter to transport them into overlying formations. This is confirmed by the occurrence of older pollen in young sediments. The vapor–water mixture forms secondary porosity due to hydraulic fracturing and gradients of formation pressures, which substantially exceed gradients in normal conditions providing prerequisites required for migration of deep fluids in all directions.

(3) Under changed thermodynamic conditions, stratal fluid intrusions (adjacent to the main conduit) are subjected to differentiation of their matter with the formation of oil and gas accumulations, preservation of which is provided by the development

of impermeable or poorly permeable boundaries due to the formation of secondary minerals, which are unavoidably deposited in such conditions. It is not incidental that the uppermost and basal parts of hydrocarbon accumulations host desalinated groundwater, the previously dissolved portion of which passed into a solid phase.

(4) In addition, the intruding vapor–water mixture contains a wide spectrum of mantle hydrocarbons (Earth's degassing), which mix with microoil available in sediments and that formed during intrusion to form different-scale hydrocarbon accumulations, giant fields included. The study of fluid inclusions in minerals of vein, metamorphic, and igneous rocks reveals that they could not form without the mantle fluid influx.

Thus, ascending hydrothermal fluids include carbon and oxygen compounds, which can participate in complex reactions with biogenic organic matter in the sedimentary cover. Hydrocarbon accumulations may be formed in all the lithologies, crystalline rocks included. Mixing and capture of biogenic oil impart to mantle hydrocarbons geochemical features inherent in oil of biogenic origin and vice versa. The location of hydrocarbon accumulation in the vertical section and their preservation are controlled by two factors: weakening energy of the vapor–water mixture of mantle origin and availability of confining beds, which may develop in all the lithologies due to the formation of secondary minerals.

Geochemical properties of oils are also variable due to many factors: quantity of microoil in sediments (existed prior to intrusion and formed after the latter) and hydrocarbon compounds of mantle origin, content of organic matter in sediments, and others. These variations are sometimes observable even within the same field.

The proposed hypothesis for explaining the formation of oil and hydrocarbon accumulations may be termed as *mineral–organic*. It combines all the arguments of sedimentary-migratory and mineral theories of hydrocarbon formation and is consistent with general laws of the Earth's evolution.

The basement is a connecting link between the sedimentary cover, the crust, and the upper mantle. Therefore, oil and gas occurrences as well as hydrocarbon accumulations in the basement serve as direct evidence in favor of both mineral and mineral–organic oil origin and the formation of hydrocarbon accumulations. Explanation of oil origin by its migration into positive structures of the basement from surrounding depressions filled with sediments is incorrect, since both the basement and the lower part of the sedimentary cover are characterized by the stratum-block structure.

Let us consider some examples of oil and gas occurrences and hydrocarbon accumulations in the basement (Chapter 5).

In the Timan region, oil occurrences in basement rocks are established for the Chib'yus, Verkhne-Chut, and Izkos'gor fields, and in the Zelenets, Chernaya Rechka, Lekkem, Timan, and other areas as well as in the weathering crust developed after the basement (0–25 m) and 194–244 m above the latter. In the Yarega structure of the Ukhta-Izhma Swell, Riphean fissured rocks host inclusions of thick oil, asphaltene, and solid bitumen. In this area, oil occurrences are recorded up to 300 m above the roof of the Riphean complex [35]. The uppermost Riphean section contains bituminous sandstones, which form the zone 4.5 km long and 0.3–1.2 km

wide. In some boreholes drilled in the Yarega structure, blowouts of hydrocarbon gas from carbonaceous shales occurred at 30 m above the roof of the Riphean section, while gas emanations (methane up to 90%) from groundwater were registered practically through the entire recovered section. In Borehole 700 drilled in the same area, bituminosity and elevated gas content are traceable to depths of 1,661 m [64]. In the initial 1940s, drilling of exploration boreholes for oil and gas of the Vodnyi Promysel area yielded the commercial gas influx containing up to 96% of methane from Riphean sediments. Gas occurrences in this borehole are traceable up to 430 m downward the Riphean sequence with most intense of them observable at a depth of 150 m. The minimal initial yield of gas was 21,000 m<sup>3</sup>/day. Liquid oil filling fissures in quartzites and schists is also registered in some boreholes drilled in southern Timan. Saturation of thin presumably Riphean sandstone beds with bitumen is recorded in the Storozhevsk area of the Vycheгда Trough (Borehole 1, interval of 2,549–2,533 m). In southern Timan, gas with the yield of 1,00,000 m<sup>3</sup>/day gushed during 2 years from Borehole 3 drilled in the Baikalian basement. The composition of gas was the following (%): methane 87–96; heavy hydrocarbons 0.4–1.5; nitrogen with inert gases 2.5–11.8; He 0.24; Ar 0.02–0.04; CO<sub>2</sub>–H<sub>2</sub>S 1.3 [64].

Over 1 billion square meters of gas was released into the atmosphere from oil mines of the Yarega area during 20 years of their exploitation.

According to [42], over 450 hydrocarbon accumulations, 40 giant fields included (3,703 bln m<sup>3</sup> of gas and 3,160 mln tons of oil, which constitutes 23% of world reserves for January 1, 2000), are discovered in the crystalline basement. The thickness of the oil-bearing section is 1.5 km. The upper boundary of the oil-bearing section is located at depths of 800–1,500 m from the basement roof. For example, the oil production of some boreholes in the White Tiger field amounted to 1.0–1.5 mln tons and total production of deposit exceeded 50 mln tons. In the Rengin field of China, production of oil from the basement is as high as 160 mln tons. In the La Pas field of Venezuela, this parameter is 14 mln tons. Hydrocarbon fluxes along basement faults are established in the Nep-Botuoba Anticline, where oil influx from the weathering crust developed after the crystalline basement is obtained in the Verkhne-Chon field.

Hydrocarbon accumulations with abnormally high formation pressures are also established in the basement in the Tyumen super-deep borehole and boreholes drilled in the Urengoi field. This area is characterized by formation pressure gradient of 1.5–1.64 mPa/100 m at depths of 5.0–6.3 km and hydrochemical anomaly at depths exceeding 5.5 km reflected in the replacement of chloride-calcic waters by hydrocarbonate ones [60], which indicates the influx of carbon dioxide.

The scientific and practical attention to the petroleum resource potential of the basement is so high that this problem was discussed at the special scientific-practical conference in Tatarstan [65], where hydrocarbon prospecting in the basement is particularly intense; similar works are also conducted in other regions.

The study of reservoir properties of Paleozoic sedimentary, metamorphic, and igneous rocks constituting the basement of West Siberia shows that they are highly heterogeneous and characterized by fissure-cavernous structure due to metasomatic transformation by hydrothermal solutions. The spores-and-pollen spectra



from Mesozoic oil include Paleozoic and Triassic microfossils (prior to sedimentary cover deposition) forms: up to 50 and 10% in Jurassic and Cretaceous rocks, respectively. In this connection, further hydrocarbon prospecting should be connected with fractured zones in deep Paleozoic formations constituting the basement (A.N. Guseva and L.P. Klimushkina, 1995).

The similar situation is also characteristic of the Shaim oil-bearing area of West Siberia, where numerous oil occurrences and small oil pools are documented in the uppermost part of pre-Jurassic sediments: Tolum, Mortym'ya-Teterev, Ubin, Danilovskoe, Potanaikos, and others in the basement weathering crust. The basement is composed of volcanics, siliceous shales, and shales with signs of intense secondary alterations of zoned patterns determined by hydrolysis and leaching [39].

The ascending migration is confirmed by wide development of past- and present-day hydrothermal systems in both the continental and oceanic segments of the Earth.

### ***14.2.8 Subaqueous Hydrothermal Vents***

The hydrothermal activity discovered in the Red Sea is characterized by temperatures of 60°C and mineralization of discharging fluids amounting to 180 g/l. Bottom sediments contain ore minerals. The similar hydrothermal activity is established in the northwestern Atlantic, eastern Pacific (Galapagos rift), Gulf of Mexico, and other basins. In mid-oceanic ridges occupying approximately 12% of the oceanic bottom, the interval of temperature anomalies is frequently as thick as 1 km [2].

Several mud volcanoes and cone-shaped clay diapirs with flows of mud breccia on slopes are discovered in the Black and Mediterranean seas. The Mediterranean mud volcanoes are larger as compared with their Black sea counterparts (5.0–7.5 km versus 1.5–2.5 km across). The volcanoes demonstrate different activity stages. Most active of them is the Tredmar Volcano (Black Sea), which shows the presence of gas hydrate aggregates. Gas and fluid seeps are established in the Napoli Volcano (Mediterranean Swell). The swell hosts also abandoned mud volcanoes and clay diapirs buried under thickness-variable sediments. The central part of the Black Sea is characterized by numerous normal faults, which implies the development of extension zones. In contrast, the bottom of the Mediterranean Sea is characterized by wide development of reversed faults, which indicates compression zones [28]. The authors interpret these facts in the following manner. The Black Sea was characterized by intense accumulation of the Maikop Group sediments, which resulted in the formation of abnormally high formation pressures with subsequent “exhumation of these sediments along normal faults to the surface.” In the Mediterranean Sea, “plastic sequences were squeezed to the sea bottom by horizontal compression” [28].

The quantitative assessments show (see above) that increment rates of the overburden pressure are significantly lower as compared with the relaxation velocities of interstitial pressures in compacting sediments and that compaction of clayey sediments itself is a stationary process in terms of geological time. Therefore, the

authors' assumption not confirmed by calculations is suspicious. In our opinion, clay diapirs, mud volcanoes, and other manifestations of the hydrothermal activity should be related to recent geodynamic processes and near-vertical ascending migration of fluids.

The concentrated deep fluids widespread in deepwater margins of continents (in the junction zones between lithospheric plates) are characterized by anomalously high contents of hydrocarbons and form various anomalies in geophysical and geochemical fields. They are widespread in the Cascadian, Makran, Barbados, Nankai, Indonesian, Chilean, Peruvian accretionary prisms, Mediterranean Swell, northern Californian borderland, and many other world regions. They are also known in passive margins: the Gulf of Mexico, Carolina margin, Blake Plateau, northern margin of Norway, Black Sea, Southern Caspian basin, and other areas.

Migrating hydrocarbons are partly trapped to form accumulations. Some of them migrate to near-surface sediments to form gas hydrates stable under appropriate thermobaric conditions. Some hydrocarbons reach the sea bottom to discharge in the form of jets of free gas ("gas torches"). The redox potential in areas of the fluid discharge shifts toward reducing conditions to result in intense reduction of metal oxides and sulfates and conservation of organic matter in sediments. "Complex biochemical processes with participation of hydrogen sulfide, carbon dioxide, and hydrocarbon gases (primarily methane) result in the formation of specific communities of chemosynthetic organisms, which take active part in consumption and transformation of ascending fluids" [27]. These processes proceed at depths of 2,000 m in oxygen-free conditions. Such organisms or chemosynthetic communities [27, p. 38] are documented in both hot and cold hydrothermal springs against the background of unpopulated bottom of deep sea basins. Hydrogen sulfide and hydrocarbon gases serve as a food source for such a symbiosis of micro- and microorganisms. "By their size and structure, these organisms differ from their 'normal' counterparts and some of them populate only these zones or were never found" [27]. Such organisms (tubular worms, chemoautotrophic bacteria, mollusks, and others) are established by the underwater television survey and sampling in many world areas.

The precipitation of secondary minerals results in the formation of carbonate concretions, aggregates, crusts, and carbonate buildups. These deepwater buildups are observed in many world areas, where they are composed of massive limestones with carbonate "tubes" inside, which serve as conduits for fluids. Carbonate buildups are up to hundreds of meters high and several kilometers across (Gulf of Mexico, northwestern Australia, deep part of Ireland, Norwegian Sea, and other areas "representing true deepwater reef massifs") [27]. The carbon isotope composition in these rocks is usually lighter as compared with that in normal marine carbonates being close to the isotope composition of methane in sediments.

The concentrated deep sea discharges of fluids are locally accompanied by the formation of tube-shaped structures composed of barite, pyrite, Fe oxides, and other minerals. The geochemical analysis of >1,000 samples of deep-sea sediments and approximately 300 samples of rock fragments revealed two groups among them: with background geochemical parameters and with abnormally high hydrocarbon

content. In the first of them, geochemical parameters are relatively uniform within the same area, although may be characterized by significant differences in concentrations of some components and compounds in different regions. The hydrocarbon content increases in sediments enriched in organic matter (sapropels, clays). In samples with abnormally high hydrocarbon content, their concentrations and composition are substantially variable in different regions and even within the same area at short distances depending on the remoteness from the discharge center and its intensity. The hydrocarbon concentration in the last group is orders of magnitude higher as compared with the background one being independent of lithology and  $C_{org}$  content. The notable share in the hydrocarbon composition belongs to heavy homologues of methane interpreted as fat oil gases. Interstitial waters demonstrate anomalies in the chemical components and ions. The carbon isotope in these samples indicates thermogenic and mixed nature of hydrocarbon gases and implies the discharge of oil and gas condensate accumulations in these areas [55].

The hydrocarbon content in the epicenter of deep-sea hydrothermal vents amounts to 1–3% to decrease beyond the latter up to 0.3% (isoprenoid hydrocarbons with admixture (up to 50%) of phytane ( $C_{20}$ ) representing hydrocarbon of the regular structure, squalane ( $C_{30}$ ), and difitile ( $C_{40}$ ) or hydrocarbon of the irregular structure) against the background of complete lack of sediments. At the same time, “discovery of bacterial life in high-temperature hydrothermal vents and products of bacterial activity in ores of deep oceanic zones widens significantly boundaries of the biosphere. . . in time and space” that increases possibilities of biogenic oil formation [7, p. 11]. The last statement is characterized by the one-sided approach, which was discussed in the Introduction section.

The above-mentioned facts may be interpreted in two ways: (1) as initiation of new life under oxygen- and illumination-free conditions from inflowing fluids during Earth’ degassing and (2) as adaptation of existing species to new thermodynamic conditions and habitat environments.

Calculations based on oceanological observations show that 60 bln tons of lavas and approximately 5 bln tons of water, gases, and salts are supplied annually to mid-oceanic ridges, whose values are higher as compared with that transported from continents (V.N. Zelenov-Ivanenkov, 1982). These areas are also characterized by intense hydrothermal activity that accompanies volcanic eruptions (postvolcanic activity). The latter is responsible for the formation of an autonomous type of ore deposits (“exhalation-sedimentary”), which are formed by ore components contained in hydrothermal solutions inflowing from deep spheres of the Earth [1]. According to [8], active structures of the East Pacific belt release annually up to  $1.6 \cdot 10^8$  of methane and  $1.3 \cdot 10^9$  of hydrogen, which is comparable with the quantity of biogenic methane released by bogs of West Siberia.

Many deep-sea studies in the World Ocean revealed numerous centers of the subaqueous fluid discharge at depths reaching 2 km and deeper, which are frequently accompanied by accumulations of gas hydrates discovered in active and passive continental margins. The distribution of gas hydrate is characterized by the following peculiar features: (1) extreme spatial irregularity and scale variability; (2) impossibility of lateral migration (prevalence of vertical migration) and, consequently,

accumulation from large areas; (3) lack of conditions for conserving biochemical gases to protect them from oxidation; (4) impossibility of thermocatalysis in many cases (temperature of 10–20°C); (5) lack of conditions for mass hydrocarbon generation from sediments due to their insignificant thickness; (6) confinement of localized ascending migration to faults, diapirs, mud volcanoes, and zones of deep detachments at the base of the sedimentary sequence; (7) wide-range variations in carbon and hydrogen isotope values (from –37 to –80 and from –150 to –260‰, respectively) in the zone saturated with gas hydrates; (8) waters of gas hydrates are highly desalinated and contain anomalous concentrations of NH<sub>4</sub>, Br, Sr, D, and other microcomponents; and (9) gas hydrates are formed by liquid hydrocarbons, not dry methane [17].

The recent studies of mud volcano activity at the bottom of seas and oceans demonstrate that the composition of discharged gas-saturated waters differs usually from that of seawater, which is impossible to explain by interstitial water release. Mud torches stimulate the formation of gas hydrates at the bottom of seas and oceans (“ice caps”) [2].

In opinion of [17], which is difficult to argue, gas hydrates are formed on account of local inflows of deep hydrocarbons. This assumption is consistent with the  $\delta^{13}\text{C}$  content, which varies from –36.1 to –94.0, from –0 to –75, from –0 to –55, and from –20 to –30‰ in gas hydrates, natural gas, gas accompanying oil fields, and natural oils, respectively. V.A. Krayushkin believes that this represents “an unavoidable result of isotope composition fractionation, which is confirmed by the Fischer-Tropsch oil syntheses” [18]. The latter shows that  $\delta^{13}\text{C}$  varies from –65 to –20‰ under respective temperatures of 127 and 227°C (synthesis from hydrogen and carbon oxide) [43]. According to Geological Survey of the United States, methane reserves in marine gas hydrates amount to 113 quadrillion cubic meters, which exceeds  $77 \cdot 10^3$  times world reserves of natural gas (1,45,740 bln m<sup>3</sup> for January 1, 2000). “Although some geologists consider methane from these gas hydrates biogenic in origin because of its  $\delta^{13}\text{C}$  values ranging from –36.1 to 94‰, their distribution through 95% of the World Ocean bottom, reserves, and recent age of their reservoirs (bottom sediments) are inconsistent with the hypothesis of source sedimentary facies as resulting from catagenesis–methanogenesis of dispersed organic matter and gas-accumulating sedimentary basins” [42].

Based on the study of over 20 thermal fields in mid-oceanic ridges, it is established that the hydrocarbon component exceeds  $1.6 \cdot 10^8$  m<sup>3</sup>/year (N.S. Beskrovnyi, 1985). According to G.I. Voitov (1986), the specific density of hydrocarbon flows amounts to 750, 300, 650, and 150 m<sup>3</sup>/m<sup>2</sup> per year in mid-oceanic ridges, abyssal basins, transitional zones, and underwater margins, respectively.

### ***14.2.9 Hydrothermal Springs on Continents***

Hydrocarbons in recent hydrothermal solutions are established in the Uzon Volcano caldera in Kamchatka, fumaroles of Santiago, Atlantis II Deep in the Red Sea,

Hawaiian lava lakes, thermal fields of the Yellowstone National Park, and other areas. Eruption of the Tolbachik Volcano in 1975–1976 was accompanied by the release of  $2.5 \cdot 10^6$  tons of hydrocarbons [2].

Oil shows in the Uzon Volcano caldera in eastern Kamchatka are known for a long time. Oil drops are delivered to the lake surface and concentrated in excavations. The Uzon oil is considered in [6] as an extract of hydrocarbons from organic matter of source rock by thermal waters, not as a product of Earth's degassing. The base of the caldera is composed of Pleistocene (38–70 ka) volcanogenic-sedimentary rocks [6]. Unfortunately, the authors received no answers to the following questions: (1) Is thermal water discharge through the entire caldera area or their springs limited to separate fractured or weakened zones? (2) What is the thickness of sediments relative to volcanogenic facies, i.e., is the reservoir potential sufficient for the discharge of hydrocarbons during centuries?

The intense recent hydrothermal activity is known in depressions surrounding Lake Baikal and in the lake proper. The united Baikal rift zone [29, 30] comprises several depressions (Ust-Selenga, Ust-Barguzin, Kichera) representing a single system (“lithological body”) and separate negative structures such as Barguzin, Verkhniy and Nizhniy Mui, Verkhnyaya Angara, and other depressions. The Baikal rift system is characterized by high sedimentation rates, large thickness of Cenozoic sediments (up to 7.5 km) containing 1–3% of dispersed organic matter (on average), elevated content of juvenile hydrogen, numerous fractures, and high seismic activity as well as development of a member with gas hydrates, the thickness of which decreases toward the shore. Due to their accumulations, the region in question is considered to be promising with respect to hydrocarbon accumulations. Numerous surface seeps of hydrocarbon gases along the lake periphery, which were first established over 250 years ago, represent their direct indications. The most intense discharge of hydrocarbon gases is observed in mouth areas of the Selenga, Barguzin, and Verkhnyaya Angara rivers. The study of the gas composition defined four of their groups (900 analyses): methane, nitrogen–methane, methane–nitrogen, and nitrogen with different contents of helium, hydrogen, oxygen, carbon dioxide, and methane. Gases of all types contain helium. The helium content in nitrogen-type gas indicates juvenile nature of gases. Methane gases are attributed to the mixed type, which contains helium as well [29, 30].

Based on the occurrence of numerous underwater mounts, hills, and banks at the lake bottom, it is inferred that subaqueous gas discharged during past geological epochs as well (gas volcanism was accompanied by ejection of solid material). For example, the Posol'skaya Bank located approximately in the middle of Baikal towers above the bottom for almost 1,000 m. In opinion of the last authors, some features allow assumption that the latter represented formerly an island. The bank slopes are composed of alternating clays, siltstones, and sandstones. Gas gryphons, which occur usually by groups, are from a few tens of meters to 1–2 km in size, being recorded in winter seasons owing to glade in ice near coasts. Gryphon yields vary from tens to  $1,000 \text{ m}^3/\text{day}$ .

Iceland representing an example of Earth's "hot" degassing site is largely (90%) composed of basalts altered to a variable extent by hydrothermal solutions. Lavas and hydrothermal minerals contain polycyclic aromatic hydrocarbons, which are "a logical result of volcanic and postvolcanic hydrothermal activity, not exotic or incidental phenomenon" [19, p. 112].

The study of the metasomatic activity in the East Sayany and Baikal regions shows that precipitation of native carbon in metasomatic zones occurred due to the influx of reduced high-carbonaceous mantle fluids under the multiple change of the fluid regime. Younger metasomatites could destroy their predecessors. These inferences are confirmed by the carbon isotope composition [9].

In opinion of most researchers, volatile mantle elements enter the crust together with magma, crystallization of which is accompanied by the release primarily of H<sub>2</sub>O, CO<sub>2</sub>, and other gases, which form convective flows. H<sub>2</sub>O and CO<sub>2</sub> are also formed due to oxidation of reduced fluids that enter the upper mantle and crust. The fluid composition also changes with time within aseismic zones, in addition to geodynamically active areas. For example, the content of methane and heavy hydrocarbons in fluids in the Khibiny Mountains varied during a week from 49.52 to 65.98 and from 1.08 to 11.08%, respectively; the  $\delta^{13}\text{C}$  value in methane during the same period ranged from 7.7 to 16.5‰ (I.G. Kissin, 2002).

Bagdasarova [4] described the influence of hydrothermal solutions on the formation of carbonate reservoirs. Regardless of the geological structure of different regions, capacity of carbonate rocks is secondary, which is explained by jointing and superimposed epigenetic processes related to ascending vertical migration of hydrothermal solutions that disturb the thermodynamic equilibrium in the fluid-rock system. Hydrothermal fluids are characterized by mineralization of 200–600 g/l and contain ore and non-ore elements of deep origin. Gas contains H, H<sub>2</sub>S, CO<sub>2</sub>, He, N, and other gases, in addition to hydrocarbons. In opinion of [4], gas saturation degree is determined by recent and past hydrothermal processes "related to mafic and ultramafic (sometimes, alkaline) volcanism."

The recent hydrothermal activity is established in the Pripyat Depression and other areas of old platform. In the Tengiz field, repeated geochemical studies established geochemical anomalies "indicating the pulsating flow of deep fluids along fractures." Gas from this field contains up to 20% of hydrogen sulfide and carbon dioxide, "which determines its aggressiveness particularly relative to readily soluble carbonate rocks." Dissolution of carbonate rocks is accompanied by the release of carbon dioxide and formation of sulfates, which determines the irregular gas composition and temperature field through the field. In Alpine fold zones, secondary porosity is largely determined by jointing and secondary processes are accompanied by hydraulic fracturing. The secondary mineral formation is evident from secondary calcite recrystallization and silicification. Gas contains hydrogen and much carbon dioxide in addition to hydrocarbons.

The mud volcano activity on continents may be arbitrarily attributed to hydrothermal processes. Mud volcanoes of Azerbaijan confined to deep-seated fault zones discharge at least 400 mln m<sup>3</sup> of methane annually, which constitutes 175 trillion cubic meters during the Quaternary.

In petroliferous basins, hydrothermal solutions are registered primarily based on thermal anomalies, which are usually confined to deep-seated faults and characterized by intense geodynamic processes. The thermal anomalies are accompanied by abnormally high formation pressures.

The composition and the temperature of hydrothermal solutions as well as their discharge intensity experience variations through the geological history of regions. "This is accompanied by the formation of complex 'block' patterns of fluids within separate structures" [2, p. 112] both under nonequilibrium and equilibrium geochemical states.

The hydrothermal activity inside the sedimentary cover of petroliferous basins results in significant rock transformation. For example, all the petroliferous complexes of the Siberian Platform (Riphean, Vendian, Vendian–Lower Cambrian) are substantially transformed by hydrothermal metasomatism [40]. Hydrothermal processes stimulated formation of lithological screens (mineralogical–geochemical boundaries, after [10–16]), cementation, and "sealing" of hydrocarbon accumulations. Silicification, argillization, and calcitization zones are characterized by zoned-circular (stratum-block) patterns with differently oriented boundaries. Special studies revealed that the accumulated production of hydrocarbons and their proven reserves are comparable with the quantity of infused matter [40, p. 361]. Vertical migration is also confirmed by transformation of near-surface sediments. Concluding, the author notes that "hydrothermal nature of formation fluids allows accumulation of hydrocarbons, secondary alterations of rocks, development of neotectonic structures, and formation of anomalous surface geochemical fields above oil and gas accumulations to be considered as an integral process continuous in time and space and related to the Earth's degassing" [40, p. 362].

The study of the Romashkino field brought interesting results [25]. The field is characterized by insignificant thickness of the sedimentary cover and low maturity degree of organic matter and is surrounded by troughs free of hydrocarbon accumulations. It is established that the Romashkino field was formed during three stages. Moreover, the same reservoir contains locally oils generated at all three stages. In opinion of the last authors, the period of planetary plume magmatism, which corresponds to the Triassic in the Tatar Arch region, was followed by the additional influx of matter from the basement into the field. This is evident, for example, from the occurrence of light oils in the southeastern slope of the Tatar Arch (Uruktamak area). The long-term studies (1982–1999) of oils from the Romashkino field show the following [49]: changes in oil properties (density) occurred during several periods of 5.0–5.5 years long, which is explained by recent tectonic processes and changes in baric conditions and strain state during field exploitation; (2) variations in isobutane and *n*-butane proportions demonstrate periodicity of approximately 5 years; (3) observable variations are correlated with solar activity variations: peaks of solar activity coincide with peaks in butane–*n*-butane values (minimums with minimums and maximums with maximums). The latter is explainable by the influence of extension and compression on vertical migration of hydrocarbons. The authors assume that the strengthened fluidodynamic activity in the Earth interior reduces this ratio. These first observations are insufficient for reliable inferences on processes,

resulting in changes in oil properties. Therefore, it is logical that the authors propose to organize monitoring in hydrocarbon accumulations.

Long exploitation periods of small fields (up to 50–100 years and longer) serve as an important evidence for the recent hydrothermal activity in petroliferous basins. “At later stages of exploitation, the production decreases up to 20–10% of the maximal one and becomes stable, i.e., extracted oil is balanced by the influx of deep fluid. . . some wells retain relatively high yields and their accumulated production amounts to millions tons. Such an anomalous phenomenon is likely explainable by location of these wells near the powerful oil-conducting channel” [37, p. 369]. In opinion of the authors, existence of such channels makes drilling of super-deep holes into the basement unnecessary. It is more reasonable to define such channels (faults in the basement) and drill two holes: one in the zone of a presumable fault and another immediately near the latter.

### ***14.2.10 Hydrothermal Hydrocarbon Accumulations***

In 1955, P.N. Kropotkin put forward an idea on hydrocarbon and inorganic components of the deep Earth’s degassing. Subsequently, it received an irrefutable proof. The fact of fluid vertical migration from the basement is now universally accepted. Only proportions of mantle and organic hydrocarbons are debatable. In this connection, the concept of hydrothermal types of hydrocarbon accumulations became widespread.

Wide development of ore and hydrocarbon accumulations in the paragenesis made it possible to define ore-naphthide deposits [50, 72 and others]. There are ore–gas and ore–oil deposits with commercial concentrations of metals. V, Ni, Co, Cr, Mo, B, and other metals associate with heavy asphalt–tarry components, while Fe, Cu, Pb, J, Br, and others are connected with liquid fractions of hydrocarbons. This is exemplified by the Yarega oil–titanium deposit in the Timan-Pechora petroliferous basin, widespread ore–carbonaceous bitumen deposits, which are exploited for V, Ni, U, S, and other elements, and high-carbonaceous tectonites of the Ospa-Kitoy Massif of East Sayany with Au and Pt concentrations up to 0.53 and 1.2 g/t, respectively.

Practically all the oil and gas fields (eastern Kamchatka, Ciscaucasia, Carpathian Foredeep, Cheleken, and other regions) are characterized by high Hg concentrations. For example, in the Mirnenskoe, Takhta-Kugul’ta, and Severo-Stavropol fields of the Caucasus, it amounts to  $7 \cdot 10^{-5}$  g/m<sup>3</sup>. Maximal Hg concentrations are recorded in the Saltzwesel-Pokensen and Vustrov fields, where their background and maximal values are 3 and 14 mg/l, respectively. Cleaning of gas from Hg in the Saltzwesel-Pokensen field provides large quantities of liquid mercury. The Hg content in the Poznan basin (Poland) ranges from 0.2 to 2.0 mg/m<sup>3</sup>.

There are a lot of examples demonstrating co-occurrence of ore and hydrocarbon accumulations. This phenomenon is particularly widespread in mid-oceanic ridges (East Pacific and others), island arcs (Kurile-Kamchatka and others), and in



petroliferous basins of Africa, America, West and East Siberia, Uralian ore belt, and Angara-Ilim iron-ore province. Petroliferous basins enclose solid bitumens with V, Mo, Pb, Ag, Zn, Cr, and other metals [37]. Locally, thick tarry oil fills free cavities with walls composed of quartz druses and pyrite or ilmenite crystals. The last author considers hydrothermal solutions as both a transporting agent and a reacting system interacting with the rock matrix at all the stages of fluid formation.

The ore formation related to hydrothermal solutions is established in some areas of the Alpine fold belt [59]. Some hydrocarbon accumulations of the Dnieper-Donets Depression are marked by precipitation of  $\text{SiO}_2$ ,  $\text{CaCO}_3$ , and Fe oxides, in addition to hydrodynamic, temperature, and hydrochemical anomalies. Gas accumulations enclosed in Lower Carboniferous and Lower Permian formations contain mercury in concentrations of  $0.05\text{--}5 \cdot 10^{-5} \text{ g/m}^3$ . Numerous ore deposits and occurrences are confined to salt domes, where they demonstrate two formation stages: barite-galenite-sphalerite (first stage) and bitumen-mercury-carbonate (second stage) mineralization. The Central Donbas concealed fault is accompanied along its strike by Hg-metallic, As-Hg with Zn and Pb, Sb-Hg, H-Au-pyrite, and Au-Ag polymetallic deposits. Beyond the depression, ore deposits are barren of bitumen; the latter occurs only in vapor-liquid inclusions. Similar deposits are also established in the Trans-Carpathian Trough [59].

Thus, existence of hydrothermal hydrocarbon accumulations is an undoubted fact; moreover, some of them are forming nowadays.

### 14.3 Principal Inferences

(1) The sedimentary-migratory hypothesis of oil origin gradually loses ground, which is reflected in (a) widening of main oil-generation phase boundaries from depths of 1,800–2,000 m to several kilometers and temperatures from 90–120°C to several hundreds of degrees; (b) supplement of this hypothesis by the fluidodynamic concept, i.e., admission of hydrothermal activity, which leads unavoidably to admission of a certain contribution of mantle hydrocarbons. This contribution is now admitted, although its role is still considered insignificant (B.A. Sokolov); (c) admission of the fact that not all the sedimentary rocks form source sequences. At present, the following question is unanswered: Why only some sedimentary rocks represent source formations under the same conditions?

(2) The available data on isotope compositions of different gases are insufficient for unambiguous solution of the hydrocarbon genesis problem. The spectrum of isotope ratios for different geological mediums is permanently widening.

(3) The widening spectrum of initial substances, chemical elements, catalysts, and thermodynamic conditions provides progressively additional possibilities for synthesizing hydrocarbons approaching by their compositions and properties to natural varieties.

(4) The lack of optical anisotropy in artificial oils is already insufficient for inferences on oil genesis. Optically active hydrocarbon compounds may be transformed into inert phases and their proportions are changeable with time.

(5) Thus, main arguments favoring the sedimentary-migratory hypothesis of oil genesis and the formation of hydrocarbon accumulations are gradually losing their efficiency under pressure of new data obtained in different knowledge fields and additional facts confirming the mineral or the mixed hypothesis of the hydrocarbon formation.

(6) Monitoring organized in exploited fields would help to solving many disputable questions and the problem of oil origin and formation of hydrocarbon accumulations. Such monitoring should be aimed at obtaining time series, observations over changes in physical and geochemical oil properties during exploitation, geodynamic, hydrodynamic, palynological, and other features.

(7) The observable increment of exploitation reserves in fields and differences in geochemical properties of oil within the same field favor against the sedimentary-migratory hypothesis of oil origin and need explanation.

## References

1. Anikeev V A (1964) Abnormally high formation pressures in oil and gas fields. Hedra, Leningrad
2. Bagdasarova M V (2000) Recent hydrothermal systems and their relation with formation of oil and gas fields. In: Basics of new technologies in oil and gas industry. Nauka, Moscow
3. Bagdasarova M V (2001) Fluid systems of oil accumulation zones and geodynamic oil and gas fields. *Geologiya nefi i gaza* 3:50–56
4. Bagdasarova M V (2001) Interaction between carbonate rocks and hydrothermal systems during formation of oil and gas reservoirs. In: Lithology and petroleum resource potential. Materials of the 2nd All-Russian Lithological Meeting and 8th All-Russian Symposium on Fossil Corals and Reefs. Syktyvkar
5. Bashilov V I, Kuprin V F, Gottikh R P et al. (1991) Hydrocarbon degassing of fault zones in the western slope of the North Urals. *Geologiya nefi i gaza* 11:17–21
6. Bazhenova O K, Aref'ev O A, Frolov E B (1997) Hydrothermal oil of Kamchatka. In: Materials of the annual scientific conference "Lomonosov's Readings." MGU, Moscow
7. Bazhenova O K, Sokolov B A (2001) Oil origin: Fundamental problem of natural science. In: Abstracts of the International Conference "Oil and gas genesis and formation of their fields in Ukraine as a scientific basis for predicting and prospecting new fields." Chernigov
8. Betelev N P (2002) Influence of gas in rocks and mud on stability of offshore drill and oil- and gas-field infrastructure. In: Earth degassing: Geodynamics, geofluids, oil, and gas. Geos, Moscow
9. Danilova Yu V, Danilov B S (2002) Reduced fluids of metasomatic systems. In: Earth degassing: Geodynamics, geofluids, oil, and gas. Geos, Moscow
10. Djunin V I (1981) Investigation methods and principles of deep formation hydrodynamics. VIEMS, Moscow
11. Djunin V I (1985) Investigation methods of the deep subsurface flow. Nedra, Moscow
12. Djunin V I (2000) Hydrodynamics of deep formations in petroliferous basins. Nauchnyi mir, Moscow
13. Djunin V I, Korzun A V (2001) Geological formation model of deep groundwaters and origin of hydrocarbon accumulations. In: Proceedings of the 5th International conference "New ideas in geosciences." Moscow
14. Djunin V I, Korzun A V (2001) Fluidodynamics and formation of hydrocarbon accumulations. Mineral recourse base of Russia in 21st century. In: Materials of the scientific-practical conference. Arkhangel'sk

15. Djunin V I, Korzun A V (2003) Fluid migration: Oil origin and formation of hydrocarbon accumulations. Nauchnyi mir, Moscow
16. Djunin V I, Korzun A V, Kiryukhina (1999) Hydrodynamics of deep formations and petroleum resource potential (exemplified by the northern Pechora Depression). In: Abstracts of the 13th geological meeting of the Komi Republic "Geology and mineral resources of northwestern European Russia." Syktyvkar
17. Dmitrievskii A N, Valyaev B M (2002) Localized flows of deep hydrocarbon fluids. In: Earth degassing: Geodynamics, geofluids, oil, and gas. Geos, Moscow
18. Dmitrovskii S V, Kim E K, Malakhov V D, Ostrovskii V N (1993) Influence of the block structure in the Alma-Ata Depression on formation of groundwater resources. *Otechestvennaya geologiya* 3:67–73
19. Geptner A R, Pikovskii Yu I, Alekseeva T A, Sorokina N S (2002) Polycyclic aromatic hydrocarbons in volcanics and hydrothermal minerals of the Iceland rift zone. In: Earth degassing: Geodynamics, geofluids, oil, and gas. Geos, Moscow
20. Goncharov V S, Esikov A D, Il'chenko V P (2000) On preservation of hydrocarbons in the Earth interior. In: Materials of the 6th International conference "New ideas in petroleum geology and geochemistry." Toward development of the general theory of the Earth petroleum resource potential. Geos, Moscow
21. Goncharov V S, Esikov A D, Il'chenko V P (2002) The distribution of carbon isotope composition in natural gases from fields of northern west Siberia. In: Earth degassing: Geodynamics, geofluids, oil, and gas. Geos, Moscow
22. Gorbachev V F, Kovalenko V S (2001) Lithosphere plate tectonics as a source of information on formation conditions, formation, localization, predicting and prospecting of oil and gas fields. In: Abstracts of the International Conference "Oil and gas genesis and formation of their accumulations in Ukraine as a scientific basis for predicting and prospecting new fields." Chernigov
23. Gorgadze G N, Aref'ev O A (2002) Some important inconsistencies between compositions of organic matter in source rocks and oils. In: Materials of the 6th International conference "New ideas in petroleum geology and geochemistry." Toward development of the general theory of the Earth petroleum resource potential. Geos, Moscow
24. Gorgadze G N, Rusinova G V (2002) Hydrocarbons-biomarkers in products of soft asphaltene and tar thermolysis. In: Materials of the 6th International conference "New ideas in petroleum geology and geochemistry." Toward development of the general theory of the Earth petroleum resource potential. Geos, Moscow
25. Gottikh R P, Pisotskii B I, Muslimov R Kh (2002) To the problem of phased formation of the Romashkino field based on deep fluidization. In: Earth degassing: Geodynamics, geofluids, oil, and gas. Geos, Moscow
26. Ione K G (2002) Abiogenic synthesis of hydrocarbon masses at biofunctioning catalysts modeling the crust composition. In: Materials of the 6th International conference "New ideas in petroleum geology and geochemistry." Toward development of the general theory of the Earth petroleum resource potential. Geos, Moscow
27. Ivanov M K (2000) Hydrocarbon fluid flows in deep margins of Europe and related phenomena. *Vestnik MGU. Ser Geol* 5:31–44
28. Ivanov M K, Limonov A F (1995) Mud volcanism and clay diapirism of the Black and Mediterranean seas. In: Materials of the annual scientific conference "Lomonosov's Readings." MGU, Moscow
29. Isaev V P (2001) On gas paleovolcanism in Lake Baikal. *Geologiya nefi i gaza* 5:45–50
30. Isaev V P (2002) Recent sediments degassing in Cenozoic depressions of the Baikal rift zone. *Geologiya nefi i gaza* 4:5–9
31. Kabyshev B P, Kabyshev Yu B (2002) Fluidodynamics: Factor of formation or destruction and reorganization of hydrocarbon accumulations. In: Materials of the 6th International conference "New ideas in petroleum geology and geochemistry." Toward development of the general theory of the Earth petroleum resource potential. Geos, Moscow

32. Karnyushina E E (1995) Role of structural–mineral associations in the formation different-type reservoirs in the catagenesis zone. In: Materials of the annual scientific conference “Lomonosov’s Readings.” MGU, Moscow
33. Kartsev A A, Lopatin N V, Sokolov B A, Chakhmakhchev V A (2001) Triumph of the organic (sedimentary-migratory) theory of oil genesis by the end of the 20th century. *Geologiya nefi i gaza* 3:2–5
34. Kiryukhina T A (1995) Oil types in the Timan-Pechora basin. *Vestnik MGU Ser geol* 2:39–49
35. Kochetkov O S, Alisievich L N, Gaideek V I, Yudin V M (2000) On formation ways of oil and gas (exemplified by the Timan-Pechora Province. *Geologiya nefi i gaza* 5:44–49
36. Konishchev V S, Kovtukha A M (2002) Petroleum resource potential and geodynamics of the Pripyat paleorift. In: Materials of the 6th International conference “New ideas in petroleum geology and geochemistry”. Toward development of the general theory of the Earth petroleum resource potential. Geos, Moscow
37. Korchagin V I, Trofimov V A (2002) Oil-conducting channels and current replenishment of oil fields. In: Earth degassing: Geodynamics, geofluids, oil, and gas. Geos, Moscow
38. Korobkov Yu. I (2002) Age of hydrocarbon accumulations in connection with the problem of prospecting oil and gas fields. In: Materials of the 6th International conference “New ideas in petroleum geology and geochemistry.” Toward development of the general theory of the Earth petroleum resource potential. Geos, Moscow
39. Korobov A D, Korobova L A (2002) Zone of unique natural reservoirs: basement rocks of taphrogenic areas. In: Materials of the 6th International conference “New ideas in petroleum geology and geochemistry.” Toward development of the general theory of the Earth petroleum resource potential. Geos, Moscow
40. Korobov Yu. I, Malyshko L D (2002) Fluidogeodynamic formation model of hydrocarbon accumulations: A theoretical basis for prospecting oil and gas fields. In: Earth degassing: Geodynamics, geofluids, oil, and gas. Geos, Moscow
41. Korolev V I (2002) Geodynamics of the Siberian Platform and its role in the formation of dispersed and concentrated matter. In: Earth degassing: Geodynamics, geofluids, oil, and gas. Geos, Moscow
42. Krayushkin V A (2001) Non biotic petroleum resource potential. In: Abstracts of the International Conference “Oil and gas genesis and formation of their accumulations in Ukraine as a scientific basis for predicting and prospecting new fields.” Chernigov
43. Krayushkin V A (2002) On oil and gas origin. In: Earth degassing: Geodynamics, geofluids, oil, and gas. Geos, Moscow
44. Krivosheya V A. (2001) Mineral synthesis of hydrocarbons: A leading concept of petroleum geology development. In: Abstracts of the International Conference “Oil and gas genesis and formation of their accumulations in Ukraine as a scientific basis for predicting and prospecting new fields.” Chernigov
45. Kucher M I (2002) Evolution of the carbon isotope composition in mantle degassing and differentiation. In: Earth degassing: Geodynamics, geofluids, oil, and gas. Geos, Moscow
46. Kucherov V G, Bendeliani N A, Alekseev V A (2002) Hydrocarbon synthesis from minerals under high thermobaric conditions. In: Earth degassing: Geodynamics, geofluids, oil, and gas. Geos, Moscow
47. Kulakov I I, Rudenko A P (2002) Fractionation of carbon isotopes in its global cycle. In: Earth degassing: Geodynamics, geofluids, oil, and gas. Geos, Moscow
48. Nivin V A, Ikorskii S V (2002) He isotopes as indicators of sources and degree of mantle degassing during the formation of Paleozoic alkali and carbonate complexes of the Kola Province. In: Earth degassing: Geodynamics, geofluids, oil, and gas. Geos, Moscow
49. Nurgaliev D K, Plotnikova I N, Sidorova N N, Nurgaliev R K (2002) Influence of the global seismic activity on compositional changes of oils in the Romashkino field. In: Materials of the 6th International conference “New ideas in petroleum geology and geochemistry.” Toward development of the general theory of the Earth petroleum resource potential. Geos, Moscow

50. Ozerova N A (2002) Mercury resource potential of gas and gas-oil fields. In: Materials of the 6th International conference "New ideas in petroleum geology and geochemistry." Toward development of the general theory of the Earth petroleum resource potential. Geos, Moscow
51. Perchuk L L (2000) Fluids in the lower crust and upper mantle. *Vestnik MGU. Ser Geol* 4:25–45
52. Petrov A I, Shein V S (2001) On necessity of accounting recent geodynamics for the assessment and recalculation of commercial oil and gas reserves. *Geologiya nefi i gaza* 3:6–13
53. Pikovskii Yu I (2002) Conception of oil and gas formation: Practical consequences as criterion for assessing. In: Materials of the 6th International conference "New ideas in petroleum geology and geochemistry." Toward development of the general theory of the Earth petroleum resource potential. Geos, Moscow
54. Prasolov E M et al. (2002) Carbon and oxygen isotope composition in carbonates from the distribution area of underwater mud volcanoes (Black Sea). In: Earth degassing: Geodynamics, geofluids, oil, and gas. Geos, Moscow
55. Prasolov E M et al. (2002) Carbon and oxygen isotope composition in natural carbonate tubes from the underwater fluid discharge area (Kadiz Bay, Atlantic Ocean). In: Earth degassing: Geodynamics, geofluids, oil, and gas. Geos, Moscow
56. Pushkarev Yu D (2002) Isotopic-geochemical aspects of the oil and gas origin problem. In: Earth degassing: Geodynamics, geofluids, oil, and gas. Geos, Moscow
57. Rodkina M V (2002) On the accuracy of the method used for determining contribution of the mantle component into the composition of natural hydrocarbon gases. In: Materials of the 6th International conference "New ideas in petroleum geology and geochemistry." Toward development of the general theory of the Earth petroleum resource potential. Geos, Moscow
58. Shchekaturov A V (2002) Peculiarities in the formation of oil fields in the Severo-Surgut homocline (West Siberia). In: Materials of the 6th International conference "New ideas in petroleum geology and geochemistry." Toward development of the general theory of the Earth petroleum resource potential. Geos, Moscow
59. Shumlyanskii V A (2002) Hydrogeological inversion, oil accumulation, and ore formation. In: Earth degassing: Geodynamics, geofluids, oil, and gas. Geos, Moscow
60. Sirotenko L V, Sirotenko O I (2002) Influence of gas-fluid flows on the reservoir and hydrocarbon potentials of clayey rocks at deep levels. In: Earth degassing: Geodynamics, geofluids, oil, and gas. Geos, Moscow
61. Slavkin V S, Shik N S, Saprykina A Yu (2001) On disjunctive-block structure of natural reservoirs in the West Siberian oil and gas basins. *Geologiya nefi i gaza* 4:40–46
62. Sokolov B A (2001) New ideas in petroleum geology. MGU, Moscow
63. Sokolov B A, Konyukhov A I (1995) Injection geology of sedimentary basins and petroleum resource potential. In: Materials of the annual scientific conference "Lomonosov's Readings." MGU, Moscow
64. Teplov E L, Abramovich A P (1998) Petroleum resource potential of the basement in the Timan Range and Mezen Syncline. In: The petroleum resource potential of the crystalline basement in Tatarstan and Volga-Kama region (1998) *Novoe znanie*, Kazan
65. The petroleum resource potential of the crystalline basement in Tatarstan and Volga-Kama region (1998) *Novoe znanie*, Kazan
66. Uremin V I, Pashkova N T, Krivosheya V A (2001) Geothermobaric model of oil and gas accumulation in the Dnieper-Donets Depression. In: Abstracts of the International Conference "Oil and gas genesis and formation of their accumulations in Ukraine as a scientific basis for predicting and prospecting new fields." Chernigov
67. Vakin E A, Kutjev F Sh (1979) Deep generation of the fluid component in recent hydrothermal solutions. In: Study and use of geothermal resources in volcanic domains. Nauka, Moscow
68. Vassoevich N B (1986) Selected papers. Geochemistry of organic matter and oil genesis. Nauka, Moscow

69. Vitvitskii V V, Efstaf'ev V P, Fed'kushkov Yu I (1982) Gas formation from chloride brines of the Moscow artesian basin DAN SSSR 2264:470–473
70. Zapivalov N P (2002) Assessment, prospects, and technology for prospecting hydrocarbon accumulations based on fluid geodynamics. In: Earth degassing: Geodynamics, geofluids, oil, and gas. Geos, Moscow
71. Zav'yalov V M, Kuchma L M (2002) To development of the general theory of the Earth interior petroleum resource potential. In: Materials of the 6th International conference "New ideas in petroleum geology and geochemistry". Toward development of the general theory of the Earth petroleum resource potential. Geos, Moscow
72. Zubkov V S, Andreev V V (2002) Role of mantle metalloorganic compounds in the formation of ore-naphthide deposits. In: Earth degassing: Geodynamics, geofluids, oil, and gas. Geos, Moscow
73. Zubkov Yu M, Sonich V P, Zaripov O G (1986) Geological and lithological criteria for estimating petroleum resource potential of the Bazhenovka Formation in West Siberia. In: Problems of the petroleum resource potential of the Bazhenovka Formation in West Siberia. Moscow

## Conclusion

Classical ideas of the artesian flow in deep sedimentary formations that admit (1) the significant role of folded orogenic structures and periphery of petroliferous basins in the formation of deep fluids, (2) the transfer of formation pressures over significant distances and depths, (3) hydrodynamic interaction within separate elements of the section in stratified negative structures (petroliferous complexes or aquifers), and (4) regional flows of deep fluids are inconsistent with available geological factual material and require revision.

(1) The *regional flows* in deep formations of petroliferous basins *cannot exist* in principle. The subsurface flow formed in peripheral parts of stratified negative structures discharges in the immediate proximity to regional centers of the infiltration recharge owing mainly to diffused ascending discharge through poorly permeable rocks; the same is true of “elision flows.” *The mass transfer in deep sedimentary sequences of negative structures (zone of the very slow water exchange) is formed independently from marginal zones of petroliferous basins* under influence of internal, mainly endogenic factors.

(2) Deep aquifers (petroliferous complexes) are characterized by the *stratum-block structure with separate blocks lacking or having weak hydrodynamic connection between each other* in all the directions. Such a situation originates under combined action of many factors, primarily tectonics (geodynamics) and physicochemical processes in the fluid-rock system included.

The stratum-block structure is a constitutive feature of deep formations in petroliferous basins, i.e., it represents a general regularity. Only the heterogeneity scale is variable. Lateral block sizes vary from tens and hundreds of meters in tectonically active areas (junction areas between platforms and surrounding orogenic structures, marginal troughs, intraplateform aulacogens, recent geosynclines) to a few tens of kilometers in areas with the calm geodynamic regime. Upward the section, blocks are gradually increasing in size to disappear in the uppermost part of the section, where hydrodynamic connection between its separate elements becomes restored.

The development of formation pressures in individual blocks is related to brief or long quasi-periodical changes of the strain state in the sedimentary cover induced by endogenic forces and activated hydrothermal activity. During the geological history, hydrodynamic interaction between blocks is changeable to become restored or

strengthened in active tectonic epochs and under intense anthropogenic load (substantial decrease in formation pressures during exploitation of mineral deposits or, to the contrary, their substantial increase under edge water flooding, construction of water reservoirs, or burial of liquid industrial wastes). These processes are accompanied by substantial changes in the field of formation pressures in individual blocks and hydraulic fracturing.

(3) Due to the stratum-block structure of deep formations, the notion “petroliferous complex” becomes senseless in the accepted understanding and reflects only stratigraphic position of the particular section element. In other words, different parts of the same stratigraphic element of the platform sedimentary cover are characterized by *different formation conditions of deep subsurface fluids*. This is confirmed by substantial differences in formation pressures, temperatures, hydrochemical fields, and other parameters in neighboring blocks. It is likely more correct to speak about subsurface fluids confined to particular stratigraphic units rather than about aquifers (petroliferous complexes).

(4) The existence of hydrodynamically isolated blocks prevents from wide development of lateral migration, which is likely limited to individual blocks. The remarkable feature of deep formations is *dominant vertical migration*, which is provided by the hydrothermal activity and is most intensive in periods of tectonic activation. In calm tectonic epochs, the mass transfer is evidently realized at the molecular level, while the convective transfer occurs along open faults (between blocks) connected with the crust (probably, with the upper mantle) and near-surface aquifers in platform sedimentary sequences.

(5) The formation of deep fluids in the zone of slow water exchange may be presented as the *pulsation-fluid geothermodynamic model*. During active tectonic periods, the vapor–liquid mixture intrudes the sedimentary cover of negative stratified structures under high pressure and, similar to magmatic intrusion, breaks its lower part to form inter- and intralayer fluid intrusions that spread over distances of tens of kilometers away from the intrusion center.

In the course of expansion of vapor–liquid mixture, its energy is spent for overcoming overburden pressure, rock deformation, hydraulic fracturing, formation of secondary minerals and the stratum-block structure of deep formations, and other processes.

Intrusion of the vapor–liquid mixture disturbs thermodynamic equilibrium in the fluid-rock system. This stimulates physicochemical processes in the system, which are accompanied by phase transitions. Under certain thermodynamic conditions, tectonic and hydraulic fractures are healed in the elastically deforming medium by secondary minerals, which are observable in natural conditions practically everywhere.

Precipitation of secondary minerals is most intense at geochemical barriers, which correspond usually with lithological-facies boundaries in the vertical section and with extreme lateral gradients in formation pressures and temperatures.

Rapid intrusion of the vapor–liquid mixture may be culminated in prolonged attenuating hydrothermal activity with gradual decrease in the solution influx and changes in their chemical compositions and temperatures (up to their cooling).



The redistribution of the newly formed field of formation pressures and tendency of the fluid-rock system for the thermodynamic equilibrium result in the formation of impermeable boundaries (completely healed interstices and fissures) and hydrodynamically isolated blocks, which became “sealed” due to precipitation of secondary minerals at their boundaries. Precisely these processes determine heterogeneity in capacity and filtration properties of rocks at deep levels and in the field of formation pressures in all the directions. They are also responsible for variations in mineralization, concentrations of microcomponents and palynomorphs, gas composition, organic matter type, and other anomalies at short distances.

(6) Passing through the long and complex transformation during their subsidence (compacting, mineralogical, textural–structural changes in the successions of montmorillonite–chlorite and clay–argillite–shale), clayey rocks are transformed into rocks with rigid structural–crystalline bonds, lose their plasticity, and acquire capacity to jointing formation. At depths exceeding 2,500 m (locally deeper), they should be considered as fissure reservoirs. Clayey rocks are permeable at all levels of the geological sedimentary section of negative structures, except for situations, when interstices and fissures are filled with secondary minerals. In the last case, they may play the role of confining beds for migrating fluids, hydrocarbons included at certain stages of geological development of artesian (petroliferous) structures.

(7) Complex and diverse catagenetic transformations of terrigenous and carbonate reservoirs lead to practically complete impermeability in some areas. *At deep levels, permeability of reservoirs is largely provided by fissures of different genesis.* The vertical migration of solutions “alien” by their chemical and gas compositions may result in partial or complete healing of fissures and transform reservoirs into impermeable formations or confining beds for hydrocarbon accumulations and groundwater. To the contrary, rocks traditionally considered being impermeable or poorly permeable (largely clayey) may serve as reservoirs. Thus, at large depths, *regardless of their genesis and lithology the same rocks may serve as either reservoirs or confining beds in different periods of geological development of artesian (petroliferous) structure.*

Most favorable conditions for fissure healing exist at lithological boundaries. Therefore, in the vertical section, well-permeable rocks (central parts of the block) alternate with practically impermeable varieties (its marginal parts). Exceptions are near-vertical zones of long-living faults, which are marked by low-amplitude and low-velocity movements resulting in disturbed continuity of rocks in fault zones. The faults that become activated during some geological epochs appear to be healed during most geological history. Filtration and capacity properties of rocks at deep levels of platform sedimentary sections are characterized by distinct anisotropy in all directions, which is yet poorly known.

(8) Hydrogeological reconstructions based on the concept of the dominant elision role in development of deep fluid formation pressures at deep levels of negative structures are insufficiently substantiated.

Transformation of clayey rocks is undoubtedly accompanied by the release of large volumes of interstitial and crystallization waters. This process is however as long as millions of years and is, in fact, stationary. As follows from

filtration consolidation modeling, the redistribution rate of interstitial pressures during compaction of clayey rocks in normal conditions (lack of hydrodynamically impermeable boundaries of different genesis) is substantially higher as compared with the rate of overburden pressure increment that provides compression. *Therefore, elision cannot determine development of formation pressures in the zone of very slow water exchange.*

In this connection, paleohydrodynamic maps based only on elision concepts (without account for boundary conditions, filtration properties of water-hosting poorly permeable rocks) do not reflect situation in natural objects. With the present-day knowledge of the study object, one should be careful when compiling paleohydrological maps. Even higher precaution degree is required, when paleohydrological reconstructions are used for substantiating criteria for prospecting deposits of mineral resources (oil, gas, groundwater for different purposes).

In our opinion, elision should be understood as ascending migration of interstitial and crystallization waters diffused in time and space, the share of which in the time and space units is extremely low in the integral balance of artesian (petroliferous) structures.

(9) *The stratum-block structure of deep formations in the petroliferous (artesian) structures (inter- and intramontane depressions) should be taken into consideration in interpreting formation or reduced pressures as well as the role of surface factors (rivers, lakes, springs, and others) in compiling maps of level surface for aquifers of the intense water exchange zones.*

It is known that water levels in boreholes located on conjugate watersheds separated by a river or in boreholes located on different sides of the same watershed are not interpolative linearly. Fractures and structural–tectonic conditions are usually ignored in practical compiling regional piezometric maps of deep aquifers (petroliferous complexes). Nevertheless, the analogy between aquifers of intense and very slow water exchange zones is obvious. The difference is only in factors that control the formation of the piezometric surface: surface factors in the first case and largely (but not completely) internal boundaries (fractures and structural–tectonic features of the region, geodynamic processes, recent and past hydrothermal solutions) in the second one.

Therefore, when compiling piezometric maps for deep aquifers (petroliferous complexes), we should take into consideration primarily available information on separate well-studied structures, not averaging and not selecting a single (of many) value of formation pressure, i.e., the study of formation pressures should be performed separately for every structure (area), which will allow internal boundaries within structures and between them to be defined. Only such an approach will make it possible to correctly interpret movement directions of deep fluids both at the regional scale for artesian (petroliferous) basins as a whole and their separate parts and perform reliable interpolation between individual points.

(10) The available experience in the study of hydrogeodynamics of deep formations demonstrates the necessity in the study of internal boundaries, genesis of which may be substantially variable (tectonic, lithological-facies, mineralogical–geochemical, hydrodynamic).

(11) The hypothesis of the layer–block structure of deep formations, development of which is explained by the pulsation-fluid geothermodynamic model is proposed instead of widely accepted infiltration and elision hypotheses explaining the formation of deep fluids in the zone of the very slow water exchange. This model unites two hypotheses of oil origin and formation of hydrocarbon accumulations (giant fields included) located at different levels of the sedimentary cover and in the crystalline basement of negative stratified structures.

# Index

## A

- Abiogenic origin of oil, 359
- Abnormally high formation pressures (AHFP)
  - and anomaly coefficient, 60
  - Bukhara-Karshi petroliferous basin, 298–303
  - definition of, 59
  - development of, 60
    - catagenetic processes on, 83
    - chemical processes on, 84
    - elision processes on, 72–73
    - tectonic forces on, 74–81
    - temperature changes, 84–86
  - distribution of, 80, 81
  - Eastern Ciscaucasia petroliferous basin, 276–278
  - in Pechora petroliferous basin, 215–218
  - permeability of boundary layer for, 63
  - process for developing, 86
  - pressure relaxation period, 61–63
- AHFP, *see* Abnormally high formation pressures (AHFP)
- Akchagylian aquifer, 256–257
- Albian-Cenomanian aquifer, 63
- Albian-Cenomanian petroliferous complex, 292
  - groundwater lateral gradient in, 294, 296
  - potentiometric surface in, 295, 303
- Albian sediments, 289
- Amirkhanov, Sh. Kh., 75
- Anikeev, V. A., 73
- Anomaly coefficient
  - and AHFP, 60
  - clayey sediments, 68–70
  - in Inzyrei structure, 217
- Apsheonian aquifer
  - elision recharge, 262–263
  - groundwater formation pressures in, 263

- Apsheonian Peninsula, vertical tectonic movements in, 74
- Aptian-Cenomanian aquifer, 137–138
  - chemical compositions, 137
- Aptian-Cenomanian complex, groundwater flow, 153
- Ardala structures
  - mineralization, 227
  - temperature field, 219
- Arie, A. G., 9
- Artesian basins
  - geostatic stage of, 6
  - groundwater dynamics, 9–10
  - groundwater formation of, 7
  - hydrodynamic isolated stages of, 5
  - hydrodynamic zones in, 1, 4
  - hydrostatic stage, 7
  - transitional stage, 7
  - types of, 2–3
- Arzgir-Prikumsk zone, potentiometric levels in, 285

## B

- Babkov, K. V., 310
- Bagdasarova, M. V., 362, 372
- Baikal rift zone, thermal anomalies in, 308
- Bakuan aquifer, 256
- Bazhenova O. K., 349
- Bazhenovka formation
  - argillites of, 101
  - reservoir properties of, 122
- Beskrovnyi, V. S., 300
- Bezrodnyi, V. D., 337
- Bochever, F. M., 151
- Bogomolovs, Yu. G., 339
- Brecciation zones, deep fluid discharge by, 154
- Brilling, I. A., 114
- Bukhara-Karshi petroliferous basin
  - AHFP in, 298–303

- anomaly coefficients, 302
- hydrogeological conditions in
  - Albian-Cenomanian complex, 292
  - Jurassic complex, 292–293
  - Turonian-Paleocene complex, 292
- local fluidodynamics in, 296–298
- regional fluidodynamics in, 303–304
- stratigraphy of
  - Cenozoic group, 289–290
  - Cretaceous, 289–290
  - Mesozoic group, 287–288
- tectonics in
  - Bukhara step, 290–291
  - Chardzhou step, 291–292
- Butov, P. I., 1
- C**
- Cambrian system, 187–189
- Carbonate rocks
  - capacity properties, 90, 109, 111
  - developing reservoir properties in, 109–112
  - factors for transformation of, 109
  - filtration properties, 109, 111
    - deterioration in, 108
    - tectonics on, 111
  - fissure permeability, 110
  - hydraulic fracturing, 111
  - permeability coefficient of, 111
  - porosity, 110, 111
  - post-sedimentary transformations, 111, 125
  - tectonic processes in, 111
  - See also* Terrigenous rocks
- Carboniferous system, 191
- Catagenetic processes, 83
  - velocities of, 83
- Catagenetic transformations
  - of clayey rocks, 73, 146
  - effect of, 101
- Caucasian Mineral Waters (CMW), 258
- Cenomanian sediments, 289
- Cenozoic sediments, 193–194, 289–290
- Cenozoic tectonic fractures, 195
- Clayey reservoirs
  - catagenetic zones, 117
  - compaction, 113
    - coefficients of, 126
  - fissures in, 118, 122, 125, 147
  - formation of
    - by geostatic compaction, 113
    - by mineralization, 113–115
  - high interstitial pressures, 124
  - hydraulic fracturing, 111, 124
  - microheterogeneity (jointing) of, 118–120
  - mineralogical composition of, 115–126
    - change of permeability by, 115
    - mineral transformations of, 118
    - montmorillonite hydration in, 116
    - non-uniform compression of, 123
  - permeability, 112, 118, 143
    - coefficient of, 113, 114, 120, 121
    - porosity, 113
- Clayey rocks, *see* Clayey reservoirs
- Clayey sediments
  - anomaly coefficient, 68–70
  - compaction of, 70
  - dehydration of, 73–74
  - fluidodynamic horizontal boundaries in, 63–71
  - interstitial pressure, 64, 65, 67–69
  - permeability, 54
    - coefficient of, 67, 69, 71
    - sedimentation rate, 66, 67, 69
    - volume of water released from, 161–165
- Cretaceous sediments, 193, 241, 289
- Crystallization of water, 328
- D**
- Dagadzhik oil field, 82
- Danian sediments, 289
- Deep fluids
  - changes in lateral expenditures of, 154–157
  - characteristic of discharge areas, 150–151
  - elision recharge of, 47–56
  - factors influencing on formation of, 200
  - flow
    - density variable, 25–27
    - modeling methods in, 27–30
  - formation pressures, elision recharge
    - influence on, 261–263
  - hydrodynamics of, 159–160
  - hydrogeological cycle, 152
  - infiltration recharge of, 147
  - influx of, 81
  - integral vertical filtration of, 38
  - in Kharasavei field, 174–175
  - migration, 81
    - by low-permeability rocks, 154–160
    - regularities in, 48
  - mineralization in
    - Ardala structures, 227
    - Eastern Kolva, 227
    - Northern Khosedayu structure, 228
    - Western Khosedayu structure, 228
  - paleomigration of, 47–56, 180–183

- pulsation-fluid geothermodynamic model of, 333
- pulsation-fluid thermodynamic model of, 332
- regional flows, 31
- regional infiltration recharge in, 37–40, 255
- in Salym field, 165–170
- in Ust-Balyk field, 176–180
- vertical migration of, 309, 311, 316
  - features of, 314–315
  - palynological analysis for, 305–307
  - in saliferous sediments, 313
  - in Western Surgut field, 170–174
- Deep formations
  - elision process, 165
  - gas composition anomalies, 310
  - geochemical anomalies, 310
  - geothermal anomalies, 307
  - hydrochemical anomalies, 308
  - fluid dynamics in, 208–210
  - mineral anomalies, 307
  - in Pechora basin, geodynamic analysis, 200–208
  - regional flows in, 8, 344, 381
  - in Salym field, 166–170
  - stratum-block structure of, 26, 103, 183, 208–209
    - fluidodynamic boundaries in, 324–325
    - formation pressures analysis in, 319
    - lithological-facies boundaries in, 321–323
    - parameters for, 231
    - tectonic boundaries in, 321–322
  - temperature field in, 218–215
  - thermal anomalies, 308, 309
  - vertical migration of fluids in, 315
- Dehydration of clay minerals, 73–74
- Denk, S. A., 111
- Density convection, 9
- Density variable fluid flows, assessing
  - directions of, 26–27
- Depolymerization of complex hydrocarbons, 84
- Derpgolts, V. F., 312
- Devonian rocks
  - Famennian sediments in, 191
  - Frasnian sediments in, 190
  - strata in, 189–190
- Djunin, V. I., 8
- Dmitriev, L. P., 314
- Dolenko, G. N., 104
- Dorofeeva, A. K., 117
- Durmish'yan, A. G., 126
- Dvorov, V. I., 309
- E**
- Earthquake
  - Arvia Tekhachani, 75
  - Dagestan, 75
  - Sakhalin, 75
  - Tashkent, 75
- East Pereval'noe field, 346–347
- Eastern Ciscaucasia petroliferous basin
  - AHFP in, 241, 276–278
  - fluid mineralization in, 245–249
  - formation pressures in, 251–254, 276–278
  - geological structure of
    - Cretaceous sediments, 241
    - Jurassic sediments, 239–241
    - Maikop aquifer, 245
    - Paleogene-Neogene sediments, 241–242
    - Quaternary sandy-clayey, 242
    - tectonics, 242–244
  - hydrogeological conditions in
    - lower Cretaceous complex, 247
    - lower-middle Jurassic complex, 248–249
    - Maikop aquifer, 245
    - Paleocene-Eocene aquifer, 245–246
    - Permian-Triassic complex, 249–250
    - upper Jurassic complex, 247–248
- Eastern Kolva structure
  - mineralization in, 227
  - temperature field of, 219
- Eastern Kuban depression, grain size of
  - sediments in, 92
- Elastic deformations, 144
- Elision recharge, 72–73
  - Apsheronian aquifer, 262–263
  - assessing influence of
    - on fluid formation, 50
    - parameters used in, 50
  - of deep fluids, 47–56
  - influence on formation pressure, 160–165, 261–263
  - sedimentation rates of, 328
- Engel'gardt, V., 95
- Eocene sediments, 242
- Erosion, groundwater discharge by, 152–153
- Ershova, S. B., 134
- F**
- Famennian carbonate rocks, fissures in, 324
- Famennian sediments, 191
- Fartukov, A. M., 12

- Fedorov, V. K., 124  
 Fergana depression, Paleogene clays of, 115  
 Filippovskii, N. A., 308  
 Filtration equation for petroliferous formation, 28  
 Filtration force  
   calculation of, 25, 265, 267  
   method, 25–26  
     for directions of density-variable flows, 25–26  
   vectors, 25  
 Filtration resistance, horizontal *versus* vertical, 38  
 Filulation movement, 9  
 First law of thermodynamics, 330  
 Fischer-Tropsch reaction, 360  
 Fissure healing, 315  
 Flow bands, 33  
 Fluid densities, changes in, 23  
 Fluid unit expenditures, 40  
 Fluidodynamic boundaries  
   in clayey sediments, 63–71  
   horizontal, 324–325  
 Fomin, A. A., 124  
 Formation pressure  
   in Achikulak area, 273  
   distribution of, 30  
   Eastern Ciscaucasia petroliferous basin, 251–254, 276–278  
   hydrodynamic blocks, 233  
   Inzyrei structure, 217, 218  
   measurement of, 204, 207, 208  
   Neocomian sediments, 298  
   reduction  
     errors in, 20–24, 201–204  
     Gurevich method of, 19, 23  
     inaccuracy in, 20  
   relaxation of, 80, 324  
   in sandy lens, 62, 63  
   Russkii Khutor Severnyi settlement, 267–268  
   in stratum-block structure, 319  
   Ust-Balyk field, 176–177  
   Western Surgut field, 171  
   Zapadno-Mekteb field, 271  
 Fossilization coefficients, 11  
 Frasnian sediments, 190  
 Furies equation, 66
- G**  
 Gaeva, A. Ya., 8  
 Gan'kino clay formation, changes in grain-size, 93
- Gas composition anomalies, 310  
 Gas-water mixture, intrusion of, 323, 333  
 Gatal'skii, M. A., 1, 5  
 Geochemical anomalies, 310  
 Geofiltration modeling, 28  
 Geothermal anomalies, 307  
 Groundwater discharge by erosion, 152–153  
 Groundwater dynamics, artesian basins, 9–10  
 Gurevich, A. E., 19, 61, 64  
 Gurova, T. I., 311
- H**  
 Horizontal filtration resistance *vs.* vertical resistance, 38, 39  
 Hydraulic fracturing, 334  
   formation of fissures by, 106–108  
 Hydrocarbon  
   accumulation, 373  
   factors to control, 365  
   geodynamic, 362  
   hydrothermal, 374–375  
   synthesis by Fischer-Tropsch reaction, 36  
 Hydrochemical anomalies  
   characteristic feature, 308  
   *See also* Thermal anomalies  
 Hydrodynamic blocks  
   fissure permeability in, 234, 235  
   formation pressure in, 233, 235  
   hydraulic fracturing in, 235  
   typification of, 232–236  
 Hydrodynamic layers, 8  
 Hydrodynamic zones  
   in artesian basins, 1, 4  
   boundaries of, 3, 41–44  
   2D model for, 45  
   groundwater migration in, 4, 5  
   period of water exchange for, 5  
   in petroliferous basins, 41–45  
   subsurface flow in, 41  
 Hydrogeodeformation field (HGDF), 9, 331  
 Hydrogeodynamic maps  
   compiling methods, 33–34  
   *See also* Potentiometric maps  
 Hydromica clays, permeability of, 73  
 Hydrostatic pressure, 16  
 Hydrothermal mineralization, 339  
 Hydrothermal solutions on continents, 370–374  
 Hydrovolcanism, 340
- I**  
 Ibragimov, D. S., 313  
 Ignatovich, N. K., 1

- Infiltration recharge in Ob-Yenisei interfluvium, 149
- Inzyrei structure  
 AHFP in, 217  
 anomaly coefficients in, 217  
 measured formation pressures in, 217, 218  
 subsurface fluids in, 218
- Isotopic composition of gases, 353–357
- Ivanchuk P. P., 340
- J**
- Jurassic aquifers, 196
- Jurassic petroliferous complex, 292–293  
 groundwater lateral gradients in, 296, 297  
 influence of basin periphery on, 296  
 potentiometric surface of, 285, 296, 297, 301  
 pressure gradients in, 260  
 regional fluidodynamics in, 284–285
- Jurassic sediments, 95, 193, 239–241, 287
- K**
- Kalinko, M. K., 61
- Kalyuzhnyi, Yu. V., 61, 72
- Kamenskii, A. N., 3
- Kaolinization, 145
- Karetnikov, L. G., 307
- Khamraev, M. R., 308
- Kharasavei field, deep formation pressure in, 174–175
- Khodzhaikuliev, A. Ya., 18
- Khometovski, A. S., 8
- Khoreiver depression, 213  
 fluid mineralization in, 225–226, 229  
 gradients of, 229  
 reduced formation pressures for, 204  
 temperature changes in, 222  
 temperature field in, 220–221  
 mineralization gradients in, 229  
 oils of, 230
- Kichk, A. A., 358
- Kirkinskaya, V. N., 235
- Kiryukhina, T. A., 210
- Kiselev, A. E., 104
- Kissin, I. G., 62, 261, 337
- Kolodii, V. V., 6, 61, 72
- Kortsenshtein, V. N., 255
- Korzun, A. V., 8
- Kosenkova, N. N., 210
- Krayushkin, V. A., 355, 356, 370
- Kropotkin, P. N., 374, 357
- Krotova, V. A., 311, 312
- Kudryavtsev, E. I., 311
- Kudryavtsev, N. A., 312
- Kungurian sediments, 192
- Kushnareva, T. I., 324
- Kustovskoe field, 346
- Kuvaev, A. A., 9
- Kynov-Sargaev sequence, 198–199
- L**
- Lateral fluid expenditures, 40
- Le Chatelier principle for depolymerization, 84
- Linetskii, V. F., 61
- Lithological-facies boundaries, 321–323
- Lithological-mineralogical composition, 143
- Local fluidodynamics  
 in Achikulak area, 269–272  
 formation pressures in, 273  
 Ozek-Suat area, 272–274  
 Russkii Khutor Severnyi settlement, 267–269  
 Velichaevsk area, 269  
 lateral pressure gradients in, 272  
 Zapadno-Mekteb field, 269  
*See also* Regional fluidodynamics
- Local gradient, calculation of, 18
- Lomonosov, I. S., 308
- Lower Cretaceous-Cenomanian complex, 133–134
- Lower Cretaceous petroliferous complex, 247  
 pressure gradients in, 259  
 sediments, 92
- Lower Devonian rocks, 189–190
- Lower-middle Jurassic complex, 248–249  
 chemical composition of, 139, 140  
 hydrogeological characteristic of, 141  
 terrigenous sediments in, 131  
 thicknesses of, 132  
 transmissibility of, 161
- Lower Permian confining sequence, 197
- Lyulinvor clay formation, 92
- M**
- Maikop aquifer, 245
- Maikop sediments, 242
- Makarenko, F. F., 1
- Mediterranean mud volcanoes, 367
- Mendelev, D. I., 357
- Mesozoic sediments, 192, 287
- Middle Devonian rock, 190
- Middle-upper Devonian petroliferous complex, 7
- Mikulenko, K. I., 122
- Mineral anomalies, 307
- Mineralization field, 35
- Mineralogical-geochemical boundaries, 323–324



- Mineral-organic hypothesis, 364–367  
 Mineral (inorganic) theory, 353–359  
 Miropol'skaya, G. A., 121  
 Mokienko, V. F., 310  
 Mongol-Baikal seismic zone, 75  
 Montmorillonite hydration, 116  
 Montmorillonite transformation, 328
- N**  
 Neocomian petroliferous complex, 138–139  
 Neocomian sediments, 95, 289  
   formation pressure in, 298  
 Neogene sediments, 289  
 Northern Khosedayu structure  
   mineralization in, 228  
   reduced pressures in, 208  
   temperature field in, 221  
 Novopokur field, 346
- O**  
 Ogil'vi, N. A., 85  
 Ordovician-lower Devonian aquifer, 199–200  
 Ordovician system, 189  
 Ovchinnikov, A. M., 5
- P**  
 Paleogene-Eocene aquifer, 245–246  
 Paleogene-Quaternary complex, 134  
 Paleogene sediments, 241, 289  
 Paleohydrodynamic reconstructions, shocks in,  
   49  
 Paleomigration  
   characteristic of, 48  
   of deep fluids, 47–56  
 Paleozoic group, 187  
 Palynological analysis for vertical fluid  
   migration, 305–307  
 Panakhi, Sh. A., 308  
 Pashkovskii, I. S., 44  
 Pechora petroliferous basin  
   AHFP in, 215–218  
   analysis of fluid geodynamics  
     in deep formations, 200–208  
   Carboniferous system, 191  
   Cenozoic sediments, 193–194  
   Cretaceous system, 193  
   Devonian rocks  
     Famennian sediments in, 191  
     Frasnian sediments in, 190  
     strata in, 189–190  
   hydrogeological conditions  
     Jurassic aquifer, 196  
     Kynov-Sargaevo confining sequence,  
       198–199  
     lower Permian confining sequence, 197  
     middle Devonian-lower Frasnian  
       aquifer, 199  
     Ordovician-lower Devonian aquifer,  
       199–200  
     Riphean aquifer, 200  
     upper Frasnian-Tournaisian complex,  
       198  
     upper Jurassic-Cretaceous confining  
       sequence, 196  
     upper Permian-Triassic aquifer, 197  
     upper Viséan-Artinskian aquifer, 197  
     Vendian-lower Cambrian aquifer, 200  
     Viséan confining sequence, 198  
   Jurassic system, 193  
   Khoreiver depression in, 194  
   Kolva Megaswell in, 194  
   Kungurian sediments, 192  
   Mesozoic sediments, 192  
   Permian system, 191–192  
   Sorokin Swell in, 194  
   tectonic zoning of, 195–196  
   Triassic sediments, 192–193  
   *See also* West Siberian petroliferous basin  
 Pecle criterion, 44  
 Permian system, 191–192  
 Permian-Triassic petroliferous complex,  
   249–250  
 Petrenko, V. P., 337  
 Petroliferous basins  
   hydrodynamic zones in, 41–45  
   role of peripheral parts of, 37–40  
   transmissibility of reservoirs of, 39  
 Pikovskii, Yu. I., 351  
 Pinneker, E. V., 5, 6  
 Plate tectonics, 11  
 Pliocene sediments, 242  
 Pulsation-fluid thermodynamic model, 340,  
   341, 364–365  
 Porfir'ev, V. B., 82  
 Potentiometric maps, 15, 279  
   of lower-middle Jurassic surface, 140  
   of Paleozoic sediment surface, 140  
   regional, compilation methods of, 30–33  
 Prasolov, E. M., 349, 353–354  
 Pre-Jurassic terrigenous sediments, 100  
 Prikumsk petroliferous basin, potentiometric  
   level, 285  
 Pulsating-fluid geothermodynamic model, 323,  
   333  
 Pulsating-fluid thermodynamic model, 340,  
   341, 364–365  
 Pushkarev, Yu. D., 361

**R**

- Radiocarbon analysis of bottom sediments, 52
- Rechinskii fault zone, gravity field change in, 76
- Rechitsa fault, 362
- Reduced pressure, conditionalities in calculations of, 17–18
- Regional fluidodynamics
  - Bukhara-Karshi petroliferous basin, 303–304
  - hydrogeological stages in, 3–4
  - Jurassic petroliferous complex, 284–285
  - lower Cretaceous petroliferous complex, 283–284
  - upper Cretaceous petroliferous complex, 279–283
- Regional hydrogeodynamics, 27
- Regional infiltration recharge sources, 37–40
- Regional potentiometric maps
  - compilation methods of, 30–33
  - in groundwater surface, 32–33
- Regional recharge centers, 260
- Reservoir transmissibility, 50, 51
- Riftogenic sedimentary basins, 11
- Riphean aquifer, 200
- Rodkina, M. V., 354–355
- Romashkino field, 373
- Rozin, A. A., 145
- Russkii Khutor Severnyi settlement
  - formation pressures in, 267–268
  - lateral pressure gradients of, 269, 271
- Rustamov, R. I., 8
- S**
- Sabirov, K. A., 313
- Saliferous rock, permeability of, 126–127
- Salym field
  - Bazhenovka formation pressures in, 166, 167
  - deep formations in, 166–170
  - hydrogeochemical anomalies, 169
  - mineralogical anomalies, 170
  - oil anomalies, 170
  - temperature anomalies, 169
  - Tyumen formation, 166
- Secondary mineral formation, 145
- Second law of thermodynamics, 330
- Sedimentary-migratory oil origin, 348–353
- Sedimentation rate in geosynclinal regions, 52
- Sedimentation waters, 6
- Semikhatov, A. N., 6
- Senonian sediments, 289
- Shagoyants, S. G., 250
- Shestakov, V. M., 18
- Shtengelov, R. S., 105
- Shumovsk hydrocarbon field, 309
- Sidorov, V. A., 76
- Silin-Bekchurin's equation, 17
- Silurian-lower Devonian petroliferous complex, 212–214
  - distribution of pressure in, 212
- Silurian system, 189
- Smekhov, E. M., 235
- Smyslov, A. A., 82
- Sokolov, B. A., 349, 350
- Sokolov, V. Ya., 300
- Sorokin Swell, 212, 214
  - water density change in, 201
- Spreading sedimentary basins, 11
- Stratum-block structure
  - deep formations of, 208–209
  - fluidodynamic boundaries, 324–325
  - formation pressures analysis in, 319
  - lithological-facies boundaries, 321–323
  - Northern Khosedayu, 210
  - tectonic boundaries, 321–322
- Strelko, I. Sh., 301
- Subaqueous hydrothermal activity, 367–370
  - in Black Sea, 367
  - in Mediterranean Sea, 367
  - in Red Sea, 367
- Subsurface fluids
  - compression-induced migration of, 47
  - deformation of, 45
  - distribution of, 53
  - flow, 42
  - migration of, 44
    - velocity of, 52
  - paleodistribution of, 164
  - paleomigration of, 48
- T**
- Tectonic boundaries, 321–322
- Tectonic forces, 74–81
  - in Alpine fold belt, 74
- Tectonic fractures, deep fluid discharge by, 154
- Tectonic movements
  - in Apsheron Peninsula, 74
  - temperature fields, 85
  - velocities of, 74
- Tectonics, 134–137
  - in Bukhara-Karshi petroliferous basin, 290–292
  - in Eastern Ciscaucasia petroliferous basin, 242–244

- fractures, 135–136
  - velocity of, 135
  - Temperature field
    - analysis of, 35
    - Ardala area, 219
    - deep formations, 218–225
    - Eastern Kolva structure, 219
    - Khoreiver depression, 220–221
    - in Northern Khosedayu, 221
    - Western Khosedayu, 219
  - Terek-Caspian trough, 362
    - anomalous altitude levels of, 284, 285
  - Terek-Sunzha uplift
    - AHFP in, 264
    - block structure of, 264
    - potentiometric levels of, 285
  - Tereshchenko, A. A., 314
  - Terrigenous rocks
    - capacity properties, 90, 104
    - of Dnieper-Donets depression, 99
    - filtration properties, 90, 104, 322
      - tectonic stresses on, 105
    - grain size change in, 93
    - interstitial permeability, 101
    - interstitial space in, 99
    - minerals in, 100
    - permeability coefficient of, 97, 104
    - porosity, 97, 101, 102, 104
    - regeneration textures in, 101
    - regional regularities in grain-size, 92, 94
    - regional transformation of, 97
    - reservoir properties in
      - catagenetic transformations, 90–94
      - cementation, 99–105
      - compaction, 94–97
      - dissolution, 97–99
      - hydraulic fracturing, 106–108
      - sedimentation settings, 94
      - tectonics, 105–106
  - Timan-Pechora petroliferous basin, 21
    - grain size of terrigenous rocks in, 92
  - Terrigenous sediments, grain-size change, 93–94
  - Thermal anomalies
    - in Baikal rift zone, 308
    - in deep formations, 308, 309
  - Transmissibility of reservoirs, 39
  - Triassic sediments, 192–193
  - Turonian-Paleocene groundwater complex, 292, 303
    - groundwater lateral gradients in, 294
    - influence of basin periphery on, 293–294
    - potentiometric surface of, 293
  - Turonian sediments, 289
  - Tyumen formation, 166
- U**
- Ulmi, M., 313
  - Upper Cretaceous-Paleogene complex, 133–134
    - clay composition of, 133
  - Upper Cretaceous petroliferous complex, 246–247
    - potentiometric levels, 282
    - pressure gradients in, 258
    - regional fluidodynamics in, 279–283
  - Upper Devonian rock, 190
  - Upper Devonian-Tournaisian complex, 198
    - filtration and capacity properties, 109
  - Upper Frasnian-Tournaisian complex, 198
  - Upper Jurassic-Cretaceous confining sequence, 196
  - Upper Jurassic petroliferous complex, 247–248
    - AHFP in sediments of, 302
  - Upper Permian-Triassic aquifer, 196
  - Upper Permian-Triassic petroliferous complex, 214–215
  - Upper Visean-Artinskian aquifer, 197
  - Ust-Balyk field
    - AHFP in, 180
    - deep formation in, 176–180
    - formation pressures in, 176–177
    - groundwater chemical composition in, 178
    - mineralization in, 178
      - gradients of, 178
- V**
- van der Waals' equation, 85
  - Vartanyan, G. S., 9
  - Vendian-lower Cambrian aquifer, 200
  - Vertical filtration resistance *vs.* horizontal resistance, 38, 39
  - Visean confining sequence, 198
  - Vsevolozhskii, V. A., 3, 163
  - Vyintoi field, 346
- W**
- Water balance calculations, 148, 149
  - Water density in normal and formation conditions, 23–24
  - West Siberian petroliferous basin
    - changes in sedimentation rates by, 135
    - filtration properties of rocks in, 141–147
      - average permeability, 143
      - factors and processes for, 143–145
      - permeability coefficients, 142
      - transmissibility, 142–143

- geological and tectonic structure
    - lower Cretaceous-Cenomanian complex, 133–134
    - lower-middle Jurassic complex, 131–133
    - Paleogene-Quaternary complex, 134
    - tectonics, 134–137
    - upper Jurassic-lower Valanginian complex, 134
  - hydrocarbons migration in, 306
  - hydrogeological conditions of
    - Aptian-Cenomanian aquifer, 137–138
    - lower-middle Jurassic complex, 139–140
    - Neocomian complex, 138–139
  - modeling of, 27–28
  - sandy-silty sediments of, 101
  - See also* Eastern Ciscaucasia petroliferous basin
  - Western Khosedayu structure
    - mineralization in, 228
    - temperature field in, 219
  - Western Surgut field
    - deep formation in, 170–174
    - formation pressures in, 171
    - ground water composition in, 171, 172
    - mineralization in, 171, 172
- Y**
- Yakobson, G. P., 5
- Z**
- Zaitsev, I. K., 2
- Zalazaeva, L. V., 96
- Zapadno-Mekteb field, 269
  - chemical composition in, 271
  - formation pressures, 271
- Zelentsova, N. I., 329
- Zerchaninov, I. K., 17